BEILSTEIN JOURNAL OF ORGANIC CHEMISTRY

Organofluorine chemistry VI

Edited by David O'Hagan

Imprint

Beilstein Journal of Organic Chemistry
www.bjoc.org
ISSN 1860-5397
Email: journals-support@beilstein-institut.de

The *Beilstein Journal of Organic Chemistry* is published by the Beilstein-Institut zur Förderung der Chemischen Wissenschaften.

Beilstein-Institut zur Förderung der Chemischen Wissenschaften
Trakehner Straße 7–9
60487 Frankfurt am Main
Germany
www.beilstein-institut.de

BEILSTEIN JOURNAL OF ORGANIC CHEMISTRY

Visible-light-induced nickel-catalyzed α-hydroxytrifluoroethylation of alkyl carboxylic acids: Access to trifluoromethyl alkyl acyloins

Feng Chen[1], Xiu-Hua Xu[1], Zeng-Hao Chen[1], Yue Chen[2] and Feng-Ling Qing[*1]

Full Research Paper

Open Access

Address:
[1]Key Laboratory of Organofluorine Chemistry, Shanghai Institute of Organic Chemistry, University of Chinese Academy of Sciences, Chinese Academy of Sciences, 345 Lingling Lu, Shanghai 200032, China and [2]Shandong Dongyue Polymer Material Co., Ltd., Zibo 256401, China

Email:
Feng-Ling Qing[*] - flq@mail.sioc.ac.cn

* Corresponding author

Keywords:
alkyl carboxylic acids; cross coupling; EDA complex; nickel catalysis; trifluoromethyl acyloins

Beilstein J. Org. Chem. **2023,** *19,* 1372–1378.
https://doi.org/10.3762/bjoc.19.98

Received: 29 June 2023
Accepted: 30 August 2023
Published: 11 September 2023

This article is part of the thematic issue "Organofluorine chemistry VI".

Guest Editor: D. O'Hagan

Abstract

A visible-light-induced nickel-catalyzed cross coupling of alkyl carboxylic acids with *N*-trifluoroethoxyphthalimide is described. Under purple light irradiation, an α-hydroxytrifluoroethyl radical generated from a photoactive electron donor–acceptor complex between Hantzsch ester and *N*-trifluoroethoxyphthalimide was subsequently engaged in a nickel-catalyzed coupling reaction with in situ-activated alkyl carboxylic acids. This convenient protocol does not require photocatalysts and metal reductants, providing a straightforward and efficient access to trifluoromethyl alkyl acyloins in good yields with broad substrate compatibility. The complex bioactive molecules were also compatible with this catalytic system to afford the corresponding products.

Introduction

Acyloins (also known as α-hydroxy ketones) are widely found as structural motif in natural products [1-7] and bioactive molecules [8-11] (Figure 1). They can also be used as building blocks in organic synthesis [12-14], involved in numerous transformations to other important functional groups such as dicarbonyls [15], diols [16], amino ketones [17] and so on. Recently, the introduction of a trifluoromethyl group into organic molecules has received great attention due to their wide applicability in medicinal [18,19] and materials [20,21] chemistry. The toxicological experiments showed that trifluoromethyl acyloins can selectively induce apoptosis in human oral cancer cells [22,23] and have therefore attracted much more attention. However, trifluoromethyl acyloins were not widely used due to the challenge associated with their synthesis.

Certain progress has been made in the synthesis of trifluoromethyl aromatic acyloins. Maekawa's group [24] developed a tandem reaction of the reductive coupling between arylalde-

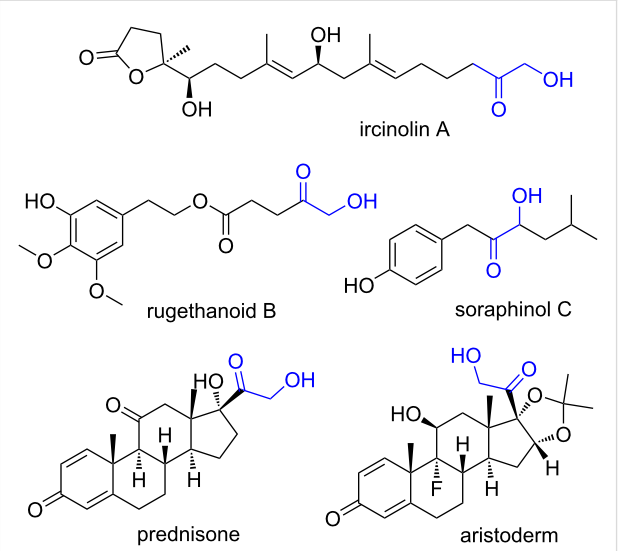

Figure 1: Selected natural products and pharmaceuticals bearing acyloins.

hydes and ethyl trifluoroacetate in the presence of magnesium and chlorotrimethylsilane, followed by desilylation to produce the trifluoromethyl aromatic acyloins (Scheme 1a). Anand's group [25] demonstrated that a NHC-catalyzed selective acyloin condensation between aromatic aldehydes and trifluoroacetaldehyde ethyl hemiacetal afforded the analogous products (Scheme 1b). In comparison, the synthesis of trifluoromethyl aliphatic acyloins is still challenging, and to the best of our knowledge, only Kawase's group [26] reported the preparation of such compounds starting from α-hydroxy acids or α-amino acids in the presence of trifluoroacetic anhydride and pyridine with very limited substrate scope (Scheme 1c). Therefore, the development of a more general and practical method for the synthesis of trifluoromethyl aliphatic acyloins is highly desirable.

Carboxylic acids are widely used in organic reactions because they are chemically stable, less toxic, and commercially available in a large structural variety [27-30]. The nickel-catalyzed direct conversion of carboxylic acids to ketones is an important chemical transformation [31-38]. However, to the best of our knowledge, this protocol has not been used for the synthesis of fluoroalkylated ketones so far. Very recently, we have developed a visible-light-induced nickel-catalyzed coupling of aryl bromides with an α-hydroxytrifluoroethyl radical for the synthesis of trifluoromethyl aryl alcohols [39]. Encouraged by this work, we envisioned that the nickel-catalyzed coupling of carboxylic acids-derived acyl electrophiles with an α-hydroxytrifluoroethyl radical might be feasible. Herein, we disclose a visible-light-induced nickel-catalyzed cross-coupling of alkyl

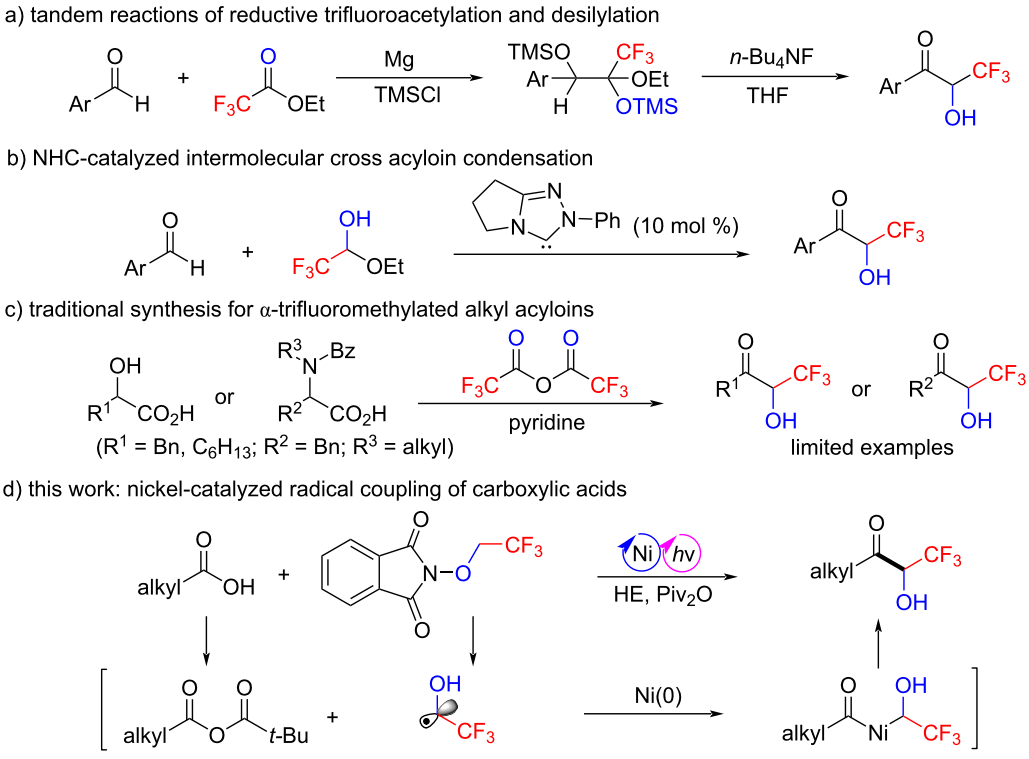

Scheme 1: Strategies for the synthesis of α-trifluoromethyl acyloins.

carboxylic acids with *N*-trifluoroethoxyphthalimide to deliver trifluoromethyl aliphatic acyloins under mild conditions (Scheme 1d). Furthermore, this platform bypasses the need for exogenous photocatalysts, providing a direct and robust access to trifluoromethyl aliphatic acyloins.

Results and Discussion

Initially, we commenced our exploration by choosing 4-phenylbutyric acid (**1a**) as the model substrate to react with *N*-trifluoroethoxyphthalimide (**2**, Table 1). On basis of the previously reported elegant strategies on direct conversion of in situ-activated carboxylic acids for ketone synthesis [27,35,38], we chose dimethyl dicarbonate (DMDC, **A1**) as the activating reagent. To our delight, the reaction of **1a** and **2** in the presence of $NiBr_2$(dtbbpy) (10 mol %), Hantzsch ester (HE) and **A1** in DMAc under the irradiation of purple LEDs afforded the desired coupling product **3a** in 50% yield (Table 1, entry 1). Further screening of other activators (Table 1, entries 2–5) indicated that pivalic anhydride (**A3**) was optimal, delivering **3a** in 56% yield. The yield of **3a** was increased to 74% when 3.0 equiv of H_2O were added to the reaction mixture [40] (Table 1, entry 6), but the addition of more water did not improve the reaction efficiency further (Table 1, entry 7). The structure of nickel catalysts played a significant role in the reaction efficiency. Switching the Ni catalyst to $NiCl_2$(dtbbpy), $NiBr_2$(bpy), $NiBr_2$(phen) or other nickel salts led to comparable or dramatically decreased yields (Table 1, entries 8–12). Other polar non-protonic solvents such as NMP and DMF led to diminished yields (Table 1, entries 13 and 14).

Having identified the optimal reaction conditions, we sought to evaluate the substrate scope of this photoinduced nickel-catalyzed cross coupling reaction. As illustrated in Scheme 2, a broad array of aliphatic carboxylic acids reacted smoothly in this protocol, providing the corresponding trifluoromethyl aliphatic acyloins in moderate to excellent yields. This mild reaction showed a good tolerance of a diverse range of functional groups, including methoxy (**3b**), methyl (**3c**), chloro (**3d**,**i**),

Table 1: Optimization of the reaction conditions.[a]

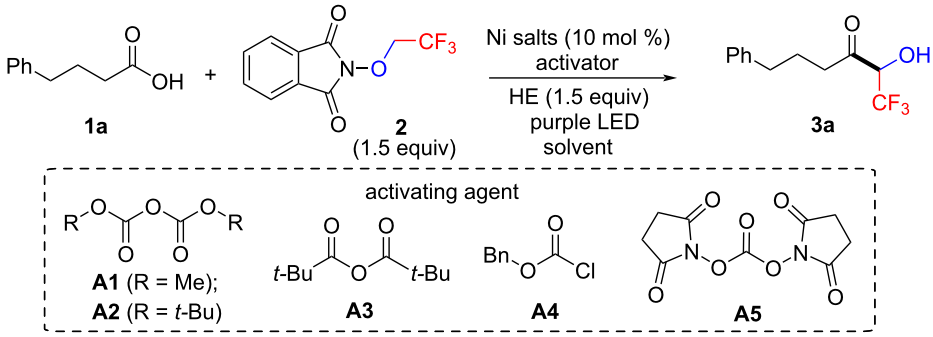

entry	Ni salt (ligand)	activator	solvent	yield (%)[b]
1	$NiBr_2$(dtbbpy)	**A1**	DMAc	50
2	$NiBr_2$(dtbbpy)	**A2**	DMAc	0
3	$NiBr_2$(dtbbpy)	**A3**	DMAc	56
4	$NiBr_2$(dtbbpy)	**A4**	DMAc	0
5	$NiBr_2$(dtbbpy)	**A5**	DMAc	0
6[c]	$NiBr_2$(dtbbpy)	**A3**	DMAc	74
7[d]	$NiBr_2$(dtbbpy)	**A3**	DMAc	68
8[c]	$NiCl_2$(dtbbpy)	**A3**	DMAc	37
9[c]	$NiBr_2$(bpy)	**A3**	DMAc	67
10[c]	$NiBr_2$(phen)	**A3**	DMAc	8
11[c]	$NiBr_2$diglyme/4,4-dCO_2Me-bpy	**A3**	DMAc	61
12[c]	$NiBr_2$diglyme/4,4-dMeO-bpy	**A3**	DMAc	65
13[c]	$NiBr_2$(dtbbpy)	**A3**	NMP	53
14[c]	$NiBr_2$(dtbbpy)	**A3**	DMF	trace

[a]Reaction conditions: **1a** (0.1 mmol), **2** (0.15 mmol), Ni catalyst (0.01 mmol), Hantzsch ester (0.15 mmol), solvent (1.0 mL), activator (0.15 mmol), purple LEDs, 7 h. [b]Yields determined by ^{19}F NMR spectroscopy using trifluoromethoxybenzene as an internal standard. [c]Adding 3.0 equiv H_2O. [d]Adding 10.0 equiv H_2O.

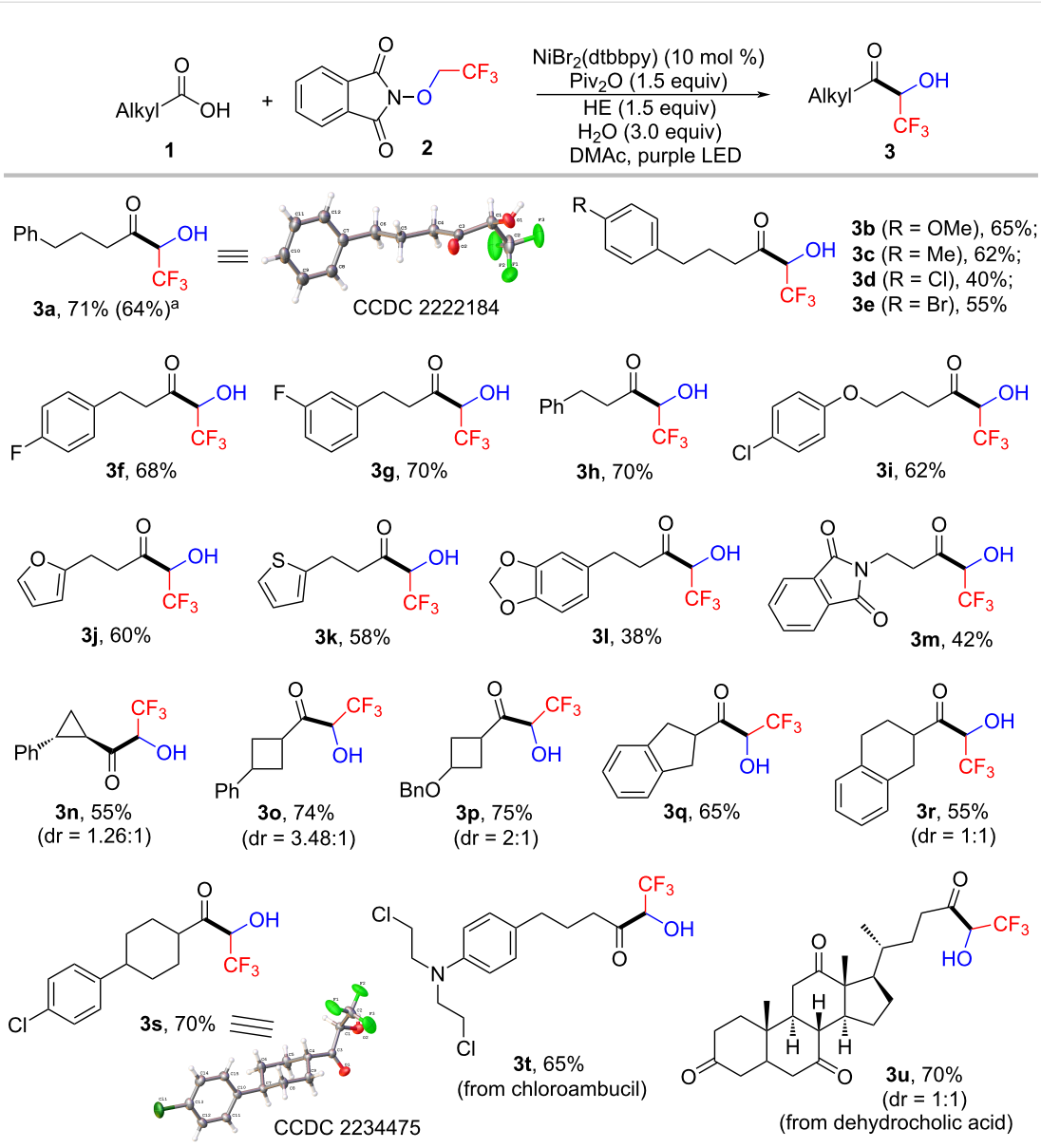

Scheme 2: Substrate scope. Standard conditions: a solution of alkyl carboxylic acid **1** (0.4 mmol), **2** (0.6 mmol), $NiBr_2$(dtbbpy) (0.04 mmol), Hantzsch ester (0.6 mmol), Piv_2O (0.6 mmol) and H_2O (1.2 mmol) in DMAc (4.0 mL) was irradiated by purple LEDs for 7 h. Isolated yields are presented. [a]The reaction was performed in a 1.0 mmol scale.

fluoro (**3f**,**g**), and ethers (**3i**,**l**,**p**). Notably, aryl bromide (**3e**) was also tolerated in this protocol, probably due to the higher reactivity of the mixed anhydride formed between carboxylic acid and pivalic anhydride than aryl bromide. The halides provided versatile synthetic handles for further transformations. Substrates bearing thiophene (**3k**) furan (**3j**) and other heterocycle (**3l**,**m**) moieties were also applicable to this reaction. This protocol allowed for the coupling of not only primary carboxylic acids but also secondary carboxylic acids (**3n**–**s**). We were pleased to find that cyclic carboxylic acids, including strained 3- and 4-membered rings, participated in this transformation and delivered the corresponding products in good yields. It should be mentioned that aromatic and more sterically hindered tertiary carboxylic acids were unfortunately not compatible with the reaction conditions. The structures of products **3a** and **3s** were unambiguously confirmed by single-crystal X-ray diffraction. Notably, the reaction of **1a** could be easily scaled up to 1.0 mmol scale, affording **3a** in a slightly lower yield. To further demonstrate the amenability toward pharmaceutically active molecules, chloroambucil (**1t**) and dehydrocholic acid (**1u**) were successfully subjected to the reaction conditions, delivering the desired products in moderate yields.

However, the analogous reaction with *N*-difluoroethoxyphthalimide as the fluoroalkylating reagent failed to afford the desired product.

According to our previous work [39] and literature precedent [27,35,38], a possible mechanism is proposed in Figure 2. The interaction between **2** and HE generates an electron donor–acceptor (EDA) complex **A**, which undergoes a light-induced charge transfer event to give trifluoroethoxyl radical **B**, followed by a 1,2-hydrogen atom transfer (HAT), producing the stable radical **C**. For the nickel cycle, it is initiated by oxidative addition of Ni(0) catalyst **E** to acyl electrophile **D** formed in situ from carboxylic acid **1** with pivalic anhydride as activator to afford Ni(II) intermediate **F**. Subsequently, trapping of the alkyl radical **C** generates high-valent Ni(III) intermediate **G**, which undergoes facile reductive elimination to furnish the final coupling product **3** and Ni(I) intermediate **H**. The single-electron transfer (SET) reduction of intermediate **H** ($E_{red}(Ni^{I}/Ni^{0})$ = −1.17 V vs SCE [41]) by photoexcited HE* ($E_{red}(HE^{*}/HE^{\bullet+})$ = −2.28 V vs SCE [42]) regenerates the active Ni(0) species **E** and closes the catalytic cycle.

Conclusion

In conclusion, we have demonstrated a visible-light-induced nickel-catalyzed radical cross coupling of readily available alkyl carboxylic acids with *N*-trifluoroethoxyphthalimide. The present study provides a mild and efficient method for the preparation of trifluoromethyl alkyl acyloins in moderate to high yields and with good functional group compatibility. Further studies on expansion of the reaction scope and development of related enantioselective photoinduced nickel-catalyzed radical cross-coupling reactions are currently underway in our laboratory.

Experimental

General procedure for the visible-light-induced nickel-catalyzed cross coupling of alkyl carboxylic acids with *N*-trifluoroethoxyphthalimide: In the glove box with nitrogen atmosphere, to an 8 mL vial equipped with a magnetic stir bar, $NiBr_2$(dtbbpy) (19.6 mg, 0.04 mmol, 10 mol %), alkyl carboxylic acid **1** (0.4 mmol, 1.0 equiv), *N*-trifluoroethoxyphthalimide (**2**, 147.1 mg, 0.6 mmol, 1.5 equiv), Hantzsch ester (152.0 mg, 0.6 mmol, 1.5 equiv), and anhydrous *N*,*N*-dimethylacetamide (4.0 mL) were added. The vial was then re-capped and taken out of the glove box, and Piv_2O (111.8 mg, 0.6 mmol, 1.5 equiv) and H_2O (21.6 mg, 1.2 mmol, 3.0 equiv) were added. The vial was sealed and the reaction mixture was then stirred under irradiation by purple LEDs (λ_{max} = 399 nm) for 7 h. After the reaction was complete, the reaction mixture was poured into water and extracted with EtOAc. The combined organic phase

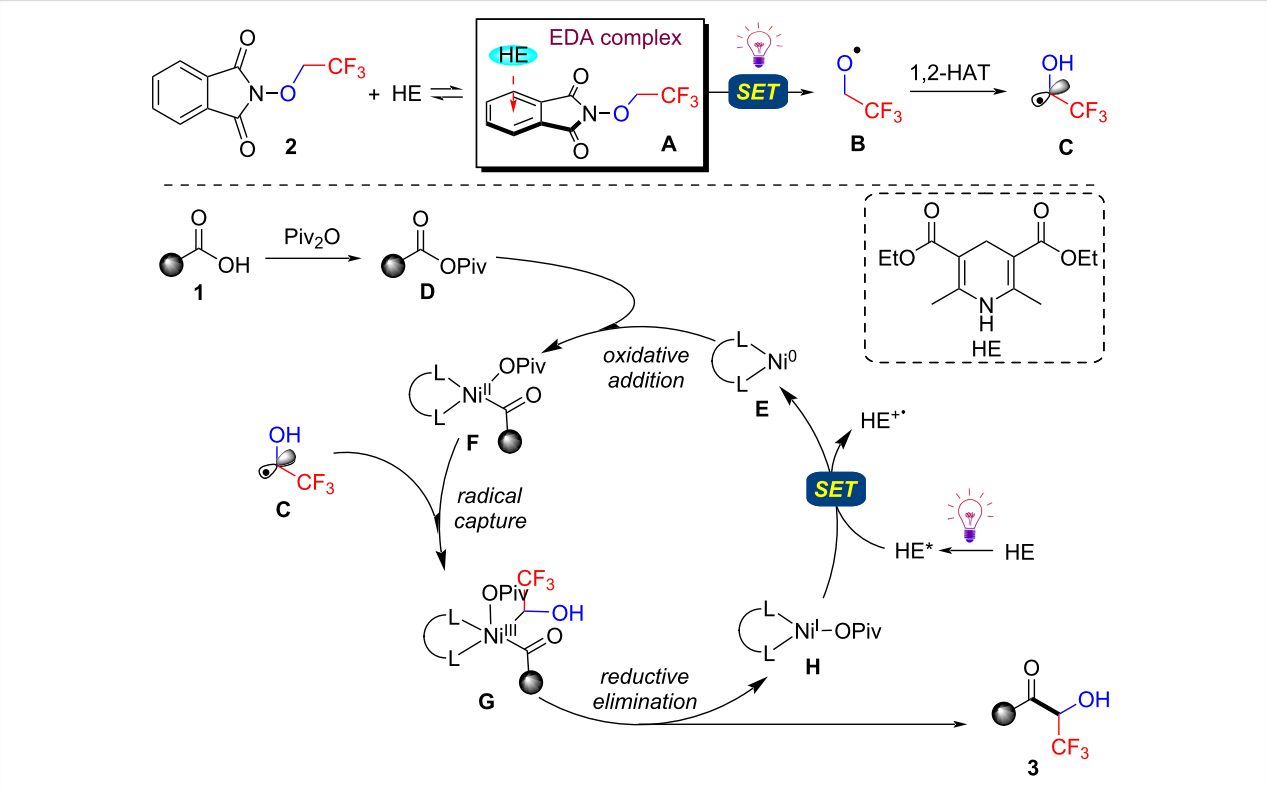

Figure 2: Proposed reaction mechanism.

was separated and washed with brine, dried over Na_2SO_4, and concentrated under vacuum. The resulting residue was purified by silica gel flash column chromatography to give the coupling product **3**.

Supporting Information

Supporting Information File 1

Experimental procedures, product characterization, and copies of NMR spectra.
[https://www.beilstein-journals.org/bjoc/content/supplementary/1860-5397-19-98-S1.pdf]

Funding

National Natural Science Foundation of China (21991121), National Key Research and Development Program of China (2021YFF0701700), Natural Science Foundation of Shandong Province (ZR2021LFG009) and Key R&D Program of Shandong Province (2022CXGC010306) are greatly acknowledged for funding this work.

References

1. Uchida, R.; Shiomi, K.; Sunazuka, T.; Inokoshi, J.; Nishizawa, A.; Hirose, T.; Tanaka, H.; Iwai, Y.; Omura, S. *J. Antibiot.* **1996,** *49,* 886–889. doi:10.7164/antibiotics.49.886
2. Wee, J. L.; Sundermann, K.; Licari, P.; Galazzo, J. *J. Nat. Prod.* **2006,** *69,* 1456–1459. doi:10.1021/np060258o
3. Chen, H.-D.; Yang, S.-P.; Wu, Y.; Dong, L.; Yue, J.-M. *J. Nat. Prod.* **2009,** *72,* 685–689. doi:10.1021/np800811b
4. Su, J.-H.; Tseng, S.-W.; Lu, M.-C.; Liu, L.-L.; Chou, Y.; Sung, P.-J. *J. Nat. Prod.* **2011,** *74,* 2005–2009. doi:10.1021/np2004209
5. Gao, X.-M.; Shu, L.-D.; Yang, L.-Y.; Shen, Y.-Q.; Zhang, Y.-J.; Hu, Q.-F. *Bull. Korean Chem. Soc.* **2013,** *34,* 246–248. doi:10.5012/bkcs.2013.34.1.246
6. Lin, Z.; Marett, L.; Hughen, R. W.; Flores, M.; Forteza, I.; Ammon, M. A.; Concepcion, G. P.; Espino, S.; Olivera, B. M.; Rosenberg, G.; Haygood, M. G.; Light, A. R.; Schmidt, E. W. *Bioorg. Med. Chem. Lett.* **2013,** *23,* 4867–4869. doi:10.1016/j.bmcl.2013.06.088
7. Terekhov, R. P.; Selivanova, I. A.; Tyukavkina, N. A.; Ilyasov, I. R.; Zhevlakova, A. K.; Dzuban, A. V.; Bogdanov, A. G.; Davidovich, G. N.; Shylov, G. V.; Utenishev, A. N.; Kovalev, D. Y.; Fenin, A. A.; Kabluchko, T. G. *Molecules* **2020,** *25,* 5437. doi:10.3390/molecules25225437
8. Wallace, O. B.; Smith, D. W.; Deshpande, M. S.; Polson, C.; Felsenstein, K. M. *Bioorg. Med. Chem. Lett.* **2003,** *13,* 1203–1206. doi:10.1016/s0960-894x(02)01058-2
9. Tanaka, T.; Kawase, M.; Tani, S. *Bioorg. Med. Chem.* **2004,** *12,* 501–505. doi:10.1016/j.bmc.2003.10.017
10. Escandón-Rivera, S.; González-Andrade, M.; Bye, R.; Linares, E.; Navarrete, A.; Mata, R. *J. Nat. Prod.* **2012,** *75,* 968–974. doi:10.1021/np300204p
11. Scott, K. A.; Qureshi, M. H.; Cox, P. B.; Marshall, C. M.; Bellaire, B. C.; Wilcox, M.; Stuart, B. A. R.; Njardarson, J. T. *J. Med. Chem.* **2020,** *63,* 15449–15482. doi:10.1021/acs.jmedchem.0c01502
12. Hoyos, P.; Sinisterra, J.-V.; Molinari, F.; Alcántara, A. R.; Domínguez de María, P. *Acc. Chem. Res.* **2010,** *43,* 288–299. doi:10.1021/ar900196n
13. Palomo, C.; Oiarbide, M.; García, J. M. *Chem. Soc. Rev.* **2012,** *41,* 4150–4164. doi:10.1039/c2cs35046g
14. Yang, K.; Zhang, F.; Fang, T.; Li, C.; Li, W.; Song, Q. *Nat. Commun.* **2021,** *12,* 441. doi:10.1038/s41467-020-20727-7
15. Zheng, S.; Smit, W.; Spannenberg, A.; Tin, S.; de Vries, J. G. *Chem. Commun.* **2022,** *58,* 4639–4642. doi:10.1039/d2cc00773h
16. Nakata, T.; Tanaka, T.; Oishi, T. *Tetrahedron Lett.* **1983,** *24,* 2653–2656. doi:10.1016/s0040-4039(00)87969-1
17. Frongia, A.; Secci, F.; Capitta, F.; Piras, P. P.; Sanna, M. L. *Chem. Commun.* **2013,** *49,* 8812–8814. doi:10.1039/c3cc45278f
18. Inoue, M.; Sumii, Y.; Shibata, N. *ACS Omega* **2020,** *5,* 10633–10640. doi:10.1021/acsomega.0c00830
19. Ogawa, Y.; Tokunaga, E.; Kobayashi, O.; Hirai, K.; Shibata, N. *iScience* **2020,** *23,* 101467. doi:10.1016/j.isci.2020.101467
20. Sicard, A. J.; Baker, R. T. *Chem. Rev.* **2020,** *120,* 9164–9303. doi:10.1021/acs.chemrev.9b00719
21. Zhang, C.; Yan, K.; Fu, C.; Peng, H.; Hawker, C. J.; Whittaker, A. K. *Chem. Rev.* **2022,** *122,* 167–208. doi:10.1021/acs.chemrev.1c00632
22. Kawase, M.; Sakagami, H.; Kusama, K.; Motohashi, N.; Saito, S. *Bioorg. Med. Chem. Lett.* **1999,** *9,* 3113–3118. doi:10.1016/s0960-894x(99)00548-x
23. Ideo, A.; Sasaki, M.; Nakamura, C.; Mori, K.; Shimada, J.; Kanda, Y.; Kunii, S.; Kawase, M.; Sakagami, H. *Anticancer Res.* **2006,** *26,* 4335–4341.
24. Maekawa, H.; Kudo, M.; Nishiyama, Y.; Shimizu, K.; Abe, M. *Tetrahedron* **2014,** *70,* 2081–2087. doi:10.1016/j.tet.2014.02.016
25. Ramanjaneyulu, B. T.; Mahesh, S.; Vijaya Anand, R. *Org. Lett.* **2015,** *17,* 6–9. doi:10.1021/ol502581b
26. Kawase, M.; Saito, S.; Kurihara, T. *Chem. Pharm. Bull.* **2000,** *48,* 1338–1343. doi:10.1248/cpb.48.1338
27. Gooßen, L. J.; Rodríguez, N.; Gooßen, K. *Angew. Chem., Int. Ed.* **2008,** *47,* 3100–3120. doi:10.1002/anie.200704782
28. Beil, S. B.; Chen, T. Q.; Intermaggio, N. E.; MacMillan, D. W. C. *Acc. Chem. Res.* **2022,** *55,* 3481–3494. doi:10.1021/acs.accounts.2c00607
29. Sakai, H. A.; MacMillan, D. W. C. *J. Am. Chem. Soc.* **2022,** *144,* 6185–6192. doi:10.1021/jacs.2c02062
30. Li, J.; Huang, C.-Y.; Li, C.-J. *Angew. Chem., Int. Ed.* **2022,** *61,* e202112770. doi:10.1002/anie.202112770
31. Yin, H.; Zhao, C.; You, H.; Lin, K.; Gong, H. *Chem. Commun.* **2012,** *48,* 7034–7036. doi:10.1039/c2cc33232a
32. Zhao, C.; Jia, X.; Wang, X.; Gong, H. *J. Am. Chem. Soc.* **2014,** *136,* 17645–17651. doi:10.1021/ja510653n
33. Amani, J.; Alam, R.; Badir, S.; Molander, G. A. *Org. Lett.* **2017,** *19,* 2426–2429. doi:10.1021/acs.orglett.7b00989
34. Badir, S. O.; Dumoulin, A.; Matsui, J. K.; Molander, G. A. *Angew. Chem., Int. Ed.* **2018,** *57,* 6610–6613. doi:10.1002/anie.201800701
35. Shu, X.; Huan, L.; Huang, Q.; Huo, H. *J. Am. Chem. Soc.* **2020,** *142,* 19058–19064. doi:10.1021/jacs.0c10471
36. Wei, Y.; Lam, J.; Diao, T. *Chem. Sci.* **2021,** *12,* 11414–11419. doi:10.1039/d1sc03596g
37. Huan, L.; Shu, X.; Zu, W.; Zhong, D.; Huo, H. *Nat. Commun.* **2021,** *12,* 3536. doi:10.1038/s41467-021-23887-2

38. Whyte, A.; Yoon, T. P. *Angew. Chem., Int. Ed.* **2022,** *61,* e202213739. doi:10.1002/anie.202213739
39. Chen, F.; Xu, X.-H.; Chu, L.; Qing, F.-L. *Org. Lett.* **2022,** *24,* 9332–9336. doi:10.1021/acs.orglett.2c03943
40. Gooßen, L. J.; Ghosh, K. *Eur. J. Org. Chem.* **2002,** 3254–3267. doi:10.1002/1099-0690(200210)2002:19<3254::aid-ejoc3254>3.0.co;2-6
41. Shields, B. J.; Doyle, A. G. *J. Am. Chem. Soc.* **2016,** *138,* 12719–12722. doi:10.1021/jacs.6b08397
42. Jung, J.; Kim, J.; Park, G.; You, Y.; Cho, E. J. *Adv. Synth. Catal.* **2016,** *358,* 74–80. doi:10.1002/adsc.201500734

License and Terms

BEILSTEIN JOURNAL OF ORGANIC CHEMISTRY

Morpholine-mediated defluorinative cycloaddition of *gem*-difluoroalkenes and organic azides

Tzu-Yu Huang‡, Mario Djugovski‡, Sweta Adhikari, Destinee L. Manning and Sudeshna Roy*

Letter

Open Access

Address:
Department of BioMolecular Sciences, School of Pharmacy, University of Mississippi, University, MS 38677, USA

Email:
Sudeshna Roy* - roy@olemiss.edu

* Corresponding author ‡ Equal contributors

Keywords:
[3 + 2] cycloaddition; defluorination; fully decorated 1,2,3-triazoles; *gem*-difluoroalkenes; organic azides

Beilstein J. Org. Chem. **2023,** *19,* 1545–1554.
https://doi.org/10.3762/bjoc.19.111

Received: 04 July 2023
Accepted: 12 September 2023
Published: 05 October 2023

This article is part of the thematic issue "Organofluorine chemistry VI".

Guest Editor: D. O'Hagan

Abstract

Here, we report the first transition-metal-free defluorinative cycloaddition of *gem*-difluoroalkenes with organic azides in morpholine as a solvent to construct fully decorated morpholine-substituted 1,2,3-triazoles. Mechanistic studies revealed the formation of an addition–elimination intermediate of morpholine and *gem*-difluoroalkenes prior to the triazolization reaction via two plausible pathways. Attractive elements include the regioselective and straightforward direct synthesis of fully substituted 1,2,3-triazoles, which are otherwise difficult to access, from readily available starting materials.

Introduction

gem-Difluoroalkenes and their synthetic preparations soared in the last decade, driven by the high demand for carbonyl mimics in medicinal chemistry and drug discovery [1]. Although a wide array of functionalization strategies for *gem*-difluoroalkenes are available [2,3], only a couple of cycloaddition reactions has been reported [4]. For example, [3 + 2] dipolar cycloadditions to form saturated difluoroisoxazolidines [5,6] and difluoropyrrolidines [7] and [4 + 2] cycloaddition reactions with *gem*-difluoro-1,3-dienes [8]. The overall landscape of cycloaddition or addition–elimination reactions with 1,3-dipoles and *gem*-difluoroalkenes is largely unexplored and the only report of a cycloaddition is with 2-fluoroindolizines (Figure 1A) via a β-fluoride elimination in an S_NV (nucleophilic vinylic substitution)-like transformation [9]. Nucleophilic addition reactions with azoles and amines (Figure 1B) are also well-precedented [10]. Herein, we address a critical gap in the literature and report the discovery of a cycloaddition of *gem*-difluoroalkenes and organic azides mediated by a base and with morpholine as a solvent. The cycloaddition adducts, 1,4,5-trisubstituted-1,2,3-triazoles, with a pendant morpholine at the C-4 position are formed with complete regiocontrol via β-fluoride elimination in an S_NV-like transformation (Figure 1C).

1,2,3-Triazoles are a privileged scaffold in medicinal chemistry with a myriad of pharmacological activities against cancer [11,12], inflammation [13], bacterial [14,15], and viral infec-

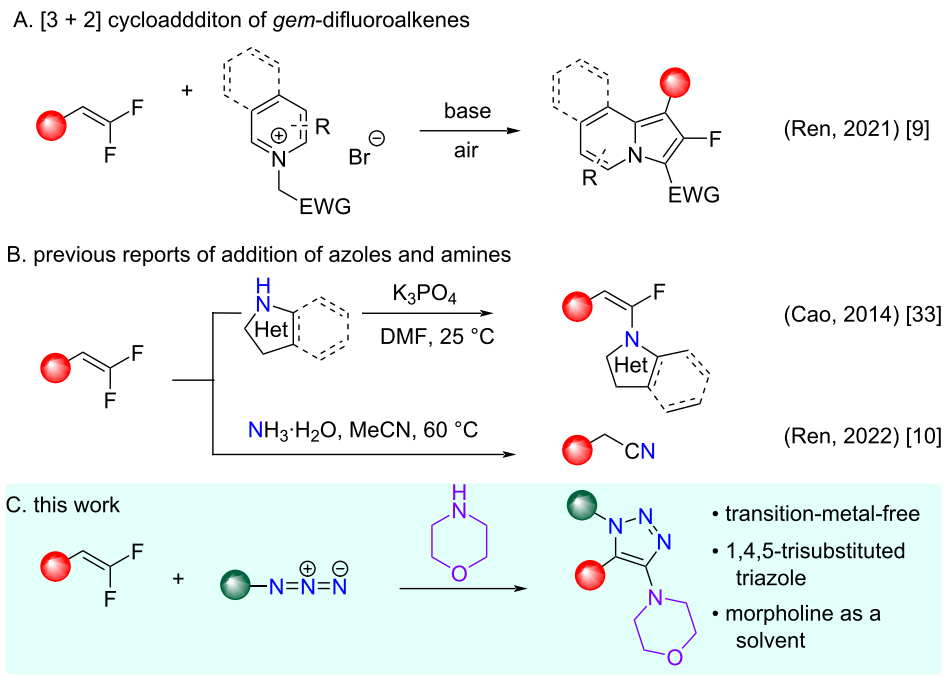

Figure 1: Functionalization of *gem*-difluoroalkenes with 1,3-dipoles and *N*-nucleophiles.

tions [16]. Hence, new ways to rapidly and efficiently access 1,2,3-triazole heterocyclic motifs are still in demand. However, methods for the direct synthesis of 1,4,5-trisubstituted-1,2,3-triazoles are limited [17]. This is highly desirable since the selective introduction of substituents at three different positions on the 1,2,3-triazole ring can augment the features of the molecule. Triazoles are also found in many biologically important molecules and functionalized materials [11-16]. 1,4,5-Trisubstituted-1,2,3-triazoles are typically accessed in two ways: (1) direct synthesis using metal or metal-free catalysis and (2) post-functionalization of disubstituted-1,2,3-triazoles [17,18]. The direct synthesis of fully substituted triazoles entails either metal-free carbonyl-based [19-21] or metal-mediated and strain-promoted [22] azide–alkyne cycloaddition reactions [17,23,24]; however, most of these strategies use high temperatures [21,25]. Herein, we report the discovery of a novel, one-step regioselective method under mild conditions to obtain 1,4,5-trisubstituted-1,2,3-triazoles from *gem*-difluoroalkenes, organic azides, and morpholine.

Terminal *gem*-difluoroalkenes exhibit unique reactivity toward nucleophiles. The two σ-withdrawing fluorine atoms at the α-position and the strong polar nature of the double bond make *gem*-difluoroalkenes susceptible to a nucleophilic attack that is followed by a β-fluoride elimination, resulting in an S_NV-like transformation [26]. We previously reported that α-fluoronitroalkenes could be effectively used as surrogates of α-fluoroalkynes in cycloaddition reactions with organic azides to construct 4-fluoro-1,5-disubstituted 1,2,3-triazoles regioselectively [27]. This two-step process involves an attack of the organic azide nucleophile to the β-position of α-fluoronitroalkenes. The polarity of *gem*-difluoroalkenes is reversed in comparison to α-fluoronitroalkenes since the nucleophile attacks at the α-position of the *gem*-difluoroalkenes. A cycloaddition reaction between organic azides and *gem*-difluoroalkenes in the presence of morpholine generates 1,5-disubstituted-1,2,3-triazoles with a pendant C-4 morpholine moiety. The regioselectivity of the triazole formation is dictated by morpholine preferentially making the first nucleophilic attack over azide at the α-position of *gem*-difluoroalkenes that subsequently undergoes a cycloaddition reaction.

Results and Discussion

While investigating 1,3-dipolar cycloaddition reactions between organic azides and *gem*-difluoroalkenes to obtain the 4-fluoro-1,4-disubstituted 1,2,3-triazole regioisomers, we observed an interesting reactivity while screening different bases. In our optimization, we discovered, when morpholine was used in excess as a base, it generated fully substituted 1,2,3-triazole cycloaddition products with morpholine at the C-4 position instead of forming 5-fluorotriazoles. The fully substituted 1,2,3-triazoles are typically generated via an azide–alkyne cycloaddition or a multicomponent reaction between carbonyls and azides [17]. α-Trifluoromethyl (α-CF_3) carbonyls were recently utilized to generate NH-1,2,3-triazoles and fully substituted 1,2,3-triazoles [28,29]. However, there are no reports of a

formal [3 + 2] cycloaddition reaction utilizing *gem*-difluoroalkenes, which inherently exhibit attenuated activity compared to the activated α-CF_3 carbonyls. This report provides a highly regioselective and novel way to access C-4-morpholine-functionalized fully decorated 1,2,3-triazoles from *gem*-difluoroalkenes and organic azides without the requirement of alkynes or late-stage modifications.

Our initial investigations led us to identify that adding morpholine as a solvent (0.34–0.4 M) in a reaction with 1-(2,2-difluoroethenyl)-4-methylbenzene (1 equiv) and phenyl azide (1.5 equiv) results in the formation of morpholine-substituted triazole **3'a** (entry 1, Table 1), in 21% yield, using $NiCl_2(PCy_3)_2$ as a catalyst and K_3PO_4 as a base. A methyl handle on the *gem*-difluoroalkene **1** was used to aid in ^{1}H NMR analysis. The *gem*-difluoroalkenes were synthesized in one step using sodium 2-chloro-2,2-difluoroacetate and triphenylphosphine in DMF at 100 °C for 5 h [30].

We hypothesized that electron-withdrawing *p*-cyanophenyl azide **2b**, would be better suited for optimizing the reaction conditions compared to the unsubstituted phenyl azide **2a**. Taking a clue from the literature, we looked at transition metals that facilitate defluorinative processes in *gem*-difluoroalkenes. $NiCl_2(PCy_3)_2$ and $NiCl_2(dppp)_2$ were chosen for our initial investigations since they have been used in both the defluorination of *gem*-difluoroalkenes and the coordination with the azides to promote [3 + 2] cycloaddition reactions [2,31,32].

Table 1: Optimization of reaction conditions.[a]

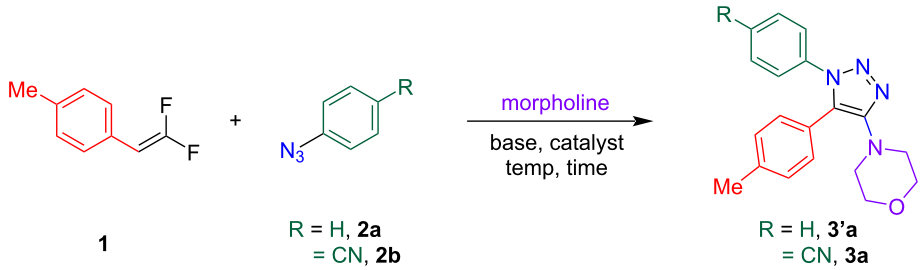

1 R = H, **2a** = CN, **2b** R = H, **3'a** = CN, **3a**

entry	R	catalyst[b] + additive (equiv)	base (equiv)	*T* (°C)	*t* (h)	yield (%)[c]
1	H[d]	$NiCl_2(PCy_3)_2$	K_3PO_4 (2)	110	48	21
2	CN	$NiCl_2(PCy_3)_2$	K_3PO_4 (2)	110	48	30
3	CN	$NiCl_2(dppp)_2$	K_3PO_4 (2)	110	48	54
4	CN	$NiCl_2(dppp)_2$	K_3PO_4 (2)	110	24	26
5	CN	$NiCl_2(dppp)_2$ + TMSCl (1)	K_3PO_4 (2)	110	24	11
6	CN	$Cu(OAc)_2$	K_3PO_4 (2)	110	48	14
7	CN	CuCl (0.15)	K_3PO_4 (2)	110	48	11
8	CN[e]	$NiCl_2(dppp)_2$	NaH (1.2)	50	24	53
9	CN[e]	$NiCl_2(dppp)_2$	Cs_2CO_3 (2)	50	24	61
10	CN[e]	$NiCl_2(dppp)_2$	LiHMDS (0.4)	50	24	61
11	CN	$NiCl_2(dppp)_2$	LiHMDS (1)	50	24	28
12	CN	–	LiHMDS (0.4)	50	48	31
13	**CN**	**–**	**LiHMDS (0.4)**	**75**	**48**	**70**
14	CN	–	LiHMDS (0.2)	75	48	49
15	CN	–	LiHMDS (0.7)	75	48	41
16	CN	–	LiHMDS (1)	75	48	36
17	CN	–	Cs_2CO_3 (2)	75	48	61
18	CN[d]	–	K_3PO_4 (2)	110	48	57
19	H[d]	–	K_3PO_4 (2)	110	48	42
20	CN	–	LiHMDS (0.4)	75	24	36
21	CN	–	–	75	48	20

[a]Standard reaction conditions: 1 equiv of *gem*-difluoroalkene **1** (0.14 mmol), 1.5 equiv of aryl azide **2a** or **2b** (0.21 mmol) 0.4 equiv of LiHMDS (1 M in THF), and 0.3 mL morpholine (0.4 M) were mixed and heated at 75 °C. Changes in the molarity of morpholine did not affect the yield; [b]0.1 equiv of catalyst used unless otherwise noted; [c]isolated yield; [d]2 equiv of azides, **2a** or **2b** were used; [e]azide was added in two portions: first portion at *t* = 0 min and second portion at *t* = 6 h. For azide safety, please refer to Supporting Information File 1. The LiHMDS reagent was acquired from Thermo Scientific Chemicals as a 1 M solution in THF.

Based on our hypothesis, we observed that *p*-cyanophenyl azide (**2b**) gave a better yield (30%, Table 1, entry 2) compared to the unsubstituted phenyl azide (**2a**, 21% yield, entry 1). Among the nickel catalysts screened, $NiCl_2(dppp)_2$ gave a better yield (Table 1, entry 2 vs entry 3). K_3PO_4 was used as a base since it has been reported to facilitate the addition of azoles to *gem*-difluoroalkenes (Figure 1B) [9,33]. An elevated temperature (110 °C) was required along with 48 h reaction time (Table 1, entry 3 vs entry 4) due to the sluggish nature of the reaction and poor reactivity of the *gem*-difluoroalkenes. The decomposition of azides at higher temperatures required the use of **2a** or **2b** in excess. No significant difference in yields between 1.5 equiv and 2 equiv of the aryl azide was observed.

Adding fluorophilic additives (TMSCl, Table 1, entry 5) or using copper as other transition metal (CuCl or $Cu(OAc)_2$, Table 1, entries 6 and 7) resulted in poor yields. Since the *gem*-difluoroalkenes are volatile compounds and as we observed decomposition of the azides at high temperatures resulting in reduced yields, we wanted to monitor the temperature and time course of this reaction. The time course study was carried out via ^{19}F NMR spectroscopy to monitor the consumption of the *gem*-difluoro starting material **1**, which was completely consumed within 16 h (Figure 3). However, a 48 h time course gave a superior yield (Table 1, entry 13 vs entry 20). We hypothesize this might be due to the volatile nature of the *gem*-difluoroalkene and its existence in the vapor phase over the course of the reaction to facilitate reaction with the remainder of the azide. With the information on the temperature and time in hand, we next screened different bases (NaH, Cs_2CO_3, and LiHMDS) with the $NiCl_2(dppp)_2$ catalyst, which resulted in similar or improved yields up to 61% (Table 1, entries 8–10). We accidentally added 0.4 equiv of LiHMDS (1 M in THF) in the screening, which afforded the product with 61% yield (Table 1, entry 10). When 1 equiv of LiHMDS was used under otherwise identical conditions, we observed a lower yield of 28% (Table 1, entry 11). To determine the role of the catalyst, we next ran the reaction without catalyst using 0.4 equiv of LiHMDS at 50 °C, which afforded the product in 31% yield (Table 1, entry 12). In order to ascertain whether a higher temperature would improve the yield, we increased the temperature of the reaction to 75 °C, which afforded the best results (70%, Table 1, entry 13). When 0.2 equiv, 0.7 equiv, and 1 equiv of LiHMDS was used, a lower product yield of 58%, 50%, and 36%, respectively, was observed (Table 1, entries 14–16). This was surprising because there was no correlation between the amount of LiHMDS used versus the yields of the product formed.

Other bases, such as Cs_2CO_3 or K_3PO_4, resulted in slightly lower yields (Table 1, entries 17–19). Without any base or catalyst, the reaction yield was much lower (20%, Table 1, entry 21). A further screen of the concentration of the solvent (morpholine) or molarity of the reaction did not improve the yield (same or within 5%, see Supporting Information File 1, Table S1). We believe that LiHMDS gave the best results primarily because it is more miscible, resulting in a homogenous reaction mixture. LiHMDS being a strong base ($pK_a \approx 25.8$) [34], facilitates the direct deprotonation of morpholine as opposed to acting as a scavenger base. Due to the significant difference in pK_a values between the conjugate acids of morpholine (pK_a of the conjugate acid is 8.3) [35] and LiHMDS, we posit that LiHMDS directly deprotonates morpholine. However, we cannot rule out that morpholine is acting as a scavenger base since it is used in large excess (0.4 M, which is equal to 30 equiv) compared to 0.4 equiv of LiHMDS and would buffer LiHMDS. Inorganic solid bases gave slightly decreased yields compared to LiHMDS (Table 1, entries 17–19 vs entry 13). Among the liquid bases that were screened, *N*,*N*-diisopropylethylamine ($pK_a \approx 9$) gave the product in 38% yield, whereas NaHMDS afforded a 24% yield. Since LiHMDS gave the best yield thus far, we wanted to examine if Li^+ ions play a role in the reaction. When the reaction was carried out with a different Li^+ source (LiCl, 0.1 equiv) with a weaker base (Cs_2CO_3, pK_a of the conjugate acid 10.3) [36], it afforded the product in 29% yield, which is much poorer than under the previously optimized conditions (see Supporting Information File 1, Table S1). This observation suggests that Li^+ ions act as a bystander and do not play a role in the reaction.

The reaction under the optimized conditions resulted in the formation of 4-(4-morpholino-5-(*p*-tolyl)-1*H*-1,2,3-triazole-1-yl)benzonitrile (**3a**) in 70% yield from 1 equiv of 1-(2,2-difluorovinyl)-4-methylbenzene and 1.5 equiv of 4-azidobenzonitrile with morpholine as solvent (0.4 M) and 0.4 equiv LiHMDS as a base at 75 °C for 48 h. The only byproducts observed are anilines as a result of thermal decomposition of the organic azides via reactive nitrene species. No other byproducts were observed by TLC or crude ^1H NMR. The volatility of the *gem*-difluoroalkenes and the co-elution of the aniline byproducts during column chromatography with the desired products affected the overall yield of the reaction. For a complete optimization list with all conditions that were screened, see Supporting Information File 1.

With the optimized conditions in hand, we started exploring the substrate scope around the *gem*-difluoroalkene handle. As shown in Figure 2, electron-donating groups in the *para*-position, for instance, methyl (**3a**), *tert*-butyl (**3b**), and methoxy (**3c**) were tolerated affording the products in 40–70% yields. Also electron-withdrawing groups, such as cyano (**3d**) at the *para*-position, were amenable to the reaction conditions affording the

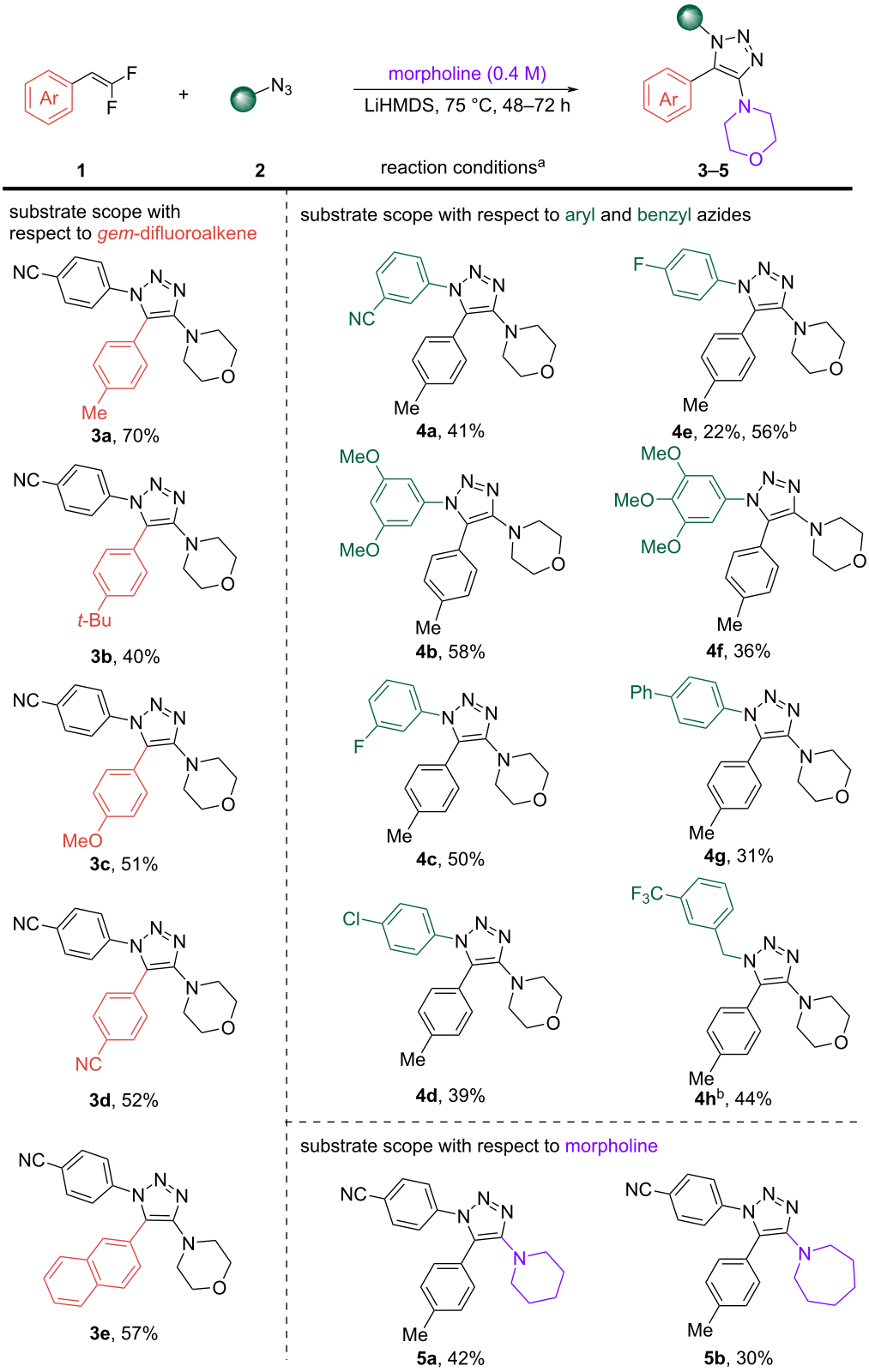

Figure 2: Substrate scope. Reaction conditions: **1** (1 equiv), **2** (1.5 equiv) 0.4 equiv of LiHMDS (1 M in THF), morpholine (0.34–0.4 M), 75 °C, 48 h. Isolated yields are reported. [a]1 Equiv of $CuSO_4$ was used as an additive. [b]Modified reaction conditions for benzyl azides: **1** (1 equiv), **2** (1.5 equiv) 0.4 equiv of LiHMDS (1 M in THF), morpholine (0.34–0.4 M), 110 °C, 72 h.

product in 52% yield. Bulky groups, such as naphthalene were also suitable forming product **3e** in 57% yield, highlighting the functional group tolerability of this reaction.

Next, the scope of the reaction for aryl and benzyl azides was examined. An array of *para*- and *meta*-substituted aryl azides was amenable to the optimized conditions. The presence of electron-withdrawing groups worked well affording the products with *m*-cyano (**4a**), 3,5-dimethoxy (**4b**), *m*-fluoro (**4c**), and *p*-chloro (**4d**) substitution in 39–58% yields. It has to be noted, that $CuSO_4$ (1 equiv) was used as an additive for the synthesis of product **4e** containing a *p*-fluoro substituent which improved the yield to 56%. Under regular optimized conditions without $CuSO_4$, product **4e** was formed in only 22% yield. However, $CuSO_4$ or any other Cu additives did not improve the yields when a cyano group was present on the azide handle. In fact, the use of $CuSO_4$ with the cyano group lowered the yield (31%, see entry 12 in Table 1) which might be due to a coordination of the copper catalyst with the cyano group hindering the triazole formation [37]. The product **4f** containing a 3,4,5-trimethoxyphenyl substituent was afforded in a moderate 36% yield.

Electron-donating groups on the aryl azide, such as biphenyl at the *para*-position gave product **4g** in 31% yield. A clear trend was observed: electron-withdrawing groups on the aryl azides facilitated the reaction faster than electron-donating groups. Similar trends were observed for benzyl azides; however, this substituent was much less reactive compared to its aryl counterparts. It required a higher temperature of 110 °C and a longer duration of the reaction (72 h). The product with an electron-withdrawing group, such as trifluoromethyl (**4h**), was obtained in 44% yield. When morpholine was replaced with piperidine (**5a**) or seven-membered azepane (**5b**) as a solvent, a decreased yield was observed (30–42%). The addition of piperidine offers an advantage in expanding the substrate scope to medicinal chemistry applications. In the reaction with piperidine, we observed unreacted organic azide **2b** by TLC and ^{1}H NMR analyses. Based on the ^{1}H NMR analysis, 0.4 equiv of **2b** had reacted to form the product, 0.9 equiv of **2b** had decomposed to form aniline, and the remaining 0.2 equiv of **2b** was unreacted. Additionally, 30% of the aniline byproduct was also isolated, which explains the modest yields of this reaction and the sluggish nature.

To investigate the mechanism of the current transformation, we conducted a series of experiments including a time course of the reaction using ^{19}F NMR spectroscopy (Figure 3). We observed addition–elimination intermediate of morpholine and *gem*-

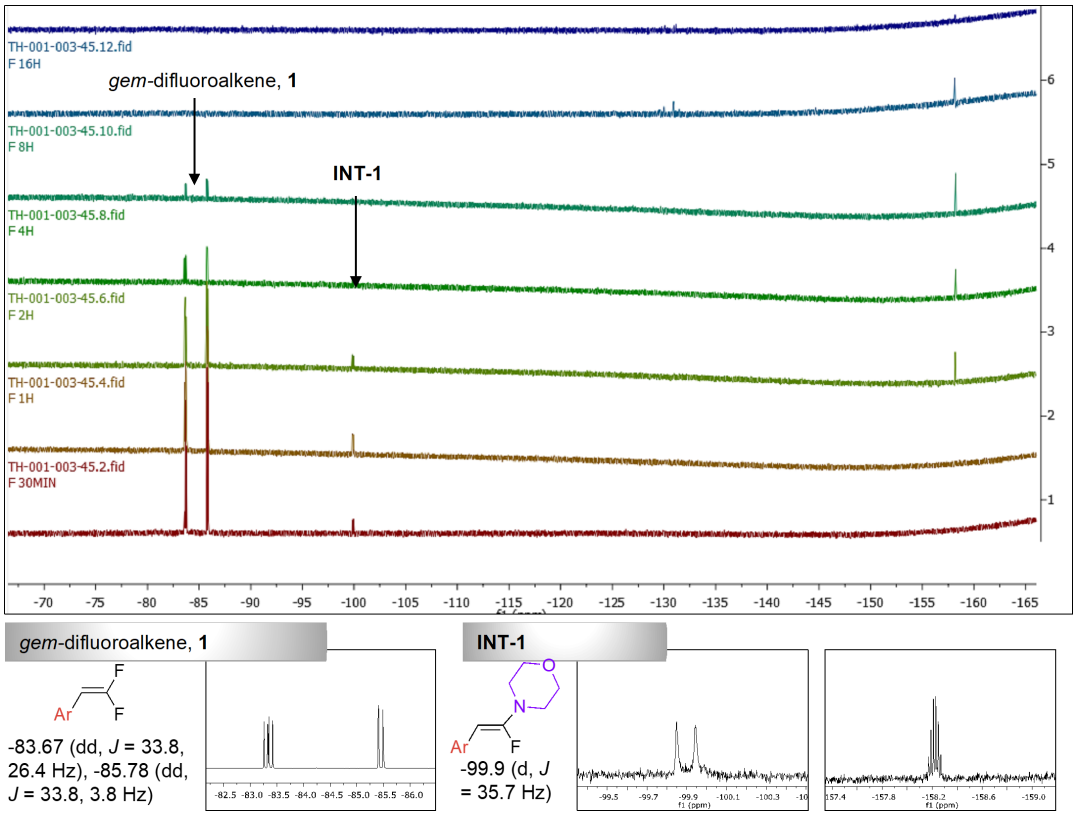

Figure 3: Time course profile monitored by ^{19}F NMR spectroscopy.

difluoroalkenes INT-1, (−99.9 ppm, d, J = 35.7 Hz) within 30 min of the reaction and a gradual consumption of the *gem*-difluoroalkene **1** (−83.67 ppm, dd, J = 33.8, 26.4 Hz and −85.78, dd, J = 33.8, 3.8 Hz) throughout the course of 8 h and beyond. The *Z*-geometry of **INT-1** was determined from its $^{3}J_{H-F}$ coupling constant of 35.7 Hz in the ^{1}H NMR with a matching J value in the ^{19}F NMR. This is in agreement with Cao's report on the geometry of *N*-(α-fluorovinyl)azoles [33]. The configurations of the *E*- and *Z*-isomers were determined by their $^{3}J_{H-F}$ coupling constants in the ^{1}H NMR spectra, circa 32.0 Hz for *Z*-isomers and 8.0 Hz for *E*-isomers [33]. A peak was observed at −158.2 ppm in the ^{19}F NMR spectrum after 2 h of the reaction, which could be the fluoride salt of the dimorpholine adduct. This peak was also found when the reaction was run in the absence of azide using optimized conditions (see Supporting Information File 1, mechanistic study, section 8). However, its further characterization was not possible because it disappeared upon workup. Finally, a 2D NOESY experiment was utilized to confirm the regiochemistry of 4-(1-(4-fluorophenyl)-5-(*p*-tolyl)-1*H*-1,2,3-triazol-4-yl)morpholine (**4e**), one of the fully decorated 1,2,3-triazoles (Figure 4). The peak at 7.59 ppm (d, J = 8.1 Hz) in the ^{1}H NMR spectrum corresponding to the H_1 protons of the C-5-aryl substituent on the 1,2,3-triazole ring shows a cross-peak with the protons of the C-4-morpholine unit (H_a = 3.68–3.59 ppm, m and H_b = 2.94–2.86 ppm, m). This suggests they are adjacent in space, thereby confirming the 1,5-disubstituted pattern on the 1,2,3-triazole ring with the morpholine moiety attached at the C-4 position. The distance between the H_1 aryl proton and the morpholine protons was determined to be 2.3 Å ($H_1 \leftrightarrow H_a$), 2.6 Å ($H_1 \leftrightarrow H_a'$), and 4.5 Å ($H_1 \leftrightarrow H_b$), 4.7 Å ($H_1 \leftrightarrow H_b'$) (see Supporting Information File 1, regioisomer study, section 9, for more details).

Based on these experiments and literature reports [28,33], we propose a base-mediated nucleophilic addition–elimination of morpholine to *gem*-difluoroalkene **1** affording **INT-1**, which can generate product **3** via two routes (Figure 5). Route A entails the formation of an aminoalkyne intermediate, **INT-2**, which can participate in a [3 + 2] azide–alkyne cycloaddition to

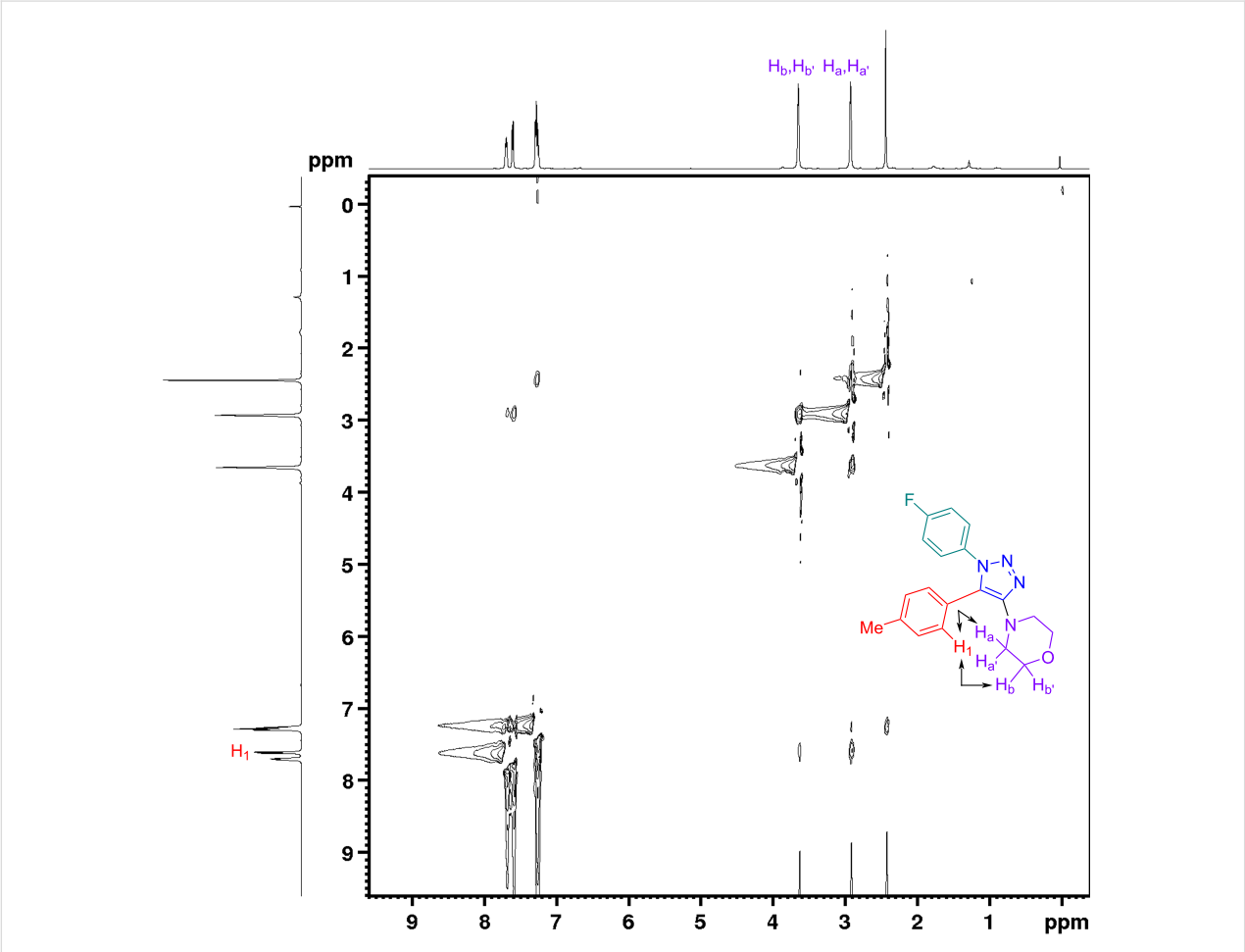

Figure 4: NOESY of **4e** confirming the regiochemistry of the product.

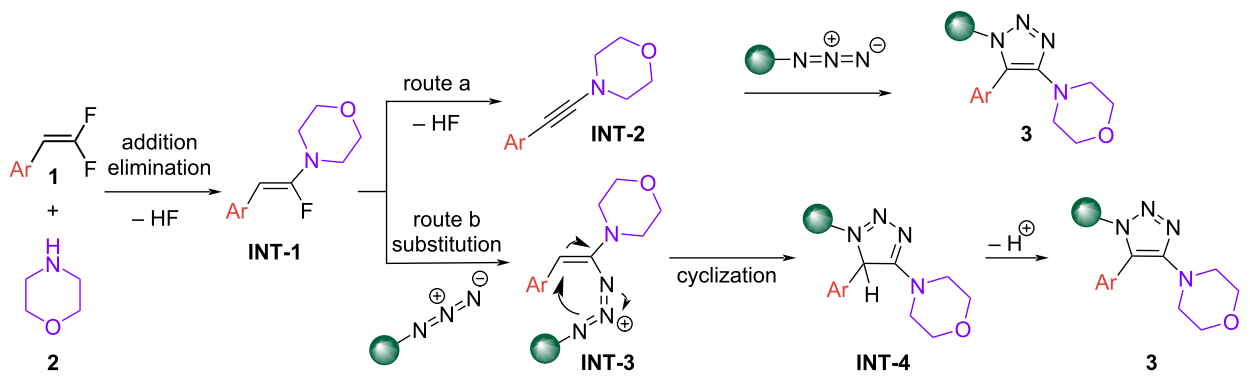

Figure 5: Proposed mechanism.

form the final product **3**. Alternatively, vinylic azido amine intermediate **INT-3** can be formed via vinylic substitution of **INT-1** with an azide which can cyclize to form **INT-4** that subsequently aromatizes to afford product **3** (route B).

To demonstrate the applicability of this method, a scale-up reaction was performed using 150 mg of the limiting reagent, which is five times the usual reaction scale used in substrate scope screening or optimization experiments (Figure 6). In this scale-up experiment, we obtained the product with 57% yield , which is slightly lower than 70% using 1-(2,2-difluorovinyl)-4-methylbenzene (**1**, 154 mg, 1 mmol, 1 equiv), 4-azidobenzonitrile (**2b**, 216 mg, 1.5 mmol, 1.5 equiv), and LiHMDS (0.4 mL, 1 M in THF, 0.4 mmol, 0.4 equiv) in morpholine (1.1 mL, 0.4 M) at 75 °C. The 4-azidobenzonitrile (**2b**) was added in two portions of 0.75 equiv at t = 0 min and the remainder 0.75 equiv were added at t = 16 h. This addition strategy aimed to mitigate the decomposition of 4-azidobenzonitrile (**2b**) during the extended reaction duration. The progress of the reaction was monitored via TLC, and starting material **1** was still observed at 48 h. The reaction ran for a total of 90 h until all the starting materials were consumed and 195 mg (57%) of product **3a** was obtained. This shows the synthetic utility of this method; however, additional investigations into process chemistry may be necessary to accommodate a larger reaction scale.

Conclusion

In conclusion, we have shown for the first time a [3 + 2] cycloaddition of *gem*-difluoroalkenes with organic azides in morpholine as a solvent forming C-4-morpholine functionalized fully decorated 1,2,3-triazoles with potential applications in pharmaceutical, biomedical, agrichemical, and materials sciences. This study fills a critical gap in the literature as it is a transition-metal-free and regioselective reaction that does not rely on carbonyl- or alkyne-based methods or late-stage modifications to access 1,4,5-trisubstituted-1,2,3-triazoles. However, carbonyl chemistry was utilized to synthesize the *gem*-difluoroalkene starting material [30]. In fact, our findings offer a straightforward direct synthesis of fully substituted 1,2,3-triazoles, which are otherwise difficult to access, from readily available starting materials. ^{19}F NMR studies indicate a mechanism involving an addition–elimination intermediate of morpholine and *gem*-difluoroalkenes that subsequently undergoes a [3 + 2] cycload-

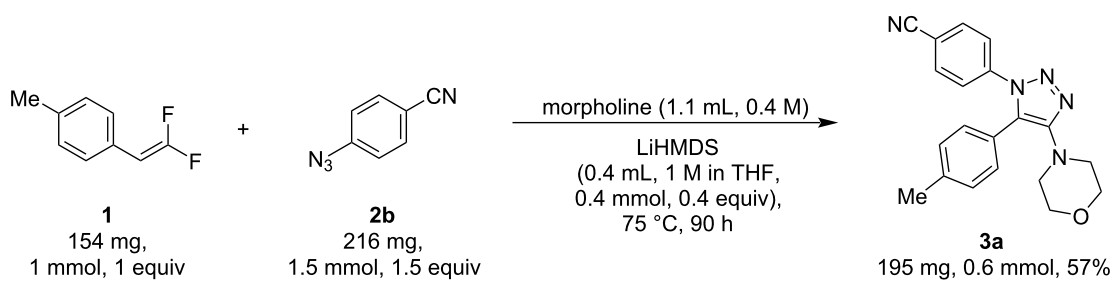

Figure 6: Scale-up experiment.

dition with an organic azide. A relatively wide range of 1,4,5-trisubstituted-1,2,3-triazoles was obtained in 30–70% yields with high regioselectivity and modest functional group tolerability. This work demonstrates that *gem*-difluoroalkenes can serve as versatile fluorinated building blocks in lieu of alkynes to access a set of fully decorated 1,2,3-triazoles.

Supporting Information

Supporting Information File 1

General information, experimental procedures for all the substrates and intermediates, characterization data, and NMR spectra (^{1}H, ^{19}F, and ^{13}C NMR).
[https://www.beilstein-journals.org/bjoc/content/supplementary/1860-5397-19-111-S1.pdf]

Funding

Research reported in this publication was supported by the National Institute of General Medical Sciences of the National Institutes of Health under Award Number R35GM150768. The content is solely the responsibility of the authors and does not necessarily represent the official views of the National Institutes of Health.

ORCID® iDs

Tzu-Yu Huang - https://orcid.org/0000-0002-8170-7117
Mario Djugovski - https://orcid.org/0000-0002-0339-8806
Sweta Adhikari - https://orcid.org/0000-0002-9052-4072
Destinee L. Manning - https://orcid.org/0000-0001-7825-5896
Sudeshna Roy - https://orcid.org/0000-0003-0237-4156

Preprint

A non-peer-reviewed version of this article has been previously published as a preprint: https://doi.org/10.26434/chemrxiv-2023-w2r84

References

1. Fujita, T.; Fuchibe, K.; Ichikawa, J. *Angew. Chem., Int. Ed.* **2019,** *58,* 390–402. doi:10.1002/anie.201805292
2. Lu, X.; Wang, Y.; Zhang, B.; Pi, J.-J.; Wang, X.-X.; Gong, T.-J.; Xiao, B.; Fu, Y. *J. Am. Chem. Soc.* **2017,** *139,* 12632–12637. doi:10.1021/jacs.7b06469
3. Du, B.; Chan, C.-M.; Lee, P.-Y.; Cheung, L.-H.; Xu, X.; Lin, Z.; Yu, W.-Y. *Nat. Commun.* **2021,** *12,* 412. doi:10.1038/s41467-020-20725-9
4. Sorrentino, J. P.; Altman, R. A. *Synthesis* **2021,** *53,* 3935–3950. doi:10.1055/a-1547-9270
5. Purrington, S. T.; Sheu, K.-W. *Tetrahedron Lett.* **1992,** *33,* 3289–3292. doi:10.1016/s0040-4039(00)92069-0
6. Loska, R.; Szachowicz, K.; Szydlik, D. *Org. Lett.* **2013,** *15,* 5706–5709. doi:10.1021/ol402735m
7. Frost, A. B.; Brambilla, M.; Exner, R. M.; Tredwell, M. *Angew. Chem., Int. Ed.* **2019,** *58,* 472–476. doi:10.1002/anie.201810413
8. Taguchi, T.; Kodama, Y.; Kanazawa, M. *Carbohydr. Res.* **1993,** *249,* 243–252. doi:10.1016/0008-6215(93)84072-e
9. Zhang, J.-Q.; Hu, D.; Song, J.; Ren, H. *J. Org. Chem.* **2021,** *86,* 4646–4660. doi:10.1021/acs.joc.0c03041
10. Zhang, J.-Q.; Liu, J.; Hu, D.; Song, J.; Zhu, G.; Ren, H. *Org. Lett.* **2022,** *24,* 786–790. doi:10.1021/acs.orglett.1c04336
11. Pokhodylo, N.; Shyyka, O.; Matiychuk, V. *Sci. Pharm.* **2013,** *81,* 663–676. doi:10.3797/scipharm.1302-04
12. Xu, Z.; Zhao, S.-J.; Liu, Y. *Eur. J. Med. Chem.* **2019,** *183,* 111700. doi:10.1016/j.ejmech.2019.111700
13. Kim, T. W.; Yong, Y.; Shin, S. Y.; Jung, H.; Park, K. H.; Lee, Y. H.; Lim, Y.; Jung, K.-Y. *Bioorg. Chem.* **2015,** *59,* 1–11. doi:10.1016/j.bioorg.2015.01.003
14. Zhang, B. *Eur. J. Med. Chem.* **2019,** *168,* 357–372. doi:10.1016/j.ejmech.2019.02.055
15. Wales, S. M.; Hammer, K. A.; King, A. M.; Tague, A. J.; Lyras, D.; Riley, T. V.; Keller, P. A.; Pyne, S. G. *Org. Biomol. Chem.* **2015,** *13,* 5743–5756. doi:10.1039/c5ob00576k
16. da Silva, F. d. C.; de Souza, M. C. B. V.; Frugulhetti, I. I. P.; Castro, H. C.; Souza, S. L. d. O.; de Souza, T. M. L.; Rodrigues, D. Q.; Souza, A. M. T.; Abreu, P. A.; Passamani, F.; Rodrigues, C. R.; Ferreira, V. F. *Eur. J. Med. Chem.* **2009,** *44,* 373–383. doi:10.1016/j.ejmech.2008.02.047
17. Shiri, P.; Amani, A. M.; Mayer-Gall, T. *Beilstein J. Org. Chem.* **2021,** *17,* 1600–1628. doi:10.3762/bjoc.17.114
18. de Albuquerque, D. Y.; de Moraes, J. R.; Schwab, R. S. *Eur. J. Org. Chem.* **2019,** 6673–6681. doi:10.1002/ejoc.201901249
19. Guo, N.; Liu, X.; Xu, H.; Zhou, X.; Zhao, H. *Org. Biomol. Chem.* **2019,** *17,* 6148–6152. doi:10.1039/c9ob01156k
20. Zhang, D.; Fan, Y.; Yan, Z.; Nie, Y.; Xiong, X.; Gao, L. *Green Chem.* **2019,** *21,* 4211–4216. doi:10.1039/c9gc01129c
21. Deng, L.; Cao, X.; Liu, Y.; Wan, J.-P. *J. Org. Chem.* **2019,** *84,* 14179–14186. doi:10.1021/acs.joc.9b01817
22. Li, K.; Fong, D.; Meichsner, E.; Adronov, A. *Chem. – Eur. J.* **2021,** *27,* 5057–5073. doi:10.1002/chem.202003386
23. Wang, W.; Peng, X.; Wei, F.; Tung, C.-H.; Xu, Z. *Angew. Chem., Int. Ed.* **2016,** *55,* 649–653. doi:10.1002/anie.201509124
24. Punzi, A.; Zappimbulso, N.; Farinola, G. M. *Eur. J. Org. Chem.* **2020,** 3229–3234. doi:10.1002/ejoc.201901305
25. Ferlin, F.; Yetra, S. R.; Warratz, S.; Vaccaro, L.; Ackermann, L. *Chem. – Eur. J.* **2019,** *25,* 11427–11431. doi:10.1002/chem.201902901
26. Ichikawa, J.; Wada, Y.; Miyazaki, H.; Mori, T.; Kuroki, H. *Org. Lett.* **2003,** *5,* 1455–1458. doi:10.1021/ol034192p
27. Jana, S.; Adhikari, S.; Cox, M. R.; Roy, S. *Chem. Commun.* **2020,** *56,* 1871–1874. doi:10.1039/c9cc09216a
28. Lv, L.; Gao, G.; Luo, Y.; Mao, K.; Li, Z. *J. Org. Chem.* **2021,** *86,* 17197–17212. doi:10.1021/acs.joc.1c02288
29. Gao, G.; Kuantao; Mao; Lv, L.; Li, Z. *Adv. Synth. Catal.* **2022,** *364,* 1402–1408. doi:10.1002/adsc.202200094
30. Hayashi, S.-i.; Nakai, T.; Ishikawa, N.; Burton, D. J.; Naae, D. G.; Kesling, H. S. *Chem. Lett.* **1979,** *8,* 983–986. doi:10.1246/cl.1979.983
31. Kim, W. G.; Kang, M. E.; Lee, J. B.; Jeon, M. H.; Lee, S.; Lee, J.; Choi, B.; Cal, P. M. S. D.; Kang, S.; Kee, J.-M.; Bernardes, G. J. L.; Rohde, J.-U.; Choe, W.; Hong, S. Y. *J. Am. Chem. Soc.* **2017,** *139,* 12121–12124. doi:10.1021/jacs.7b06338

32. Zhou, M.; Zhang, J.; Zhang, X.-G.; Zhang, X. *Org. Lett.* **2019,** *21,* 671–674. doi:10.1021/acs.orglett.8b03841
33. Xiong, Y.; Zhang, X.; Huang, T.; Cao, S. *J. Org. Chem.* **2014,** *79,* 6395–6402. doi:10.1021/jo5005845
34. Fraser, R. R.; Mansour, T. S.; Savard, S. *J. Org. Chem.* **1985,** *50,* 3232–3234. doi:10.1021/jo00217a050
35. Hall, H. K., Jr. *J. Am. Chem. Soc.* **1957,** *79,* 5441–5444. doi:10.1021/ja01577a030
36. Perrin, D. D. *Dissociation constants of inorganic acids and bases in aqueous solution;* Butterworth: London, UK, 1969.
37. Bell, N. L.; Xu, C.; Fyfe, J. W. B.; Vantourout, J. C.; Brals, J.; Chabbra, S.; Bode, B. E.; Cordes, D. B.; Slawin, A. M. Z.; McGuire, T. M.; Watson, A. J. B. *Angew. Chem., Int. Ed.* **2021,** *60,* 7935–7940. doi:10.1002/anie.202016811

License and Terms

BEILSTEIN JOURNAL OF ORGANIC CHEMISTRY

Trifluoromethylated hydrazones and acylhydrazones as potent nitrogen-containing fluorinated building blocks

Zhang Dongxu

Review

Open Access

Address:
Department of Fire Protection Engineering, China Fire and Rescue Institute, Beijing 102202, P. R. of China

Email:
Zhang Dongxu - zhangdongxu@cfri.edu.cn

Keywords:
acylhydrazones; difluoromethylation; dihydropyridazine; fluorinated building blocks; hydrazones; imidazolidines; pyrazoles; pyrazolidines; pyrazolines; trifluoromethylation

Beilstein J. Org. Chem. **2023,** *19,* 1741–1754.
https://doi.org/10.3762/bjoc.19.127

Received: 02 September 2023
Accepted: 03 November 2023
Published: 15 November 2023

This article is part of the thematic issue "Organofluorine chemistry VI".

Guest Editor: D. O'Hagan

Abstract

Nitrogen-containing organofluorine derivatives, which are prepared using fluorinated building blocks, are among the most important active fragments in various pharmaceutical and agrochemical products. This review focuses on the reactivity, synthesis, and applications of fluoromethylated hydrazones and acylhydrazones. It summarizes recent methodologies that have been used for the synthesis of various nitrogen-containing organofluorine compounds.

Introduction

The introduction of fluorine into pharmaceuticals, agrochemicals, and materials can significantly enhance lipophilicity and metabolic stability compared to nonfluorinated compounds [1-5]. At present, about 300 drug molecules and over 400 pesticides on the market contain at least one fluorine atom [6,7]. Therefore, the development of novel and effective synthetic methodologies for the synthesis of organofluorine compounds has become a major research focus.

The use of difluoromethylating and trifluoromethylating reagents is a popular approach applied to prepare di/trifluoromethyl-containing molecules [8-18]. Also the reaction of diverse di/trifluoromethyl-containing building blocks offers another mainstream approach to introducing fluorine. Among these, di/trifluorodiazoethane [19-22], trifluoromethyl aldimines [23-25], trifluoroacetimidoyl halides [26], and fluoroalkyl *N*-sulfonyl hydrazones [27] have emerged as powerful nitrogen-containing fluorinated building blocks that have been used to construct organofluorine derivatives. To the best of our knowledge, the synthetic applications of fluoromethylated hydrazones and acylhydrazones as useful building blocks, has not yet been summarized. Hence, the present review highlights recent advancements enabling the synthesis of diverse di/trifluoromethyl-containing molecules by using di/trifluoromethylated hydrazones, acylhydrazones, and their related compounds.

Review

Trifluoroacetaldehyde hydrazones

Hydrazones possess diverse biological and pharmacological properties and have been employed in the treatment of several diseases [28-30]. They have also been applied in the field of materials science, especially for the synthesis of metal and covalent organic frameworks, dyes, hole-transporting materials and sensors, and in dynamic combinatorial chemistry [31], indicating a wide applicability. Hydrazones can be regarded as electrophilic and nucleophilic imine equivalents, and thus they represent valuable and versatile building blocks in synthetic chemistry [32-36].

Trifluoroacetaldehyde hydrazones can be regarded as an equivalent of fluorine-containing azomethine imines in the presence of Brønsted acid. In their pioneering research, Tanaka et al. reported the [3 + 2] cycloaddition reactions of trifluoroacetaldehyde hydrazones and glyoxals to give 4-hydroxy-3-trifluoromethylpyrazoles. The resultant pyrazoles containing a free 4-hydroxy group were easily converted to a variety of other derivatives in good yields [37] (Scheme 1).

Later, Wu et al. described a diastereoselective 1,3-dipolar cycloaddition of trifluoroacetaldehyde hydrazones with α,β-ethenyl ketones to obtain polysubstituted pyrazolidines and pyrazolines. These reactions were carried out under two different sets of conditions [38] (Scheme 2).

Moreover, a chiral Brønsted acid-catalyzed asymmetric 6π electrocyclization of trifluoroacetaldehyde hydrazones for the synthesis of enantiomerically enriched 3-trifluoromethyl-1,4-dihydropyridazines was first developed by Rueping et al. [39]. The strategy involves chiral ion pairs and provides a good basis and scope for further extensions and explorations [39] (Scheme 3).

Based on the work by Wu et al. and extending their previous work, Rueping and co-workers explored the effects of fluorine in organocatalytic reactions. They developed an asymmetric Brønsted acid–Lewis base catalysis, for the synthesis of trifluoromethylated dihydropyridazines under simple reaction conditions and the chemistry displayed very good enantioselectivities and high functional group tolerance (Scheme 4) [40].

Zhan et al. reported an efficient and highly selective method for the synthesis of CF_3-pyrazoles and CF_3-1,6-dihydropyridazines from readily available trifluoromethylated *N*-propargylic hydrazones. These reactions proceed through intermediate diazoallenes, and were conducted with catalytic $PtCl_4$ [41] or AgOTf [42] (Scheme 5).

Their study explored the effects of fluorine through reactions with trifluoroacetaldehyde hydrazones. Jasiński et al. demonstrated that the CF_3 group offered an appropriate electronic balance through experimental spectral analysis and computational DFT methods, and the hydrazones could be readily used

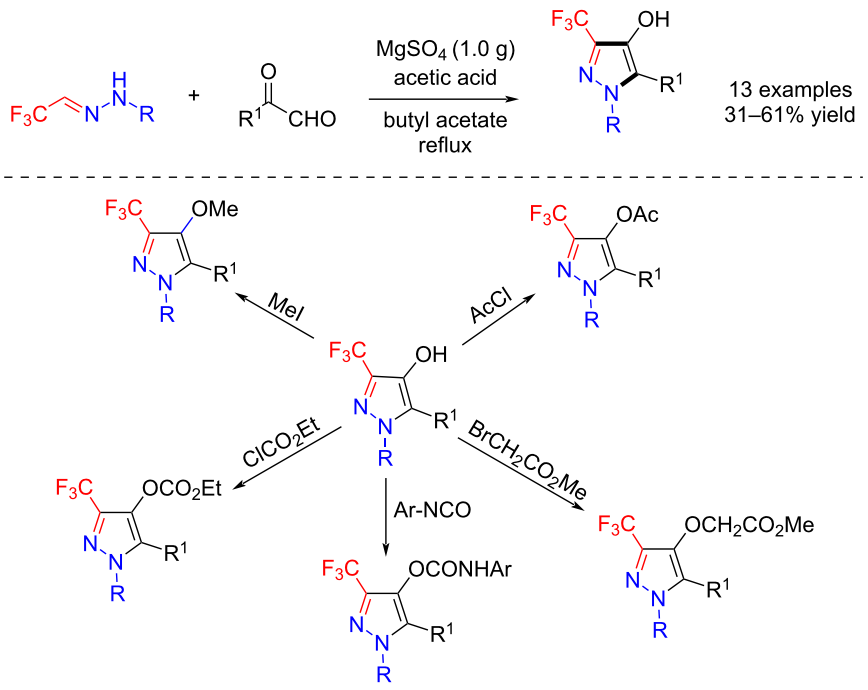

Scheme 1: Synthesis of trifluoromethylpyrazoles from trifluoroacetaldehyde hydrazones.

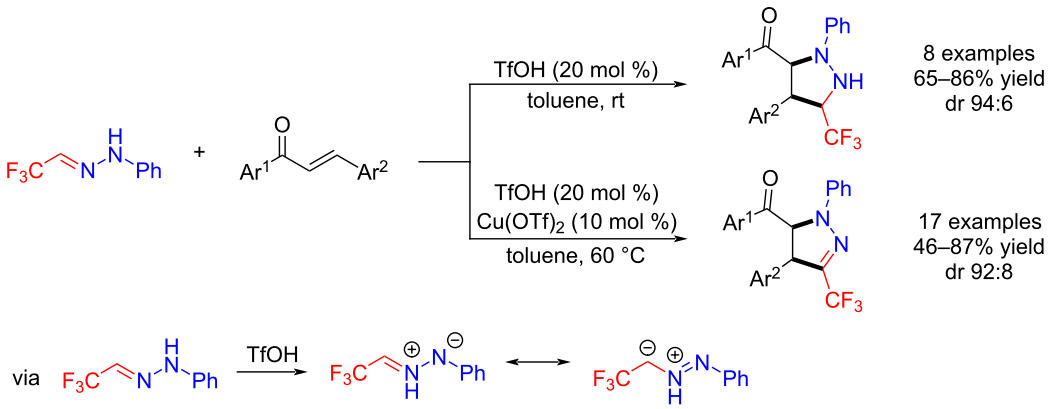

Scheme 2: Synthesis of polysubstituted pyrazolidines and pyrazolines.

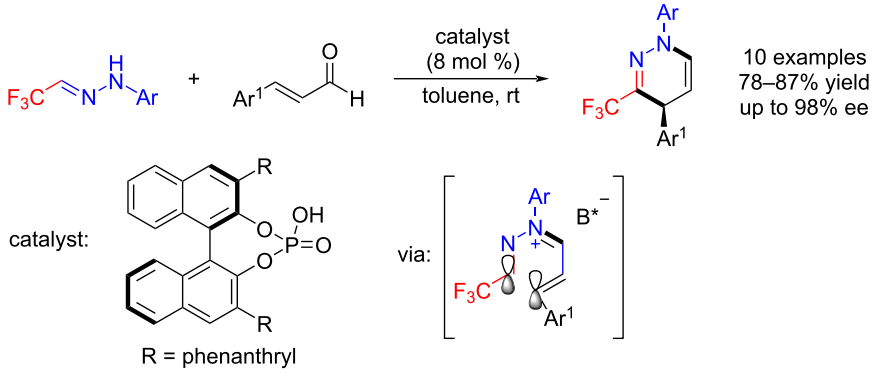

Scheme 3: Asymmetric synthesis of 3-trifluoromethyl-1,4-dihydropyridazines reported by Rueping et al. [39].

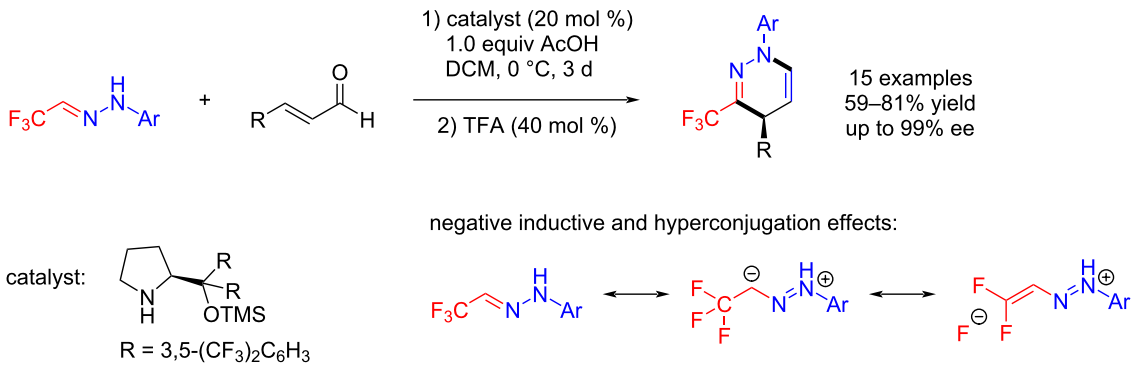

Scheme 4: Synthesis of 3-trifluoromethyl-1,4-dihydropyridazine with Brønsted acid-assisted Lewis base catalysis.

to provide convenient access to azo tautomers under the acidic conditions [43].

The C=N motif within hydrazones gives them both electrophilic and nucleophilic character. In 2005, Brigaud et al. developed a highly stereoselective method for the synthesis of α-trifluoromethylamines with organometallic reagents to extend the asymmetric methodologies of trifluoroacetaldehyde hydrazones [44] (Scheme 6).

El Kaim and Jia reported a Mannich-type reaction of trifluoroacetaldehyde hydrazones with formaldehyde and aromatic alde-

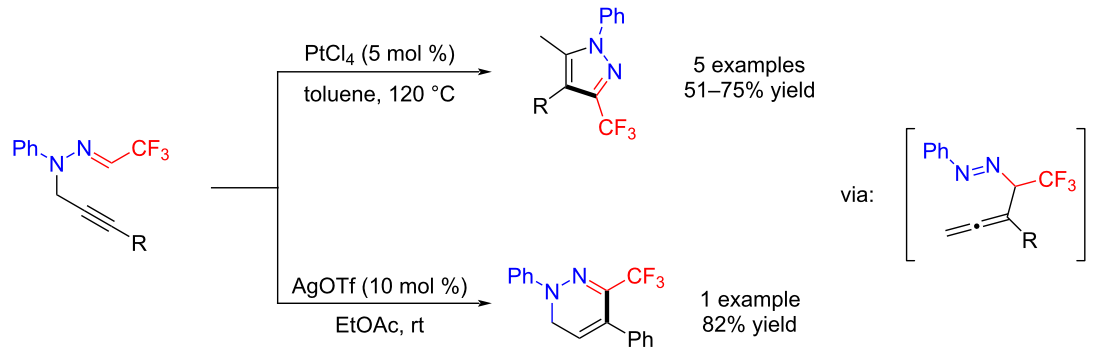

Scheme 5: Synthesis of CF_3-pyrazoles and CF_3-1,6-dihydropyridazines.

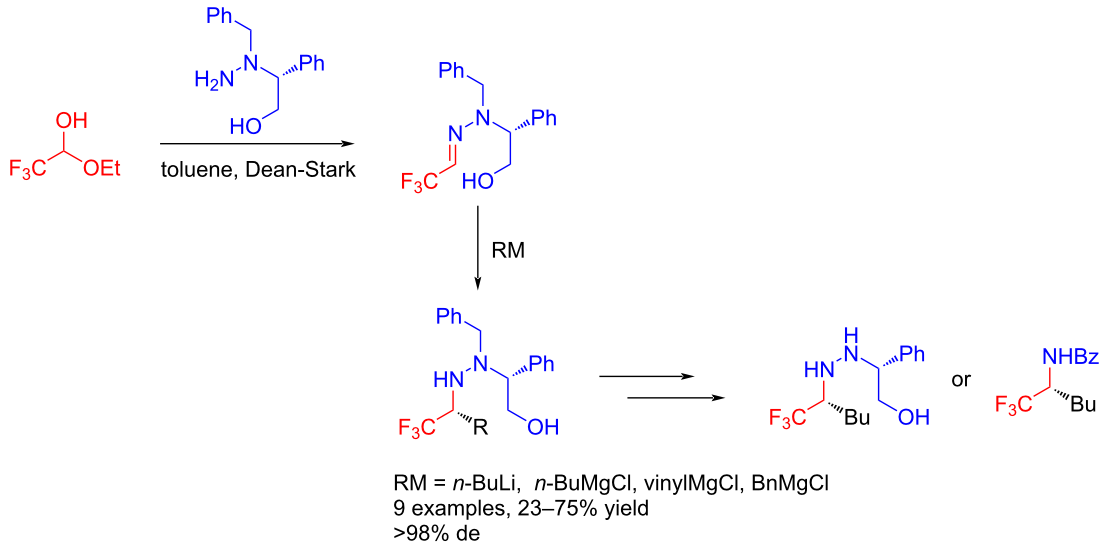

Scheme 6: Asymmetric reactions of trifluoromethylimines with organometallic reagents.

hydes to obtain valuable starting materials for the generation of other trifluoromethyl-substituted heterocycles. The study demonstrated that the electron-withdrawing property of the trifluoromethyl group is key to this coupling reaction [45] (Scheme 7).

Trifluoromethylated hydrazonoyl halides

Hydrazonoyl halides, which offer a reactive 1,3-dipole, can easily be transformed to nitrile imines in the presence of a base, and they have shown to be useful building blocks for the synthesis of heterocycles [46,47]. The resultant heterocycles bearing a fluorine or fluorine-containing group have been used in a broad array of pharmaceutical applications [48,49]. The use of di/trifluoromethylated hydrazonoyl halides as building blocks for the synthesis of di/trifluoromethylated organic molecules is equally attractive and proven to be important.

Generally, the reaction of trifluoroacetaldehyde hydrazones with *N*-chloro- and *N*-bromosuccinimide is used to prepare trifluoromethylated hydrazonoyl halides (Scheme 8a), or alternatively trichloroisocyanuric acid (TCCA) can be used as a chloride source for the preparation of these compounds [50] (Scheme 8b).

As early as in 1982, the reactivity of trifluoromethylated hydrazonoyl halides in the presence of base has been systematically studied by Tanaka et al. The trifluoromethylated hydrazonoyl halides, as the precursors of trifluoroacetonitrile imine, are highly versatile in that they react with olefins, acetylenes, dimethyl fumarate, dimethyl maleate, β-diketones, β-keto esters, bicyclic olefins, and potassium isothiocyanate and isocyanate affording the corresponding trifluoromethyl-containing compounds, generally with good yields [51-58] (Scheme 9).

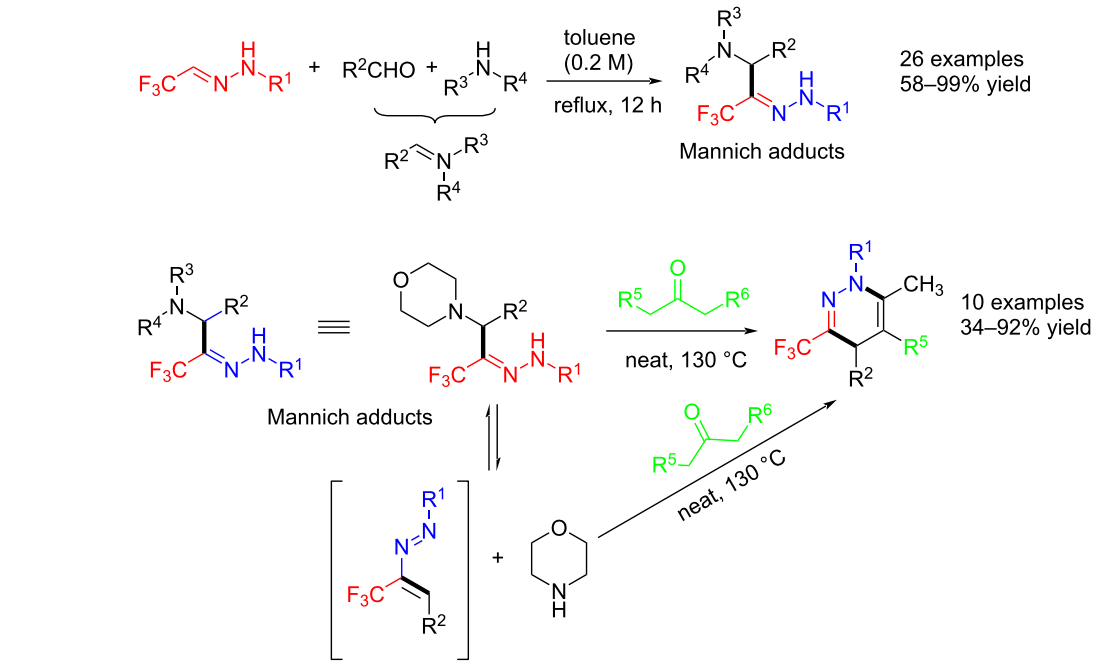

Scheme 7: Mannich-type reaction of trifluoroacetaldehyde hydrazones.

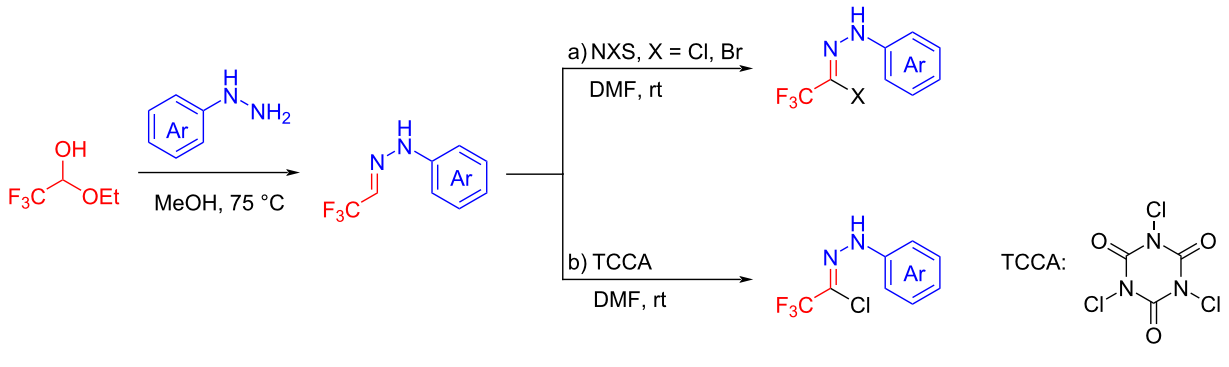

Scheme 8: Synthesis of trifluoromethylated hydrazonoyl halides.

Thioketones, thiochalcones, and tertiary thioamides react as C=S super dipolarophilic agents. Jasiński et al. reported that these thiocarbonyl compounds react with trifluoromethylated hydrazonoyl halides to give trifluoromethylated 1,3,4-thiadiazoles via regioselective [3 + 2] cycloadditions [59-63] (Scheme 10a). Similarly, trifluoroacetonitrile imine reacted with mercaptoacetaldehyde and mercaptocarboxylic acids to generate fluorinated 1,3,4-thiadiazines with good yields via a [3 + 3] annulation [64] (Scheme 10b).

Meanwhile, mercaptoacetaldehyde as a surrogate of acetylene reacted with trifluoroacetonitrile imine to form 1-aryl-3-trifluoromethylpyrazoles, followed by a series of cascade annulation/dehydration/ring contraction reactions when treated with *p*-TsCl [65] (Scheme 10b).

The chemistry of pyrazoles with a fluorine or a fluoroalkylated group has attracted a significant level of attention, and many trifluoromethylated pyrazoles have been used in medicinal products or in pesticides [66]. The [3 + 2] cycloaddition reactions are considered among the most powerful tools for the synthesis of versatile fluoroalkylated pyrazoles. Enol ethers, 1,4-naphthoquinones, *o*-trimethylsilylphenyl triflate and chalcones have all been reacted with fluorinated nitrile imines to give a series of fluoroalkylated pyrazoles by Jasiński's team [67-72] (Scheme 11a).

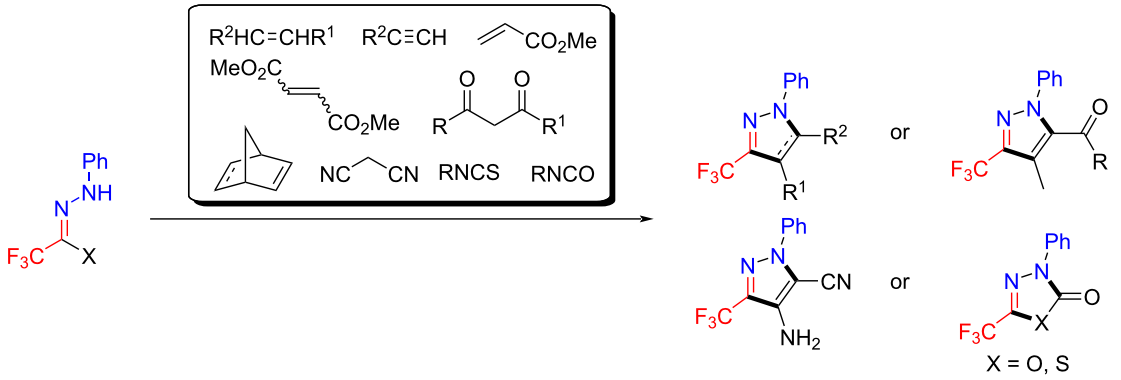

Scheme 9: Early work of trifluoromethylated hydrazonoyl halides.

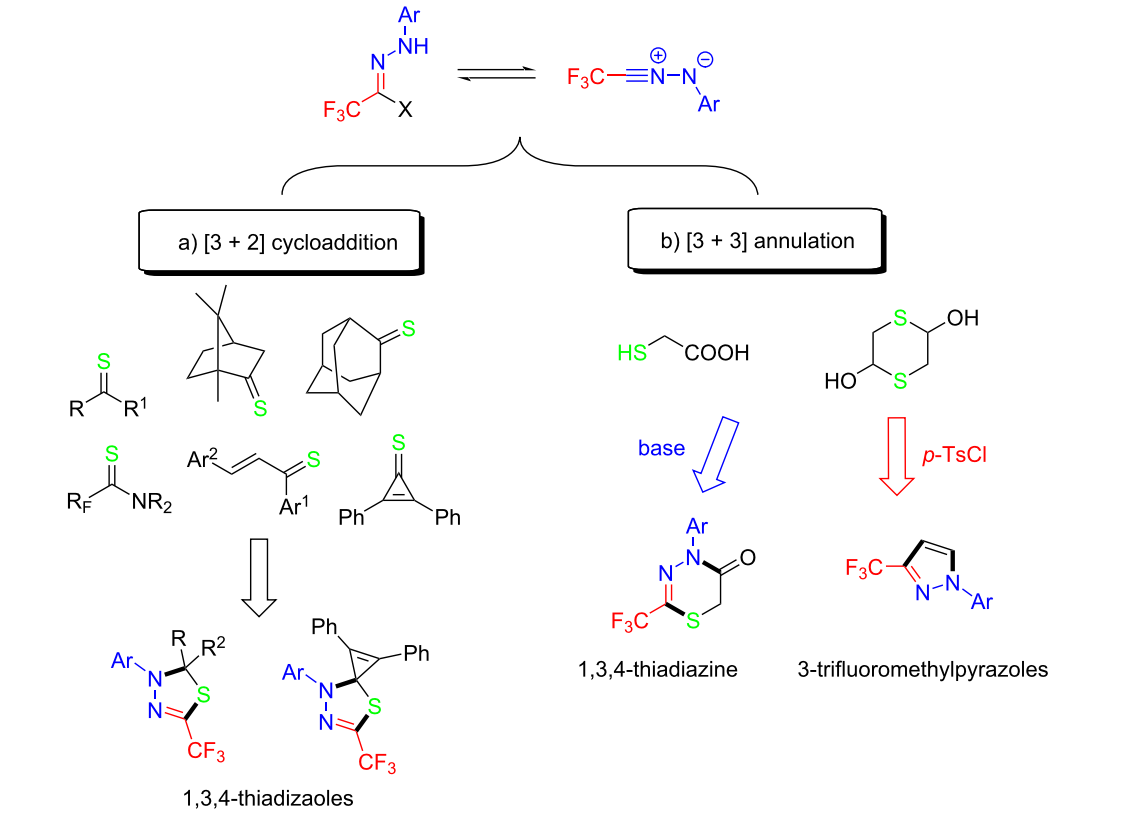

Scheme 10: [3 + 2]/[3 + 3] Cycloadditions of trifluoromethylated hydrazonoyl halides.

Subsequently, Hu et al., Nie et al., and Ma et al. have all independently reported practical methods, which extended the structural scope of such dipoles. This has allowed the synthesis of trifluoromethylpyrazoles by a range of regioselective [3 + 2] cycloadditions of trifluoroacetonitrile imines with electron-poor olefins [73-76] (Scheme 11b).

Moreover, the trifluoromethylated 1,2,4-triazoles were synthesized with excellent regioselectivities in [3 + 2] cycloaddition reactions of trifluoromethylated hydrazonoyl chlorides with imidates, amidine and 1*H*-benzo[*d*]imidazole-2-thiols, all of which were individually reported by Wang, Deng and Cai, respectively [77-79] (Scheme 12a). Meanwhile, the Jasiński

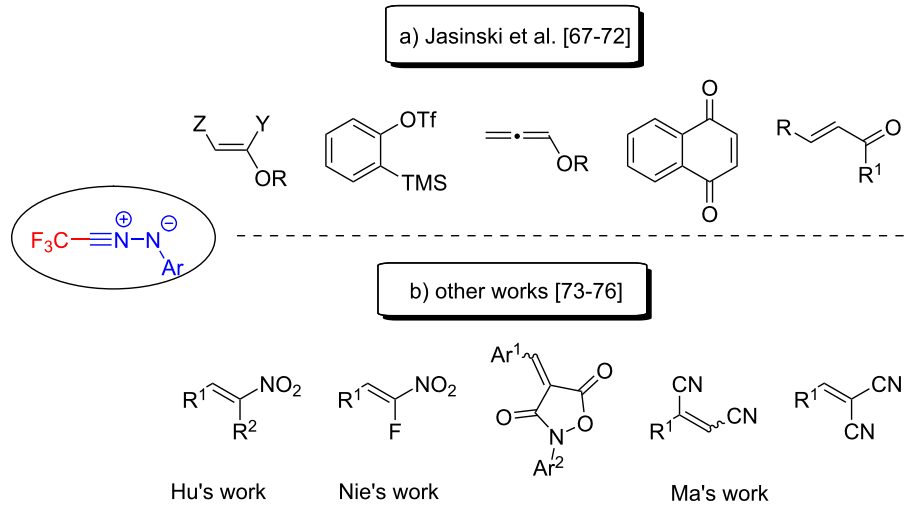

Scheme 11: Substrate scope for [3 + 2] cycloadditions with trifluoroacetonitrile imines reported by Jasiński's team and other groups.

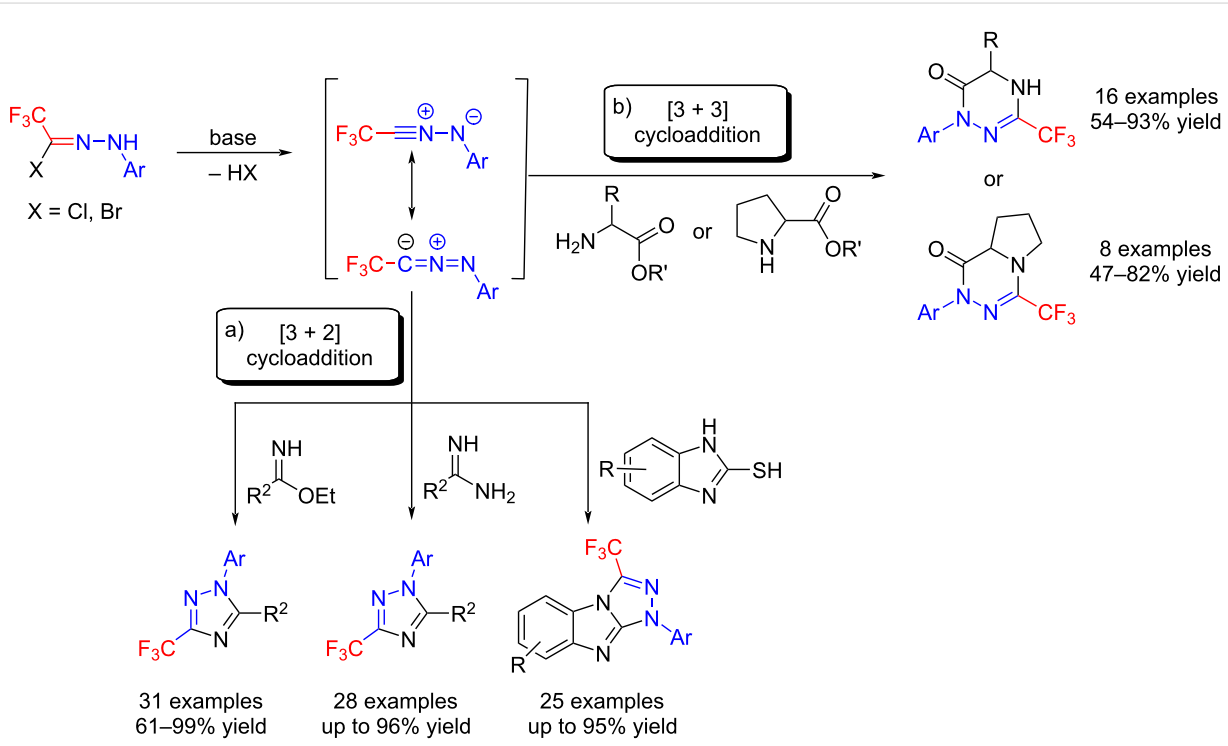

Scheme 12: Synthesis of trifluoromethylated 1,2,4-triazole and 1,2,4-triazine derivatives.

group turned their attention to the [3 + 3] cycloaddition of α-amino esters and trifluoromethylated hydrazonoyl halides and demonstrated the efficient synthesis of trifluoromethylated 1,2,4-triazine derivatives [80] (Scheme 12b).

Difluoromethylated compounds play an indispensable role in drug discovery and design since the hydrogen atom can act as lipophilic hydrogen-bond donor and act as a bioisostere for the alcohol moiety [81-83]. Thus, many effective difluoromethylation strategies have been developed in recent years. Difluoroacetohydrazonoyl bromides were chosen as fluorinated building blocks for the synthesis of difluoromethylated pyrazole derivatives by such [3 + 2] cycloaddition reactions [73,84,85] (Scheme 13).

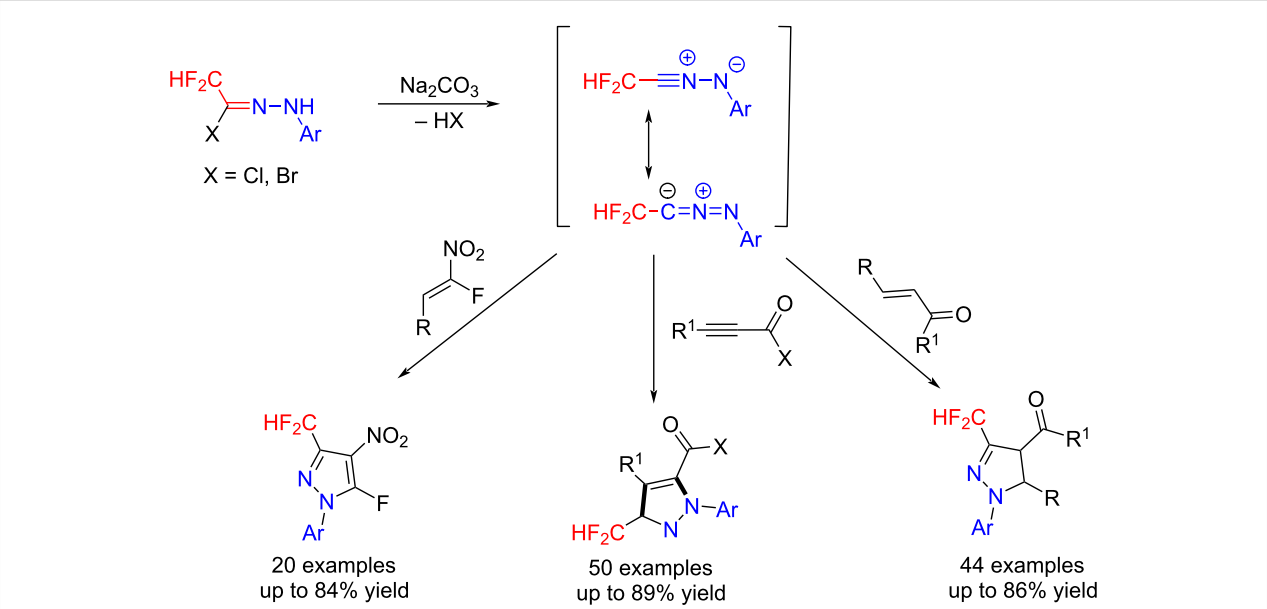

Scheme 13: [3 + 2] Cycloadditions of difluoromethylated hydrazonoyl halides.

These studies therefore emphasize that fluoromethylated nitrile imines are versatile building blocks for [3 + 2] and [3 + 3] cycloaddition reactions and indicate their potential offering an efficient approach to fluoroalkylated heterocycles in drug design.

Trifluoromethylated acylhydrazonoes

Acylhydrazones are a well-established class of organic compounds with the –CONH–N=CH– structure, and some variants show potential pesticidal and pharmacological activities [86,87]. Acylhydrazones can exist in either *E* or *Z* forms in solution, and they can exhibit good optical properties for applications as photoswitches, in luminescence sensing, and as metallo-assemblies [88,89]. In organic synthesis, acylhydrazones have served as stable imine equivalents to react with various nucleophilic reagents [90].

In 2014, Heimgartner et al. first developed the condensation reaction of a commercially available fluoral hemiacetal with acylhydrazides to yield trifluoromethylated acylhydrazones, and these fluorinated compounds underwent heterocyclization reactions with mercaptoacetic acid and acetic anhydride leading to trifluoromethylated 1,3-thiazolidin-4-ones and 3-acetyl-2,3-dihydro-1,3,4-oxadiazoles, respectively. It was found that the C=N reactivity of the trifluoromethylated acylhydrazones is similar to that of other nitrogen-containing fluorinated building blocks [91] (Scheme 14).

Inspired by previous accounts and this work [92,93], Hu et al. explored 1,2- nucleophilic addition reactions of trifluoromethylated acylhydrazones with organometallic reagents for the synthesis of trifluorinated homoallylic acylhydrazines [94-98], trifluorinated α-methylene-γ-lactams [99,100], and β-trifluoromethyl-β-acylhydrazonyl carbonyl compounds [101] (Scheme 15).

Among these fluorinated products, the trifluoromethylated homoallylic acylhydrazines were easily transformed to CF_3-

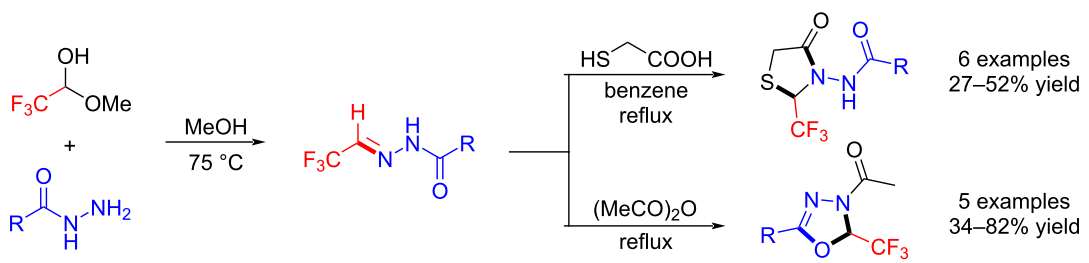

Scheme 14: Preparation and early applications of trifluoromethylated acylhydrazones.

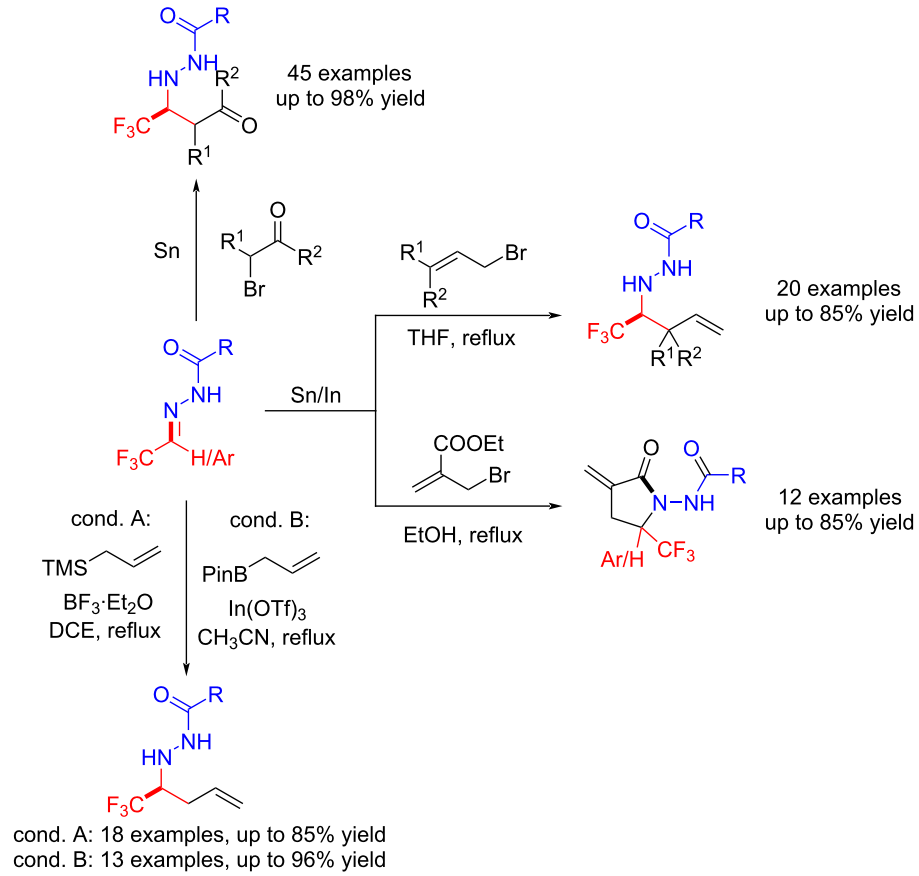

Scheme 15: 1,2-Nucleophilic addition reactions of trifluoromethylated acylhydrazones.

substituted pyrazolines and 1,6-dihydropyridazines via a cascade oxidation/cyclization with NXS or $Cu(OAc)_2$. Notably, some of the resultant CF_3-substituted 1,6-dihydropyridazines exhibited aggregation-induced emission [102,103] (Scheme 16).

The hydrocyanation of acylhydrazones is an important method for the preparation of α-hyrazino acids. Hu et al. reported a Lewis acid-catalyzed hydrocyanation of trifluoromethylated acylhydrazones, in which the product was the precursor for

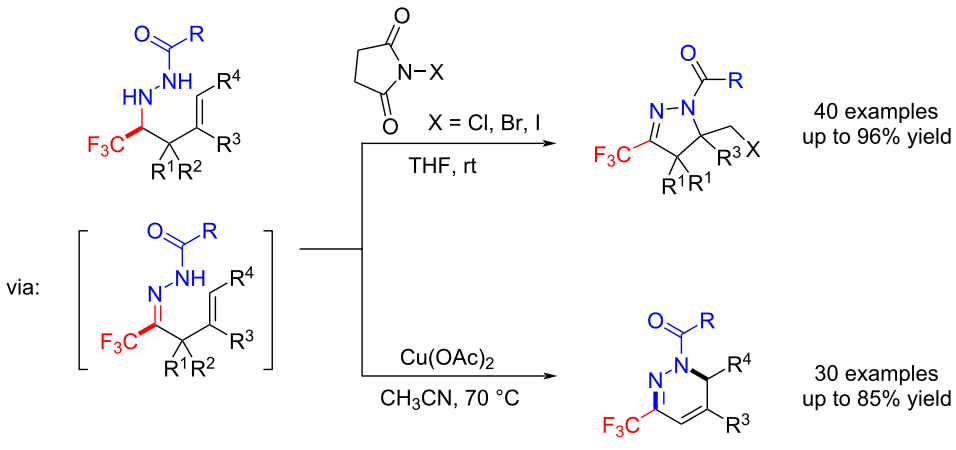

Scheme 16: Cascade oxidation/cyclization reactions of trifluoromethylated homoallylic acylhydrazines.

the preparation of chiral fluorinated amino acids [104] (Scheme 17a).

Meanwhile, Hu et al. provided a novel and efficient process for the synthesis of polysubstituted 3-trifluoromethyl-1,2,4-triazolines and their derivatives via tandem 1,2-addition/cyclization reactions between trifluoromethyl acylhydrazones and cyanamide [105] (Scheme 17b).

Afterwards, Hu et al. developed a method for the *N*-arylation and *N*-alkylation of trifluoromethyl acylhydrazones with diaryliodonium salts and alkyl halides under basic conditions, and expanded the synthetic method to N-substituted acylhydrazones [106,107] (Scheme 18).

In the early development of 1,3-dipolar cycloadditions of azomethine imines, the acyclic azomethine imines were unstable and their in situ preparation required Brønsted acid or thermal activation [108-110]. Besides, pyrazolidine and pyrazoline compounds are highly valuable hereocycles which are found in many natural products and bioactive compounds. Among them, CF_3-substituted pyrazolidines have already been shown to be

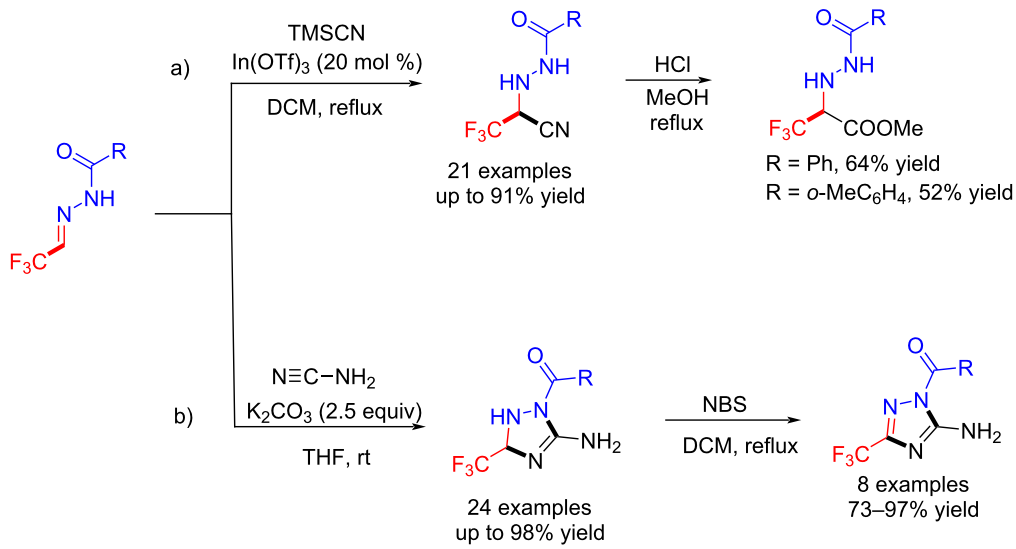

Scheme 17: Synthesis of trifluoromethylated cyanohydrazines and 3-trifluoromethyl-1,2,4-triazolines.

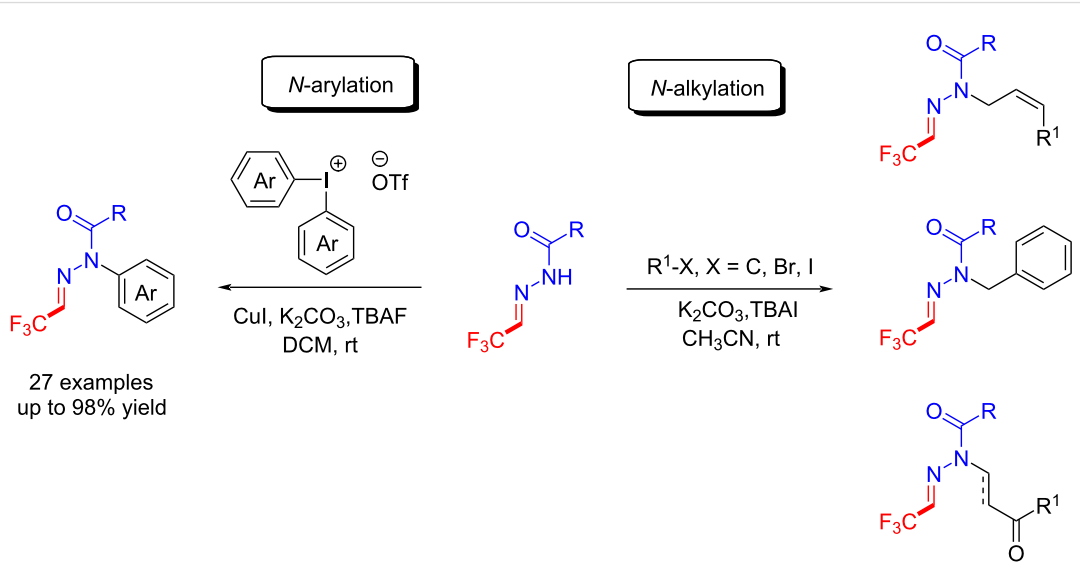

Scheme 18: *N*-Arylation and *N*-alkylation of trifluoromethyl acylhydrazones.

highly bioactive [111-113]. Thus, Hu et al. chose trifluoromethyl acylhydrazones as 1,3-dipolar agents to react with β-nitrostyrenes [114], maleates [115], cyclopentadiene [116] and maleimides [117] for the synthesis of CF_3-substituted pyrazolidine derivatives. These reactions were conducted under basic conditions and in the presence of $Cu(OTf)_2$ (Scheme 19a).

As an extension of their trifluoromethyl acylhydrazone synthesis, Hu et al. reported that trifluoromethyl acylhydrazones react with azomethine ylides [118] and ethyl isocyanoacetate [119] to generate trifluoromethylated imidazolidines. They demonstrated then that trifluoromethyl acylhydrazones act as dipolarophiles in the [3 + 2]-cycladditions (Scheme 19b).

Conclusion

Fluorine-containing molecules have attracted widespread attention as important components of agrochemicals, pharmaceuticals, and advanced materials. Abundant and fruitful progress in the applications of fluoromethylated hydrazones and acylhydrazones in recent years have been summarized and discussed. The resultant fluorinated building blocks provided a facile and rapid approach to directly construct valuable nitrogen-containing

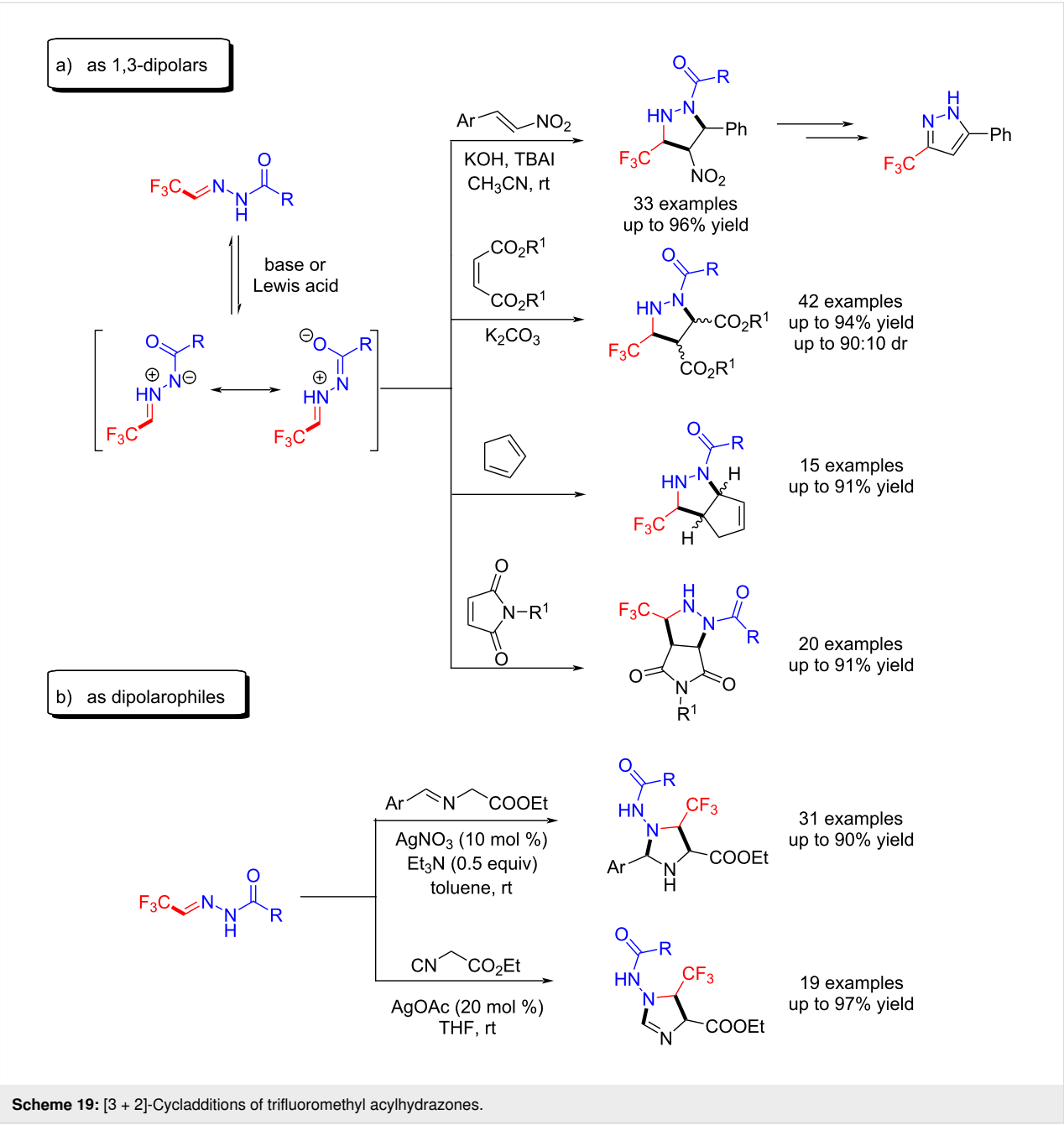

Scheme 19: [3 + 2]-Cycladditions of trifluoromethyl acylhydrazones.

fluorinated compounds. Apart from the regular involvement of addition and annulation reactions, the exploitation of more in-depth applications of fluoromethylated hydrazones and acylhydrazones to synthesize natural product analogues and fluorinated drugs is highly desirable. These methods should encourage the introduction of these difluoromethylated nitrogen-containing building blocks in future bioactives discovery programs.

ORCID® iDs

Zhang Dongxu - https://orcid.org/0009-0005-8137-7102

References

1. O'Hagan, D. *Chem. Soc. Rev.* **2008,** *37,* 308–319. doi:10.1039/b711844a
2. Hunter, L. *Beilstein J. Org. Chem.* **2010,** *6,* No. 38. doi:10.3762/bjoc.6.38
3. Meanwell, N. A. *J. Med. Chem.* **2018,** *61,* 5822–5880. doi:10.1021/acs.jmedchem.7b01788
4. Hagmann, W. K. *J. Med. Chem.* **2008,** *51,* 4359–4369. doi:10.1021/jm800219f
5. Zhou, Y.; Wang, J.; Gu, Z.; Wang, S.; Zhu, W.; Aceña, J. L.; Soloshonok, V. A.; Izawa, K.; Liu, H. *Chem. Rev.* **2016,** *116,* 422–518. doi:10.1021/acs.chemrev.5b00392
6. Inoue, M.; Sumii, Y.; Shibata, N. *ACS Omega* **2020,** *5,* 10633–10640. doi:10.1021/acsomega.0c00830
7. Ogawa, Y.; Tokunaga, E.; Kobayashi, O.; Hirai, K.; Shibata, N. *iScience* **2020,** *23,* 101467. doi:10.1016/j.isci.2020.101467
8. Ma, R.; Deng, Z.; Wang, K.; Huang, D.; Hu, Y.; Lü, X. *Chin. J. Org. Chem.* **2022,** *42,* 353–362. doi:10.6023/cjoc202108058
9. Qing, F.-L.; Liu, X.-Y.; Ma, J.-A.; Shen, Q.; Song, Q.; Tang, P. *CCS Chem.* **2022,** *4,* 2518–2549. doi:10.31635/ccschem.022.202201935
10. Xie, Q.; Hu, J. *Chin. J. Chem.* **2020,** *38,* 202–212. doi:10.1002/cjoc.201900424
11. Reichel, M.; Karaghiosoff, K. *Angew. Chem., Int. Ed.* **2020,** *59,* 12268–12281. doi:10.1002/anie.201913175
12. Zhang, C. *Org. Biomol. Chem.* **2014,** *12,* 6580–6589. doi:10.1039/c4ob00671b
13. Chu, L.; Qing, F.-L. *Acc. Chem. Res.* **2014,** *47,* 1513–1522. doi:10.1021/ar4003202
14. Liu, X.; Xu, C.; Wang, M.; Liu, Q. *Chem. Rev.* **2015,** *115,* 683–730. doi:10.1021/cr400473a
15. Zhang, C. *Adv. Synth. Catal.* **2014,** *356,* 2895–2906. doi:10.1002/adsc.201400370
16. Kaboudin, B.; Ghashghaee, M.; Bigdeli, A.; Farkhondeh, A.; Eskandari, M.; Esfandiari, H. *ChemistrySelect* **2021,** *6,* 12998–13014. doi:10.1002/slct.202103867
17. Charpentier, J.; Früh, N.; Togni, A. *Chem. Rev.* **2015,** *115,* 650–682. doi:10.1021/cr500223h
18. Ni, C.; Hu, M.; Hu, J. *Chem. Rev.* **2015,** *115,* 765–825. doi:10.1021/cr5002386
19. Mykhailiuk, P. K. *Chem. Rev.* **2020,** *120,* 12718–12755. doi:10.1021/acs.chemrev.0c00406
20. Kumar, A.; Khan, W. A.; Ahamad, S.; Mohanan, K. *J. Heterocycl. Chem.* **2022,** *59,* 607–632. doi:10.1002/jhet.4416
21. Mykhailiuk, P. K.; Koenigs, R. M. *Chem. – Eur. J.* **2019,** *25,* 6053–6063. doi:10.1002/chem.201804953
22. Bos, M.; Poisson, T.; Pannecoucke, X.; Charette, A. B.; Jubault, P. *Chem. – Eur. J.* **2017,** *23,* 4950–4961. doi:10.1002/chem.201604564
23. Nie, J.; Guo, H.-C.; Cahard, D.; Ma, J.-A. *Chem. Rev.* **2011,** *111,* 455–529. doi:10.1021/cr100166a
24. Fioravanti, S. *Tetrahedron* **2016,** *72,* 4449–4489. doi:10.1016/j.tet.2016.06.015
25. Sun, Z.; Zhang, C.; Chen, L.; Xie, H.; Liu, B.; Liu, D. *Chin. J. Org. Chem.* **2021,** *41,* 1789–1803. doi:10.6023/cjoc202011005
26. Chen, Z.; Hu, S.; Wu, X.-F. *Org. Chem. Front.* **2020,** *7,* 223–254. doi:10.1039/c9qo01167f
27. Sivaguru, P.; Bi, X. *Sci. China: Chem.* **2021,** *64,* 1614–1629. doi:10.1007/s11426-021-1052-7
28. de Oliveira Carneiro Brum, J.; França, T. C. C.; LaPlante, S. R.; Villar, J. D. F. *Mini-Rev. Med. Chem.* **2020,** *20,* 342–368. doi:10.2174/1389557519666191014142448
29. Verma, G.; Marella, A.; Shaquiauzzaman, M.; Akhtar, M.; Ali, M. R.; Alam, M. M. *J. Pharm. BioAllied Sci.* **2014,** *6,* 69–80. doi:10.4103/0975-7406.129170
30. Rollas, S.; Küçükgüzel, Ş. G. *Molecules* **2007,** *12,* 1910–1939. doi:10.3390/12081910
31. Su, X.; Aprahamian, I. *Chem. Soc. Rev.* **2014,** *43,* 1963–1981. doi:10.1039/c3cs60385g
32. Kobayashi, S.; Mori, Y.; Fossey, J. S.; Salter, M. M. *Chem. Rev.* **2011,** *111,* 2626–2704. doi:10.1021/cr100204f
33. Kölmel, D. K.; Kool, E. T. *Chem. Rev.* **2017,** *117,* 10358–10376. doi:10.1021/acs.chemrev.7b00090
34. Xu, P.; Li, W.; Xie, J.; Zhu, C. *Acc. Chem. Res.* **2018,** *51,* 484–495. doi:10.1021/acs.accounts.7b00565
35. Lv, Y.; Meng, J.; Li, C.; Wang, X.; Ye, Y.; Sun, K. *Adv. Synth. Catal.* **2021,** *363,* 5235–5265. doi:10.1002/adsc.202101184
36. Latrache, M.; Hoffmann, N. *Chem. Soc. Rev.* **2021,** *50,* 7418–7435. doi:10.1039/d1cs00196e
37. Iwata, S.; Namekata, J.; Tanaka, K.; Mitsuhashi, K. *J. Heterocycl. Chem.* **1991,** *28,* 1971–1976. doi:10.1002/jhet.5570280830
38. Xie, H.; Zhu, J.; Chen, Z.; Li, S.; Wu, Y. *Synthesis* **2011,** 2767–2774. doi:10.1055/s-0030-1260127
39. Das, A.; Volla, C. M. R.; Atodiresei, I.; Bettray, W.; Rueping, M. *Angew. Chem., Int. Ed.* **2013,** *52,* 8008–8011. doi:10.1002/anie.201301638
40. Volla, C. M. R.; Das, A.; Atodiresei, I.; Rueping, M. *Chem. Commun.* **2014,** *50,* 7889–7892. doi:10.1039/c4cc03229b
41. Wen, J.-J.; Tang, H.-T.; Xiong, K.; Ding, Z.-C.; Zhan, Z.-P. *Org. Lett.* **2014,** *16,* 5940–5943. doi:10.1021/ol502968c
42. Ding, Z.-C.; Ju, L.-C.; Yang, Y.; An, X.-M.; Zhou, Y.-B.; Li, R.-H.; Tang, H.-T.; Ding, C.-K.; Zhan, Z.-P. *J. Org. Chem.* **2016,** *81,* 3936–3941. doi:10.1021/acs.joc.6b00428
43. Wojciechowska, A.; Jasiński, M.; Kaszyński, P. *Tetrahedron* **2015,** *71,* 2349–2356. doi:10.1016/j.tet.2015.03.015
44. Fries, S.; Pytkowicz, J.; Brigaud, T. *Tetrahedron Lett.* **2005,** *46,* 4761–4764. doi:10.1016/j.tetlet.2005.05.040
45. Jia, S.; El Kaim, L. *Org. Biomol. Chem.* **2018,** *16,* 1457–1460. doi:10.1039/c7ob02840g
46. Sayed, A. R.; Ali, S. H.; Gomha, S. M.; Al-Faiyz, Y. S. *Synth. Commun.* **2020,** *50,* 3175–3203. doi:10.1080/00397911.2020.1799016

47. Farghaly, T. A.; Abdallah, M. A.; Mahmoud, H. K. *Curr. Org. Synth.* **2017,** *14,* 430–461. doi:10.2174/1570179413666160624105624
48. Fustero, S.; Sanz-Cervera, J. F.; Aceña, J. L.; Sánchez-Roselló, M. *Synlett* **2009,** 525–549. doi:10.1055/s-0028-1087806
49. Zheng, Z.; Dai, A.; Jin, Z.; Chi, Y. R.; Wu, J. *J. Agric. Food Chem.* **2022,** *70,* 11019–11030. doi:10.1021/acs.jafc.1c08383
50. Zong, W.; Hu, Y.; Wang, X.; Liu, J.; Huang, D.; Wang, K. *Chin. J. Org. Chem.* **2019,** *39,* 1396–1403. doi:10.6023/cjoc201811039
51. Tanaka, K.; Maeno, S.; Mitsuhashi, K. *Chem. Lett.* **1982,** *11,* 543–546. doi:10.1246/cl.1982.543
52. Tanaka, K.; Maeno, S.; Mitsuhashi, K. *J. Heterocycl. Chem.* **1985,** *22,* 565–568. doi:10.1002/jhet.5570220271
53. Tanaka, K.; Maeno, S.; Mitsuhashi, K. *Bull. Chem. Soc. Jpn.* **1985,** *58,* 1841–1842. doi:10.1246/bcsj.58.1841
54. Tanaka, K.; Kishida, M.; Maeno, S.; Mitsuhashi, K. *Bull. Chem. Soc. Jpn.* **1986,** *59,* 2631–2632. doi:10.1246/bcsj.59.2631
55. Tanaka, K.; Suzuki, T.; Maeno, S.; Mitsuhashi, K. *J. Heterocycl. Chem.* **1986,** *23,* 1535–1538. doi:10.1002/jhet.5570230556
56. Tanaka, K.; Masuda, H.; Mitsuhashi, K. *Bull. Chem. Soc. Jpn.* **1986,** *59,* 3901–3904. doi:10.1246/bcsj.59.3901
57. Tanaka, K.; Honda, O.; Minoguchi, K.; Mitsuhashi, K. *J. Heterocycl. Chem.* **1987,** *24,* 1391–1396. doi:10.1002/jhet.5570240532
58. Tanaka, K.; Suzuki, T.; Maeno, S.; Mitsuhashi, K. *Bull. Chem. Soc. Jpn.* **1987,** *60,* 4480–4482. doi:10.1246/bcsj.60.4480
59. Mlostoń, G.; Urbaniak, K.; Utecht, G.; Lentz, D.; Jasiński, M. *J. Fluorine Chem.* **2016,** *192,* 147–154. doi:10.1016/j.jfluchem.2016.10.018
60. Utecht, G.; Sioma, J.; Jasiński, M.; Mlostoń, G. *J. Fluorine Chem.* **2017,** *201,* 68–75. doi:10.1016/j.jfluchem.2017.07.014
61. Grzelak, P.; Utecht, G.; Jasiński, M.; Mlostoń, G. *Synthesis* **2017,** *49,* 2129–2137. doi:10.1055/s-0036-1588774
62. Heimgartner, H.; Jasiński, M.; Utecht-Jarzyńska, G.; Świątek, K.; Mlostoń, G. *Heterocycles* **2020,** *101,* 251–262. doi:10.3987/com-19-s(f)20
63. Utecht-Jarzyńska, G.; Mykhaylychenko, S. S.; Rusanov, E. B.; Shermolovich, Y. G.; Jasiński, M.; Mlostoń, G. *J. Fluorine Chem.* **2021,** *242,* 109702. doi:10.1016/j.jfluchem.2020.109702
64. Utecht-Jarzyńska, G.; Michalak, A.; Banaś, J.; Mlostoń, G.; Jasiński, M. *J. Fluorine Chem.* **2019,** *222–223,* 8–14. doi:10.1016/j.jfluchem.2019.04.012
65. Świątek, K.; Utecht-Jarzyńska, G.; Palusiak, M.; Ma, J.-A.; Jasiński, M. *Org. Lett.* **2023,** *25,* 4462–4467. doi:10.1021/acs.orglett.3c01437
66. Mykhailiuk, P. K. *Chem. Rev.* **2021,** *121,* 1670–1715. doi:10.1021/acs.chemrev.0c01015
67. Utecht, G.; Mlostoń, G.; Jasiński, M. A. *Synlett* **2018,** *29,* 1753–1758. doi:10.1055/s-0037-1610454
68. Utecht, G.; Fruziński, A.; Jasiński, M. *Org. Biomol. Chem.* **2018,** *16,* 1252–1257. doi:10.1039/c7ob03126b
69. Utecht-Jarzyńska, G.; Nagła, K.; Mlostoń, G.; Heimgartner, H.; Palusiak, M.; Jasiński, M. *Beilstein J. Org. Chem.* **2021,** *17,* 1509–1517. doi:10.3762/bjoc.17.108
70. Kowalczyk, A.; Utecht-Jarzyńska, G.; Mlostoń, G.; Jasiński, M. *J. Fluorine Chem.* **2021,** *241,* 109691. doi:10.1016/j.jfluchem.2020.109691
71. Kowalczyk, A.; Utecht-Jarzyńska, G.; Mlostoń, G.; Jasiński, M. *Org. Lett.* **2022,** *24,* 2499–2503. doi:10.1021/acs.orglett.2c00521
72. Utecht-Jarzyńska, G.; Kowalczyk, A.; Jasiński, M. *Molecules* **2022,** *27,* 8446. doi:10.3390/molecules27238446
73. Wang, K.-H.; Liu, H.; Liu, X.; Bian, C.; Wang, J.; Su, Y.; Huang, D.; Hu, Y. *Asian J. Org. Chem.* **2022,** e202200103. doi:10.1002/ajoc.202200103
74. Zhang, N.; Ma, H.; Cheung, C. W.; Zhang, F.-G.; Jasiński, M.; Ma, J.-A.; Nie, J. *Org. Biomol. Chem.* **2023,** *21,* 5040–5045. doi:10.1039/d3ob00644a
75. Tian, Y.-C.; Li, J.-K.; Zhang, F.-G.; Ma, J.-A. *Adv. Synth. Catal.* **2021,** *363,* 2093–2097. doi:10.1002/adsc.202100091
76. Zhou, Y.; Gao, C.-F.; Ma, H.; Nie, J.; Ma, J.-A.; Zhang, F.-G. *Chem. – Asian J.* **2022,** *17,* e202200436. doi:10.1002/asia.202200436
77. Zhang, Y.; Zeng, J.-L.; Chen, Z.; Wang, R. *J. Org. Chem.* **2022,** *87,* 14514–14522. doi:10.1021/acs.joc.2c01926
78. Wang, D.; Wan, X.; Zhou, Y.; Liu, J.; Cai, J.; Deng, G.-J. *Asian J. Org. Chem.* **2023,** *12,* e202200674. doi:10.1002/ajoc.202200674
79. Cen, K.; Wei, J.; Feng, Y.; Liu, Y.; Wang, X.; Liu, Y.; Yin, Y.; Yu, J.; Wang, D.; Cai, J. *Org. Biomol. Chem.* **2023,** *21,* 7095–7099. doi:10.1039/d3ob01133j
80. Kowalczyk, A.; Świątek, K.; Celeda, M.; Utecht-Jarzyńska, G.; Jaskulska, A.; Gach-Janczak, K.; Jasiński, M. *Materials* **2023,** *16,* 856. doi:10.3390/ma16020856
81. Zafrani, Y.; Yeffet, D.; Sod-Moriah, G.; Berliner, A.; Amir, D.; Marciano, D.; Gershonov, E.; Saphier, S. *J. Med. Chem.* **2017,** *60,* 797–804. doi:10.1021/acs.jmedchem.6b01691
82. Sessler, C. D.; Rahm, M.; Becker, S.; Goldberg, J. M.; Wang, F.; Lippard, S. J. *J. Am. Chem. Soc.* **2017,** *139,* 9325–9332. doi:10.1021/jacs.7b04457
83. Zafrani, Y.; Saphier, S.; Gershonov, E. *Future Med. Chem.* **2020,** *12,* 361–365. doi:10.4155/fmc-2019-0309
84. Han, T.; Wang, K.-H.; Yang, M.; Zhao, P.; Wang, F.; Wang, J.; Huang, D.; Hu, Y. *J. Org. Chem.* **2022,** *87,* 498–511. doi:10.1021/acs.joc.1c02521
85. Ren, Y.; Ma, R.; Feng, Y.; Wang, K.-H.; Wang, J.; Huang, D.; Lv, X.; Hu, Y. *Asian J. Org. Chem.* **2022,** *11,* e202200438. doi:10.1002/ajoc.202200438
86. Xie, J.; Xu, W.; Song, H.; Liu, Y.; Zhang, J.; Wang, Q. *J. Agric. Food Chem.* **2020,** *68,* 5555–5571. doi:10.1021/acs.jafc.0c00875
87. Thota, S.; Rodrigues, D. A.; de Sena Murteira Pinheiro, P.; Lima, L. M.; Fraga, C. A. M.; Barreiro, E. J. *Bioorg. Med. Chem. Lett.* **2018,** *28,* 2797–2806. doi:10.1016/j.bmcl.2018.07.015
88. Moreno, M.; Gelabert, R.; Lluch, J. M. *Phys. Chem. Chem. Phys.* **2019,** *21,* 16075–16082. doi:10.1039/c9cp03324f
89. de Oliveira, W. A.; Mezalira, D. Z.; Westphal, E. *Liq. Cryst.* **2021,** *48,* 88–99. doi:10.1080/02678292.2020.1766135
90. Sugiura, M.; Kobayashi, S. *Angew. Chem., Int. Ed.* **2005,** *44,* 5176–5186. doi:10.1002/anie.200500691
91. Mlostoń, G.; Urbaniak, K.; Jacaszek, N.; Linden, A.; Heimgartner, H. *Heterocycles* **2014,** *88,* 387–401. doi:10.3987/com-13-s(s)40
92. Kobayashi, S.; Sugiura, M.; Ogawa, C. *Adv. Synth. Catal.* **2004,** *346,* 1023–1034. doi:10.1002/adsc.200404101
93. Elaas, N. A.; Elaas, W. A.; Huang, D.; Hu, Y.; Wang, K.-H. *Curr. Org. Synth.* **2017,** *14,* 1156–1171. doi:10.2174/1570179414666170201150313
94. Du, G.; Huang, D.; Wang, K.-H.; Chen, X.; Xu, Y.; Ma, J.; Su, Y.; Fu, Y.; Hu, Y. *Org. Biomol. Chem.* **2016,** *14,* 1492–1500. doi:10.1039/c5ob02260f

95. Li, J.; Yang, T.; Zhang, H.; Huang, D.; Wang, K.; Su, Y.; Hu, Y. *Chin. J. Org. Chem.* **2017,** *37,* 925–935. doi:10.6023/cjoc201611009
96. Wang, K.; Wang, Y.; Yin, X.; Peng, X.; Huang, D.; Su, Y.; Hu, Y. *Chin. J. Org. Chem.* **2017,** *37,* 1764–1773. doi:10.6023/cjoc201612042
97. Liu, J.; Huang, D.; Wang, X.; Zong, W.; Su, Y.; Wang, K.; Hu, Y. *Chin. J. Org. Chem.* **2019,** *39,* 1767–1775. doi:10.6023/cjoc201901007
98. Hu, Y.; Huang, D.; Wang, K.; Zhao, Z.; Zhao, F.; Xu, W.; Hu, Y. *Chin. J. Org. Chem.* **2020,** *40,* 1689–1696. doi:10.6023/cjoc201912006
99. Li, J.; Huang, D.; Zhang, H.; Zhang, X.; Wang, J.; Wang, K.-H.; Su, Y.; Hu, Y. *Chin. J. Org. Chem.* **2017,** *37,* 2985–2992. doi:10.6023/cjoc201703050
100. Wang, K.-H.; Wang, J.; Wang, Y.; Su, Y.; Huang, D.; Fu, Y.; Du, Z.; Hu, Y. *Synthesis* **2018,** *50,* 1907–1913. doi:10.1055/s-0036-1591909
101. Wang, K.-H.; Shi, B.; Wang, Y.; Wang, J.; Huang, D.; Su, Y.; Hu, Y. *Asian J. Org. Chem.* **2019,** *8,* 716–721. doi:10.1002/ajoc.201800693
102. Wang, Y.; Wang, K.-H.; Su, Y.; Yang, Z.; Wen, L.; Liu, L.; Wang, J.; Huang, D.; Hu, Y. *J. Org. Chem.* **2018,** *83,* 939–950. doi:10.1021/acs.joc.7b02934
103. Yang, T.; Deng, Z.; Wang, K.-H.; Li, P.; Huang, D.; Su, Y.; Hu, Y. *J. Org. Chem.* **2020,** *85,* 12304–12314. doi:10.1021/acs.joc.0c01568
104. Xu, W.; Huang, D.; Wang, K.; Zhao, F.; Zhao, Z.; Hu, Y.; Su, Y.; Hu, Y. *Chin. J. Org. Chem.* **2020,** *40,* 922–929. doi:10.6023/cjoc201910011
105. Liu, X.; Liu, H.; Bian, C.; Wang, K.-H.; Wang, J.; Huang, D.; Su, Y.; Lv, X.; Hu, Y. *J. Org. Chem.* **2022,** *87,* 5882–5892. doi:10.1021/acs.joc.2c00176
106. Zhang, H.; Wang, K.-H.; Wang, J.; Su, Y.; Huang, D.; Hu, Y. *Org. Biomol. Chem.* **2019,** *17,* 2940–2947. doi:10.1039/c9ob00236g
107. Yang, J.; Huang, D.; Wang, K.; Wang, J.; Su, Y.; Deng, Z.; Yang, T.; Hu, Y. *Chin. J. Org. Chem.* **2021,** *41,* 2029–2037. doi:10.6023/cjoc202011001
108. Nájera, C.; Sansano, J. M.; Yus, M. *Org. Biomol. Chem.* **2015,** *13,* 8596–8636. doi:10.1039/c5ob01086a
109. Hashimoto, T.; Maruoka, K. *Chem. Rev.* **2015,** *115,* 5366–5412. doi:10.1021/cr5007182
110. Yue, G.; Liu, B. *Chin. J. Org. Chem.* **2020,** *40,* 3132–3153. doi:10.6023/cjoc202005092
111. Behr, L. C.; Fusco, R.; Jarboe, C. H. In *Pyrazoles, Pyrazolines, Pyrazolidines, Indazoles and Condensed Rings;* Wiley, R. H., Ed.; *The Chemistry of Heterocyclic Compounds*, Vol. 22; Interscience Publishers: New York, NY, USA, 1967. doi:10.1002/9780470186848
112. Zhang, X.; Li, X.; Allan, G. F.; Sbriscia, T.; Linton, O.; Lundeen, S. G.; Sui, Z. *J. Med. Chem.* **2007,** *50,* 3857–3869. doi:10.1021/jm0613976
113. Reddy, M. V. R.; Billa, V. K.; Pallela, V. R.; Mallireddigari, M. R.; Boominathan, R.; Gabriel, J. L.; Reddy, E. P. *Bioorg. Med. Chem.* **2008,** *16,* 3907–3916. doi:10.1016/j.bmc.2008.01.047
114. Peng, X.; Huang, D.; Wang, K.-H.; Wang, Y.; Wang, J.; Su, Y.; Hu, Y. *Org. Biomol. Chem.* **2017,** *15,* 6214–6222. doi:10.1039/c7ob01299c
115. Wen, L.; Huang, D.; Wang, K.-H.; Wang, Y.; Liu, L.; Yang, Z.; Su, Y.; Hu, Y. *Synthesis* **2018,** *50,* 1979–1990. doi:10.1055/s-0036-1591768
116. Liu, L.; Huang, D.; Wang, Y.; Wen, L.; Yang, Z.; Su, Y.; Wang, K.; Hu, Y. *Chin. J. Org. Chem.* **2018,** *38,* 1469–1476. doi:10.6023/cjoc201712036
117. Feng, Y.; Chang, B.; Ren, Y.; Zhao, F.; Wang, K.-H.; Wang, J.; Huang, D.; Lv, X.; Hu, Y. *Tetrahedron* **2023,** *136,* 133353. doi:10.1016/j.tet.2023.133353
118. Zhao, F.; Wang, K.-H.; Wen, L.; Zhao, Z.; Hu, Y.; Xu, W.; Huang, D.; Su, Y.; Wang, J.; Hu, Y. *Asian J. Org. Chem.* **2020,** *9,* 1036–1039. doi:10.1002/ajoc.202000057
119. Yang, M.; Huang, D.; Wang, K.; Han, T.; Zhao, P.; Wang, F.; Wang, J.; Su, Y.; Hu, Y. *Chin. J. Org. Chem.* **2022,** *42,* 1509–1519. doi:10.6023/cjoc202111009

License and Terms

BEILSTEIN JOURNAL OF ORGANIC CHEMISTRY

Copper-catalyzed multicomponent reaction of β-trifluoromethyl β-diazo esters enabling the synthesis of β-trifluoromethyl *N*,*N*-diacyl-β-amino esters

Youlong Du[1], Haibo Mei[*1], Ata Makarem[2], Ramin Javahershenas[3], Vadim A. Soloshonok[4,5] and Jianlin Han[*1]

Letter

Open Access

Address:
[1]Jiangsu Co-Innovation Center of Efficient Processing and Utilization of Forest Resources, College of Chemical Engineering, Nanjing Forestry University, Nanjing 210037, China, [2]Department of Chemistry, University of Hamburg, Martin-Luther-King-Platz 6, 20146 Hamburg, Germany, [3]Department of Organic Chemistry, Faculty of Chemistry, Urmia University, Urmia, Iran, [4]Department of Organic Chemistry I, Faculty of Chemistry, University of the Basque Country (UPV/EHU), Paseo Manuel Lardizábal 3, San Sebastián, 20018, Spain and [5]IKERBASQUE, Basque Foundation for Science, Alameda Urquijo 36-5, Plaza Bizkaia, 48011 Bilbao, Spain

Email:
Haibo Mei[*] - meihb@njfu.edu.cn; Jianlin Han[*] - hanjl@njfu.edu.cn

* Corresponding author

Keywords:
β-carbonyl diazo; copper catalyst; fluoroalkyl diazo; Mumm rearrangement; unsymmetrical β-diacylamino esters

Beilstein J. Org. Chem. **2024,** *20,* 212–219.
https://doi.org/10.3762/bjoc.20.21

Received: 12 October 2023
Accepted: 23 January 2024
Published: 02 February 2024

This article is part of the thematic issue "Organofluorine chemistry VI".

Guest Editor: D. O'Hagan

Abstract

An efficient multicomponent reaction of newly designed β-trifluoromethyl β-diazo esters, acetonitrile, and carboxylic acids via an interrupted esterification process under copper-catalyzed conditions has been developed, which affords various unsymmetrical β-trifluoromethyl *N*,*N*-diacyl-β-amino esters in good to excellent yields. The reaction features mild conditions, a wide scope of β-amino esters and carboxylic acids, and also applicability to large-scale synthesis, thus providing an efficient way for the synthesis of β-trifluoromethyl β-diacylamino esters. Furthermore, this reaction represents the first example of a Mumm rearrangement of β-trifluoromethyl β-diazo esters.

Introduction

The insertion of fluorine-containing components frequently confers desirable physical and biological properties to organic molecules, and the development of fluorine-containing drugs is an important field of research [1-9]. It is estimated that 30% of drugs and over 50% of agricultural chemicals contain at least one fluorine atom, among which architectural motifs contain-

ing fluorine and amino acid residues are a fast-growing segment of modern pharmaceuticals [10-13].

Fluoroalkyldiazo compounds belong to the most versatile and valuable reagents in organic synthesis, as they can be used as diazo intermediates or carbene precursors for the rapid construction of complex molecules along with the introduction of fluoroalkyl groups [14-16]. Although the reaction of trifluorodiazoethane [17-27] as well as α-diazo esters [28-30] have been widely explored, β-trifluoromethyl β-diazo esters have been less investigated, mainly due to the instability of such structures. Therefore, methods for the synthesis of β-trifluoromethyl β-diazo esters and their applications in organic synthesis are needed but remain challenging.

On the other hand, several interesting transformations of nitrile ylides from diazo compounds have been developed in the past years [31-38]. In particular, acylglycine esters could be easily constructed with ester-containing diazo compounds as the starting materials. For example, Wan and co-workers developed a cascade reaction of α-diazo esters, nitriles, and carboxylic acids via the generation of nitrile ylides and Mumm rearrangement affording unsymmetric diacyl α-amino acid esters as products (Scheme 1a) [39]. In 2017, Zhang, Hu, and co-workers developed a Cu-catalyzed reaction of CF_3CHN_2 with carboxylic acids and acetonitrile via a similar process to afford a series of *N*-trifluoroethylimides (Scheme 1b) [40,41]. Inspired by these elegant works [31-41] and based on our continuous interest in reactions of fluoroalkyldiazo compounds [42-49], we sought to develop reactions of the unexplored β-trifluoromethyl β-diazo esters. We hypothesized that nitrile ylides, in situ generated from nitriles and β-trifluoromethyl β-amino esters, could also react with carboxylic acids to give nitriliums, which then could undergo a Mumm rearrangement to provide unsymmetrical β-trifluoromethyl diacyl-β-amino esters as products (Scheme 1c). Herein, we report our results on the design of β-trifluoromethyl β-diazo esters and their application in a three-component reaction with nitriles and carboxylic acids under mild conditions. A variety of unnatural unsymmetrical β-trifluoromethyl diacyl-β-amino esters were obtained in good yields, which are useful synthetic scaffolds [50-52] but difficult to obtain by other methods [53-57]. This work is the first example of the reaction of β-trifluoromethyl β-diazo esters, which enriches the studied content of fluoroalkyl diazo compounds.

Results and Discussion

Due to the instability of β-carbonyl diazo compounds and the occurrence of possible side reactions [58-61], screening of reaction conditions to optimize this conversion and inhibit the occurrence of side reactions was carried out with benzyl 3-amino-4,4,4-trifluorobutanoate (**1a**) and benzoic acid (**3a**) as model

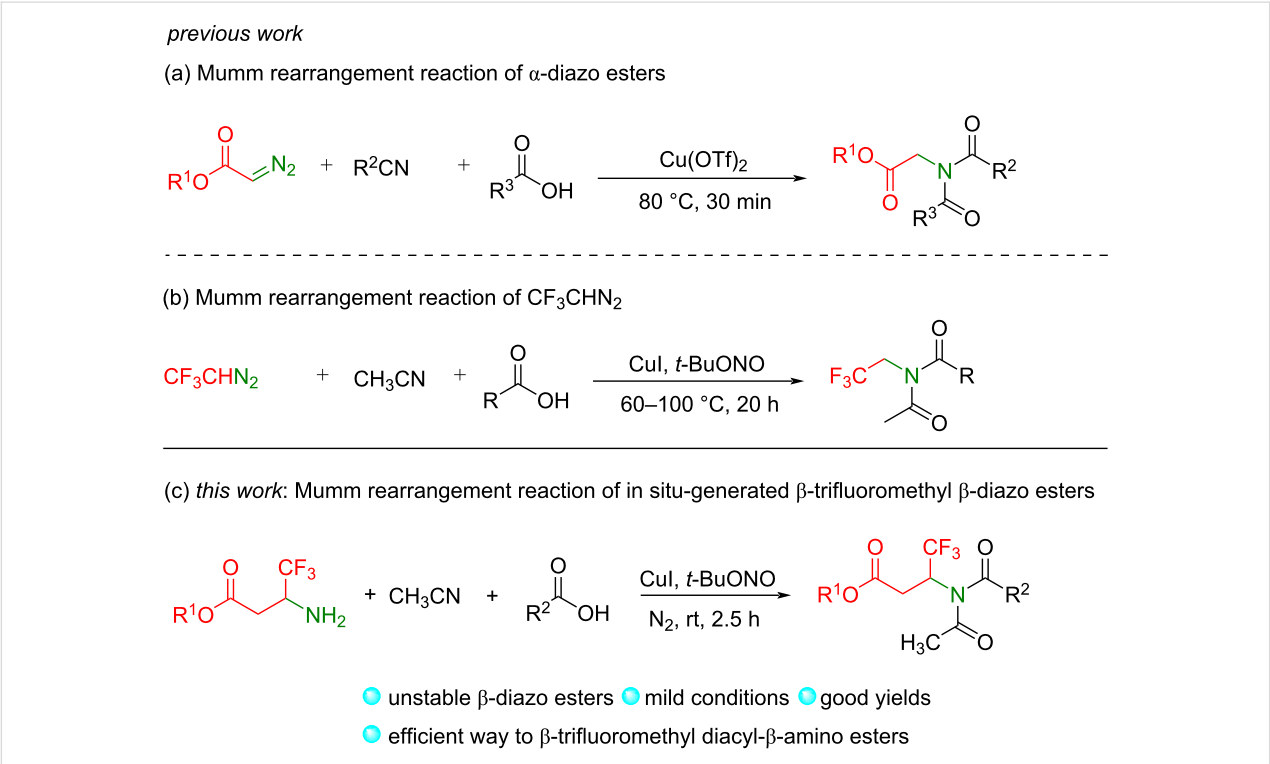

Scheme 1: Mumm-type rearrangement of diazo compounds.

substrates. The initial reaction of amine **1a** and acid **3a** in acetonitrile in the presence of diazotization reagent *tert*-butyl nitrite with CuI (10 mol %) as catalysts for 2.5 h at room temperature proceeded to afford the desired unsymmetrical β-trifluoromethyl diacyl-β-amino ester **4a** in 54% yield (Table 1, entry 1). The loading amount of catalyst CuI plays a crucial role in the formation of the desired product **4a**. Increasing the loading amount of CuI, the yield could be raised to 66% when 20 mol % of CuI was used as catalyst (Table 1, entries 2 and 3). However, further increasing the amount of the catalyst led to an obvious decrease in the yield of product **4a** (Table 1, entries 4 and 5). Variation on the reaction temperature also afforded the corresponding product **4a** but failed to bring any improvement on the reaction outcome (Table 1, entries 6 and 7). Further optimization of the reaction conditions focused on the variation of the amounts of amine **1a** and *tert*-butyl nitrite (Table 1, entries 8–12). Considering the instability of the diazo structure generated from amine **1a**, we increased the amount of amine **1a** and *tert*-butyl nitrite to 4 equivalents. Pleasingly, the yield of product **4a** was further increased to 74% (Table 1, entry 12). Furthermore, we optimized the reaction time and found that shortening the reaction time resulted in a decreased yield (Table 1, entry 13). Increasing the reaction time to 3 h also did not lead to any better result mainly due to the decomposition of product **4a** (Table 1, entry 14).

With the optimized reaction conditions in hand, we next evaluated the substrate scope by using a variety of structurally diverse carboxylic acids **3** to react with β-trifluoromethyl β-amino esters **1**. As shown in Scheme 2, all the substituted benzoic acids **3** tested were well tolerated in this reaction, and the corresponding product **4** was successfully prepared at moderate to excellent yields (**4a–e**, **4h–m**, 31–86% yields). The benzoic acids featuring a wide range of functional groups, including alkyl (**4a–e**), halogen (**4h–l**), and phenyl (**4m**), were all suitable substrates for this reaction. However, the benzoic acid with *ortho*-substituent did not afford the expected product (**4f**) mainly due to the steric hindrance effect. Notably, substrates with electron-withdrawing groups (**4h–l**, 76–86% yields) provided better chemical yields in this reaction compared with those containing electron-donating groups (**4b–e**, 31–84% yields). For the case with a strong electron-donating group (methoxy, **3g**) only traces of **4g** were produced. Besides benzoic acid, the current Cu-catalyzed reaction was also applicable to other aromatic acid substrates. Using 2-naphthoic and 1-naphthoic acid as substrates, the corresponding products **4n** and **4o** were produced well with yields of 78% and 54%, respectively. Unfortunately, the tested aliphatic acid, such as cyclohexanecarboxylic acid, did not work in the system to produce the expected product (**4p**). In addition, the β-trifluoromethyl β-amino benzyl ester substrates **1** with different ester groups were tried to react with benzoic acid (**3a**) to further extend the substrate range. To our

Table 1: Optimization of reaction conditions.[a]

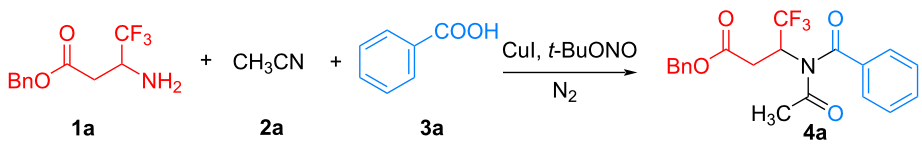

1a **2a** **3a** **4a**

Entry	**1a** (equiv)	CuI (mol %)	*t*-BuONO (equiv)	*T* (°C)	Time (h)	Yield[b] (%)
1	2	10	2	rt	2.5	54
2	2	15	2	rt	2.5	57
3	2	20	2	rt	2.5	66
4	2	30	2	rt	2.5	32
5	2	40	2	rt	2.5	trace
6	2	20	2	0	2.5	20
7	2	20	2	60	2.5	38
8	2	20	1	rt	2.5	38
9	2	20	3	rt	2.5	41
10	1	20	2	rt	2.5	27
11	3	20	2	rt	2.5	43
12	4	20	4	rt	2.5	74
13	4	20	4	rt	1.5	43
14	4	20	4	rt	3	60

[a]Reaction conditions: amine **1a** (0.4 mmol), benzoic acid **3a** (0.1 mmol), CuI (20 mol %), *t*-BuONO (0.4 mmol) and CH_3CN (2 mL) under nitrogen atmosphere. [b]Isolated yield based on acid **3a**.

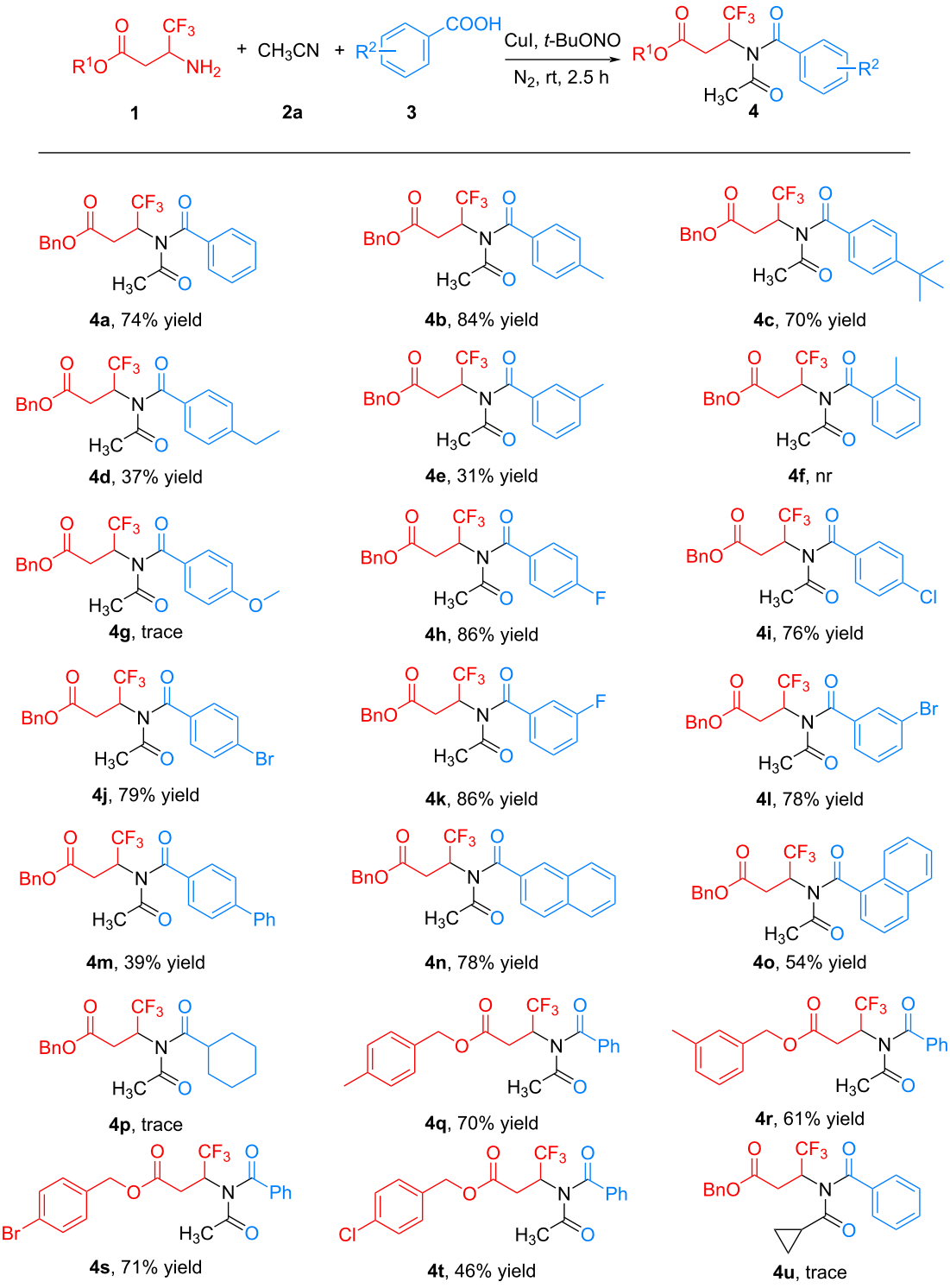

Scheme 2: Substrate scope study of this Cu-catalyzed reaction.

delight, both the amines with electron-donating groups (**4q** and **4r**) and electron-withdrawing groups (**4s** and **4t**) could generate the target products with moderate to good yields (46–71%). We also tried another nitrile substrate, such as cyclopropyl acetonitrile, which yielded only very small amounts of the expected product (**4u**).

To gain insight into the mechanism of this reaction, several control experiments were performed. First, the reaction was conducted under the optimized conditions without the addition of CuI. The conversion of the starting substrates to the desired product **4a** was decreased and only 14% yield of **4a** was obtained (Scheme 3a). However, as shown in entry 1 of Table 1, 54% yield product **4a** was produced by this reaction in the presence of 10 mol % CuI. These results demonstrate that copper catalysis plays a crucial role in the generation of the desired product **4a**. Moreover, we performed this reaction without the addition of *tert*-butyl nitrite (Scheme 3b). The expected three-component tandem reaction did not occur, and the target **4a** was not observed with almost all of the starting amine **1a** remaining. This result indicates the reaction proceeds through the diazo intermediate.

According to the above experimental results and literature reports [39-41,58,59], a possible mechanism for this Cu-catalyzed reaction of β-trifluoromethyl β-amino esters was proposed in Scheme 4. Initially, β-trifluoromethyl β-amino ester **1a** reacts with *tert*-butyl nitrite to form trifluoromethylated β-carbonyl diazo intermediate **A**. Then, the diazo intermediate **A** reacts with the copper catalyst generating the Cu-carbene intermediate **B**, which undergoes nucleophilic attack by acetonitrile to form the intermediate **C**. Subsequently, nucleophilic addition of benzoic acid to intermediate **C** affords the acetimidic anhydride **D** with the release of Cu^I catalyst for the next catalytic cycle. Finally, the acetimidic anhydride **D** undergoes a Mumm rearrangement to furnish the desired β-trifluoromethyl diacylamino ester **4a**.

The final goal of this work is the examination of the scale-up applicability of this three-component tandem reaction (Scheme 5). To our delight, the reaction also proceeded smoothly when the amount of β-trifluoromethyl β-amino ester **1a** was increased ten-fold to 988.8 mg. The corresponding β-tri-

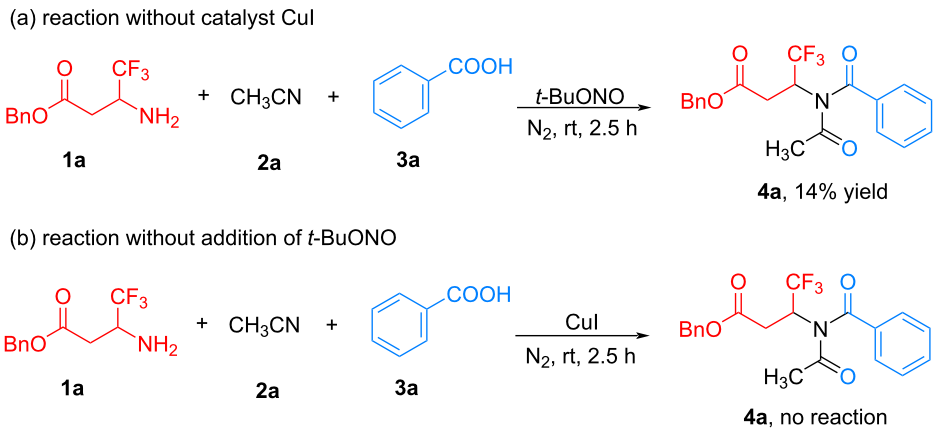

Scheme 3: Control experiments.

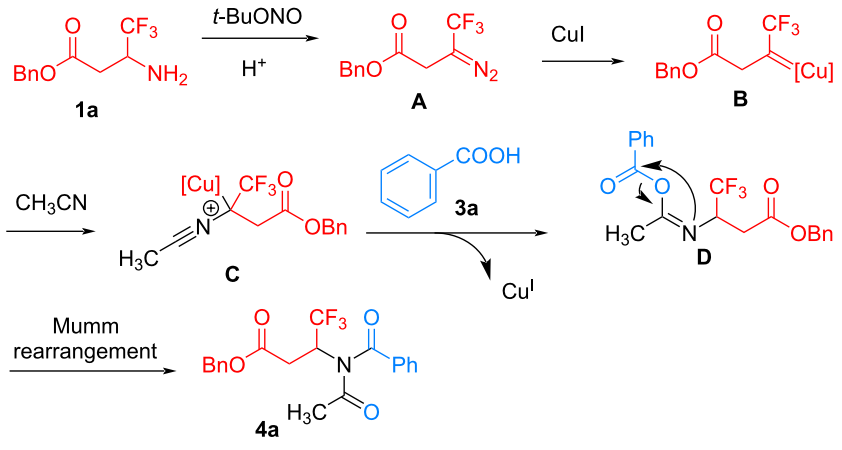

Scheme 4: Proposed reaction mechanism.

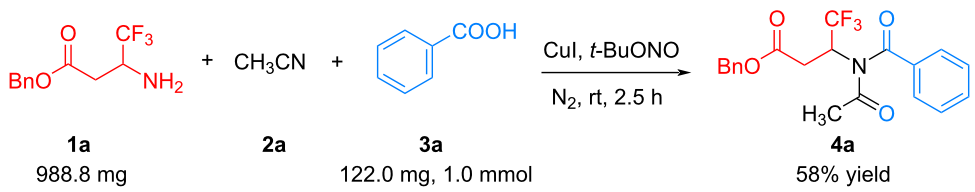

Scheme 5: Scale-up synthesis.

fluoromethyl diacylamino ester **4a** was obtained in 58% chemical yield. This result indicates the wide synthesis utility of the reactions reported in this work.

Conclusion

In summary, a series of new β-trifluoromethyl β-diazo esters have been designed, which are applied for the first time in a cascade reaction through an interrupted esterification with nitrile ylides as the key intermediates under copper-catalysis conditions. Varieties of unsymmetric trifluoromethyl diacyl β-amino esters can be easily constructed with good chemical yields. The reaction is conducted under mild conditions and shows good applicability to different series of substrates, which provides an efficient way for the preparation of unsymmetric trifluoromethyl diacyl β-amino esters.

Experimental

General procedure for copper-catalyzed multicomponent reaction of β-amino esters

Into a flask were added amines **1** (0.4 mmol), acids **3** (0.1 mmol), CuI (20 mol %), and CH_3CN (2 mL). Then, the mixture was stirred at room temperature under a nitrogen atmosphere and *t*-BuONO (0.4 mmol) was added dropwise. Stirring was continued at room temperature for 2.5 h and the solvent was removed in vacuum. Products **4** were purified on a TLC plate of 20 cm × 20 cm using petroleum ether/ethyl acetate 7:1 (v/v) as eluent.

Supporting Information

Supporting Information File 1

Experimental details and spectral data.
[https://www.beilstein-journals.org/bjoc/content/supplementary/1860-5397-20-21-S1.pdf]

Funding

We gratefully acknowledge the financial support from the National Natural Science Foundation of China (No. 21761132021) and Qing Lan Project of Jiangsu Province. IKERBASQUE, Basque Foundation for Science (for Soloshonok) is also acknowledged.

ORCID® iDs

Ramin Javahershenas - https://orcid.org/0000-0001-5771-7203
Jianlin Han - https://orcid.org/0000-0002-3817-0764

Data Availability Statement

The data that supports the findings of this study is available from the corresponding author upon reasonable request.

References

1. Zhou, Y.; Wang, J.; Gu, Z.; Wang, S.; Zhu, W.; Aceña, J. L.; Soloshonok, V. A.; Izawa, K.; Liu, H. *Chem. Rev.* **2016,** *116,* 422–518. doi:10.1021/acs.chemrev.5b00392
2. Wang, J.; Sánchez-Roselló, M.; Aceña, J. L.; del Pozo, C.; Sorochinsky, A. E.; Fustero, S.; Soloshonok, V. A.; Liu, H. *Chem. Rev.* **2014,** *114,* 2432–2506. doi:10.1021/cr4002879
3. Kirk, K. L. *J. Fluorine Chem.* **2006,** *127,* 1013–1029. doi:10.1016/j.jfluchem.2006.06.007
4. Bégué, J.-P.; Bonnet-Delpon, D. *J. Fluorine Chem.* **2006,** *127,* 992–1012. doi:10.1016/j.jfluchem.2006.05.006
5. O'Hagan, D. *J. Fluorine Chem.* **2010,** *131,* 1071–1081. doi:10.1016/j.jfluchem.2010.03.003
6. He, J.; Li, Z.; Dhawan, G.; Zhang, W.; Sorochinsky, A. E.; Butler, G.; Soloshonok, V. A.; Han, J. *Chin. Chem. Lett.* **2023,** *34,* 107578. doi:10.1016/j.cclet.2022.06.001
7. Yu, Y.; Liu, A.; Dhawan, G.; Mei, H.; Zhang, W.; Izawa, K.; Soloshonok, V. A.; Han, J. *Chin. Chem. Lett.* **2021,** *32,* 3342–3354. doi:10.1016/j.cclet.2021.05.042
8. Mei, H.; Remete, A. M.; Zou, Y.; Moriwaki, H.; Fustero, S.; Kiss, L.; Soloshonok, V. A.; Han, J. *Chin. Chem. Lett.* **2020,** *31,* 2401–2413. doi:10.1016/j.cclet.2020.03.050
9. Gillis, E. P.; Eastman, K. J.; Hill, M. D.; Donnelly, D. J.; Meanwell, N. A. *J. Med. Chem.* **2015,** *58,* 8315–8359. doi:10.1021/acs.jmedchem.5b00258
10. Mei, H.; Han, J.; White, S.; Graham, D. J.; Izawa, K.; Sato, T.; Fustero, S.; Meanwell, N. A.; Soloshonok, V. A. *Chem. – Eur. J.* **2020,** *26,* 11349–11390. doi:10.1002/chem.202000617
11. Mei, H.; Han, J.; Klika, K. D.; Izawa, K.; Sato, T.; Meanwell, N. A.; Soloshonok, V. A. *Eur. J. Med. Chem.* **2020,** *186,* 111826. doi:10.1016/j.ejmech.2019.111826
12. Wang, Q.; Han, J.; Sorochinsky, A.; Landa, A.; Butler, G.; Soloshonok, V. A. *Pharmaceuticals* **2022,** *15,* 999. doi:10.3390/ph15080999
13. Wang, N.; Mei, H.; Dhawan, G.; Zhang, W.; Han, J.; Soloshonok, V. A. *Molecules* **2023,** *28,* 3651. doi:10.3390/molecules28093651

14. Mykhailiuk, P. K.; Koenigs, R. M. *Chem. – Eur. J.* **2019,** *25,* 6053–6063. doi:10.1002/chem.201804953
15. Mertens, L.; Koenigs, R. M. *Org. Biomol. Chem.* **2016,** *14,* 10547–10556. doi:10.1039/c6ob01618a
16. Ollevier, T.; Carreras, V. *ACS Org. Inorg. Au* **2022,** *2,* 83–98. doi:10.1021/acsorginorgau.1c00027
17. Mykhailiuk, P. K. *Chem. Rev.* **2020,** *120,* 12718–12755. doi:10.1021/acs.chemrev.0c00406
18. Britton, J.; Jamison, T. F. *Angew. Chem., Int. Ed.* **2017,** *56,* 8823–8827. doi:10.1002/anie.201704529
19. Hock, K. J.; Mertens, L.; Metze, F. K.; Schmittmann, C.; Koenigs, R. M. *Green Chem.* **2017,** *19,* 905–909. doi:10.1039/c6gc03187k
20. Chen, Y.-J.; Zhang, F.-G.; Ma, J.-A. *Org. Lett.* **2021,** *23,* 6062–6066. doi:10.1021/acs.orglett.1c02139
21. Jonker, S. J. T.; Jayarajan, R.; Kireilis, T.; Deliaval, M.; Eriksson, L.; Szabó, K. J. *J. Am. Chem. Soc.* **2020,** *142,* 21254–21259. doi:10.1021/jacs.0c09923
22. Zhang, X.; Liu, Z.; Yang, X.; Dong, Y.; Virelli, M.; Zanoni, G.; Anderson, E. A.; Bi, X. *Nat. Commun.* **2019,** *10,* 284. doi:10.1038/s41467-018-08253-z
23. Li, J.; Zhang, D.; Chen, J.; Ma, C.; Hu, W. *ACS Catal.* **2020,** *10,* 4559–4565. doi:10.1021/acscatal.0c00972
24. Gao, C.-F.; Zhou, Y.; Ma, H.; Zhang, Y.; Nie, J.; Zhang, F.-G.; Ma, J.-A. *CCS Chem.* **2022,** *4,* 3693–3704. doi:10.31635/ccschem.022.202201923
25. Liu, Y.; Pang, T.; Yao, W.; Zhong, F.; Wu, G. *Org. Lett.* **2023,** *25,* 1958–1962. doi:10.1021/acs.orglett.3c00464
26. Dhami, A.; Chandrasekharan, S. P.; Mohanan, K. *Org. Lett.* **2023,** *25,* 3018–3022. doi:10.1021/acs.orglett.3c00801
27. Schaus, L.; Das, A.; Knight, A. M.; Jimenez-Osés, G.; Houk, K. N.; Garcia-Borràs, M.; Arnold, F. H.; Huang, X. *Angew. Chem., Int. Ed.* **2023,** *62,* e202208936. doi:10.1002/anie.202208936
28. Ford, A.; Miel, H.; Ring, A.; Slattery, C. N.; Maguire, A. R.; McKervey, M. A. *Chem. Rev.* **2015,** *115,* 9981–10080. doi:10.1021/acs.chemrev.5b00121
29. Xia, Y.; Qiu, D.; Wang, J. *Chem. Rev.* **2017,** *117,* 13810–13889. doi:10.1021/acs.chemrev.7b00382
30. Che, J.; Niu, L.; Jia, S.; Xing, D.; Hu, W. *Nat. Commun.* **2020,** *11,* 1511. doi:10.1038/s41467-020-15345-2
31. Horneff, T.; Chuprakov, S.; Chernyak, N.; Gevorgyan, V.; Fokin, V. V. *J. Am. Chem. Soc.* **2008,** *130,* 14972–14974. doi:10.1021/ja805079v
32. Austeri, M.; Rix, D.; Zeghida, W.; Lacour, J. *Org. Lett.* **2011,** *13,* 1394–1397. doi:10.1021/ol2000815
33. Zibinsky, M.; Fokin, V. V. *Org. Lett.* **2011,** *13,* 4870–4872. doi:10.1021/ol201949h
34. Billedeau, R. J.; Klein, K. R.; Kaplan, D.; Lou, Y. *Org. Lett.* **2013,** *15,* 1421–1423. doi:10.1021/ol400062w
35. Lonzi, G.; López, L. A. *Adv. Synth. Catal.* **2013,** *355,* 1948–1954. doi:10.1002/adsc.201300346
36. Karad, S. N.; Liu, R.-S. *Angew. Chem., Int. Ed.* **2014,** *53,* 5444–5448. doi:10.1002/anie.201403015
37. Li, H.; Wu, X.; Hao, W.; Li, H.; Zhao, Y.; Wang, Y.; Lian, P.; Zheng, Y.; Bao, X.; Wan, X. *Org. Lett.* **2018,** *20,* 5224–5227. doi:10.1021/acs.orglett.8b02172
38. Cai, B.-G.; Yao, W.-Z.; Li, L.; Xuan, J. *Org. Lett.* **2022,** *24,* 6647–6652. doi:10.1021/acs.orglett.2c02671
39. Chen, J.; Shao, Y.; Ma, L.; Ma, M.; Wan, X. *Org. Biomol. Chem.* **2016,** *14,* 10723–10732. doi:10.1039/c6ob02037b
40. Peng, S.-Q.; Zhang, X.-W.; Zhang, L.; Hu, X.-G. *Org. Lett.* **2017,** *19,* 5689–5692. doi:10.1021/acs.orglett.7b02866
41. Hu, X.-G.; Qiu, X.-F.; Liu, D.-Y.; Zhang, W.-F. *Synthesis* **2021,** *53,* 961–970. doi:10.1055/a-1339-3227
42. Mei, H.; Wang, L.; Pajkert, R.; Wang, Q.; Xu, J.; Liu, J.; Röschenthaler, G.-V.; Han, J. *Org. Lett.* **2021,** *23,* 1130–1134. doi:10.1021/acs.orglett.1c00150
43. Mei, H.; Liu, J.; Pajkert, R.; Wang, L.; Röschenthaler, G.-V.; Han, J. *Org. Chem. Front.* **2021,** *8,* 767–772. doi:10.1039/d0qo01394c
44. Liu, J.; Xu, J.; Pajkert, R.; Mei, H.; Röschenthaler, G.-V.; Han, J. *Acta Chim. Sin. (Chin. Ed.)* **2021,** *79,* 747–750. doi:10.6023/a21030096
45. Liu, J.; Pajkert, R.; Wang, L.; Mei, H.; Röschenthaler, G.-V.; Han, J. *Chin. Chem. Lett.* **2022,** *33,* 2429–2432. doi:10.1016/j.cclet.2021.10.066
46. Wang, Q.; Liu, J.; Mei, H.; Pajkert, R.; Röschenthaler, G.-V.; Han, J. *Adv. Synth. Catal.* **2023,** *365,* 2883–2887. doi:10.1002/adsc.202300595
47. Wang, Q.; Liu, J.; Mei, H.; Pajkert, R.; Kessler, M.; Röschenthaler, G.-V.; Han, J. *Org. Lett.* **2022,** *24,* 8036–8040. doi:10.1021/acs.orglett.2c03268
48. Wang, Q.; Liu, J.; Wang, N.; Pajkert, R.; Mei, H.; Röschenthaler, G.-V.; Han, J. *Adv. Synth. Catal.* **2022,** *364,* 1969–1974. doi:10.1002/adsc.202200330
49. Xu, J.; Liu, J.; Mei, H.; Soloshonok, V. A.; Han, J. *Chem. Heterocycl. Compd.* **2023,** *59,* 465–471. doi:10.1007/s10593-023-03217-8
50. Meng, G.; Zhang, J.; Szostak, M. *Chem. Rev.* **2021,** *121,* 12746–12783. doi:10.1021/acs.chemrev.1c00225
51. Chen, J.; Xia, Y.; Lee, S. *Org. Lett.* **2020,** *22,* 3504–3508. doi:10.1021/acs.orglett.0c00958
52. Ferreira, P. M. T.; Maia, H. L. S.; Monteiro, L. S. *Eur. J. Org. Chem.* **2003,** 2635–2644. doi:10.1002/ejoc.200300103
53. Soloshonok, V. A.; Ono, T.; Soloshonok, I. V. *J. Org. Chem.* **1997,** *62,* 7538–7539. doi:10.1021/jo9710238
54. Soloshonok, V. A.; Kukhar, V. P. *Tetrahedron* **1996,** *52,* 6953–6964. doi:10.1016/0040-4020(96)00300-6
55. Zhou, S.; Wang, J.; Chen, X.; Aceña, J. L.; Soloshonok, V. A.; Liu, H. *Angew. Chem., Int. Ed.* **2014,** *53,* 7883–7886. doi:10.1002/anie.201403556
56. Shibata, N.; Nishimine, T.; Shibata, N.; Tokunaga, E.; Kawada, K.; Kagawa, T.; Sorochinsky, A. E.; Soloshonok, V. A. *Chem. Commun.* **2012,** *48,* 4124–4126. doi:10.1039/c2cc30627a
57. Soloshonok, V. A.; Kirilenko, A. G.; Kukhar', V. P.; Resnati, G. *Tetrahedron Lett.* **1993,** *34,* 3621–3624. doi:10.1016/s0040-4039(00)73652-5
58. Wang, N.; Qiao, Y.; Du, Y.; Mei, H.; Han, J. *Org. Biomol. Chem.* **2022,** *20,* 7467–7471. doi:10.1039/d2ob01391f
59. Mei, H.; Wang, N.; Li, Z.; Han, J. *Org. Lett.* **2022,** *24,* 2258–2263. doi:10.1021/acs.orglett.2c00738
60. Jiang, L.; Wang, Z.; Armstrong, M.; Suero, M. G. *Angew. Chem., Int. Ed.* **2021,** *60,* 6177–6184. doi:10.1002/anie.202015077
61. Barluenga, J.; Lonzi, G.; Riesgo, L.; Tomás, M.; López, L. A. *J. Am. Chem. Soc.* **2011,** *133,* 18138–18141. doi:10.1021/ja208965b

BEILSTEIN JOURNAL OF ORGANIC CHEMISTRY

(*E*,*Z*)-1,1,1,4,4,4-Hexafluorobut-2-enes: hydrofluoroolefins halogenation/dehydrohalogenation cascade to reach new fluorinated allene

Nataliia V. Kirij[1], Andrey A. Filatov[1], Yurii L. Yagupolskii[*1], Sheng Peng[*2] and Lee Sprague[2]

Full Research Paper

Open Access

Address:
[1]Institute of Organic Chemistry, National Academy of Sciences of Ukraine, Academician Kukhar Str., 5, Kyiv-94, 02660, Ukraine and [2]The Chemours Company, Chemours Discovery Hub, Newark, DE 19713, United States

Email:
Yurii L. Yagupolskii[*] - yagupolskii@ioch.kiev.ua; Sheng Peng[*] - sheng.peng@chemours.com

* Corresponding author

Keywords:
allenes; dehydrohalogenation; halogenation; 1,1,1,4,4,4-hexafluorobut-2-enes; isomerization

Beilstein J. Org. Chem. **2024,** *20,* 452–459.
https://doi.org/10.3762/bjoc.20.40

Received: 09 November 2023
Accepted: 25 January 2024
Published: 27 February 2024

This article is part of the thematic issue "Organofluorine chemistry VI".

Guest Editor: D. O'Hagan

Abstract

A series of 2,3-dihalo-1,1,1,4,4,4-hexafluorobutanes and 2-halo-1,1,1,4,4,4-hexafluorobut-2-enes were prepared from commercially available hydrofluoroolefins 1,1,1,4,4,4-hexafluorobut-2-enes and their ^{1}H, ^{19}F and ^{13}C chemical shifts measured. Some reactions of synthesized 2-halo-1,1,1,4,4,4-hexafluorobut-2-enes have been investigated. A simple, one-pot procedure for the preparation of a new allene (1,1,4,4,4-pentafluorobuta-1,2-diene) and some of its transformations is presented.

Introduction

The first publication using (*E*)-1,1,1,4,4,4-hexafluorobut-2-ene (**1a**) was published in the middle of the 20th century [1]. Despite this, the real opportunity to study the properties of 1,1,1,4,4,4-hexafluorobut-2-ene appeared only after (*Z*)-1,1,1,4,4,4-hexafluorobut-2-ene (**1b**) began to be produced on an industrial scale [2]. These hydrofluoroolefins belong to the newest 4th generation of fluorocarbon refrigerants and are promising compounds and starting materials. Due to this, interest in the use of (*E*)- and (*Z*)-butenes **1a**,**b** as synthons in various organic transformations has recently grown significantly. One of the new and budding directions in recent years is the stereoselective olefin metathesis processes based on catalysis by complexes of molybdenum, tungsten and ruthenium [3-5]. The first publications have recently appeared that molybdenum complexes can catalyze cross-metathesis of butene **1b**. Wherein various alkyl and aryl olefins, including those that contain Lewis basic esters, carbamates and amines or α-branched moieties, may be used in efficient and exceptionally Z-selective

cross-metathesis reactions [6-8]. A few years ago, some publications devoted to the cleavage of the C–F bond in butenes **1a**,**b** have been presented in the literature. First, Crimmin et al. investigated the reaction of an aluminum(I) complex with fluoroalkenes. Unlike all the presented fluoroolefins, the reaction of the Al(I) complex with (*Z*)-butene **1b** did not allow isolating the intermediate organoaluminum compound, but led to the elimination of two fluorine atoms with the formation of 1,1,4,4-tetrafluorobuta-1,3-diene [9]. It was also shown that the reactions of the boron reagent (CAACMe)$BH_2Li(thf)_3$ with hydrofluoroolefins, including (*Z*)-1,1,1,4,4,4-hexafluorobut-2-ene, results in defluoroborylation to form the corresponding $=CF_2$ containing products [10]. In addition to complexes of aluminum and boron, several magnesium and lithium silyl reagents were prepared and proved to be good nucleophiles in reactions with (*Z*)-1,1,1,4,4,4-hexafluorobut-2-ene, as a result of which the corresponding defluorosilylation product was obtained [11]. In a related study of the hydrosilylation reaction of olefins **1a**,**b**, it was shown that, depending on the catalyst used, platinum or rhodium compounds, along with the products of the addition of silane to the double bond, the elimination of the fluorine atom occurs with the formation of the corresponding olefin [12]. Another area of application of olefins **1a,b** is based on C=C double bond addition reactions. As early as 1968, Atherton and Fields showed that (*Z*)- and (*E*)-butenes **1a**,**b** reacted with diazotrifluoroethane to give 3,4,5-tris(trifluoromethyl)pyrazoline [13]. A few decades later, several new publications in this direction appeared in the literature. In a Chemours' patent, it has been shown that the oxidation of (*E*)-butene **1a** with sodium hypochlorite in the presence of tetrabutylphosphonium bromide leads to the formation of a bistrifluoromethyl containing oxirane [14]. A related study has demonstrated that (*E*)-butene **1a** reacts with potassium persulfate to form 4,5-bistrifluoromethyl)-1,3,2-dioxathiolane 2,2-dioxide [15]. In 2021 Petrov published an article on the interaction of fluorinated olefins with fluorinated thioketones. In this publication it was demonstrated that 1,1,1,4,4,4-hexafluorobut-2-ene reacts with dithietane, sulfur and KF with the formation of the corresponding 1,3-dithiole [16]. Also, a recent patent presents a method for the preparation of 5,6-bis(trifluoromethyl)-1,2,4-triazine-3-carboxylic acid ethyl ester starting from 1,1,1,4,4,4-hexafluorobut-2-ene and an oxalamide hydrazone [17].

In the present study, we investigated the reactions of commercially available butenes **1a**,**b** with halogens, as well as subsequent transformations of the resulting compounds.

Results and Discussion

In 1952 Haszeldine found that the reaction of bromine with (*E*)-1,1,1,4,4,4-hexafluorobut-2-ene (**1a**) under UV irradiation leads to the formation of 2,3-dibromo-1,1,1,4,4,4-hexafluorobutane (**2**) [1]. Subsequent dehydrobromination of compound **2** by treatment with alcoholic potassium hydroxide formed a mixture of isomers 2-bromo-1,1,1,4,4,4-hexafluorobut-2-ene (**3a**,**b**) with a yield in two stages of 48%. It should be noted, that only boiling points and elemental analysis data were given for the obtained substances. Ten years later Knunyants and co-workers also synthesized compound **2** and density, refractive index and mass spectra were added to the already available data [18]. However, until now there was no information about the structure and spectral characteristics of the obtained compounds. We have now synthesized these compounds, fully characterized them, and studied some of their transformations.

We found that not only (*E*)-butene **1a** but also (*Z*)-butene **1b** reacted with bromine in the same manner under the influence of ultraviolet irradiation or sunlight with the formation of 2,3-dibromo-1,1,1,4,4,4-hexafluorobutane (**2**) in 95% yield (Scheme 1).

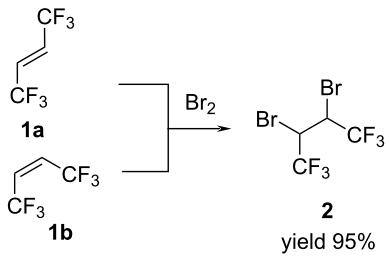

Scheme 1: Synthesis of 2,3-dibromo-1,1,1,4,4,4-hexafluorobutane (**2**).

The only difference was that under UV irradiation, the reaction proceeded faster. In both cases, product **2** represented a mixture of stereoisomers in 2:1 ratio. After isolation by distillation, 2,3-dibromo-1,1,1,4,4,4-hexafluorobutane (**2**) was characterized by ^1H, ^{19}F, ^{13}C NMR and mass spectra.

We studied the reaction of dibromoalkane **2** with various bases such as DBU, Hünig's base (iPr_2NEt), and potassium hydroxide (Table 1).

In all cases, except the reaction in diglyme (Table 1, entry 5), a mixture of (*E*)- and (*Z*)-2-bromo-1,1,1,4,4,4-hexafluorobut-2-enes (**3a**,**b**) in a ratio of 2:1 was formed. The configuration of the isomers was determined by the $^5J_{FFcis}$ coupling constant in the $^{19}F\{H\}$ NMR spectrum (ca. 0 Hz for (*Z*)-isomer and ca. 11 Hz for (*E*)-isomer). The best results were obtained in Et_2O with Hünig's and DBU bases (Table 1, entries 2 and 3), but unfortunately in these cases the product olefins could not be separated from Et_2O. Therefore, we decided to use high-boiling diglyme instead of ether. The reaction of a butane **2** with one equivalent of DBU (Table 1, entry 4) led to the same results as

Table 1: The reaction of 2,3-dibromo-1,1,1,4,4,4-hexafluorobutane (**2**) with bases.

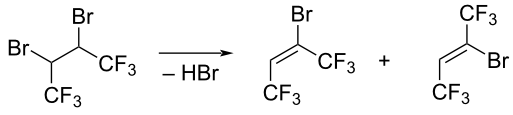

2 **3a** **3b**

yield 89% (**3a** + **3b**)

Entry	Solvent	Base (equiv)	Conditions (°C/h)	Conversion (%)
1	Et_2O	iPr_2NEt (1)	20/18	60
2	Et_2O	iPr_2NEt (1)	20/18	95
3	Et_2O	DBU (1)	20/1	95
4	diglyme	DBU (1)	20/18	60
5	diglyme	DBU (2)	20/1	100
6	H_2O	KOH (1)	20/18	55
7	H_2O	KOH (1.3)	20/2	100

for the Hünig's base (Table 1, entry 1). The use of two equivalents of DBU (Table 1, entry 6) led to the complete conversion of the initial substrate, but the selectivity of the reaction was significantly reduced in this case. The reaction mixture gave a complex mixture, in which (*E*)-butene **3a** was identified as a major component. Product **3a** was removed from bulk diglyme in vacuum and after subsequent distillation it was isolated with a yield of 23%. As the isolation of the 2-dehydrobromination products from organic bases was complex, we focused our attention on carrying out the reaction with KOH. The best result was obtained by treatment of 1 equivalent of butane **2** with 1.3 equivalents of KOH in the presence of 5 mol % of Bu_4NBr as an interfacial carrier in water at room temperature for 2 h (Table 1, entry 7). After completion of the reaction the mixture of isomers **3a**,**b** was separated from the water phase and distilled at 55 °C.

Further increase in the amount of KOH led to the elimination of the second mole of HBr with the formation of hexafluorobut-2-yne (**4**). By controlling the course of the reaction by the ^{19}F NMR method it was possible to achieve complete dehydrobromination of (*Z*)-isomer **3b** and isolation of (*E*)-isomer **3a** in pure form in 35% yield (Scheme 2).

Unexpectedly the (*E*)-isomer **3a**, upon long-term storage, transforms into the (*Z*)-isomer **3b**. Therefore, we studied the isomerization of olefin **3a** in the presence of $SbCl_5$, $AlCl_3$, Bu_4NOH/MeOH and under UV irradiation. We found that under UV irradiation for several hours, the (*E*)-isomer **3a** completely transformed into (*Z*)-isomer **3b** in quantitative yield (Scheme 3).

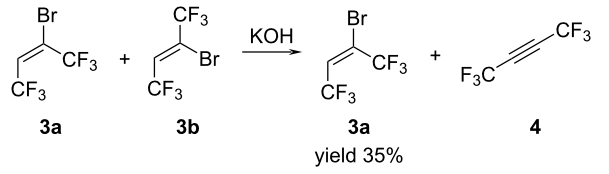

3a **3b** **3a** **4**

yield 35%

Scheme 2: Synthesis of (*E*)-butene **3a**.

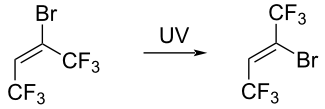

3a **3b**

yield 100%

Scheme 3: Isomerization reaction of (*E*)-butene **3a** to (*Z*)-butene **3b**.

Next, our attention was directed toward the reaction of (*E*)- and (*Z*)-butenes **1a**,**b** with iodine monochloride (ICl). We found that olefins **1a** and **1b** reacts with ICl under the influence of sunlight to form previously unknown 2-chloro-3-iodo-1,1,1,4,4,4-hexafluorobutane (**5**, Scheme 4).

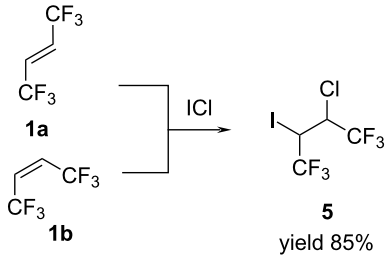

5

yield 85%

Scheme 4: Synthesis of 2-chloro-3-iodo-1,1,1,4,4,4-hexafluorobutane (**5**).

Pure final product **5** was isolated by distillation at 112 °C in 85% yield. NMR analysis as in the case of bromo derivative **2** showed a mixture of stereoisomers with a 2:1 ratio.

The dehydrohalogenation reaction of 2-chloro-3-iodo-1,1,1,4,4,4-hexafluorobutane (**5**) was studied. Like the dehydrobromination of alkane **2**, the reaction of compound **5** with 1.3 equivalents of KOH in water in the presence of 5 mol % of Bu_4NBr was carried out. In this case, a mixture of 2-chloro-1,1,1,4,4,4-hexafluorobut-2-enes (**6a**,**b**) and 2-iodo-1,1,1,4,4,4-hexafluorobut-2-enes (**7a**,**b**) in a ratio of 3:2 was formed from the concurrent elimination reactions of hydrogen iodide and hydrogen chloride (Scheme 5).

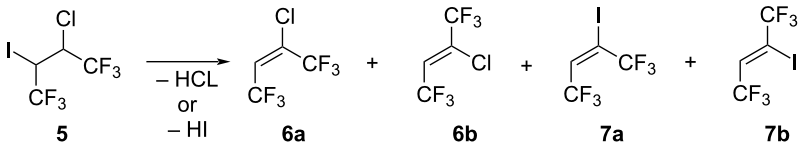

Scheme 5: Dehydrohalogenation reaction of 2-chloro-3-iodo-1,1,1,4,4,4-hexafluorobutane (**5**).

The chloro- and iodobutenes were separated by distillation in 52% yield for **6a**,**b** and 34% yield for **7a**,**b**. NMR analysis showed the mixtures of (*E*)- and (*Z*)-isomers in both cases with the ratio *E*/*Z* = ≈4:5 for **6a**,**b** and *E*/*Z* = ≈1:2 for **7a**,**b**. The configuration of the isomers was determined by the $^5J_{FFcis}$ coupling constant in the $^{19}F\{H\}$ NMR spectrum (ca. 0 Hz for (*Z*)-isomer and ≈11 Hz for (*E*)-isomer). The 2-chloro-1,1,1,4,4,4-hexafluorobut-2-enes were first described by Haszeldine in 1952 [1] and only then the (*Z*)-isomer. We report here the isolation and complete characterization of both (*E*)- and (*Z*)-isomers. The spectral characteristics of product **6b** obtained by us fully correspond to the literature data [19,20]. The ^1H and ^{19}F NMR spectra of compounds **7a**,**b** also corresponded to the data given in the literature [21,22]. We present here the spectral data for isomer **6a**, as well as the missing data of ^{13}C NMR spectra for iodoolefins **7a**,**b**.

It should be noted that the reaction of alkane **5** with DBU or Hünig's base in Et_2O or dimethoxyethane (DME) as a solvent, resulted only in the formation of 2-chloro-1,1,1,4,4,4-hexafluorobut-2-enes **6a**,**b** (Scheme 5). Unfortunately, due to difficulties in separation from solvent, olefins **6a**,**b** in this case were not isolated in a pure state.

For iodoolefin **7a**, we found an alternative route for its synthesis. We have previously shown that hydrosilylation reaction of hexafluorobut-2-yne with triethylsilanes gave (*E*)-1,1,1,4,4,4-hexafluoro-2-triethylsilylbut-2-ene (**8**) [23]. Going back to the study of the obtained silane reactivity we performed the reaction with iodine. All experiments were carried out in THF, *N*-methylpyrrolidone and sulfolane with iodine in the presence of a source of fluoride ion. The best result was observed when the reaction was carried out in dry sulfolane with a two-fold excess of iodine and 1.5-fold excess of anhydrous KF (Scheme 6).

The mixture was stirred at 30 °C for several days until none of the starting **8** was detected in ^{19}F NMR spectra. The desired iodoolefin **7a** together with byproduct triethylfluorosilane (Et_3SiF) were removed from sulfolane under vacuum and after double distillation with column **7a** was isolated in 67% yield. The $^{19}F\{1H\}$ NMR spectra of **7a**, showed the coupling constant of CF_3 and CF_3 to be 11.3 Hz, suggesting strongly that product **7a** like the original silane **8** has (*E*)-configuration.

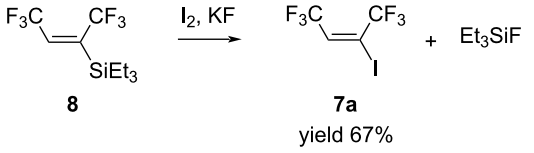

Scheme 6: The reaction of silane **8** with I_2/KF.

Although some olefins presented above were obtained several decades ago, there was almost no information about their reactivity in the literature. Therefore, we became interested in exploring the synthetic potential of halo-bistrifluoromethyl-containing olefins **3**, **6** and **7**, which are readily available and can be synthesized in the laboratory in appreciable amounts.

Fluorinated organic compounds are important synthons, which are widely used in agrochemicals, pharmaceuticals and other fields [24-26]. Fluoroorganic lithium and Grignard reagents have been obtained by the metalation reactions of organofluorine compounds containing bromine and iodine atoms with alkyllithium and Grignard reagents.

Although olefin **3** has been available for many decades, only one paper describes its lithiation with methyllithium and the subsequent reaction of the lithium compound with trifluoroacetophenone [27]. We began our research on the reactivity of the bromobutenes **3a**,**b** with isopropylmagnesium chloride (iPrMgCl) and butyllithium (BuLi), as well as the reactions of the resulting organometallic compounds.

1.2 Equivalents of a solution of iPrMgCl in THF were added to bromoolefin **3a** in Et_2O or THF at −78 °C and then after 1 h at the same temperature 1 equivalent of 4-fluorobenzaldehyde (**9**) was added. After completion of the reaction and subsequent treatment of the reaction mixture with 2 N hydrochloric acid, 2,3-bis(trifluoromethyl)-1-(4-fluorophenyl)prop-2-ene-1-ol (**10**) was detected in the ^{19}F NMR spectrum. It should be noted that, in addition to the unreacted starting aldehyde **9**, the formation of olefin **1b** and previously unknown product **11** were also re-

corded in the reaction mixture (Scheme 7). The ^{19}F NMR spectrum of compound **11** showed two signals at −65.6 and −99.1 ppm in a ratio of 3:2 and in the ^{1}H NMR spectrum, a multiplet at 6.5 ppm was detected. Based on the received data, we assumed that product **11** had an allene structure. It was also important to note that the reaction proceeded more selectively in ether, which significantly reduced the amount of byproducts.

Pure final alcohol **10** was isolated by column chromatography on SiO_2 in 46% yield and ^{1}H, ^{19}F and ^{13}C NMR spectra were in full agreement with the published data [23].

The most interesting outcome from our point of view was the formation of 1,1,4,4,4-pentafluorobuta-1,2-diene (**11**). 1,1-Difluoroallenes are building blocks for a great number of valuable transformations [28]. Therefore, the synthesis of new fluorinated allenes continues to be relevant. One of the methods for the synthesis of allenes was based on the interaction of bromoolefins with organolithium compounds, followed by the elimination of lithium fluoride [29-31]. It was logical to assume that in our case a similar reaction of the Grignard reagent **12** with aldehyde **9**, elimination of MgBrF results in the formation of allene **11**. To confirm our hypothesis, we studied the reaction of haloolefins **3** and **7** with iPrMgCl and BuLi.

Thus, olefin **3a** in Et_2O reacted with iPrMgCl solution in THF at −80 °C to form Grignard reagent **12** and by heating the reaction mixture to room temperature MgBrF was produced together with allene **11** (Scheme 8). In addition to the allene, the formation of olefin **1b** was also recorded in the ^{19}F NMR spectrum.

Unfortunately, due to difficulties in separating from olefin **1b** and diethyl ether, allene **11** was not isolated in a pure state. Therefore, we turned to study the reaction of adduct **3a** with butyllithium.

Unlike the reaction of bromobutene **3a** with iPrMgCl, the reaction mixture with BuLi in hexane solution did not contain olefin **1b** and only desired allene **11** was identified with 95% purity in the ^{19}F NMR spectra (Scheme 9).

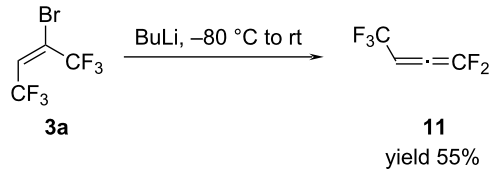

Scheme 9: The reaction of (*E*)-butene **3a** with BuLi.

The volatile product **11** was removed from the reaction mixture at 20 °C for 2 hours with a slow flow of argon through the system. Unfortunately, we failed to completely separate it from the hexane and allene **11** was produced with 80–85% purity. We managed to partially solve this problem by replacing hexane with the higher-boiling heptane. In this case, the desired product was isolated by double distillation at 7 °C in 50% yield and >90% purity and was fully characterized by ^{1}H, ^{19}F, ^{13}C NMR and IR spectra. The presence of a characteristic band at 2038 cm^{-1} in the IR spectrum confirmed the allene structure of product **11**. As expected, allene **11** is extremely reactive and therefore it decomposes rather quickly during storage both in solvent and in the individual state.

Since we were able to obtain both isomers **3a** and **3b** in the individual state, we investigated the reaction of (*Z*)-isomer **3b** with BuLi. Thus, **3b** also reacted with butyllithium to form

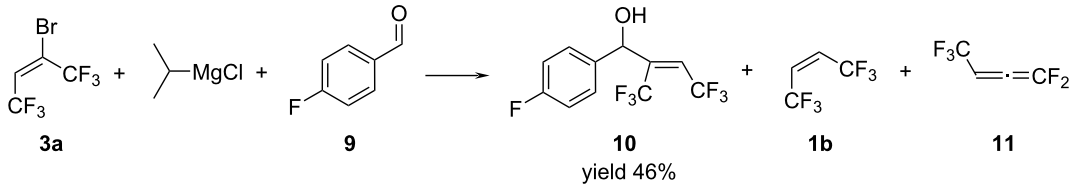

Scheme 7: The reaction of **3a** with iPrMgCl and 4-fluorobenzaldehyde (**9**).

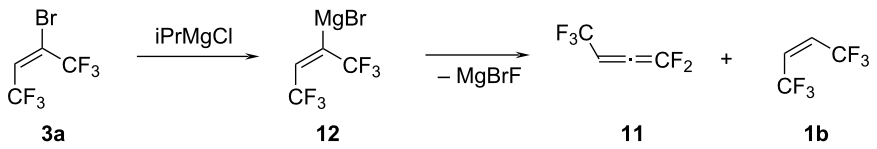

Scheme 8: The reaction of olefin **3a** with iPrMgCl.

allene **11**. However, when studying the reaction of each of the isomers under the same conditions, it turned out that the (*Z*)-isomer reacts faster than the (*E*)-isomer. Therefore, in the case of the (*E*)-isomer, to achieve its complete conversion, it was necessary to increase the lithiation reaction time. Based on the results obtained, it was logical to assume that the reaction can be carried out with a mixture of **3a**,**b**. We found that the reaction of **3a**,**b** with 1.2 equivalents of BuLi in heptane at −80 °C for 1 hour, followed by warming to room temperature, led to the complete conversion of the original olefins and the formation of allene **11**.

Thus, we have developed a method for the synthesis of the previously unknown allene **11**. In addition, the possibility of using a mixture of olefins **3a**,**b** made the allene **11** a more accessible synthon for studying its further transformations.

We started studying the reactivity of allene **11** with the bromination reaction. The reaction was carried out without a solvent at a reagent ratio of 1:1. Bromine was added dropwise to allene **11** at −30 °C and the reaction mixture was stirred at the same temperature until colorless. The bromination of allene resulted in the formation of (*Z*)-1,2-dibromo-1,1,4,4,4-pentafluorobut-2-ene (**13**) in 92% yield, which was isolated as a colorless liquid and fully characterized by NMR spectroscopy (Scheme 10).

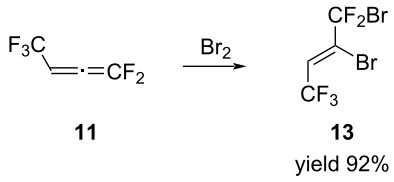

Scheme 10: The reaction of allene **11** with bromine.

The ^{19}F NMR spectrum showed two signals with the integrated intensity ratio 3:2, a doublet for a CF_3 group at δ −57.7 ppm with the coupling constant $^3J_{FH}$ = 6.8 Hz and the characteristic signal of a CF_2Br group as a singlet at δ −50.1 ppm. In the ^{1}H NMR spectrum, there was a signal attributed to the CH proton at 6.9 ppm as a quartet with the coupling constant of $^3J_{HF}$ = 6.8 Hz. The (*Z*)-configuration of product **13** was determined by the absence of the F–F constant in the ^{19}F NMR spectra. It should be noted that the bromination reaction could also be carried out in diethyl ether. In this case, the bromo derivative **13** could be isolated in pure form only after several distillations, which significantly reduces its yield.

Continuing to study the reactivity of allene **11**, we investigated its reaction with ICl. The reaction was carried out at a reagent ratio of 1:1. ICl was added to a solution of allene in pentane at −20 °C and then the reaction mixture was stirred at rt until the color disappeared. In contrast to bromination, the reaction with ICl is less selective and leads to the formation of addition products at both double bonds. At the same time, the reaction proceeded predominantly at the terminal double bond with the formation of a mixture of isomers (*Z*)-**14a** and (*E*)-**14b**. The content of the addition product **15** at the second double bond in the reaction mixture was about 15% (Scheme 11).

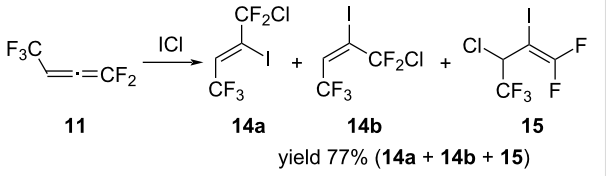

Scheme 11: The reaction of allene **11** with ICl.

It should be noted that we failed to isolate the pure product **15** from reaction mixtures because of the small difference in boiling points and volatiles between isomers **14a**,**b** and product **15**. Nevertheless, it was tentatively identified in the mixture, based on ^{1}H, ^{19}F and ^{13}C NMR data. The ^{19}F NMR spectrum showed three signals with the integrated intensity ratio 3:1:1, a doublet for a CF_3 group at δ −71.5 ppm with a coupling constant of $^3J_{FH}$ = 6 Hz and two highly characteristic signals of geminal fluorine atoms of the CF_2 group as doublets of multiplets at δ −66.7 and −70.3 ppm with a coupling constant of $^2J_{FF}$ = 15 Hz. In the ^{1}H NMR spectrum, there was a signal attributed to CH proton at 4.9 ppm as a quartet of multiplets with a coupling constant of $^3J_{HF}$ = 6 Hz.

Thus, during the study of reactions of allene **11** with Br_2 and ICl, we obtained new synthons, which due to the presence of several reaction centers, could be of particular interest in various kinds of transformations. Therefore, we decided to synthesize a bistrifluoromethyl containing olefin with bromine and chlorine atoms and explore the possibility of using it to obtain another allene.

We found that 2-chloro-1,1,1,4,4,4-hexafluorobut-2-enes (**6a**,**b**) react with bromine under the influence of sunlight with the formation of 2,3-dibromo-2-chloro-1,1,1,4,4,4-hexafluorobutane **16** in 84% yield (Scheme 12).

As in the case of alkanes **2** and **5**, product **16** represented a mixture of stereoisomers in 2:1 ratio. After isolation by distillation butane **16** was characterized by ^{1}H, ^{19}F, ^{13}C NMR and mass spectra.

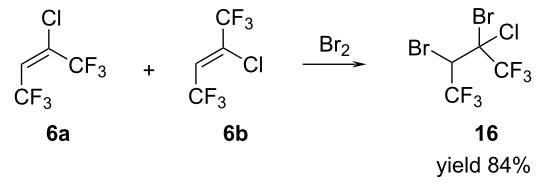

Scheme 12: Synthesis of 2,3-dibromo-2-chloro-1,1,1,4,4,4-hexafluorobutane (**16**).

The reaction of alkane **16** with DBU in pentane as a solvent led exclusively to dehydrobromination with the formation of a mixture of (*Z*)- and (*E*)-2-bromo-3-chloro-1,1,1,4,4,4-hexafluorobut-2-enes (**17a**,**b**) in a ratio of 2:1 (Scheme 13).

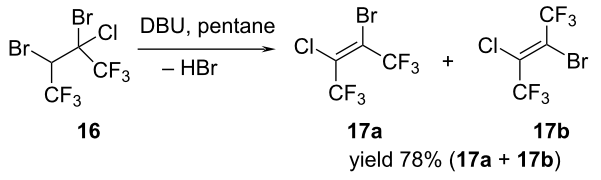

Scheme 13: Synthesis of (*Z*, *E*)-2-bromo-3-chloro-1,1,1,4,4,4-hexafluorobut-2-enes (**17a**,**b**).

After completion of the reaction the mixture of isomers **17a**,**b** was isolated by distillation at 79 °C and fully characterized. The configuration of the isomers was determined by the $^{5}J_{\mathrm{FFcis}}$ coupling constant in the ^{19}F{H} NMR spectrum (ca. 0 Hz for (*Z*)-isomer and ca. 13 Hz for (*E*)-isomer).

Like the reaction of bromobutenes **3a**,**b** with BuLi, the reaction of olefins **17a**,**b** with BuLi was carried out. Unfortunately, we were unable to detect the formation of allene **18** in this reaction. In the ^{19}F NMR spectrum, along with the unreacted starting olefins **17a**,**b**, the main reaction product is hexafluorobut-2-yne (**4**, Scheme 14).

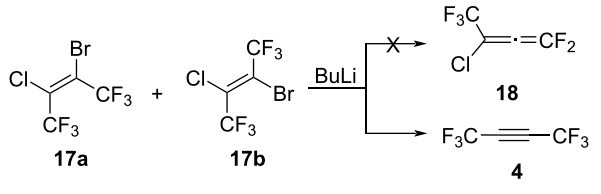

Scheme 14: The reaction of olefins **17a**,**b** with BuLi.

Although attempts to obtain allene **18** were unsuccessful, olefins **17a**,**b** may be of great interest as synthons due to the presence of several reaction centers in the molecule.

Conclusion

In conclusion, we synthesized a series of synthons from available industrial starting compounds – (*E*,*Z*)-1,1,1,4,4,4-hexafluorobut-2-enes (**1a**,**b**) using simple procedures. We demonstrated the halogenation reactions of butenes **1a**,**b** with bromine and iodine monochloride to form 2,3-dihalo-1,1,1,4,4,4-hexafluorobutanes. Dehydrohalogenation of the obtained butanes leads to the formation of a number of bistrifluoromethyl-containing haloolefins, which are widely used in subsequent transformations. Based on bromoolefins **3a**,**b**, a new polyfluoro-containing allene **11** was synthesized and its reactions with bromine and iodine monochloride were also studied.

Supporting Information

Supporting Information File 1

Experimental part and copies of NMR spectra.
[https://www.beilstein-journals.org/bjoc/content/supplementary/1860-5397-20-40-S1.pdf]

ORCID® iDs

Nataliia V. Kirij - https://orcid.org/0009-0004-1118-3305
Andrey A. Filatov - https://orcid.org/0000-0001-7050-8131
Yurii L. Yagupolskii - https://orcid.org/0000-0002-5179-4096

References

1. Haszeldine, R. N. *J. Chem. Soc.* **1952,** 2504–2513. doi:10.1039/jr9520002504
2. Sicard, A. J.; Baker, R. T. *Chem. Rev.* **2020,** *120,* 9164–9303. doi:10.1021/acs.chemrev.9b00719
3. Malcolmson, S. J.; Meek, S. J.; Sattely, E. S.; Schrock, R. R.; Hoveyda, A. H. *Nature* **2008,** *456,* 933–937. doi:10.1038/nature07594
4. Yu, M.; Wang, C.; Kyle, A. F.; Jakubec, P.; Dixon, D. J.; Schrock, R. R.; Hoveyda, A. H. *Nature* **2011,** *479,* 88–93. doi:10.1038/nature10563
5. Herbert, M. B.; Grubbs, R. H. *Angew. Chem., Int. Ed.* **2015,** *54,* 5018–5024. doi:10.1002/anie.201411588
6. Koh, M. J.; Nguyen, T. T.; Lam, J. K.; Torker, S.; Hyvl, J.; Schrock, R. R.; Hoveyda, A. H. *Nature* **2017,** *542,* 80–85. doi:10.1038/nature21043
7. Mu, Y.; Nguyen, T. T.; van der Mei, F. W.; Schrock, R. R.; Hoveyda, A. H. *Angew. Chem., Int. Ed.* **2019,** *58,* 5365–5370. doi:10.1002/anie.201901132
8. Hoveyda, A. H.; Ming, J.; Nauyen, T. T.; Schrock, R. R.; Hyvl, J. Halogen-containing metathesis catalysts and methods thereof. WO Patent WO2018/013943, Jan 18, 2018.
9. Bakewell, C.; White, A. J. P.; Crimmin, M. R. *Angew. Chem., Int. Ed.* **2018,** *57,* 6638–6642. doi:10.1002/anie.201802321
10. Phillips, N. A.; Coates, G. J.; White, A. J. P.; Crimmin, M. R. *Chem. – Eur. J.* **2020,** *26,* 5365–5368. doi:10.1002/chem.202000636
11. Coates, G.; Tan, H. Y.; Kalff, C.; White, A. J. P.; Crimmin, M. R. *Angew. Chem., Int. Ed.* **2019,** *58,* 12514–12518. doi:10.1002/anie.201906825

12. Pavlenko, N. V.; Peng, S.; Petrov, V.; Jackson, A.; Sun, X.; Sprague, L.; Yagupolskii, Y. L. *Eur. J. Org. Chem.* **2020,** 5425–5435. doi:10.1002/ejoc.202000853
13. Atherton, J. H.; Fields, R. *J. Chem. Soc. C* **1968,** 1507–1513. doi:10.1039/j39680001507
14. Petrov, V. A.; Brandt, D. R.; Minor, B. H.; Kontomaris, K.; Robin, M. L.; Wysong, E. B.; Musyimi, H. K.; Glatt, C. M. Uses of fluorinated epoxides and novel mixtures thereof. WO Patent WO2018/165623, Sept 13, 2018.
15. Long, Z.; Xiaodong, G.; Xiaolong, W.; Zheng, L. Preparation method of ethylene sulfate and derivatives thereof. Chin. Patent CN114805291, July 29, 2022.
16. Petrov, V. *J. Fluorine Chem.* **2021,** *248,* 109775. doi:10.1016/j.jfluchem.2021.109775
17. Wissler, M.; Mueller, E.; Lorenz, P.; Kliem, C.; Fleischhacker, H. Process for the covalent coupling of two molecules by means of a Diels-Alder reaction with inverse electron requirement. U.S. Patent US2010/0016545, Jan 21, 2010.
18. Knunyants, I. L.; German, L. S.; Rozhkov, I. N. *Russ. Chem. Bull.* **1962,** *11,* 1587–1588. doi:10.1007/bf00907244
19. Bo, Z.; Jian, L.; Wei, Z.; Jijun, Z.; Sheng, H.; Zhiqiang, Y.; Xiaobo, T.; Zhijun, H.; Jianping, K.; Fengxian, L. Catalytic conversion method for hexachlorobutadiene. Chin. Patent CN110372471, Oct 25, 2019.
20. Jian, L.; Bo, Z.; Wei, Z.; Jijun, Z.; Sheng, H.; Zhiqiang, Y.; Xiaobo, T.; Zhijun, H.; Jianping, K.; Fengxian, L. Synthesis method of 2-chloro-1,1,1,4,4,4-hexafluoro-2-butene. Chin. Patent CN110372472, Oct 25, 2019.
21. Leedham, K.; Haszeldine, R. N. *J. Chem. Soc.* **1954,** 1634–1638. doi:10.1039/jr9540001634
22. El Soueni, A.; Tedder, J. M.; Walton, J. C. *J. Chem. Soc., Faraday Trans. 1* **1981,** *77,* 89–100. doi:10.1039/f19817700089
23. Kirij, N. V.; Filatov, A. A.; Yagupolskii, Yu.. L.; Peng, S.; Jackson, A. *J. Fluorine Chem.* **2022,** *253,* 109922. doi:10.1016/j.jfluchem.2021.109922
24. Kirsch, P. *Modern Fluoroorganic Chemistry: Synthesis, Reactivity and Applications;* Wiley-VCH: Weinheim, Germany, 2004. doi:10.1002/352760393x
25. Purser, S.; Moore, P. R.; Swallow, S.; Gouverneur, V. *Chem. Soc. Rev.* **2008,** *37,* 320–330. doi:10.1039/b610213c
26. Zhou, Y.; Wang, J.; Gu, Z.; Wang, S.; Zhu, W.; Aceña, J. L.; Soloshonok, V. A.; Izawa, K.; Liu, H. *Chem. Rev.* **2016,** *116,* 422–518. doi:10.1021/acs.chemrev.5b00392
27. Gassman, P. G.; Ray, J. A.; Wenthold, P. G.; Mickelson, J. W. *J. Org. Chem.* **1991,** *56,* 5143–5146. doi:10.1021/jo00017a029
28. Fuchibe, K.; Ichikawa, J. *Sci. Synth., Knowl. Updates* **2014,** *2,* 217–231. doi:10.1055/sos-sd-124-00001
29. Drakesmith, F. G.; Stewart, O. J.; Tarrant, P. *J. Org. Chem.* **1968,** *33,* 280–285. doi:10.1021/jo01265a055
30. Zens, A. P.; Ellis, P. D.; Ditchfield, R. *J. Am. Chem. Soc.* **1974,** *96,* 1309–1312. doi:10.1021/ja00812a008
31. Dolbier, W. R., Jr.; Burkholder, C. R.; Piedrahita, C. A. *J. Fluorine Chem.* **1982,** *20,* 637–647. doi:10.1016/s0022-1139(00)82289-7

License and Terms

BEILSTEIN JOURNAL OF ORGANIC CHEMISTRY

Synthesis of 2,2-difluoro-1,3-diketone and 2,2-difluoro-1,3-ketoester derivatives using fluorine gas

Alexander S. Hampton[1], David R. W. Hodgson[*1], Graham McDougald[2], Linhua Wang[3] and Graham Sandford[1]

Full Research Paper

Open Access

Address:
[1]Durham University, Department of Chemistry, Lower Mountjoy, South Road, Durham, DH1 3LE, UK, [2]Syngenta, Huddersfield Manufacturing Centre, PO Box A38, Huddersfield, West Yorkshire, HD2 1FF, UK and [3]Syngenta USA, 410 Swing Road, Greensboro, North Carolina, NC 27409, USA

Email:
David R. W. Hodgson[*] - d.r.w.hodgson@durham.ac.uk

* Corresponding author

Keywords:
difluorination; difluoromethylene; direct fluorination; electrophilic fluorination; organofluorine

Beilstein J. Org. Chem. **2024,** *20,* 460–469.
https://doi.org/10.3762/bjoc.20.41

Received: 27 November 2023
Accepted: 15 February 2024
Published: 28 February 2024

This article is part of the thematic issue "Organofluorine chemistry VI".

Guest Editor: D. O'Hagan

Abstract

Solutions of 1,3-diketones and 1,3-ketoester derivatives react with fluorine to give the corresponding 2,2-difluoro-1,3-dicarbonyl derivatives in the presence of quinuclidine. Quinuclidine reacts with fluorine in situ to generate a fluoride ion that facilitates limiting enolization processes, and an electrophilic N–F fluorinating agent that is reactive towards neutral enol species.

Introduction

Fluorine is present in many agrochemical and pharmaceutical products owing to the beneficial properties imparted such as increased metabolic stability, lipophilicity and bioavailability of the bioactive entity [1-3]. In 2018, 30% of FDA approved drugs contained at least one fluorine atom, with an average of 2.7 fluorine atoms per fluorinated drug, and fluorine is also present in the structures of 50% of marketed agrochemicals [4]. In the context of the research reported here, the incorporation of difluoromethylene (CF_2) units into life science products is growing in importance and a number of commercially significant pharmaceuticals [lubiprostone (constipation), maraviroc (HIV), tafluproct (anti-inflamatory), ledipasvir (hepatitis-C)] and agrochemicals [isopyrazam (fungicide), riodipine (calcium channel blocker), primisulfuron-methyl (pesticide)] owe their enhanced bioactivity, in part, to the presence of difluoromethylene units.

To meet the demands of synthetic chemists within the life science discovery and manufacturing arenas, many fluorination methods have been developed over the years to introduce

difluoromethylene groups into organic systems. Approaches using nucleophilic fluorination include halogen exchange of *gem*-dihalo groups to corresponding CF_2 derivatives using silver tetrafluoroborate [5] or mercury(II) fluoride [6], deoxyfluorination of carbonyl derivatives using diethylaminosulfur trifluoride (DAST) or related Deoxo-Fluor and Xtalfluor reagents [7,8]. Alternatively, oxidative fluorodesulfurizations of carbonyl derivatives using a combination of sources of halonium and fluoride ions such as 1,3-dibromo-5,5-dimethylhydantoin (DBH) and tetrabutylammonium dihydrogen trifluoride have been achieved [9-11].

The transformation of methylene to difluoromethylene using electrophilic fluorinating agents offers an alternative fluorination route, for example, the reactions of MeCN solutions of 1,3-diketones with electrophilic fluorinating agents such as Selectfluor eventually give the corresponding 2,2-difluoro-1,3-diketone derivatives [12]. Monofluorination of the 1,3-diketone substrates is rapid, but the second fluorination step occurs only after reaction for several days. In the solid phase, mechanical milling of the diketone substrate with solid Selectfluor in the presence of sodium carbonate [13,14], and reaction of ketones with a strong base and an N–F reagent give rise to the corresponding 2,2-difluoroketones [15]. In related kinetic studies concerning the electrophilic 2-fluorination of 1,3-diketones with Selectfluor [16,17], we demonstrated that the rate-determining step for difluorination was enolization of the intermediate 2-fluoro-1,3-diketone. Monofluorination of 1,3-diketones occurs rapidly because the substrates lie predominantly in their enol tautomeric forms. The resulting 2-difluoro-1,3-diketones, on the other hand, are formed in their keto-tautomeric forms. Thus, we found difluorination could only be achieved upon addition of water or a base to accelerate the enolization of the monofluoro-diketone intermediates. In addition, imines and α-diboryl ketone derivatives can also be transformed to 2,2-difluoroketones using an N–F electrophilic fluorinating reagent [18]. Alternatively, building blocks containing CF_2 units such as ethyl bromodifluoroacetate and difluoromethylphenyl sulfoxide offer the possibility of transferring difluoromethylene groups directly into organic systems [19-25] and there is now a very extensive literature on carbon–carbon bond-forming reactions using these and other difluoromethylated building blocks [3,26-32].

Since profit margins in the life science industries are always under constant pressure, less expensive methods of introducing fluorine selectively into active intermediates for manufacture on the industrial scale are required and, as a relatively inexpensive strategy, direct fluorination of substrates using fluorine gas has been used successfully for the production of 5-fluorouracil (generic, anticancer) and voriconazole (V-FEND, Pfizer, antifungal) [33]. Methods have been developed for the selective monofluorination of 1,3-dicarbonyl derivatives by fluorine gas using batch and continuous flow techniques [34-36]. Difluorination occurs very slowly in comparison to monofluorination, although some difluorinated by-products are, in general, formed upon fluorination of dicarbonyl substrates and difluorinated products can be readily separated from monofluorinated systems [34]. Direct fluorination of diazo compounds using F_2 [37] is the only report of a useful synthetic procedure to selectively prepare a difluoromethylene containing product using F_2 but, in these cases, CFCs, now banned under the Montreal protocol, were used as the reaction medium.

Here, we demonstrate that the addition of quinuclidine to direct fluorination reactions of 1,3-diketone and 1,3-ketoester substrates using fluorine gas can give difluorinated products by a simple batch process, offering a potentially valuable route to the synthesis of difluoromethylene compounds that is suitable for inexpensive scale-up.

Results

2-Fluorinations of 1,3-diaryldiketone derivatives such as 1,3-diphenylpropane-1,3-dione (dibenzoylmethane, DBM, **1a**) using electrophilic fluorinating reagents such as Selectfluor, NFSI, and NFOBS under a range of conditions have been described extensively [3,12,13,30,38-43]. We confirmed that reaction of compound **1a** with Selectfluor in acetonitrile (MeCN) gave high yields of the monofluorinated product **2a** with no difluorinated product being observed by ^{19}F NMR analysis of the product mixture after 5 h (Scheme 1).

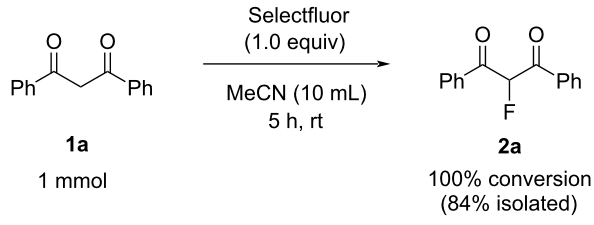

Scheme 1: Monofluorination of 1,3-diphenylpropane-1,3-dione with Selectfluor.

In contrast, attempts to fluorinate **1a** with one equivalent of fluorine gas in MeCN gave no noticeable conversion on analysis by ^{19}F NMR spectroscopy, and a large excess of fluorine led to formation of a dark brown tar from which no useful product could be isolated. On the bases of these failed attempts, coupled with our previous experiences with the DBM scaffold [16,17,36], we used the difluorination of **1a** with fluorine gas as a model process to assess how direct fluorination reactions could be achieved using reaction additives.

The lack of reactivity of **1a** towards one equiv of fluorine gas when compared with strong reactivity towards Selectfluor suggested the use of a cationic, electrophilic reagent to be important. Given the structural similarity of 1,4-diazabicyclo[2.2.2]octane (DABCO) to the Selectfluor system, a 10% v/v mixture of fluorine in nitrogen was passed through a solution of **1a** in acetonitrile containing one equivalent of DABCO, using a fluorination apparatus and gas flow controller equipment described previously [35]. Our aim was to form a N–F system in situ and thus mimic the successful monofluorination observed between **1a**-enol and Selectfluor. After purging the product mixture with nitrogen, a known quantity of α,α,α-trifluorotoluene was added to the product mixture and the crude yields of fluorinated products were estimated by ^{19}F NMR integration (monofluoro product **2a**, δ_F −189.9 ppm; difluoro product **3a**, δ_F −102.7 ppm) (Table 1, entry 3).

Using excess fluorine or DABCO (entries 5 and 6 in Table 1) led to the formation of tars, while 0.1 equiv of DABCO (entry 7) gave only relatively low conversions to **2a** and **3a**. Other organic nitrogen bases were tested, and we found that quinuclidine (entries 8 and 9, Table 1) gave high conversion to difluorinated product **3a**, with very little monofluorinated product **2a** being observed. Suspensions of caesium carbonate or sodium chloride (entries 11 and 12 in Table 1) also gave some **2a** and **3a**, but also unwanted tar.

This set of reactions showed that the basic species we screened all facilitated mono- and difluorination to some degree. The quinuclidine-mediated fluorination of **1a** led to the highest conversion to difluorinated product **3a** so we next sought to optimize this process at a preparative scale by varying the reaction stoichiometry. We found that 2.3 equiv of fluorine and 1.1 equiv of quinuclidine gave 99% conversion of **1a** with **2a** and **3a** being the only products observed by ^{19}F NMR spectroscopy in a 16:120 ratio (see Supporting Information File 1). To isolate the main difluorinated product **3a**, the reaction vessel was purged with nitrogen and the product mixture was partitioned between water and DCM to remove HF and salt by-products. Purification of **3a** by column chromatography gave **3a** as a white crystalline solid in 65% isolated yield (Scheme 2) and the structure was confirmed by NMR spectroscopy and X-ray crystallography (Figure 1).

To expand the substrate scope of this difluorination method, a range of DBM derivatives **1b**–**n** was synthesized from *para*-substituted acetophenones, *para*-substituted benzoyl chlorides and lithium hexamethyldisilazane following a literature proce-

Table 1: Screening conditions for the fluorination of 1,3-diphenylpropane-1,3-dione (**1a**).[a]

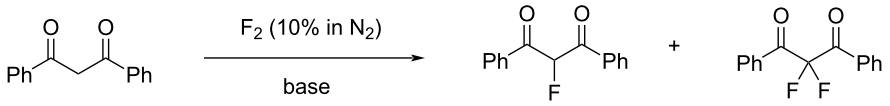

1a 1 mmol — **2a** — **3a**

Entry	Base additive	Equiv of additive	Equiv of F_2	Crude yield by ^{19}F NMR spectroscopy[a,b]		
				1a [%]	**2a** [%]	**3a** [%]
1	–	–	1	100	0	0
2	–	–	20	polyfluorinated tar		
3	DABCO	1	1	32	4	20
4	DABCO	1	2	1	1	37
5	DABCO	1	3	polyfluorinated tar		
6	DABCO	2	2	many fluorinated products		
7	DABCO	0.1	1	22	28	8
8	quinuclidine	1	1	42	10	43
9	quinuclidine	1.2	1	54	1	43
10	Et_3N	1	1	56	25	6
11	Cs_2CO_3	1	1	0	4	14
12	NaCl	1	1	0	33	12

[a]Conversion levels determined by NMR spectroscopy by comparing the integrals (CF dp at –189.9 ppm, CF_2 s at –102.7 ppm) to α,α,α-trifluorotoluene standard. [b]The mass balances included mixtures of soluble, unidentified products, and insoluble materials.

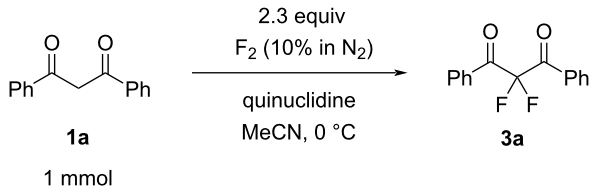

Scheme 2: Synthesis of 2,2-difluoro-1,3-diphenylpropane-1,3-dione (**3a**).

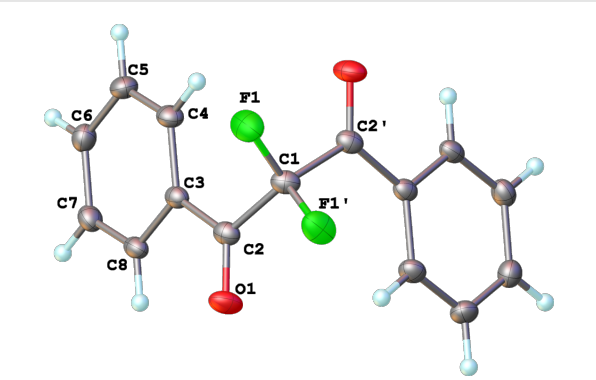

Figure 1: Molecular structure of 2,2-difluoro-1,3-diphenylpropane-1,3-dione (**3a**).

dure reported by Liu and co-workers (see Supporting Information File 1) [44]. Subsequently, difluorinations of DBM substrates **1b**–**n** were performed under conditions similar to those optimized for the preparation of **3a**. The desired difluorinated products **3b**–**n** were synthesized and isolated in good yields (Table 2).

Unfortunately, substrates bearing electron-donating groups **1b** (–Me) and **1c** (–OMe) reacted with fluorine to give tarry materials and products arising from fluorination of both the desired enolic sites and the aryl rings. No products could be isolated from these complex mixtures and yields were estimated by ^{19}F NMR spectroscopy.

In contrast, substrates bearing electron-withdrawing groups deactivated the aryl rings sufficiently to suppress competing ring fluorination and difluorinated products **3d**–**i** could be isolated in high yields. Again, purification by column chromatography gave the products **3** as white crystalline solids and the structures of compounds **3f** and **3i** were confirmed by X-ray crystallography (Figure 2 and Supporting Information File 1). Molecules **3a, f**, and **i** all exist in the solid state with the dicarbonyl moiety rotated to maximize the distances between the lone pairs of the electron-rich fluorine and oxygen atoms. Usually, one of the fluorine atoms lies in a *syn* orientation to an oxygen (e.g., **3f** has an F–C–C–O dihedral angle of 15.6°) creating a dipole. This dipole appears to aid crystal packing by forming weak intermolecular interactions with an aryl ring in an adjacent molecule. The two aryl rings within the molecule are near-perpendicular to each other and this conformation leads to enhanced, orthogonal π-stacking interactions.

We next turned our attention to difluorination of related 2-ketoester substrates. Monofluorination of 2-ketoesters using fluorine gas has been scaled up to the manufacturing level [33], whereas preparative methods for the synthesis of 2,2-difluoro-3-ketoesters using fluorine gas have not been realized. Ethyl benzoylacetate (**4a**) was used as a model system for the devel-

Table 2: Difluorination of dibenzoylmethane derivatives **3a–n** using fluorine gas and quinuclidine.

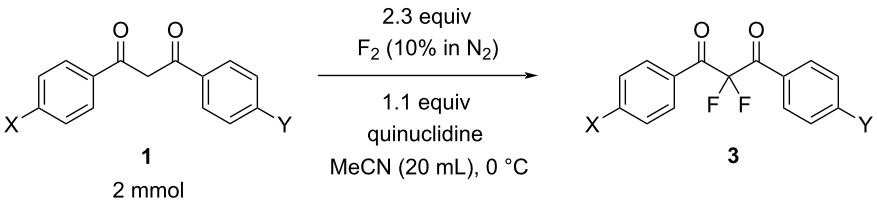

Entry	1,3-Diketone	Product	Structure	Isolated yield [%]
1	**1a**	**3a**	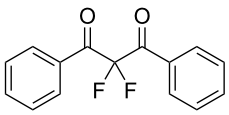	65
2	**1b**	**3b**	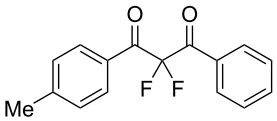	41[a] 10[a] (**7a**) 12[a] (Ar–F)

Table 2: Difluorination of dibenzoylmethane derivatives **3a–n** using fluorine gas and quinuclidine. (continued)

3	**1c**	**3c**	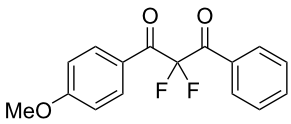	31[a] 16[a] (Ar–F)
4	**1d**	**3d**	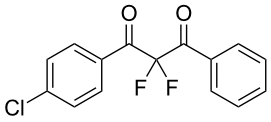	60
5	**1e**	**3e**	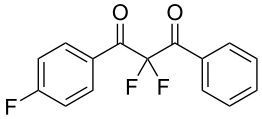	59
6	**1f**	**3f**	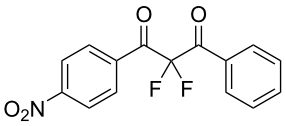	50
7	**1g**	**3g**	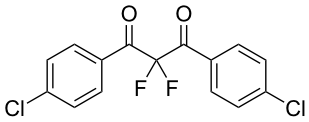	72
8	**1h**	**3h**	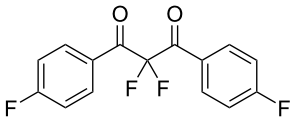	76
9	**1i**	**3i**	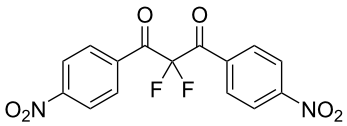	77

[a]Conversion estimated by NMR spectroscopy.

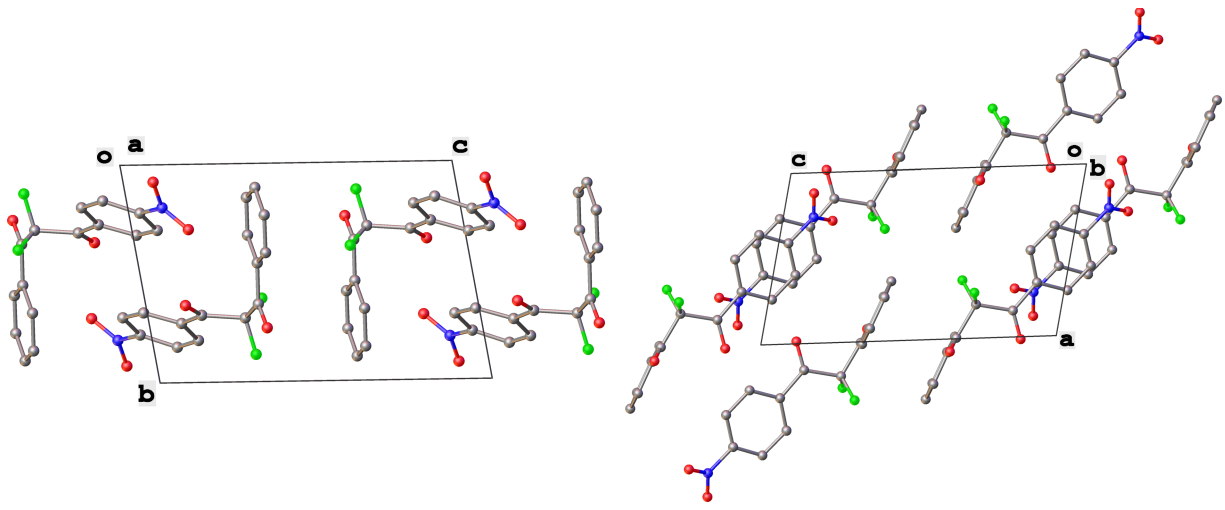

Figure 2: Crystal packing structure of **3f** as determined by SXRC.

opment of conditions for selective difluorination using fluorine gas. After screening basic additives as mediating agents and subsequent optimization (see Supporting Information File 1), we found that reaction of ethyl benzoylacetate (**4a**), quinuclidine (1.5 equiv), and fluorine (3 equiv) in acetonitrile gave the desired difluorinated product **5a** in 85% isolated yield. Purification of **5a** was achieved very readily by eluting the reaction mixture through a small quantity of silica gel with chloroform and evaporating the residual solvent to leave the crude product which could be further purified by recrystallization. Subsequently, a range of ethyl benzoylacetate derivatives was prepared (see Supporting Information File 1) [45,46] and successfully subjected to difluorination conditions (Table 3).

Purification by column chromatography using the minimum amount of silica gel with chloroform as the eluent yielded **5c**–**g** in high yields. As was observed in attempted fluorination reaction of **1c** towards difluorodiketone **3c**, methoxy ketoester derivative **4b** gave substantial amounts of product arising from competing fluorination of the aromatic ring. Structures of difluorinated ketoesters **5a**–**h** were confirmed by NMR spectroscopy. The $^{13}C\{^1H\}$ NMR spectra contained signals supporting the presence of ketone (e.g., δ_C = 185.6 ppm for **5a**) and ester (δ_C = 161.9 ppm for **5a**) functionalities. Difluoroketoester products were found to hydrate readily to give *gem*-diol derivatives during aqueous work-up [39], thus reducing the efficiency of extraction. Indeed, attempts to grow a single crystal of **5e** from a mixture of EtOH and water led to the isolation of the corresponding *gem*-diol (Figure 3). There are very few examples of organic structures containing a $C(OH)_2$–CF_2–C fragment in the CCDC and only three acyclic examples (CSD 5.43 (Nov. 2021); ref codes IZICEA [47], XOPZEK and XOPZIO [48]) are

Table 3: Quinuclidine-mediated direct fluorination of ethyl benzoylacetate derivatives **4a**–**g**.

Entry	Product	Structure	Yield/%
1	**5a**	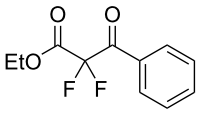	85
2	**5b**	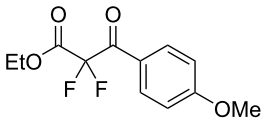	not isolated
3	**5c**	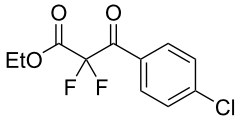	89
4	**5d**	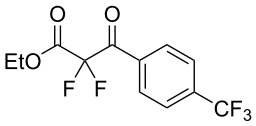	87
5	**5e**	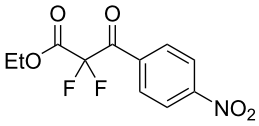	83
6	**5f**	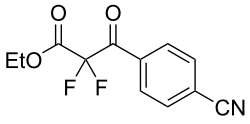	67
7	**5g**	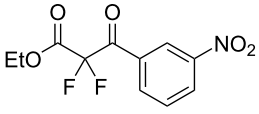	84
8	**5h**	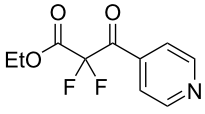	not isolated

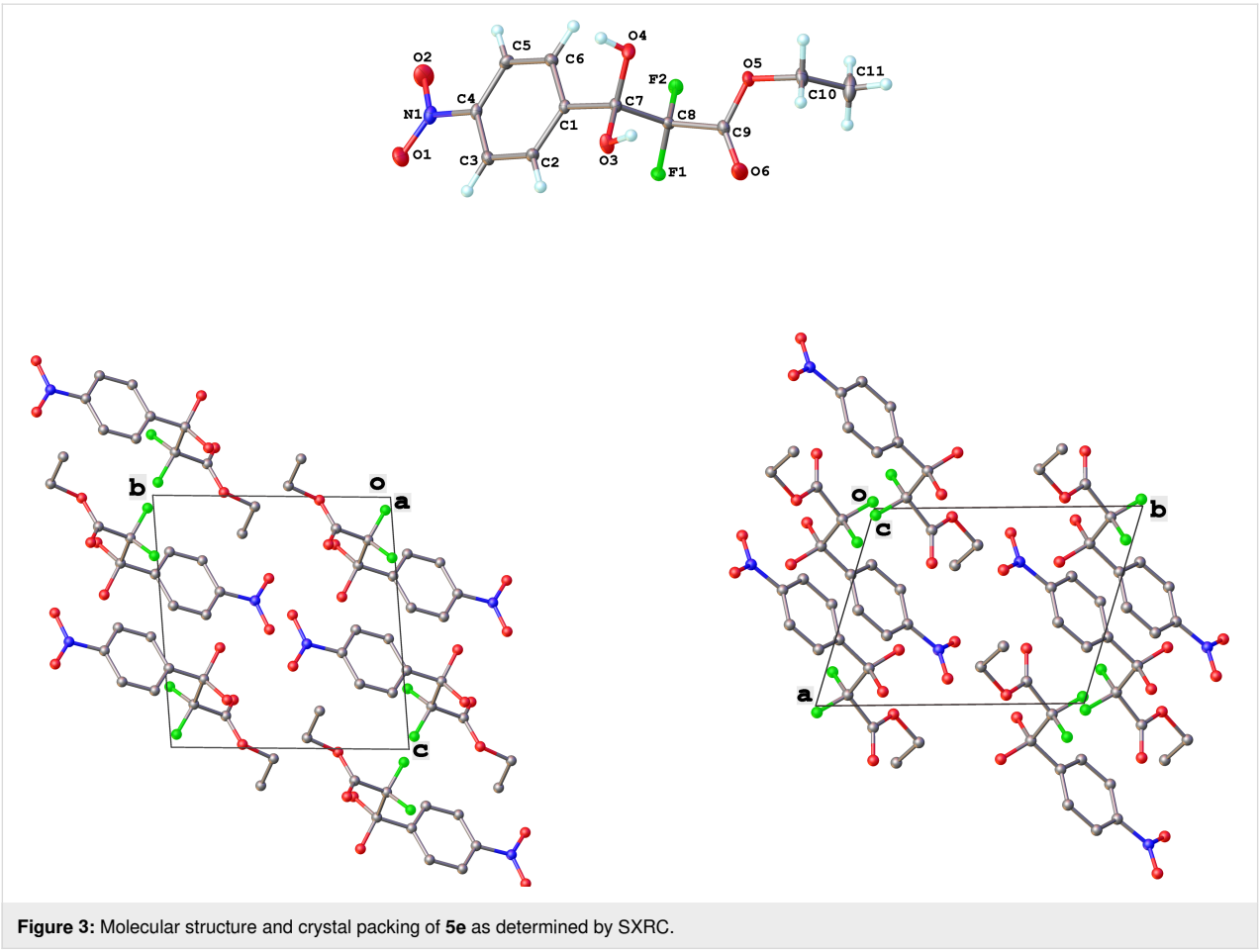

Figure 3: Molecular structure and crystal packing of **5e** as determined by SXRC.

known. Interestingly, in contrast to the previously described acyclic structures no OH···O(H) hydrogen bonds are present in structure **5e** – the molecules are linked by OH···O(NO_2) interactions.

Discussion

Keto–enol tautomer studies have shown that DBM **1a** and related systems **1b**–**i** exist almost entirely (ca. 90%) in their enolic forms in MeCN [17]. Our initial experiments showed **1a** to be unreactive towards 1 equiv of fluorine gas, suggesting that the neutral enol group and neutral, elemental fluorine do not react to give the desired 2-fluoro-1,3-diketone **2a**. Supplementation of the reaction mixture with either a tertiary amine or inorganic base led to varying mixtures of mono- and difluoro products **2a** and **3a**, respectively, with the tertiary amines proving most effective. Inorganic bases offer the possibility of deprotonating **1a**-enol to form a more reactive enolate **1a**-enolate. Nitrogen-centered bases react with fluorine gas to form *N*-fluoroammonium fluorides and fluoride ion [49]. Thus, on addition of tertiary amines, fluorine can react to generate basic fluoride ions and deliver reactive, electrophilic N–F species. Given that Selectfluor is sufficiently electrophilic to react with the neutral enol forms of dicarbonyls **1a**–**i**, we believe that *N*-fluoroammonium ion **6** (Scheme 3) reacts with **1a**–**i**-enol, whereas fluorine does not appear to react with neutral **1a**–**i**-enol to give 2-fluoro products **2a**–**i**. Conversely, fluorine could react directly with the anionic **1a**–**i**-enolate species in parallel with *N*-fluoroammonium ion **6**. Fluoride ions formed through the reactions between fluorine and quinuclidine or fluorine and enolate species, may deprotonate **1a**–**i**-enol, to form enolates of **1a**–**i** that are reactive towards both fluorine and *N*-fluoroammonium ion **6**. The fluorination of **1a**–**i** affords monofluoro products **2a**–**i** in their keto tautomeric forms. For difluorodiketones **3a**–**i** to be formed, enolization of **2a**–**i**-keto must occur through deprotonation at the 2-position, and this process is a key limiting factor [17]. The challenge posed by enolization of **2a**–**i**-keto may be estimated from pK_a differences between acidic species and potential base species. The pK_a(MeCN) for dibenzoylmethane (**1a**) can be estimated from pK_a(DMSO) [50], where pK_a(MeCN) = pK_a(DMSO) + 12.9 = 13.4 + 12.9 = 26.3. Mayr and co-workers have shown the 2-fluoro-substituted species to be only slightly less acidic than their non-fluorinated homologues owing to the dominant π-donor effect of the 2-fluoro group [51,52]. On this basis, quinuclidine with

pK_{aH}(MeCN) ≈ 18.0–19.5 (estimated using pK_{aH}(water) = 11.0 and pK_{aH}(DMSO) = 9.8), is not predicted to be sufficiently basic to offer significant acceleration of the enolization processes of residual **1a**–**i**-keto or, more critically, the 2-fluoro-keto intermediates **2a**–**i**-keto that are formed after monofluorination [50,53,54]. Consequently, we believe a stronger base must be formed during the fluorination process in the presence of quinuclidine, and it is this base that accelerates enolization of **2a**–**i**-keto to allow difluorination to occur. The fluoride ion is a relatively strong base (pK_a(MeCN) of HF is ≈25 based on pK_a(DMSO) [55,56]), especially when formed in situ under anhydrous conditions, where solvation of fluoride ion is not possible. Since the pK_a(MeCN) of **1a**-keto is ≈26.3, and we expect a pK_a(MeCN) of **2a**-keto to be similar in value [51,52], we suggest fluoride ion may be sufficiently basic to cause significant acceleration of the deprotonation of **2a**–**i**-keto and allow formation of **2a**–**i**-enolates, which then react rapidly with fluorine gas, or *N*-fluoroammonium ion **6**, to form difluoroketones **3a**–**i**. Quinuclidine hydrofluoride has independently been shown to be an effective form of soluble fluoride ion in a variety of carbon–fluorine bond-forming processes [57,58]. Enols are, in general, significantly more acidic than their isomeric keto forms, for example, the pK_a(DMSO) of acetone is ≈26.5, whereas the pK_a(DMSO) of acetone enol is ≈18.2 [59]. Thus, assuming a similar difference in pK_a values between **1a**-keto and **1a**-enol, we expect pK_a(MeCN) of **1a**-enol to be ≈18. On this basis, quinuclidine with pK_{aH}(MeCN) ≈ 18.0–19.5, could also be an effective base to facilitate the formation of **1a**-enolate from **1a**-enol and thus facilitate the initial monofluorination step by either fluorine or *N*-fluoroammonium ion **6**.

Carbonate ions are also expected to be highly basic in MeCN, however, their limited solubility is likely to inhibit their ability to act as an effective base for the formation of enolates of **1a** and **2a**, and this is reflected in the modest levels of formation of **3a** (Scheme 4). Chloride ion, on the other hand, is less basic (pK_a(MeCN) of HCl is 10.30 [60]), however, its greater solubility seemingly allows some level of deprotonation of **1a**-enol to occur, where the enolate of **1a** can react with fluorine to afford **2a** and fluoride ion (Scheme 4). The resulting fluoride ion can then act as an additional, stronger base catalyst to facilitate further enolization processes and thus form **3a**. Similar arguments are also applicable to the fluorinations of ethyl benzoylacetate derivatives **4a**–**g**.

Conclusion

From our experiments, we conclude that quinuclidine is the most effective mediating agent for the difluorination of 1,3-dicarbonyl species using fluorine. Difluorinations of 1,3-diketones **1** and 1,3-ketoesters **4** were achieved by the addition of two equivalents of quinuclidine. We propose that the fluoride ion, generated in situ, deprotonates enolic forms of 1,3-dicarbonyls and accelerates the rate-limiting enolization of 2-fluoro-1,3-dicarbonyl intermediates. The resulting enolates are nucleophilic and could react with fluorine or in situ-generated *N*-fluoroammonium ion **7** to form 2-fluoro- and 2,2-difluoro-1,3-dicarbonyl products.

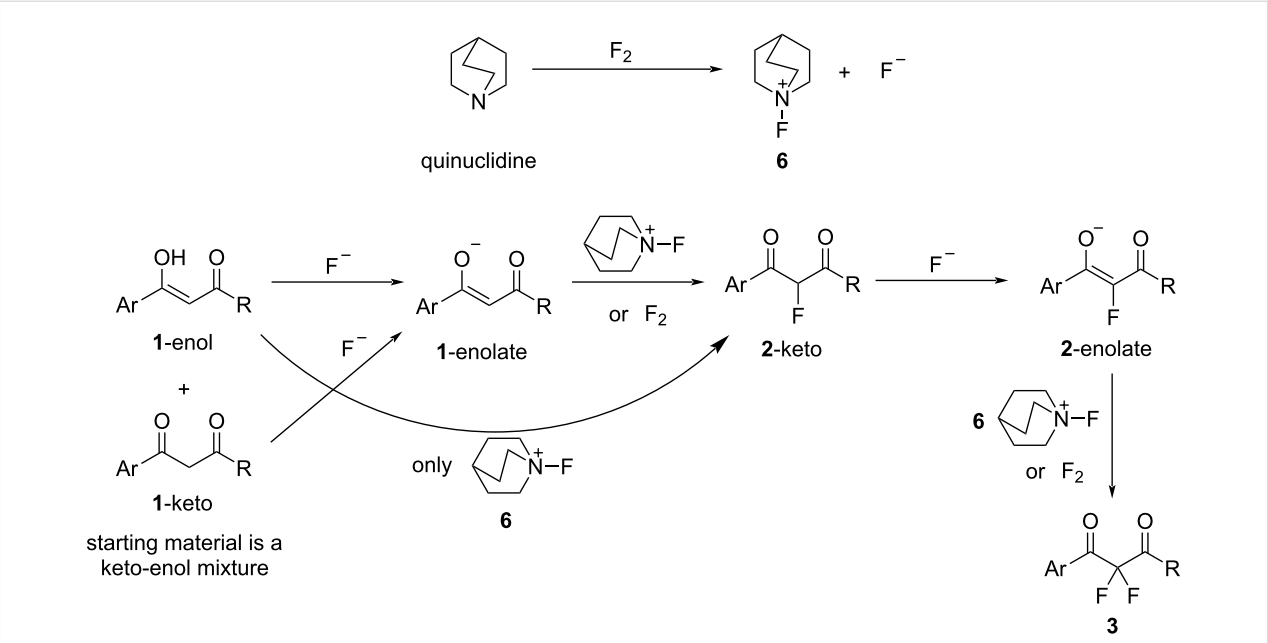

Scheme 3: Proposed mechanism of the quinuclidine-mediated difluorination of 1,3-dicarbonyl substrates.

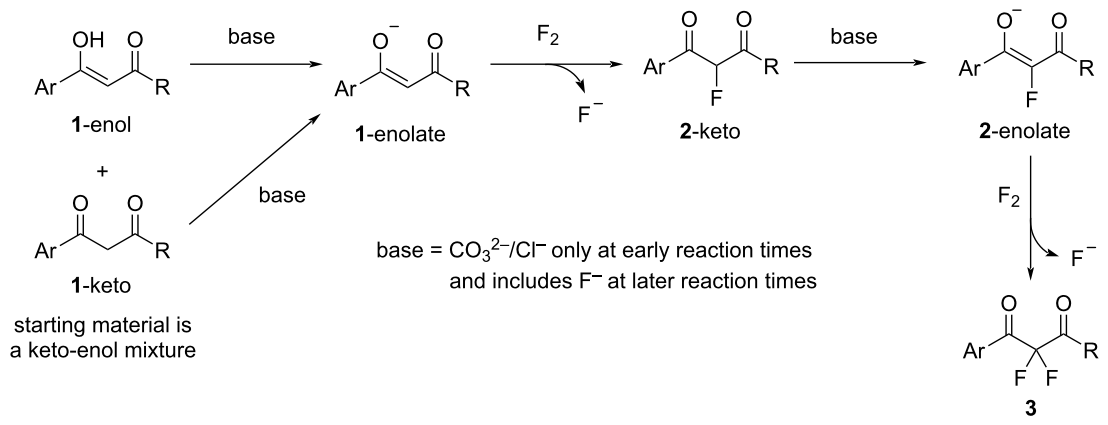

Scheme 4: Proposed mechanisms of carbonate and chloride ion-mediated difluorination of 1,3-dicarbonyl substrates.

Supporting Information

Associated CDCC submission numbers: 2288841–2288848.

Supporting Information File 1

Experimental procedures, characterization data, and copies of ^{1}H, ^{19}F and $^{13}C\{^{1}H\}$ NMR spectra.
[https://www.beilstein-journals.org/bjoc/content/supplementary/1860-5397-20-41-S1.pdf]

Acknowledgements

We thank Dr Dmitry S. Yufit for conducting X-ray crystallographic studies. Parts of this work have already been published in Alexander Hampton's Ph.D. thesis [61].

Funding

We thank Syngenta and Durham University Faculty of Science for studentship funding (to ASH).

ORCID® iDs

David R. W. Hodgson - https://orcid.org/0000-0003-4517-9166

Data Availability Statement

All data that supports the findings of this study are available in the published article and/or the supporting information to this article.

References

1. Purser, S.; Moore, P. R.; Swallow, S.; Gouverneur, V. *Chem. Soc. Rev.* **2008,** *37,* 320–330. doi:10.1039/b610213c
2. Müller, K.; Faeh, C.; Diederich, F. *Science* **2007,** *317,* 1881–1886. doi:10.1126/science.1131943
3. Liang, T.; Neumann, C. N.; Ritter, T. *Angew. Chem., Int. Ed.* **2013,** *52,* 8214–8264. doi:10.1002/anie.201206566
4. de la Torre, B. G.; Albericio, F. *Molecules* **2019,** *24,* 809. doi:10.3390/molecules24040809
5. Bloodworth, A. J.; Bowyer, K. J.; Mitchell, J. C. *Tetrahedron Lett.* **1987,** *28,* 5347–5350. doi:10.1016/s0040-4039(00)96726-1
6. Modarai, B.; Khoshdel, E. *J. Org. Chem.* **1977,** *42,* 3527–3531. doi:10.1021/jo00442a017
7. Fäh, C.; Mathys, R.; Hardegger, L. A.; Meyer, S.; Bur, D.; Diederich, F. *Eur. J. Org. Chem.* **2010,** 4617–4629. doi:10.1002/ejoc.201000712
8. Markovskij, L. N.; Pashinnik, V. E.; Kirsanov, A. V. *Synthesis* **1973,** 787–789. doi:10.1055/s-1973-22302
9. Middleton, W. J.; Bingham, E. M. *J. Org. Chem.* **1980,** *45,* 2883–2887. doi:10.1021/jo01302a025
10. Singh, R. P.; Majumder, U.; Shreeve, J. M. *J. Org. Chem.* **2001,** *66,* 6263–6267. doi:10.1021/jo0157674
11. Singh, R. P.; Shreeve, J. M. *Org. Lett.* **2001,** *3,* 2713–2715. doi:10.1021/ol016319l
12. Banks, R. E.; Lawrence, N. J.; Popplewell, A. L. *J. Chem. Soc., Chem. Commun.* **1994,** 343–344. doi:10.1039/c39940000343
13. Howard, J. L.; Sagatov, Y.; Repusseau, L.; Schotten, C.; Browne, D. L. *Green Chem.* **2017,** *19,* 2798–2802. doi:10.1039/c6gc03139k
14. Howard, J. L.; Sagatov, Y.; Browne, D. L. *Tetrahedron* **2018,** *74,* 3118–3123. doi:10.1016/j.tet.2017.11.066
15. Differding, E.; Rüegg, G. M.; Lang, R. W. *Tetrahedron Lett.* **1991,** *32,* 1779–1782. doi:10.1016/s0040-4039(00)74328-0
16. Rozatian, N.; Ashworth, I. W.; Sandford, G.; Hodgson, D. R. W. *Chem. Sci.* **2018,** *9,* 8692–8702. doi:10.1039/c8sc03596b
17. Rozatian, N.; Beeby, A.; Ashworth, I. W.; Sandford, G.; Hodgson, D. R. W. *Chem. Sci.* **2019,** *10,* 10318–10330. doi:10.1039/c9sc04185k
18. Iacono, C. E.; Stephens, T. C.; Rajan, T. S.; Pattison, G. *J. Am. Chem. Soc.* **2018,** *140,* 2036–2040. doi:10.1021/jacs.7b12941
19. Prakash, G. K. S.; Hu, J.; Wang, Y.; Olah, G. A. *Org. Lett.* **2004,** *6,* 4315–4317. doi:10.1021/ol048166i
20. Zhu, L.; Li, Y.; Ni, C.; Hu, J.; Beier, P.; Wang, Y.; Prakash, G. K. S.; Olah, G. A. *J. Fluorine Chem.* **2007,** *128,* 1241–1247. doi:10.1016/j.jfluchem.2007.05.003
21. Furuta, S.; Kuroboshi, M.; Hiyama, T. *Bull. Chem. Soc. Jpn.* **1998,** *71,* 2687–2694. doi:10.1246/bcsj.71.2687
22. Hallinan, E. A.; Fried, J. *Tetrahedron Lett.* **1984,** *25,* 2301–2302. doi:10.1016/s0040-4039(01)80239-2

23. Curran, T. T. *J. Org. Chem.* **1993,** *58,* 6360–6363. doi:10.1021/jo00075a033
24. Iseki, K.; Kuroki, Y.; Asada, D.; Kobayashi, Y. *Tetrahedron Lett.* **1997,** *38,* 1447–1448. doi:10.1016/s0040-4039(97)00044-0
25. Sato, K.; Omote, M.; Ando, A.; Kumadaki, I. *J. Fluorine Chem.* **2004,** *125,* 509–515. doi:10.1016/j.jfluchem.2003.11.023
26. Hiyama, T. In *Organofluorine Compounds: Chemistry and Applications;* Yamamoto, H., Ed.; Springer: Berlin, Heidelberg, Germany, 2000. doi:10.1007/978-3-662-04164-2
27. Campbell, M. G.; Ritter, T. *Chem. Rev.* **2015,** *115,* 612–633. doi:10.1021/cr500366b
28. Champagne, P. A.; Desroches, J.; Hamel, J.-D.; Vandamme, M.; Paquin, J.-F. *Chem. Rev.* **2015,** *115,* 9073–9174. doi:10.1021/cr500706a
29. Liu, X.; Xu, C.; Wang, M.; Liu, Q. *Chem. Rev.* **2015,** *115,* 683–730. doi:10.1021/cr400473a
30. Yang, X.; Wu, T.; Phipps, R. J.; Toste, F. D. *Chem. Rev.* **2015,** *115,* 826–870. doi:10.1021/cr500277b
31. Pattison, G. *Eur. J. Org. Chem.* **2018,** 3520–3540. doi:10.1002/ejoc.201800532
32. Adler, P.; Teskey, C. J.; Kaiser, D.; Holy, M.; Sitte, H. H.; Maulide, N. *Nat. Chem.* **2019,** *11,* 329–334. doi:10.1038/s41557-019-0215-z
33. Butters, M.; Ebbs, J.; Green, S. P.; MacRae, J.; Morland, M. C.; Murtiashaw, C. W.; Pettman, A. J. *Org. Process Res. Dev.* **2001,** *5,* 28–36. doi:10.1021/op0000879
34. Chambers, R. D.; Greenhall, M. P.; Hutchinson, J. *J. Chem. Soc., Chem. Commun.* **1995,** 21–22. doi:10.1039/c39950000021
35. Harsanyi, A.; Sandford, G. *Green Chem.* **2015,** *17,* 3000–3009. doi:10.1039/c5gc00402k
36. Lisse, E.; Sandford, G. *J. Fluorine Chem.* **2018,** *206,* 117–124. doi:10.1016/j.jfluchem.2017.12.012
37. Patrick, T. B.; Scheibel, J. J.; Cantrell, G. L. *J. Org. Chem.* **1981,** *46,* 3917–3918. doi:10.1021/jo00332a034
38. Stavber, G.; Zupan, M.; Jereb, M.; Stavber, S. *Org. Lett.* **2004,** *6,* 4973–4976. doi:10.1021/ol047867c
39. Stavber, G.; Stavber, S. *Adv. Synth. Catal.* **2010,** *352,* 2838–2846. doi:10.1002/adsc.201000477
40. Stavber, G.; Zupan, M.; Stavber, S. *Tetrahedron Lett.* **2007,** *48,* 2671–2673. doi:10.1016/j.tetlet.2007.02.077
41. Davis, F. A.; Han, W.; Murphy, C. K. *J. Org. Chem.* **1995,** *60,* 4730–4737. doi:10.1021/jo00120a014
42. Xiao, J.-C.; Shreeve, J. M. *J. Fluorine Chem.* **2005,** *126,* 473–476. doi:10.1016/j.jfluchem.2004.10.043
43. Lal, G. S. *J. Org. Chem.* **1993,** *58,* 2791–2796. doi:10.1021/jo00062a023
44. Yang, N.-Y.; Li, Z.-L.; Ye, L.; Tan, B.; Liu, X.-Y. *Chem. Commun.* **2016,** *52,* 9052–9055. doi:10.1039/c6cc00364h
45. Clay, R. J.; Collom, T. A.; Karrick, G. L.; Wemple, J. *Synthesis* **1993,** 290–292. doi:10.1055/s-1993-25849
46. Venkat Ragavan, R.; Vijayakumar, V.; Rajesh, K.; Palakshi Reddy, B.; Karthikeyan, S.; Suchetha Kumari, N. *Bioorg. Med. Chem. Lett.* **2012,** *22,* 4193–4197. doi:10.1016/j.bmcl.2012.04.008
47. Han, C.; Kim, E. H.; Colby, D. A. *J. Am. Chem. Soc.* **2011,** *133,* 5802–5805. doi:10.1021/ja202213f
48. Khatri, H. R.; Han, C.; Luong, E.; Pan, X.; Adam, A. T.; Alshammari, M. D.; Shao, Y.; Colby, D. A. *J. Org. Chem.* **2019,** *84,* 11665–11675. doi:10.1021/acs.joc.9b01595
49. Banks, R. E.; Mohialdin-Khaffaf, S. N.; Lal, G. S.; Sharif, I.; Syvret, R. G. *J. Chem. Soc., Chem. Commun.* **1992,** 595–596. doi:10.1039/c39920000595
50. Olmstead, W. N.; Bordwell, F. G. *J. Org. Chem.* **1980,** *45,* 3299–3305. doi:10.1021/jo01304a033
51. Zhang, Z.; Puente, Á.; Wang, F.; Rahm, M.; Mei, Y.; Mayr, H.; Prakash, G. K. S. *Angew. Chem., Int. Ed.* **2016,** *55,* 12845–12849. doi:10.1002/anie.201605616
52. Zhang, Z.; Puente, Á.; Wang, F.; Rahm, M.; Mei, Y.; Mayr, H.; Prakash, G. K. S. *Angew. Chem., Int. Ed.* **2016,** *55,* 14494. doi:10.1002/anie.201609842
53. Coetzee, J. F.; Padmanabhan, G. R. *J. Am. Chem. Soc.* **1965,** *87,* 5005–5010. doi:10.1021/ja00950a006
54. Cox, B. G. *Acids and Bases: Solvent Effects on Acid-Base Strength;* Oxford University Press: Oxford, UK, 2013. doi:10.1093/acprof:oso/9780199670512.001.0001
55. Bordwell, F. G. *Acc. Chem. Res.* **1988,** *21,* 456–463. doi:10.1021/ar00156a004
56. Ashworth, I. W.; Frodsham, L.; Moore, P.; Ronson, T. O. *J. Org. Chem.* **2022,** *87,* 2111–2119. doi:10.1021/acs.joc.1c01768
57. Chambers, R. D.; Holmes, T. F.; Korn, S. R.; Sandford, G. *J. Chem. Soc., Chem. Commun.* **1993,** 855–856. doi:10.1039/c39930000855
58. Okoromoba, O. E.; Han, J.; Hammond, G. B.; Xu, B. *J. Am. Chem. Soc.* **2014,** *136,* 14381–14384. doi:10.1021/ja508369z
59. Bordwell, F. G.; Zhang, S.; Eventova, I.; Rappoport, Z. *J. Org. Chem.* **1997,** *62,* 5371–5373. doi:10.1021/jo970404i
60. Raamat, E.; Kaupmees, K.; Ovsjannikov, G.; Trummal, A.; Kütt, A.; Saame, J.; Koppel, I.; Kaljurand, I.; Lipping, L.; Rodima, T.; Pihl, V.; Koppel, I. A.; Leito, I. *J. Phys. Org. Chem.* **2013,** *26,* 162–170. doi:10.1002/poc.2946
61. Hampton, A. S. Fluorine Gas as a Selective Difluorinating Reagent. Ph.D. Thesis, Durham University, Durham, U.K., 2020.

License and Terms

BEILSTEIN JOURNAL OF ORGANIC CHEMISTRY

Direct synthesis of acyl fluorides from carboxylic acids using benzothiazolium reagents

Lilian M. Maas[‡1,2], Alex Haswell[‡2], Rory Hughes[2] and Matthew N. Hopkinson[*1,2]

Full Research Paper

Open Access

Address:
[1]Institute of Chemistry and Biochemistry, Freie Universität Berlin, Fabeckstrasse 34–36, 14195 Berlin, Germany and [2]School of Natural and Environmental Sciences, Newcastle University, Bedson Building, Newcastle upon Tyne, NE1 7RU, United Kingdom

Email:
Matthew N. Hopkinson[*] - matthew.hopkinson@newcastle.ac.uk

* Corresponding author ‡ Equal contributors

Keywords:
acyl fluorides; amides; benzothiazolium salts; carboxylic acids; deoxygenative reactions

Beilstein J. Org. Chem. **2024,** *20,* 921–930.
https://doi.org/10.3762/bjoc.20.82

Received: 09 February 2024
Accepted: 05 April 2024
Published: 23 April 2024

This article is part of the thematic issue "Organofluorine chemistry VI".

Guest Editor: D. O'Hagan

Abstract

2-(Trifluoromethylthio)benzothiazolium triflate (BT-SCF_3) was used as deoxyfluorinating reagent for the synthesis of versatile acyl fluorides directly from the corresponding carboxylic acids. These acyl fluorides were reacted with amines in a one-pot protocol to form different amides, including dipeptides, under mild and operationally simple conditions in high yields. Mechanistic studies suggest that BT-SCF_3 can generate acyl fluorides from carboxylic acids via two distinct pathways, which allows the deoxyfluorinating reagent to be employed in sub-stoichiometric amounts.

Introduction

Acyl fluorides are attracting much attention as versatile reagents for different applications in organic synthesis. In addition to their use as sources of fluoride ions, they are most commonly employed as acylation reagents [1-3]. The strong C–F bond makes acyl fluorides relatively stable towards hydrolysis and easier to handle than other acyl halides [4-8]. Their reactions with nucleophiles are typically less violent than for the corresponding acyl chlorides with acyl fluorides exhibiting comparable electrophilicity to activated esters; however, with considerably fewer steric restrictions [9,10]. Acylations with acyl fluorides also typically proceed with fewer side-reactions while derivatives bearing an α-stereocentre generally undergo little racemisation [11,12]. The combination of all these properties mean that acyl fluorides can provide significant advantages over acyl chlorides, especially for challenging acylation reactions [13,14].

Nevertheless, acyl chlorides still dominate in the literature; however, the recent development of safer and more practical synthetic routes to acyl fluorides are inspiring greater interest in these compounds. Various synthetic approaches have been investigated with two main strategies being pursued: fluorine-transfer to acyl radicals and nucleophilic fluorination of acyl electrophiles [15]. The latter approach is the most intensively

studied due to the easy accessibility of fluoride ions with many methods directly employing the parent carboxylic acid as substrate. These processes avoid an additional pre-functionalisation step and have been reported using a range of deoxyfluorinating reagents including (diethylamino)sulfur trifluoride (DAST) [16-18], bis(2-methoxyethyl)aminosulfur trifluoride (Deoxo-Fluor®) [10,19,20], (diethylamino)difluorosulfonium tetrafluoroborate (XtalFluor-E®) [21-24], $(Me_4N)SCF_3$ [9,25], pentafluoropyridine (PFP) [26] and cyanuric fluoride [27,28] among others [15].

Since 2019, our group has developed a series of 2-(fluoroalkylthio)benzothiazolium (BT-SR_F) reagents for the deoxygenative transfer of SR_F (R_F = poly- or perfluoroalkyl) groups into organic molecules (Figure 1). In an initial report, the trifluoromethylthio-containing salt, BT-SCF_3, was reacted with unactivated aliphatic alcohols to afford (trifluoromethyl)thioethers, while subsequent work focused on the direct deoxygenative synthesis of fluorinated thioesters from carboxylic acids [29-31]. In each case, the reactions proceeded smoothly under operationally simple conditions while BT-SCF_3 and related BT-SR_F reagents are easy-to-handle solids that can be readily produced on a multigram scale from relatively inexpensive starting materials. During the optimisation studies for the latter process with carboxylic acid substrates, in addition to the desired (trifluoromethyl)thioester products, small amounts of the corresponding acyl fluorides were also observed as by-products. Given the increasing interest in acyl fluorides in organic synthesis and the attractive features of BT-SR_F salts as reagents for organofluorine chemistry, we considered whether optimisation of the reaction conditions could allow for the selective synthesis of acyl fluoride products directly from carboxylic acids. Here, we report the results of this study, which led to the development of a practical and high yielding methodology for the synthesis of acyl fluorides and their subsequent one-pot conversion into amides. Moreover, by virtue of BT-SCF_3's ability to deliver acyl fluorides via two distinct deoxyfluorination pathways, an efficient process could be achieved using only substoichiometric amounts of the fluorinating reagent.

Results and Discussion

In an initial test reaction, 4-methylbenzoic acid (**1a**) was reacted with 1.25 equiv of BT-SCF_3 and 2.0 equiv of NaH in DCM under conditions similar to our previous reports on the deoxygenative trifluoromethylthiolation of carboxylic acids [31]. ^{19}F NMR analysis of the crude reaction mixture after 2 h at rt

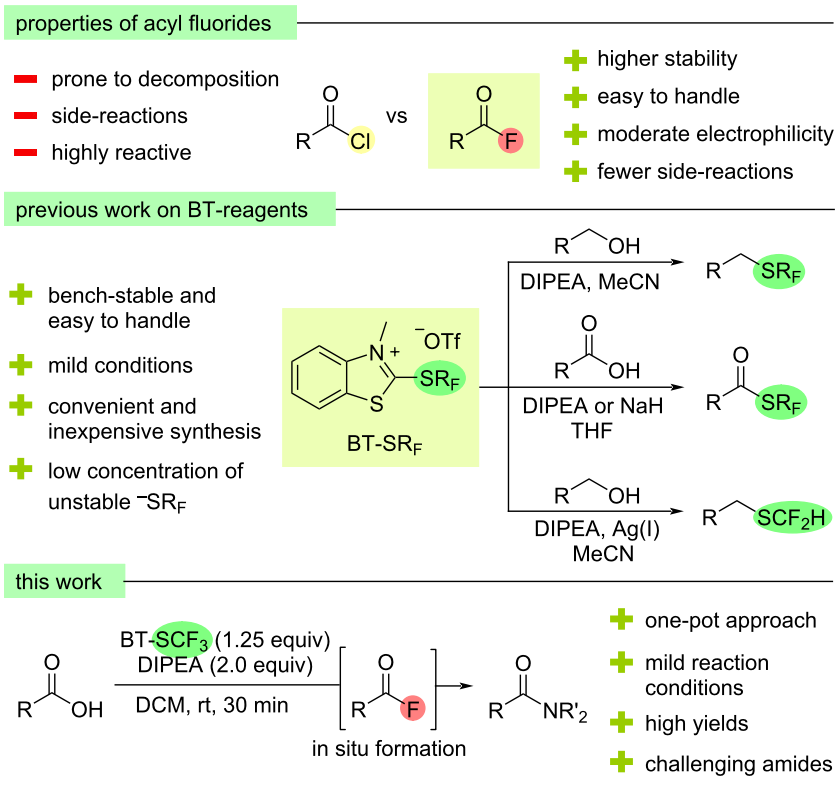

Figure 1: Advantages of acyl fluorides compared to acyl chlorides, previous work on BT-SR_F reagents [29-33] and a summary of this work on the BT-SCF_3-mediated in situ formation of acyl fluorides and their use for the synthesis of amides.

revealed no conversion towards the desired acyl fluoride product **2a**, however, 30% of thioester **3a** was formed (internal standard: $PhCF_3$, Table 1, entry 1). Pleasingly, changing the base to K_2CO_3 led to the formation of **2a** in 7% ^{19}F NMR yield (Table 1, entry 2), while the selectivity of the reaction could be switched significantly upon employing organic amine bases (Table 1, entries 3 and 4). Using 2.0 equiv of diisopropylethylamine (DIPEA), **2a** could be obtained in quantitative ^{19}F NMR yield although a reduction to 1.5 equiv led to a significant drop in efficiency, delivering the acyl fluoride in only 30% ^{19}F NMR yield together with 45% of thioester **3a** (Table 1, entries 4 and 5). At this stage, we were interested in the reactivity of other BT-SR_F reagents developed in our group and tested three longer-chain derivatives under deoxyfluorination conditions. Employing BT-SC_4F_9 and BT-SC_8F_{17}, ^{19}F NMR yields of **2a** of 84% and 81% were achieved (Table 1, entries 6 and 7), however, BT-$SCF(CF_3)_2$, which features a branched perfluoroalkyl chain, gave a comparatively moderate ^{19}F NMR yield of 67% (Table 1, entry 8). BT-SCF_3 still led to the highest ^{19}F NMR yield of **2a** among all the tested reagents and was therefore used throughout the subsequent optimisation and scope studies. An interesting observation was made upon varying the equivalents of BT-SCF_3. Rather than reducing the yield to 50% or lower, conducting the reaction with 0.5 equiv of BT-SCF_3 provided **2a** in 55% ^{19}F NMR yield, suggesting that each equivalent of the benzothiazolium reagent can deliver more than one equivalent of the acyl fluoride product (Table 1, entry 9). Although representing a considerable drop in efficiency compared to using 1.25 equiv of BT-SCF_3, this observation provides an interesting insight into the reaction mechanism (vide infra). Changing the solvent from DCM to THF or MeCN resulted in no significant change in the efficiency of the reaction, whereas a ^{19}F NMR yield of only 11% was achieved in DMF (Table 1, entries 10–12). Increasing the reaction concentration to 0.2 M in DCM led to a reduction in the ^{19}F NMR yield of **2a** to 74% (Table 1, entry 13). Finally, optimisation of the reaction time revealed the starting material was completely converted after only 30 min at rt (Table 1, entry 14).

With the optimised conditions in hand, the scope of the reaction was investigated to assess the practical utility of BT-SCF_3-mediated deoxyfluorination as a method for preparing diverse acyl fluorides. As shown in Scheme 1, the reaction showed excellent functional group tolerance with a range of aromatic carboxylic acids **1**, delivering the corresponding acyl fluorides **2** in very good ^{19}F NMR yields above 75% for all substrates tested. Both electron-withdrawing and electron-donating substituents were tolerated while substituents could be present at

Table 1: Optimisation of the reaction conditions for the deoxygenative fluorination of 4-methylbenzoic acid using benzothiazolium reagents.

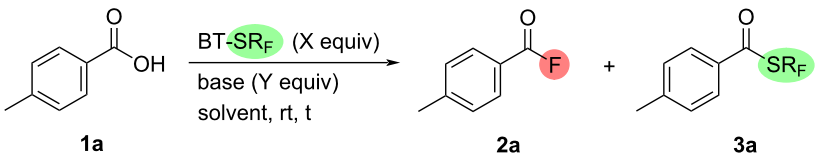

1a **2a** **3a**

Entry	R_F (X equiv)	Base (Y equiv)	Solvent (conc.)	*t* (h)	Yield **2a**[a]	Yield **3a**[a]
1	CF_3 (1.25)	NaH (2.0)	DCM (0.1 M)	2	–	30
2	CF_3 (1.25)	K_2CO_3 (2.0)	DCM (0.1 M)	2	7	37
3	CF_3 (1.25)	NEt_3 (2.0)	DCM (0.1 M)	2	96	traces
4	CF_3 (1.25)	DIPEA (2.0)	DCM (0.1 M)	2	quant.	–
5	CF_3 (1.25)	DIPEA (1.5)	DCM (0.1 M)	2	30	45
6	C_4F_9 (1.25)	DIPEA (2.0)	DCM (0.1 M)	2	84	–
7	C_8F_{17} (1.25)	DIPEA (2.0)	DCM (0.1 M)	2	81	–
8	$CF(CF_3)_2$ (1.25)	DIPEA (2.0)	DCM (0.1 M)	2	67	–
9	CF_3 (0.5)	DIPEA (2.0)	DCM (0.1 M)	2	55	–
10	CF_3 (1.25)	DIPEA (2.0)	DMF (0.1 M)	2	11	–
11	CF_3 (1.25)	DIPEA (2.0)	MeCN (0.1 M)	2	88	–
12	CF_3 (1.25)	DIPEA (2.0)	THF (0.1 M)	2	91	–
13	CF_3 (1.25)	DIPEA (2.0)	DCM (0.2 M)	2	74	–
14	CF_3 (1.25)	DIPEA (2.0)	DCM (0.1 M)	0.5	quant.	–

[a]As internal standard for ^{19}F NMR yields α,α,α-trifluorotoluene was used.

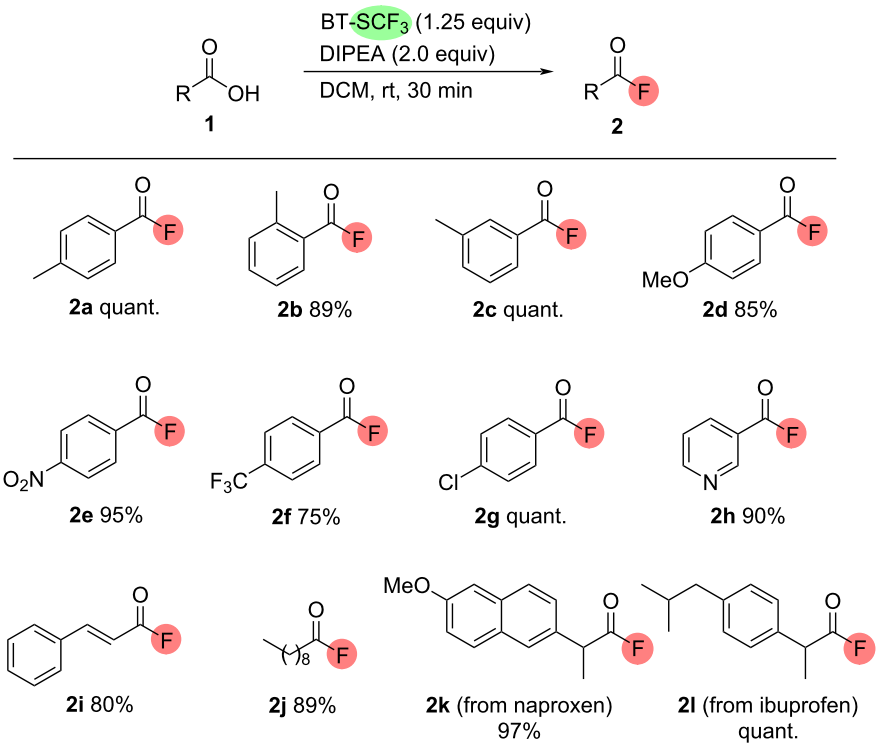

Scheme 1: Scope of the BT-SCF_3-mediated deoxygenative fluorination of carboxylic acids **1**. Reactions were performed on a 0.2 mmol scale. ^{19}F NMR yields using α,α,α-trifluorotoluene as the internal standard.

the *ortho*-, *meta*- or *para*-positions. The heteroaromatic acyl fluoride **2h** could be prepared efficiently while deoxyfluorination of representative olefinic and aliphatic carboxylic acids proceeded smoothly, affording cinnamoyl and decanoyl acyl fluorides **2i** and **2j** in 80% and 89% ^{19}F NMR yields, respectively. Furthermore, the widely available drug molecules naproxen and ibuprofen could be efficiently converted into their acyl fluoride derivatives **2k** and **2l** in 97% and quantitative yields, respectively.

To improve the practicality of the methodology and to avoid the often unreliable isolation of acyl fluoride intermediates, we next considered whether BT-SCF_3-mediated deoxyfluorination of carboxylic acids could be coupled with a subsequent acylation in an overall one-pot process. Selecting amines as nucleophilic coupling partners, a short optimisation study was carried out to identify suitable conditions compatible with the deoxyfluorination process. Pleasingly, adding 2.0 equiv of benzylamine (**4a**) to the standard reaction between 4-methylbenzoic acid (**1a**) and BT-SCF_3 (1.25 equiv) in DCM (0.1 M) and increasing the amount of DIPEA to 3.0 equiv allowed for the efficient formation of the desired amide **5a** after 16 h at rt, which could be isolated in 80% yield after column chromatography. A survey of carboxylic acids **1** revealed that the one-pot approach is efficient for a variety of substitution profiles (Scheme 2). Aromatic acids bearing methyl substituents at the *para*-, *ortho*- or *meta*-positions all reacted smoothly with **4a** to afford the corresponding benzylamides **5a–c** in very good isolated yields up to 81%. Electron-donating and -withdrawing groups at the *para*-position were well tolerated (**5d–f**), including halogen substituents that could serve as handles for follow-up functionalisation chemistry such as coupling reactions (**5g**, **5m**, **5n**). Heteroaromatic (**5o**) and aliphatic carboxylic acids (**5j**, **5p**, **5q**) also reacted smoothly under the optimised conditions. As demonstrated by the efficient formation of amide **5q** in 84% yield, the process is tolerant of significant steric bulk at the carboxyl α-position. Finally, to assess the influence of the reaction on the stereochemical integrity of chiral carboxylic acid substrates, the deoxyfluorination was performed on the enantiopure (*S*)-isomer of ibuprofen (er = 99:1). Pleasingly, efficient conversion to the corresponding amide (*S*)-**5l** was observed (yield = 72%) with analysis by chiral HPLC revealing no erosion of the enantiomeric ratio (er = 99:1).

At this stage, the suitability of BT-SCF_3-mediated deoxyfluorination for the one-pot formation of peptide linkages between amino acids was investigated (Scheme 3). Treatment of *N*-Boc-valine under the optimised one-pot conditions with benzylamine (**4a**) resulted in the formation of the desired amide product, however, significant by-products were also observed.

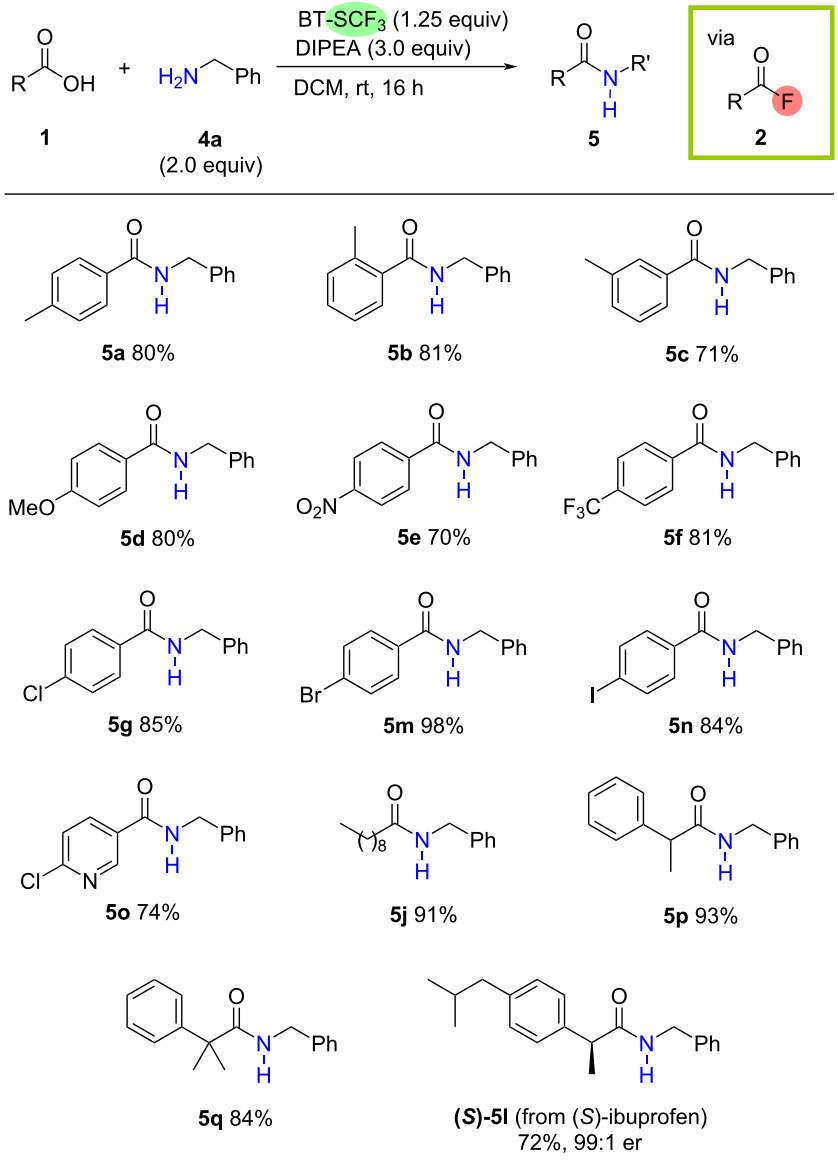

Scheme 2: Scope of the one-pot BT-SCF_3-mediated deoxygenative coupling of carboxylic acids and amines via acyl fluoride derivatives. Reactions conducted on a 0.5 mmol scale, isolated yields after column chromatography.

Careful column chromatography of the crude reaction mixture allowed for the partial isolation and characterisation of the benzothiazolimine species **6** which results from Boc-deprotection and subsequent condensation of the amide product onto the benzothiazolium core. Although the other identified by-product, thiourea **7**, is not derived from the limiting carboxylic acid substrate, it was found to coelute with the amide product, complicating isolation (Scheme 3a). As Boc-deprotection is seemingly feasible under the reaction conditions, to avoid formation of by-product **6**, the process was tested using the *N*-Cbz-valine (**1s**). Moreover, the BT-SCF_3 reagent was substituted for the longer chain BT-reagent BT-SC_5F_{11}. The use of this benzothiazolium species would avoid the formation of thiocarbonyl difluoride, which is most likely responsible for the generation of thiourea **7**. Pleasingly, under these conditions, amide **5s** was formed smoothly with isolation by column chromatography providing the pure product in 71% yield (Scheme 3b). Furthermore, replacing the benzylamine coupling partner with phenylalanine methyl ester provided dipeptide **5t** in 67% yield (Scheme 3b).

With the scope of the deoxyfluorination process established, our attention turned to an investigation of the reaction mechanism (Scheme 4). As demonstrated in our previous work, reacting

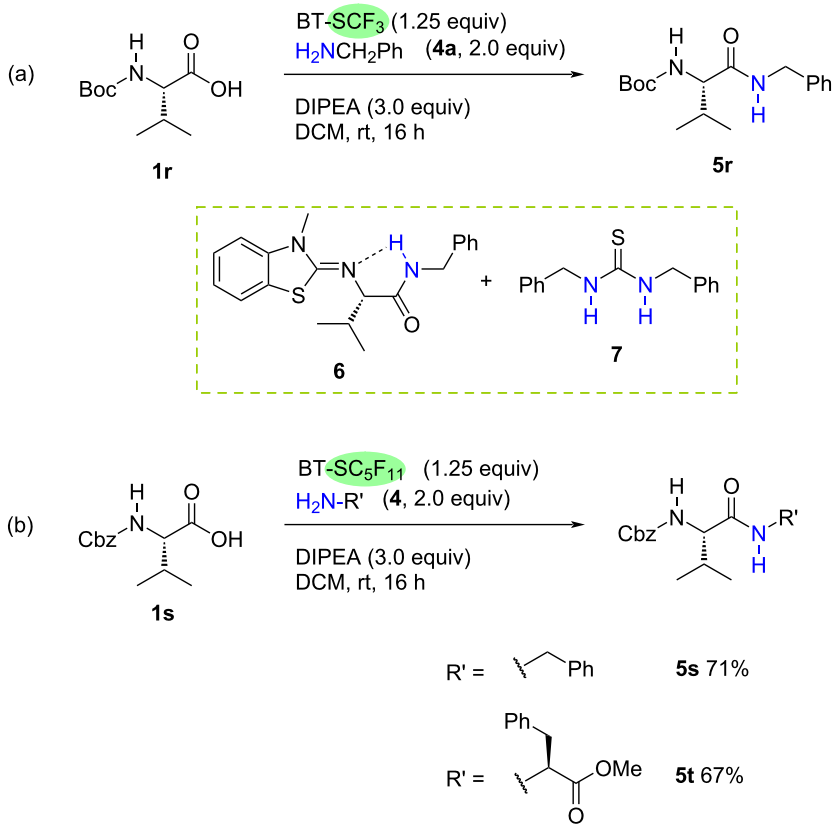

Scheme 3: One-pot BT-SCF_3-mediated deoxygenative coupling of amino acids. Isolated yields after column chromatography.

BT-SCF_3 with carboxylic acids **1** under similar conditions provides (trifluoromethyl)thioesters **3** via a concerted deoxytrifluoromethylthiolation process from tetrahedral intermediate **A** affording thiocarbamate by-product **B** [31]. To test whether thioester species could act as intermediates in the formation of acyl fluorides, **3a** was prepared independently and treated with DIPEA (1.1 equiv) in DCM (Scheme 5a). After 1 h at rt, complete consumption of the thioester was observed with acyl fluoride **2a** being obtained as the only product in quantitative ^{19}F NMR yield. Conversion of **3** into **2** could result from a self-propagating process initiated by addition of an adventitious nucleophile to the electrophilic thioester. This results in elimination of a (trifluoromethyl)thiolate ($^-SCF_3$) anion (**C**, Scheme 4), which can subsequently undergo β-fluoride elimination, releasing a fluoride anion. Addition of F^- to another molecule of thioester **3** thus sets off a chain process, delivering acyl fluoride **2** and regenerating the fluoride nucleophile. A series of experiments conducted with thioester **3a** suggest a number of nucleophiles feasibly present in the reaction mixture can initiate the chain process [34]. Stirring **3a** in the presence of the sodium carboxylate salt of acid **1a** resulted in the formation of **2a** in 18% ^{19}F NMR yield while only 10 mol % of tetramethylammonium fluoride (TMAF) provided the acyl fluoride in 59% yield (Scheme 5b). Moreover, efficient conversion of **3a** into **2a** could be achieved using only 10 mol % of DIPEA (92% ^{19}F NMR yield, Scheme 5b). This reaction could result from base-assisted nucleophilic attack of adventitious water present in the reaction mixture.

In addition to addition/elimination of fluoride ions to thioesters **3**, a second potential mechanistic pathway exists for the formation of acyl fluorides **2**. Alongside a fluoride ion, β-fluoride elimination from a (trifluoromethyl)thiolate ($^-SCF_3$) anion (**C**) also generates a thiocarbonyl difluoride species **D**. As previously demonstrated by Schoenebeck and co-workers in a deoxyfluorination of carboxylic acids with NMe_4SCF_3, this highly electrophilic compound can react with the carboxylic acid in the presence of DIPEA via addition/elimination affording a thioic anhydride species **E** and a fluoride ion [9]. Addition of F^- to the carboxyl carbon followed by fluoride elimination from the resulting thiocarboxylate would provide acyl fluoride **2**, carbonyl sulfide and another fluoride ion. As a result of this pathway, each molecule of the BT-SCF_3 reagent can in principle lead to the formation of two molecules of acyl fluoride **2**. Indeed, a yield of **2a** above 50% was observed during the optimisation studies using 0.5 equiv of BT-SCF_3 (Table 1, entry 9). To

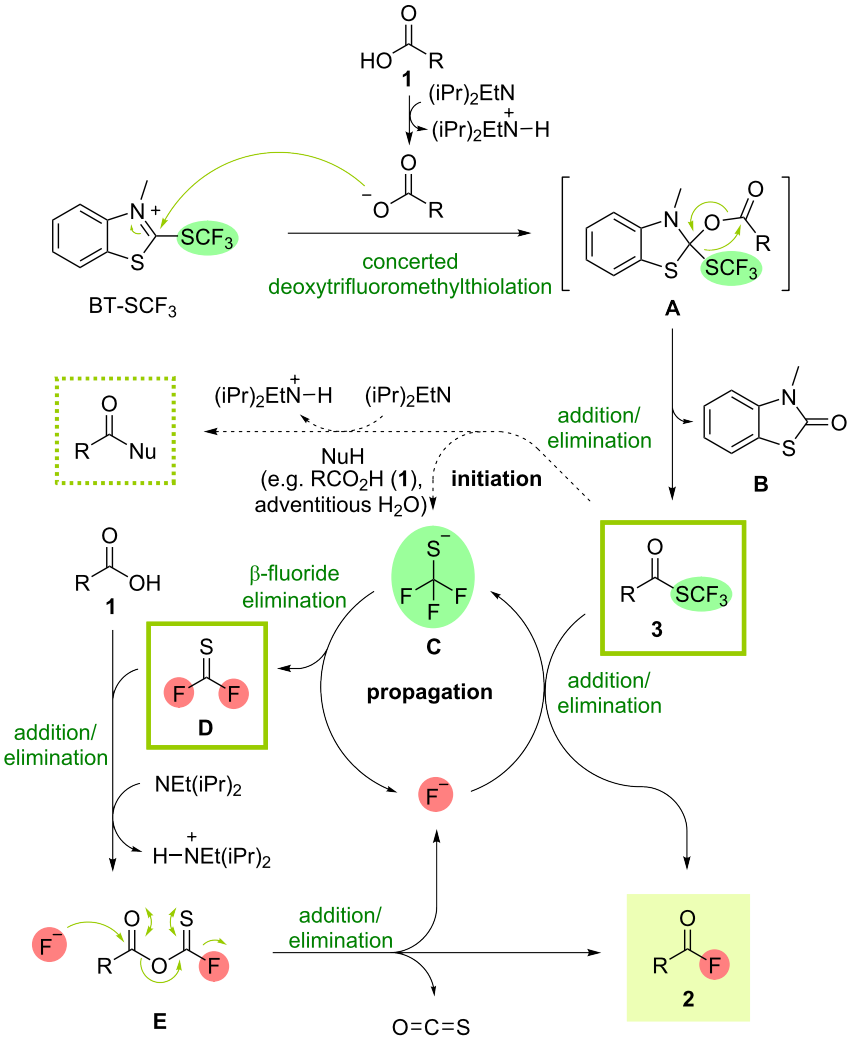

Scheme 4: Plausible mechanism for the deoxyfluorination of carboxylic acids with BT-SCF_3.

further investigate the potential for reducing the loading of the deoxyfluorinating reagent, 0.5 equiv of the carboxylic acid substrate **1a** was reacted with 0.5 equiv of both BT-SCF_3 and DIPEA in DCM for 30 min at rt. ^{19}F NMR analysis of the mixture indicated the clean formation of thioester **3a** and the remaining 0.5 equiv of **1a** and 0.5 equiv of DIPEA were then added (Scheme 5c). According to the mechanism shown in Scheme 4, self-propagating conversion of **3a** into **2a**, presumably initiated by a carboxylate nucleophile, would account for half of the acyl fluoride formed with the remaining product resulting from addition of **1** to thiocarbonyl difluoride. After a further 30 minutes at rt, ^{19}F NMR analysis of the crude mixture indeed indicated the formation of **2a** in an overall yield of 74%, implying both pathways are feasible and that sub-stoichiometric amounts of BT-SCF_3 relative to the carboxylic acid can lead to good overall yields of acyl fluorides.

Conclusion

In conclusion, a practical method for the direct synthesis of acyl fluorides from carboxylic acids using BT-SCF_3 as a deoxyfluorinating reagent has been developed. In a one-pot process, direct access to various amides was achieved under mild and operationally simple conditions while peptide coupling between two amino acids could be efficiently conducted using the longer-chain perfluoroalkyl reagent BT-SC_5F_{11}. Mechanistic studies revealed that each equivalent of the benzothiazolium reagent can feasibly generate two equivalents of the acyl fluoride with addition/elimination of fluoride to a thioester intermediate and independent deoxyfluorination of a second equivalent of the acid substrate by the released $^{-}SCF_3$ anion both operating under the reaction conditions. This allows for the reduction in the loading of BT-SCF_3 to sub-stoichiometric levels, further increasing the attractiveness of the method.

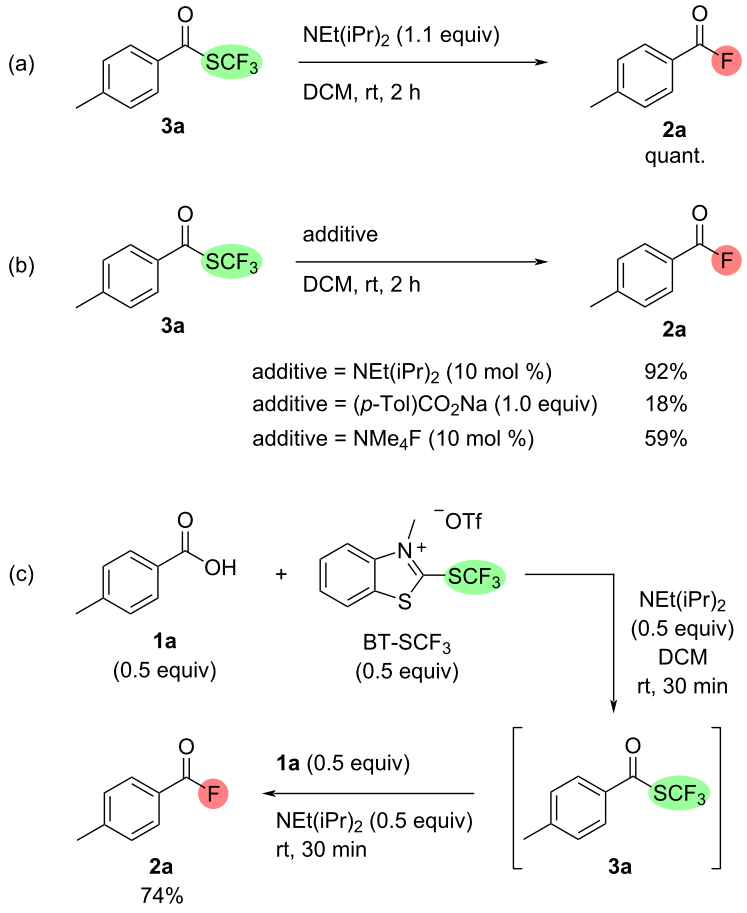

Scheme 5: Mechanistic experiments. (a) Conversion of thioester **3a** into acyl fluoride **2a** in the presence of DIPEA. (b) Conversion of thioester **3a** into acyl fluoride **2a** in the presence of carboxylate and fluoride nucleophiles. (c) Two-stage deoxyfluorination reaction using 0.5 equiv of BT-SCF_3. ^{19}F NMR yields using α,α,α-trifluorotoluene as internal standard.

Supporting Information

Supporting Information File 1

Experimental procedures, characterisation data of all isolated products as well as copies of NMR spectra for novel compounds.
[https://www.beilstein-journals.org/bjoc/content/supplementary/1860-5397-20-82-S1.pdf]

Acknowledgements

We would like to acknowledge the assistance of the Core Facility BioSupraMol supported by the DFG and the analytical services at Newcastle University. We also thank Andreas Mavroskoufis (FU Berlin) for conducting some initial experiments and Aaron Campbell (Newcastle University) for assistance with chiral HPLC measurements.

Funding

This work is funded by the Friedrich Ebert Stiftung (scholarship to L.M.M.) and the School of Natural and Environmental Sciences at Newcastle University (studentship to A.H.). Financial support from Deutsche Forschungsgemeinschaft (DFG, German Research Foundation), Project-ID 387284271-SFB 1349 (gefördert durch die Deutsche Forschungsgemeinschaft (DFG) - Projektnummer 387284271 - SFB 1349), and the Fonds der Chemischen Industrie (Sachkostenzuschuss) is also gratefully acknowledged.

Author Contributions

Lilian M. Maas: conceptualization; investigation; methodology; project administration; resources; supervision; validation; writing – original draft; writing – review & editing. Alex Haswell: conceptualization; investigation; methodology; project administration; resources; supervision; validation; writing – review & editing. Rory Hughes: investigation; methodology;

resources; writing – review & editing. Matthew N. Hopkinson: conceptualization; funding acquisition; methodology; project administration; supervision; writing – original draft; writing – review & editing.

ORCID® iDs

Lilian M. Maas - https://orcid.org/0000-0002-1399-947X
Alex Haswell - https://orcid.org/0000-0001-7067-7840
Rory Hughes - https://orcid.org/0009-0003-5990-9403
Matthew N. Hopkinson - https://orcid.org/0000-0002-0183-0466

Data Availability Statement

The data that supports the findings of this study is available from the corresponding author upon reasonable request.

References

1. Ogiwara, Y.; Sakai, N. *Angew. Chem., Int. Ed.* **2020,** *59,* 574–594. doi:10.1002/anie.201902805
2. Blanchard, N.; Bizet, V. *Angew. Chem., Int. Ed.* **2019,** *58,* 6814–6817. doi:10.1002/anie.201900591
3. Prabhu, G.; Narendra, N.; Basavaprabhu, B.; Panduranga, V.; Sureshbabu, V. V. *RSC Adv.* **2015,** *5,* 48331–48362. doi:10.1039/c4ra16142d
4. Munoz, S. B.; Dang, H.; Ispizua-Rodriguez, X.; Mathew, T.; Prakash, G. K. S. *Org. Lett.* **2019,** *21,* 1659–1663. doi:10.1021/acs.orglett.9b00197
5. Schindler, C. S.; Forster, P. M.; Carreira, E. M. *Org. Lett.* **2010,** *12,* 4102–4105. doi:10.1021/ol1016977
6. O'Hagan, D. *Chem. Soc. Rev.* **2008,** *37,* 308–319. doi:10.1039/b711844a
7. Swain, C. G.; Scott, C. B. *J. Am. Chem. Soc.* **1953,** *75,* 246–248. doi:10.1021/ja01097a520
8. Satchell, D. P. N. *J. Chem. Soc.* **1963,** 555–557. doi:10.1039/jr9630000555
9. Scattolin, T.; Deckers, K.; Schoenebeck, F. *Org. Lett.* **2017,** *19,* 5740–5743. doi:10.1021/acs.orglett.7b02516
10. White, J. M.; Tunoori, A. R.; Turunen, B. J.; Georg, G. I. *J. Org. Chem.* **2004,** *69,* 2573–2576. doi:10.1021/jo035658k
11. Carpino, L. A.; Beyermann, M.; Wenschuh, H.; Bienert, M. *Acc. Chem. Res.* **1996,** *29,* 268–274. doi:10.1021/ar950023w
12. Montalbetti, C. A. G. N.; Falque, V. *Tetrahedron* **2005,** *61,* 10827–10852. doi:10.1016/j.tet.2005.08.031
13. Due-Hansen, M. E.; Pandey, S. K.; Christiansen, E.; Andersen, R.; Hansen, S. V. F.; Ulven, T. *Org. Biomol. Chem.* **2016,** *14,* 430–433. doi:10.1039/c5ob02129d
14. Kangani, C. O.; Kelley, D. E. *Tetrahedron Lett.* **2005,** *46,* 8917–8920. doi:10.1016/j.tetlet.2005.10.068
15. Gonay, M.; Batisse, C.; Paquin, J.-F. *Synthesis* **2021,** *53,* 653–665. doi:10.1055/s-0040-1705951
16. Markovskij, L. N.; Pashinnik, V. E.; Kirsanov, A. V. *Synthesis* **1973,** 787–789. doi:10.1055/s-1973-22302
17. Gustafsson, T.; Gilmour, R.; Seeberger, P. H. *Chem. Commun.* **2008,** 3022–3024. doi:10.1039/b803695k
18. Kaduk, C.; Wenschuh, H.; Beyermann, M.; Forner, K.; Carpino, L. A.; Bienert, M. *Lett. Pept. Sci.* **1996,** *2,* 285–288. doi:10.1007/bf00142240
19. Lal, G. S.; Pez, G. P.; Pesaresi, R. J.; Prozonic, F. M. *Chem. Commun.* **1999,** 215–216. doi:10.1039/a808517j
20. Tunoori, A. R.; White, J. M.; Georg, G. I. *Org. Lett.* **2000,** *2,* 4091–4093. doi:10.1021/ol000318w
21. Beaulieu, F.; Beauregard, L.-P.; Courchesne, G.; Couturier, M.; LaFlamme, F.; L'Heureux, A. *Org. Lett.* **2009,** *11,* 5050–5053. doi:10.1021/ol902039q
22. L'Heureux, A.; Beaulieu, F.; Bennett, C.; Bill, D. R.; Clayton, S.; LaFlamme, F.; Mirmehrabi, M.; Tadayon, S.; Tovell, D.; Couturier, M. *J. Org. Chem.* **2010,** *75,* 3401–3411. doi:10.1021/jo100504x
23. Vandamme, M.; Bouchard, L.; Gilbert, A.; Keita, M.; Paquin, J.-F. *Org. Lett.* **2016,** *18,* 6468–6471. doi:10.1021/acs.orglett.6b03365
24. Gonay, M.; Batisse, C.; Paquin, J.-F. *J. Org. Chem.* **2020,** *85,* 10253–10260. doi:10.1021/acs.joc.0c01377
25. Kremlev, M. M.; Tyrra, W.; Naumann, D.; Yagupolskii, Y. L. *Tetrahedron Lett.* **2004,** *45,* 6101–6104. doi:10.1016/j.tetlet.2004.06.073
26. Brittain, W. D. G.; Cobb, S. L. *Org. Lett.* **2021,** *23,* 5793–5798. doi:10.1021/acs.orglett.1c01953
27. Olah, G. A.; Nojima, M.; Kerekes, I. *Synthesis* **1973,** 487–488. doi:10.1055/s-1973-22238
28. Groß, S.; Laabs, S.; Scherrmann, A.; Sudau, A.; Zhang, N.; Nubbemeyer, U. *J. Prakt. Chem.* **2000,** *342,* 711–714. doi:10.1002/1521-3897(200009)342:7<711::aid-prac711>3.0.co;2-m
29. Dix, S.; Jakob, M.; Hopkinson, M. N. *Chem. – Eur. J.* **2019,** *25,* 7635–7639. doi:10.1002/chem.201901607
30. Ariamajd, A.; Gerwien, N. J.; Schwabe, B.; Dix, S.; Hopkinson, M. N. *Beilstein J. Org. Chem.* **2021,** *17,* 83–88. doi:10.3762/bjoc.17.8
31. Tironi, M.; Maas, L. M.; Garg, A.; Dix, S.; Götze, J. P.; Hopkinson, M. N. *Org. Lett.* **2020,** *22,* 8925–8930. doi:10.1021/acs.orglett.0c03328
32. Haswell, A.; Tironi, M.; Wang, H.; Hopkinson, M. N. *J. Fluorine Chem.* **2024,** *273,* 110231. doi:10.1016/j.jfluchem.2023.110231
33. Tironi, M.; Hopkinson, M. N. *Eur. J. Org. Chem.* **2022,** e202101557. doi:10.1002/ejoc.202101557
34. Notably, similar reactivity was observed with longer-chain (perfluoroalkyl)thioesters generated upon deoxygenative perfluoroalkylthiolation of carboxylic acids with BT-SR_F reagents. With these very electrophilic compounds, conversion into the corresponding acyl fluorides was often observed as a decomposition pathway during purification or extended storage (see ref. [32]).

License and Terms

BEILSTEIN JOURNAL OF ORGANIC CHEMISTRY

Benzylic C(sp^3)–H fluorination

Alexander P. Atkins, Alice C. Dean and Alastair J. J. Lennox*

Review

Open Access

Address:
University of Bristol, School of Chemistry, Bristol, BS8 1TS, U.K.

Email:
Alastair J. J. Lennox* - a.lennox@bristol.ac.uk

* Corresponding author

Keywords:
benzylic; C–H functionalization; fluorination; photoredox catalysis

Beilstein J. Org. Chem. **2024,** *20,* 1527–1547.
https://doi.org/10.3762/bjoc.20.137

Received: 24 April 2024
Accepted: 26 June 2024
Published: 10 July 2024

This article is part of the thematic issue "Organofluorine chemistry VI".

Guest Editor: D. O'Hagan

Abstract

The selective fluorination of C(sp^3)–H bonds is an attractive target, particularly for pharmaceutical and agrochemical applications. Consequently, over recent years much attention has been focused on C(sp^3)–H fluorination, and several methods that are selective for benzylic C–H bonds have been reported. These protocols operate via several distinct mechanistic pathways and involve a variety of fluorine sources with distinct reactivity profiles. This review aims to give context to these transformations and strategies, highlighting the different tactics to achieve fluorination of benzylic C–H bonds.

Introduction

The development of new fluorination methodologies is driven largely by the beneficial effects of including fluorine into bioactive molecules. These advantages include the modulation of potency, bioavailability and physical properties of drug and agrochemical compounds [1-3]. The significance of fluorination is reflected in the fact that a large number of agrochemicals contain fluorine, and that almost a quarter of drug molecules approved by the FDA between 2018 and 2022 contained at least one fluorine atom, for example belzutifan and quinofumelin, Figure 1A [4,5].

The fluorination of functionalised carbon centres is a reliable strategy to incorporate fluorine into compounds of interest, with regio and site selectivity pre-determined by the nature of the functionalised carbon. However, the development of C(sp^3)–H fluorination methods represents a more sustainable and versatile approach, as there is no requirement to pre-functionalise the compound, carry that functional group through synthesis and also protect any potentially labile group that would otherwise displace during the installation of the fluorine atom [6-8]. Therefore, methodologies for the selective C–H fluorination represent a valuable class of reactions [1,9,10], for which several have been disclosed in the chemical literature [11,12].

Benzylic C(sp^3)–H bonds are comparatively weaker compared to unactivated C(sp^3)–H bonds, with bond dissociation enthalpies (BDEs) falling in the range of 76–90 kcal mol^{-1} (Figure 1B), due to the increased stability of benzylic radicals

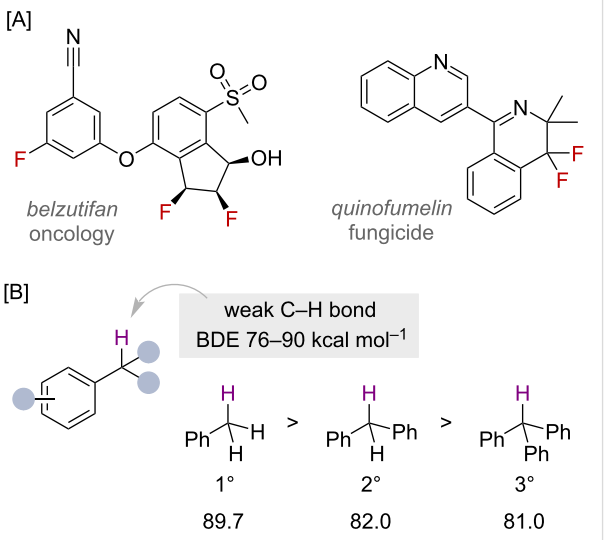

Figure 1: A) Benzylic fluorides in bioactive compounds, with B) the relative BDEs of different benzylic C–H bonds reported in kcal mol^{-1}.

and ions imparted through delocalisation with the adjacent π-system [13-15]. In general, the more stabilised the benzylic radical, the weaker the C(sp^3)–H bond, as demonstrated when considering the BDEs of a series of phenyl-substituted methanes (Figure 1B). The changes in BDE correlate with the relative stability of primary, secondary and tertiary benzylic radicals and cations. As a result, the presence of benzylic C(sp^3)–H bonds in bioactive molecules can be problematic as they are particularly labile to enzymatic oxidation [16], and hence, their functionalisation has become a strategy to overcome this [17]. For this reason, the fluorination of benzylic C(sp^3)–H bonds has become particularly important in biologically relevant situations. Benzylic C(sp^3)–H bonds are also present in a large portion of commercially available building blocks, highlighting the appeal for benzylic C(sp^3)–H functionalisation reactions in drug-discovery campaigns [17]. Although much is unknown about the precise details, several benzylic fluorides have been reported to be unstable, which is an effect that is apparently dependent on the substitution of the ring. While primary benzylic fluorides are predominately considered to be stable to isolation conditions, secondary and tertiary suffer from the elimination of HF, especially in the presence of silica gel or glass vessels. Therefore, benzyl fluorides have been derivatised, for example in C–O, C–N and C–C bond-forming reactions [18-20], thereby also demonstrating their suitability, as precursors for further functionalisation.

Reviews on the broad area of C–H fluorination have been written [11,12,21-29] with the focus varying, for example between aliphatic fluorination [23], α-fluorination of carbonyl compounds [30], photosensitised C–H fluorination [21,26], recent advances [24] and mechanistic approaches [11]. Examples of specifically benzylic C(sp^3)–H fluorination reactions are included into many of these reports, as well as in sections of reviews with a much broader scope [12,27,28], and alternative routes to benzylic fluorides have also been reviewed, such as through deoxyfluorination, C–X fluorination, or decarboxylative fluorination [22,31-33]. However, a comprehensive review that focusses specifically on benzylic C–H bonds is still currently missing in the literature. Therefore, we aim to cover reports that focus specifically on benzylic C(sp^3)–H fluorination, emphasising the most recent protocols but with also some historical context. We also signpost readers to reports where benzylic C–H fluorination has been included, but is not the focus of the work. We have organised the review into different mechanistic strategies, namely, electrophilic, radical and nucleophilic approaches, and highlighted when emerging technologies, such as photo- and electrochemistry effect the desired transformation [22,27].

Review

Electrophilic benzylic C(sp^3)–H fluorination

Base mediated

Electrophilic fluorinating reagents have been used to effect the transformation of benzylic C(sp^3)–H to C(sp^3)–F bonds [22]. Shreeve and co-workers reported the use of KOH or *n*-BuLi to deprotonate acidic protons at benzylic positions adjacent to electron-withdrawing nitro or nitrile groups, respectively, generating benzylic anions that subsequently attack electrophilic Selectfluor to afford the benzyl fluoride (Figure 2) [34]. The methodology was demonstrated on eight *para*-substituted benzylic substrates. The authors noted that resubjecting the monofluorinated compound **1** to the same reaction conditions afforded the difluorinated compound **2** in good yield. The requirement of adjacent to nitro or nitrile groups limits the scope of this approach. Furthermore, the use of strong bases, particularly *n*-BuLi, prevents the application of this methodology on any substrate bearing sensitive functional groups.

An analogous method for monofluorination of tertiary benzylic C(sp^3)–H bonds adjacent to nitro groups was reported by Loghmani-Khouzani and co-workers in 2006, in which ammonium acetate and Selectfluor were employed under sonochemical conditions to effect the fluorination (Figure 3) [35]. The authors noted that the use of sonochemistry afforded higher yields and shorter reaction times compared to standard stirring conditions with DBU. When employing substrates bearing secondary benzylic sites in the reaction conditions, the difluorinated products were observed exclusively in high yields.

In 2016, Britton and co-workers reported a method for the efficient monofluorination of 4- and 2-alkylpyridines (Figure 4 –

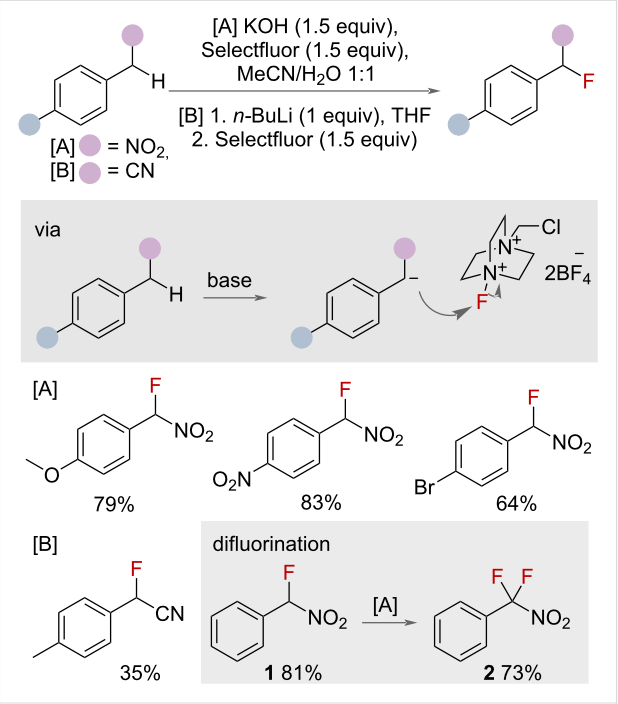

Figure 2: Base-mediated benzylic fluorination with Selectfluor.

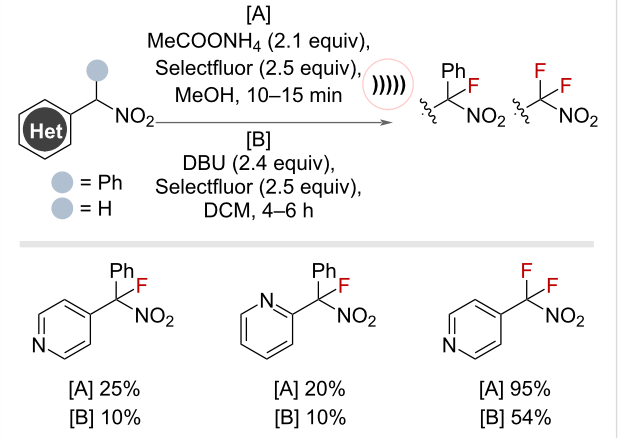

Figure 3: Sonochemical base-mediated benzylic fluorination with Selectfluor.

conditions [A]) [36]. The transformation relied on the polarisation of the heterobenzylic C–H bond, via the intermediate formation of an *N*-sulphonylpyridinium salt, to promote deprotonation. Following a polar mechanism with excess NFSI, the heterobenzyl fluoride is obtained. In the case of product **3**, the authors suggested that the absence of radical clock rearrangement products supported a polar mechanism. Conveniently, when both benzylic and heterobenzylic C–H bonds were present in a substrate, the reaction was selective for the heterobenzylic position, as shown by compound **4**. In 2018, a subsequent publication by the same group detailed the use of increased lithium carbonate and NFSI loadings (conditions [B]) to access the difluorinated products [37]. This report also demonstrated a single example of ^{18}F monofluorination radiolabelling using [^{18}F]NFSI.

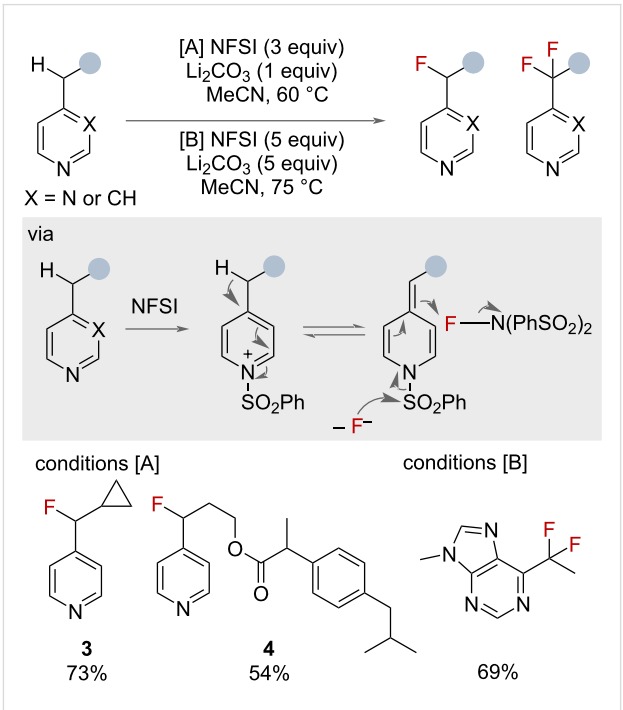

Figure 4: Mono- and difluorination of nitrogen-containing heteroaromatic benzylic substrates.

Electrophilic fluorination of benzylic C–H bonds has been demonstrated as a powerful approach. However, these techniques can be constrained to defined substrate classes and the requirement of using strong bases.

Palladium catalysis

Palladium-catalysed chemistry is pervasive in organic synthesis and can also be used to efficiently fluorinate benzylic C(sp^3)–H bonds. The general blueprint for this transformation follows a metal insertion into the C(sp^3)–H bond followed by C–F reductive elimination [11,22,38].

In 2006, Sanford and co-workers published a seminal and pioneering report into palladium(II)/(IV)-catalysed C–H fluorination of 8-methylquinolines using *N*-fluoro-2,4,6-trimethylpyridinium tetrafluoroborate as an electrophilic "F^+" source under microwave conditions (Figure 5) [39]. Benzylic fluorination was achieved in good yields on three examples, each bearing different functional groups at the 5-position.

The Shi group reported the use of Pd(II) and Selectfluor to enable the enantioselective β-fluorination of α-amino acids

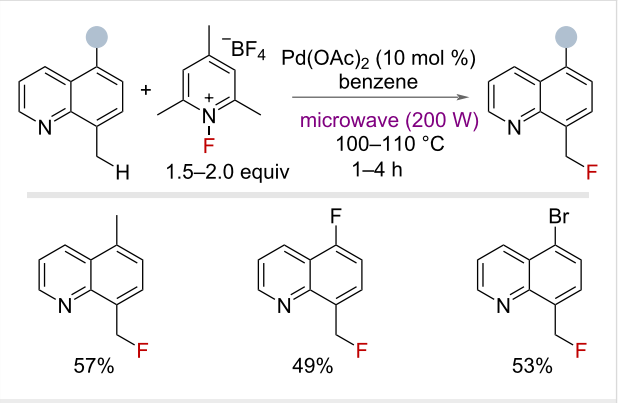

Figure 5: Palladium-catalysed benzylic C–H fluorination with *N*-fluoro-2,4,6-trimethylpyridinium tetrafluoroborate.

(Figure 6) [40]. The presence of 2-(pyridin-2-yl)isopropylamine (PIP) as directing group was essential for the formation of a four-coordinate palladacycle intermediate, defining the stereochemical outcome. Subsequent oxidation to the Pd(IV)–F species, which triggered reductive elimination, afforded the fluorinated product. The non-innocent behaviour of the isobutyrylnitrile co-solvent aided in stabilising the palladacycle through occupying the vacant coordination site. By installing a cleavable directing group, the authors were able to extend the scope reported by Sanford and co-workers outside of 8-aminoquinoline substrates. Multiple electron-donating and withdrawing groups on the ring were tolerated, including the pinacolborane group; however, the methodology was only shown on secondary benzylic positions.

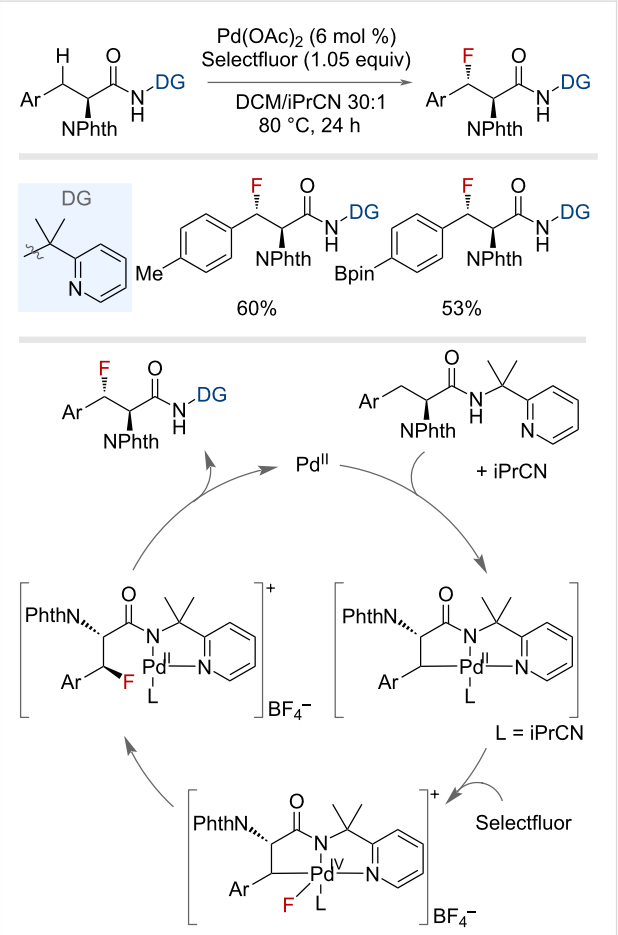

Figure 6: Palladium-catalysed, PIP-directed benzylic C(sp^3)–H fluorination of α-amino acids and proposed mechanism.

The stereoselective benzylic monofluorination of α-amino acids was also reported by Yu and co-workers, employing a similar directing group strategy (Figure 7) [41]. The use of the monodentate directing group 2,3,5,6-tetrafluoro-4-(trifluoromethyl)aniline in conjunction with external ligand **5** facilitated the formation of a series of fluorinated α-amino acids.

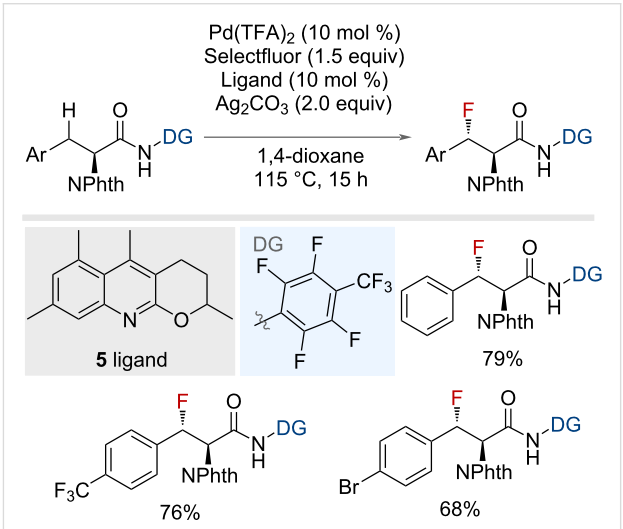

Figure 7: Palladium-catalysed monodentate-directed benzylic C(sp^3)–H fluorination of α-amino acids.

Xu and co-workers also disclosed a palladium-catalysed protocol for the fluorination of simple benzylic substrates bearing a bidentate directing group (Figure 8) [42]. Yields varied from 61–75% across a series of nine benzylic substrates with various substitution patterns on the aromatic ring.

In 2018, Yu and co-workers reported a palladium-catalysed enantioselective fluorination of benzylic C(sp^3)–H bonds with the use of a transient chiral directing group **6** [43]. This approach was effective for the stereoselective fluorination of benzylic positions *ortho* to aldehyde substituents (Figure 9). The choice of a bulky amino, transient, directing group dictated the stereochemical outcome and promoted the C–F reductive elimination through an inner-sphere pathway. A competitive C–O bond formation to afford the acyloxylation product was observed, and

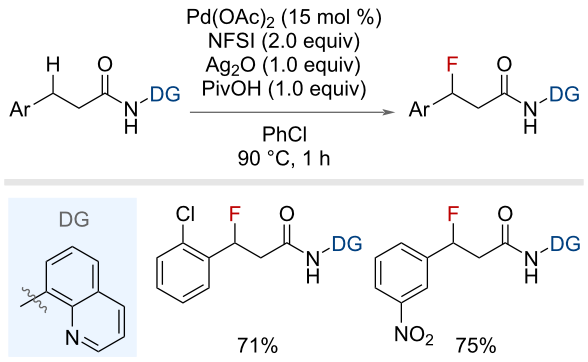

Figure 8: Palladium-catalysed bidentate-directed benzylic C(sp^3)–H fluorination.

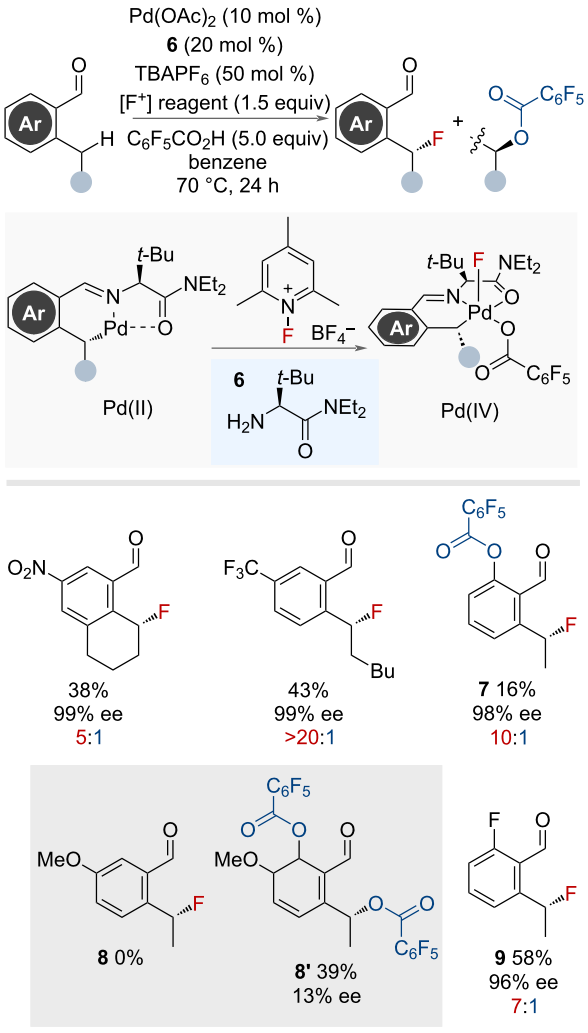

Figure 9: Palladium-catalysed benzylic fluorination using a transient directing group approach. Ratio refers to fluorination (red) vs oxygenation (blue) product.

favoured when using directing groups with less steric bulk. This product had the opposite stereochemistry to the fluorination product suggesting it occurred via a competitive S_N2 pathway. This is supported by the selectivity for C–O bond formation for substrates bearing primary benzylic positions, attributed to the faster rate of S_N2 at the less hindered carbon. The scope was limited to substrates bearing secondary benzylic sites, with various functional groups tolerated. However, substrates bearing electron-donating substituents on the arene were unsuccessful. Without substituents on the ring, aryl C–H activation and subsequent C–O bond formation occurred along with benzylic fluorination (**7**) (low efficiency). The presence of a *p*-methoxy group resulted in a switch in selectivity to acyloxylation **8'** as the major product. The authors displayed the stability of the secondary benzyl fluoride **9** to various S_NAr conditions.

While these methods demonstrate excellent application of palladium catalysts to perform benzylic fluorinations, the need to install a directing group can limit substrate scope. Therefore, methods that can achieve the same transformation in the absence of a directing group are particularly attractive.

Radical benzylic C(sp^3)–H fluorination

Radical fluorination techniques are an attractive approach for benzylic C–H fluorinations that are shown to proceed without a directing group. Carbon-centred radical generation at the benzylic position is known to occur via multiple pathways [44-47]. These radicals can then undergo fluorination via fluorine-atom-transfer (FAT) with various reagents capable of SET pathways, such as Selectfluor and NFSI (Figure 10) [48]. By avoiding the need for strong bases and directing group strategies, this approach opens the door to fluorinating a wider range of benzylic substrates.

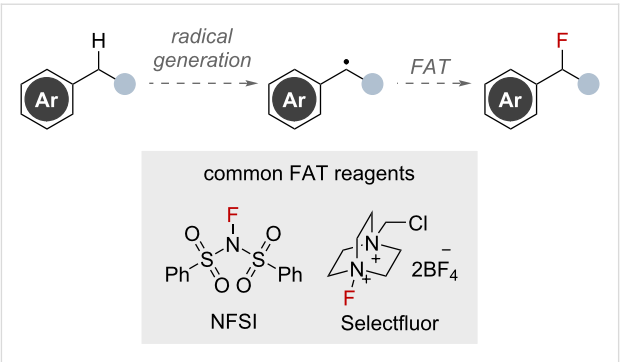

Figure 10: Outline for benzylic C(sp^3)–H fluorination via radical intermediates.

Metal catalysed

In 2013, Lectka and co-workers reported an iron(II)-catalysed benzylic fluorination with Selectfluor (Figure 11) [49]. The

authors were able to use an inexpensive iron source to promote the fluorination of a range of primary and secondary benzylic substrates that were not too electron-rich nor too electron-poor. Interestingly, selectivity for the benzylic position was observed over α-halogenation in substrates bearing carbonyl groups (41% yield for **10**). The conditions were selective for primary benzylic fluorination (**11**) and secondary benzylic fluorination (**12**) in the presence of tertiary benzylic sites. Although no mechanism has been proposed, the authors concluded it likely proceeded via a radical pathway [23].

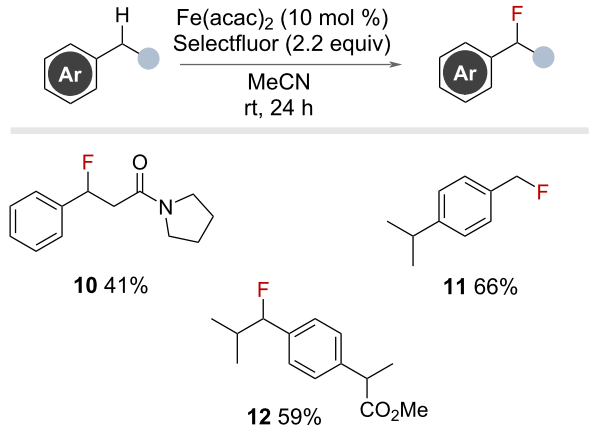

Figure 11: Iron(II)-catalysed radical benzylic C(sp^3)–H fluorination using Selectfluor.

In 2017, Baxter and co-workers introduced a silver-catalysed benzylic fluorination method that employed unprotected amino acids as radical precursors, Figure 12 [50]. Oxidation of glycine by Ag(II) promotes decarboxylation and results in the α-amino radical, which performs a HAT on the benzylic substrate to furnish the benzylic radical. This subsequently undergoes FAT with Selectfluor to produce the desired benzyl fluoride. Increasing amino acid and Selectfluor loadings achieved difluorination of the benzylic substrates. This procedure was demonstrated predominately on primary benzylic substrates, but could be used to effect the fluorination of several secondary and tertiary substrates too.

In 2012, Lectka reported a fluorination of mostly aliphatic C–H bonds that used a molecularly defined copper catalyst with a bis imine ligand, along with co-catalytic *N*-hydroxyphthalimide and a phase-transfer catalyst [51]. Although only a few benzylic substrates were shown, this report provided important precedent for the ability of copper fluoride species to deliver fluorine to carbon radicals. Following on from this, Stahl and co-workers reported in 2020 an efficient synthesis of secondary and tertiary benzyl fluorides via a copper-catalysed radical relay mechanism. Excess NFSI functioned as both a fluorine source

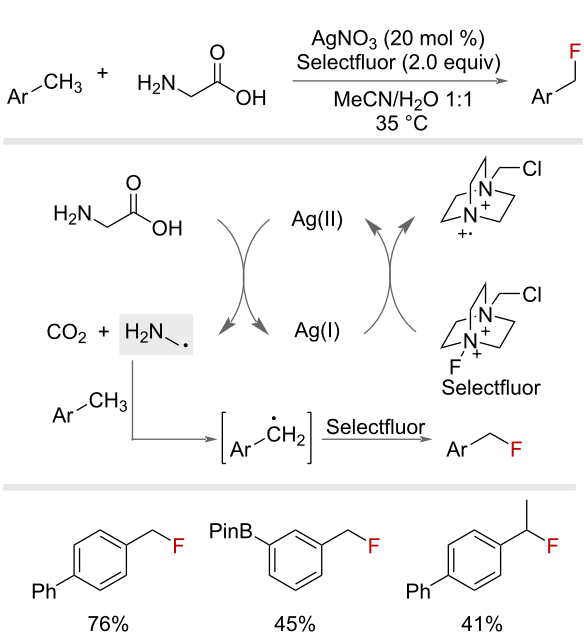

Figure 12: Silver and amino acid-mediated benzylic fluorination.

and HAT reagent precursor (Figure 13) [20]. Fluorine abstraction from NFSI by copper(I) generates an *N*-centred radical that is selective for benzylic C(sp^3)–H bonds [52,53], affording the benzylic radical via HAT. Subsequent FAT with the in situ-generated Cu(II)F or NFSI affords the benzyl fluoride. Substrates bearing secondary and tertiary benzylic sites were successful in the reaction. However, primary benzylic substrates were not tolerated, instead affording the $N(SO_2Ph)_2$ adduct (e.g., product **13**) in moderate yields. The authors noted that several secondary and tertiary benzyl fluorides were unstable to silica during isolation or storage in glass vessels, and therefore, demonstrated several downstream diversifications of the benzyl fluorides.

Sevov, Zhang and co-workers reported in 2023 a stable copper(III) fluoride complex that was capable of C(sp^3)–H activation and fluorination, including on one tertiary and five secondary benzylic substrates (Figure 14) [54]. This work utilised electrochemical oxidation with a nucleophilic source of fluoride, CsF, to regenerate the trisligated copper(III) fluoride complex.

In 2016, Silas reported an intramolecular fluorine-atom-transfer (FAT) from an *N*-fluorinated amide to a pendant carbon-based radical formed from an iron catalyst (Figure 15) [55,56]. This concept of fluorine transfer through a 6-membered transition state was shown to work efficiently from primary, as well as secondary, benzylic radicals that have an *ortho*-substituted *tert*-butylamide moiety.

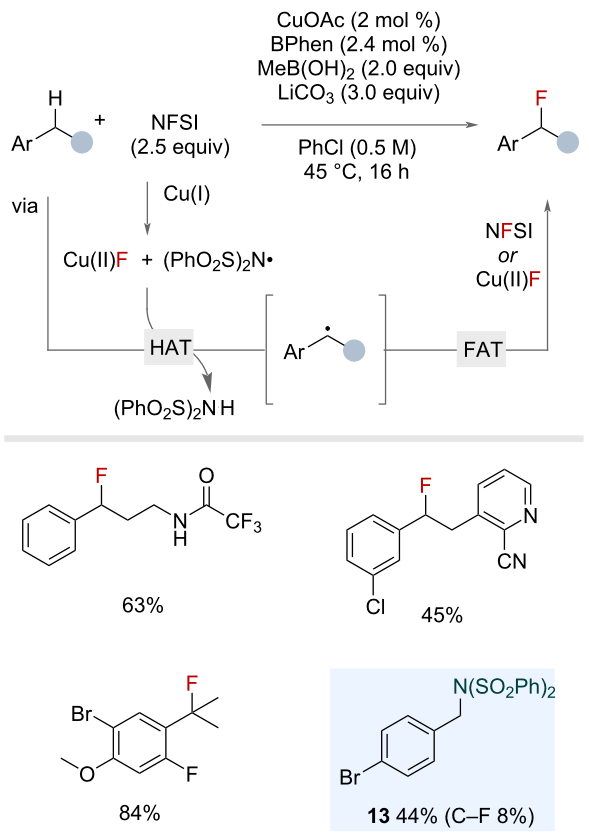

Figure 13: Copper-catalysed radical benzylic C(sp^3)–H fluorination using NFSI.

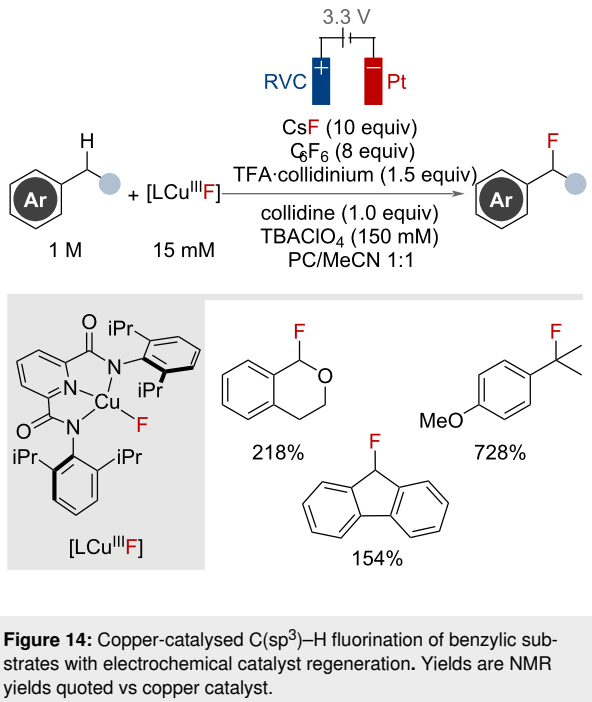

Figure 14: Copper-catalysed C(sp^3)–H fluorination of benzylic substrates with electrochemical catalyst regeneration. Yields are NMR yields quoted vs copper catalyst.

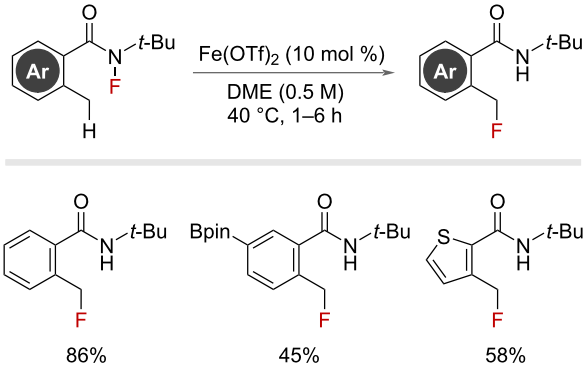

Figure 15: Iron-catalysed intramolecular fluorine-atom-transfer from N–F amides.

Finally, while not focussing on benzylic substrates, a vanadium-mediated fluorination of aliphatic C–H bonds was reported by Chen and co-workers, which also included five benzylic substrates (Figure 16) [57].

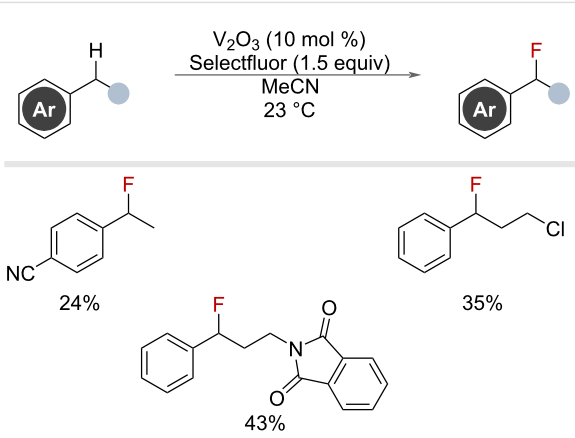

Figure 16: Vanadium-catalysed benzylic fluorination with Selectfluor.

Metal free

Numerous reports have detailed metal-free radical C(sp^3)–H fluorinations suitable for benzylic substrates. These typically involve the generation of a HAT reagent that is selective for benzylic C–H bonds and facilitates the generation of a benzylic radical. Subsequent FAT, from a fluorinating reagent, yields the desired benzyl fluorides. In 2013, Inoue and co-workers demonstrated the use of catalytic *N*,*N*-dihydroxypyromellitimide (NDHPI) as a precursor for *N*-oxyl radicals that serve as the HAT reagent. Selectfluor was employed as the FAT reagent, generating an *N*-centred radical on the spent Selectfluor that can regenerate the *N*-oxyl radicals from NDHPI (Figure 17) [58]. The secondary and tertiary substrates selected were shown to undergo this transformation in moderate to good yields.

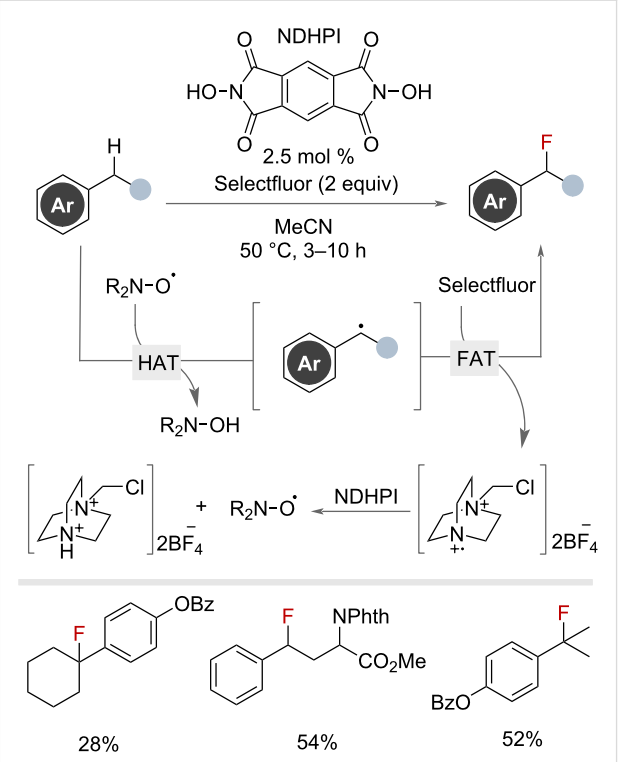

Figure 17: NDHPI-catalysed radical benzylic C(sp^3)–H fluorination with Selectfluor.

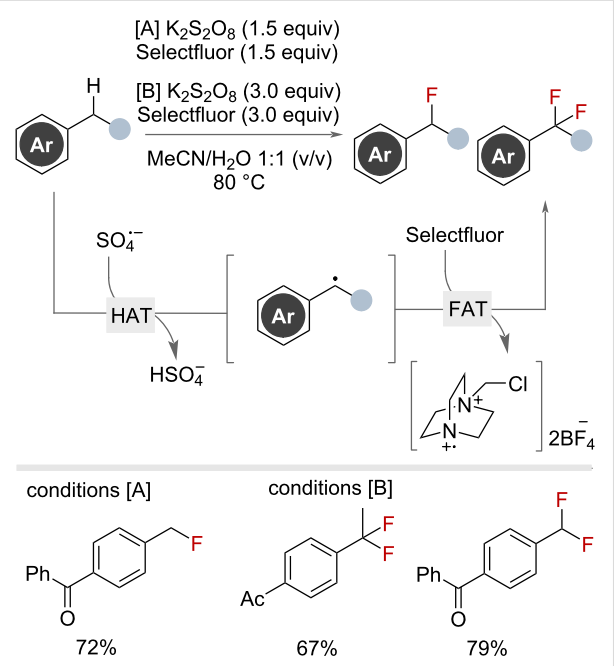

Figure 18: Potassium persulfate-mediated radical benzylic C(sp^3)–H fluorination with Selectfluor.

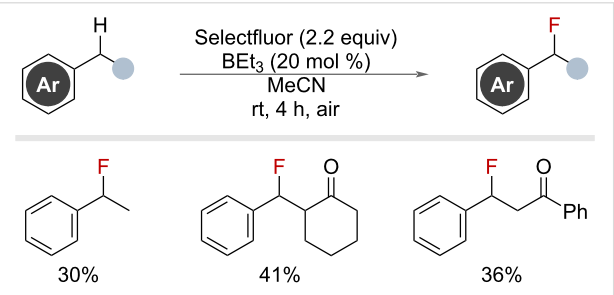

Figure 19: Benzylic fluorination using triethylborane as a radical chain initiator.

The Yi group published a complementary method using stoichiometric potassium persulfate as the HAT reagent precursor (Figure 18) [59]. The authors proposed that under heating $K_2S_2O_8$ decomposed to $SO_4^{\bullet-}$ which could then abstract the benzylic hydrogen to generate the benzylic radical. Fluorine-atom-transfer with Selectfluor then afforded the benzyl fluoride. Other fluorinating reagents such as NFSI or DAST did not perform as well. By varying the loadings of $K_2S_2O_8$ and Selectfluor, selectivity for the mono- (conditions A) or difluorination (conditions B) products could be achieved.

Building on their previous iron-catalysed work, Figure 11, Lectka and co-workers reported in 2014 the use of triethylborane as a radical chain initiator for C(sp^3)–H fluorination. They demonstrated this reaction primarily on alkyl substrates, but 5 secondary benzylic substrates were also shown to undergo the reaction effectively (Figure 19) [60]. The authors proposed the transformation occurred via established triethylborane autoxidation initiation and propagation methods, noting the importance of high purity reagents and the presence of O_2.

Radical fluorination of hetereobenzylic C(sp^3)–H bonds was demonstrated by Van Humbeck and co-workers in 2018, who enabled the fluorination of aza-heterocycles at the benzylic position using Selectfluor (Figure 20) [61]. The authors proposed the formation of a charge-transfer complex between the heterocycle and Selectfluor, capable of promoting an ET/PT or PCET pathway to furnish the carbon-centred radical at the heterobenzylic position. Fluorine-atom-transfer with Selectfluor then afforded the desired product. Secondary and tertiary substrates worked well under the reaction conditions, whereas primary positions afforded low yields (**14**). No additive was required to achieve the desired selectivity, but in some cases the addition of small amounts of iron salt $[FeCl_4][FeCl_2(dmf)_3]$ improved yields.

In 2022, Pieber and co-workers reported a benzylic fluorination of phenylacetic acids via a charge-transfer complex (Figure 21) [62]. The authors proposed that the combination of Selectfluor and DMAP spontaneously produced the Selectfluor radical dication ($TEDA^{2+\bullet}$), which served as a radical chain carrier

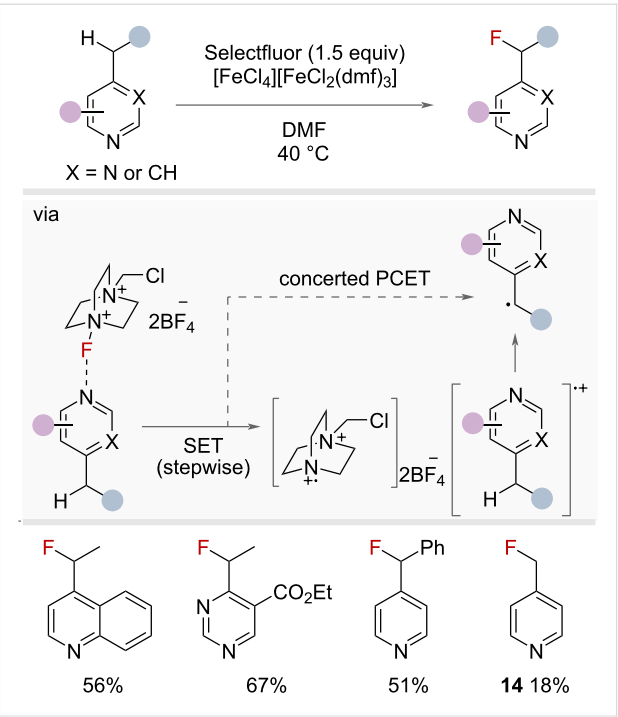

Figure 20: Heterobenzylic C(sp^3)–H radical fluorination with Selectfluor.

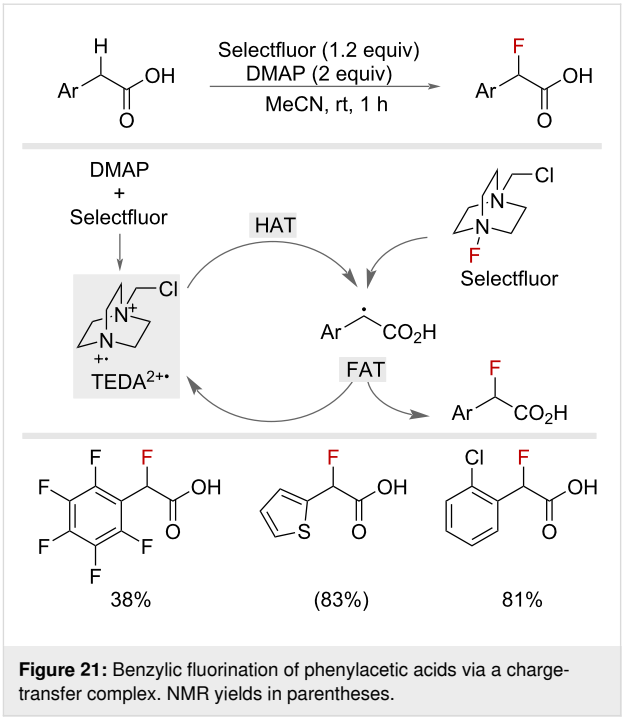

Figure 21: Benzylic fluorination of phenylacetic acids via a charge-transfer complex. NMR yields in parentheses.

capable of facilitating HAT to produce a benzylic radical. Fluorine-atom-transfer (FAT) with Selectfluor then gave the benzyl fluoride. The low acidity of phenylacetic acids in polar aprotic solvents disfavoured decarboxylation (via an SET pathway) promoting HAT from the benzylic position. By using a mixture of 1:1 MeCN/H_2O and heating, the decarboxylation pathway could be enabled to afford primary benzyl fluorides.

In the same year, Barham and co-workers also showed that the radical dication $TEDA^{2+\bullet}$ was capable of HAT on unactivated C(sp^3)–H, enabling fluorination at these positions [63]. This work utilised *para*-fluorobenzoates as both photocatalysts or photo-auxiliaries and was demonstrated on a number of benzylic examples.

Photochemical

Photochemical methods have proven to be powerful tools in the generation of reactive intermediates, including benzylic radicals [64-67]. Oxidative photochemical functionalisation of benzylic C–H bonds to benzylic radicals can be envisaged to occur through three different pathways (Figure 22). Upon excitation by light, photoredox reagents can induce a number of changes in benzylic substrate **I**, either directly or via mediated processes. Hydrogen-atom-transfer (HAT) results in the concerted transfer of an electron and a proton from the benzylic substrate resulting in the benzylic radical **II** – pathway [A] [67]. This radical can also be accessed via sequential oxidative single-electron-transfer (SET) and proton-transfer (PT) steps (pathway [B]), or concerted proton-coupled electron transfer (PCET) (pathway [C]). Benzylic radicals can then react with FAT reagents to give the desired benzyl fluoride products [66,68].

Several photochemical benzylic fluorination methodologies proposed to proceed via radical pathways have been reported. Chen and co-workers published a pioneering report in 2013 that used photocatalyst 9-fluorenone under visible-light irradiation to generate a photoexcited aryl ketone, capable of HAT to

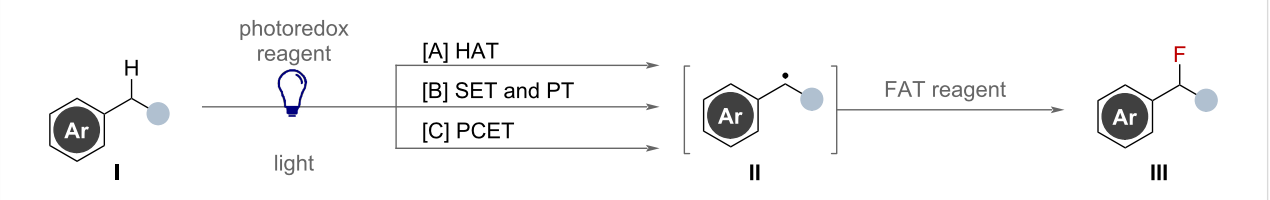

Figure 22: Oxidative radical photochemical benzylic C(sp^3)–H strategies.

promote benzylic fluorination with Selectfluor (Figure 23) [69]. The reaction tolerated an exceptional range of functional groups and enabled the fluorination of primary, secondary and tertiary benzylic substrates. The methodology was amenable to scale up, demonstrating the gram-scale synthesis of product **15** in 85% yield.

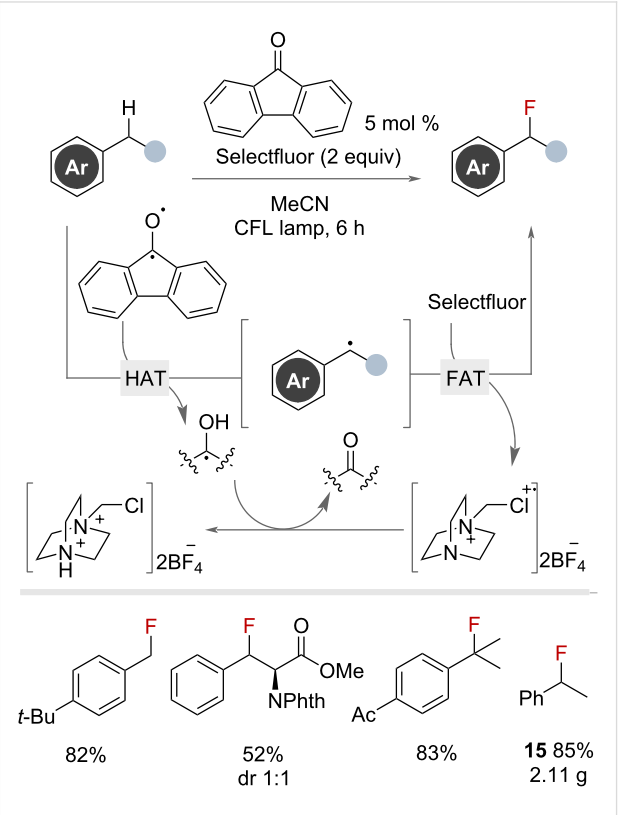

Figure 23: 9-Fluorenone-catalysed photochemical radical benzylic fluorination with Selectfluor.

The authors recognised the difficulty in sequential fluorination and noted that the use of a more electron-rich photocatalyst would be required to promote hydrogen abstraction. By changing the photocatalyst to xanthone and replacing Selectfluor with 3 equivalents of Selectfluor II, the authors afforded *gem*-difluoride products of primary and secondary benzylic substrates in high yields (Figure 24).

In 2014, Lectka and co-workers showed that 1,2,4,5-tetracyanobenzene could be used under ultraviolet light irradiation as a photocatalyst in the fluorination of benzylic C(sp^3)–H bonds (Figure 25) [70]. Selectfluor was used as the FAT reagent to furnish a selection of primary, secondary and tertiary benzyl fluorides with different functional groups on the aromatic ring and adjacent to the benzylic position. Mechanistic investigations suggested an initial electron transfer to generate a radical cation en route to the intermediate benzylic radical, rather than a

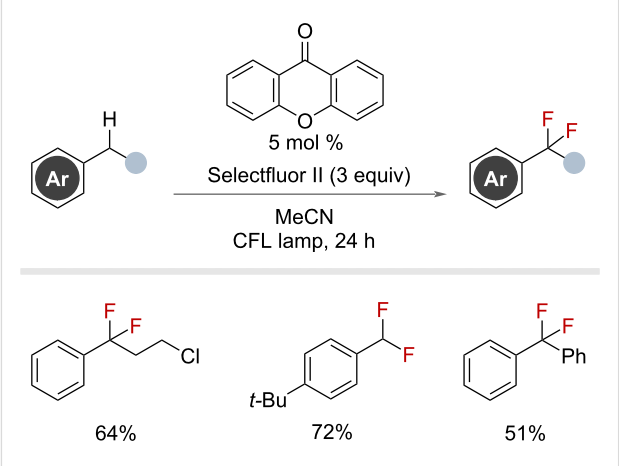

Figure 24: Xanthone-photocatalysed radical benzylic fluorination with Selectfluor II.

HAT process, however, the authors did not distinguish between a stepwise SET and subsequent PT or concerted PCET mechanism. The yields observed using this approach were broadly similar to the same group's iron-catalysed method (Figure 11).

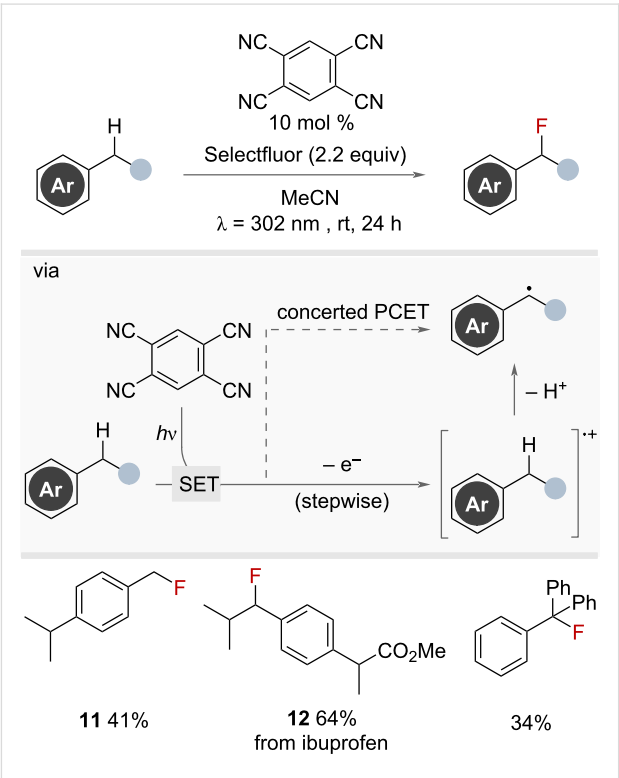

Figure 25: 1,2,4,5-Tetracyanobenzene-photocatalysed radical benzylic fluorination with Selectfluor.

In the same year, Cantillo, de Frutos, Kappe and co-workers reported a similar approach, using xanthone as their photocatalyst in a continuous flow system (Figure 26) [71]. The authors were

able to demonstrate rapid benzylic fluorination of 13 substrates, requiring residence times below 30 min.

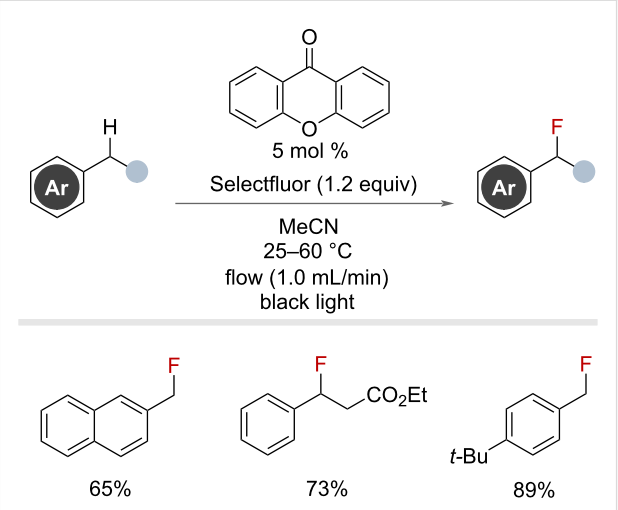

Figure 26: Xanthone-catalysed benzylic fluorination in continuous flow.

The use of photoexcited aryl ketones was further expanded in 2016 by Lectka and co-workers who reported the use of 5-dibenzosuberenone as a photosensitive arylketone catalyst in the fluorination of phenylalanine residues in peptides (Figure 27) [72]. This work demonstrated high yields and selectivity for peptides bearing phenylalanine residues, including tripeptides, such as **16**.

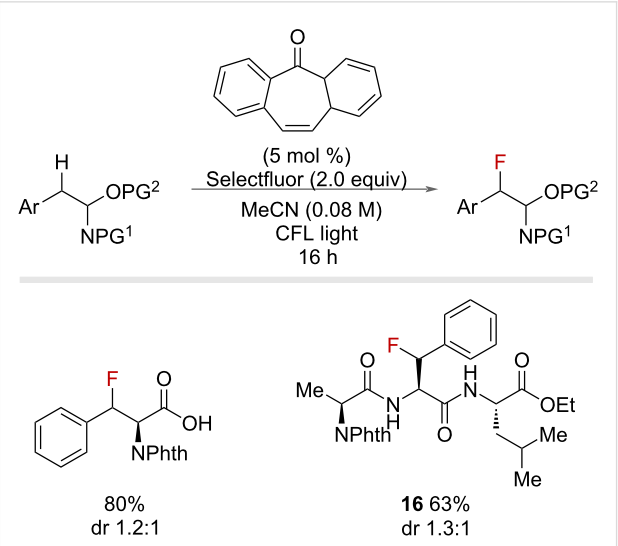

Figure 27: Photochemical phenylalanine fluorination in peptides.

In 2015, Britton and co-workers reported a photochemical HAT-guided approach using NFSI as their fluorine source [73]. The authors demonstrated the use of a decatungstate photocatalyst as a species capable of hydrogen-atom abstraction and use it to access a range of secondary and tertiary benzyl fluorides in moderate to excellent yields. AIBN was also demonstrated as a suitable radical initiator for this transformation, albeit in reduced yields. Interestingly, for substrates bearing both primary and secondary benzylic C(sp^3)–H bonds, AIBN exhibited selectivity for the primary position and the opposite was seen for the decatungstate catalyst (Figure 28). The authors attributed this to the increased solubility and concentration of NFSI in the AIBN conditions, which were performed at elevated temperatures, promoting facile trapping of a primary radical. In contrast, the decatungstate conditions, which operated at room temperature where NFSI is not completely dissolved and is therefore not as concentrated in solution, allows for equilibration between benzylic radicals towards the more stable secondary radical. This switch in selectivity provides an interesting tool for selective fluorination in substrates with multiple benzylic sites.

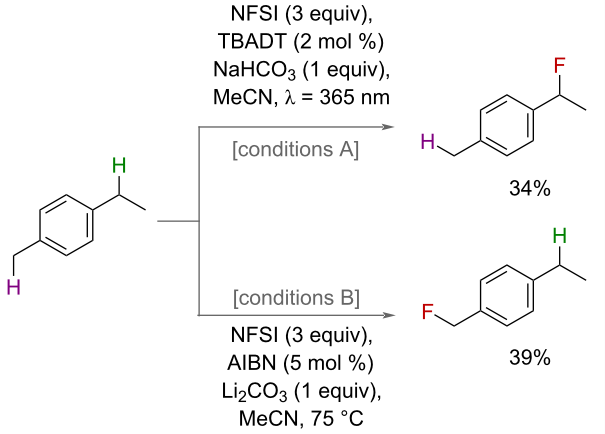

Figure 28: Decatungstate-photocatalyzed versus AIBN-initiated selective benzylic fluorination.

In 2017, Wu and co-workers disclosed the use of catalytic amounts of the organic dye Acr^+-Mes under visible-light irradiation in combination with stoichiometric amounts of Selectfluor to achieve benzylic fluorination (Figure 29) [74]. It was proposed that a SET between Selectfluor and the photoexcited catalyst liberated fluoride and a potent HAT reagent capable of generating the benzylic radical, which then performs FAT with Selectfluor to generate the desired benzyl fluoride. Alternatively, the benzylic radical could further be oxidized to the cation, and in the process, regenerating the ground-state catalyst. The benzylic cation would then be trapped by the previously liberated fluoride. This reactivity was demonstrated on one primary, one tertiary and eight secondary substrates. When diphenylmethane substrates were subjected to the reaction conditions benzylic ketone products were observed.

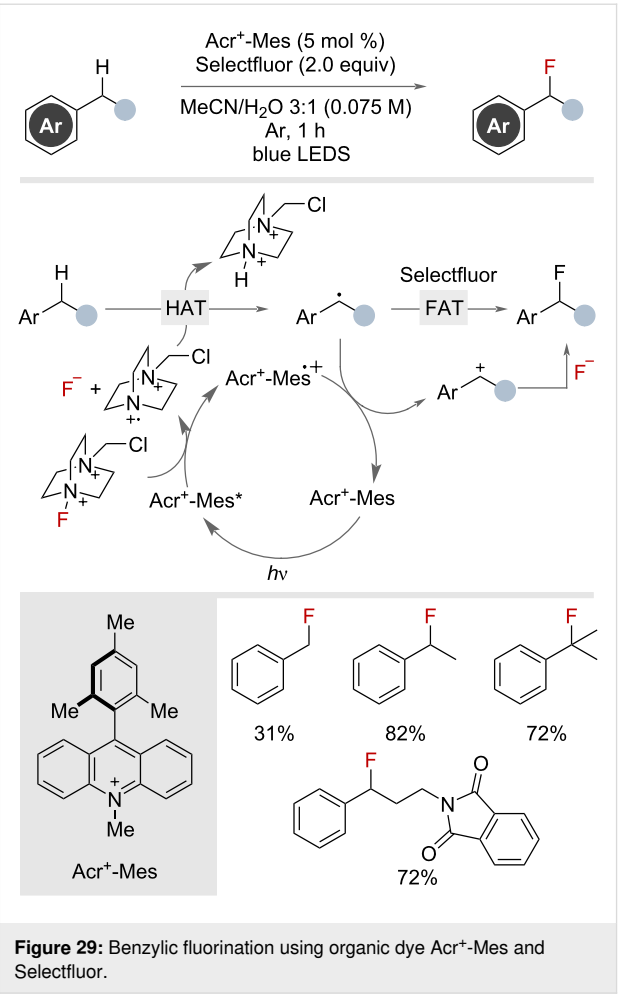

Figure 29: Benzylic fluorination using organic dye Acr$^+$-Mes and Selectfluor.

As highlighted by the examples in this section, radical-based approaches enable the fluorination of a diverse range of benzylic substrates, which rely on the use of FAT reagents, such as Selectfluor, NFSI or copper fluoride complexes.

Nucleophilic benzylic C(sp^3)–H fluorination

Nucleophilic fluorine sources can be more economical from financial and waste perspectives when compared to reagents such as Selectfluor and NFSI [75-77]. This type of fluorine source is also preferred for positron emission tomography (PET) imaging with [^{18}F]fluoride [78]. Despite the challenges associated with nucleophilic fluoride, including solubility issues of metal fluoride salts, safety issues with hydrogen fluoride, poor nucleophilicity [79], and side reactivity as a base [75,79], a few elegant examples of nucleophilic benzylic C(sp^3)–H fluorination have been reported.

Metal catalysis

Fluoride sources have been used in combination with transition-metal complexes to generate metal–fluorine bonds capable of FAT to benzylic substrates. In a follow-up to their work using electrophilic fluorine sources for palladium-catalysed benzylic C–H fluorination (Figure 5), the Sanford group demonstrated in 2012 the same transformation could be achieved with nucleophilic fluoride sources too (Figure 30) [77]. This process involved an initial quinoline-directed C–H activation by Pd(II), followed by oxidation to generate a Pd(IV)–fluoride complex capable of C–F reductive elimination to generate the primary benzyl fluoride. Under this protocol, eleven 8-methylquinoline derivatives could be fluorinated in yields of up to 70%.

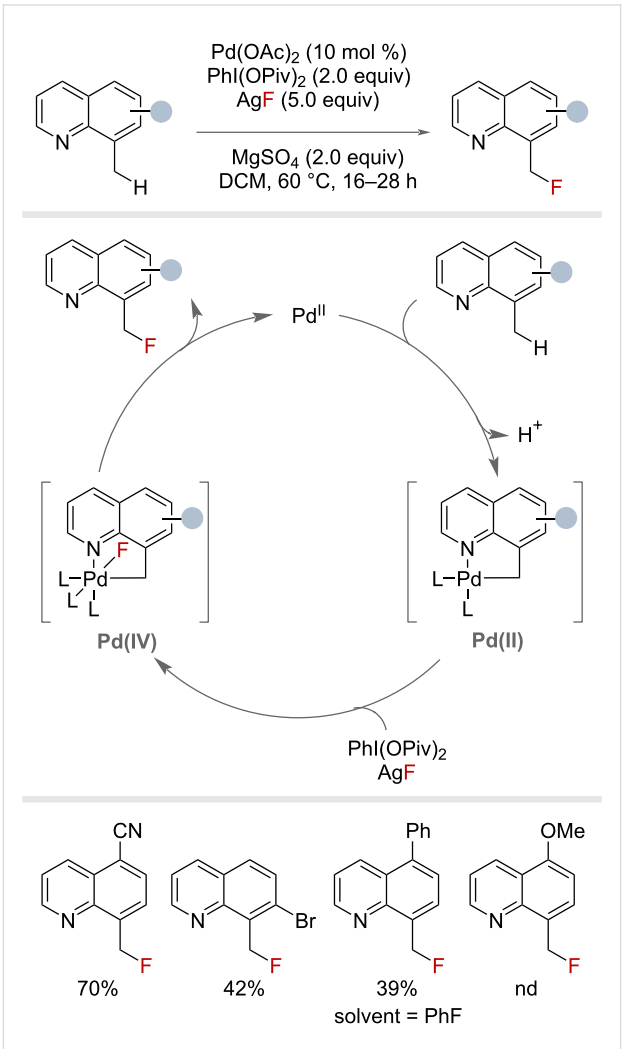

Figure 30: Palladium-catalysed benzylic C(sp^3)–H fluorination with nucleophilic fluoride.

In 2013, Groves and co-workers reported the use of manganese salen and manganese porphyrin catalysts in the preparation of a range of secondary benzyl fluorides via C–H fluorination (Figure 31) [80]. Substrates bearing electron-withdrawing substituents on the aryl group benefitted from fewer HF equivalents and the addition of silver fluoride. A follow-up report showed that only minor alterations to the conditions were

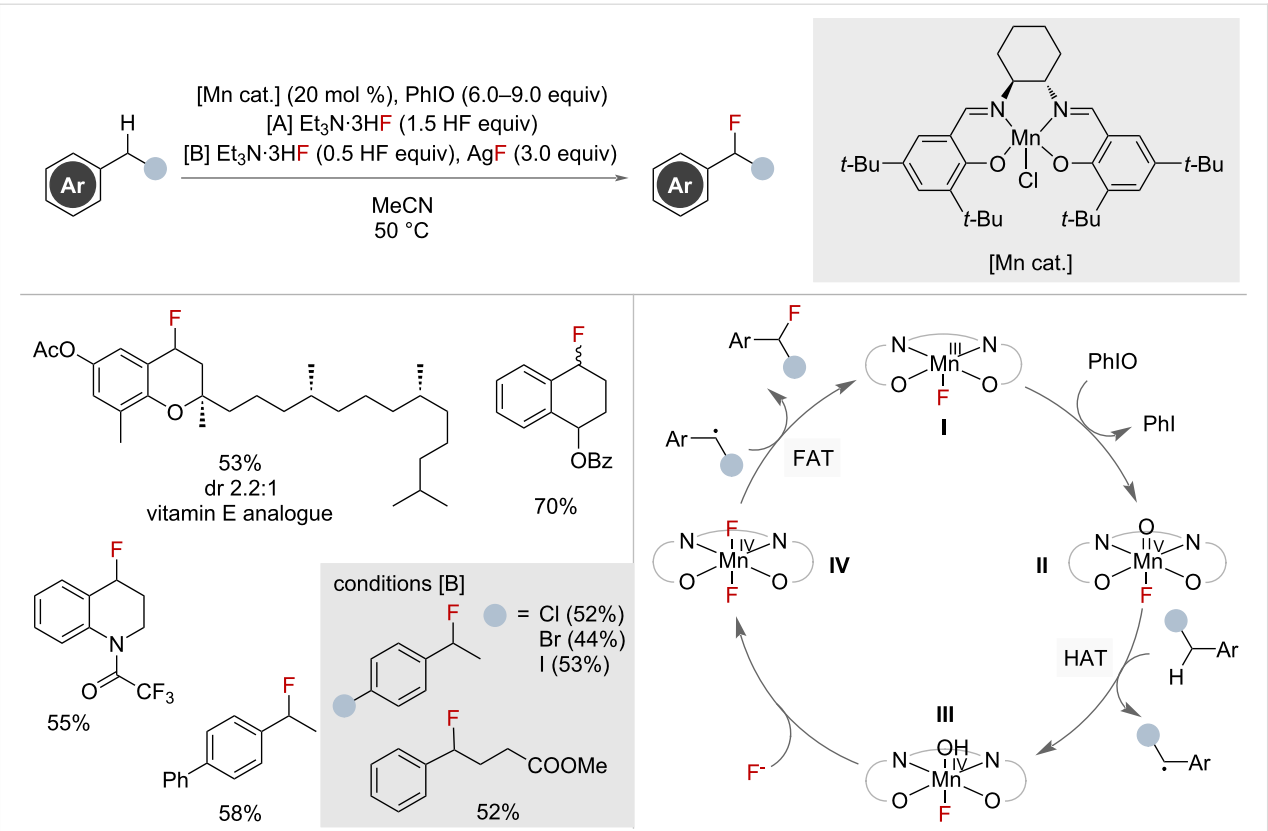

Figure 31: Manganese-catalysed benzylic C(sp^3)–H fluorination with AgF and $Et_3N·3HF$ and proposed mechanism. ^{19}F NMR yields in parentheses.

needed to make the process amenable to the use of [^{18}F]KF, facilitating radiofluorination [81]. Both reports used hypervalent iodine as a super-stoichiometric oxidant. The catalyst system has precedent for also facilitating oxygenation reactions [82], which was observed as a competing pathway under these conditions.

The catalytic cycle proposed by the authors begins at resting state **I** (Figure 31), which is generated in situ and is subsequently oxidised to Mn(V)-oxo species **II** by hypervalent iodine oxidant PhIO. This can perform a HAT from the benzylic substrate, in turn generating a benzylic radical and Mn(IV)-hydroxy species **III**. Ligand exchange with the fluoride source affords complex **IV**, which performs FAT with the benzylic radical furnishing the desired product and regenerating **I**.

Photochemical methods

Photochemical methods that make use of fluoride to quench benzylic carbocations in order to form a new C–F bond have proved effective for functionalising a broad range of benzylic substrates. Two concurrent publications by the Doyle and Musacchio groups in 2021 and 2022 demonstrated the effective use of photochemical oxidative radical-polar crossover mechanisms to achieve this.

The Doyle group reported the use of an iridium-catalysed system in this context with $Et_3N·3HF$ as the fluoride source (Figure 32) [83]. Photoexcitation of the Ir(III) catalyst **I** with blue light resulted in the photoexcited Ir(III)* catalyst, which was capable of performing a single-electron reduction on *N*-acyloxyphthalimide, promoting decarboxylation, releasing CO_2, a methyl radical, anionic phthalimide and an Ir(IV) species. The resultant methyl radical displayed high affinity for benzylic HAT, in turn affording a benzylic radical and methane. The Ir(IV) species then oxidised the benzylic radical to the benzylic cation regenerating the ground-state iridium species, completing the catalytic cycle. Attack of the benzylic cation by fluoride, from $Et_3N·3HF$, provided the benzylic fluoride product. Although a majority of examples were performed with an excess of benzylic substrate (up to 6 equivalents with respect to methyl radical precursor), a broad scope with excellent functional group tolerance was demonstrated. Difluorination was possible under these conditions, but required first generating the monobenzyl fluoride in situ from the corresponding benzyl chloride before undergoing the photochemical transformation to give the difluorination product. The authors showed that this HAT-radical-polar crossover approach could be applied to other nucleophiles, including water to give benzylic alcohols, or methanol to give methoxy products.

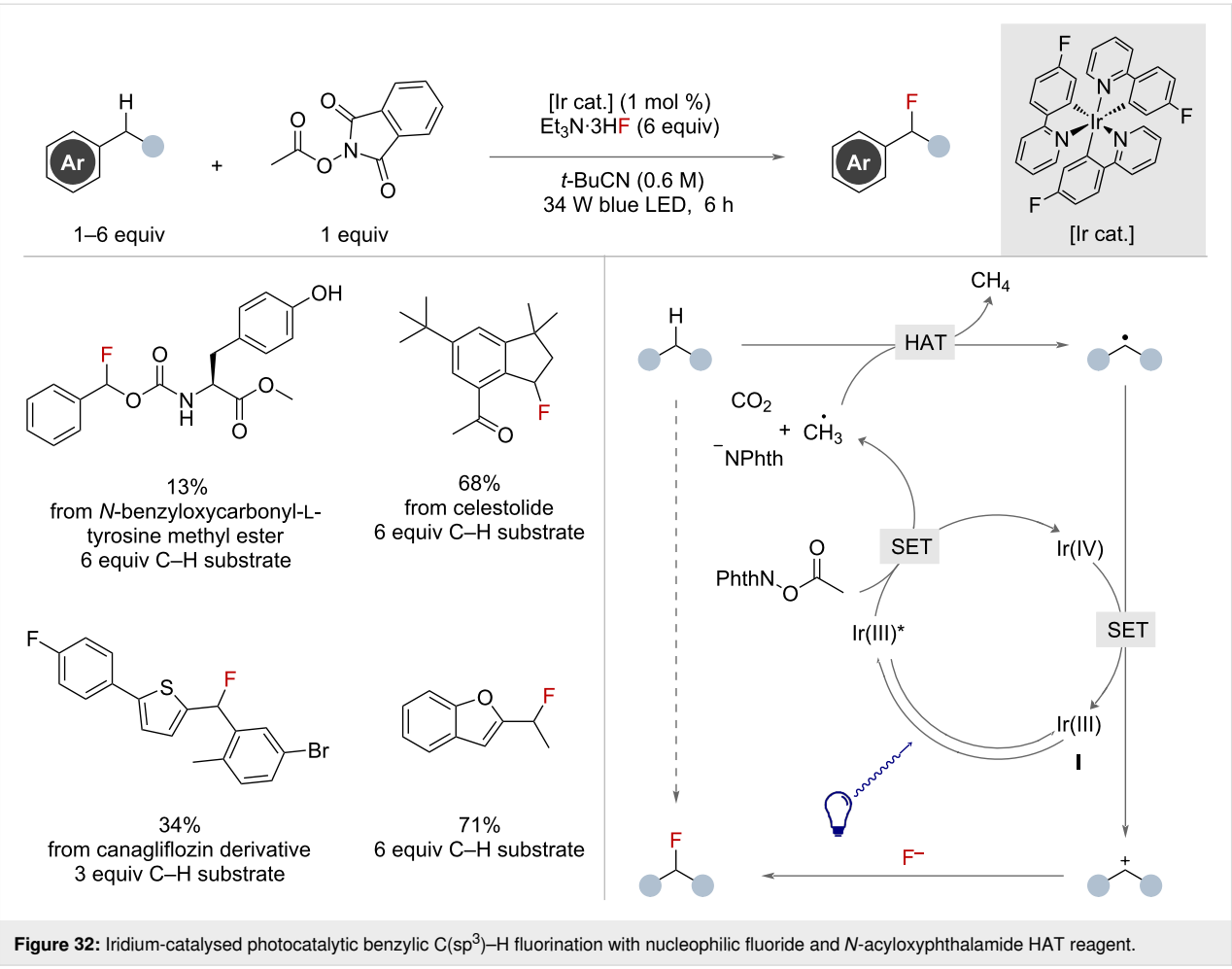

Figure 32: Iridium-catalysed photocatalytic benzylic C(sp^3)–H fluorination with nucleophilic fluoride and *N*-acyloxyphthalamide HAT reagent.

Musacchio and co-workers reported a similar approach for benzylic fluorination (Figure 33) [84], which followed a similar mechanistic blueprint to that reported by the Doyle group. Using *tert*-butoxide radicals, generated from reduction of *tert*-butyl benzoperoxoate (TBPB), selective benzylic HAT afforded the benzylic radical. Subsequent oxidation by Ir(IV) generated the benzylic cation that could be trapped by fluoride to afford the benzyl fluorides. An impressive scope with broad functional group tolerance, including bioactive molecules, was detailed in their work. Similar to the Doyle report, excess C–H substrate (up to 3 equivalents with respect to HAT reagent) was required in many cases, with the exception of tertiary benzylic substrates, which required only 1 equivalent of substrate and 2 equivalents of HAT reagent. Difluorination could be achieved using excess fluoride and HAT reagent. Other nucleophiles were amenable to the reaction conditions, allowing various benzylic functionalisation reactions, including acetoxylation and chlorination.

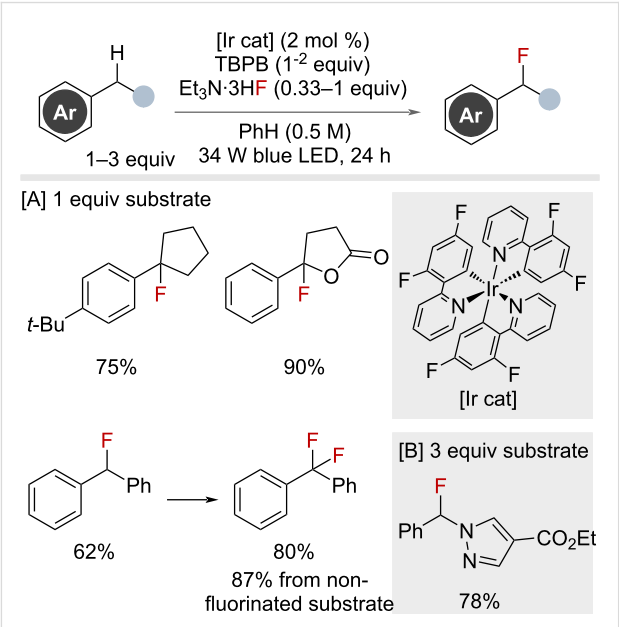

Figure 33: Iridium-catalysed photocatalytic benzylic C(sp^3)–H fluorination with TBPB HAT reagent.

In 2023, Hamashima and co-workers disclosed an analogous, non-photochemical, silver-catalysed HAT radical-polar

crossover mechanism for nucleophilic benzylic fluorination (Figure 34) [85]. The authors proposed a similar mechanistic pathway to the photochemical methods, citing the use of amide ligands as important for modulating the silver catalyst stability and oxidation potentials.

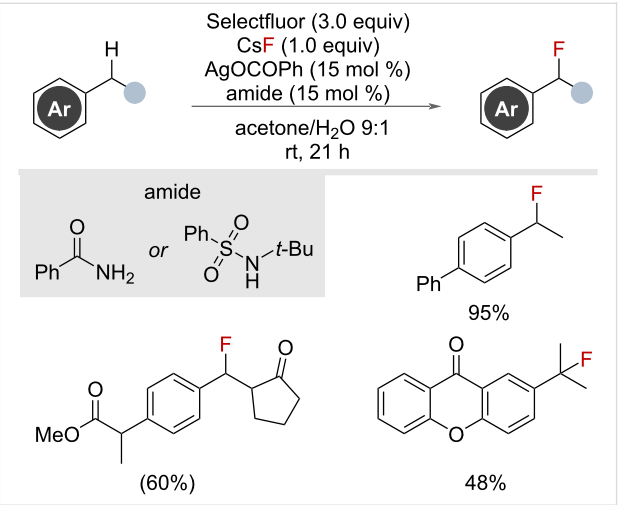

Figure 34: Silver-catalysed, amide-promoted benzylic fluorination via a radical-polar crossover pathway.

Electrochemical methods

Synthetic electrochemistry is a powerful tool offering excellent control over reaction kinetics and selectivity [86]. Electrochemical oxidation has been demonstrated as an efficient means for generating benzylic cations, allowing for the introduction of a host of functional groups [68]. This approach can also be applied for nucleophilic fluorination of benzylic substrates. This occurs via sequential electron-transfer and proton-transfer steps, as outlined in Figure 35 [87].

Single-electron oxidation of benzylic substrate **I** at the anode generates radical cation **II**. The acidity of benzylic protons is augmented after oxidation of the adjacent π-system, facilitating rapid proton transfer at this position, resulting in benzylic radical **III** [13,88]. Single-electron oxidation of the resulting benzylic radical is facile and expected to occur readily under the cell potentials required to initiate the first single-electron transfer, resulting in benzylic cation **IV** [89,90]. This species can then be captured by fluoride to give benzylic fluoride product **V**.

HF·amine ionic liquids are a popular choice of fluoride source in organic electrochemistry as their function is three-fold; as a fluoride source, as a supporting electrolyte and as a proton source, allowing for the hydrogen-evolution reaction as the counter electrode process [91]. Benzylic fluorination with these reagents has been observed as a side-product in the electrochemical generation of hypervalent fluoroiodane reagents [92,93].

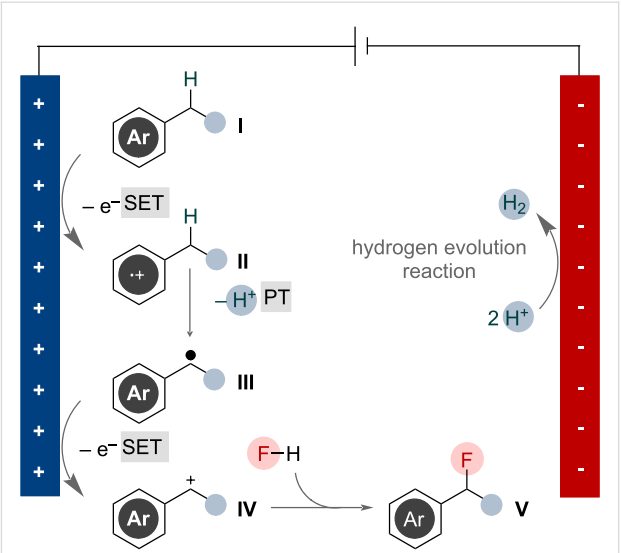

Figure 35: General mechanism for oxidative electrochemical benzylic C(sp^3)–H fluorination.

In 2000, Fuchigami and co-workers demonstrated the effectiveness of these reagents in the oxidative electrochemical fluorination of benzylic positions adjacent to thiocyanate groups (Figure 36) [94]. The authors proposed anodic oxidation to generate a radical cation that can undergo facile α-proton elimination facilitated by the strongly electron-withdrawing thiocyanate group. Subsequent anodic oxidation affords a cationic species that can be trapped by fluoride to afford the product. This reaction was demonstrated on four substrates in yields of 47–71%. The authors noted a sensitivity to the fluoride source, with $Et_3N{\cdot}5HF$ determined to be superior, and reaction temperature, as demonstrated by fluctuations in the yield of product **17** depending on the reaction temperature.

In 2003, Fuchigami and co-workers also reported the use of $Et_3N{\cdot}5HF$ in combination with the ionic liquid 1-ethyl-3-methylimidazolium trifluoromethanesulfonate ([emim][OTf]) for the fluorination of phthalides at the benzylic position (Figure 37) [95]. It was considered that the zwitterionic nature of the ionic liquid served two purposes. Firstly, to enhance the nucleophilicity of fluoride, and secondly, to improve the electrophilicity of the phthalide cationic intermediate generated by the SET/PT/SET sequence. Model substrate **18** could be fluorinated in excellent yield, but the yields decreased upon variation of the substrate. A poor selectivity for primary and secondary benzylic positions was observed when both positions were present, as highlighted by the formation of **19** and **20** in equal yields from the same substrate.

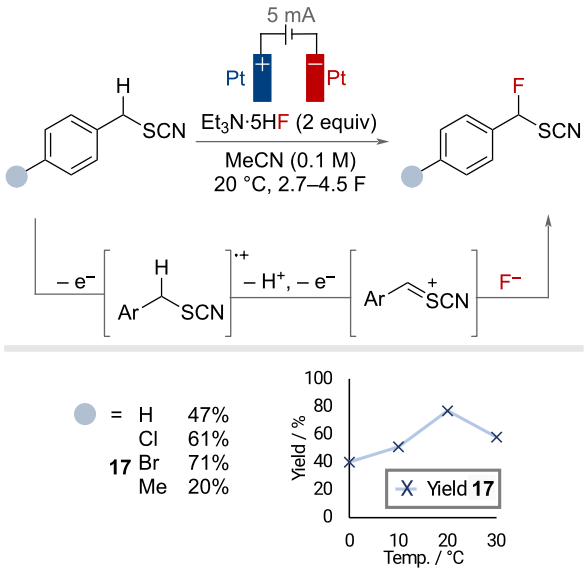

Figure 36: Electrochemical benzylic C(sp^3)–H fluorination with HF·amine reagents.

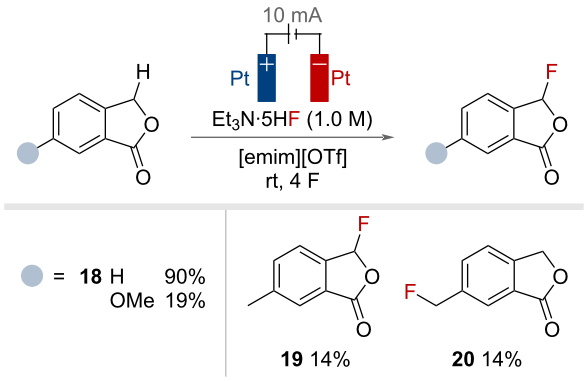

Figure 37: Electrochemical benzylic C(sp^3)–H fluorination with 1-ethyl-3-methylimidazolium trifluoromethanesulfonate ([emim][OTf]) and HF·amine reagents.

In the same year, Yoneda and co-workers reported the electrochemical benzylic fluorination of four phenylacetic acid esters and 1-tetralone (Figure 38) [96]. $Et_4N{\cdot}2HF$ proved to be the best of the HF·amine reagents screened. The reaction was conducted under constant potential conditions, using cyclic voltammetry prior to electrolysis to determine the appropriate oxidation potential required for each substrate. Under these conditions, yields of up to 65% were achieved. Product **21** could be resubjected to the reaction conditions, affording difluoride **22** in 46% yield.

Metal fluorides are an economical source of nucleophilic fluorine, but are sparingly soluble in organic solvents. To overcome this, in 2012, Fuchigami and co-workers used polyethylene

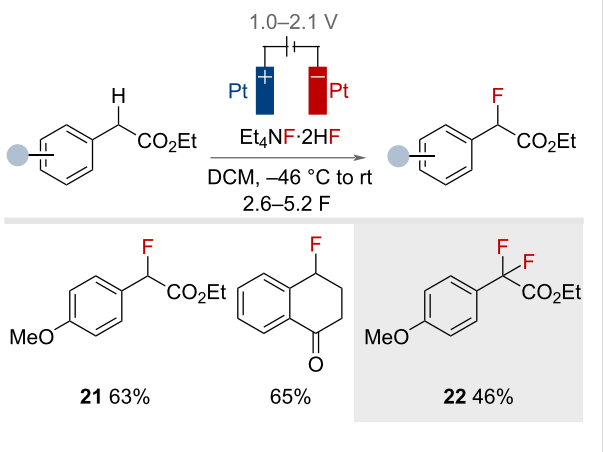

Figure 38: Electrochemical benzylic C(sp^3)–H fluorination of phenylacetic acid esters with HF·amine reagents.

glycol (PEG) to dissolve caesium fluorides and facilitate an electrochemical benzylic C(sp^3)–H fluorination of triphenylmethane (Figure 39) [97]. The authors suggested that PEG complexed the metal ion, increasing the nucleophilicity of the fluoride ion. Product **23** was achieved in 85% isolated yield after a small optimisation campaign.

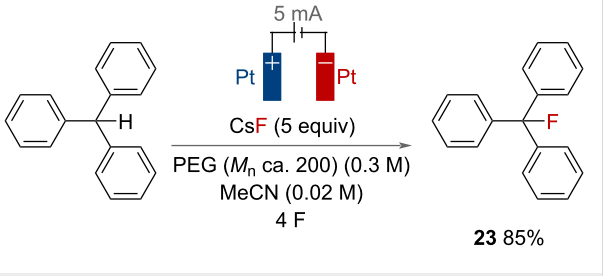

Figure 39: Electrochemical benzylic C(sp^3)–H fluorination of triphenylmethane with PEG and CsF.

The fluorinated alcohol HFIP was used to dissolve caesium fluoride allowing for the electrochemical benzylic fluorination by Fuchigami, Inagi and co-workers in 2021 (Figure 40) [98]. The HFIP/CsF system functioned as both a fluoride source and as supporting electrolyte, enabling the passage of current through the reaction medium. Heavily stabilised **23** was afforded in quantitative yield. The protocol could be extended to other substrates to give **24** and **25**, albeit in reduced yields. The addition of molecular sieves and an atmosphere of argon ensured the best yields.

Building on the work of Fuchigami, a more general electrochemical method for the nucleophilic fluorination of secondary and tertiary benzylic C(sp^3)–H bonds was reported by Ackermann and co-workers in 2022 (Figure 41) [99]. A solvent mix-

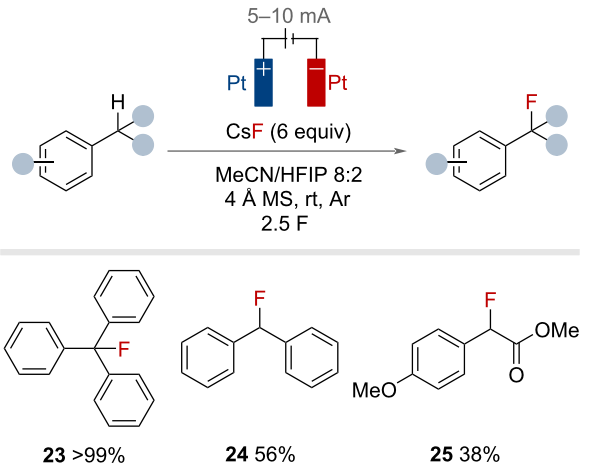

Figure 40: Electrochemical benzylic C(sp^3)–H fluorination with caesium fluoride and fluorinated alcohol HFIP.

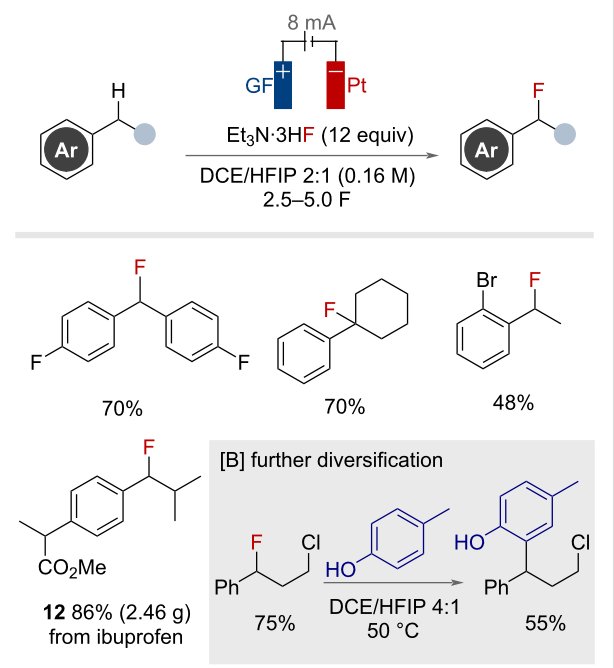

Figure 41: Electrochemical secondary and tertiary benzylic C(sp^3)–H fluorination. GF = graphite felt. DCE = 1,2-dichloroethane.

ture of DCE and HFIP (2:1) and 12 equivalents of $Et_3N{\cdot}3HF$ resulted in the highest yields, with the authors proposing that HFIP aided in stabilising the electrochemically generated benzylic radical cation intermediates. Secondary and tertiary benzylic substrates bearing halogen, ester, protected amine and alkyl functional groups tolerated the reaction conditions well. The authors showed they were able to scale-up and selectively fluorinate the ibuprofen methyl ester at the methylene group to produce over 2 g of product **12**. The utility of the benzyl fluoride products as strategic intermediates for benzylation of electron-rich arenes was demonstrated by the authors (Figure 41B). Overall, this work demonstrates the broadest range of secondary and tertiary benzylic substrates for electrochemical nucleophilic fluorination.

As highlighted by the previous examples, electrochemical oxidation is a useful tool for preparing benzylic fluorides. However, a number of reports highlight the fragility of secondary and tertiary benzyl fluorides, as they observe elimination and hydrolysis in many cases [20,100], thereby raising question marks over their suitability as synthetic targets. Monofluorinated methyl arenes, however, are much more stable to these decomposition pathways. The nucleophilic fluorination of primary benzylic substrates is a highly challenging reaction, due to the lower stability of the reactive intermediates involved in the mechanism. This is reflected in the fact that very few papers have been reported beyond the work on methylquinolines by the Sanford group (Figure 30), and a few preliminary electrochemical examples [93,101]. Middleton and co-workers described an alternating polarity approach for the fluorination of simple toluene derivatives in neat pyridine·HF (Figure 42) [102,103]. Poor conductivity necessitated the use of this waveform type. The benzylic fluorination was proposed to proceed via the classical ET/PT/ET pathway (pathway [A]). Nitro, cyano and sulphonyl fluoride substituents on the ring afforded ring fluorination–migration byproducts (via pathway [B]). In total, 14 substrates were fluorinated with yields ranging from 12–58%. Difluorination was observed under prolonged reaction times or upon increasing the applied cell potentials.

In 2024, Lennox and co-workers reported their investigation in exploring how alternative electrolysis waveforms might assist in the generation of reactive primary benzylic cations for nucleophilic fluorination (Figure 43) [104]. The challenge involved avoiding over-oxidation of the monofluorination product and overcoming mass transportation issues. It was found that the use of pulsed electrolysis waveforms, via the introduction of resting periods during electrolysis, was beneficial for the reaction outcome. This was demonstrated on a series of primary benzylic biphenyls and two secondary substrates by comparing to the pulsed technique (pDC) to the traditional direct current (DC) technique (Figure 43B and C). Under a constant potential (CP) regime no product was observed, but it was demonstrated that the introduction of a resting period, to generate a pulsed step–constant potential waveform (pSCP), assisted in the formation of benzyl fluoride product. The positive effect of the pulsed waveforms was attributed to a modulation of the electrical double layer, which results in improved mass transport, and subsequently decreases over-oxidation and decomposition to improve the reaction efficiency overall.

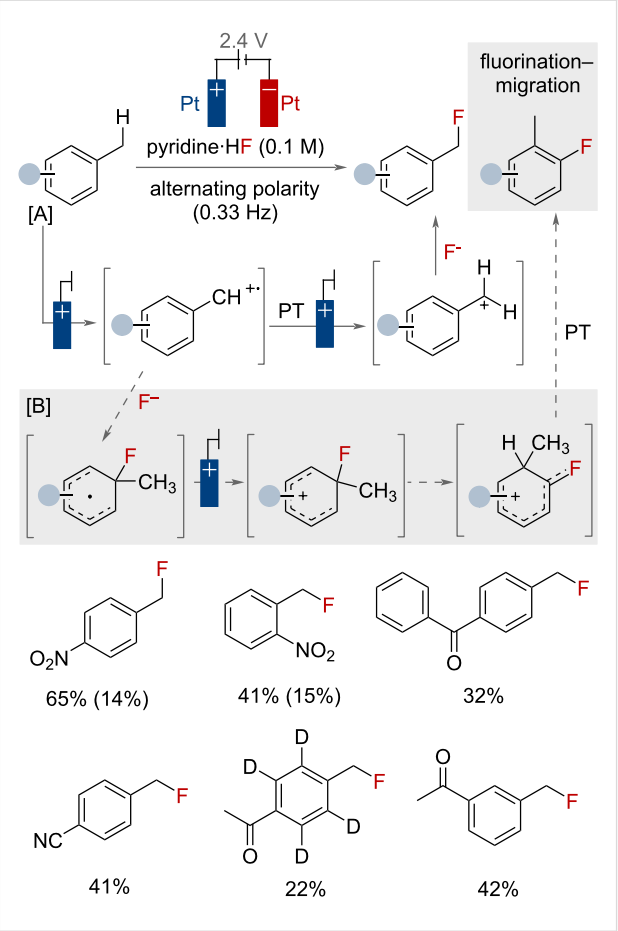

Figure 42: Electrochemical primary benzylic C(sp^3)–H fluorination of electron-poor toluene derivatives. Ring fluorination–migration product yields in parentheses.

Conclusion

The fluorination of benzylic C(sp^3)–H bonds provides rapid access to an important functional group used in medicinal chemistry to control the pharmacokinetic profile of drug candidates. Historical and recent research efforts have resulted in a collection of protocols for the benzylic C(sp^3)–H fluorination that demonstrate a broad tolerance of substrate classes. Electrophilic fluorination protocols are effective for specific substrate classes. Metal-catalysed processes operating via C–F reductive elimination pathways demonstrate stereospecificity, again on predefined substrate classes. Radical fluorination methods offer an expansion to substrate scopes and rely on the use of more expensive fluorine-atom-transfer reagents. Finally, oxidative benzylic activation methods, often in tandem with enabling technologies, such as photoredox catalysis and electrochemistry, open up the use of nucleophilic fluoride sources, complementing the broader scopes demonstrated by radical methods. All these approaches highlight the multiple reactivity modes of benzylic C(sp^3)–H bond functionalisation, and provide context on the state of the art and will hopefully encourage further development in key areas. This is particularly pertinent to the late-stage benzylic fluorination of complex molecules, which will require exceptionally mild conditions in order to tolerate a broad range of functional groups.

Acknowledgements

We would like to acknowledge Dr Joseph Tate (Syngenta) for discussions.

Funding

We would like to thank the Royal Society (University Research Fellowship and Enhancement Awards to AJJL), the EPSRC (EP/T51763X/1, EP/S024107/1), the European Research Council (949821, SENF) and Syngenta for generous funding.

Author Contributions

Alexander P. Atkins: writing – original draft; writing – review & editing. Alice C. Dean: writing – original draft; writing – review & editing. Alastair J. J. Lennox: conceptualization;

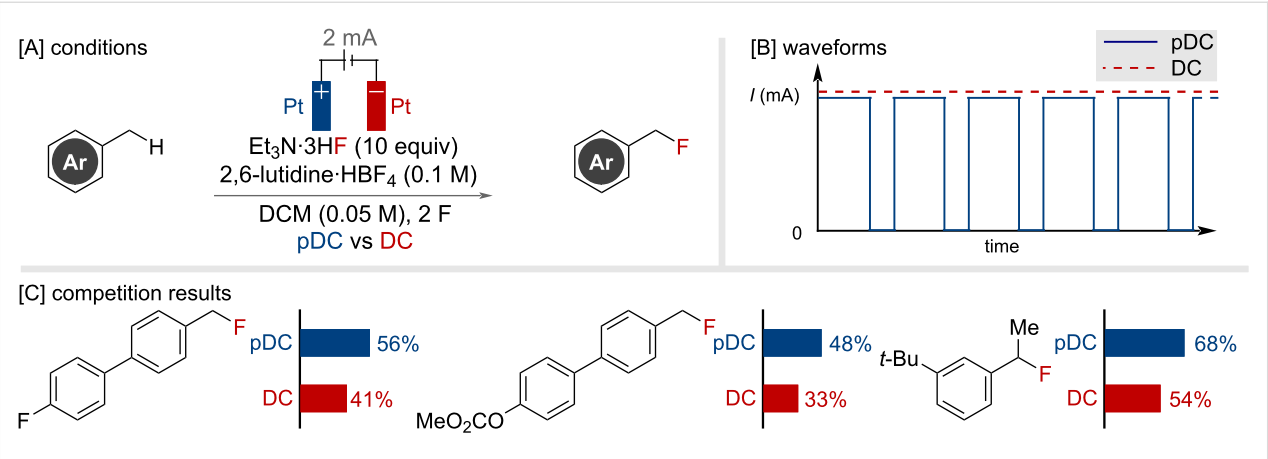

Figure 43: Electrochemical primary benzylic C(sp^3)–H fluorination utilizing pulsed current electrolysis.

funding acquisition; project administration; supervision; writing – review & editing.

ORCID® iDs

Alexander P. Atkins - https://orcid.org/0000-0002-9799-6881
Alice C. Dean - https://orcid.org/0000-0001-8735-9654
Alastair J. J. Lennox - https://orcid.org/0000-0003-2019-7421

Data Availability Statement

Data sharing is not applicable as no new data was generated or analyzed in this study.

References

1. Johnson, B. M.; Shu, Y.-Z.; Zhuo, X.; Meanwell, N. A. *J. Med. Chem.* **2020,** *63,* 6315–6386. doi:10.1021/acs.jmedchem.9b01877
2. Gillis, E. P.; Eastman, K. J.; Hill, M. D.; Donnelly, D. J.; Meanwell, N. A. *J. Med. Chem.* **2015,** *58,* 8315–8359. doi:10.1021/acs.jmedchem.5b00258
3. Meanwell, N. A. *J. Med. Chem.* **2018,** *61,* 5822–5880. doi:10.1021/acs.jmedchem.7b01788
4. Purser, S.; Moore, P. R.; Swallow, S.; Gouverneur, V. *Chem. Soc. Rev.* **2008,** *37,* 320–330. doi:10.1039/b610213c
5. Jeffries, B.; Wang, Z.; Felstead, H. R.; Le Questel, J.-Y.; Scott, J. S.; Chiarparin, E.; Graton, J.; Linclau, B. *J. Med. Chem.* **2020,** *63,* 1002–1031. doi:10.1021/acs.jmedchem.9b01172
6. Constable, D. J. C.; Dunn, P. J.; Hayler, J. D.; Humphrey, G. R.; Leazer, J. L., Jr.; Linderman, R. J.; Lorenz, K.; Manley, J.; Pearlman, B. A.; Wells, A.; Zaks, A.; Zhang, T. Y. *Green Chem.* **2007,** *9,* 411–420. doi:10.1039/b703488c
7. Bryan, M. C.; Dunn, P. J.; Entwistle, D.; Gallou, F.; Koenig, S. G.; Hayler, J. D.; Hickey, M. R.; Hughes, S.; Kopach, M. E.; Moine, G.; Richardson, P.; Roschangar, F.; Steven, A.; Weiberth, F. J. *Green Chem.* **2018,** *20,* 5082–5103. doi:10.1039/c8gc01276h
8. Jana, R.; Begam, H. M.; Dinda, E. *Chem. Commun.* **2021,** *57,* 10842–10866. doi:10.1039/d1cc04083a
9. Fujiwara, T.; O'Hagan, D. *J. Fluorine Chem.* **2014,** *167,* 16–29. doi:10.1016/j.jfluchem.2014.06.014
10. O'Hagan, D.; Young, R. J. *Med. Chem. Res.* **2023,** *32,* 1231–1234. doi:10.1007/s00044-023-03094-y
11. Szpera, R.; Moseley, D. F. J.; Smith, L. B.; Sterling, A. J.; Gouverneur, V. *Angew. Chem., Int. Ed.* **2019,** *58,* 14824–14848. doi:10.1002/anie.201814457
12. Leibler, I. N.-M.; Gandhi, S. S.; Tekle-Smith, M. A.; Doyle, A. G. *J. Am. Chem. Soc.* **2023,** *145,* 9928–9950. doi:10.1021/jacs.3c01824
13. Xue, X.-S.; Ji, P.; Zhou, B.; Cheng, J.-P. *Chem. Rev.* **2017,** *117,* 8622–8648. doi:10.1021/acs.chemrev.6b00664
14. Clayden, J.; Greeves, N.; Warren, S. *Organic Chemistry,* 2nd ed.; Oxford University Press: Oxford, UK, 2012. doi:10.1093/hesc/9780199270293.001.0001
15. Zhang, X.; Bordwell, F. G. *J. Org. Chem.* **1992,** *57,* 4163–4168. doi:10.1021/jo00041a020
16. Rosenblum, S. B.; Huynh, T.; Afonso, A.; Davis, H. R.; Yumibe, N.; Clader, J. W.; Burnett, D. A. *J. Med. Chem.* **1998,** *41,* 973–980. doi:10.1021/jm970701f
17. Chen, S.-J.; Krska, S. W.; Stahl, S. S. *Acc. Chem. Res.* **2023,** *56,* 3604–3615. doi:10.1021/acs.accounts.3c00580
18. Garg, A.; Gerwien, N. J.; Fasting, C.; Charlton, A.; Hopkinson, M. N. *Angew. Chem., Int. Ed.* **2023,** *62,* e202302860. doi:10.1002/anie.202302860
19. Willcox, D. R.; Nichol, G. S.; Thomas, S. P. *ACS Catal.* **2021,** *11,* 3190–3197. doi:10.1021/acscatal.1c00282
20. Vasilopoulos, A.; Golden, D. L.; Buss, J. A.; Stahl, S. S. *Org. Lett.* **2020,** *22,* 5753–5757. doi:10.1021/acs.orglett.0c02238
21. Bui, T. T.; Hong, W. P.; Kim, H.-K. *J. Fluorine Chem.* **2021,** *247,* 109794. doi:10.1016/j.jfluchem.2021.109794
22. Koperniku, A.; Liu, H.; Hurley, P. B. *Eur. J. Org. Chem.* **2016,** 871–886. doi:10.1002/ejoc.201501329
23. Bume, D. D.; Harry, S. A.; Lectka, T.; Pitts, C. R. *J. Org. Chem.* **2018,** *83,* 8803–8814. doi:10.1021/acs.joc.8b00982
24. Lin, A.; Huehls, C. B.; Yang, J. *Org. Chem. Front.* **2014,** *1,* 434–438. doi:10.1039/c4qo00020j
25. Cheng, Q.; Ritter, T. *Trends Chem.* **2019,** *1,* 461–470. doi:10.1016/j.trechm.2019.04.001
26. Yakubov, S.; Barham, J. P. *Beilstein J. Org. Chem.* **2020,** *16,* 2151–2192. doi:10.3762/bjoc.16.183
27. Champagne, P. A.; Desroches, J.; Hamel, J.-D.; Vandamme, M.; Paquin, J.-F. *Chem. Rev.* **2015,** *115,* 9073–9174. doi:10.1021/cr500706a
28. Yerien, D. E.; Bonesi, S.; Postigo, A. *Org. Biomol. Chem.* **2016,** *14,* 8398–8427. doi:10.1039/c6ob00764c
29. Yan, H.; Zhu, C. *Sci. China: Chem.* **2017,** *60,* 214–222. doi:10.1007/s11426-016-0399-5
30. Pihko, P. M. *Angew. Chem., Int. Ed.* **2006,** *45,* 544–547. doi:10.1002/anie.200502425
31. Aggarwal, T.; Sushmita; Verma, A. K. *Org. Chem. Front.* **2021,** *8,* 6452–6468. doi:10.1039/d1qo00952d
32. Hu, W.-L.; Hu, X.-G.; Hunter, L. *Synthesis* **2017,** *49,* 4917–4930. doi:10.1055/s-0036-1590881
33. Qiao, Y.; Zhu, L.; Ambler, B.; Altman, R. *Curr. Top. Med. Chem.* **2014,** *14,* 966–978. doi:10.2174/1568026614666140202210850
34. Peng, W.; Shreeve, J. M. *Tetrahedron Lett.* **2005,** *46,* 4905–4909. doi:10.1016/j.tetlet.2005.05.056
35. Sadeghi, M. M.; Loghmani-Khouzani, H.; Ranjbar-Karimi, R.; Golding, B. T. *Tetrahedron Lett.* **2006,** *47,* 2455–2457. doi:10.1016/j.tetlet.2006.01.037
36. Meanwell, M.; Nodwell, M. B.; Martin, R. E.; Britton, R. *Angew. Chem., Int. Ed.* **2016,** *55,* 13244–13248. doi:10.1002/anie.201606323
37. Meanwell, M.; Adluri, B. S.; Yuan, Z.; Newton, J.; Prevost, P.; Nodwell, M. B.; Friesen, C. M.; Schaffer, P.; Martin, R. E.; Britton, R. *Chem. Sci.* **2018,** *9,* 5608–5613. doi:10.1039/c8sc01221k
38. Furuya, T.; Benitez, D.; Tkatchouk, E.; Strom, A. E.; Tang, P.; Goddard, W. A., III; Ritter, T. *J. Am. Chem. Soc.* **2010,** *132,* 3793–3807. doi:10.1021/ja909371t
39. Hull, K. L.; Anani, W. Q.; Sanford, M. S. *J. Am. Chem. Soc.* **2006,** *128,* 7134–7135. doi:10.1021/ja061943k
40. Zhang, Q.; Yin, X.-S.; Chen, K.; Zhang, S.-Q.; Shi, B.-F. *J. Am. Chem. Soc.* **2015,** *137,* 8219–8226. doi:10.1021/jacs.5b03989
41. Zhu, R.-Y.; Tanaka, K.; Li, G.-C.; He, J.; Fu, H.-Y.; Li, S.-H.; Yu, J.-Q. *J. Am. Chem. Soc.* **2015,** *137,* 7067–7070. doi:10.1021/jacs.5b04088
42. Zhu, Q.; Ji, D.; Liang, T.; Wang, X.; Xu, Y. *Org. Lett.* **2015,** *17,* 3798–3801. doi:10.1021/acs.orglett.5b01774
43. Park, H.; Verma, P.; Hong, K.; Yu, J.-Q. *Nat. Chem.* **2018,** *10,* 755–762. doi:10.1038/s41557-018-0048-1
44. Zhang, Z.; Chen, P.; Liu, G. *Chem. Soc. Rev.* **2022,** *51,* 1640–1658. doi:10.1039/d1cs00727k

45. Lubov, D. P.; Talsi, E. P.; Bryliakov, K. P. *Russ. Chem. Rev.* **2020,** *89,* 587–628. doi:10.1070/rcr4918
46. Yazaki, R.; Ohshima, T. *Tetrahedron Lett.* **2019,** *60,* 151225. doi:10.1016/j.tetlet.2019.151225
47. Golden, D. L.; Suh, S.-E.; Stahl, S. S. *Nat. Rev. Chem.* **2022,** *6,* 405–427. doi:10.1038/s41570-022-00388-4
48. Chatalova-Sazepin, C.; Hemelaere, R.; Paquin, J.-F.; Sammis, G. *Synthesis* **2015,** *47,* 2554–2569. doi:10.1055/s-0034-1378824
49. Bloom, S.; Pitts, C. R.; Woltornist, R.; Griswold, A.; Holl, M. G.; Lectka, T. *Org. Lett.* **2013,** *15,* 1722–1724. doi:10.1021/ol400424s
50. Hua, A. M.; Mai, D. N.; Martinez, R.; Baxter, R. D. *Org. Lett.* **2017,** *19,* 2949–2952. doi:10.1021/acs.orglett.7b01188
51. Bloom, S.; Pitts, C. R.; Miller, D. C.; Haselton, N.; Holl, M. G.; Urheim, E.; Lectka, T. *Angew. Chem., Int. Ed.* **2012,** *51,* 10580–10583. doi:10.1002/anie.201203642
52. Zhang, W.; Wang, F.; McCann, S. D.; Wang, D.; Chen, P.; Stahl, S. S.; Liu, G. *Science* **2016,** *353,* 1014–1018. doi:10.1126/science.aaf7783
53. Hu, H.; Chen, S.-J.; Mandal, M.; Pratik, S. M.; Buss, J. A.; Krska, S. W.; Cramer, C. J.; Stahl, S. S. *Nat. Catal.* **2020,** *3,* 358–367. doi:10.1038/s41929-020-0425-1
54. Hintz, H.; Bower, J.; Tang, J.; LaLama, M.; Sevov, C.; Zhang, S. *Chem Catal.* **2023,** *3,* 100491. doi:10.1016/j.checat.2022.100491
55. Pinter, E. N.; Bingham, J. E.; AbuSalim, D. I.; Cook, S. P. *Chem. Sci.* **2020,** *11,* 1102–1106. doi:10.1039/c9sc04055b
56. Groendyke, B. J.; AbuSalim, D. I.; Cook, S. P. *J. Am. Chem. Soc.* **2016,** *138,* 12771–12774. doi:10.1021/jacs.6b08171
57. Xia, J.-B.; Ma, Y.; Chen, C. *Org. Chem. Front.* **2014,** *1,* 468–472. doi:10.1039/c4qo00057a
58. Amaoka, Y.; Nagatomo, M.; Inoue, M. *Org. Lett.* **2013,** *15,* 2160–2163. doi:10.1021/ol4006757
59. Ma, J.-j.; Yi, W.-b.; Lu, G.-p.; Cai, C. *Org. Biomol. Chem.* **2015,** *13,* 2890–2894. doi:10.1039/c4ob02418d
60. Pitts, C. R.; Ling, B.; Woltornist, R.; Liu, R.; Lectka, T. *J. Org. Chem.* **2014,** *79,* 8895–8899. doi:10.1021/jo501520e
61. Danahy, K. E.; Cooper, J. C.; Van Humbeck, J. F. *Angew. Chem., Int. Ed.* **2018,** *57,* 5134–5138. doi:10.1002/anie.201801280
62. Madani, A.; Anghileri, L.; Heydenreich, M.; Möller, H. M.; Pieber, B. *Org. Lett.* **2022,** *24,* 5376–5380. doi:10.1021/acs.orglett.2c02050
63. Yakubov, S.; Stockerl, W. J.; Tian, X.; Shahin, A.; Mandigma, M. J. P.; Gschwind, R. M.; Barham, J. P. *Chem. Sci.* **2022,** *13,* 14041–14051. doi:10.1039/d2sc05735b
64. Romero, N. A.; Nicewicz, D. A. *Chem. Rev.* **2016,** *116,* 10075–10166. doi:10.1021/acs.chemrev.6b00057
65. Murray, P. R. D.; Cox, J. H.; Chiappini, N. D.; Roos, C. B.; McLoughlin, E. A.; Hejna, B. G.; Nguyen, S. T.; Ripberger, H. H.; Ganley, J. M.; Tsui, E.; Shin, N. Y.; Koronkiewicz, B.; Qiu, G.; Knowles, R. R. *Chem. Rev.* **2022,** *122,* 2017–2291. doi:10.1021/acs.chemrev.1c00374
66. Capaldo, L.; Ravelli, D.; Fagnoni, M. *Chem. Rev.* **2022,** *122,* 1875–1924. doi:10.1021/acs.chemrev.1c00263
67. Capaldo, L.; Ravelli, D. *Eur. J. Org. Chem.* **2017,** 2056–2071. doi:10.1002/ejoc.201601485
68. Oliva, M.; Coppola, G. A.; Van der Eycken, E. V.; Sharma, U. K. *Adv. Synth. Catal.* **2021,** *363,* 1810–1834. doi:10.1002/adsc.202001581
69. Xia, J.-B.; Zhu, C.; Chen, C. *J. Am. Chem. Soc.* **2013,** *135,* 17494–17500. doi:10.1021/ja410815u
70. Bloom, S.; McCann, M.; Lectka, T. *Org. Lett.* **2014,** *16,* 6338–6341. doi:10.1021/ol503094m
71. Cantillo, D.; de Frutos, O.; Rincón, J. A.; Mateos, C.; Kappe, C. O. *J. Org. Chem.* **2014,** *79,* 8486–8490. doi:10.1021/jo5016757
72. Bume, D. D.; Pitts, C. R.; Jokhai, R. T.; Lectka, T. *Tetrahedron* **2016,** *72,* 6031–6036. doi:10.1016/j.tet.2016.08.018
73. Nodwell, M. B.; Bagai, A.; Halperin, S. D.; Martin, R. E.; Knust, H.; Britton, R. *Chem. Commun.* **2015,** *51,* 11783–11786. doi:10.1039/c5cc04058b
74. Xiang, M.; Xin, Z.-K.; Chen, B.; Tung, C.-H.; Wu, L.-Z. *Org. Lett.* **2017,** *19,* 3009–3012. doi:10.1021/acs.orglett.7b01270
75. Liang, T.; Neumann, C. N.; Ritter, T. *Angew. Chem., Int. Ed.* **2013,** *52,* 8214–8264. doi:10.1002/anie.201206566
76. Hollingworth, C.; Gouverneur, V. *Chem. Commun.* **2012,** *48,* 2929. doi:10.1039/c2cc16158c
77. McMurtrey, K. B.; Racowski, J. M.; Sanford, M. S. *Org. Lett.* **2012,** *14,* 4094–4097. doi:10.1021/ol301739f
78. Bejot, R.; Fowler, T.; Carroll, L.; Boldon, S.; Moore, J. E.; Declerck, J.; Gouverneur, V. *Angew. Chem., Int. Ed.* **2009,** *48,* 586–589. doi:10.1002/anie.200803897
79. Clark, J. H. *Chem. Rev.* **1980,** *80,* 429–452. doi:10.1021/cr60327a004
80. Liu, W.; Groves, J. T. *Angew. Chem., Int. Ed.* **2013,** *52,* 6024–6027. doi:10.1002/anie.201301097
81. Huang, X.; Liu, W.; Ren, H.; Neelamegam, R.; Hooker, J. M.; Groves, J. T. *J. Am. Chem. Soc.* **2014,** *136,* 6842–6845. doi:10.1021/ja5039819
82. Jacobsen, E. N.; Zhang, W.; Muci, A. R.; Ecker, J. R.; Deng, L. *J. Am. Chem. Soc.* **1991,** *113,* 7063–7064. doi:10.1021/ja00018a068
83. Leibler, I. N.-M.; Tekle-Smith, M. A.; Doyle, A. G. *Nat. Commun.* **2021,** *12,* 6950. doi:10.1038/s41467-021-27165-z
84. Zhang, Y.; Fitzpatrick, N. A.; Das, M.; Bedre, I. P.; Yayla, H. G.; Lall, M. S.; Musacchio, P. Z. *Chem Catal.* **2022,** *2,* 292–308. doi:10.1016/j.checat.2021.12.010
85. Yamashita, K.; Fujiwara, Y.; Hamashima, Y. *J. Org. Chem.* **2023,** *88,* 1865–1874. doi:10.1021/acs.joc.2c02575
86. Yan, M.; Kawamata, Y.; Baran, P. S. *Chem. Rev.* **2017,** *117,* 13230–13319. doi:10.1021/acs.chemrev.7b00397
87. Hou, Z.-W.; Liu, D.-J.; Xiong, P.; Lai, X.-L.; Song, J.; Xu, H.-C. *Angew. Chem., Int. Ed.* **2021,** *60,* 2943–2947. doi:10.1002/anie.202013478
88. Schmittel, M.; Burghart, A. *Angew. Chem., Int. Ed. Engl.* **1997,** *36,* 2550–2589. doi:10.1002/anie.199725501
89. Roth, H.; Romero, N.; Nicewicz, D. *Synlett* **2015,** *27,* 714–723. doi:10.1055/s-0035-1561297
90. Wayner, D. D. M.; McPhee, D. J.; Griller, D. *J. Am. Chem. Soc.* **1988,** *110,* 132–137. doi:10.1021/ja00209a021
91. Fuchigami, T.; Inagi, S. *Acc. Chem. Res.* **2020,** *53,* 322–334. doi:10.1021/acs.accounts.9b00520
92. Doobary, S.; Sedikides, A. T.; Caldora, H. P.; Poole, D. L.; Lennox, A. J. J. *Angew. Chem., Int. Ed.* **2020,** *59,* 1155–1160. doi:10.1002/anie.201912119
93. Winterson, B.; Rennigholtz, T.; Wirth, T. *Chem. Sci.* **2021,** *12,* 9053–9059. doi:10.1039/d1sc02123k
94. Hou, Y.; Higashiya, S.; Fuchigami, T. *Electrochim. Acta* **2000,** *45,* 3005–3010. doi:10.1016/s0013-4686(00)00379-0
95. Hasegawa, M.; Ishii, H.; Fuchigami, T. *Green Chem.* **2003,** *5,* 512–515. doi:10.1039/b304617f
96. Dinoiu, V.; Fukuhara, T.; Miura, K.; Yoneda, N. *J. Fluorine Chem.* **2003,** *121,* 227–231. doi:10.1016/s0022-1139(03)00037-x

97. Sawamura, T.; Takahashi, K.; Inagi, S.; Fuchigami, T. *Angew. Chem., Int. Ed.* **2012,** *51,* 4413–4416. doi:10.1002/anie.201200438
98. Shida, N.; Takenaka, H.; Gotou, A.; Isogai, T.; Yamauchi, A.; Kishikawa, Y.; Nagata, Y.; Tomita, I.; Fuchigami, T.; Inagi, S. *J. Org. Chem.* **2021,** *86,* 16128–16133. doi:10.1021/acs.joc.1c00692
99. Stangier, M.; Scheremetjew, A.; Ackermann, L. *Chem. – Eur. J.* **2022,** *28,* e202201654. doi:10.1002/chem.202201654
100. Liu, W.; Huang, X.; Groves, J. T. *Nat. Protoc.* **2013,** *8,* 2348–2354. doi:10.1038/nprot.2013.144
101. Tajima, T.; Ishii, H.; Fuchigami, T. *Electrochem. Commun.* **2002,** *4,* 589–592. doi:10.1016/s1388-2481(02)00381-8
102. Savett, S. C.; Lee, S. M.; Bradley, A. Z.; Kneizys, S. P.; Lobue, J. M.; Middleton, W. J. *Microchem. J.* **1993,** *48,* 192–199. doi:10.1006/mchj.1993.1090
103. Lee, S. M.; Roseman, J. M.; Blair Zartman, C.; Morrison, E. P.; Harrison, S. J.; Stankiewicz, C. A.; Middleton, W. J. *J. Fluorine Chem.* **1996,** *77,* 65–70. doi:10.1016/0022-1139(95)03379-3
104. Atkins, A. P.; Chaturvedi, A. K.; Tate, J. A.; Lennox, A. J. J. *Org. Chem. Front.* **2024,** *11,* 802–808. doi:10.1039/d3qo01865b

License and Terms

BEILSTEIN JOURNAL OF ORGANIC CHEMISTRY

Regio- and stereochemical stability induced by anomeric and *gauche* effects in difluorinated pyrrolidines

Ana Flávia Candida Silva[1], Francisco A. Martins[2] and Matheus P. Freitas[*1]

Full Research Paper

Open Access

Address:
[1]Department of Chemistry, Institute of Natural Sciences, Federal University of Lavras, 37200-900, Lavras, MG, Brazil and [2]Department of Chemistry, University of Houston, Houston, TX, USA

Email:
Matheus P. Freitas[*] - matheus@ufla.br

* Corresponding author

Keywords:
anomeric effect; fluoropyrrolidine; *gauche* effect; stereochemistry

Beilstein J. Org. Chem. **2024,** *20,* 1572–1579.
https://doi.org/10.3762/bjoc.20.140

Received: 22 April 2024
Accepted: 01 July 2024
Published: 12 July 2024

This article is part of the thematic issue "Organofluorine chemistry VI".

Guest Editor: D. O'Hagan

Abstract

Selective fluorination of the pyrrolidine ring in proline motifs has been found to induce significant conformational changes that impact the structure and biological roles of modified peptides and proteins. Vicinal difluorination of fluoroproline, for example, in (3*S*,4*R*)-3,4-difluoroproline, serves to mitigate the inherent conformational bias of the pyrrolidine ring by inducing stereoelectronic effects that attenuate this conformational bias. In this investigation, we present a quantumchemical analysis of the conformational equilibrium and effects that are induced in difluorinated pyrrolidines, with a particular focus on exploring the impact of *gauche* and anomeric effects on the conformer stabilities of different stereo- and regioisomers. Initially, we conducted a benchmark assessment comparing the optimal density functional theory method with coupled cluster with single and double excitations (CCSD) calculations and crystallographic data using the 3-fluoropyrrolidinium cation and 3-fluoropyrrolidine. Subsequently, we explored the relative energy of all favored conformations of all different stereoisomers of 2,3-, 2,4-, and 3,4-difluoropyrrolidines at the B3LYP-D3BJ/6-311++G** level. A generalized anomeric effect, arising from $n_N \rightarrow \sigma^*_{CF}$ electron delocalization, is particularly important in modulating the energetics of the α-fluoro isomers and imparts a strong conformational bias. In contrast, the fluorine *gauche* effect assumes a secondary role, as it is overshadowed by steric and electrostatic interactions, referred to as Lewis interactions from a natural bond orbital perspective.

Introduction

The pyrrolidine ring structure is prevalent in numerous natural alkaloids and is an important feature of the proline and hydroxyproline residues that pervade biochemistry in peptides and proteins. The chemical and biological properties of substituted pyrrolidine derivatives, along with many other compounds, hinge on the relative stereochemistry. It is well estab-

lished that the presence of fluorine in an organic molecule can significantly influence the stereochemical behavior. Consequently, various molecular properties, such as polarity, viscosity, and intra- and intermolecular interactions, are impacted by the C–F bond. These features underlie the important role of selective fluorination in pharmaceuticals and agrochemicals development [1].

For instance, substituted 3-fluoropyrrolidines, particularly in the form of 2-carboxy derivatives (fluoroprolines), have been extensively explored. These compounds represent valuable non-natural amino acids, and depending on the regio- and stereochemistry of fluorine substitution, fluoroproline substututions can enhance the conformational stability of proline-rich proteins such as collagen [2]. Therefore, pyrrolidine derivatives are particularly susceptible to conformational control induced by a fluorine substituent.

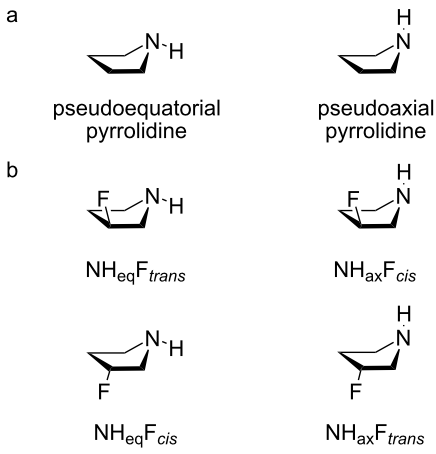

Figure 1: a) Pseudoequatorial and pseudoaxial conformations of pyrrolidine. b) *Cis*- and *trans*-isomers of 3-fluoropyrrolidine.

The 5-membered pyrrolidine ring is a cyclic alkylamine that adopts a conformation that resembles the familiar envelope of cyclopentane, with an NH unit occupying either a pseudoaxial or pseudoequatorial position (Figure 1a). When a hydrogen atom of the pyrrolidine at C-3 is replaced with fluorine, a conformational interconversion can occur within the *cis*- and *trans*-isomers, as illustrated in Figure 1b. The fluorine *gauche* effect, commonly observed in compounds containing the F–C–C–X fragment (where X is an electron-withdrawing substituent, such as nitrogen), typically favors a conformation where F and X are *gauche* to each other. This preference is attributed to stabilizing $\sigma_{CH} \rightarrow \sigma^*_{CF}$ and $\sigma_{CH} \rightarrow \sigma^*_{CX}$ hyperconjugative interactions [3]. However, it is noteworthy that 3-fluoropiperidine does not exhibit such a fluorine *gauche* effect. In this case, the axial conformer is similarly populated to the equatorial conformer, despite the favorable antiperiplanar arrangement of orbitals that would facilitate these interactions [4].

Protonation of 3-fluoropyrrolidine generates the 3-fluoropyrrolidinium cation, and this typically results in a highly favored conformation in both the gas phase and solution where the fluorine and nitrogen atoms are *cis*, mirroring the behavior observed in analagous 4- and 6-membered ring systems [5]. This conformational preference is attributed to an electrostatic *gauche* effect, where an attractive $NH_2^+ \cdots F^{\delta-}$ interaction reinforces the well-known hyperconjugative *gauche* effect. Additionally, NH···F hydrogen bonding has been proposed to play a role in stabilizing conformers of certain 3-fluoroalkylamines and the respective cations [6].

Intramolecular hydrogen bonds involving either the carboxy or hydroxy group of 4*R*- and 4*S*-hydroxyproline have been identified as key factors in stabilizing the favored conformations in the gas phase. Therein, the contribution of a *gauche* effect due to electron delocalization is considered to be secondary [7]. However, stabilization via intramolecular hydrogen bonding does not seem to significantly impact the conformational stability of 3-fluoropiperidine. In this context, the *cis*-conformer, with the axial fluorine atom facing the *N*-hydrogen atom, is either equally or only slightly more stable than the other three conformers in both the gas phase and implicit water [4]. Hence, it appears that strong intramolecular interactions, and not only hydrogen bonding, govern the orientation of the fluorine atom in the F–C–C–N fragment, favoring the *cis*-isomer of 3-fluoropyrrolidine.

To investigate potential changes in the preferred orientation of the fluorine substituent in 3-fluoropyrrolidine and the respective cation, an additional fluorine atom was introduced into the molecule for theoretic studies (Figure 2). The subsequent evaluation focused on the role of anomeric and fluorine *gauche* effects to evaluate significant conformational biases in all of the possible isomers.

Achieving conformational control upon the introduction of a second fluorine atom in fluoropyrrolidine presents challenges. Unlike the chair-like conformation of six-membered rings, five-membered rings lack the geometric arrangement necessary to most effectively accommodate anomeric and *gauche* effects [8,9]. It is noteworthy that vicinal difluorination has previously been demonstrated to minimize conformational bias in fluoroprolines [10], offering some insight into the potential outcomes of this study.

In this study, initially, the conformational equilibrium of 3-fluoropyrrolidine and the corresponding cation were analyzed to

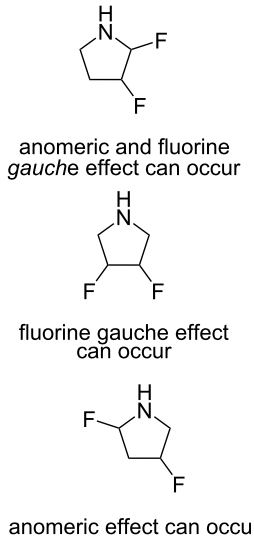

Figure 2: Flat representations of 2,3-, 3,4-, and 2,4-difluoropyrrolidines. The potential effects resulting from the addition of a second 1,2- or 1,3-fluorine atom ($n_N \rightarrow \sigma^*_{CF}$ anomeric and $\sigma_{CH} \rightarrow \sigma^*_{CF}$ fluorine *gauche* effects) on the conformation of different stereoisomers is explored.

establish a benchmark for selecting an appropriate theory level for subsequent calculations. Then, the different isomers of the 1,2- or 1,3-difluorinated pyrrolidines were each be subjected to quantum-chemical analysis.

Results and Discussion

In order to achieve the most accurate conformational depiction of the difluorinated pyrrolidines through density functional theory (DFT), a benchmark study was conducted. This study compares the crystallographic geometry of a pyrrolidinium salt [11] with the CCSD/DGTZVP geometry of the pyrrolidinium cation (with an exclusively axial C–F bond) and the energy of 3-fluoropyrrolidine conformations. Various combinations of DFT methods (B3LYP-D3BJ, ωB97XD, and PBEPBE) and basis sets (DGTZVP and 6-311++G**) were evaluated. The selection of these functionals was based on whether or not they included dispersion terms that could influence the absolute energy. These functionals are widely used and have demonstrated strong performance in numerous evaluations and validations across the literature. Similarly, for the basis sets, a comparison was made between a triple-zeta valence plus polarization basis set with diffuse and tight d-functions (DGTZVP) and a Pople-based large basis set with polarizability and diffuse functions, often referred to as high standard.

The geometry was assessed based on atom distance, bond length, dihedral angle, etc. The analysis revealed that the lowest mean absolute error (MAE) [12] was observed for the B3LYP-D3BJ/6-311++G** and ωB97XD/6-311++G** levels (Figure 3). While there were differences between the CCSD and experimental structures, attributed to intermolecular forces and counterion effects, these differences did not impact the selection of the best levels based on geometry criteria.

Regarding the conformational energy, 3-fluoropyrrolidine exhibited four conformers in the gas phase, although this was reduced to three in implicit DMSO experiments (Table 1). In both cases, a *cis*-twist ring with an axial N–H bond was the most stable conformer, allowing for an intramolecular F···H hydrogen bond. However, 3-fluoropyrrolidine displayed extensive conformational diversity (ΔG^0 among conformers

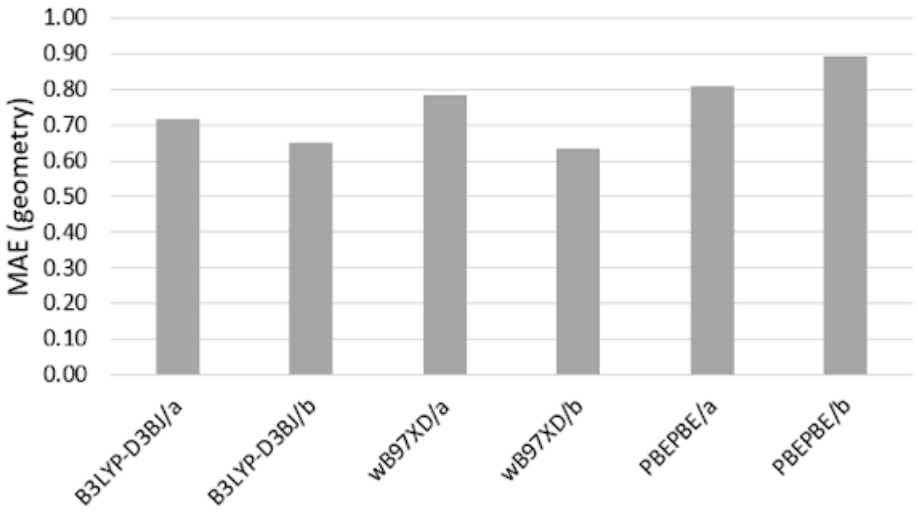

Figure 3: MAE comparing the geometry parameters (bond length, bond angle, and dihedral angle) obtained from DFT calculations at the CCSD/DGTZVP level. The MAE for the crystal structure compared to the CCSD structure is 20.3316. “a” denotes DGTZVP and “b” denotes 6-311++G**.

Table 1: Conformational energy (ΔG^0, kcal·mol^{-1}) and population (%) of 3-fluoropyrrolidine according to different theoretical levels for the gas phase and implicit DMSO (in parentheses), along with the MAE compared to the CCSD/DGTZVP level.

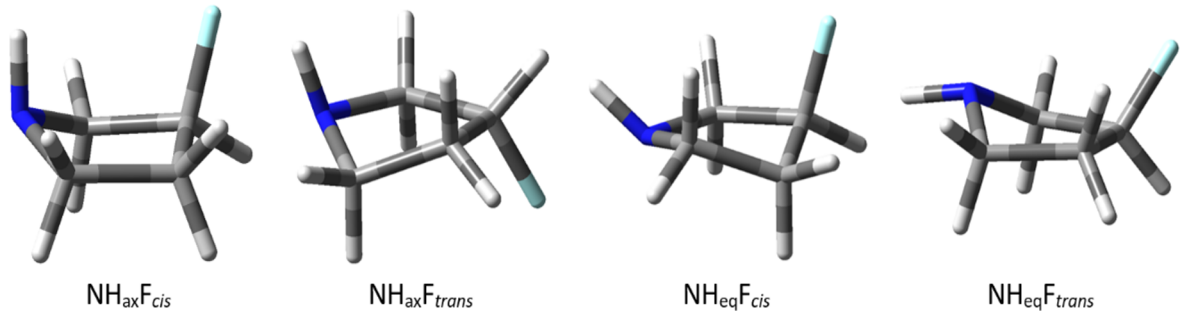

$NH_{ax}F_{cis}$ $NH_{ax}F_{trans}$ $NH_{eq}F_{cis}$ $NH_{eq}F_{trans}$

conformer	CCSD/a[a]	B3LYP-D3BJ/a	B3LYP-D3BJ/b[b]	ωB97XD/a	ωB97XD/b	PBEPBE/a	PBEPBE/b	average, %
$NH_{ax}F_{cis}$	0.00 (0.00)	0.00 (0.00)	0.00 (0.00)	0.00 (0.00)	0.00 (0.00)	0.00 (0.00)	0.00 (0.00)	54 (64)
$NH_{ax}F_{trans}$	1.00 (0.46)	0.97 (0.47)	0.94 (0.47)	0.96 (0.49)	0.91 (0.47)	0.97 (0.51)	0.96 (0.53)	11 (28)
$NH_{eq}F_{cis}$	0.28 (—)	0.31 (—)	0.28 (—)	0.20 (—)	0.09 (—)	0.61 (—)	0.56 (—)	31 (—)
$NH_{eq}F_{trans}$	1.60 (1.17)	1.59 (1.27)	1.45 (1.09)	1.57 (1.21)	1.49 (1.07)	1.64 (1.35)	1.46 (1.15)	4 (9)
MAE	—	0.02 (0.04)	0.05 (0.03)	0.04 (0.02)	0.10 (0.04)	0.10 (0.08)	0.12 (0.03)	—

[a]a = DGTZVP. [b]b = 6-311++G**.

≤1.6 kcal·mol^{-1}) as the intramolecular interactions were not sufficiently stabilizing to dictate a dominant conformation. Consequently the introduction of a second fluorine atom with an appropriate relative configuration was thought to reinforce and establish a predominant conformation.

Theoretical levels that closely approximated the CCSD outcome included B3LYP-D3BJ/6-311++G**, B3LYP-D3BJ/DGTZVP, and ωB97XD/DGTZVP (Table 1). Consequently, the B3LYP-D3BJ/6-311++G** level was selected for further calculations involving the difluorinated pyrrolidines shown in Figure 4.

From the pool of 24 potential conformational, configurational, and constitutional isomers of the difluorinated pyrrolidines (i.e., **1**–**24**), two pairs were degenerate (i.e., **10**/**11** and **14**/**15**), reducing the number of distinct structures to 22. However, due to the considerable flexibility of the five-membered ring and the low barrier for pyramidal interconversion of the N–H moiety, some inputs converged to the same isomer post-geometry optimization. Consequently, a total of 10 different structures was identified in the gas phase, with two additional structures observed in implicit DMSO (using solvation model density, SMD), bringing the total to 12.

Since the atomic composition of the compounds in Figure 4 was the same, the relative energy may be compared, and a stability landscape covering all optimized structures may be obtained from this analysis. Among these structures, only six were found to be significantly stable (<3 kcal·mol^{-1}) in either the gas phase or DMSO. Remarkably, structure **19** was the most stable, followed by structure **17**, as shown in Figure 5 and Table 2. This disparity in stability was largely attributed to the relative orientation of the nitrogen electron lone pair and the adjacent C–F bond, facilitating an anomeric interaction characterized by $n_N \rightarrow \sigma^*_{CF}$ electron delocalization. Isomer **2** also demonstrated such an orientation, but the C–F bonds in this case were vicinal. Compounds lacking α-fluorine atoms (i.e., **9**, **10**, **12**, and **16**) possessed a notably higher energy, indicating the impact of the anomeric effect.

To further illuminate these findings, a natural bond orbital (NBO) analysis was conducted across the entire array of difluorinated pyrrolidines to assess the relative energy in isodesmic relationships (Table 3). Unlike in 1,2-difluoroethane [10,13], vicinal *gauche*-oriented fluorine atoms in 5-membered rings, particularly in compounds **1**, **9**, and **12**, as well as in 6-membered rings, do not favor $\sigma_{CH} \rightarrow \sigma^*_{CF}$ interactions. Rather, less stabilizing $\sigma_{CC} \rightarrow \sigma^*_{CF}$ interactions were anticipated. Moreover, besides the anomeric interaction, the pseudoaxially oriented C–F bonds in **17** and **19** facilitated efficient electron donation from vicinal antiperiplanar C–H bonds through $\sigma_{CH} \rightarrow \sigma^*_{CF}$ interactions (Figure 6). The methylene group separating both C–F bonds in **17** and **19** enabled an additional $\sigma_{CH} \rightarrow \sigma^*_{CF}$ interaction, rather than the negligible $\sigma_{CF} \rightarrow \sigma^*_{CF}$ electron delocalization that would occur if these bonds were vicinally antiperiplanar. As discerned from the decomposition of the full elec-

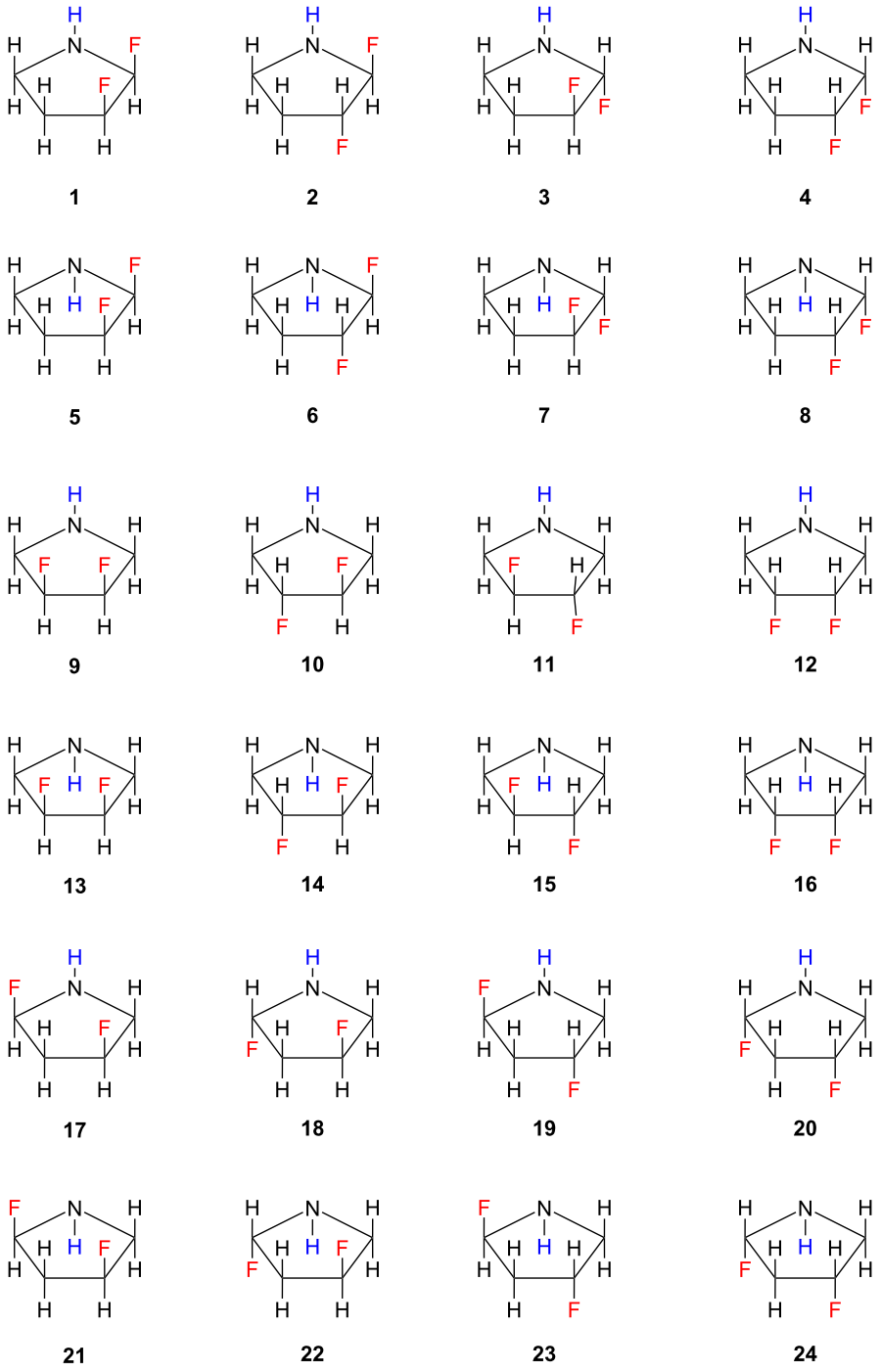

Figure 4: Exhaustive illustration of all conformational, configurational, and constitutional isomers of difluorinated pyrrolidine, illustrating the relative orientation of the C–F and N–H bonds used to build the input geometry for the calculations. The pairs **10**/**11** and **14**/**15** were degenerate. Consequently, only one structure of each pair was computed.

tronic energy into Lewis (e.g., steric effects) and non-Lewis (electron delocalization) contributions, **17** and **19** were favored by a delicate equilibrium between weak repulsion and substantial stabilization due to hyperconjugation. Conversely, structures such as **9** and **10** experienced minimal steric effects but were inadequately stabilized by electron delocalization, rendering them higher in energy when compared to the other isomers. Compounds **1** and **4**, with *syn*-C–F bonds, exhibited the highest ΔE_{Lewis} term due to significant dipolar and steric repulsions.

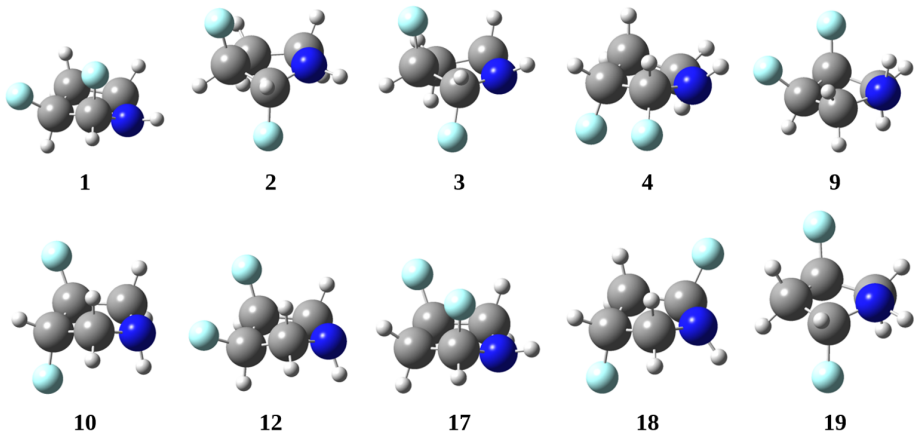

Figure 5: Stable difluorinated pyrrolidines derived from gas-phase calculations performed at the B3LYP-D3BJ/6-311++G** level. Conformers: **1**/**4**, **2**/**3**, **9**/**12**, and **18**/**19**. Stereoisomers: **1** /**4**, **9**/**12**, and **17**/**19**.

Table 2: Relative Gibbs free energy (kcal·mol^{-1}) for the geometry-optimized difluorinated pyrrolidines.

isomer	ΔG^0_{gas}	isomer	ΔG^0_{DMSO}
1	3.50	**1**	3.23
2	1.15	**2**	1.83
3	1.79	**3**	2.20
4	7.59	**4**	3.23
9	13.02	**5**	3.47
10	9.70	**6**	2.19
12	13.55	**9**	12.94
17	0.75	**10**	10.88
18	1.79	**12**	12.87
19	0.00	**17**	0.11
		18	1.01
		19	0.00

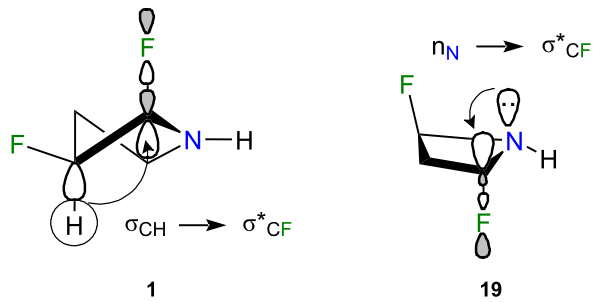

Figure 6: $\sigma_{CH} \rightarrow \sigma^*_{CF}$ fluorine *gauche* interaction, which also occurred in **19**, and anomeric interaction in isomer **19**. The $n_N \rightarrow \sigma^*_{CF}$ electron delocalization stabilized **19** by 22.43 kcal·mol^{-1}.

Conclusion

Quantum-chemical calculations were conducted at the B3LYP-GD3BJ/6-311++G(d,p) level to assess isodesmic

Table 3: Relative electronic energy ($\Delta E_{full} = \Delta E_{Lewis} + \Delta E_{non\text{-}Lewis}$) in isodesmic relationships and significant electron delocalization derived from NBO calculations (kcal·mol^{-1}) for the difluorinated pyrrolidines in the gas phase.

isomer	ΔE_{full}	ΔE_{Lewis}	$\Delta E_{non\text{-}Lewis}$	$n_N \rightarrow \sigma^*_{CF}$	$\sigma_{CH} \rightarrow \sigma^*_{CF}$[a]
1	3.27	31.68	−28.41	23.71	3.81
2	1.38	28.39	−27.01	26.97	3.82
3	1.91	27.09	−25.18	22.90	4.61
4	7.69	30.35	−22.66	17.53	4.36
9	13.09	16.87	−3.79	0.00	8.95
10	9.63	9.63	0.00	0.00	5.83
12	13.45	20.12	−6.67	1.51	6.37
17	1.00	23.20	−22.21	21.97	7.89
18	2.07	21.97	−19.90	17.31	8.37
19	0.00	22.71	−22.71	22.43	8.02

[a]Sum of antiperiplanar $\sigma_{CH} \rightarrow \sigma^*_{CF}$ interactions.

relationships for the most stable conformations of all isomers of 1,2- and 1,3- difluorinated pyrrolidines. This level of theory was chosen for its superior performance compared to other methodologies, as demonstrated through comparisons of the method with structural data on the 3-fluoropyrrolidinium cation and 3-fluoropyrrolidine. The conformational space of 2,3-, 2,4-, and 3,4-difluoropyrrolidines is notably dictated, both in the gas phase and implicit polar solution, by the N to C–F bond anomeric effect. Additionally, albeit less significant, electron delocalization from the C–H bonding orbital to the C–F antibonding orbital plays a crucial role in lowering the energy of isomers **17** and **19** relative to **1**, **2**, and **3**. These insights deepen our understanding of the energetic principles governing molecular structures and provide valuable guidance in designing selectively fluorinated stereoisomers to influence preferred conformations when designing functional molecules.

Experimental

Computational details

The benchmark study was conducted for 3-fluoropyrrolidine and 3-fluoropyrrolidinium cation to determine the optimal theoretical level for further investigations involving 2,3-, 2,4-, and 3,4-difluoropyrrolidines, compared to the CCSD/DGTZVP level [14,15]. The evaluated levels encompassed the B3LYP-GD3BJ [16-18], ωB97XD [19], and PBEPBE [20] functionals, along with the 6-311++G(d,p) [21] and DGTZVP [15] basis sets. Following the identification of B3LYP-GD3BJ/6-311++G(d,p) as the most reliable method, it was employed to optimize the geometry and compute frequencies (to derive Gibbs free energy) for the difluorinated pyrrolidines. These computations were conducted in both the gas phase and employing an implicit DMSO solvent using SMD [22]. Subsequently, a NBO [23] analysis was performed for the gas-phase-optimized geometry at the same level of theory, utilizing the DEL (NOSTAR) keyword to discern Lewis- and non-Lewis-type contributions to the total electronic energy, alongside individual electronic delocalization interactions. The calculations were all performed using the Gaussian 16 package of software [24].

Supporting Information

Supporting Information File 1

Standard orientations for the difluorinated pyrrolidines in the gas phase and DMSO.
[https://www.beilstein-journals.org/bjoc/content/supplementary/1860-5397-20-140-S1.pdf]

Funding

The authors are grateful to Coordenação de Aperfeiçoamento de Pessoal de Nível Superior (CAPES, funding code 001), Conselho Nacional de Desenvolvimento Científico e Tecnológico (CNPq, grant number 306830/2021-3), and Fundação de Amparo à Pesquisa do Estado de Minas Gerais (FAPEMIG) for the financial support of this research.

Author Contributions

Ana Flávia Candida Silva: formal analysis; investigation. Francisco A. Martins: formal analysis; investigation; supervision; writing – review & editing. Matheus P. Freitas: conceptualization; formal analysis; supervision; writing – original draft; writing – review & editing.

ORCID® iDs

Matheus P. Freitas - https://orcid.org/0000-0002-7492-1801

Data Availability Statement

All data that supports the findings of this study is available in the published article and/or the supporting information to this article.

References

1. O'Hagan, D. *J. Org. Chem.* **2012,** *77,* 3689–3699. doi:10.1021/jo300044q
2. Gakh, A. N. Monofluorinated Heterocycles. In *Halogenated Heterocycles: Synthesis, Application and Environment;* Iskra, J., Ed.; Springer: Heidelberg, Germany, 2012; pp 33–63. doi:10.1007/7081_2011_58
3. Buissonneaud, D. Y.; van Mourik, T.; O'Hagan, D. *Tetrahedron* **2010,** *66,* 2196–2202. doi:10.1016/j.tet.2010.01.049
4. Silla, J. M.; Silva, W. G. D. P.; Cormanich, R. A.; Rittner, R.; Tormena, C. F.; Freitas, M. P. *J. Phys. Chem. A* **2014,** *118,* 503–507. doi:10.1021/jp410458w
5. Gooseman, N. E. J.; O'Hagan, D.; Peach, M. J. G.; Slawin, A. M. Z.; Tozer, D. J.; Young, R. J. *Angew. Chem., Int. Ed.* **2007,** *46,* 5904–5908. doi:10.1002/anie.200700714
6. Sun, A.; Lankin, D. C.; Hardcastle, K.; Snyder, J. P. *Chem. – Eur. J.* **2005,** *11,* 1579–1591. doi:10.1002/chem.200400835
7. Lesarri, A.; Cocinero, E. J.; López, J. C.; Alonso, J. L. *J. Am. Chem. Soc.* **2005,** *127,* 2572–2579. doi:10.1021/ja045955m
8. Freitas, M. P.; Rittner, R.; Tormena, C. F.; Abraham, R. J. *Spectrochim. Acta, Part A* **2005,** *61,* 1771–1776. doi:10.1016/j.saa.2004.07.007
9. Martins, F. A.; Silla, J. M.; Freitas, M. P. *Carbohydr. Res.* **2017,** *451,* 29–35. doi:10.1016/j.carres.2017.09.007
10. Hofman, G.-J.; Ottoy, E.; Light, M. E.; Kieffer, B.; Kuprov, I.; Martins, J. C.; Sinnaeve, D.; Linclau, B. *Chem. Commun.* **2018,** *54,* 5118–5121. doi:10.1039/c8cc01493k
11. Gao, J.-X.; Zhang, W.-Y.; Wu, Z.-G.; Zheng, Y.-X.; Fu, D.-W. *J. Am. Chem. Soc.* **2020,** *142,* 4756–4761. doi:10.1021/jacs.9b13291
12. Roy, K.; Das, R. N.; Ambure, P.; Aher, R. B. *Chemom. Intell. Lab. Syst.* **2016,** *152,* 18–33. doi:10.1016/j.chemolab.2016.01.008
13. Goodman, L.; Gu, H.; Pophristic, V. *J. Phys. Chem. A* **2005,** *109,* 1223–1229. doi:10.1021/jp046290d

14. Cížek, J. On the Use of the Cluster Expansion and the Technique of Diagrams in Calculations of Correlation Effects in Atoms and Molecules. In *Advances in Chemical Physics;* LeFebvre, R.; Moser, C., Eds.; John Wiley & Sons: New York, NY, USA, 1969; Vol. 14, pp 35–89. doi:10.1002/9780470143599.ch2
15. Godbout, N.; Salahub, D. R.; Andzelm, J.; Wimmer, E. *Can. J. Chem.* **1992,** *70,* 560–571. doi:10.1139/v92-079
16. Becke, A. D. *Phys. Rev. A* **1988,** *38,* 3098–3100. doi:10.1103/physreva.38.3098
17. Lee, C.; Yang, W.; Parr, R. G. *Phys. Rev. B* **1988,** *37,* 785–789. doi:10.1103/physrevb.37.785
18. Grimme, S.; Ehrlich, S.; Goerigk, L. *J. Comput. Chem.* **2011,** *32,* 1456–1465. doi:10.1002/jcc.21759
19. Chai, J.-D.; Head-Gordon, M. *Phys. Chem. Chem. Phys.* **2008,** *10,* 6615–6620. doi:10.1039/b810189b
20. Adamo, C.; Barone, V. *J. Chem. Phys.* **1999,** *110,* 6158–6170. doi:10.1063/1.478522
21. McLean, A. D.; Chandler, G. S. *J. Chem. Phys.* **1980,** *72,* 5639–5648. doi:10.1063/1.438980
22. Marenich, A. V.; Cramer, C. J.; Truhlar, D. G. *J. Phys. Chem. B* **2009,** *113,* 6378–6396. doi:10.1021/jp810292n
23. *NBO 7.0;* Theoretical Chemistry Institute, University of Wisconsin–Madison: Madison, WI, USA, 2018.
24. *Gaussian 16,* Revision C.01; Gaussian, Inc.: Wallingford, CT, 2016.

License and Terms

BEILSTEIN JOURNAL OF ORGANIC CHEMISTRY

1,2-Difluoroethylene (HFO-1132): synthesis and chemistry

Liubov V. Sokolenko*, Taras M. Sokolenko and Yurii L. Yagupolskii

Review

Open Access

Address:
Institute of Organic Chemistry, National Academy of Sciences of Ukraine, Academician Kukhar str., 5, Kyiv-94, 02660, Ukraine

Email:
Liubov V. Sokolenko* - sokolenko.liubov@gmail.com

* Corresponding author

Keywords:
1,2-difluoroethylene; fluorinated monomers; HFO-1132; hydrofluoroolefins; radical reactions; refrigerants

Beilstein J. Org. Chem. **2024,** *20,* 1955–1966.
https://doi.org/10.3762/bjoc.20.171

Received: 10 May 2024
Accepted: 26 July 2024
Published: 12 August 2024

This article is part of the thematic issue "Organofluorine chemistry VI".

Guest Editor: D. O'Hagan

Abstract

This article provides a comprehensive overview of the synthesis and chemistry of 1,2-difluoroethylene (HFO-1132). The major routes for the preparation of the *E*- and *Z*-isomer of HFO-1132 are reviewed, along with the chemistry in radical, nucleophilic, and electrophilic reactions.

Introduction

In the 1930s, halogenated chlorofluorocarbons (CFCs) and hydrochlorofluorocarbons (HCFCs) were synthesized and have been shown to have low toxicity, which has opened the door for the application as safe refrigerants [1,2]. The development of the commercial synthesis of CFCs and HCFCs, along with new refrigeration systems in the 1930s–1960s, has led to the wide application of these materials in household and commercial refrigeration systems [1,2]. In addition, CFCs have found applications as propellants, foam-blowing agents, cleaning solvents, etc. Although these groups of fluorinated materials are non-flammable and have low toxicity, CFCs were found to be destructive to the ozone layer of the stratosphere [1,2] due to high ozone-depleting potential (ODP). This has led to the phasing out of CFCs and the replacement with hydrofluorocarbons (HFCs), which show no significant impact on stratospheric ozone [1-3]. However, as it was demonstrated in the 1980s, HFCs have significant global warming potential (GWP) [1-3]. In the 2000s, a new generation of refrigerants, namely hydrofluoroolefins (HFOs), which have a short atmospheric lifetime and low GWP [4,5], has been introduced into commercial use [1-3]. Recently, these compounds and blends thereof have replaced HFCs in refrigerants and air-conditioning systems [1-3].

The commercial production of HFOs has made these compounds available for chemists to be used as important reagents in laboratories. For example, the interest in $CF_3CH{=}CHCF_3$ (HFO-1336mzz) [6-12], $CF_3CH{=}CHCl$ (HCFO-1233zd) [13-18], $CF_3CH{=}CHF$ (HFO-1234ze) [12,19-23], and $CF_3CF{=}CH_2$ (HFO-1234yf) [12,20,21,23-39] as fluorinated building blocks has significantly increased in the last years.

Recently, the *E*-isomer of 1,2-difluoroethylene ((*E*)-HFO-1132) has attracted attention as a new refrigerant due to the low

boiling point, moderate flammability, and low toxicity [40-42]. Also, in patent literature 1,2-difluoroethylene has been claimed to be a potential monomer for the preparation of new fluoropolymers [43,44].

Despite the fact that HFO-1132 has been known for a long time, there are no publications that summarize the chemistry of the compound. With this in mind, the main methods for the preparation of (*E*/*Z*)-1,2-difluoroethylene are discussed in this Review article. Special attention is given to the role of 1,2-difluoroethylene in multiple reaction types.

Review

Preparation of HFO-1132

In scientific literature, the number of publications on the synthesis of 1,2-difluoroethylene is limited. HFO-1132 was first obtained in 1955 as a byproduct in the reaction of diborane with tetrafluoroethylene [45]. To the best of our knowledge, the first preparative route to 1,2-difluoroethylene was described in 1957 by Haszeldine and Steele [46], using trifluoroethylene as starting material (Scheme 1) [46,47].

Another approach to 1,2-difluoroethylene was based on 1,2-dichloro-1,2-difluoroethane (HCFC-132) [48-52], prepared from 1,1,2,2-tetrachloro-1,2-difluoroethane (CFC-112) by reduction using lithium aluminum hydride [48-51] or photoreduction (Scheme 2) [51]. The resulting HCFC-132 reacted with zinc [47,49,52] or magnesium [50,51] to form the desired 1,2-difluoroethylene as a mixture of *E*- and *Z*-isomers, which were separated by fractional distillation (boiling point: −53.1 °C for (*E*)-HFO-1132 and −26.0 °C for (*Z*)-HFO-1132 [47]).

In patent literature, a variety of synthetic routes to HFO-1132 starting from other available industrial halocarbons can be found. It should be pointed out that the majority of patents in this field belongs to Daikin Industries [53-60]. Scheme 3 shows the synthesis of HFO-1132 based on dehydrofluorination of 1,1,2,-trifluoroethane (HFC-143) in the presence of base (e.g., *t*-BuOK) [53] or metal (Cr, Al, Fe, Ni, Mg)-based catalyst [54-56].

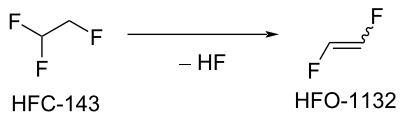

Scheme 3: 1,2-Difluoroethylene synthesis from HFC-143.

2-Chloro-1,2-difluoroethane (HCFC-142) and 1-chloro-1,2-difluoroethane (HCFC-142a) can also be used as 1,2-difluoroethene precursors (Scheme 4) [57,61]. The dehydrochlorination reaction proceeded in the presence of metal-based catalysts (Fe, Mg, Ca, Ni, Zn, Pd, Li, Na [57] or Pd, Ru [61]).

Unsaturated compounds were also applied as starting materials for 1,2-difluoroethylene preparation. Thus, chlorine atoms in 1,2-dichloro-1,2-difluoroethylene (CFO-1112) could be removed through the action of hydrogen and metal catalyst (Pd, Pd, Pt, Rh, Ru, Ir, Ni/Cu, Ag, Au, Zn, Cr, Co, Scheme 5) [62,63]. Further, 1,2-Dichloroethylene was reacted with hydro-

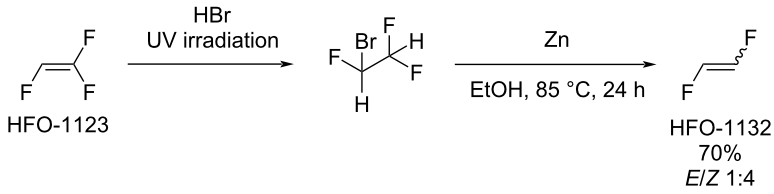

Scheme 1: 1,2-Difluoroethylene synthesis from HFO-1123.

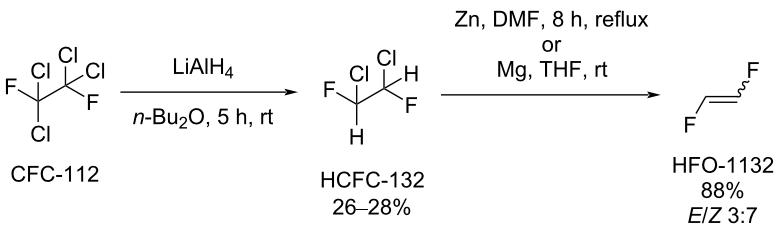

Scheme 2: 1,2-Difluoroethylene synthesis from CFC-112 and HCFC-132.

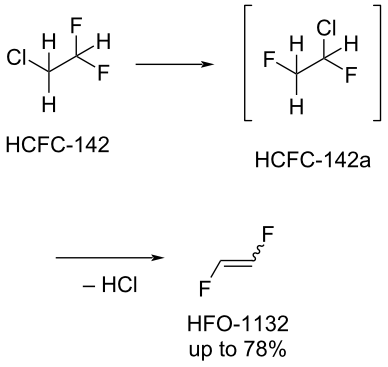

Scheme 4: 1,2-Difluoroethylene synthesis from HCFC-142 via HCFC-142a.

gen fluoride in the presence of metal fluorides or transition metals (Cr, Al, Co, Mn, Ni, Fe) to form 1,2-difluoroethylene (Scheme 6) [56,58].

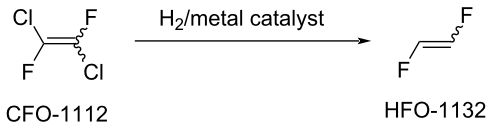

Scheme 5: 1,2-Difluoroethylene synthesis from CFO-1112.

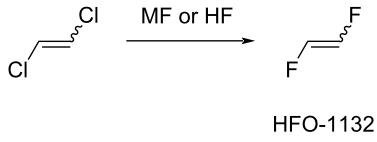

Scheme 6: 1,2-Difluoroethylene synthesis from 1,2-dichloroethylene.

In patents [59,60], an exotic synthesis of 1,2-difluoroethylene based on perfluoropropyl vinyl ether as starting material can be found (Scheme 7).

Consequently, two methods to prepare 1,2-difluoroethylene in the laboratory have been described to date. Even though at least five approaches to HFO-1132 can be found in patent literature, it is not clear which of these can be used for the commercial production of HFO-1132.

Physical properties of HFO-1132

The physical properties of the *E*- and *Z*-isomers of HFO-1132 are summarized in Table 1 [47,64-66].

IR-spectral data of (*E*)- and (*Z*)-HFO-1132 can be found in references [67] and [50], respectively, while reference [68] provides UV-spectral data of both isomers. ^{1}H, ^{19}F, and ^{13}C NMR data [69,70] are given in Table 2.

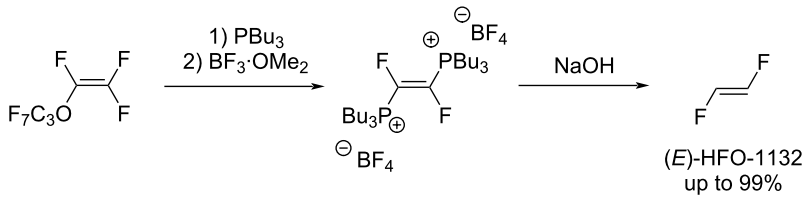

Scheme 7: 1,2-Difluoroethylene synthesis from perfluoropropyl vinyl ether.

Table 1: Physical properties of HFO-1132.

parameter	(*E*)-HFO-1132	(*Z*)-HFO-1132
boiling point, °C	–53.1 [47]	–26.0 [47]
density (at –153 °C), g/cm^3	1.592 [64]	1.556 [64]
dipole moment	0 [65]	2.81 (calculated) [65] 2.42 (experimental) [65]
ODP	0 [40]	—
GWP_{100}[a]	1.9 [66]	1.5 [66]

[a]Average GWP over 100 years.

Table 2: NMR-spectral data of HFO-1132.

compound	^{1}H NMR (300 MHz, C_6D_6, δ), ppm [69]	^{19}F NMR (282 MHz, C_6D_6, δ), ppm [69]	^{13}C NMR[1] (δ), ppm [70]
(*E*)-HFO-1132	6.68 (m)	–187.73 (dd, $^{2}J_{FH}$ = 49 Hz, $^{3}J_{FH}$ = 30 Hz)	146.0
(*Z*)-HFO-1132	5.54 (m)	–163.09 (m)	138.5

[1]CH_4 as standard.

Chemistry of HFO-1132

Isomerization

Iodine-catalyzed *cis–trans* isomerization of 1,2-difluoroethylene and corresponding equilibrium measurements were described in the 1960s [47]. Along with this, photoisomerization is described in patent literature [71-74]. It was shown that the experimentally observed enthalpy of isomerization (0.928 kcal/mol [47]) is in agreement with the calculated difference in the total energy of the two isomers (0.959 kcal/mol [65,75]). *Cis*-1,2-difluoroethylene was shown to have a lower energy compared to *trans*-1,2-difluoroethylene, which is in accordance with previously described 1,2-dihalogenated ethylene species [47].

The authors of reference [47] explained the higher stability of (*Z*)-HFO-1132 as follows: Within the family of 1,2-dihaloethylenes, when going from diiodo- and dibromo- to dichloro- and difluoroethylene, the radius of the halogen atom decreases while the electronegativity increases. As a result, the influence of halogen atom electronegativity on the double bond is more significant in 1,2-difluoroethylene, and the relative energy of the *cis*-isomer decreases, i.e., the *cis*-isomer of 1,2-difluoroethylene is thermodynamically favored [47].

Deuteration

The stereospecific reaction of (*E*/*Z*)-1,2-difluoroethylene with a 1–2 M solution of NaOD in D_2O (90–120 °C, 2 d) led to the formation of CDF=CDF with high isotopic purity (Scheme 8) [76,77].

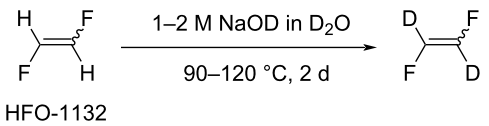

Scheme 8: Deuteration reaction of 1,2-difluoroethylene.

Additionally, when the reaction was performed using DMSO-d_6 (or CD_3CN) and CH_3ONa, H/D exchange occurred already at ambient temperature (25 °C, 20 h) [78]. The formation of CDF=CDF was confirmed by NMR spectroscopy, namely by the change of signal multiplicity in the ^{19}F NMR spectra of *E*- and *Z*-isomers of 1,2-difluoroethylene and the disappearance of vinyl protons resonances in the ^{1}H NMR spectra [78].

Addition to the C=C bond

Halogen addition: 1,2-Difluoroethylene was reported to react with chlorine [46,79] and bromine [51] under irradiation, yielding 1,2-difluoro-1,2-dihaloethanes in moderate to high yield (Scheme 9).

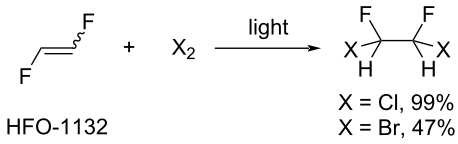

Scheme 9: Halogen addition to 1,2-difluoroethylene.

Hypohalite addition: It was shown by the DesMarteau group that different hypohalites (perfluoroalkyl-, perfluoroacyl-, perfluoroalkylsulfonyl-, and peroxyhypochlorite) easily reacted with 1,2-difluoroethylene to form addition products in high to quantitative yield (Scheme 10) [80-88]. In Table 3, reaction data are summarized to show the scope and limitations of this process.

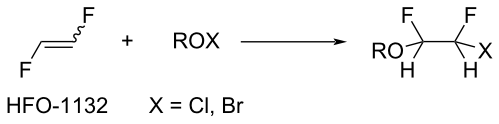

Scheme 10: Hypohalite addition to 1,2-difluoroethylene.

An interesting feature of this reaction is the high stereospecificity. In almost all cases, the addition proceeded *syn*-specific, yielding the *erythro*-isomer from *cis*- and the *threo*-isomer from *trans*-1,2-difluoroethylene, respectively, with one exception: *threo*-isomer formation from *cis*-1,2-difluoroethylene (entry 1, Table 3). Supposedly this was due to dominant steric factors, such that the reaction occurred as *anti*-addition.

Table 3: Hypohalite addition to 1,2-difluoroethylene.

entry	hypohalite	configuration	product	yield, %	Reference
1	$CF_3CF_2C(CF_3)_2OBr$	*Z* (*cis*)	*threo*-$CF_3CF_2C(CF_3)_2OCFH–CFHBr$	74	[81]
2	$FSO_2CF_2CF_2OCl$	*Z* (*cis*)	*erythro*-$FSO_2CF_2CF_2OCFH–CFHCl$	100	[80]
3	CF_3OF	*Z* (*cis*)	$CF_3OCFH–CF_2H$	100	[82]
4	CF_3OCl	*Z* (*cis*)	*erythro*-$CF_3OCFH–CFHCl$	86	[82]
		E (*trans*)	*threo*-$CF_3OCFH–CFHCl$	88	
		E/*Z* 8:5	*erythro*/*threo*-$CF_3OCFH–CFHCl$ 8:5	not stated	
5	$CF_3C(O)OCl$	*Z* (*cis*)	*erythro*-$CF_3C(O)OCFH–CFHCl$	64	[83]
		E (*trans*)	*threo*-$CF_3C(O)OCFH–CFHCl$	65	
6	CF_3SO_2OCl	*Z* (*cis*)	*erythro*-$CF_3SO_2OCFH–CFHCl$	88	[84,85]
		Z/*E* 3:2	*erythro*/*threo*-$CF_3SO_2OCFH–CFHCl$ ≈ 3:2	90	
7	CF_3SO_2OBr	*Z* (*cis*)	*erythro*-$CF_3SO_2OCFH–CFHBr$	87	[84]
		Z/*E* 3:2	*erythro*/*threo*-$CF_3SO_2OCFH–CFHBr$ ≈ 3:2	95	
8	$C_4F_9SO_2OCl$	*Z* (*cis*)	*erythro*-$C_4F_9SO_2OCFH–CFHCl$	80	[86]
9	$C_4F_9SO_2OBr$	*Z* (*cis*)	*erythro*-$C_4F_9SO_2OCFH–CFHBr$	80	[86]
10	CF_3OOCl	*Z* (*cis*)	*erythro*-$CF_3OOCFH–CFHCl$	40[a]	[87]
11	SF_5OOCl	*Z* (*cis*)	*erythro*-$SF_5OOCFH–CFHCl$	70	[88]

[a]Chloroperoxytrifluoromethane is an unstable compound that decomposed to CF_3OCl. Therefore, $CF_3OCFH–CFHCl$ byproduct was also isolated in 11% yield in this reaction.

Addition of *N*-halo compounds: It was shown by Haszeldine and Tipping that *N*-bromobis(trifluoromethyl)amine easily reacted with (*Z*)-1,2-difluoroethylene to form the addition product in high yield (Scheme 11) [89]. However, the stereochemistry of this reaction has not been reported.

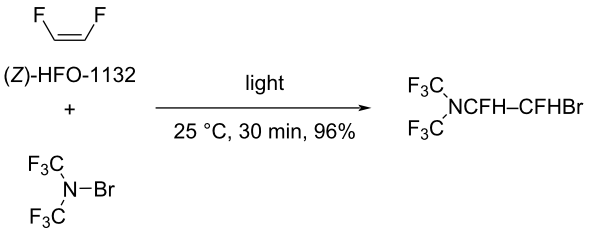

Scheme 11: *N*-Bromobis(trifluoromethyl)amine addition to 1,2-difluoroethylene.

A similar reaction of (*Z*)-1,2-difluoroethylene with *N*-chloroimidobis(sulfonyl fluoride) (Scheme 12) [90] was shown to be stereounspecific, although the addition product was reported to form in high yield.

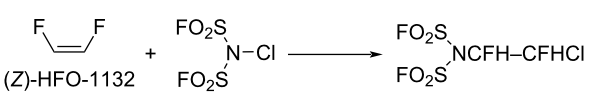

Scheme 12: *N*-Chloroimidobis(sulfonyl fluoride) addition to 1,2-difluoroethylene.

In the same publication [90], it was mentioned that $(FSO_2)_2NH$ did not form an addition product in the reaction with (*Z*)-1,2-difluoroethylene, although the reaction of $(FSO_2)_2NH$ with other olefins, including fluorinated ones, occurred similar to HF addition [90].

Miscellaneous additions: In reference [91], the addition of trichlorosilane to 1,2-difluoroethylene (Scheme 13) was reported by the Haszeldine group. The reaction under UV irradiation produced the corresponding trichlorosilane in 85% yield, and the silane that was obtained was pyrolyzed to form vinyl fluoride.

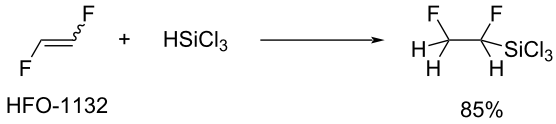

Scheme 13: Trichlorosilane addition to 1,2-difluoroethylene.

It was shown that SF_5Br easily reacted with the *E*- and *Z*-isomer, respectively, of 1,2-difluoroethylene in the presence or absence of light, yielding a mixture of *erythro*- and *threo*-isomeric addition products in both cases (Scheme 14) [92]. However, under light irradiation, conversion and product yield were higher, although the ratio of diastereomers produced in

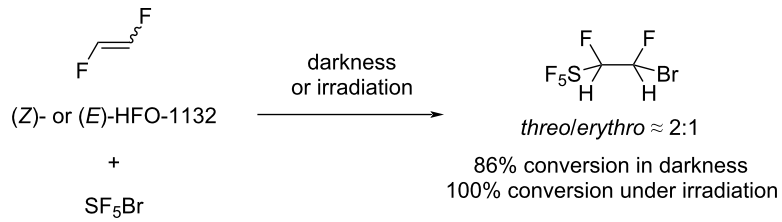

Scheme 14: SF_5Br addition to 1,2-difluoroethylene.

both cases was almost the same for the *E*- and *Z*-isomer, respectively, and did not depend on irradiation.

The reaction of 1,2-difluoroethylene with PCl_3 and O_2 was described by Boyce and co-workers [93]. Therein, a mixture of products, with diethyl 2-chloro-1,2-difluoroethylphosphonate as main compound, was formed (Scheme 15). This mixture was reacted with absolute ethanol, and the esters formed were separated by distillation and characterized. The authors did not point out which 1,2-difluoroethylene isomer (*E* and/or *Z*) was used. It was mentioned that the addition products were obtained as a mixture of diastereomers (Scheme 15).

Tetramethyldiarsine was shown to react with (*Z*/*E*)-1,2-difluoroethylene under UV irradiation, yielding the product as a mixture of the racemate and the *meso* form in high combined yield (90%, Scheme 16) [94]. The product was used as a ligand for the preparation of transitional metal carbonyl complexes.

The addition reaction of trichlorofluoromethane (CFC-11) to 1,2-difluoroethylene in the presence of aluminum chloride under pressure was described [51]. In this electrophilic reaction, two products were formed in 3:1 ratio (Scheme 17) in a very low yield of 0.4%.

In patent literature [95], radical reaction of 1,2-difluoroethylene with long-chain perfluoroalkyl iodides ($C_nF_{2n+1}I$, n = 2–8) was described (Scheme 18). Products formed were further converted into polyfluorinated olefins $R_FCF{=}CFH$ by HI elimination.

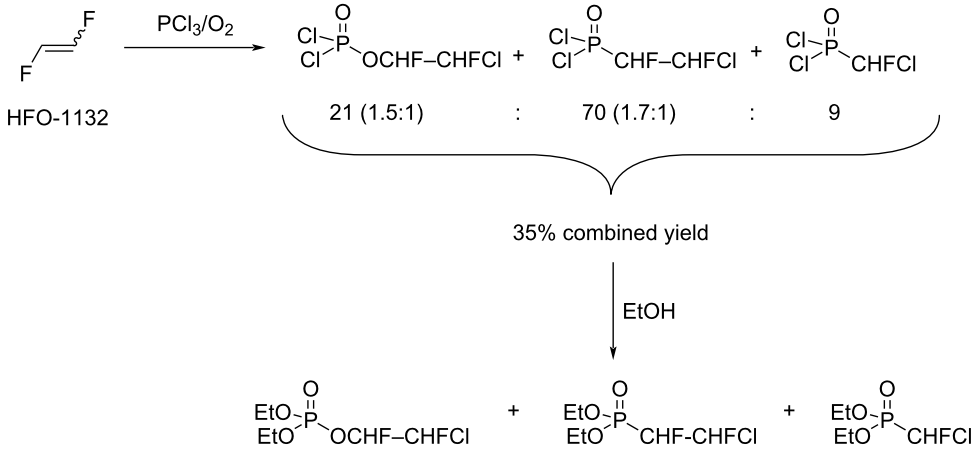

Scheme 15: PCl_3/O_2 addition to 1,2-difluoroethylene.

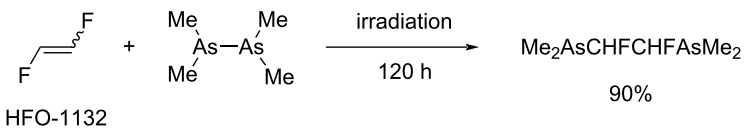

Scheme 16: Reaction of tetramethyldiarsine with 1,2-difluoroethylene.

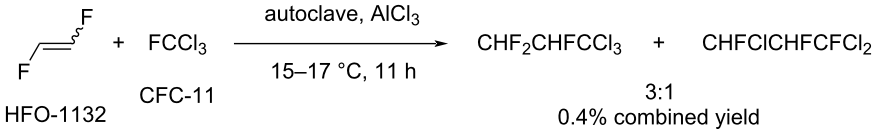

Scheme 17: Reaction of trichlorofluoromethane with 1,2-difluoroethylene.

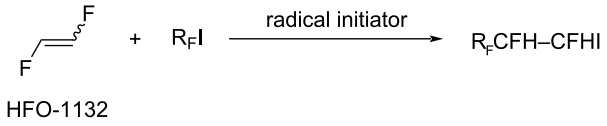

Scheme 18: Addition of perfluoroalkyl iodides to 1,2-difluoroethylene.

Cyclization reactions

Carbocyclizations: A series of articles devoted to structural investigations of 1,2-difluorocyclopropanes was published [96-98]. For this purpose, *cis*- and *trans*-1,2-difluorocyclopropanes were synthesized by liquid-phase photolysis at −80 °C from 1,2-difluoroethylene and diazomethane (Scheme 19). Unfortunately, the product yield was not reported.

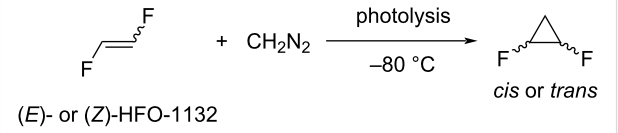

Scheme 19: Cyclopropanation of 1,2-difluoroethylene.

Diels–Alder reaction of (*E*)- and (*Z*)-1,2-difluoroethylenes with hexachlorocyclopentadiene was studied by Ihrid and Smith [99]. It was shown that (*Z*)-1,2-difluoroethylene reacted with hexachlorocyclopentadiene at 200–220 °C within 3–4 days, forming 5,6-*endo*,*endo*-difluoro-1,2,3,4,7,7-hexachlorobicyclo[2.2.1]-2-heptene (Scheme 20) in 66% yield. At the same time, (*E*)-1,2-difluoroethylene, which formed the *endo*,*exo*-adduct, reacted much slower, and completion of the reaction required 2–3 weeks at the same temperature. In this case, sufficient *E*–*Z* isomerization of the starting olefin occurred during the reaction, and the major product was 5,6-*endo*,*endo*-difluoro-1,2,3,4,7,7-hexachlorobicyclo[2.2.1]-2-heptene, which was formed from (*Z*)-1,2-difluoroethylene (Scheme 20). Both products were separated by column chromatography and characterized.

Heterocyclizations–photochemical [2 + 2]- and [2 + 4]-cycloaddition reactions: The formation of oxetanes as a result of photochemical cycloaddition of fluoroketones or fluoroaldehydes and 1,2-difluoroethylene was previously described by Haszeldine et al. [49,100]. The reaction of individual *E*- or *Z*-isomer of 1,2-difluoroethylene and fluorinated ketones (Scheme 21) led to a mixture of stereoisomers in both cases, al-

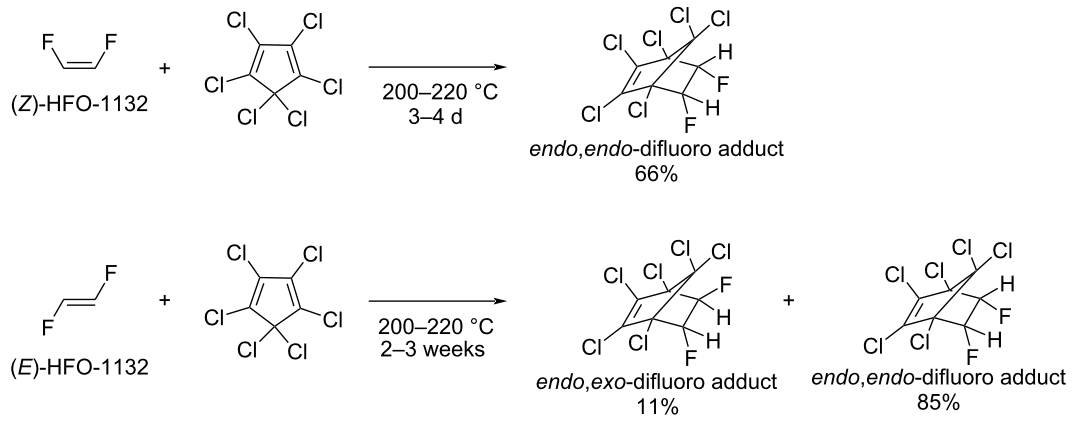

Scheme 20: Diels–Alder reaction of 1,2-difluoroethylene and hexachlorocyclopentadiene.

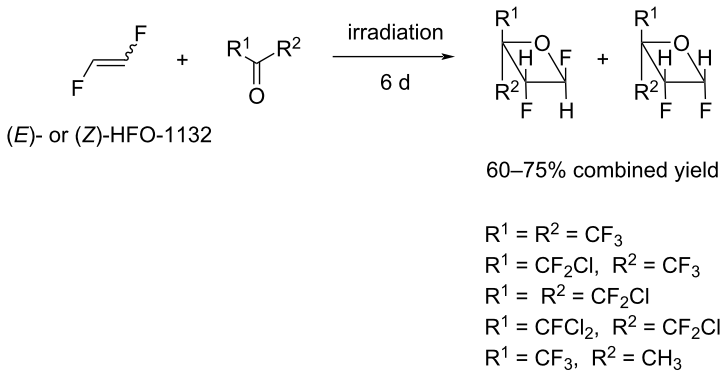

Scheme 21: Cycloaddition reaction of 1,2-difluoroethylene and fluorinated ketones.

though for the *E*-isomer, about 70% of the product retained the starting configuration. Overall, (*E*)-1,2-difluoroethylene had higher reactivity than (*Z*)-1,2-difluoroethylene in this reaction.

The reaction of either (*E*)- or (*Z*)-1,2-difluoroethylene with perfluoroaldehydes resulted in the formation of three isomeric oxetanes in a 1.0:1.7:1.3 ratio in a high yield of 78–94% (Scheme 22) [49].

All data reported for the [2 + 2]-cycloaddition reaction of fluorinated ketones and aldehydes [49,100] were indicative of the fact that under photochemical conditions, this reaction is likely to be a stepwise process involving the formation of a biradical intermediate.

Either (*Z*)- or (*E*)-1,2-difluoroethylene easily reacted with hexafluorodiacetyl under UV irradiation, yielding a mixture of five products, regardless of the configuration of the starting 1,2-difluoroethylene, in a ratio of 8.8:2.0:1.2:1.2:1.0 in 85% and 92% yield for the *Z*- and *E*-olefin, respectively (Scheme 23) [48]. Interestingly, the formation of [4 + 2]-adducts in this case was predominant over [2 + 2]-cycloadducts.

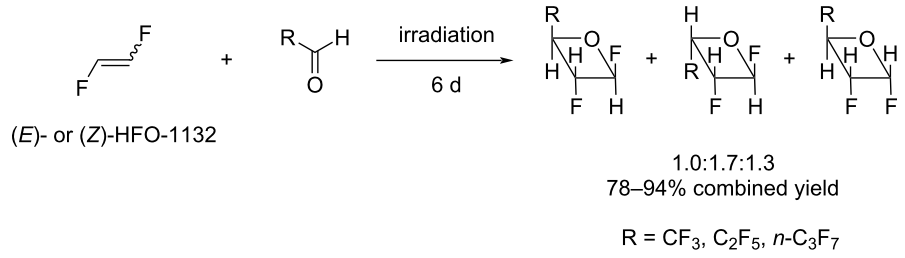

Scheme 22: Cycloaddition reaction of 1,2-difluoroethylene and perfluorinated aldehydes.

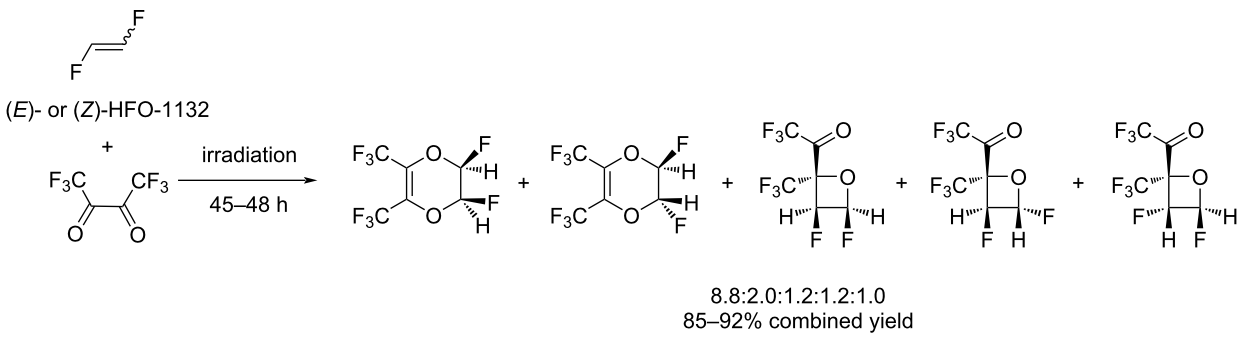

Scheme 23: Photochemical cycloaddition of 1,2-difluoroethylene and hexafluorodiacetyl.

Reactions involving C–F bonds

It was shown by Liu and co-workers that SiF_2 was able to insert into the C–F bond of 1,2-difluoroethylene, as well as into the emerging Si–F bond, leading to a mixture of fluoropolysilanes with a low combined yield (Scheme 24) [101,102].

Our group attempted to use (*E*/*Z*)-1,2-difluoroethylene in a Heck reaction [78]. The experiments were performed using 4-iodotoluene or methyl 4-iodobenzoate in DMF, $Pd(OAc)_2$ as a catalyst, and Et_3N as a base (Scheme 25). The reactions were carried out in a stainless steel autoclave at 120 °C for 24 h. Careful investigation of the product structures by ^1H and ^{19}F NMR as well as GC–MS revealed exclusive substitution of fluorine rather than hydrogen, leading to a mixture of products in the ratio 0.15:1:1:0.15 (Scheme 25), with a combined yield of 50% for 4-iodotoluene and 75% for methyl 4-iodobenzoate. Under similar conditions, 4-nitroiodobenzene produced exclusively the corresponding homocoupling product 4,4'-nitrobiphenyl.

Additional author remarks

Other attempts to utilize 1,2-difluoroethylene in reactions with N-, O-, and C- nucleophiles carried out in our group were unsuccessful [78], while S-nucleophiles, namely thiophenolates, led to products upon fluorine atom substitution, which were isolated in low yield. Corresponding disulfides were isolated as major products, even when the reaction was carried out under inert atmosphere, suggesting a radical process.

In summary, we compiled the methods for the preparation of HFO-1132 as well as reactions demonstrating the chemical behavior of this compound. From the reactions not included in this Review article, mechanistic studies on 1,2-difluoroethylene ozonolysis [77,103-108] and studies on the stability of transitional metal complexes with 1,2-difluoroethylene as a ligand should be mentioned [109-111].

Conclusion

In conclusion, our literature analysis demonstrated that radical processes are most typical for 1,2-difluoroethylene, while examples of electrophilic reactions are scarce, and nucleophilic reactions were not described at all. Nevertheless, the radical reactions are the most powerful instrument for the preparation of new molecules with a CHF–CHF fragment. For instance, the radical addition of hypohalites is a suitable high-yielding approach toward polyfluorinated aliphatic ethers and esters. Photochemical [2 + 2]-cycloaddition with fluorinated aldehydes and ketones gives access to a variety of fluorinated oxygen-containing heterocycles. We hope that this article will help chemists to utilize HFO-1132 and that this olefin will find applications as a useful synthon in organic chemistry.

Author Contributions

Liubov V. Sokolenko: conceptualization; data curation; writing – original draft; writing – review & editing. Taras M. Sokolenko: investigation; methodology; validation. Yurii L. Yagupolskii: conceptualization; funding acquisition; writing – review & editing.

ORCID® iDs

Liubov V. Sokolenko - https://orcid.org/0000-0002-4757-0305
Taras M. Sokolenko - https://orcid.org/0000-0002-3944-5571
Yurii L. Yagupolskii - https://orcid.org/0000-0002-5179-4096

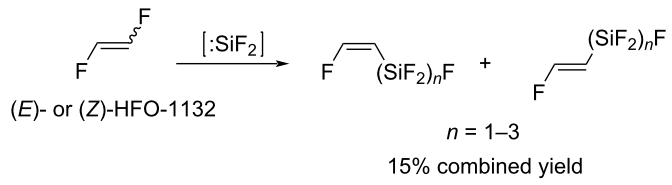

Scheme 24: Reaction of 1,2-difluoroethylene with difluorosilylene.

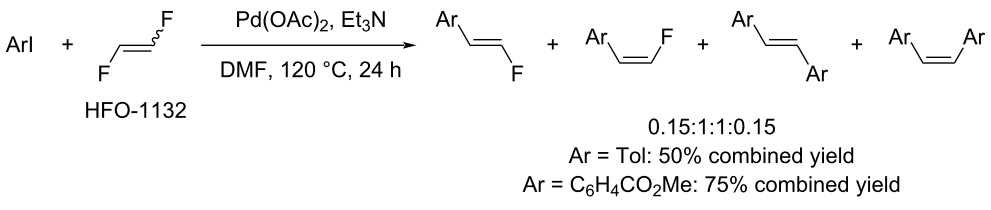

Scheme 25: Reaction of 1,2-difluoroethylene with aryl iodides.

Data Availability Statement

Data sharing is not applicable as no new data was generated or analyzed in this study.

References

1. McLinden, M. O.; Seeton, C. J.; Pearson, A. *Science* **2020,** *370,* 791–796. doi:10.1126/science.abe3692
2. McLinden, M. O.; Huber, M. L. *J. Chem. Eng. Data* **2020,** *65,* 4176–4193. doi:10.1021/acs.jced.0c00338
3. Hogue, C. *Chem. Eng. News* **2011,** *89* (49), 31–32. doi:10.1021/cen-v089n049.p031
4. Nappa, M.; Peng, S.; Sun, X. Industrial Syntheses of Hydrohaloolefins and Related Products. In *Modern Synthesis Processes and Reactivity of Fluorinated Compounds;* Groult, H.; Leroux, F. R.; Tressaud, A., Eds.; Progress in Fluorine Science Series, Vol. 3; Elsevier: Amsterdam, Netherlands, 2017; pp 27–69. doi:10.1016/b978-0-12-803740-9.00003-2
5. Søndergaard, R.; Nielsen, O. J.; Hurley, M. D.; Wallington, T. J.; Singh, R. *Chem. Phys. Lett.* **2007,** *443,* 199–204. doi:10.1016/j.cplett.2007.06.084
6. Misani, F.; Speers, L.; Lyon, A. M. *J. Am. Chem. Soc.* **1956,** *78,* 2801–2804. doi:10.1021/ja01593a041
7. Fields, R.; Haszeldine, R. N. *J. Chem. Soc.* **1964,** 1881–1889. doi:10.1039/jr9640001881
8. Atherton, J. H.; Fields, R. *J. Chem. Soc. C* **1968,** 1507–1513. doi:10.1039/j39680001507
9. Koh, M. J.; Nguyen, T. T.; Lam, J. K.; Torker, S.; Hyvl, J.; Schrock, R. R.; Hoveyda, A. H. *Nature* **2017,** *542,* 80–85. doi:10.1038/nature21043
10. VenkatRamani, S.; Schrock, R. R.; Hoveyda, A. H.; Müller, P.; Tsay, C. *Organometallics* **2018,** *37,* 1641–1644. doi:10.1021/acs.organomet.8b00168
11. Mu, Y.; Nguyen, T. T.; van der Mei, F. W.; Schrock, R. R.; Hoveyda, A. H. *Angew. Chem., Int. Ed.* **2019,** *58,* 5365–5370. doi:10.1002/anie.201901132
12. Pavlenko, N. V.; Peng, S.; Petrov, V.; Jackson, A.; Sun, X.; Sprague, L.; Yagupolskii, Y. L. *Eur. J. Org. Chem.* **2020,** 5425–5435. doi:10.1002/ejoc.202000853
13. Miyagawa, A.; Naka, M.; Yamazaki, T.; Kawasaki-Takasuka, T. *Eur. J. Org. Chem.* **2009,** 4395–4399. doi:10.1002/ejoc.200900370
14. Naka, M.; Kawasaki-Takasuka, T.; Yamazaki, T. *Beilstein J. Org. Chem.* **2013,** *9,* 2182–2188. doi:10.3762/bjoc.9.256
15. Mushta, O. I.; Kremlev, M. M.; Filatov, A. A.; Yagupolskii, Y. L. *J. Fluorine Chem.* **2020,** *232,* 109456. doi:10.1016/j.jfluchem.2020.109456
16. Li, Y.; Hao, M.; Chang, Y.-C.; Liu, Y.; Wang, W.-F.; Sun, N.; Zhu, W.-Q.; Gao, Z. *Chin. J. Chem.* **2021,** *39,* 2962–2966. doi:10.1002/cjoc.202100313
17. Petko, K. I.; Filatov, A. A.; Yagupolskii, Y. L. *Chem. Heterocycl. Compd.* **2022,** *58,* 129–134. doi:10.1007/s10593-022-03065-y
18. Cheng, J.; Zhang, C.; Quan, H. *J. Fluorine Chem.* **2023,** *270,* 110164. doi:10.1016/j.jfluchem.2023.110164
19. Gregory, R.; Haszeldine, R. N.; Tipping, A. E. *J. Chem. Soc. C* **1970,** 1750–1758. doi:10.1039/j39700001750
20. Sakaguchi, H.; Uetake, Y.; Ohashi, M.; Niwa, T.; Ogoshi, S.; Hosoya, T. *J. Am. Chem. Soc.* **2017,** *139,* 12855–12862. doi:10.1021/jacs.7b08343
21. Sakaguchi, H.; Ohashi, M.; Ogoshi, S. *Angew. Chem., Int. Ed.* **2018,** *57,* 328–332. doi:10.1002/anie.201710866
22. Schwabedissen, J.; Glodde, T.; Vishnevskiy, Y. V.; Stammler, H.-G.; Flierl, L.; Kornath, A. J.; Mitzel, N. W. *ChemistryOpen* **2020,** *9,* 921–928. doi:10.1002/open.202000172
23. Phillips, N. A.; Coates, G. J.; White, A. J. P.; Crimmin, M. R. *Chem. – Eur. J.* **2020,** *26,* 5365–5368. doi:10.1002/chem.202000636
24. Li, Y.; Sun, N.; Hao, M.; Zhang, C.-L.; Li, H.; Zhu, W.-Q. *Catal. Lett.* **2021,** *151,* 764–772. doi:10.1007/s10562-020-03334-5
25. Li, Y.; Tu, D.-H.; Gu, Y.-J.; Wang, B.; Wang, Y.-Y.; Liu, Z.-T.; Liu, Z.-W.; Lu, J. *Eur. J. Org. Chem.* **2015,** 4340–4343. doi:10.1002/ejoc.201500597
26. Yagupolskii, Y. L.; Pavlenko, N. V.; Shelyazhenko, S. V.; Filatov, A. A.; Kremlev, M. M.; Mushta, A. I.; Gerus, I. I.; Peng, S.; Petrov, V. A.; Nappa, M. *J. Fluorine Chem.* **2015,** *179,* 134–141. doi:10.1016/j.jfluchem.2015.08.001
27. Hiraoka, Y.; Kawasaki-Takasuka, T.; Morizawa, Y.; Yamazaki, T. *J. Fluorine Chem.* **2015,** *179,* 71–76. doi:10.1016/j.jfluchem.2015.05.006
28. Meyer, D.; El Qacemi, M. *Org. Lett.* **2020,** *22,* 3479–3484. doi:10.1021/acs.orglett.0c00931
29. Murray, B. J.; Ball, E. D.; Harsanyi, A.; Sandford, G. *Eur. J. Org. Chem.* **2019,** 7666–7672. doi:10.1002/ejoc.201901445
30. Murray, B. J.; Boulton, L. T.; Sandford, G. *J. Fluorine Chem.* **2021,** *245,* 109774. doi:10.1016/j.jfluchem.2021.109774
31. Luo, Y.-C.; Wang, M.-K.; Yu, L.-C.; Zhang, X. *Angew. Chem., Int. Ed.* **2023,** *62,* e202308690. doi:10.1002/anie.202308690
32. Murray, B. J.; Marsh, T. G. F.; Yufit, D. S.; Fox, M. A.; Harsanyi, A.; Boulton, L. T.; Sandford, G. *Eur. J. Org. Chem.* **2020,** 6236–6244. doi:10.1002/ejoc.202001071
33. Varga, B.; Tóth, B. L.; Béke, F.; Csenki, J. T.; Kotschy, A.; Novák, Z. *Org. Lett.* **2021,** *23,* 4925–4929. doi:10.1021/acs.orglett.1c01709
34. Csenki, J. T.; Tóth, B. L.; Béke, F.; Varga, B.; Fehér, P. P.; Stirling, A.; Czégény, Z.; Bényei, A.; Novák, Z. *Angew. Chem., Int. Ed.* **2022,** *61,* e202208420. doi:10.1002/anie.202208420
35. Bakewell, C.; White, A. J. P.; Crimmin, M. R. *Angew. Chem., Int. Ed.* **2018,** *57,* 6638–6642. doi:10.1002/anie.201802321
36. Talavera, M.; von Hahmann, C. N.; Müller, R.; Ahrens, M.; Kaupp, M.; Braun, T. *Angew. Chem., Int. Ed.* **2019,** *58,* 10688–10692. doi:10.1002/anie.201902872
37. Coates, G.; Tan, H. Y.; Kalff, C.; White, A. J. P.; Crimmin, M. R. *Angew. Chem., Int. Ed.* **2019,** *58,* 12514–12518. doi:10.1002/anie.201906825
38. Meißner, G.; Kretschmar, K.; Braun, T.; Kemnitz, E. *Angew. Chem., Int. Ed.* **2017,** *56,* 16338–16341. doi:10.1002/anie.201707759
39. Csenki, J. T.; Novák, Z. *Chem. Commun.* **2024,** *60,* 726–729. doi:10.1039/d3cc04985j
40. Gobo, K.; Tsuchiya, T.; Yamada, Y.; Nakaue, T.; Karube, D.; Komatsu, Y.; Ito, R.; Ohkubo, S.; Rydkin, I. Thermal stability of novel HFO blend refrigerant. In *HFO2021 2nd IIR Conference on HFOs and Low GWP blends,* June 16–18, 2021; Osaka, Japan; Paper ID 1043. doi:10.18462/iir.hfo.2021.1043
41. Tomoaki, T.; Mai, H.; Shuichi, O.; Masato, F. Actuation medium for heat cycle and manufacturing method therefor. Japn. Pat. App. JP2015,229,768A, Dec 21, 2015.
42. Takashi, Y.; Tomoyuki, G.; Yuki, Y. Composition, method for preserving refrigerant, and method for suppressing polymerization of refrigerant. Japn. Pat. Appl. JP2022,063,162A, April 21, 2022.

43. Yotsumoto, Y.; Ryouichi, Y.; Takahiro, F. Fluorine-containing polymer and production method thereof. U.S. Pat. Appl. US2023,220,128A1, June 13, 2023.
44. Rina, T.; Tatsuya, M.; Sota, Y.; Kouhei, T.; Masaki, I. Production method for aqueous fluorine-containing elastomer dispersion, composition, and aqueous dispersion. WO Pat. Appl. WO2022,260,139A1, Dec 15, 2022.
45. Stone, F. G. A.; Graham, W. A. G. *Chem. Ind.* **1955,** 1181–1183.
46. Haszeldine, R. N.; Steele, B. R. *J. Chem. Soc.* **1957,** 2800–2806. doi:10.1039/jr9570002800
47. Craig, N. C.; Entemann, E. A. *J. Am. Chem. Soc.* **1961,** *83,* 3047–3050. doi:10.1021/ja01475a019
48. Barlow, M. G.; Coles, B.; Haszeldine, R. N. *J. Chem. Soc., Perkin Trans. 1* **1980,** 2523–2526. doi:10.1039/p19800002523
49. Barlow, M. G.; Coles, B.; Haszeldine, R. N. *J. Chem. Soc., Perkin Trans. 1* **1980,** 2258–2267. doi:10.1039/p19800002258
50. Visinoni, R.; Giorgianni, S.; Baldan, A.; Nivellini, G. *Phys. Chem. Chem. Phys.* **2001,** *3,* 4242–4246. doi:10.1039/b102537f
51. Pošta, A.; Paleta, O.; Voves, J. *Collect. Czech. Chem. Commun.* **1974,** *39,* 2801–2807. doi:10.1135/cccc19742801
52. Durrell, W. S.; Westmoreland, G.; Moshonas, M. G. *J. Polym. Sci., Part A: Gen. Pap.* **1965,** *3,* 2975–2982. doi:10.1002/pol.1965.100030824
53. Tsubasa, N.; Takashi, U.; Takehiro, C. Fluoroolefin production method. U.S. Pat. Appl. US2021070678A1, March 11, 2021.
54. Usui, T.; Nakaue, T.; Chaki, T.; Komatsu, Y. Method for producing fluoroolefin. U.S. Pat. Appl. US20210253502A1, Aug 19, 2021.
55. Kazuhiro, T.; Takehiro, C.; Tsubasa, N.; Tomoyuki, I.; Megumi, K. Method for preparing 1,1,2-trifluoroethane. WO Pat. Appl. WO2022191185A1, Sept 15, 2022.
56. Komatsu, Y. Method for preparing 1,2-difluoroethylene and/or 1,1,2-trifluoroethane. WO Pat. Appl. WO2019216239A1, Nov 14, 2019.
57. Tsubasa, N. Production method of 1,2-difluoroethylene. WO Pat. Appl. WO2020105608A1, May 28, 2020.
58. Takashi, U.; Tsubasa, N.; Tomoyuki, I. Method for producing fluoroethylene. U.S. Pat. Appl. US2023096389A1, March 30, 2023.
59. Tsutsui, Y.; Tsubasa, N.; Takehiro, C.; Takashi, U.; Satoyuki, I.; Megumi, K. Method for purifying phosphorus-containing olefin compound salt and method for producing olefin compound using purified product obtained thereby. Japn. Pat. Appl. JP2021024816A, Feb 22, 2021.
60. Tsutsui, Y.; Tsubasa, N.; Takehiro, C.; Takashi, U.; Satoyuki, I.; Megumi, K. Olefin compound production method. Japn. Pat. Appl. JP2021024815A, Feb 22, 2021.
61. Peng, L.; Di, Z.; Yaoyao, L.; Tianzuo, G.; Wanjin, Y.; Wucan, L. Method for preparing 1,2-difluoroethylene through resource utilization of 2-chloro-1,1-difluoroethane. Chin. Patent CN116,332,721, June 27, 2023.
62. Tomoaki, T.; Mai, H.; Shuichi, O.; Masato, F. Actuation medium for heat cycle and manufacturing method therefor. Japn. Patent JP2015229768, Dec 21, 2015.
63. Hikaru, I.; Taku, Y.; Hidekazu, O. Method for producing hydrogen substitution product of 1,2-dichloro-1,2-difluoroethylene. WO Patent WO2023112433, June 22, 2023.
64. Lentz, D.; Bach, A.; Buschmann, J.; Luger, P.; Messerschmidt, M. *Chem. – Eur. J.* **2004,** *10,* 5059–5066. doi:10.1002/chem.200400223
65. Fokin, A. V.; Landau, M. A. *Russ. Chem. Bull.* **1982,** *31,* 1553–1561. doi:10.1007/bf00956891
66. McLinden, M. O.; Kazakov, A. F.; Brown, J. S.; Domanski, P. A. *Int. J. Refrig.* **2014,** *38,* 80–92. doi:10.1016/j.ijrefrig.2013.09.032
67. Craig, N. C.; Brandon, D. W.; Stone, S. C.; Lafferty, W. J. *J. Phys. Chem.* **1992,** *96,* 1598–1605. doi:10.1021/j100183a022
68. Belanger, G.; Sandorfy, C. *Chem. Phys. Lett.* **1969,** *3,* 661–665. doi:10.1016/0009-2614(69)87003-x
69. Andrella, N. O.; Xu, N.; Gabidullin, B. M.; Ehm, C.; Baker, R. T. *J. Am. Chem. Soc.* **2019,** *141,* 11506–11521. doi:10.1021/jacs.9b03101
70. Bernard-Moulin, P.; Rajzmann, M.; Pouzard, G. *C. R. Seances Acad. Sci., Ser. C* **1979,** *288,* 261–264.
71. Tomo, O.; Tsubasa, N.; Kazuhiro, T. Method for manufacturing 1-halo-2-fluoroethylene. WO Pat. Appl. WO2020250949A1, Dec 17, 2020.
72. Tatsuya, T.; Osamu, Y.; Daisuke, K. Method for producing difluoroethylene. WO Pat. Appl. WO2021085449A1, May 6, 2021.
73. Kazuhiro, T.; Osamu, Y. Method for producing difluoroethylene. WO Pat. Appl. WO2020250914A1, Dec 17, 2020.
74. Takashi, U.; Tsubasa, N.; Yuzo, K.; Kazuhiro, T.; Takehiro, C.; Megumi, K. Method for producing difluoroethylene. WO Pat. Appl. WO2019240233A1, Dec 19, 2019.
75. Bock, C. W.; George, P.; Mains, G. J.; Trachtman, M. *J. Chem. Soc., Perkin Trans. 2* **1979,** 814–821. doi:10.1039/p29790000814
76. Craig, N. C.; Overend, J. *J. Chem. Phys.* **1969,** *51,* 1127–1142. doi:10.1063/1.1672113
77. Hillig, K. W., II; Kuczkowski, R. L.; Cremer, D. *J. Phys. Chem.* **1984,** *88,* 2025–2030. doi:10.1021/j150654a019
78. Unpublished results in our group.
79. Tomoaki, T.; Shoji, F. Method for producing 1-chloro-1,2-difluoroethylene. Japn. Pat. Appl. JP2015120670A, July 2, 2015.
80. Storzer, W.; DesMarteau, D. D. *J. Fluorine Chem.* **1992,** *58,* 59–69. doi:10.1016/s0022-1139(00)82793-1
81. Anderson, J. D. O.; DesMarteau, D. D. *J. Fluorine Chem.* **1996,** *77,* 147–152. doi:10.1016/0022-1139(96)03400-8
82. Johri, K. K.; DesMarteau, D. D. *J. Org. Chem.* **1983,** *48,* 242–250. doi:10.1021/jo00150a019
83. Tari, I.; DesMarteau, D. D. *J. Org. Chem.* **1980,** *45,* 1214–1217. doi:10.1021/jo01295a009
84. Katsuhara, Y.; DesMarteau, D. D. *J. Org. Chem.* **1980,** *45,* 2441–2446. doi:10.1021/jo01300a035
85. Katsuhara, Y.; DesMarteau, D. D. *J. Am. Chem. Soc.* **1979,** *101,* 1039–1040. doi:10.1021/ja00498a045
86. Johri, K. K.; DesMarteau, D. D. *J. Org. Chem.* **1981,** *46,* 5081–5086. doi:10.1021/jo00338a006
87. Walker, N.; DesMarteau, D. D. *J. Am. Chem. Soc.* **1975,** *97,* 13–17. doi:10.1021/ja00834a004
88. Hopkinson, M. J.; Walker, N. S.; DesMarteau, D. D. *J. Org. Chem.* **1976,** *41,* 1407–1410. doi:10.1021/jo00870a025
89. Haszeldine, R. N.; Tipping, A. E. *J. Chem. Soc.* **1965,** 6141–6149. doi:10.1039/jr9650006141
90. Colburn, C. B.; Hill, W. E.; Verma, R. D. *J. Fluorine Chem.* **1981,** *17,* 75–84. doi:10.1016/s0022-1139(00)85252-5
91. Haszeldine, R. N.; Pool, C. R.; Tipping, A. E. *J. Chem. Soc., Dalton Trans.* **1975,** 2177–2181. doi:10.1039/dt9750002177

92. Berry, A. D.; Fox, W. B. *J. Org. Chem.* **1978,** *43,* 365–367. doi:10.1021/jo00396a050
93. Boyce, C. B. C.; Webb, S. B.; Phillips, L.; Ager, I. R. *J. Chem. Soc., Perkin Trans. 1* **1974,** 1644–1650. doi:10.1039/p19740001644
94. Cullen, W. R.; Hall, L. D.; Ward, J. E. H. *J. Am. Chem. Soc.* **1974,** *96,* 3422–3431. doi:10.1021/ja00818a014
95. Tingjian, Z.; Jianxin, Z.; Bin, L.; Xianrong, W.; Jinlong, Y.; Jun, L. Preparation method of long-chain fluorine-containing alkene. Chin. Pat. Appl. CN104529694A, April 22, 2015.
96. Craig, N. C.; Chao, T.-N. H.; Cuellar, E.; Hendriksen, D. E.; Koepke, J. W. *J. Phys. Chem.* **1975,** *79,* 2270–2282. doi:10.1021/j100588a014
97. Sengupta, S. K.; Justnes, H.; Gillies, C. W.; Craig, N. C. *J. Am. Chem. Soc.* **1986,** *108,* 876–880. doi:10.1021/ja00265a004
98. Justnes, H.; Zozom, J.; Gillies, C. W.; Sengupta, S. K.; Craig, N. C. *J. Am. Chem. Soc.* **1986,** *108,* 881–887. doi:10.1021/ja00265a005
99. Ihrig, A. M.; Smith, S. L. *J. Am. Chem. Soc.* **1970,** *92,* 759–763. doi:10.1021/ja00707a003
100. Tarrant, P.; Bull, R. N. *J. Fluorine Chem.* **1988,** *40,* 201–215. doi:10.1016/s0022-1139(00)83066-3
101. Liu, C.-S.; Hwang, T.-L. *J. Chin. Chem. Soc.* **1978,** *25,* 203–208. doi:10.1002/jccs.197800033
102. Hwang, T.-L.; Pai, Y.-M.; Liu, C.-S. *J. Am. Chem. Soc.* **1980,** *102,* 7519–7524. doi:10.1021/ja00545a021
103. LaBarge, M. S.; Hillig, K. W., II; Kuczkowski, R. L. *J. Phys. Chem.* **1986,** *90,* 3092–3097. doi:10.1021/j100405a012
104. Toby, S.; Toby, F. S. *J. Phys. Chem.* **1981,** *85,* 4071–4073. doi:10.1021/j150626a024
105. Agopovich, J. W.; Gillies, C. W. *J. Am. Chem. Soc.* **1982,** *104,* 813–817. doi:10.1021/ja00367a027
106. LaBrecque, G.; Gillies, C. W.; Raw, T. T.; Agopovich, J. W. *J. Am. Chem. Soc.* **1984,** *106,* 6171–6175. doi:10.1021/ja00333a008
107. Beauchamp, R. N.; Agopovich, J. W.; Gillies, C. W. *J. Am. Chem. Soc.* **1986,** *108,* 2552–2560. doi:10.1021/ja00270a011
108. Moss, S. J.; Rattanaphani, S. *J. Chem. Soc., Faraday Trans. 1* **1982,** *78,* 3053–3061. doi:10.1039/f19827803053
109. Tolman, C. A. *J. Am. Chem. Soc.* **1974,** *96,* 2780–2789. doi:10.1021/ja00816a020
110. Jones, M. T.; McDonald, R. N. *Organometallics* **1988,** *7,* 1221–1223. doi:10.1021/om00095a032
111. Ristic-Petrovic, D.; Anderson, D. J.; Torkelson, J. R.; McDonald, R.; Cowie, M. *Organometallics* **2003,** *22,* 4647–4657. doi:10.1021/om030328b

License and Terms

BEILSTEIN JOURNAL OF ORGANIC CHEMISTRY

From perfluoroalkyl aryl sulfoxides to *ortho* thioethers

Yang Li, Guillaume Dagousset, Emmanuel Magnier* and Bruce Pégot*

Full Research Paper

Open Access

Address:
Université Paris-Saclay, UVSQ, CNRS, UMR 8180, Institut Lavoisier de Versailles, 78035 Versailles Cedex, France

Email:
Emmanuel Magnier* - emmanuel.magnier@uvsq.fr; Bruce Pégot* - bruce.pegot@uvsq.fr

* Corresponding author

Keywords:
ortho functionalization; rearrangement; sulfoxide

Beilstein J. Org. Chem. **2024,** *20,* 2108–2113.
https://doi.org/10.3762/bjoc.20.181

Received: 05 May 2024
Accepted: 02 August 2024
Published: 23 August 2024

This article is part of the thematic issue "Organofluorine chemistry VI".

Guest Editor: D. O'Hagan

Abstract

Access to original *ortho* thioether derivatives was achieved through a [3,3]-rearrangement in a one-pot two-step protocol. Several aryl-SCF_3 compounds are reported by variation of the nitrile or of the trifluoroalkyl sulfoxide starting material. The variation of the perfluoroalkyl chain was also possible.

Introduction

Since decades, sigmatropic rearrangements have established themselves as robust and versatile tools for many transformations in organic synthesis [1-3]. They were widely employed with a wide range of substrates. With a peculiar type of scaffold, *S*-perfluoroalkyl aryl sulfoxides, in 2009, we were the first to demonstrate their ability to be engaged in such a rearrangement [4,5]. Upon activation with trifluoromethanesulfonic anhydride and under heating, we showed their transformation to *ortho* thioethers with a fairly acceptable selectivity towards the pathway of sulfilimine synthesis (Scheme 1b). Following our seminal study, many research groups described a strategy for *ortho*-C–H functionalization of aryl sulfoxides with various nucleophiles via a cascade reaction of interrupted Pummerer reaction/sigmatropic rearrangement (Scheme 1a) [6-11]. A large range of nucleophiles, such as phenols [12-16], anilines [17], carbonyls [18-21], propargyl/allylsilanes [22-34], ynamides [35-37], and alkyl nitriles [38-40], were found to be suitable for this process. Whereas the addition of fluorine atoms to molecules is a well-established strategy to improve or modulate their physicochemical and biological properties [41-45], only few publications have reported a [3,3]-rearrangement with fluorinated molecules (Scheme 1c). In 2020, Wang and co-workers have developed a one-pot [3,3]-sigmatropic rearrangement/Haller–Bauer reaction of aryl sulfoxides with difluoroenoxysilanes as nucleophile under mild reaction conditions [46]. This provided access to organosulfur compounds *ortho*-functionalized by CF_2H. At the same time Peng and co-workers described the dearomatization of aryl sulfoxides using the same difluoroenol silyl ether with trifluoromethanesulfonic anhydride, allowing the incorporation of two difluoroalkyl groups [47]. By blocking the rearomatization after the [3,3]-rearrangement, external nucleophiles could be trapped to give mono-difluoroalkylated cycles. More recently, in 2019, Peng's group reported also the *ortho*-cyanoalkylation of benzoyl or ester group-substi-

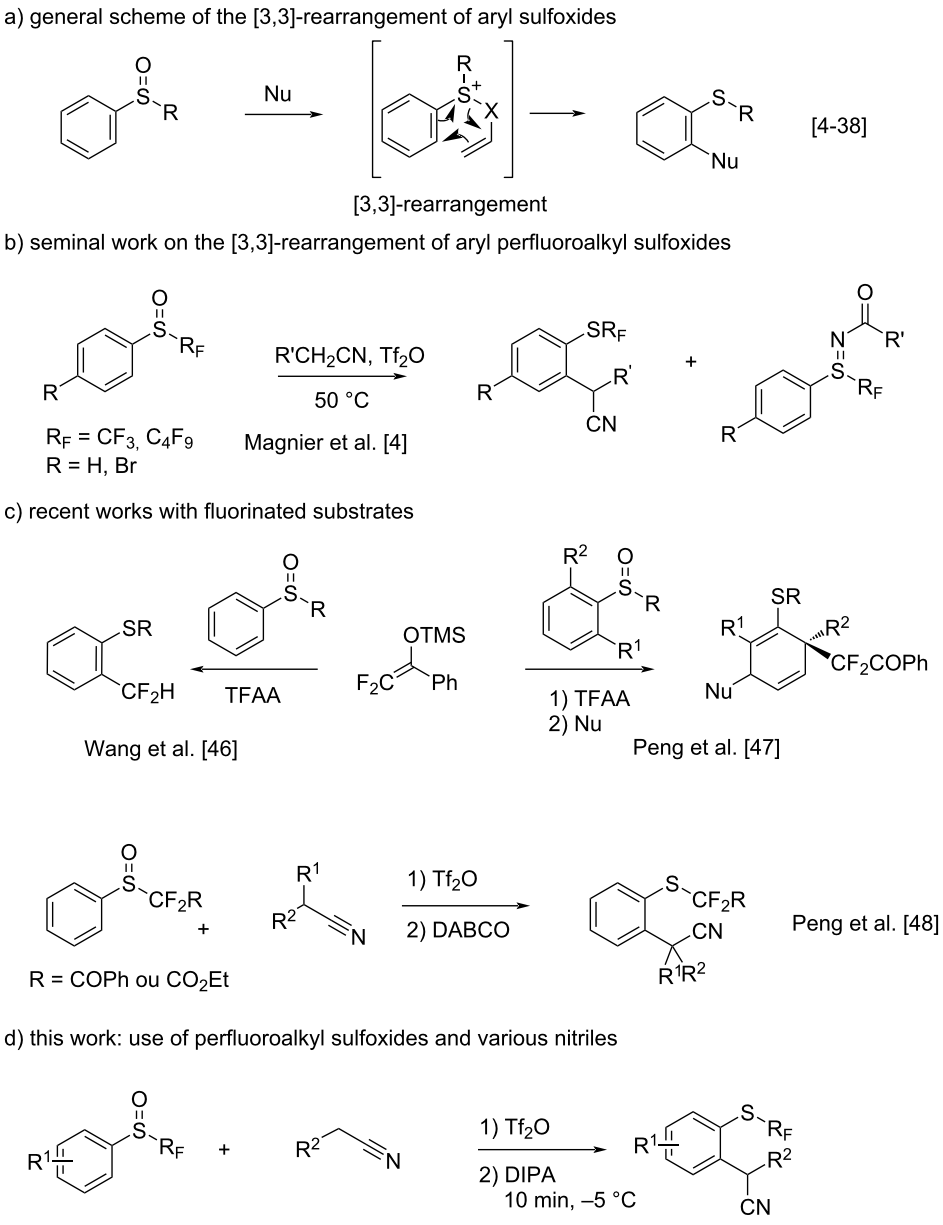

Scheme 1: [3,3]-Rearrangement of aryl sulfoxides.

tuted fluoroalkyl aryl sulfoxides with various alkyl nitriles in two steps [48]. The addition of a base in the second step easily enabled the [3,3]-rearrangement, allowing for the addition of two functional groups – the cyano group and difluoromethylthio group – to arenes in good yield.

Inspired and stimulated by this abundant literature, and as part of our research program focused on creating novel perfluoroalkylsulfur derivatives, we became interested in a reappraisal of our previous study with the aim of increasing its scope as well as the yield and selectivity (Scheme 1d). It is important to mention that during the preparation of this paper, a similar study appeared. Peng and co-workers demonstrated the efficient use of acetonitrile as nucleophile with various aryl difluoroalkyl sulfoxides but only one example of an SCF_3 compound was reported [49].

Results and Discussion

We started our optimization with the reaction between acetonitrile and phenyl trifluoromethyl sulfoxide (**1a**, Table 1). We firstly chose the same stoichiometry as described in our previous study and tried to reduce the reaction time by the help of microwave heating (Table 1, entry 1). Under these conditions, a significant amount of degradation products was ob-

Table 1: Optimization of the reaction conditions.

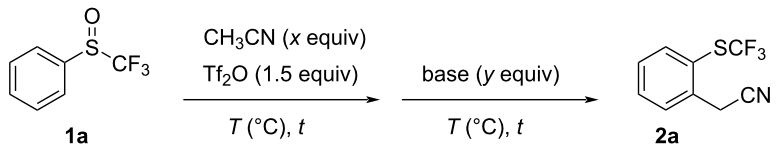

Entry	*T* (°C)	*t*	*x*	base	*y*	NMR yield (%)[a,b]
1	50 °C (MW)	1 h	1.5	–		21
2	0 to 50 °C (MW)	1 h	1.5	–		21
3	−15 to 20 °C	12 h	3	–		38
4	−15 °C	10 min	3	DIPEA	2	74
5	−30 °C	10 min	3	DIPEA	2	41
6	−5 °C	10 min	3	DIPEA	2	77
7	0 °C	10 min	3	DIPEA	2	75
8	−5 °C	10 min	5	DIPEA	2.5	80
9	−5 °C	10 min	5	DIPEA	5	95 (79)
10	−5 °C	10 min	5	Et_3N	5	85
11	−5 °C	10 min	5	DBU	5	48
12	−5 °C	10 min	5	K_2CO_3	5	2

[a]Experimental conditions: **1a** (0.5 mmol), Tf_2O (1.5 equiv), *T* (°C), *t* (min or h), then addition of base (*y* equiv) at the same temperature and time as the first step (*T*, *t*). [b]^{19}F NMR spectroscopic yields, isolated yields in parentheses.

served and the yield was rather low. The same result was obtained when the reagent was first added at 0 °C and then heated for one hour under microwave irradiation (Table 1, entry 2). To avoid degradation, the temperature was reduced while the reaction time was increased with twice the number of equivalents of acetonitrile (−15 °C to rt, for 12 hours, entry 3 in Table 1) without any significant improvement in the yield. As previously reported, the use of an organic base can improve the yield of this reaction [26,38,40,48]. Therefore, we decided to use 2 equivalents of DIPEA at low temperature. After ten minutes at −15 °C to allow for the reaction between phenyl trifluoromethyl sulfoxide (**1a**) and acetonitrile, the base was added and the reaction was stirred for the same amount of time. To our delight, a good NMR yield of 74% was received under these conditions (Table 1, entry 4). The importance of the temperature was then evaluated (Table 1, entries 5–7). A too low value was deleterious to the yield, whereas −5 °C appeared as the conditions of choice. Finally, by adjusting to 5 equivalents of nitrile and base, resulted in the optimal conditions (Table 1, entry 9). Other organic nitrogenous bases were tested (Table 1, entries 10–12). Et_3N gave nearly the same result, while DBU seemed less efficient. The use of the inorganic base K_2CO_3 resulted in poor outcomes.

With the optimized conditions in hand, a scale-up was successfully performed, resulting in the production of 1.88 g of product **2a** corresponding to 84% yield (Scheme 2). The reaction with other aryl sulfoxides was then investigated. We observed that the rearrangement product was isolated in good yield (**2b**–**d**) when the sulfoxide is *para*-substituted whereas the *meta* or difunctionalization led to lower yields (**2e**,**f**). The product of rearrangement **2a** was oxidized into the sulfoxide and re-engaged under the optimized conditions to afford the compound of bis-rearrangement **2g** in a good yield of 49%. This compound is then the result of an iterative rearrangement. Difluorinated sulfoxides **1h**–**j** proved also efficient for this rearrangement giving rise to the corresponding thioethers **2h**–**j** in good NMR yields and lower isolated yield in the case of the more volatile adduct **2i**. Finally, trifluoromethyl selenoxide **1k** was tested as a substrate, and the rearranged product was obtained in a low yield of 15%. The main product obtained was phenyl(trifluoromethyl)selane, a reduction product of the selenoxide. Despite a low yield, this result is encouraging because it is the first example of rearrangement with aryl trifluoromethyl selenoxide.

We further investigated the generality of the reaction using a series of nitriles with the sulfoxide **1a** (Scheme 3). We noticed that the length of the alkyl chain has no impact on the yield (**3a**,**b**). However, the use of benzyl cyanide is completely deleterious for the reaction as no product was observed (**3c**). The presence of a chlorine atom at the alpha-position of the nitrile is

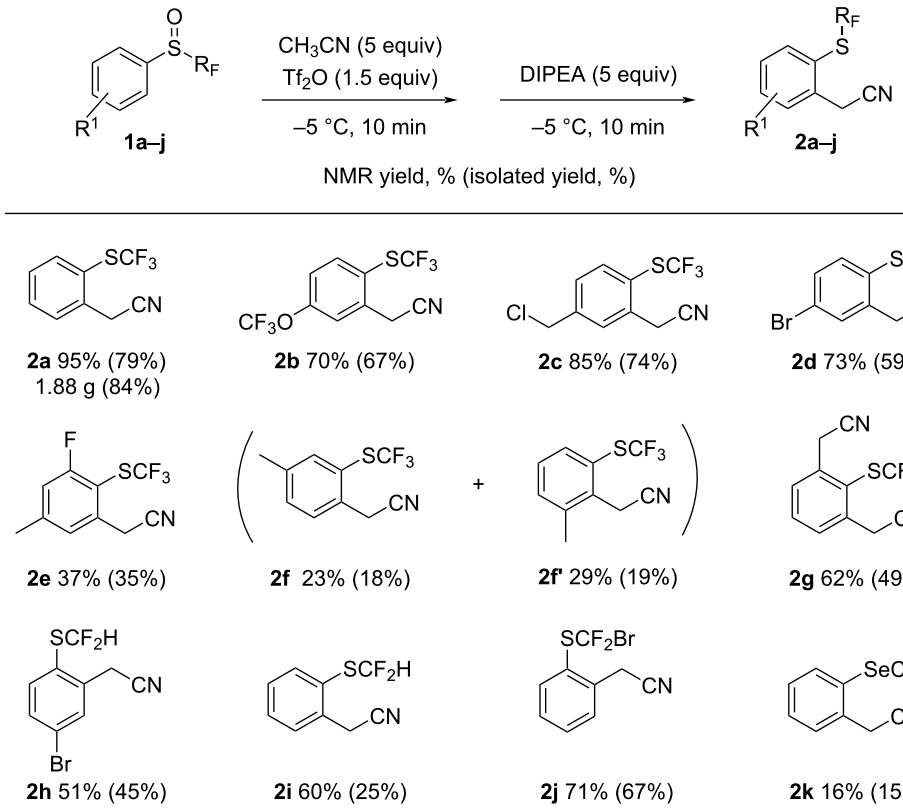

Scheme 2: The scope of aryl perfluoromethyl sulfoxides and a selenoxide.

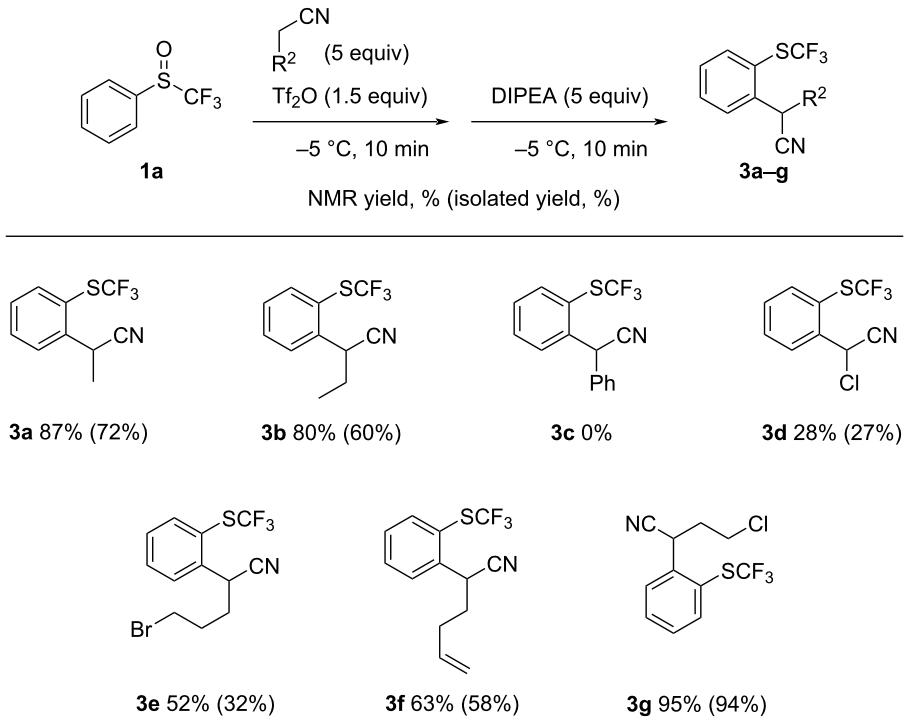

Scheme 3: The scope of alkyl nitriles.

also detrimental to the reaction, resulting in less than 30% yield of the desired product **3d**. Nevertheless, the reaction is compatible with halogens elsewhere in longer nitrile alkyl chains (**3e**,**g**). Finally, it was possible to obtain the terminal alkene **3f** with a yield of 58% using hex-5-enenitrile.

Conclusion

In summary, fine-tuning of the experimental conditions gave us access to original *ortho*-cyanoalkylated aryl perfluoroalkylsulfur derivatives. We have also shown that structural diversity is possible by varying the substituents on the aromatic ring, the perfluoroalkyl chain, and the alkyl chain linking the cyano functional groups. The [3,3]-sigmatropic rearrangement of perfluoroalkyl selenoxides needs to be optimized to improve the yield and decrease the amount of reduction product. The complete evaluation of the potential of these new compounds will be provided in the future.

Experimental

General procedure for the rearrangement process

Sulfoxide (0.5 mmol, 1 equiv), nitrile (5 equiv) and Tf_2O (1.5 equiv) were added in the described order to a 5 mL flask under an argon atmosphere, maintained at −5 °C. The reaction mixture was stirred for 10 min, then DIPEA (5 equiv) was slowly added to the flask with a syringe and the reaction was stirred for another 10 min. At the end of the reaction, 1 mL of chloroform and a known amount of trifluoromethoxybenzene were added to the flask in order to determine the ^{19}F NMR yield. To purify the product, the reaction mixture was mixed with a sufficient volume of a saturated NH_4Cl solution, then extracted 3 times with diethyl ether. The combined organic layers were dried over $MgSO_4$, filtered, concentrated under reduced pressure, and purified by preparative TLC or flash chromatography.

Supporting Information

Supporting Information File 1

Experimental procedures, characterization data of all isolated products as well as copies of NMR spectra for novel compounds.
[https://www.beilstein-journals.org/bjoc/content/supplementary/1860-5397-20-181-S1.pdf]

Acknowledgements

We thank Matthias George for preparing some of the initial material during his master's degree.

Funding

Y.L. thanks the CNRS for Ph.D. grant. French Fluorine Network (GIS Fluor) is acknowledged for financial support.

ORCID® iDs

Yang Li - https://orcid.org/0000-0002-8494-1873
Guillaume Dagousset - https://orcid.org/0000-0001-8720-3828
Emmanuel Magnier - https://orcid.org/0000-0003-3392-3971
Bruce Pégot - https://orcid.org/0000-0001-5137-5548

Data Availability Statement

The data that supports the findings of this study is available from the corresponding author upon reasonable request.

References

1. Hiersemann, M.; Nubbemeyer, U., Eds. *The Claisen Rearrangement: Methods and Applications;* Wiley-VCH: Weinheim, Germany, 2007. doi:10.1002/9783527610549
2. Martín Castro, A. M. *Chem. Rev.* **2004,** *104,* 2939–3002. doi:10.1021/cr020703u
3. Ito, H.; Taguchi, T. *Chem. Soc. Rev.* **1999,** *28,* 43–50. doi:10.1039/a706415b
4. Macé, Y.; Urban, C.; Pradet, C.; Blazejewski, J.-C.; Magnier, E. *Eur. J. Org. Chem.* **2009,** 5313–5316. doi:10.1002/ejoc.200900873
5. Pégot, B.; Urban, C.; Diter, P.; Magnier, E. *Eur. J. Org. Chem.* **2013,** 7800–7808. doi:10.1002/ejoc.201301017
6. Zhang, L.; Hu, M.; Peng, B. *Synlett* **2019,** *30,* 2203–2208. doi:10.1055/s-0039-1690212
7. Yorimitsu, H. *Chem. Rec.* **2017,** *17,* 1156–1167. doi:10.1002/tcr.201700017
8. Yanagi, T.; Nogi, K.; Yorimitsu, H. *Tetrahedron Lett.* **2018,** *59,* 2951–2959. doi:10.1016/j.tetlet.2018.06.055
9. Pulis, A. P.; Procter, D. J. *Angew. Chem., Int. Ed.* **2016,** *55,* 9842–9860. doi:10.1002/anie.201601540
10. Kaiser, D.; Klose, I.; Oost, R.; Neuhaus, J.; Maulide, N. *Chem. Rev.* **2019,** *119,* 8701–8780. doi:10.1021/acs.chemrev.9b00111
11. Smith, L. H. S.; Coote, S. C.; Sneddon, H. F.; Procter, D. J. *Angew. Chem., Int. Ed.* **2010,** *49,* 5832–5844. doi:10.1002/anie.201000517
12. Yanagi, T.; Otsuka, S.; Kasuga, Y.; Fujimoto, K.; Murakami, K.; Nogi, K.; Yorimitsu, H.; Osuka, A. *J. Am. Chem. Soc.* **2016,** *138,* 14582–14585. doi:10.1021/jacs.6b10278
13. Murakami, K.; Yorimitsu, H.; Osuka, A. *Angew. Chem., Int. Ed.* **2014,** *53,* 7510–7513. doi:10.1002/anie.201403288
14. Shrives, H. J.; Fernández-Salas, J. A.; Hedtke, C.; Pulis, A. P.; Procter, D. J. *Nat. Commun.* **2017,** *8,* 14801. doi:10.1038/ncomms14801
15. Okamoto, K.; Hori, M.; Yanagi, T.; Murakami, K.; Nogi, K.; Yorimitsu, H. *Angew. Chem., Int. Ed.* **2018,** *57,* 14230–14234. doi:10.1002/anie.201809035
16. Kobatake, T.; Fujino, D.; Yoshida, S.; Yorimitsu, H.; Oshima, K. *J. Am. Chem. Soc.* **2010,** *132,* 11838–11840. doi:10.1021/ja1030134
17. Yanagi, T.; Nogi, K.; Yorimitsu, H. *Chem. – Eur. J.* **2020,** *26,* 783–787. doi:10.1002/chem.201903570
18. Peng, B.; Geerdink, D.; Farès, C.; Maulide, N. *Angew. Chem., Int. Ed.* **2014,** *53,* 5462–5466. doi:10.1002/anie.201402229

19. Huang, X.; Maulide, N. *J. Am. Chem. Soc.* **2011,** *133,* 8510–8513. doi:10.1021/ja2031882
20. Huang, X.; Patil, M.; Farès, C.; Thiel, W.; Maulide, N. *J. Am. Chem. Soc.* **2013,** *135,* 7312–7323. doi:10.1021/ja4017683
21. Meng, X.; Chen, D.; Cao, X.; Luo, J.; Wang, F.; Huang, S. *Chem. Commun.* **2019,** *55,* 12495–12498. doi:10.1039/c9cc06505a
22. Kaiser, D.; Veiros, L. F.; Maulide, N. *Chem. – Eur. J.* **2016,** *22,* 4727–4732. doi:10.1002/chem.201600432
23. Šiaučiulis, M.; Sapmaz, S.; Pulis, A. P.; Procter, D. J. *Chem. Sci.* **2018,** *9,* 754–759. doi:10.1039/c7sc04723a
24. Akai, S.; Kawashita, N.; Satoh, H.; Wada, Y.; Kakiguchi, K.; Kuriwaki, I.; Kita, Y. *Org. Lett.* **2004,** *6,* 3793–3796. doi:10.1021/ol0484310
25. Hu, L.; Gui, Q.; Chen, X.; Tan, Z.; Zhu, G. *J. Org. Chem.* **2016,** *81,* 4861–4868. doi:10.1021/acs.joc.6b00535
26. Fernández-Salas, J. A.; Eberhart, A. J.; Procter, D. J. *J. Am. Chem. Soc.* **2016,** *138,* 790–793. doi:10.1021/jacs.5b12579
27. Eberhart, A. J.; Procter, D. J. *Angew. Chem., Int. Ed.* **2013,** *52,* 4008–4011. doi:10.1002/anie.201300223
28. Eberhart, A. J.; Imbriglio, J. E.; Procter, D. J. *Org. Lett.* **2011,** *13,* 5882–5885. doi:10.1021/ol2025197
29. Eberhart, A. J.; Cicoira, C.; Procter, D. J. *Org. Lett.* **2013,** *15,* 3994–3997. doi:10.1021/ol401786d
30. Baldassari, L. L.; Mantovani, A. C.; Senoner, S.; Maryasin, B.; Maulide, N.; Lüdtke, D. S. *Org. Lett.* **2018,** *20,* 5881–5885. doi:10.1021/acs.orglett.8b02544
31. Kaiser, D.; Veiros, L. F.; Maulide, N. *Adv. Synth. Catal.* **2017,** *359,* 64–77. doi:10.1002/adsc.201600860
32. Akai, S.; Kawashita, N.; Wada, Y.; Satoh, H.; Alinejad, A. H.; Kakiguchi, K.; Kuriwaki, I.; Kita, Y. *Tetrahedron Lett.* **2006,** *47,* 1881–1884. doi:10.1016/j.tetlet.2006.01.090
33. Eberhart, A. J.; Shrives, H. J.; Álvarez, E.; Carrĕr, A.; Zhang, Y.; Procter, D. J. *Chem. – Eur. J.* **2015,** *21,* 7428–7434. doi:10.1002/chem.201406424
34. Pons, A.; Michalland, J.; Zawodny, W.; Chen, Y.; Tona, V.; Maulide, N. *Angew. Chem., Int. Ed.* **2019,** *58,* 17303–17306. doi:10.1002/anie.201909381
35. Peng, B.; Huang, X.; Xie, L.-G.; Maulide, N. *Angew. Chem., Int. Ed.* **2014,** *53,* 8718–8721. doi:10.1002/anie.201310865
36. Kaldre, D.; Maryasin, B.; Kaiser, D.; Gajsek, O.; González, L.; Maulide, N. *Angew. Chem., Int. Ed.* **2017,** *56,* 2212–2215. doi:10.1002/anie.201610105
37. Maryasin, B.; Kaldre, D.; Galaverna, R.; Klose, I.; Ruider, S.; Drescher, M.; Kählig, H.; González, L.; Eberlin, M. N.; Jurberg, I. D.; Maulide, N. *Chem. Sci.* **2018,** *9,* 4124–4131. doi:10.1039/c7sc04736c
38. Shang, L.; Chang, Y.; Luo, F.; He, J.-N.; Huang, X.; Zhang, L.; Kong, L.; Li, K.; Peng, B. *J. Am. Chem. Soc.* **2017,** *139,* 4211–4217. doi:10.1021/jacs.7b00969
39. Luo, F.; Lu, Y.; Hu, M.; Tian, J.; Zhang, L.; Bao, W.; Yan, C.; Huang, X.; Wang, Z.-X.; Peng, B. *Org. Chem. Front.* **2018,** *5,* 1756–1762. doi:10.1039/c8qo00268a
40. Zhang, L.; He, J.-N.; Liang, Y.; Hu, M.; Shang, L.; Huang, X.; Kong, L.; Wang, Z.-X.; Peng, B. *Angew. Chem., Int. Ed.* **2019,** *58,* 5316–5320. doi:10.1002/anie.201900434
41. Gillis, E. P.; Eastman, K. J.; Hill, M. D.; Donnelly, D. J.; Meanwell, N. A. *J. Med. Chem.* **2015,** *58,* 8315–8359. doi:10.1021/acs.jmedchem.5b00258
42. Inoue, M.; Sumii, Y.; Shibata, N. *ACS Omega* **2020,** *5,* 10633–10640. doi:10.1021/acsomega.0c00830
43. Nair, A. S.; Singh, A. K.; Kumar, A.; Kumar, S.; Sukumaran, S.; Koyiparambath, V. P.; Pappachen, L. K.; Rangarajan, T. M.; Kim, H.; Mathew, B. *Processes* **2022,** *10,* 2054. doi:10.3390/pr10102054
44. Johnson, B. M.; Shu, Y.-Z.; Zhuo, X.; Meanwell, N. A. *J. Med. Chem.* **2020,** *63,* 6315–6386. doi:10.1021/acs.jmedchem.9b01877
45. Kirsch, P. *Modern Fluoroorganic Chemistry: Synthesis, Reactivity, Applications;* Wiley-VCH: Weinheim, Germany, 2013. doi:10.1002/9783527651351
46. Li, J.; Chen, Y.; Zhong, R.; Zhang, Y.; Yang, J.; Ding, H.; Wang, Z. *Org. Lett.* **2020,** *22,* 1164–1168. doi:10.1021/acs.orglett.0c00018
47. Huang, X.; Zhang, Y.; Liang, W.; Zhang, Q.; Zhan, Y.; Kong, L.; Peng, B. *Chem. Sci.* **2020,** *11,* 3048–3053. doi:10.1039/d0sc00244e
48. Hu, M.; He, J.-N.; Liu, Y.; Dong, T.; Chen, M.; Yan, C.; Ye, Y.; Peng, B. *Eur. J. Org. Chem.* **2020,** 193–197. doi:10.1002/ejoc.201901577
49. Ye, S.; Wang, H.; Liang, G.; Hu, Z.; Wan, K.; Zhang, L.; Peng, B. *Org. Biomol. Chem.* **2024,** *22,* 1495–1499. doi:10.1039/d3ob02102e

License and Terms

BEILSTEIN JOURNAL OF ORGANIC CHEMISTRY

Facile preparation of fluorine-containing 2,3-epoxypropanoates and their epoxy ring-opening reactions with various nucleophiles

Yutaro Miyashita[1], Sae Someya[1], Tomoko Kawasaki-Takasuka[1], Tomohiro Agou[2] and Takashi Yamazaki[*1]

Full Research Paper

Open Access

Address:
[1]Division of Applied Chemistry, Institute of Engineering, Tokyo University of Agriculture and Technology, 2-24-16 Nakamachi, Koganei 184-8588, Japan and [2]Department of Material Science, Graduate School of Science, University of Hyogo, 3-2-1 Koto, Kamigori-cho, Ako-gun, Hyogo 678-1297, Japan

Email:
Takashi Yamazaki* - tyamazak@cc.tuat.ac.jp

* Corresponding author

Keywords:
α,β-unsaturated esters; epoxyesters; fluorine; Grignard-based cuprates; nucleophiles

Beilstein J. Org. Chem. **2024,** *20,* 2421–2433.
https://doi.org/10.3762/bjoc.20.206

Received: 13 July 2024
Accepted: 12 September 2024
Published: 25 September 2024

This article is part of the thematic issue "Organofluorine chemistry VI".

Guest Editor: D. O'Hagan

Abstract

We describe herein a facile method to access 2,3-epoxyesters with fluorine-containing substituents at their 3-position starting from the corresponding enoates by utilization of the low-costed and easy-to-handle reagent, $NaOCl·5H_2O$. Because very little has been disclosed about the reactivity of such 2,3-epoxyesters, their epoxy ring opening by a variety of nucleophiles was carried out and we succeeded in clarifying these chemo- as well as regioselective processes proceeding via the S_N2 mechanism to mainly afford 2-substituted 3-hydroxyesters usually in a highly *anti* selective manner.

Introduction

Fluorine-containing compounds have been utilized in diverse fields due to their special character originating from unique fluorine atoms or fluorinated groups [1-7]. During our study in this area, ethyl 4,4,4-trifluorobut-2-enoate (**1a**) has been frequently employed as a potent and convenient Michael acceptor towards a variety of enolates [8-15] as well as organometallic species [16-19]. At least in part, its high reactivity was considered to be due to the significantly lower-lying LUMO energy level by the attachment of electron-withdrawing trifluoromethyl (CF_3) and ethoxycarbonyl groups [20]. As we previously pointed out [10,21], the effective intramolecular interaction between fluorine and metals would also facilitate the smooth progress of these reactions. Such high potential of **1a** allowed us to apply it to nucleophilic epoxidation because the

resultant epoxyester **2a** is recognized as an intriguing building block (Scheme 1).

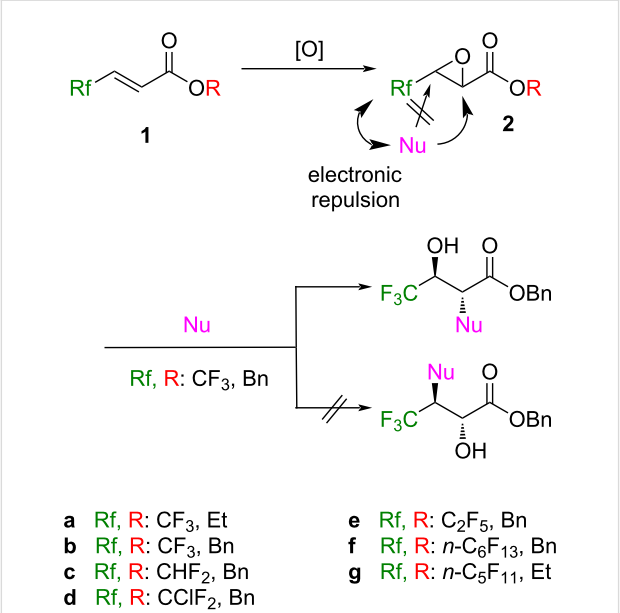

Scheme 1: Expectation of the regio- as well as stereoselective reactions of **2**.

Another expectation to **2a** is the high regio- and stereoselectivities of its epoxy ring opening specifically occurring at the 2 position in an S_N2 manner, when it is treated with appropriate nucleophiles (Nu), leading to the formation of the 2-substituted 3-hydroxyesters with 2,3-*anti* stereochemistry. These characteristic outcomes would stem from a result of the electronically repulsive interaction between the incoming nucleophiles and an electronically strongly negative CF_3 group, and the anticipated clean S_N2 mechanism of epoxides in general, respectively. This is interestingly compared with the case of **2a** with nonfluorinated Rf groups which sometimes suffered from the contamination of the regioisomers as a consequence of the regiorandom attack of nucleophiles [22-26].

Despite such significant advantage, compound **2a** was previously prepared only by 1) the LDA-mediated iodination-intramolecular ring closure sequence from the corresponding chiral 4,4,4-trifluoro-3-hydroxybutyrate at low temperature [27-30], and 2) *t*-BuO_2Li-mediated transformation of the enoates like **1g** at −78 °C [31,32] and, to the best of our knowledge, no report has appeared on the convenient methods applicable to the larger scale synthesis to get access to the synthetically quite useful compounds like **2a** [33,34].

Under such situations, we envisaged that the high electrophilicity of compound **1a** would permit the usage of the extraordinarily convenient and mild reagent NaOCl [35-38] which opens the promising route for the preparation of **2a**. Moreover, the fact that only very limited examples are known for their synthetic application except for the synthesis of 4,4,4-trifluorothreonine [29,33], stereoselective ring opening with organometallic species [29], and so on [32] also stimulated our interest. In this article, we would like to describe in detail the results of the preparation of epoxyesters **2** with various Rf groups as well as their reactivity with diverse nucleophiles [39].

Results and Discussion

Preparation of (*E*)-2,3-epoxypropanoates **2** with Rf groups at the 3 position

Because the urea·H_2O_2 complex proved its usefulness for the epoxidation of the β-CF_3-α,β-unsaturated ketones [40], we applied this method at first for the epoxidation of **1b**. However, contrary to our anticipation, only a total recovery of the substrate was observed, and further search for an oxidant reached the usage of a NaClO aqueous solution with its convenient handling and availability at a low cost. Following to the reported protocol [41], although a catalytic amount of Al_2O_3 and MgO worked nicely (entries 1 and 2 in Table 1), it was clarified that these additives were not necessary for the attainment of the same level of chemical yields (entries 3 vs 1 and 2). The drawback of this sequence was the isolated yield of **2b** no more than 70% which was, at least in part, due to the production of the undesired hydrolyzed products from **1b** and/or **2b** under the alkaline conditions of this epoxidation reagent. This was experimentally proved by the detection of benzaldehyde which was considered to be formed by the NaClO-mediated oxidation of benzyl alcohol generated by hydrolysis. Changing the oxidizing reagent to crystalline NaClO·$5H_2O$ nicely solved the problem with the realization of 86% isolated yield of **2b** by the utilization of this oxidant (2 equiv) at 0 °C with 6 h stirring (entry 8 in Table 1). We also tried to apply these conditions to other fluorine-containing substrates **1c**–**f** and successfully obtained good to high yields of the desired products **2c**–**f**, respectively (entries 10–13 in Table 1). The requirement of longer reaction time and higher temperature especially in the case of compounds **1e** and **1f** as well as the high loading of the oxidant in the latter might be due to their higher oleophobicity by possessing longer Rf chains. For all instances, epoxyesters **2** were obtained as single *E*-isomers, and based on the result obtained by the *t*-BuO_2Li reagent [31], we speculated that NaClO·$5H_2O$ would similarly work for the corresponding *Z*-**1** with retention of stereochemistry.

The procedure found here was also applied to the three representative CF_3-containing α,β-unsaturated esters,**1h**–**j** [42] with different substitution patterns (Scheme 2).

Table 1: Optimization of epoxidation conditions of **1**.

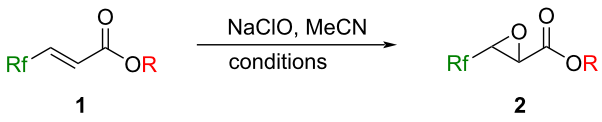

1 **2**

Entry	Sub.	NaClO[a]	(equiv)	Conditions	Isolated yield[b] (%)
1[c]	**1b**	AQ	1.0	25 °C, 6 h	59 (67)
2[d]	**1b**	AQ	1.0	25 °C, 5 h	(69)
3	**1b**	AQ	1.0	25 °C, 4.5 h	60 (63)
4	**1b**	S	1.0	20 °C, 3 h	(65)
5	**1b**	S	1.5	20 °C, 3 h	(83)
6	**1b**	S	1.5	20 °C, 6 h	(84)
7	**1b**	S	1.5	0 °C, 6 h	(89)
8	**1b**	S	2.0	0 °C, 6 h	86 (94)
9	**1b**	S	3.0	0 °C, 6 h	(83)
10	**1c**	S	2.0	0 °C, 6 h	79
11	**1d**	S	2.0	0 °C, 6 h	78
12	**1e**	S	2.0	0 °C, 6 h: 20 °C, 12 h	73
13	**1f**	S	5.0	20 °C, 48 h	61

[a]AQ: a 5% aqueous solution, S: solid of NaClO·5H_2O; [b]the yields determined by ^{19}F NMR were described in the parentheses; [c]10 mol % of Al_2O_3 was added; [d]20 mol % of MgO was added.

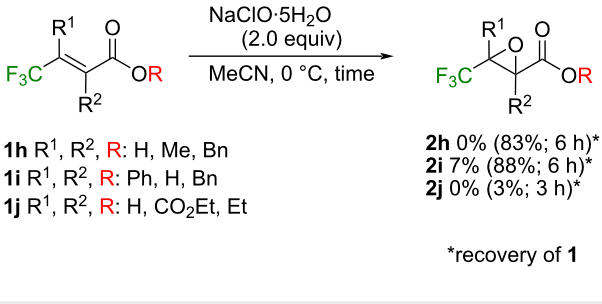

Scheme 2: Attempts of the present epoxidation to other α,β-unsaturated esters, **1h–j**.

The subjection of the compounds **1h** and **1i** to the standard conditions described above resulted in high recovery of the substrates, which could be explained by their higher LUMO + 1 energy levels responsible for the epoxidation [43]. Extensive decomposition was observed in the case of **1j** even in a shorter period possibly because of its significantly high electrophilicity by the attachment of three strongly electron-withdrawing moieties.

Reactions of (*E*)-3-Rf-2,3-epoxypropanoates **2** with amines, thiols, and metal halides

Because the epoxide ring opening is known to occur in an S_N2 fashion, compounds **2** were recognized as versatile building blocks for the construction of 2-amino-3-hydroxypropanoates with 2,3-*anti* stereochemistry, if appropriate amines work nicely in a nucleophilic manner [44].

After the brief optimization of the conditions for the reaction of **2b** and *p*-anisidine, good yields with high stereoselectivity were similarly recorded for the other substrates **2c** and **2d** possessing different Rf groups at the 3 position (Table 2, entries 1–3). Mixing of **2b** with different primary (entries 4–7 in Table 2) and secondary (entries 8 and 9) amines led to the formation of the respective products in high to excellent yields without detection of any regio- as well as stereoisomers. The chirality contained in amines did not work efficiently for the stereochemical induction of the products (entries 6 and 7 in Table 2). In the case of secondary amines, the sterically demanding dibenzylamine failed in this transformation and recovery of **2b** was observed (Table 2, entry 10). As was pointed out in the introductory section, the highly regioselective epoxy ring opening is well compared with the case when the nonfluorinated substrate (Ph instead of CF_3 in **2b**) was employed [25,26].

With the successful employment of amines as nucleophiles for the epoxy ring opening in a highly stereoselective fashion, we next turned our attention to thiols. Optimization of the reaction conditions based on the ones for amines clarified the tendency that the longer reaction time and the higher temperature decreased the chemical yields as well as the diastereomeric ratios (Table 3, entries 1–4). The higher pK_a values of the carbonyl

Table 2: Reactions of **2** with a variety of amines.

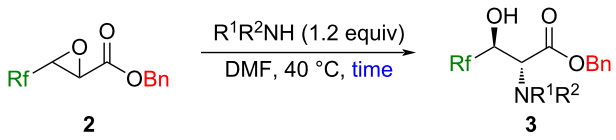

2 **3**

Entry	Rf	R^1	R^2	Time (h)	Isolated yield (%)
1[a]	**CF_3**	4-$MeOC_6H_4$	H	19	78 (**3ba**)
2[a]	**CHF_2**	4-$MeOC_6H_4$	H	19	59 (**3ca**)
3[a]	**$CClF_2$**	4-$MeOC_6H_4$	H	19	76 (**3da**)
4	**CF_3**	$PhCH_2$	H	7	86 (**3bb**)
5	**CF_3**	*n*-Bu	H	7	48 (**3bc**)
6	**CF_3**	$PhCH(CH_3)$	H	18	77[c] (**3bd**)
7[b]	**CF_3**	$EtCH(Me)CH(CO_2Bn)$	H	24	72[c] (**3be**)
8	**CF_3**	Et	Et	7	83 (**3bf**)
9	**CF_3**	$(CH_2)_4$		7	56 (**3bg**)
10	**CF_3**	Bn	Bn	7	–[d]

[a]EtOH was used as the solvent and the reaction temperature was 50 °C; [b]reaction was performed with 2.5 equiv of benzyl isoleucinate·TsOH and Et_3N; [c]consisted of 53:47 diastereomers in both cases; [d]no reaction was observed.

Table 3: Reactions of **2** with a variety of thiols.

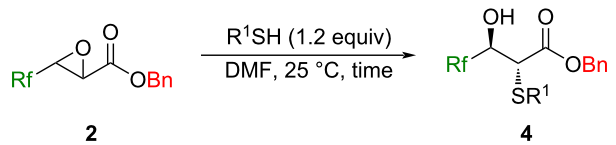

2 **4**

Entry	Rf	R^1	Time (h)	Isolated yield (%)	dr[a]
1[b]	**CF_3**	$PhCH_2$	3	92 (**4ba**)	87:13
2[b]	**CF_3**	$PhCH_2$	12	75 (**4ba**)	75:25
3[c]	**CF_3**	$PhCH_2$	3	80 (**4ba**)	61:39
4	**CF_3**	$PhCH_2$	5	90 (**4ba**)	94:6
5[d]	**CF_3**	$PhCH_2$	5	90 (**4ba**)	94:6
6	**CHF_2**	$PhCH_2$	48	76 (**4ca**)	>99:1
7	**$CClF_2$**	$PhCH_2$	24	87 (**4da**)	90:10
8	**C_2F_5**	$PhCH_2$	81	72 (**4ea**)	69:31
9	**CF_3**	$CH_3(CH_2)_9$	10	59[e] (**4bb**)	95:5
10	**CF_3**	Ph	5	92 (**4bc**)	93:7
11	**CF_3**	$CH_3OC(O)CH_2$	5	94 (**4bd**)	95:5

[a]Determined by ^{19}F NMR; [b]reaction at 40 °C; [c]reaction at 60 °C; [d]utilization of 1.0 equiv of $PhCH_2SH$ resulted in the observation of 9% recovery of **2b** by ^{19}F NMR; [e]7% recovery of **2a** was observed by ^{19}F NMR.

α-proton of **4** (for example, the p*K*a values of the protons of X-CH_2C(O)Ph in DMSO were reported to be 17.1 (X: PhS) [45] and 20.3 (X: Ph_2N) [46]) would result in the contamination of the stereoisomers when compared with the case of the compounds **3** [47,48]. Because control of the amount of $PhCH_2SH$ to 1.0 equiv did not give a positive effect, the conditions in entry 4 (Table 3) were eventually determined as the best.

The different epoxyesters **2c**–**e** were also applied for this ring-opening reaction with the same thiol (entries 6–8 in Table 3). It is interesting to note that a longer reaction time was required for

these substrates which would be the major reason for the relatively low diastereomeric ratio (especially in the case of entry 8 in Table 3) while the CHF_2-possessing epoxyester **2b** furnished a single stereoisomer (entry 6) whose reason was not clear yet. Other thiols like decanethiol, thiophenol, and thioglycolate all worked nicely to furnish the corresponding products **4bb**–**bd** in good to excellent chemical yields with high stereoselectivities (Table 3, entries 9–11).

The stereostructure of the products was confirmed by X-ray crystallographic analysis using the minor diastereomer of **3bd**, nicely separated from the major isomer by recrystallization, and the major product **4ba**. As was our expectation, these compounds [49] possess the *anti* relationship between the 2 and 3 positions which clearly proved the epoxy ring opening taking place at the 2 position in an S_N2 fashion (Figure 1).

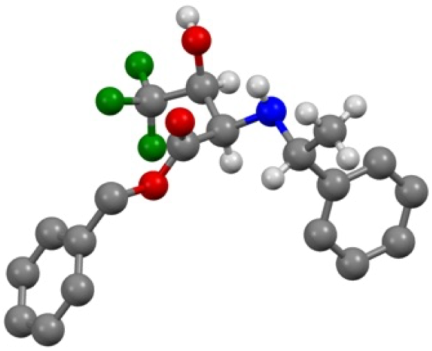

the minor diastereomer of **3bd**

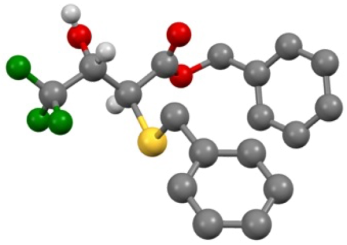

4ba

Figure 1: Crystallographic structure of the epoxy ring-opening products by $PhCH(NH_2)Me$ (**3bd**) and $PhCH_2SH$ (**4ba**).

The introduction of an additional halogen atom was considered to be possible by treatment of **2b** with an appropriate metal salt, and actually, similar results to the case of amines and thiols were obtained by using the corresponding MgX_2 [23,24]. It was proved that a larger amount of nucleophiles, higher temperature, and longer time all led to a decrease in the diastereomeric ratio of the products **5** (ca 10%) like the case of thiols described above. This is the reason why the three examples shown in Scheme 3 stopped before completion, and, for example, 24 h stirring in the case of the Cl atom entry furnished 67% yield of **5ba** [32,34] and 19% recovery of **2b** with the diastereomeric ratio of the former of 97:3. Contamination by the deiodinated 3-hydroxyester [50] was noticed during the synthesis of **5bc** using LiI.

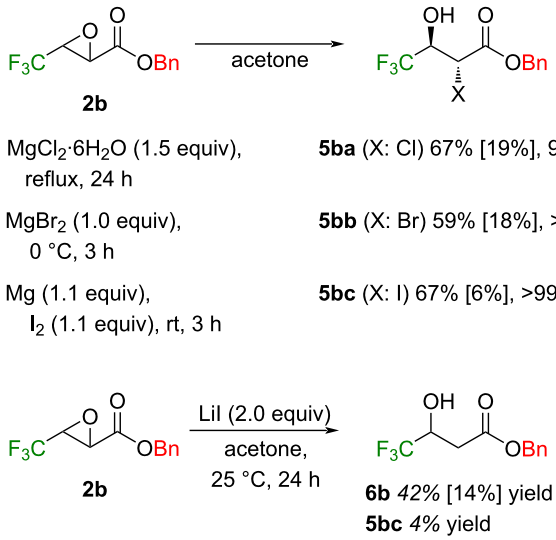

Scheme 3: Introduction of additional halogen atoms at the 2-position of the compound **2b**.

Reactions of (*E*)-4,4,4-trifluoro-2,3-epoxybutanoate **2b** with compounds possessing an acidic proton

It was very interesting to know that there were scarce examples in the literature [51] on the ring opening of 2,3-epoxyesters in general by the stabilized anionic species from, for example, malonate. One reason could be because of the formation of the less stable alkoxide by the progress of the nucleophilic addition. If this is really the case, the presence of the strongly electron-withdrawing fluorine-containing groups in our instance should nicely affect the characteristics of the resultant intermediate which could lead to the realization of the addition of such nucleophilic species.

First of all, as shown in Table 4, we started to investigate the reactivity of **2b** toward sodium malonate as the representative nucleophile. Because a brief solvent search indicated DMSO as the best for the attainment of high yields and diastereoselectivity (entries 1–5 vs 6 in Table 4), we further examined bases in

Table 4: Reactions of **2b** with the anionic species from diethyl malonate.

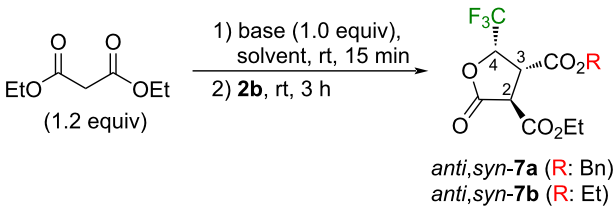

anti,*syn*-**7a** (R: Bn)
anti,*syn*-**7b** (R: Et)

Entry	Base	Solvent	Yield[a] (%)	dr	Recovery (%)
1[b]	NaH	THF	20	>99:1	0
2[b]	NaH	Toluene	6	>99:1	13
3[b]	NaH	Et_2O	12	>99:1	13
4[b]	NaH	MeCN	45	98:2	7
5[b]	NaH	DMF	75	96:4	0
6	NaH	DMSO	78	99:1	0
7	Et_3N	DMSO	0	–	83
8	TMG	DMSO	22	14:86	3
9	DBU	DMSO	13	23:77	2
10	CsF	DMSO	34	91:9	21
11	K_2CO_3	DMSO	50	98:2	13
12	*t*-BuOK	DMSO	85	98:2	0
13[c]	*t*-BuOK	DMSO	91	99:1	0
14[d]	*t*-BuOK	DMSO	94	98:2	0
15[c,e]	*t*-BuOK	DMSO	93	99:1	0
16[b,c,e]	*t*-BuONa	DMF	56	98:2	5
17[b,c,e]	*t*-BuOLi	DMF	trace	–	32

[a]Combined yields of *anti*,*syn*-**7a** and -**7b** were determined by ^{19}F NMR and isolated yield of *anti*,*syn*-**7a** was shown in parentheses; [b]0 °C for 30 min were employed for the step 1 instead of rt, 15 min; [c]2.0 equiv of malonate was used; [d]3.0 equiv of malonate was used; [e]stirring for 0.5 h for step 2.

this solvent to find out that *t*-BuOK behaved nicely, and the reaction of **2b** with 2.0 equiv of diethyl malonate for 0.5 h at room temperature furnished 93% yield of the product (Table 4, entry 15). During this optimization process, the obtained product was uncovered not to be a single component but a mixture of two compounds, *anti*,*syn*-**7a** and *anti*,*syn*-**7b**, the latter of which seemed to be produced from the former by the attack of the ethoxide ion released during the lactone-forming process. Their close structural resemblance led to a significant peak overlap both in the ^1H and ^{19}F NMR spectra which made it difficult to obtain their exact ratio and thus, the combined ^{19}F NMR yields were shown in Table 4. Separation of these two compounds was eventually succeeded by the usual hydrogenolysis to furnish the carboxylic acid *anti*,*syn*-**8a** in 79% isolated yield and the lactone *anti*,*syn*-**7b** was recovered in 13% yield (Scheme 4) which was considered to be the reflection of the original composition of *anti*,*syn*-**7a** and -**7b**. The relative stereochemistry of *anti*,*syn*-**8a** was confirmed as 2,3-*anti*-3,4-*syn* by its X-ray crystallographic analysis [49] (Figure 2) whose construction could be readily understood as the result of a highly stereoselective S_N2-type epoxy ring opening of **2a**, followed by the intramolecular lactone formation with the pro-*R* ethoxycarbonyl group possibly due to the higher steric congestion by the selection of the other CO_2Et moiety.

As shown in entries 8 or 9 in Table 4, it was proved that the usage of tetramethylguanidine (TMG) or DBU as the base provided a different stereoisomer as the major component. For the

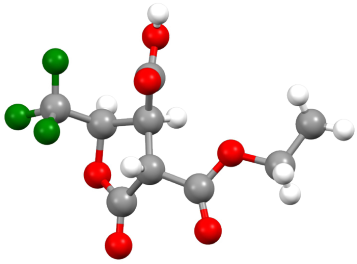

Figure 2: Crystallographic structure of *anti*,*syn*-**8a**.

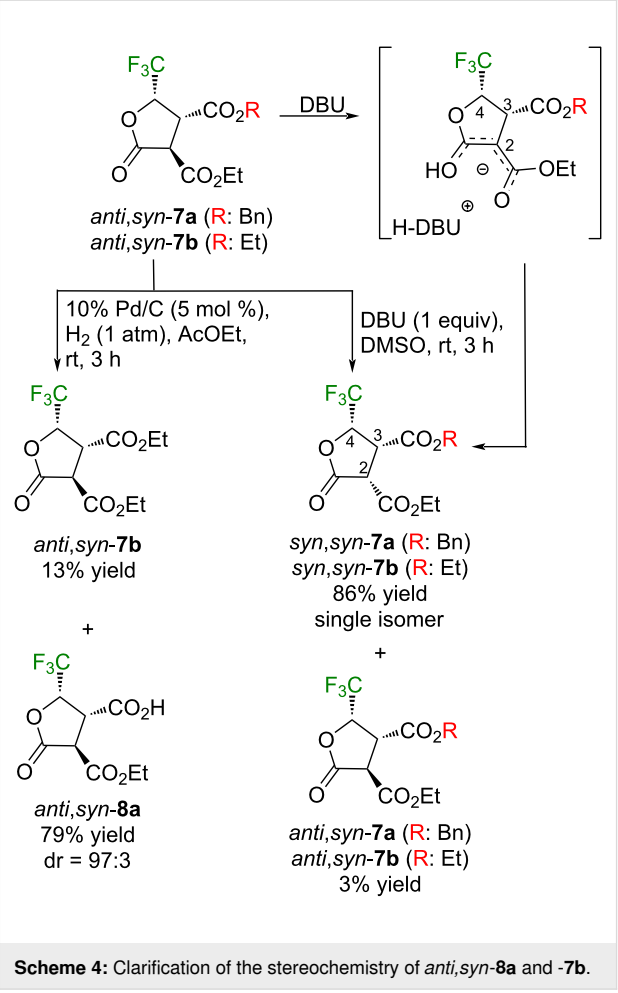

Scheme 4: Clarification of the stereochemistry of *anti,syn*-**8a** and -**7b**.

confirmation of its stereostructure, the isolated inseparable mixture of *anti*,*syn*-**7a** and -**7b** by the reaction of **2b** and diethyl malonate was treated with an equimolar amount of DBU in DMSO (rt, 3 h) to furnish products which were identical to the ones obtained in entries 8 or 9 (Table 4). The relative stereochemistry of the isomerized products was concluded by the observed NOESY cross peaks between H^2-H^4 and H^3-H^4, clearly demonstrating the relationship between these three hydrogen atoms as *cis*. Formation of *syn*,*syn*-**7a** and -**7b** by the above tertiary amines would be mechanistically elucidated by the deprotonation of the most acidic H^2 from the initially formed *anti*,*syn*-**7a** and -**7b**, followed by the re-protonation by the sterically bulky [H·amine]$^+$ from the less congested top side.

These results prompted us to further investigate the ring opening of **2b** by other nucleophiles with active hydrogen whose results are summarized in Scheme 5. If the in situ conversion of *anti*,*syn*-**7a** to *anti*,*syn*-**7b** follows the above ester alcohol exchange mechanism, employment of dibenzyl malonate should afford a single compound. This is actually the case and the expected dihydrofuran *anti,syn*-**7c** was obtained in 53% yield as a 98:2 diastereomer mixture, and stereochemistry of the major isomer was deduced from the above result as *anti*,*syn*. Although malononitrile also furnished the dihydrofuran *syn*-**7d** in good yield as a sole stereoisomer, a sharp contrast to these results was observed when **2b** was subjected to the anionic species from cyanoacetate, allowing to isolate the acyclic hydroxyester *anti*-**9e** in 76% yield. Smooth conversion to the dihydrofuran *syn*-**7e** was observed from this intermediary compound *anti*-**9e** by refluxing the crude solution in AcOEt.

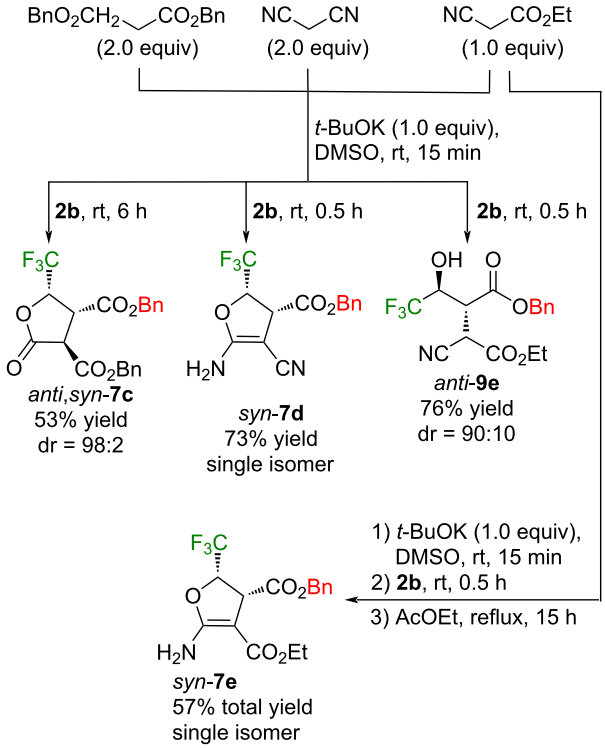

Scheme 5: Reaction of **2b** with other stabilized nucleophiles.

Different from these outcomes, other possible nucleophilic candidates like acetylacetone (pK_a value of the active hydrogen in DMSO: 13.3 [52]), nitromethane (17.2 [53]), ethyl (diethylphosphono)acetate (18.6 [52]), malononitrile (11.1 [53]), ethyl 2-nitroacetate (9.1 [54]), ethyl 2-cyanoacetate (13.1 [55]), and diethyl malonate (16.4 [56]) all failed to afford the desired addition products. From the complex mixture after mixing **2b** with *t*-BuOK and nitroacetate in DMSO at 80 °C, the unexpected compound 2,3-dihydroxybutyrate *anti*-**10a** was isolated as a single isomer. Its production was also detected by ^{19}F NMR from the reaction mixture when nitromethane (16%) and ethyl (diethylphosphono)acetate (17%) were employed instead of nitroacetate, while no other compound was separated from these mixtures due to their complexity (Scheme 6).

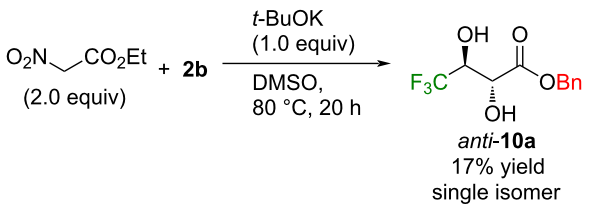

Scheme 6: Production of 4,4,4-trifluoro-2,3-dihydroxybutanoate *anti*-**10a**.

Reactions of (*E*)-4,4,4-trifluoro-2,3-epoxybutanoate **2b** with Grignard-based copper reagents

Despite the previous report by the Seebach group on the intriguing reactivity of the CF_3-containing ethyl 2,3-epoxybutanoate **2a** towards a variety of organometallic species [27-29], because relatively readily accessible Grignard-based cuprates were not involved, their applicability to **2b** as the representative partner was investigated here (Table 5).

The 1:2 ratio of CuI and *n*-$C_{10}H_{21}$MgBr was selected due to the better material balance than the case of 1:1 (entries 1 and 2 in Table 5), the latter of which afforded an almost equimolar amount of the hydroxyketone **11a** and epoxyalcohol **12a**. A decrease of the temperature to −40 °C resulted in the better preference of **11a** (Table 5, entry 3), and 1.6 and 3.2 equiv of CuI and *n*-$C_{10}H_{21}$MgBr, respectively, were concluded as the best amounts for the synthesis of the nucleophilic species (entries 3–5). The shorter reaction time led to a slightly better ratio of **11a** to **12a** with a lower combined yield along with the detection of the epoxyketone **13a** at the same instance (entry 6 in Table 5). We recognized compound **13a** as the precursor for the formation of **11a** and **12a**. The conditions in the absence of CuI afforded **12a** as the sole product (entry 7 in Table 5) whose result was nicely compared with the one previously reported [29]. Changing the solvent to THF (Table 5, entry 8) or the Cu species to CuCN (entry 9) both did not have a positive effect on the present reaction, and we eventually found out that the temperature for the preparation of the cuprate was important and lowering it to −40 °C nicely allowed to record 79% isolated yield of **11a** with only 6% of the byproduct **12a** (entry 10).

The conditions described in entry 10 in Table 5 were applied to the reactions of **2b** with other Grignard reagents in the presence of CuI (Table 6).

Table 5: Optimization of the reaction conditions of **2b** with the *n*-$C_{10}H_{21}$MgBr-based cuprate.

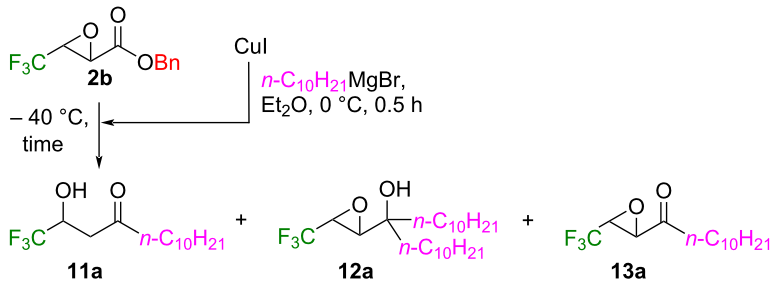

	Amount (equiv)			^{19}F NMR yield[a] (%)	
Entry	CuI	*n*-$C_{10}H_{21}$MgBr	Time (h)	**11a**	**12a**
1[b]	2.0	2.0	1	47	4
2	2.0	4.0	1	30	40
3	2.0	4.0	4	64	12
4	1.6	3.2	4	66	16
5	1.2	2.4	4	49	19
6[c]	1.6	3.2	1	56	7
7	–	3.2	0.5	0	84 (73)
8[d]	1.6	3.2	3	3	13
9[e]	1.6	3.2	3	7	14
10[f]	1.6	3.2	3	(79)	6

[a]Isolated yields are described in parentheses; [b]reaction at 0 °C when the cuprate was added to **2b**; [c]19% of the epoxy ketone **13a** was detected by ^{19}F NMR; [d]the reaction was carried out in THF; [e]CuCN was employed instead of CuI; [f]the cuprate was prepared at –40 °C.

Table 6: Reactions of Grignard-based cuprates with **2b**.

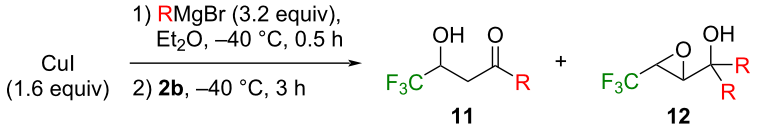

	Isolated yield (%)	
R	**11**	**12**
n-$C_{10}H_{21}$- (**a**)	79	6[a]
$PhCH_2CH_2$- (**b**)	57	13[a]
c-Hex- (**c**)	55	4[a]
Ph- (**d**)	trace[a]	77
4-$MeOC_6H_4$- (e)	0[a]	80

[a]Determined by ^{19}F NMR.

$PhCH_2CH_2MgBr$ and *c*-$C_6H_{11}MgBr$ produced the β-hydroxyketones **11b** and **11c** in 57% and 55% yields, respectively, along with small amounts of the corresponding epoxyalcohols **12b** and **12c**. On the other hand, **12d** and **12e** were substantially formed by ArMgBr (Ar: Ph and 4-$MeOC_6H_4$, respectively), the former of which was reported to be obtained by the action of PhLi alone [29]. It was intriguing to note that the present method yielded the unprecedented products **11** by the reaction of the epoxyester **2b** with other organometallic species.

For the mechanistic clarification of the present reactions, two additional experiments were executed which are shown in Scheme 7. Employment of the epoxyketone **13f** (R: *n*-C_6H_{13}), structurally analogous to **13a**, to the reaction with $(n\text{-}C_{10}H_{21})_2CuMgBr$ furnished a mixture of the hydroxyketone **11f** and epoxyalcohol **12f** in 32% and 52% yields, respectively. This experimental result clearly indicated that the conversion of **13a** to **11a** is one of the possible routes.

The second reaction was carried out for the verification of the intermediate leading to the product **11**. Although we initially assumed that the epoxy ring opening occurred by hydride generated through the β-elimination of the *n*-$C_{10}H_{21}MgBr$-based cuprate species, the TLC analysis of the reaction mixture did not show any evidence of the production of the possible olefinic product *n*-$C_8H_{17}CH{=}CH_2$. Moreover, when the reaction mixture was quenched with D_2O, incorporation of deuterium was observed to give **11a**-D in a high yield which allowed us to conclude the possible presence of the *C*-copper species just before quenching. Our result well compares with the one by Alexakis et al. [57]. In their instance, the reaction of *t*-$Bu_2CuCNLi_2$ and cyclohexene oxide afforded a mixture of products in 10 and 50% yields as a result of the epoxy ring opening by *t*-Bu group and hydride, respectively. Their additional experiment to quench the corresponding intermediate by D_2O proved that no deuteration occurred. This result clearly indicated that hydride was released from the *t*-Bu group of the Cu(III) species formed after the nucleophilic attack of the epoxy ring. In our case, since the strongly electron-withdrawing CF_3 group would render the rate of the reductive elimination very slow, the intermediary Cu(III) species safely existed until the addition of D_2O. Because the significant overlap of NMR peaks was observed due to the quite similar structure of **11a** and **11a**-D, quantitative analysis of the deuterium content of **11a**-D

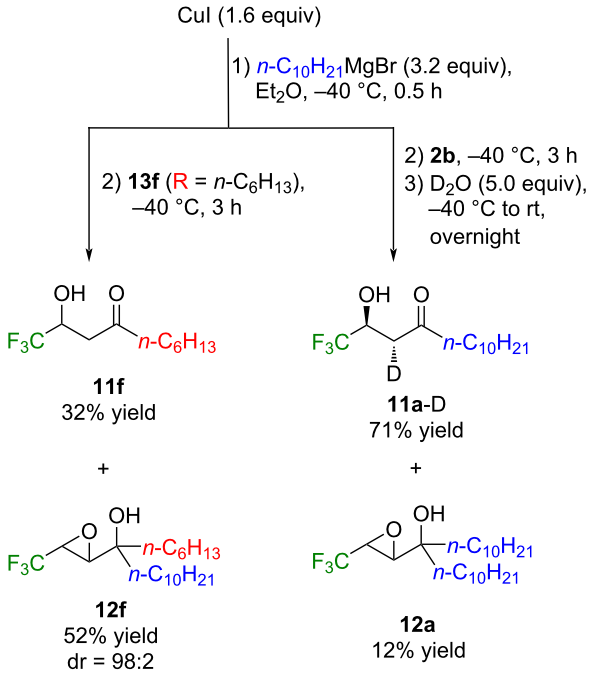

Scheme 7: Reactions of *n*-$C_{10}H_{21}MgBr$-based cuprate with **13f** as well as **2b** with/without D_2O quenching.

was not possible. However, the comparison of their specific region of the ^{13}C NMR charts and sharp peaks readily led us to qualitative understanding of the high purity of **11a**-D possibly as a single diastereomer (Figure 3).

Conclusion

As described above, we have succeeded in the facile preparation of 2,3-epoxyesters **2** with a variety of Rf groups at the 3 position starting from the corresponding 3-Rf-acrylates **1** by the action of the low cost and easy-to-handle reagent, $NaOCl{\cdot}5H_2O$. The special feature of this process is the requirement of a very mild temperature of 0 °C which can be well compared to the previous one executed at −78 °C under the action of LDA [29]. Moreover, by using the epoxyester **2b** as the representative substrate, clarification of its reactivity was carried out by mixing with 1) heteronucleophiles like amines, thiols, and magnesium halides, 2) softer carbon nucleophiles such as malonates, and 3) Grignard-based cuprates. These processes usually yielded the addition products along with the epoxy ring opening at the 2 position via the S_N2 mechanism, affording 3-Rf-3-hydroxyesters with the incorporation of a variety of substituents at the 2-position in a highly *anti*-selective fashion. We believe that the facile procedure presented here opens novel routes to the application of these intriguing products in a variety of fields.

Experimental

General procedure for the formation of the epoxyesters (GP-1): Benzyl (*E*)-2,3-epoxy-4,4,4-trifluorobutanoate (**2b**)

GP-1A (by use of aqueous NaClO): To a solution of compound **1b** [42] (0.23 g, 1.00 mmol) in 3.0 mL of CH_3CN was added NaClO aq. (5% in H_2O, 1.50 g, 1.00 mmol) and the solution was stirred for 4.5 h at room temperature. This mixture was extracted with CH_2Cl_2 and the usual workup and purification afforded 0.15 g (0.60 mmol) of the pure title compound in 60% yield.

GP-1B (by use of $NaClO{\cdot}5H_2O$): To a solution of compound **1b** [42] (0.2302 g, 1.00 mmol) in 3.0 mL of CH_3CN was added $NaClO{\cdot}5H_2O$ (0.3290 g, 2.00 mmol) at 0 °C, and the solution was stirred for 6 h at the same temperature. After the same workup process and purification with silica gel column chromatography using AcOEt/Hex 1:20 as an eluent, 0.2117 g (0.86 mmol) of the title compound (86% yield) were isolated. R_f 0.52 (Hex/AcOEt 5:1); ^1H NMR (300.40 MHz, $CDCl_3$) δ 3.71–3.76 (m, 2H), 5.21 (d, J = 12.3 Hz, 1H), 5.28 (d, J = 12.3 Hz, 1H), 7.34–7.44 (m, 5H); ^{13}C NMR (75.45 MHz, $CDCl_3$) δ 49.4 (q, J = 2.5 Hz), 52.7 (q, J = 42.2 Hz), 68.0, 121.4 (q, J = 276.0 Hz), 128.5, 128.7, 128.8, 134.3, 165.6; ^{19}F NMR (282.65

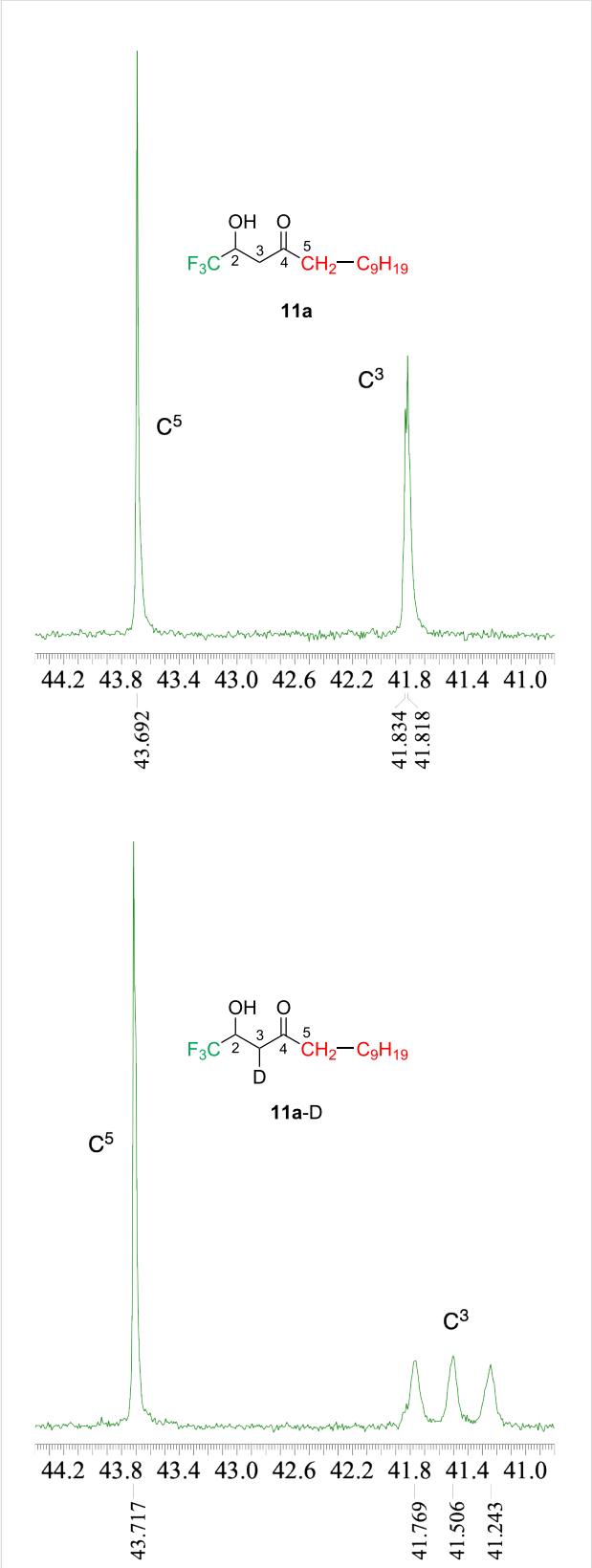

Figure 3: A part of ^{13}C NMR spectra for the compounds **11a** and **11a**-D.

MHz, $CDCl_3$) δ −75.12 (d, *J* = 4.5 Hz); IR (neat) ν: 3944, 3689, 3054, 2987, 2685, 2306, 1756, 1456, 1422, 1382, 1341, 1265, 1169, 1089, 988, 929, 896, 664 cm^{-1}; Anal. calcd for $C_{11}H_9F_3O_3$: C, 53.67; H, 3.68; found: C, 53.54; H, 3.89.

General procedure for the ring opening of epoxides (GP-2). Benzyl 2,3-*anti*-4,4,4-trifluoro-3-hydroxy-2-(*p*-methoxyphenyl)amino-butanoate (**3ba**)

p-Anisidine (0.07 g, 0.60 mmol) was added to an EtOH (3 mL) solution of compound **2b** (0.12 g, 0.50 mmol), and the resultant mixture was stirred at 50 °C for 19 h under the open air. After quenching the reaction with 1 M HCl aq., the mixture was extracted with AcOEt three times and the combined organic phase was washed with brine. Evaporation of the volatiles furnished crude materials which were recrystallized by use of Hex/$CHCl_3$ 3:2 as a solvent to afford 0.14 g (0.39 mmol) of the title compound **3aa** in 78% yield as a sole stereoisomer. R_f 0.30 (Hex/AcOEt 2:1); mp 95–97 °C; ^{1}H NMR (300.40 MHz, $CDCl_3$) δ 3.70 (brs, 1H), 3.76 (s, 3H), 4.31–4.33 (m, 2H), 4.39 (brs, 1H), 5.14 (dd, *J* = 12.0, 21.3 Hz, 1H), 6.74–6.81 (m, 4H), 7.26–7.36 (m, 5H); ^{13}C NMR (75.45 MHz, acetone-d_6) δ 55.5, 59.3, 67.9, 70.0 (q, *J* = 30.2 Hz), 114.8, 117.7, 124.1 (q, *J* = 283.5 Hz), 128.5, 128.6, 128.7, 134.4, 139.5, 154.3, 170.2; ^{19}F NMR (282.65 MHz, $CDCl_3$) δ −76.83 (d, *J* = 9.0 Hz); IR (KBr) ν: 3454, 3315, 2955, 2924, 2854, 2360, 1741, 1519, 1458, 1238, 1204, 1156, 1138, 1097, 1030, 822, 749 cm^{-1}; HRMS–FAB (*m/z*): $[M]^+$ calcd for $C_{18}H_{18}F_3NO_4$, 369.1182; found, 369.1209.

General procedure for the ring opening of epoxides by enolates (GP-3). 4-Benzyl 5-ethyl *anti*,*syn*-tetrahydro-2-oxo-3-(trifluoromethyl)-furan-4,5-dicarboxylate (*anti*,*syn*-**7a**) and 4,5-diethyl *anti*,*syn*-tetrahydro-2-oxo-3-(trifluoromethyl)furan-4,5-dicarboxylate (*anti*,*syn*-**7b**)

Diethyl malonate (0.18 mL, 1.20 mmol) was added to a flask containing 0.0673 g (0.60 mmol) of *t*-BuOK in DMSO (1.8 mL) under an argon atmosphere and the resultant mixture was stirred for 15 min at room temperature. Then, 0.1477 g (0.60 mmol) of **2b** in 0.8 mL of DMSO was introduced to the resultant solution and the stirring was continued for 0.5 h. The same workup process and purification furnished 0.1717 g of an inseparable mixture of *anti*,*syn*-**7a** (dr = 99:1) and *anti*,*syn*-**7b** (**7a**:**7b** = 83:17). *Anti*,*syn*-**7a**: R_f 0.34 (Hex/AcOEt 4:1); ^{1}H NMR (300.40 MHz, $CDCl_3$) δ 1.32 (t, *J* = 7.2 Hz, 3H), 4.20–4.27 (m, 2H), 4.21–4.35 (m, 2H), 5.05 (quint, *J* = 7.2 Hz, 1H), 5.15 (d, *J* = 12.3 Hz, 1H), 5.23 (d, *J* = 12.0 Hz, 1H), 7.32–7.40 (m, 5H); ^{13}C NMR (75.45 MHz, $CDCl_3$) δ 13.8, 44.4, 46.4, 63.1, 68.5, 73.5 (q, *J* = 34.1 Hz), 122.5 (q, *J* = 282.9 Hz), 128.61, 128.63, 128.8, 134.0, 165.1, 165.6, 167.4; ^{19}F NMR (282.65 MHz, $CDCl_3$) δ −75.84 (d, *J* = 6.8 Hz); IR (neat) ν: 2987, 1813, 1742, 1457, 1389, 1321,1218, 1182, 1128, 1023, 972, 755 cm^{-1}; HRMS–FAB+ (*m/z*): $[M + H]^+$ calcd for $C_{16}H_{16}F_3O_6$, 361.0893; found, 361.0911. Epimer at the 2 position of *anti*,*syn*-**7a** (*syn*,*syn*-**7a**): ^{1}H NMR (300.40 MHz, $CDCl_3$) δ 1.30 (t, *J* = 7.2 Hz, 3H), 4.00 (d, *J* = 8.4 Hz, 1H), 4.08 (dd, *J* = 6.3, 8.1 Hz, 1H), 4.26–4.34 (m, 2H), 5.00 (quint, *J* = 5.7 Hz, 1H), 5.22 (d, *J* = 12.0 Hz, 1H), 5.27 (d, *J* = 12.3 Hz, 1H), 7.31–7.41 (m, 5H); ^{13}C NMR (75.45 MHz, $CDCl_3$) δ 13.9, 43.2, 48.5, 63.3, 68.6, 74.9 (q, *J* = 35.4 Hz), 122.4 (q, *J* = 279.8 Hz), 128.3, 128.8, 128.9, 134.2, 164.5, 167.1, 168.2; ^{19}F NMR (282.65 Hz, $CDCl_3$) δ −79.55 (d, *J* = 4.8 Hz); HRMS–FAB+ (*m/z*): $[M + H]^+$ calcd for $C_{16}H_{16}F_3O_6$, 361.0893; found, 361.0909.

General procedure for the reaction of the epoxyester **2b** with cuprates (GP-4): 1,1,1-Trifluoro-2-hydroxytetradecan-4-one (**11a**)

1.70 mL of a 0.94 M Et_2O solution of decylmagnesium bromide (1.6 mmol) was added to an Et_2O (3.0 mL) solution containing 0.1524 g (0.80 mmol) of CuI at −40 °C under an argon atmosphere and the resultant mixture was stirred for 0.5 h at that temperature. A solution of 0.1231 g (0.50 mmol) of **2b** in Et_2O (1.0 mL) was added and the mixture was stirred for 3 h at the same temperature. After quenching the reaction with a saturated NH_4Cl aq, the usual workup afforded 0.1116 g (0.40 mmol) of the title compound in 79% yield after silica gel column chromatography using Hex/AcOEt 6:1 as an eluent. R_f 0.51 (Hex/AcOEt 4:1); ^{1}H NMR (300.40 MHz, $CDCl_3$) δ 0.88 (t, *J* = 6.9 Hz, 3H), 1.26 (brs, 14H), 1.60 (quint, *J* = 6.9 Hz, 2H), 2.49 (t, *J* = 7.5 Hz, 2H), 2.74 (dd, *J* = 3.6, 17.7 Hz, 1H), 2.83 (dd, *J* = 9.0, 17.7 Hz, 1H), 3.49 (d, *J* = 4.2 Hz, 1H), 4.43–4.56 (m, 1H); ^{13}C NMR (75.45 MHz, $CDCl_3$) δ 14.0, 15.0, 22.6, 23.4, 29.26, 29.28, 29.4, 29.5, 31.8, 41.8 (q, *J* = 1.2 Hz), 43.7, 66.4 (q, *J* = 32.2 Hz), 124.7 (q, *J* = 281.1 Hz), 208.9; ^{19}F NMR (282.65 MHz, $CDCl_3$) δ −80.79 (d, *J* = 7.1 Hz); IR (neat) ν: 3408, 2958, 2927, 2856, 1720, 1469, 1291, 1176, 1146, 899, 841, 719, 643 cm^{-1}; HRMS–FAB+ (*m/z*): $[M + H]^+$ calcd for $C_{14}H_{26}F_3O_2$, 283.1879; found, 283.1893.

Supporting Information

Supporting Information File 1

Full experimental and analytical details, copies of NMR spectra for new compounds, and crystallographic data.
[https://www.beilstein-journals.org/bjoc/content/supplementary/1860-5397-20-206-S1.pdf]

Author Contributions

Yutaro Miyashita: investigation. Sae Someya: investigation. Tomoko Kawasaki-Takasuka: investigation; resources. Tomohiro Agou: resources. Takashi Yamazaki: conceptualization; supervision; writing – original draft; writing – review & editing.

ORCID® iDs

Tomoko Kawasaki-Takasuka - https://orcid.org/0000-0002-8468-7553
Takashi Yamazaki - https://orcid.org/0000-0002-1460-3086

Data Availability Statement

All data that supports the findings of this study is available in the published article and/or the supporting information to this article.

References

1. Kirsch, P. *Modern Fluoroorganic Chemistry: Synthesis, Reactivity, Applications;* Wiley-VCH: Weinheim, Germany, 2004. doi:10.1002/352760393x
2. Uneyama, K., Ed. *Organofluorine Chemistry;* Blackwell:: Oxford, UK, 2006. doi:10.1002/9780470988589
3. Yamazaki, T.; Taguchi, T.; Ojima, I. Unique Properties of Fluorine and their Relevance to Medicinal Chemistry and Chemical Biology; Introduction: Basic Aspects of Fluorine Substituent Effect in Medicinal Chemistry. In *Fluorine in Medicinal Chemistry and Chemical Biology;* Ojima, I., Ed.; Wiley: West Sussex, UK, 2009; pp 3–46. doi:10.1002/9781444312096.ch1
4. Brittain, W. D. G.; Lloyd, C. M.; Cobb, S. L. *J. Fluorine Chem.* **2020,** *239,* 109630. doi:10.1016/j.jfluchem.2020.109630
5. O'Hagan, D. *Chem. – Eur. J.* **2020,** *26,* 7981–7997. doi:10.1002/chem.202000178
6. Remete, A. M.; Nonn, M.; Escorihuela, J.; Fustero, S.; Kiss, L. *Eur. J. Org. Chem.* **2021,** 5946–5974. doi:10.1002/ejoc.202101094
7. Decaens, J.; Couve-Bonnaire, S.; Charette, A. B.; Poisson, T.; Jubault, P. *Chem. – Eur. J.* **2021,** *27,* 2935–2962. doi:10.1002/chem.202003822
8. Yamazaki, T.; Haga, J.; Kitazume, T.; Nakamura, S. *Chem. Lett.* **1991,** 2171–2174. doi:10.1246/cl.1991.2171
9. Yamazaki, T.; Haga, J.; Kitazume, T. *Chem. Lett.* **1991,** *20,* 2175–2178. doi:10.1246/cl.1991.2175
10. Shinohara, N.; Haga, J.; Yamazaki, T.; Kitazume, T.; Nakamura, S. *J. Org. Chem.* **1995,** *60,* 4363–4374. doi:10.1021/jo00119a013
11. Yamazaki, T.; Shinohara, N.; Kitazume, T.; Sato, S. *J. Org. Chem.* **1995,** *60,* 8140–8141. doi:10.1021/jo00130a012
12. Pan, X.; Liu, Z. *Tetrahedron* **2014,** *70,* 4602–4610. doi:10.1016/j.tet.2014.05.049
13. Shu, C.; Liu, H.; Slawin, A. M. Z.; Carpenter-Warren, C.; Smith, A. D. *Chem. Sci.* **2020,** *11,* 241–247. doi:10.1039/c9sc04303a
14. Kim, B.-J.; Song, Y.-N.; Lee, S. Y.-M. *Chem. Commun.* **2021,** *57,* 11052–11055. doi:10.1039/d1cc04875a
15. Wu, J.; Young, C. M.; Watts, A. A.; Slawin, A. M. Z.; Boyce, G. R.; Bühl, M.; Smith, A. D. *Org. Lett.* **2022,** *24,* 4040–4045. doi:10.1021/acs.orglett.2c01486
16. Yamazaki, T.; Shinohara, N.; Kitazume, T.; Sato, S. *J. Fluorine Chem.* **1999,** *97,* 91–96. doi:10.1016/s0022-1139(99)00034-2
17. Yamazaki, T.; Taketsugi, M.; Kawasaki-Takasuka, T.; Agou, T.; Kubota, T. *Bull. Chem. Soc. Jpn.* **2021,** *94,* 1815–1822. doi:10.1246/bcsj.20210136
18. Morigaki, A.; Tanaka, T.; Miyabe, T.; Ishihara, T.; Konno, T. *Org. Biomol. Chem.* **2013,** *11,* 586–595. doi:10.1039/c2ob26708j
19. Zhang, L.-Y.; Zhou, J.-H.; Xu, Y.-H.; Loh, T.-P. *Chem. – Asian J.* **2015,** *10,* 844–848. doi:10.1002/asia.201403303
20. Computation of **1b** and its non-fluorinated counterpart as the methyl ester clearly showed their LUMO + 1 energy levels as 0.053 and 0.961 eV, respectively, by employment of Gaussian 09W, Revision D.01 using the B3LYP/6-311++G** level of theory.
21. Yamazaki, T.; Ando, M.; Kitazume, T.; Kubota, T.; Omura, M. *Org. Lett.* **1999,** *1,* 905–908. doi:10.1021/ol990821c
22. Gleason, J. G.; Hall, R. F.; Perchonock, C. D.; Erhard, K. F.; Frazee, J. S.; Ku, T. W.; Kondrad, K.; McCarthy, M. E.; Mong, S.; Crooke, S. T.; Chi-Rosso, G.; Wasserman, M. A.; Torphy, T. J.; Muccitelli, R. M.; Hay, D. W.; Tucker, S. S.; Vickery-Clark, L. *J. Med. Chem.* **1987,** *30,* 959–961. doi:10.1021/jm00389a001
23. Righi, G.; Rumboldt, G.; Bonini, C. *J. Org. Chem.* **1996,** *61,* 3557–3560. doi:10.1021/jo951441h
24. Righi, G.; Pescatore, G.; Bonadies, F.; Bonini, C. *Tetrahedron* **2001,** *57,* 5649–5656. doi:10.1016/s0040-4020(01)00492-6
25. Durán Pachón, L.; Gamez, P.; van Brussel, J. J. M.; Reedijk, J. *Tetrahedron Lett.* **2003,** *44,* 6025–6027. doi:10.1016/s0040-4039(03)01480-1
26. Rackl, D.; Kais, V.; Lutsker, E.; Reiser, O. *Eur. J. Org. Chem.* **2017,** 2130–2138. doi:10.1002/ejoc.201700014
27. Seebach, D.; Beck, A. K.; Renaud, P. *Angew. Chem., Int. Ed. Engl.* **1986,** *25,* 98–99. doi:10.1002/anie.198600981
28. Lin, J. T.; Yamazaki, T.; Takeda, M.; Kitazume, T. *J. Fluorine Chem.* **1989,** *44,* 113–120. doi:10.1016/s0022-1139(00)84374-2
29. von dem Bussche-Hünnefeld, C.; Seebach, D. *Chem. Ber.* **1992,** *125,* 1273–1281. doi:10.1002/cber.19921250538
30. Ishii, A.; Kanai, M.; Kuriyama, S.; Yasumoto, M.; Inomiya, N.; Otsuka, T.; Ueda, H. Preparation of 4,4,4-trifluoro-2,3-epoxybutanoic acid esters. Japanese patent JP2005047870, Feb 24, 2005. See for preparation of compound **2a** by the Bayer-Villiger oxidation of epoxyketones.
31. Lanier, M.; Haddach, M.; Pastor, R.; Riess, J. G. *Tetrahedron Lett.* **1993,** *34,* 2469–2472. doi:10.1016/s0040-4039(00)60443-4
32. Lanier, M.; Le Blanc, M.; Pastor, R. *Tetrahedron* **1996,** *52,* 14631–14640. doi:10.1016/0040-4020(96)00874-5
33. Walborsky, H. M.; Baum, M. E. *J. Am. Chem. Soc.* **1958,** *80,* 187–192. doi:10.1021/ja01534a047
34. Wakselman, C.; Tordeux, M. *J. Fluorine Chem.* **1982,** *21,* 99–106. doi:10.1016/s0022-1139(00)81235-x
35. Ooi, T.; Tayama, E.; Doda, K.; Takeuchi, M.; Maruoka, K. *Synlett* **2000,** 1500–1502. doi:10.1055/s-2000-7652
36. Moyna, G.; Williams, H. J.; Scott, A. I. *Synth. Commun.* **1996,** *26,* 2235–2239. doi:10.1080/00397919608003584
37. Yadav, V. K.; Kapoor, K. K. *Tetrahedron* **1995,** *51,* 8573–8584. doi:10.1016/0040-4020(95)00472-k
38. Semmelhack, M. F.; Jeong, N. *Tetrahedron Lett.* **1990,** *31,* 605–608. doi:10.1016/s0040-4039(00)94579-9
39. Yamazaki, T.; Someya, S. Method for the preparation of fluorine-containing epoxy ester. Japanese patent JP2010208998, Sept 24, 2010. Our patent was already published which was on the preparation of **2** by using an aqueous solution of NaOCl.
40. Yamazaki, T.; Ichige, T.; Kitazume, T. *Org. Lett.* **2004,** *6,* 4073–4076. doi:10.1021/ol048229x
41. Foucaud, A.; Bakouetila, M. *Synthesis* **1987,** 854–856. doi:10.1055/s-1987-28104

42. Yamazaki, T.; Mano, N.; Hikage, R.; Kaneko, T.; Kawasaki-Takasuka, T.; Yamada, S. *Tetrahedron* **2015,** *71,* 8059–8066. doi:10.1016/j.tet.2015.08.048
43. Our computation (B3LYP/6-311++G** by the Gaussian 09W (rev. D.01)) clarified that the LUMO+1 energy levels of the compounds of **1b**, **1h**, and **1i** (as the methyl esters) were calculated to be 0.053, 0.429, and 0.405 eV, respectively.
44. Davidge, H.; Davies, A. G.; Kenyon, J.; Mason, R. F. *J. Chem. Soc.* **1958,** 4569–4573. doi:10.1039/jr9580004569
Our literature search clarified that only one example was previously reported for the reaction of **2a** with amine.
45. Bordwell, F. G.; Zhang, X.; Alnajjar, M. S. *J. Am. Chem. Soc.* **1992,** *114,* 7623–7629. doi:10.1021/ja00046a003
46. Taft, R. W.; Bordwell, F. G. *Acc. Chem. Res.* **1988,** *21,* 456–463. doi:10.1021/ar00156a005
47. Tang, Z.; Yang, Z.-H.; Chen, X.-H.; Cun, L.-F.; Mi, A.-Q.; Jiang, Y.-Z.; Gong, L.-Z. *J. Am. Chem. Soc.* **2005,** *127,* 9285–9289. doi:10.1021/ja0510156
The epimerization for the nonfluorinated epoxysuccinate was noticed by the action of NaN_3.
48. Sugano, Y.; Naruto, S. *Chem. Pharm. Bull.* **1988,** *36,* 4619–4621. doi:10.1248/cpb.36.4619
A similar epimerization was suggested for the non-fluorinated a-sulfenylated esters.
49. CCDC 2325464 ((2*R**,3*S**,2'*R**)-**3ad**), 2325462 (*anti,syn*-**8a**), and 2325461 (**4aa**) contain the supplementary crystallographic data for this paper. These data are provided free of charge by the joint Cambridge Crystallographic Data Centre and Fachinformationszentrum Karlsruhe Access Structures service, https://www.ccdc.cam.ac.uk/structures/.
50. Zemtsov, A. A.; Levin, V. V.; Dilman, A. D.; Struchkova, M. I.; Belyakov, P. A.; Tartakovsky, V. A. *Tetrahedron Lett.* **2009,** *50,* 2998–3000. doi:10.1016/j.tetlet.2009.03.188
51. Takeda, A.; Torii, S. *Bull. Chem. Soc. Jpn.* **1967,** *40,* 1261–1263. doi:10.1246/bcsj.40.1261
52. Ripin, D. H.; Evans, D. A. http://ccc.chem.pitt.edu/wipf/MechOMs/evans_pKa_table.pdf.
53. Matthews, W. S.; Bares, J. E.; Bartmess, J. E.; Bordwell, F. G.; Cornforth, F. J.; Drucker, G. E.; Margolin, Z.; McCallum, R. J.; McCollum, G. J.; Vanier, N. R. *J. Am. Chem. Soc.* **1975,** *97,* 7006–7014. doi:10.1021/ja00857a010
54. Goumont, R.; Magnier, E.; Kizilian, E.; Terrier, F. *J. Org. Chem.* **2003,** *68,* 6566–6570. doi:10.1021/jo034244o
55. Bordwell, F. G.; Fried, H. E. *J. Org. Chem.* **1981,** *46,* 4327–4331. doi:10.1021/jo00335a001
56. Olmstead, W. N.; Bordwell, F. G. *J. Org. Chem.* **1980,** *45,* 3299–3305. doi:10.1021/jo01304a033
57. Alexakis, A.; Jachiet, D.; Normant, J. F. *Tetrahedron* **1986,** *42,* 5607–5619. doi:10.1016/s0040-4020(01)88165-5

License and Terms

BEILSTEIN JOURNAL OF ORGANIC CHEMISTRY

Phenylseleno trifluoromethoxylation of alkenes

Clément Delobel[1], Armen Panossian[2], Gilles Hanquet[2], Frédéric R. Leroux[2], Fabien Toulgoat[*1,3] and Thierry Billard[*1]

Full Research Paper

Open Access

Address:
[1]Institute of Chemistry and Biochemistry (ICBMS - UMR 5246), CNRS, University Claude Bernard-Lyon 1, CPE Lyon, Lyon, France, [2]Université de Strasbourg, Université de Haute-Alsace, CNRS, UMR 7042-LIMA, ECPM, Strasbourg, France and [3]CPE Lyon, Lyon, France

Email:
Fabien Toulgoat[*] - Fabien.toulgoat@cpe.fr; Thierry Billard[*] - Thierry.billard@univ-lyon1.fr

* Corresponding author

Keywords:
DNTFB; electrophilic addition; fluorine; selenium; trifluoromethoxy

Beilstein J. Org. Chem. **2024,** *20,* 2434–2441.
https://doi.org/10.3762/bjoc.20.207

Received: 17 July 2024
Accepted: 13 September 2024
Published: 26 September 2024

This article is part of the thematic issue "Organofluorine chemistry VI".

Guest Editor: D. O'Hagan

Abstract

Trifluoromethoxylated molecules and selenylated compounds find a wide range of interesting applications, but separately. In order to combine the potential of these two motifs and to propose a new class of compounds, we have developed an electrophilic phenylseleno trifluoromethoxylation of alkenes, which leads to β-selenylated trifluoromethoxylated compounds or, upon subsequent reduction, to the trifluoromethoxylated ones.

Introduction

Due to the specific properties of the fluorine atom [1-3], fluorinated compounds are now present in a wide range of applications, from materials to life sciences [4-11]. In order to propose new molecules with specific properties for targeted applications, the development of new fluorinated moieties is an active research field [12]. Among these emerging fluorinated groups, the association of the CF_3 moiety with chalcogens is an interesting approach. In particular, the trifluoromethoxy group (CF_3O) possesses valuable properties such as electronegativity [13,14], lipophilicity [15,16], electronic effects [17,18], and conformation [19-21]. Some trifluoromethoxylated molecules can be used as drugs in the treatment of various pathologies (Figure 1) [22-29].

On the other hand, despite its toxicity at higher doses, selenium is also an essential trace element in human physiology [30,31]. Moreover, several selenylated molecules have found applications in various fields such as materials or bioactive compounds [32-43]. Some selenylated compounds exhibit fascinating biological properties.

Despite these separate converging interests, no methods have been described to synthesize both trifluoromethoxylated and phenylselenylated molecules.

The introduction of a CF_3O moiety into organic molecules remains poorly described in the literature, especially the direct

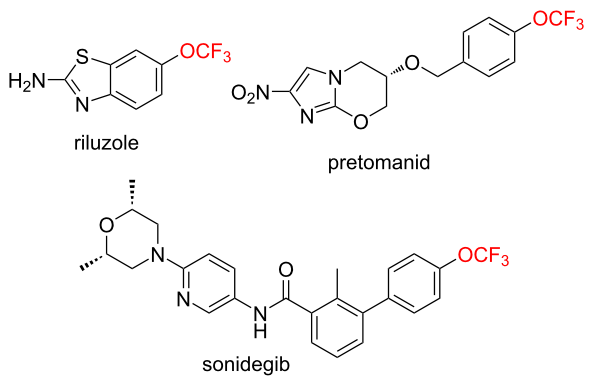

Figure 1: Examples of trifluoromethoxylated drugs.

trifluoromethoxylation [44-46]. Only few radical trifluoromethoxylations of (hetero)aromatics [47-52], enol carbonates [53] or silyl enol ethers and allyl silanes [54] have been reported. Most of the methods described have used the trifluoromethoxide anion (CF_3O^-) [45]. Many sources of the CF_3O^- anion have been described, but with certain drawbacks such as their volatility, their tedious and expensive synthesis and the use of toxic reagents [55-65]. Recently, we reported the preparation of a stable solution of the CF_3O^- anion (**DDPyOCF$_3$**) from the cheap and commercially available 2,4-dinitro(trifluoromethoxy)benzene (**DNTFB**) [66,67]. This **DDPyOCF$_3$** solution has shown a good reactivity to obtain various fluorinated compounds and especially trifluoromethoxylated molecules [68-71].

As another chapter of this research program, we propose here an easy and complementary access to CF_3O-substituted alkyl compounds from alkenes and **DDPyOCF$_3$**, more precisely to α-trifluoromethoxylated, β-phenylselenylated compounds.

Results and Discussion

The electrophilic addition of phenylselenyl halides to alkenes to form a selenonium intermediate that can be intercepted by an external nucleophile is a well-known method to obtain 1,2-disubstituted compounds [72-74]. Therefore, the reaction of alkenes with electrophilic sources of phenylselenyl in presence of **DDPyOCF$_3$** as a nucleophilic source of the CF_3O group was studied (Table 1).

First, we started from the optimal conditions previously established for the trifluoromethoxylation by nucleophilic substitution, using an excess of **DNTFB** as a reservoir of CF_3O^- [68]. Thus, by adding cyclohexene (**1a**) to the preformed mixture of

Table 1: Reaction of **1a** with PhSeX and **DDPyOCF$_3$**.[a]

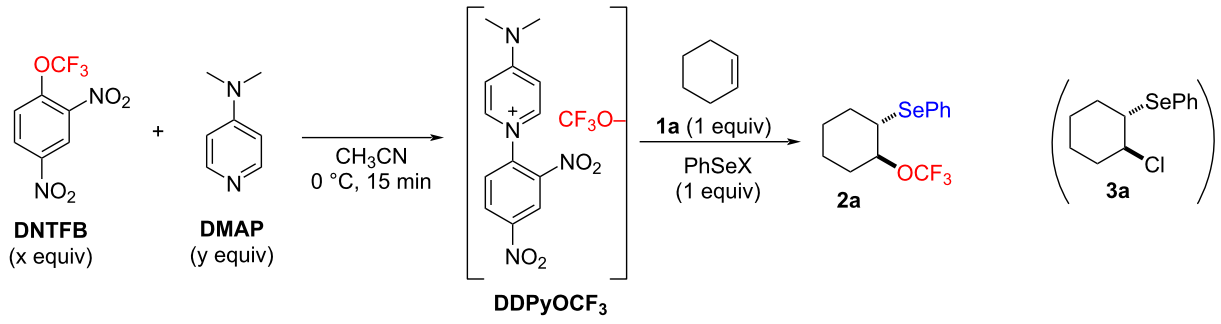

Entry	**DNTFB** (equiv)	**DMAP** (equiv)	PhSeX	Method	**2a** (%)
1	2	1	PhSeCl	**1a** then PhSeCl; 20 °C, 24 h	12
2	3	2	PhSeCl	**1a** then PhSeCl; 20 °C, 24 h	30
3	4	3	PhSeCl	**1a** then PhSeCl; 20 °C, 24 h	32
4	3	2	PhSeCl	**1a** then PhSeCl; 0 °C, 24 h	30
5	3	2	PhSeCl	1) PhSeCl, 15 min, 0 °C 2) **1a**; 20 °C, 24 h	44
6	3	2	PhSeBr	1) PhSeBr, 15 min, 0 °C 2) **1a**; 20 °C, 24 h	93
7	2	2	PhSeBr	1) PhSeBr, 15 min, 0 °C 2) **1a**; 20 °C, 24 h	85
8	2	2	PhSeBr	1) PhSeBr, 15 min, 0 °C 2) **1a**; 20 °C, 2.5 h	88

[a]Yields determined by ^{19}F NMR spectroscopy with $PhCF_3$ as internal standard.

DNTFB (2 equiv) and DMAP (1 equiv), followed by the addition of PhSeCl, only a low yield of the expected α-trifluoromethoxylated,β-phenylselenylated compound **2a** was observed (Table 1, entry 1). By increasing the amount of **DNTFB** and DMAP, the yield was doubled but remained low (entry 2 in Table 1) and did not evolve with a higher excess of reagents (entry 3). A reaction at lower temperature to possibly slow down the degradation of the CF_3O^- anion did not improve the results (Table 1, entry 4). A better yield was obtained by adding first the phenylselenyl chloride and stirring the mixture for 15 min at 0 °C before adding **1a** (Table 1, entry 5). During all these reactions the formation of compound **3a** was observed as by-product. This compound results from the competitive opening of the transient episelenonium by the more nucleophilic chloride anion competing with the less nucleophilic CF_3O^- anion.

To avoid this side reaction, the phenylselenyl chloride was replaced by phenylselenyl bromide, assuming that the bromide anion released is less nucleophilic than chloride in an aprotic solvent such as acetonitrile. Gratifyingly, an excellent yield was obtained (Table 1, entry 6) without detection of the brominated by-product. To facilitate purification, the amount of **DNTFB** was reduced to 2 equiv without significantly changing the result (Table 1, entry 7). Finally, the reaction time was reduced from 24 h to 2.5 h without affecting the yield (Table 1, entry 8).

In order to better understand the mechanism of the reaction, an NMR study of the premixing of **DDPyOCF$_3$** with PhSeBr was performed. The disappearance of the broad signal of CF_3O^- and the appearance of a new broad signal in the upper field were observed (Scheme 1). This suggests the formation of the highly reactive CF_3OSePh species, which cannot be isolated. Furthermore, since only the *trans* stereomer **2a** was observed, the transient formation of an episelenonium can be reasonably assumed. Consequently, the mechanism described in Scheme 1 can be proposed.

Under optimal conditions (Table 1, entry 8), various alkenes were functionalized (Scheme 2).

In general, the reaction gave good yields for both cyclic (**2a**–**d**, **2j**) and aliphatic alkenes (**2e**–**2i**, **2k**, **l**). Similar results were observed regardless of the position of the double bond in the molecule. Notably, a longer reaction time was required for less reactive or more hindered substrates. The reaction was stereoselective as only the *anti* products were obtained. A good regioselectivity was generally observed, as at least 80% of the main regioisomer were usually obtained when the substituents at the double bond differed significantly. When the substituent hindrance was less pronounced, the ratio was less significant (**2f**, **2j**). Interestingly, a reverse regioselectivity was observed depending on the starting alkenes. For the terminal alkenes, the Markovnikov product (i.e. with the CF_3O in the "internal" position) was predominant, whereas for the allylic alcohol derivatives, the anti-Markovnikov addition (i.e. with the CF_3O in the "terminal" position) was predominant (**2e** vs **2g** and **2h** vs **2i**). This could be rationalized by the electronic effect of the oxygen atom which disfavors the episelenonium opening with the CF_3O^- anion in the closest position to the oxygen atom. It is noteworthy that the regioisomeric ratio of terminal alkenes (**2e**, **2i**) evolved with the reaction time. The amount of the kinetic terminal regioisomer (anti-Markovnikov – **2e'**, **2i'**) decreases with time in favor of the thermodynamic Markovnikov regio-

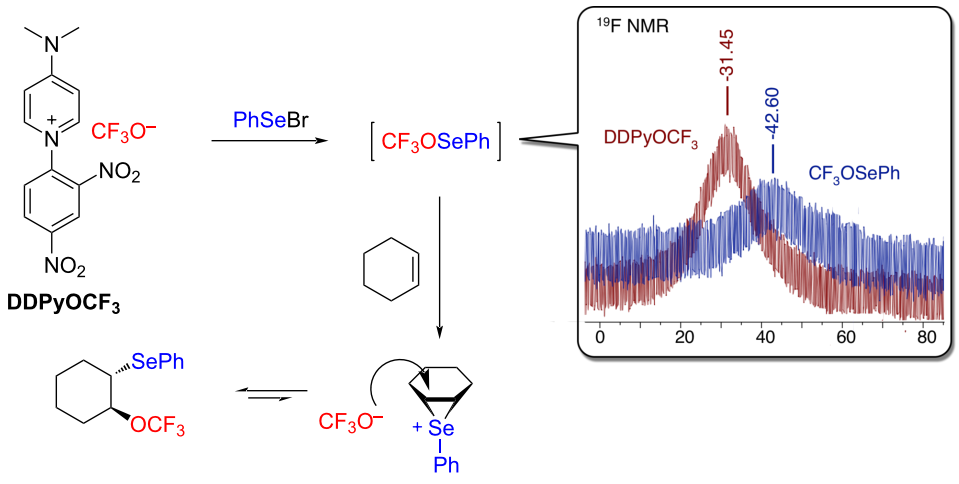

Scheme 1: Proposed mechanism of the reaction and ^{19}F NMR of the **DDPYOCF$_3$**/PhSeBr mixture.

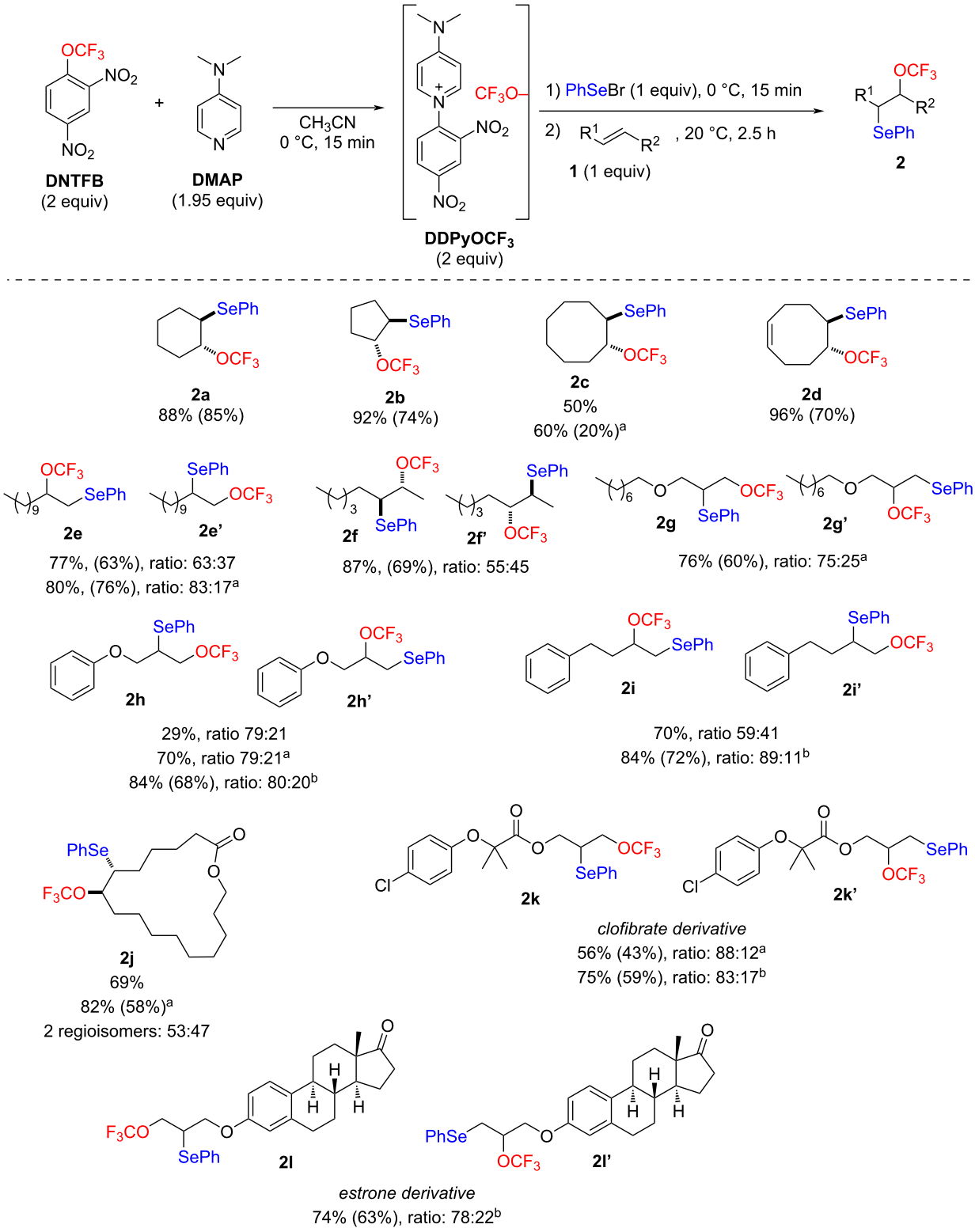

Scheme 2: Phenylseleno trifluoromethoxylation of various alkenes. Yields determined by ^{19}F NMR spectroscopy with $PhCF_3$ as internal standard (in parentheses isolated yields). [a]24 h. [b]48 h.

isomer (**2e**, **2i**). This phenomenon cannot occur for products **2g** and **2h** because the kinetic and thermodynamic products are the same. This observation confirms the existence of an equilibrium between the episelenonium and the final products **2** (Scheme 1). It should be noted that the reaction with styrene gave low yields and the resulting products appeared very unstable. Finally, the tri-substituted alkene 1-methylcyclohexene did not give the expected products.

Finally, some more elaborated molecules such as the macrolactone **2j**, the clofibrate derivative **2k**, and the estrone derivative **2l** were also successfully bis-functionalized.

Some products appeared to be sensitive during purification by chromatography on silica gel. Suspecting acid sensitivity, compound **2a** was treated with trifluoroacetic acid to confirm this hypothesis (Scheme 3). The product resulting from the substitution of the CF_3O group by the trifluoroacetoxy group was then observed. The activation of a fluorine atom from the CF_3O group by H^+ could be envisaged, which would then trigger the selenium attack to release difluorophosgene and HF, thus generating an episelenonium, which would finally be reopened by trifluoroacetate (Scheme 3).

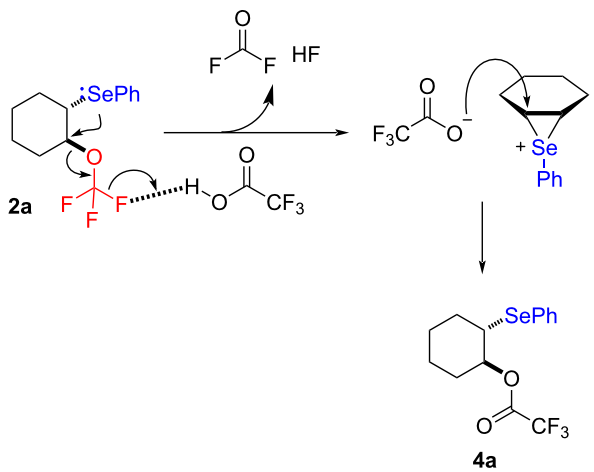

Scheme 3: Degradation of **2a** under acidic conditions.

Although the selenylated compounds **2** are of interest, the presence of the PhSe moiety allows other transformations to be considered. First, the oxidative elimination of the selenyl moiety to generate a double bond was first studied. However, regardless of the oxidative conditions used (mCPBA [75], H_2O_2 [75], selectfluor®/H_2O [76], SO_2Cl_2/$NaHCO_3$ (aq) [77,78]), in most cases a complex mixture was observed and no corresponding vinylic compound was detected by NMR.

The phenylselenyl moiety could also undergo radical reduction to produce trifluoromethoxylated molecules [79]. Using tris(trimethylsilyl)silane in the presence of AIBN [80], some compounds were successfully reduced to give the corresponding trifluoromethoxylated products with good yields (Scheme 4). This approach could be a complementary method to obtain trifluoromethoxylated compounds that are difficult to synthesize by nucleophilic substitution, such as products **5a** and **5b** [68].

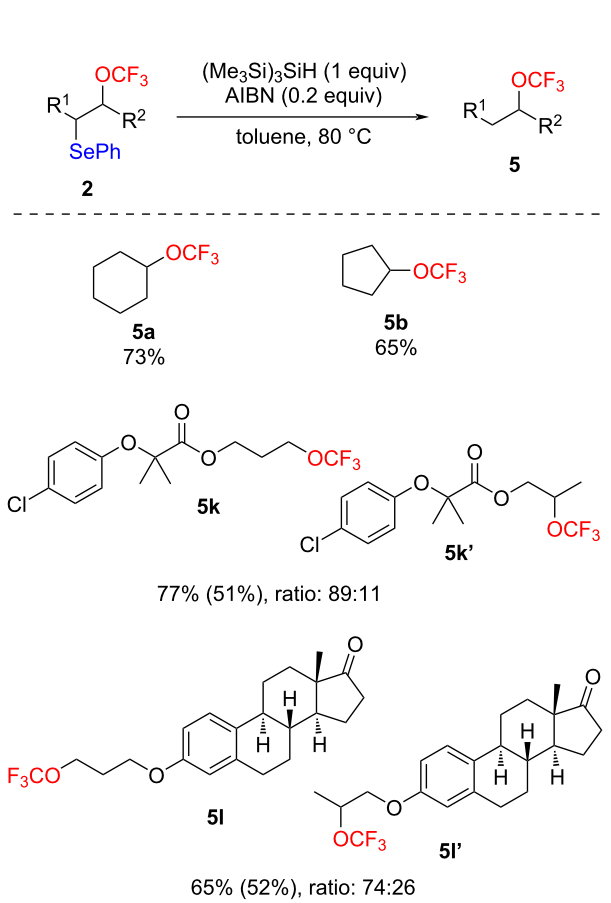

Scheme 4: Radical deselenylation of **2**. Yields determined by ^{19}F NMR spectroscopy with $PhCF_3$ as internal standard (in parentheses isolated yields).

Conclusion

In this work, an efficient phenylseleno trifluoromethoxylation of alkenes has been developed to readily obtain β-selenylated trifluoromethoxylated compounds. These compounds can also undergo radical deselenylation to provide trifluoromethoxylated molecules that can be difficult to access by nucleophilic substitution. These results contribute to the further valorization of the **DDPyOCF$_3$** salt (arising from **DNTFB**/DMAP) as an efficient tool in organic fluorine chemistry.

Experimental

Typical procedure: Synthesis of **2**. In a 10 mL vial, **DNTFB** (160 µL, 1 mmol, 2 equiv) is added in one portion to a stirred solution of **DMAP** (119 mg, 0.975 mmol, 1.95 equiv) in anhydrous MeCN (1.5 mL). The vial is closed and the reaction mixture is stirred in an ice bath for 15 minutes (the reaction rapidly turns orange after the addition of **DNTFB** and quickly turns yellow). Then, the tube is opened and PhSeBr (118 mg, 0.5 mmol, 1 equiv) is added in one portion. The resulting reaction mixture is stirred in the same ice bath for 15 minutes. Then, the tube is opened and the alkene (**1**, 0.5 mmol, 1 equiv) is added. The reaction is stirred at room temperature for 2.5 h (unless otherwise stated). Note that a yellowish precipitate is formed during the reaction for high yielding substrates. The reaction is monitored by ^{19}F NMR ($PhCF_3$ as internal standard). At the end of the reaction, the content of the vial is transferred to a separatory funnel and 10 mL of water are added. The aqueous layer is extracted three times with 10 mL of diethyl ether. The organic layers are combined and washed with 10 mL of water. The organic layer is dried with $MgSO_4$, filtered, and concentrated under vacuum. Compounds **2** are obtained after purification by chromatography.

Supporting Information

Supporting Information File 1

Additional experimental and analytical data and NMR spectra.
[https://www.beilstein-journals.org/bjoc/content/supplementary/1860-5397-20-207-S1.pdf]

Acknowledgements

The NMR Center and the Mass Spectrometry Center are acknowledged for their analysis.

Funding

The authors are grateful to the French National Research Agency (ANR; grant no. 20-CE07-0004-02, Ap-PET-I). The CNRS, the French Ministry of Education and Research and CPE Lyon are thanked for funding. The French Fluorine Network (GIS-FLUOR) is also acknowledged for its support.

ORCID® iDs

Clément Delobel - https://orcid.org/0009-0007-8447-1748
Armen Panossian - https://orcid.org/0000-0003-2317-1200
Gilles Hanquet - https://orcid.org/0000-0001-8829-1225
Frédéric R. Leroux - https://orcid.org/0000-0001-8900-5753
Fabien Toulgoat - https://orcid.org/0000-0001-7339-4985
Thierry Billard - https://orcid.org/0000-0002-2937-9523

Data Availability Statement

The data that supports the findings of this study is available from the corresponding author upon reasonable request.

References

1. Smart, B. E. *J. Fluorine Chem.* **2001,** *109,* 3–11. doi:10.1016/s0022-1139(01)00375-x
2. Kirsch, P. *Modern Fluoroorganic Chemistry;* Wiley-VCH: Weinheim, 2013. doi:10.1002/9783527651351
3. Szabó, K. J.; Selander, N., Eds. *Organofluorine Chemistry: Synthesis, Modeling, and Applications;* Wiley: Weinheim, Germany, 2021. doi:10.1002/9783527825158
4. Dolui, S.; Kumar, D.; Banerjee, S.; Ameduri, B. *Acc. Mater. Res.* **2021,** *2,* 242–251. doi:10.1021/accountsmr.1c00015
5. Wang, Y.; Yang, X.; Meng, Y.; Wen, Z.; Han, R.; Hu, X.; Sun, B.; Kang, F.; Li, B.; Zhou, D.; Wang, C.; Wang, G. *Chem. Rev.* **2024,** *124,* 3494–3589. doi:10.1021/acs.chemrev.3c00826
6. Meanwell, N. A. *J. Med. Chem.* **2018,** *61,* 5822–5880. doi:10.1021/acs.jmedchem.7b01788
7. Inoue, M.; Sumii, Y.; Shibata, N. *ACS Omega* **2020,** *5,* 10633–10640. doi:10.1021/acsomega.0c00830
8. Zhang, C.; Yan, K.; Fu, C.; Peng, H.; Hawker, C. J.; Whittaker, A. K. *Chem. Rev.* **2022,** *122,* 167–208. doi:10.1021/acs.chemrev.1c00632
9. Sheikhi, N.; Bahraminejad, M.; Saeedi, M.; Mirfazli, S. S. *Eur. J. Med. Chem.* **2023,** *260,* 115758. doi:10.1016/j.ejmech.2023.115758
10. Ogawa, Y.; Tokunaga, E.; Kobayashi, O.; Hirai, K.; Shibata, N. *iScience* **2020,** *23,* 101467. doi:10.1016/j.isci.2020.101467
11. Jeschke, P. *Eur. J. Org. Chem.* **2022,** e202101513. doi:10.1002/ejoc.202101513
12. Ma, J. A.; Cahard, D., Eds. *Emerging Fluorinated Motifs: Synthesis, Properties and Applications;* Wiley: Weinheim, Germany, 2020. doi:10.1002/9783527824342
13. Huheey, J. E. *J. Phys. Chem.* **1965,** *69,* 3284–3291. doi:10.1021/j100894a011
14. Hansch, C.; Leo, A.; Taft, R. W. *Chem. Rev.* **1991,** *91,* 165–195. doi:10.1021/cr00002a004
15. Leo, A.; Hansch, C.; Elkins, D. *Chem. Rev.* **1971,** *71,* 525–616. doi:10.1021/cr60274a001
16. Hansch, C.; Leo, A.; Unger, S. H.; Kim, K. H.; Nikaitani, D.; Lien, E. J. *J. Med. Chem.* **1973,** *16,* 1207–1216. doi:10.1021/jm00269a003
17. Taft, R. W.; Price, E.; Fox, I. R.; Lewis, I. C.; Andersen, K. K.; Davis, G. T. *J. Am. Chem. Soc.* **1963,** *85,* 3146–3156. doi:10.1021/ja00903a022
18. Taft, R. W.; Price, E.; Fox, I. R.; Lewis, I. C.; Andersen, K. K.; Davis, G. T. *J. Am. Chem. Soc.* **1963,** *85,* 709–724. doi:10.1021/ja00889a015
19. Shishkov, I. F.; Khristenko, L. V.; Vilkov, L. V.; Oberhammer, H. *J. Phys. Chem. A* **2004,** *108,* 4966–4970. doi:10.1021/jp0492671
20. Manteau, B.; Genix, P.; Brelot, L.; Vors, J.-P.; Pazenok, S.; Giornal, F.; Leuenberger, C.; Leroux, F. R. *Eur. J. Org. Chem.* **2010,** 6043–6066. doi:10.1002/ejoc.201000958
21. Kang, L.; Novick, S. E.; Gou, Q.; Spada, L.; Vallejo-López, M.; Caminati, W. *J. Mol. Spectrosc.* **2014,** *297,* 32–34. doi:10.1016/j.jms.2014.01.011
22. Liu, J.; Lin, W.; Sorochinsky, A. E.; Butler, G.; Landa, A.; Han, J.; Soloshonok, V. A. *J. Fluorine Chem.* **2022,** *257-258,* 109978. doi:10.1016/j.jfluchem.2022.109978

23. Bensimon, G.; Lacomblez, L.; Meininger, V. *N. Engl. J. Med.* **1994,** *330,* 585–591. doi:10.1056/nejm199403033300901
24. Fang, T.; Al Khleifat, A.; Meurgey, J.-H.; Jones, A.; Leigh, P. N.; Bensimon, G.; Al-Chalabi, A. *Lancet Neurol.* **2018,** *17,* 416–422. doi:10.1016/s1474-4422(18)30054-1
25. Stover, C. K.; Warrener, P.; VanDevanter, D. R.; Sherman, D. R.; Arain, T. M.; Langhorne, M. H.; Anderson, S. W.; Towell, J. A.; Yuan, Y.; McMurray, D. N.; Kreiswirth, B. N.; Barry, C. E.; Baker, W. R. *Nature* **2000,** *405,* 962–966. doi:10.1038/35016103
26. Conradie, F.; Diacon, A. H.; Ngubane, N.; Howell, P.; Everitt, D.; Crook, A. M.; Mendel, C. M.; Egizi, E.; Moreira, J.; Timm, J.; McHugh, T. D.; Wills, G. H.; Bateson, A.; Hunt, R.; Van Niekerk, C.; Li, M.; Olugbosi, M.; Spigelman, M. *N. Engl. J. Med.* **2020,** *382,* 893–902. doi:10.1056/nejmoa1901814
27. Buonamici, S.; Williams, J.; Morrissey, M.; Wang, A.; Guo, R.; Vattay, A.; Hsiao, K.; Yuan, J.; Green, J.; Ospina, B.; Yu, Q.; Ostrom, L.; Fordjour, P.; Anderson, D. L.; Monahan, J. E.; Kelleher, J. F.; Peukert, S.; Pan, S.; Wu, X.; Maira, S.-M.; García-Echeverría, C.; Briggs, K. J.; Watkins, D. N.; Yao, Y.-m.; Lengauer, C.; Warmuth, M.; Sellers, W. R.; Dorsch, M. *Sci. Transl. Med.* **2010,** *2,* 51r. doi:10.1126/scitranslmed.3001599
28. Pan, S.; Wu, X.; Jiang, J.; Gao, W.; Wan, Y.; Cheng, D.; Han, D.; Liu, J.; Englund, N. P.; Wang, Y.; Peukert, S.; Miller-Moslin, K.; Yuan, J.; Guo, R.; Matsumoto, M.; Vattay, A.; Jiang, Y.; Tsao, J.; Sun, F.; Pferdekamper, A. C.; Dodd, S.; Tuntland, T.; Maniara, W.; Kelleher, J. F., III; Yao, Y.-m.; Warmuth, M.; Williams, J.; Dorsch, M. *ACS Med. Chem. Lett.* **2010,** *1,* 130–134. doi:10.1021/ml1000307
29. Migden, M. R.; Guminski, A.; Gutzmer, R.; Dirix, L.; Lewis, K. D.; Combemale, P.; Herd, R. M.; Kudchadkar, R.; Trefzer, U.; Gogov, S.; Pallaud, C.; Yi, T.; Mone, M.; Kaatz, M.; Loquai, C.; Stratigos, A. J.; Schulze, H.-J.; Plummer, R.; Chang, A. L. S.; Cornélis, F.; Lear, J. T.; Sellami, D.; Dummer, R. *Lancet Oncol.* **2015,** *16,* 716–728. doi:10.1016/s1470-2045(15)70100-2
30. European Food Safety Authority. *EFSA Supporting Publ.* **2017,** *14,* e15121E. doi:10.2903/sp.efsa.2017.e15121
31. EFSA Panel on Dietetic Products, Nutrition and Allergies. *EFSA J.* **2014,** *12,* 3846. doi:10.2903/j.efsa.2014.3846
32. Hoover, G. C.; Seferos, D. S. *Chem. Sci.* **2019,** *10,* 9182–9188. doi:10.1039/c9sc04279b
33. Fan, B.; Lin, F.; Wu, X.; Zhu, Z.; Jen, A. K.-Y. *Acc. Chem. Res.* **2021,** *54,* 3906–3916. doi:10.1021/acs.accounts.1c00443
34. Rayman, M. P. *Lancet* **2000,** *356,* 233–241. doi:10.1016/s0140-6736(00)02490-9
35. Brown, K. M.; Arthur, J. R. *Public Health Nutr.* **2001,** *4,* 593–599. doi:10.1079/phn2001143
36. Singh, N.; Halliday, A. C.; Thomas, J. M.; Kuznetsova, O. V.; Baldwin, R.; Woon, E. C. Y.; Aley, P. K.; Antoniadou, I.; Sharp, T.; Vasudevan, S. R.; Churchill, G. C. *Nat. Commun.* **2013,** *4,* 1332. doi:10.1038/ncomms2320
37. Mousa, R.; Notis Dardashti, R.; Metanis, N. *Angew. Chem., Int. Ed.* **2017,** *56,* 15818–15827. doi:10.1002/anie.201706876
38. Rocha, J. B. T.; Piccoli, B. C.; Oliveira, C. S. *ARKIVOC* **2017,** No. ii, 457–491. doi:10.24820/ark.5550190.p009.784
39. Jain, V. K.; Priyadarsini, K. I., Eds. *Organoselenium Compounds in Biology and Medicine: Synthesis, Biological and Therapeutic Treatments;* Royal Society of Chemistry: Croydon, UK, 2017. doi:10.1039/9781788011907
40. Chen, Z.; Lai, H.; Hou, L.; Chen, T. *Chem. Commun.* **2020,** *56,* 179–196. doi:10.1039/c9cc07683b
41. Chuai, H.; Zhang, S.-Q.; Bai, H.; Li, J.; Wang, Y.; Sun, J.; Wen, E.; Zhang, J.; Xin, M. *Eur. J. Med. Chem.* **2021,** *223,* 113621. doi:10.1016/j.ejmech.2021.113621
42. Morán-Serradilla, C.; Plano, D.; Sanmartín, C.; Sharma, A. K. *J. Med. Chem.* **2024,** *67,* 7759–7787. doi:10.1021/acs.jmedchem.3c02426
43. Li, Q.; Zhang, Y.; Chen, Z.; Pan, X.; Zhang, Z.; Zhu, J.; Zhu, X. *Org. Chem. Front.* **2020,** *7,* 2815–2841. doi:10.1039/d0qo00640h
44. Tang, P.; Jiang, X. Reagents for Direct Trifluoromethoxylation. In *Emerging Fluorinated Motifs;* Cahard, D.; Ma, J. A., Eds.; Wiley: Weinheim, Germany, 2020; pp 207–224. doi:10.1002/9783527824342.ch7
45. Toulgoat, F.; Liger, F.; Billard, T. Chemistry of OCF_3, SCF_3, and $SeCF_3$ Functional Groups. In *Organofluorine Chemistry: Synthesis, Modeling, and Applications;* Szabó, K.; Selander, N., Eds.; Wiley-VCH: Weinheim, Germany, 2021; pp 49–97. doi:10.1002/9783527825158.ch3
46. Hao, B.-Y.; Han, Y.-P.; Zhang, Y.; Liang, Y.-M. *Org. Biomol. Chem.* **2023,** *21,* 4926–4954. doi:10.1039/d3ob00258f
47. Jelier, B. J.; Tripet, P. F.; Pietrasiak, E.; Franzoni, I.; Jeschke, G.; Togni, A. *Angew. Chem., Int. Ed.* **2018,** *57,* 13784–13789. doi:10.1002/anie.201806296
48. Zheng, W.; Morales-Rivera, C. A.; Lee, J. W.; Liu, P.; Ngai, M.-Y. *Angew. Chem., Int. Ed.* **2018,** *57,* 9645–9649. doi:10.1002/anie.201800598
49. Zheng, W.; Lee, J. W.; Morales-Rivera, C. A.; Liu, P.; Ngai, M.-Y. *Angew. Chem., Int. Ed.* **2018,** *57,* 13795–13799. doi:10.1002/anie.201808495
50. Lee, J. W.; Lee, K. N.; Ngai, M.-Y. *Angew. Chem., Int. Ed.* **2019,** *58,* 11171–11181. doi:10.1002/anie.201902243
51. Lee, J. W.; Lim, S.; Maienshein, D. N.; Liu, P.; Ngai, M.-Y. *Angew. Chem., Int. Ed.* **2020,** *59,* 21475–21480. doi:10.1002/anie.202009490
52. Dix, S.; Golz, P.; Schmid, J. R.; Riedel, S.; Hopkinson, M. N. *Chem. – Eur. J.* **2021,** *27,* 11554–11558. doi:10.1002/chem.202101621
53. Duhail, T.; Bortolato, T.; Mateos, J.; Anselmi, E.; Jelier, B.; Togni, A.; Magnier, E.; Dagousset, G.; Dell'Amico, L. *Org. Lett.* **2021,** *23,* 7088–7093. doi:10.1021/acs.orglett.1c02494
54. Maas, L. M.; Fasting, C.; Voßnacker, P.; Limberg, N.; Golz, P.; Müller, C.; Riedel, S.; Hopkinson, M. N. *Angew. Chem., Int. Ed.* **2024,** *63,* e202317770. doi:10.1002/anie.202317770
55. Billard, T. Methanesulfonic Acid, 1,1,1-Trifluoro-, Trifluoromethyl Ester. *Encyclopedia of Reagents for Organic Synthesis;* John Wiley & Sons, Ltd, 2016. doi:10.1002/047084289x.rn01930
56. Zhou, M.; Ni, C.; Zeng, Y.; Hu, J. *J. Am. Chem. Soc.* **2018,** *140,* 6801–6805. doi:10.1021/jacs.8b04000
57. Lei, M.; Miao, H.; Wang, X.; Zhang, W.; Zhu, C.; Lu, X.; Shen, J.; Qin, Y.; Zhang, H.; Sha, S.; Zhu, Y. *Tetrahedron Lett.* **2019,** *60,* 1389–1392. doi:10.1016/j.tetlet.2019.04.033
58. Li, Y.; Yang, Y.; Xin, J.; Tang, P. *Nat. Commun.* **2020,** *11,* 755. doi:10.1038/s41467-020-14598-1
59. Newton, J. J.; Jelier, B. J.; Meanwell, M.; Martin, R. E.; Britton, R.; Friesen, C. M. *Org. Lett.* **2020,** *22,* 1785–1790. doi:10.1021/acs.orglett.0c00099
60. Turksoy, A.; Scattolin, T.; Bouayad-Gervais, S.; Schoenebeck, F. *Chem. – Eur. J.* **2020,** *26,* 2183–2186. doi:10.1002/chem.202000116
61. Jiang, X.; Tang, P. *Chin. J. Chem.* **2021,** *39,* 255–264. doi:10.1002/cjoc.202000465

62. Lu, Z.; Kumon, T.; Hammond, G. B.; Umemoto, T. *Angew. Chem., Int. Ed.* **2021,** *60,* 16171–16177. doi:10.1002/anie.202104975
63. Saiter, J.; Guérin, T.; Donnard, M.; Panossian, A.; Hanquet, G.; Leroux, F. R. *Eur. J. Org. Chem.* **2021,** 3139–3147. doi:10.1002/ejoc.202100429
64. Chen, L.-Y.; Pan, P.-F.; Lin, J.-H.; Jin, C.-M.; Xiao, J.-C. *J. Org. Chem.* **2023,** *88,* 3346–3352. doi:10.1021/acs.joc.2c03018
65. Yuan, W.-J.; Tong, C.-L.; Xu, X.-H.; Qing, F.-L. *J. Org. Chem.* **2023,** *88,* 4434–4441. doi:10.1021/acs.joc.2c03031
66. Bonnefoy, C.; Chefdeville, E.; Panosian, A.; Hanquet, G.; Leroux, F. R.; Toulgoat, F.; Billard, T. *Chem. – Eur. J.* **2021,** *27,* 15986–15991. doi:10.1002/chem.202102809
67. Duran-Camacho, G.; Ferguson, D. M.; Kampf, J. W.; Bland, D. C.; Sanford, M. S. *Org. Lett.* **2021,** *23,* 5138–5142. doi:10.1021/acs.orglett.1c01664
68. Bonnefoy, C.; Panossian, A.; Hanquet, G.; Leroux, F. R.; Toulgoat, F.; Billard, T. *Chem. – Eur. J.* **2023,** *29,* e202301513. doi:10.1002/chem.202301513
69. Bonnefoy, C.; Chefdeville, E.; Tourvieille, C.; Panossian, A.; Hanquet, G.; Leroux, F.; Toulgoat, F.; Billard, T. *Chem. – Eur. J.* **2022,** *28,* e202201589. doi:10.1002/chem.202201589
70. Bonnefoy, C.; Gallego, A.; Delobel, C.; Raynal, B.; Decourt, M.; Chefdeville, E.; Hanquet, G.; Panossian, A.; Leroux, F. R.; Toulgoat, F.; Billard, T. *Eur. J. Org. Chem.* **2024,** *27,* e202400142. doi:10.1002/ejoc.202400142
71. Wisson, L.; Hanquet, G.; Toulgoat, F.; Billard, T.; Panossian, A.; Leroux, F. R. *Eur. J. Org. Chem.* **2024,** *27,* e202400388. doi:10.1002/ejoc.202400388
72. Paulmier, C. *Selenium Reagents & Intermediates in Organic Synthesis;* Pergamon Press: Oxford, 1986.
73. Krief, A. Selenium. In *Comprehensive Organometallic Chemistry II;* Abel, E. W.; Stone, F. G. A.; Wilkinson, G., Eds.; Elsevier: Oxford, 1995; pp 515–569. doi:10.1016/b978-008046519-7.00104-0
74. Preedy, V. R., Ed. *Selenium: Chemistry, Analysis, Function and Effects;* The Royal Society of Chemistry: Cambridge, 2015. doi:10.1039/9781782622215
75. Billard, T.; Langlois, B. R. *Tetrahedron* **1999,** *55,* 8065–8074. doi:10.1016/s0040-4020(99)00421-4
76. Guo, X.; Sun, X.; Jiang, M.; Zhao, Y. *Synthesis* **2022,** *54,* 1996–2004. doi:10.1055/a-1701-6700
77. Engman, L. *J. Org. Chem.* **1987,** *52,* 4086–4094. doi:10.1021/jo00227a026
78. Engman, L. *Tetrahedron Lett.* **1987,** *28,* 1463–1466. doi:10.1016/s0040-4039(00)95954-9
79. Renaud, P. Radical Reactions Using Selenium Precursors. In *Organoselenium Chemistry: Modern Developments in Organic Synthesis;* Wirth, T., Ed.; Springer: Berlin, Heidelberg, 2000; pp 81–112. doi:10.1007/3-540-48171-0_4
80. Ballestri, M.; Chatgilialoglu, C.; Clark, K. B.; Griller, D.; Giese, B.; Kopping, B. *J. Org. Chem.* **1991,** *56,* 678–683. doi:10.1021/jo00002a035

License and Terms

BEILSTEIN JOURNAL OF ORGANIC CHEMISTRY

Synthesis and conformational analysis of pyran inter-halide analogues of D-talose

Olivier Lessard, Mathilde Grosset-Magagne, Paul A. Johnson and Denis Giguère*

Full Research Paper

Open Access

Address:
Département de Chimie, 1045 av. De la Médecine, Université Laval, Québec City, Qc, G1V 0A6, PROTEO, Canada

Email:
Denis Giguère* - denis.giguere@chm.ulaval.ca

* Corresponding author

Keywords:
organofluorine; pyran inter-halide; solid-state conformation; solution-state conformation

Beilstein J. Org. Chem. **2024,** *20,* 2442–2454.
https://doi.org/10.3762/bjoc.20.208

Received: 05 June 2024
Accepted: 11 September 2024
Published: 27 September 2024

This article is part of the thematic issue "Organofluorine chemistry VI".

Guest Editor: D. O'Hagan

Abstract

In this work, we describe the synthesis of halogenated pyran analogues of D-talose using a halo-divergent strategy from known 1,6-anhydro-2,3-dideoxy-2,3-difluoro-β-D-mannopyranose. In solution and in the solid-state, all analogues adopt standard $^4C_1$-like conformations despite 1,3-diaxial repulsion between the F2 and the C4 halogen. Moreover, the solid-state conformational analysis of halogenated pyrans reveals deviation in the intra-annular torsion angles arising from repulsion between the axial fluorine at C2 and the axial halogen at C4, which increases with the size of the halogen at C4 (F < Cl < Br < I). Crystal packing arrangements of pyran inter-halides show hydrogen bond acceptor and nonbonding interactions for the halogen at C4. Finally, density functional theory (DFT) calculations corroborate the preference of talose analogues to adopt a $^4C_1$-like conformation and a natural bonding orbital (NBO) analysis demonstrates the effects of hyperconjugation from C–F antibonding orbitals.

Introduction

Polyfluorinated pyran analogues of carbohydrates have attracted attention over the years. This class of glycomimetics has great biological potential with useful applications [1-7]. What about other halogens? Pyran inter-halide analogues of carbohydrates were rarely investigated as new tools in glycobiology [8]. This is surprising since the incorporation of halogens can improve cellular uptakes and enhance membrane binding and permeation [9-11]. In addition, halogen bonding is an important interaction in biological systems [12-17] and the beneficial effect of the chloro substituent has been reviewed recently [18].

As a result, there is a lack of efficient synthetic strategies to access multivicinal inter-halide stereocenters (i.e., contiguous chiral halides: F, Cl, Br, I) [19]. Only a handful of natural product syntheses have been reported [20,21], despite the promising biological activity of these unique inter-halides [22]. For our

part, we recently reported the synthesis of contiguous inter-halide-bearing stereocenters using a Chiron approach from levoglucosan **1** (Figure 1a) [23]. Allopyranose inter-halides **4** incorporating the 2,3-*cis*, 3,4-*cis* relationship for the halogens were prepared via intermediates **2** and **3** from levoglucosan (**1**). Compounds **4** were the starting point to complex 2,3,4-trihalohexanetriols and 2,3,4,5-tetrahalohexanediols. Conformational analysis and lipophilicities of the latter compounds were determined and trihalogenated alkanes were incorporated into piperidines of pitolisant [23]. This work was an extension of our synthetic routes to multivicinal organofluorines to unveil some of their unique properties [24-30], such as the solution-state conformation of diastereomeric polyfluorohexitols [31].

Herein, we report the synthesis of pyran inter-halide analogues of D-talopyranose **6**, integrating also the 2,3-*cis*, 3,4-*cis* relationship for the halogens, from known intermediate **5** (Figure 1b) [24]. The solution and the solid-state conformational analysis were supplemented with DFT calculations to understand key conformational drivers. This study adds more data to the field of nuclear magnetic resonance (NMR) spectroscopy of polyhalogenated molecules. It should be noted that the NMR predictions of such compounds remain very challenging [32].

Results and Discussion

Our recent discovery that the nature of halogen atoms can have a large impact on conformation and lipophilicity motivated us to investigate novel pyran inter-halides [23]. We used a halodivergent route starting from the known 1,6-anhydro-2,3-dideoxy-2,3-difluoro-β-D-mannopyranose (**5**) readily accessible form levoglucosan (**1**, Scheme 1) [24]. Activation of the C4 hydroxy group as triflate and direct treatment with a nucleophilic halogen furnished intermediates **8–11**. The latter compounds proved to be difficult to purify, therefore we were compelled to proceed directly to the next step. Cleavage of the 1,6-anhydro bridges was achieved under acetolysis conditions providing halogenated talopyranoses **12–15** in good yield over 3 steps as α anomers.

Luckily, inter-halides **13**–**15** were crystalline, allowing the absolute configuration to be confirmed by single-crystal diffraction analysis (see below) [33]. Unfortunately, trifluorinated analogue **12** was not crystalline. Thus, we removed the acetyl protecting groups and generated the corresponding *p*-bromobenzoate derivative **17** to obtain suitable crystalline material [24,34].

In order to decipher the key physical properties of complex pyran inter-halides, we performed ^{19}F NMR analysis of halogenated talose analogues **12**–**15** (Figure 2). First, all analogues adopt standard $^{4}C_{1}$-like conformations. Comparison of the vicinal and geminal coupling constants for each organohalogen suggests that there is little change in the conformations (although there is an increasing chair distortion for larger halogens, see below). Because F3 is adjacent to the C4 halogen, ^{19}F resonance of F3 occurs at lower field than F2 for analogues **13**–**15**. There is a strong increase in chemical shift of F3 depending on the incorporated halogen on the pyran core at C4: −208.33 ppm for **12** (fluorine), −197.95 ppm for **13** (chlorine), −192.80 ppm for **14** (bromine), and −184.56 ppm for **15** (iodine). Similarly, the increase in chemical shift of F2 is smaller as exemplified with an upfield shift of −205.46 ppm for **12** to −200.55 ppm for **15**. Talopyranose analogues **12–15** incorporate a 2,3-*cis*, 3,4-*cis* relationship for the halogens. We previously prepared a small set of trihalogenated allopyranose analogues that also included the 2,3-*cis*, 3,4-*cis* relationship for

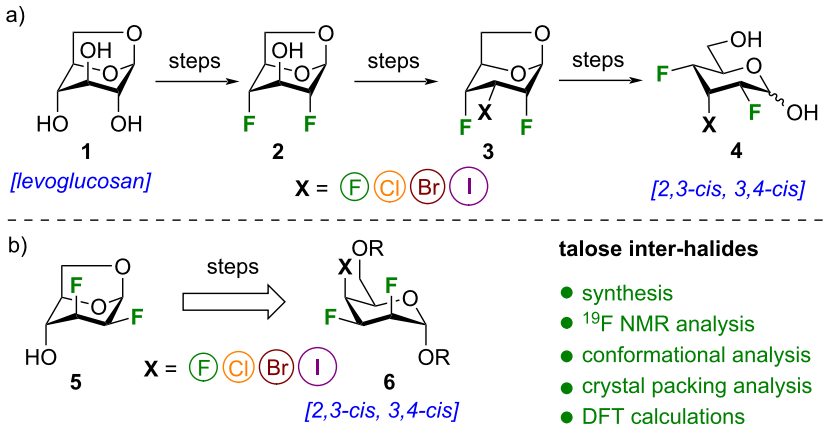

Figure 1: Synthesis of trihalogenated pyrans: a) Chiron approach to multivicinal inter-halide derived from allopyranoses; b) synthesis and conformational analysis of pyran inter-halide analogues of D-talose integrating the 2,3-*cis*, 3,4-*cis* relationship for the halogens (this work).

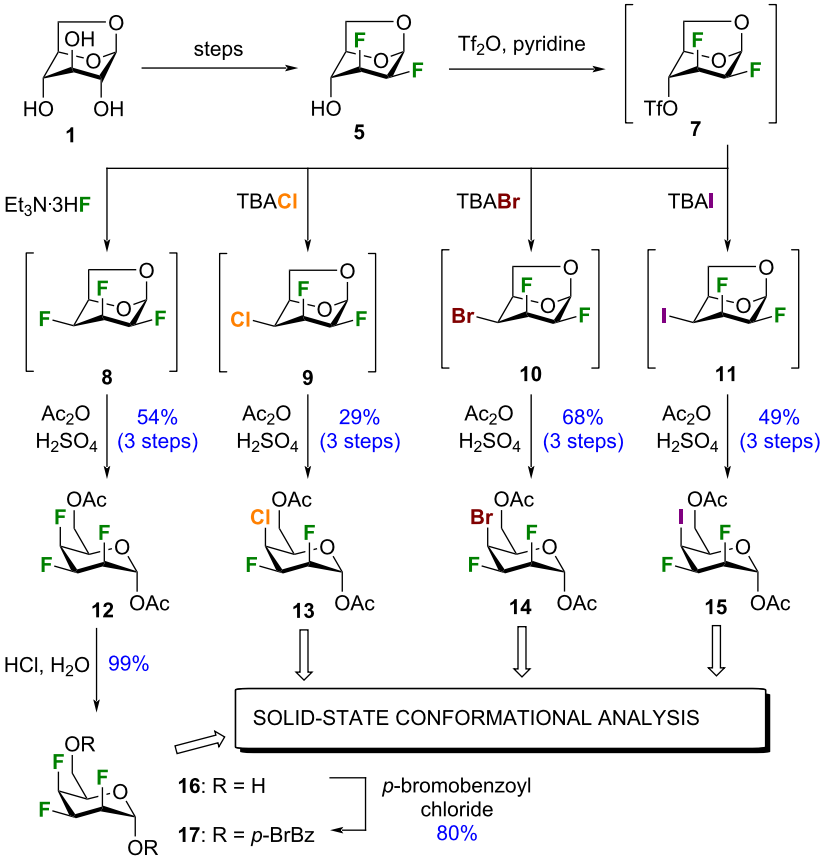

Scheme 1: Synthesis of halogenated talopyranose analogues **13–15**, and **17** that include a 2,3-*cis*, 3,4-*cis* relationship for the halogens.

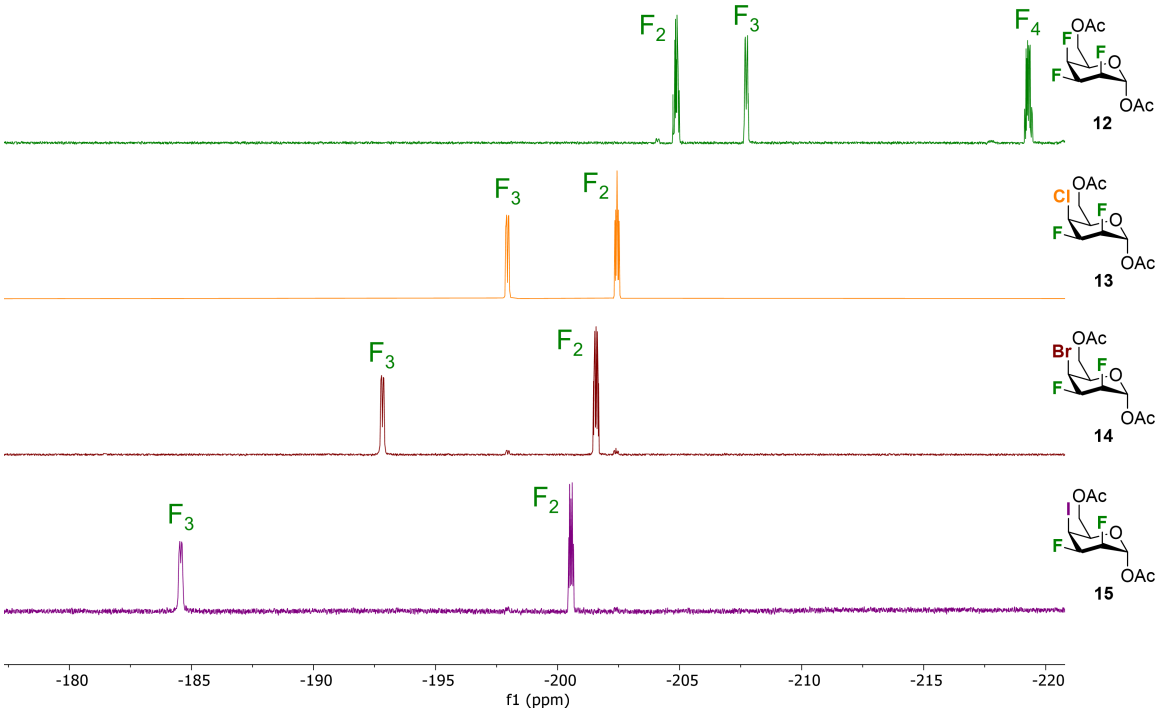

Figure 2: Direct comparison of ^{19}F resonances of halogenated talose analogues **12–15** (^{19}F NMR; 470 MHz, $CDCl_3$).

the halogens (Figure 1a) [23]. ^{19}F NMR analysis of halogenated allopyranose analogues can be found in Supporting Information File 1.

Our interest in the conformation of organohalogens motivated us to compare the solid-state conformation of halogenated pyrans **13**–**15**, and **17** [24] with α-D-talose **18** [35] (Figure 3). The crystallographic data and structural refinement details for the crystal structures can be found in Supporting Information File 1. As tosyl and benzoate groups are essential for the crystallinity of multivicinal organofluorines they influence the solid-state conformations [31,36-38]. Thus, information drawn from the crystallographic data of compound **17** might be influenced by benzoate groups. We included compound **17** in our comparative analysis in any case. All structures adopt a standard $^4C_1$-like conformation in the solid-state. This conformation occurs despite 1,3-diaxial repulsion between the F2 and the C4 halogen. The 1,3-diaxial repulsion between 2 fluorine atoms have been reported in recent years [24,39], however, the 1,3-diaxial repulsion between fluorine and other halogens is quite uncommon [40,41]. As for the C5–C6 rotamer, all analogues exhibit a *gt* conformation except for trifluorinated **17**, which possesses a *tg* conformation. An axial substituent at C4 generally leads to a *gt* conformation [42,43], with some exceptions [24]. Bond distances, bond angles, torsion angles, and key interatomic distances are listed in Tables 1–4. It is important to point out that these results compare well with previous analysis of polyfluorinated carbohydrates [44,45].

The C–C bond lengths within the pyran rings of halogenated analogues are between 1.50 and 1.54 Å, which is similar to native talose (**18**, 1.52–1.53 Å) (Table 1, entries 1–4). However, all specified bond lengths within the pyran rings are shorter for halogenated analogues compared to α-D-talose, except for the C3–C4 bond of compound **15**. This can be explained by the adjacent repulsion between CF3 with the CI4 group. Next, it has

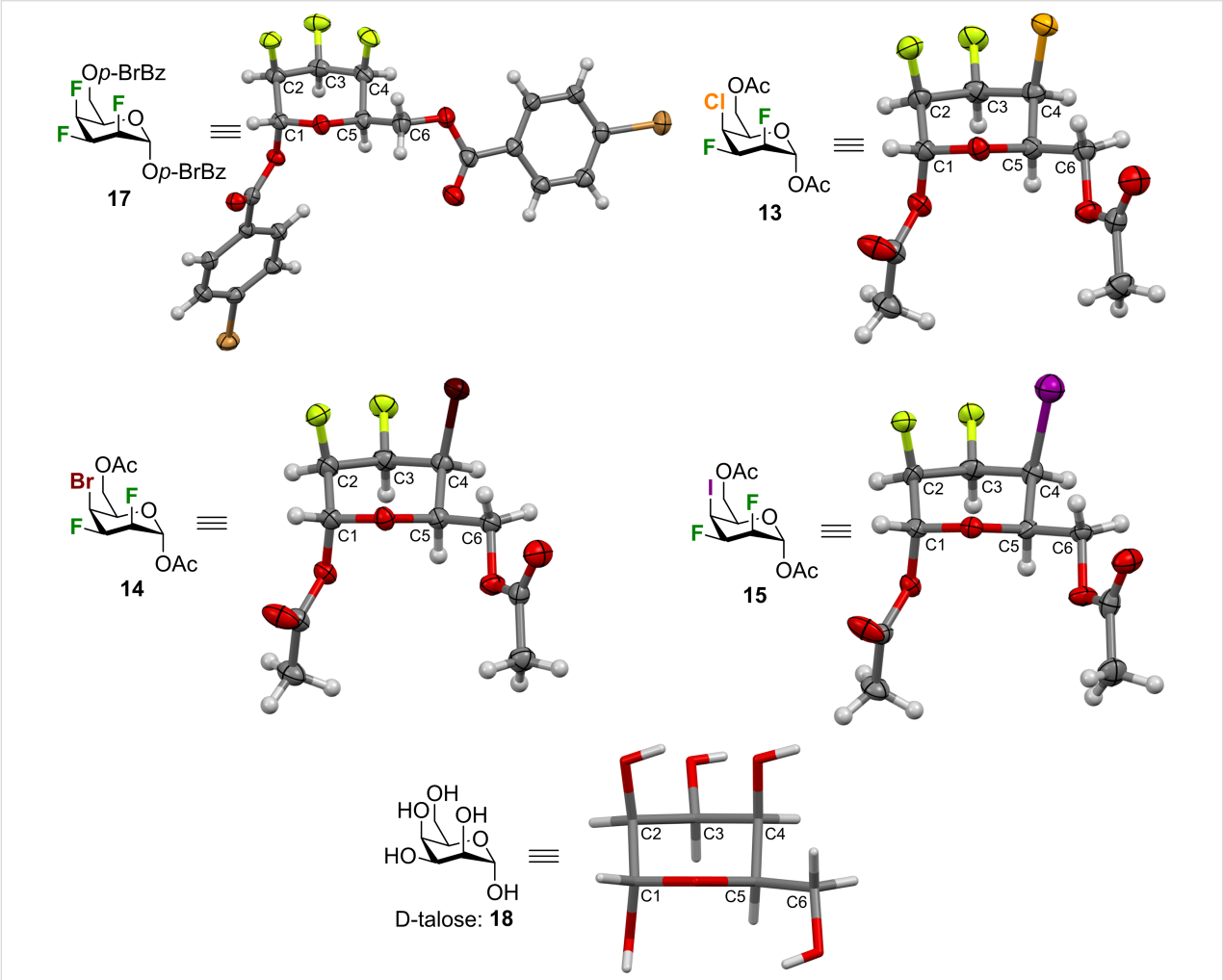

Figure 3: X-ray analysis of compound **13–15**, **17**, and α-D-talose **18**. ORTEP diagram showing 50% thermal ellipsoid probability (except for **18**): carbon (gray), oxygen (red), fluorine (green), chlorine (orange), bromine (dark red), iodine (purple), and hydrogen (white).

Table 1: Selected bond distances for compounds **13–15**, **17**, and **18**.

Entry	Bonds	Distances (Å)				
		Talose (**18**)[a]	**17**	**13**	**14**	**15**
1	C1–C2	1.5316	1.518(3)	1.526(2)	1.523(3)	1.53(1)
2	C2–C3	1.5234	1.506(3)	1.513(2)	1.508(3)	1.50(2)
3	C3–C4	1.5300	1.508(4)	1.522(2)	1.520(3)	1.54(2)
4	C4–C5	1.5325	1.524(3)	1.527(2)	1.523(3)	1.53(1)
5	C5–C6	1.5127	1.525(3)	1.507(2)	1.513(3)	1.50(1)
6	C5–O5	1.4489	1.432(3)	1.438(2)	1.435(2)	1.44(1)
7	O5–C1	1.4380	1.399(3)	1.403(2)	1.403(2)	1.40(1)
8	C1–O1	1.4028	1.442(3)	1.429(2)	1.431(2)	1.44(1)
9	O1–C(O)	na	1.361(3)	1.372(2)	1.374(3)	1.40(1)
10	C2–F2	1.4228[b]	1.393(3)	1.402(2)	1.407(2)	1.39(1)
11	C3–F3	1.4212[c]	1.397(3)	1.393(2)	1.396(2)	1.39(1)
12	C4–X4	1.4279[d]	1.395(3)	1.797(2)	1.956(2)	2.11(1)

[a]Reference [35]; [b]C2–O2; [c]C3–O3; [d]C4–O4.

been reported that the C1–O1 bond lengths are shorter than the O5–C1 for α anomers [42,46,47]. Talopyranose (**18**) follows this trend, but not the halogenated analogues (Table 1, entries 7 and 8). Also, the exocyclic C1–O1 bond lengths of compounds **13–15** and **17** are in average 0.033 Å longer than native talose (**18**). As expected, all the C–F bond lengths are shorter than the corresponding C–OH bond lengths (Table 1, entries 10–12) [48]. The C2–F2 bond lengths are in average 0.025 Å shorter than the C2–OH bond and the C3–F3 bond lengths are in average 0.027 Å shorter than the C3–OH bond. Similarly, for compound **13**–**15**, the C4–X bond lengths are longer than the C4–OH bond of native talose (1.43 Å): C4–Cl: 1.80 Å, C4–Br: 1.96 Å, and C4–I: 2.11 Å.

Table 2 shows the selected bond angles for compounds **13–15**, **17**, and **18**. All the bond angles of halogenated analogues are larger by 0.1–4.07° than talose (**18**). As such, the H2–C2–F2 bond angles are similar for compounds **13–15** and **17** (109.69–109.78°), but significantly larger than the H2–C2–O2 bond angle of talose (105.87°). Moreover, the H3–C3–F3 bond angles slightly decrease according to the nature of the atom at C4 (F: 107.97°; Cl: 107.67°; Br: 107.47°; I: 107.46°), as compared with talose (108.85°). As for the H4–C4–X4 bond angles, the angles are similar for talose and the trifluorinated analogues: 109.33° and 109.36°, respectively. However, there is a bond angle narrowing for the other analogues (Cl: 108.07°; Br: 107.94°; I: 107.78°). Finally, the angles involving the *exo*-

Table 2: Selected bond angles for compounds **13–15**, **17**, and **18**.

Entry	Bonds	Angles (°)				
		Talose (**18**)[a]	**17**	**13**	**14**	**15**
1	C1–C2–C3	109.51	110.2(2)	111.9(1)	111.9(2)	111.9(9)
2	C2–C3–C4	110.43	113.7(2)	114.0(1)	114.5(2)	114.1(9)
3	C3–C4–C5	107.80	109.9(2)	108.3(1)	108.3(2)	107.9(8)
4	C4–C5–O5	109.92	111.8(2)	111.6(1)	112.2(1)	112.0(8)
5	C5–O5–C1	113.68	114.9(2)	114.7(1)	114.7(1)	113.9(8)
6	O5–C1–C2	110.29	113.0(2)	112.2(1)	112.3(2)	112.7(9)
7	O1–C1–O5	111.87	111.1(2)	111.3(1)	110.9(2)	111.4(8)
8	O1–C1–C2	107.98	105.5(2)	106.8(1)	106.9(2)	106.6(8)
9	C1–O1–C(O)	na	116.2(2)	115.4(1)	115.3(2)	115.2(8)
10	C1–C2–F2	109.78[b]	106.9(2)	105.4(1)	105.2(1)	104.6(8)
11	C3–C2–F2	112.49[c]	110.5(2)	110.4(1)	110.5(2)	110.9(9)

Table 2: Selected bond angles for compounds **13–15**, **17**, and **18**. (continued)

12	C2–C3–F3	107.54[d]	109.3(2)	109.5(1)	109.6(1)	109.9(9)
13	C4–C3–F3	113.36[e]	109.7(2)	110.1(1)	110.0(1)	110.1(8)
14	C3–C4–X4	108.18[f]	109.7(2)	112.1(1)	112.1(1)	111.9(7)
15	C5–C4–X4	111.14[g]	109.2(2)	112.1(1)	112.5(1)	113.5(7)
16	H2–C2–F2	105.87[h]	109.75	109.69	109.72	109.78
17	H3–C3–F3	108.85[i]	107.97	107.67	107.47	107.46
18	H4–C4–X4	109.33[j]	109.36	108.07	107.94	107.78

[a]Reference [35]; [b]C1–C2–O2; [c]C3–C2–O2; [d]C2–C3–O3; [e]C4–C3–O3; [f]C3–C4–O4; [g]C5–C4–O4; [h]H2–C2–O2; [i]H3–C3–O3; [j]H4–C4–O4.

anomeric oxygen (O1–C1–O5) are similar with a difference of about 1° between the larger (compound **17**) and smaller (compound **14**) angle.

As stated above, all analogues exhibit a *gt* conformation except for compound **17**, which is a *tg* conformer. This information could also be extracted from Table 3 by looking at the O5–C5–C6–O6 torsion angles (Table 3, entry 1). Table 3 also highlights that there are significant intra-annular torsion angles for halogenated analogues. There are reductions in the C1–C2–C3–C4 torsion angles for the halogenated pyrans as compared to compound **18** (–56.58°) (Table 3, entry 4). The decrease depends on the size of the halogen at C4 (F: –49.4°; Cl: –46.9°; Br: –46.5°; I: –46°). There is also a reduction in the C2–C3–C4–C5 torsion angles of about 8.4° in average for compound **13–15** and **17** falling outside the range of an ideal pyran ring (Table 3, entry 5) [35]. However, the C4–C5–O5–C1 torsion angles are similar for all compounds except for compound **17** (Table 3, entry 7). The deviation in the intra-annular torsion angles clearly arise from repulsion of the axial fluorine at C2 and the axial halogen at C4 as exemplified with the H3–C3–C2–F2 and the X4–C4–C3–H3 torsion angles being smaller than the expected 180° (Table 3, entry 16 and 17). The 1,3-diaxial repulsion leads to a deviation from parallel alignment as shown in Table 4. The Newman projections of the halogenated analogues show deviations from parallel alignment for

Table 3: Selected torsion angles for compounds **13–15**, **17**, and **18**.

Entry	Bonds	Torsion angles (°)				
		Talose **18**[a]	**17**	**13**	**14**	**15**
1	O5–C5–C6–O6	70.35	–178.3(2)	75.4(1)	74.9(2)	75(1)
2	O5–C1–O1–C(O)	na	94.7(2)	89.0(2)	88.7(2)	88(1)
3	C2–C1–O1–C(O)	na	–142.5(2)	–148.1(1)	–148.5(2)	–148.4(9)
4	C1–C2–C3–C4	–56.58	–49.4(3)	–46.9(2)	–46.5(2)	–46(1)
5	C2–C3–C4–C5	57.88	50.1(3)	50.0(2)	49.0(2)	49(1)
6	C3–C4–C5–O5	–58.49	–51.6(3)	–55.0(2)	–53.9(2)	–55(1)
7	C4–C5–O5–C1	60.88	56.4(2)	60.5(2)	59.8(2)	61(1)
8	C5–O5–C1–C2	–58.73	–56.1(2)	–55.5(2)	–55.3(2)	–57(1)
9	O5–C1–C2–C3	55.31	51.0(3)	47.6(2)	47.6(2)	48(1)
10	O5–C1–C2–F2	–68.66[b]	–69.0(2)	–72.4(1)	–72.4(2)	–72(1)
11	C1–C2–C3–F3	179.26[c]	–172.3(2)	–170.7(1)	–170.7(1)	–170.6(8)
12	F2–C2–C3–C4	65.78[d]	68.5(3)	70.2(2)	70.4(2)	70(1)
13	F3–C3–C4–C5	178.62[e]	172.8(2)	173.5(1)	173.0(1)	173.1(8)
14	C2–C3–C4–X4	–62.40[f]	–70.0(3)	–74.2(2)	–75.6(2)	–77(1)
15	X4–C4–C5–O5	59.91[g]	68.8(2)	69.2(1)	70.5(2)	70.0(9)
16	X4–C4–C3–H3	179.05[h]	170.2	166.4	165.0	164.4
17	H3–C3–C2–F2	–175.98[i]	–171.7	–170.4	–170.3	–170.9

[a]Reference [35]; [b]O5–C1–C2–O2; [c]C1–C2–C3–O3; [d]O2–C2–C3–C4; [e]O3–C3–C4–C5; [f]C2–C3–C4–O4; [g]O4–C4–C5–O5; [h]O4–C4–C3–H3; [i]H3–C3–C2–O2.

the C2–F and C4–X substituents of 12.08° for **17**, 17.08° for **13**, 18.18° for **14**, and 18.59° for **15** (talopyranose, **18**: 5.92°). This deviation is responsible for the distance between F2 and the halogen at C4. Table 5 highlights key interatomic distances for all analogues. As such, the F2···X4 distance increases with the size of the C4 halogen (F < Cl < Br < I): 2.82 Å for **17**, 3.06 Å for **13**, 3.14 Å for **14**, and 3.23 Å for **15**. Another interesting feature can be drawn from Table 5. As such, intramolecular F2···F3, F2···X4, and F3···X4 contacts are smaller than the sum of the Van der Walls radii [49]. Taking together, all these data clearly demonstrate that the nature of one halogen can have an impact on the solid-state conformation of halogenated pyrans.

We also evaluated the Cremer–Pople ring puckering parameters (Table 6) [50]. For pyranoid rings, these parameters take the form of a spherical polar coordinate set, Q, θ, and φ, which define the point P, on a sphere of radius Q [51]. The smaller puckering amplitude (Q) values for the halogenated analogues indicate a flattened ring in comparison to the non-halogenated compound. The puckering amplitude for an ideal cyclohexane chair, with C–C bond lengths of 1.54 Å, is 0.63 Å [50]. The azimuthal angle (θ) represents the distortion of the ring. For pyranose rings, an azimuthal angle of θ = 0° represents a perfect $^4C_1$ chair, and an angle of θ = 180° is the $^1C_4$ chair. The distortion of the chair conformation increases with the size of the halogen at C4. Surprisingly, the trifluorinated analogue is less distorted than the non-halogenated talopyranose. The meridian angle (φ) indicates the nature of the distortion. The distortion of the trifluorinated analogue is in a direction somewhat between an E_5 conformation (φ ≈ 300°) and a $^OH_5$ conformation (φ ≈

Table 6: Cremer–Pople ring puckering amplitudes (Q), theta (θ) and phi (φ) parameters.

	Talose (**18**)	**17**	**13**	**14**	**15**
Q (Å)	0.588	0.514	0.521	0.514	0.523
θ (°)	2.976	1.724	6.936	6.439	7.248
φ (°)	233.600	315.204	299.454	305.438	307.711

Table 4: 1,3-Diaxial repulsion between C2–F and C4–X bonds for **13–15** and **17**.[a]

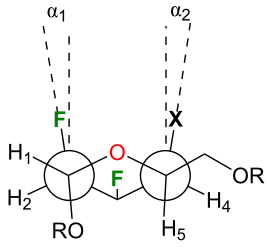

Entry	Angles (°)	**17** (X = F, R = *p*-BrBz)	**13** (X = Cl, R = Ac)	**14** (X = Br, R = Ac)	**15** (X = I, R = Ac)
1	α_1	5.99	6.77	7.05	7.06
2	α_2	6.09	10.31	11.13	11.53
3	$\alpha_1 + \alpha_2$	12.08	17.08	18.18	18.59

[a]For α-talopyranose **18**: α_1 = 5.58°, α_2 = 0.34°, and $\alpha_1 + \alpha_2$ = 5.92° (reference [35]).

Table 5: Key interatomic distances (intramolecular) for **13–15**, **17**, and **18**.

Entry	Atoms	Distances (Å)				
		Talose (**18**)[a]	**17**	**13**	**14**	**15**
1	O1···F2	3.6141[b]	3.560(2)	3.552(2)	3.557(2)	3.55(1)
2	O1···F3	4.1700[c]	4.194(2)	4.288(2)	4.285(2)	4.28(1)
3	F2···F3	2.8154[d]	2.732(3)	2.735(2)	2.741(2)	2.746(9)
4	F2···X4	2.6546[e]	2.817(2)	3.056(1)	3.143(1)	3.228(6)
5	F3···X4	2.8517[f]	2.714(2)	2.968(1)	3.052(1)	3.160(6)

[a]Reference [35]; [b]O1···O2; [c]O1···O3; [d]O2···O3; [e]O2···O4; [f]O3···O4.

330°). The other trihalogenated analogues are distorted towards an E_5 conformation (φ ≈ 300°). The distortion of the non-halogenated talopyranose is in the direction on an ^4E conformation (φ ≈ 240°).

The solid-state conformation of each of the pyran inter-halides **13–15** is unique. One would expect that compounds **13–15** would have distinct crystal packing arrangements based on the nature of the halogen. On the contrary, all analogues adopt a similar stacking pattern. Figure 4 shows the packing arrangement for compound **15** and the crystal packing of compound **13** and **14** can be found in the Supporting Information File 1. The halogens are on the same side of the pyran ring, thus increasing the overall molecular dipole moment (see Supporting Information File 1). This allows intermolecular C–X···H–C interactions responsible, in part, for the solid-state ordering [52]. Individual pyrans stack on top of one another in a manner consistent with electrostatic interactions with halogens facing H3, H4, and H5 (Figure 4a). As such, some intermolecular H···X bond distances and angles for compound **13**–**15** are listed in Table 7. Solid-state intermolecular interactions involving fluorine atoms have been well documented over the years for carbohydrate analogues [24,44,53] or other organofluorines [54]. In our case, there is a number of C–F···H–C interactions with F2 and H4 (**13**: d = 2.271 Å, **14**: d = 2.270 Å, and **15**: d = 2.356 Å) and with F3 and H4 (**13**: d = 2.867 Å, **14**: d = 2.849 Å, and **15**: d = 2.886 Å).

Does the halogen at C4 contribute to the stabilization within the crystal lattice? To answer this question, we have to look at the behavior of halogens as hydrogen bond acceptors (X···H) and nonbonding interactions (X···O/N/S). For C–X, a σ-hole arises when a valence electron is pulled into the σ-molecular orbital resulting in an electropositive crown and a flattening of the atomic radius, that accounts for the directionality of the interactions [55,56]. Thus, the halogen has an amphoteric character with an electropositive halogen bond ability along the σ-hole (C–X···O/N/S, a ≈ 180°) and an electronegative hydrogen bond acceptor perpendicular to the C–X bond (C–X···H, a ≈ 90°) [57-60]. Such halogen bonds have been detrimental in the understanding interactions of organic halogens in biological systems [61-65]. In our case, for compound **15**, I4 interacts with H4 (d = 3.521 Å, a = 93.77°) and I4 also interact with the oxygen of the carbonyl of the acetate at C6 (I4···O, d = 3.147 Å; a = 179.70°) (Figure 4b and Table 7). This result is in line with hydrogen (C–I···H) and halogen (C–I···O) interactions that show remarkable differences in term of geometrical features [66]. It is important to point out that similar interactions are also present in the packing of compound **13** (Cl4···H4 (d = 3.625 Å, a = 96.94°) and Cl4···O (d = 3.203 Å, a = 174.03°)) and compound **14** (Br4···H4 (d = 3.526 Å, a = 95.15°) and Br4···O (d = 3.143 Å, a = 177.49°)) (Table 7) (and see Supporting Information File 1). To the best of our knowledge, this is the first application of halogen bonding in the context of solid-state ordering of pyran inter-halides.

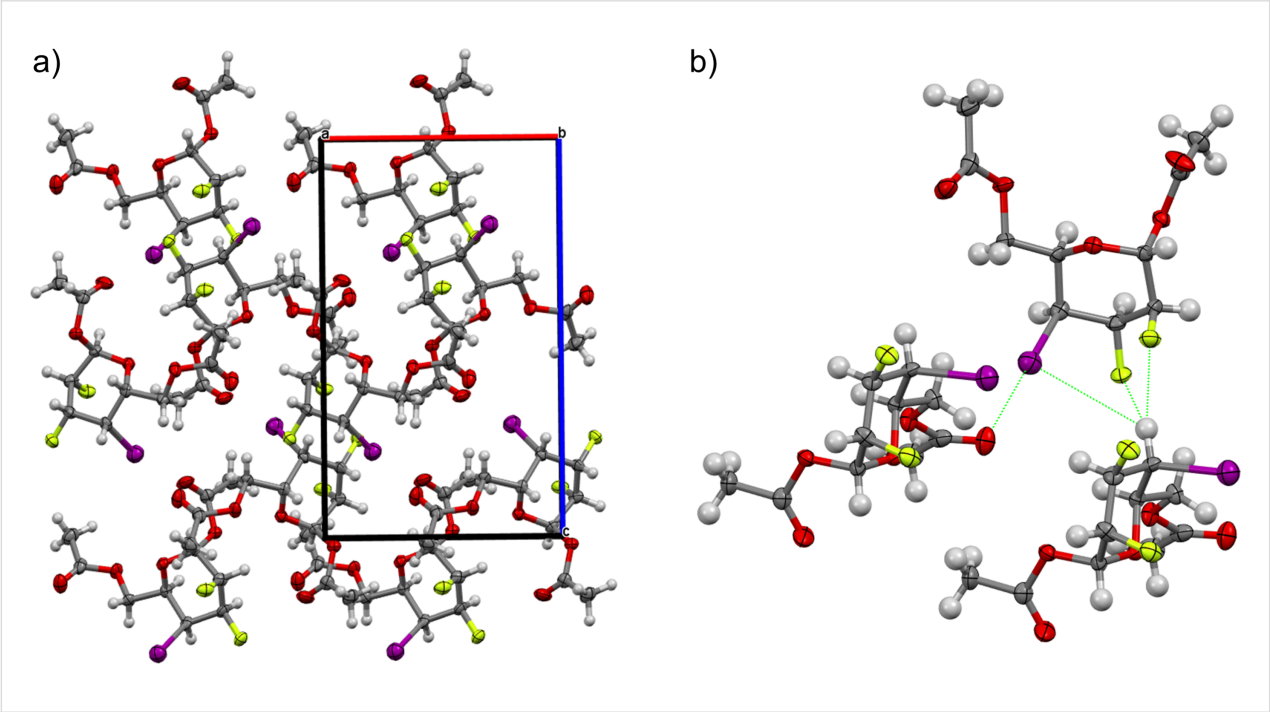

Figure 4: Packing arrangement of compound compound **15**; a) View down the *b* axis; b) proposed intermolecular interactions involving halogens. ORTEP diagram showing 50% thermal ellipsoid probability: carbon (gray), oxygen (red), fluorine (green), iodine (purple), and hydrogen (white).

Table 7: Intermolecular X···H bond distances and angles for compound **13–15**.

Entry	Compound	D–H···A	*d*(D–H) (Å)	*d*(H···A) (Å)	*d*(D···A) (Å)	*a*(D–H–A) (°)	*a*(C–X–H) (°)
1	**13**	F2···H3	0.980	3.704	3.826	89.69	na
2		F2···H4	0.980	2.271	3.222	163.14	na
3		F3···H3	0.980	4.239	4.561	103.01	na
4		F3···H4	0.980	2.867	3.614	133.69	na
5		F3···H5	0.980	3.074	3.490	107.03	na
6		Cl4···H3	0.980	3.437	4.232	139.73	133.71
7		Cl4···H4	0.980	3.625	4.298	128.02	96.94
8		Cl4···H5	0.980	3.953	4.624	128.19	103.45
9	**14**	F2···H3	1.000	3.771	3.869	88.12	na
10		F2···H4	1.000	2.270	3.233	161.19	na
11		F3···H3	1.000	4.290	4.599	101.79	na
12		F3···H4	1.000	2.849	3.626	135.07	na
13		F3···H5	1.000	3.130	3.533	105.61	na
14		Br4···H3	1.000	3.316	4.132	139.90	133.33
15		Br4···H4	1.000	3.526	4.213	127.67	95.15
16		Br4···H5	1.000	3.887	4.564	127.36	102.99
17	**15**	F2···H3	0.980	3.867	3.950	87.64	na
18		F2···H4	0.981	2.356	3.293	159.70	na
19		F3···H3	0.980	4.382	4.673	101.24	na
20		F3···H4	0.981	2.886	3.668	137.42	na
21		F3···H5	0.980	3.248	3.612	103.92	na
22		I4···H3	0.980	3.285	4.086	140.25	132.28
23		I4···H4	0.981	3.521	4.192	127.59	93.77
24		I4···H5	0.980	3.905	4.559	126.76	102.70

Our interest in the synthesis and conformation of multivicinal inter-halides motivated us to use density functional theory (DFT) calculations to understand the preference of talose analogues to adopt $^4C_1$-like conformations. DFT computations were performed using Gaussian 16 revision B.01 [67] with the CAM-B3LYP [68-70] functional and the Def2TZVP basis set [71], which includes effective core potentials for iodine. Empirical dispersion was accounted with Grimme's D3 [72,73] correction including Becke–Johnson damping [74]. Computations were performed both in the gas phase (i.e., individual molecules with thermal corrections at 298.15 K based on ideal gas assumptions) and in a chloroform solution, using the polarizable continuum model (PCM) [75]. A natural bonding orbital (NBO) analysis was performed to study the effects of hyperconjugation from C–F antibonding orbitals [76].

First, dipole moments, enthalpy and Gibbs free energy differences between $^1C_4$ and $^4C_1$ chair structures are shown in Table 8. In the gas phase, there is little difference in enthalpy between the two structures. For Cl, Br, and I, the $^1C_4$ structures are predicted to have slightly lower enthalpies. However, as these differences are much smaller than 1 kcal/mol, one should conclude that the structures are nearly degenerate. In solution, the picture is much clearer: the $^4C_1$ structure is always lower in enthalpy and Gibbs free energy, which corresponds with the experimental measurements. One can see that the gap between the two structures tends to decrease as the halogen becomes larger (the minor exception being bromine). Dipole moments for the $^4C_1$ structures are 2 Debye larger than for $^1C_4$ structures, making them substantially more stable in chloroform.

Both chair structures have multiple C–F bonds in gauche arrangements which are stable due to hyperconjugation: there is donation from C–H bonding orbitals to C–F (or C–X) antibonding orbitals that are aligned with one another. The principal difference between the two structures is that in the $^1C_4$ structure there are two such interactions whereas in the $^4C_1$

Table 8: Dipole moments (Debye), enthalpy and Gibbs free energy differences (kcal/mol) computed (CAM-B3LYP-D3BJ/Def2TZVP) for $^1C_4$ and $^4C_1$ chair structures in the gas phase and in chloroform (PCM). Thermal corrections are reported at 298.15 K.

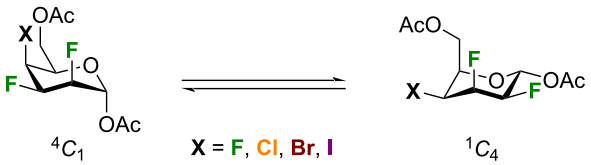

		Gas phase				Chloroform			
Entry	X	μ $^1C_4$	μ $^4C_1$	Δ*H*	Δ*G*	μ $^1C_4$	μ $^4C_1$	Δ*H*	Δ*G*
1	F	4.55	6.48	0.98	2.51	5.95	8.09	2.47	3.90
2	Cl	4.45	6.34	–0.03	1.31	5.93	7.93	1.29	2.21
3	Br	4.40	6.30	–0.13	1.18	5.89	7.94	1.19	2.55
4	I	4.32	6.07	–0.03	1.17	5.78	7.64	1.04	1.86

structure there are three. One can see that in the $^4C_1$ structure the C5–H5 bond will donate to the antibonding orbital of the C4–X4 bond, and the C3–H3 bond will donate to the antibonding orbitals of the C4–X4 and the C2–F2 bonds. In the $^1C_4$ structure, the C4–H4 and C2–H2 bonds will both donate to the antibonding orbital of the C3–F3 bond. These effects can be shown with an NBO analysis: the Kohn–Sham orbitals produced from DFT are localized to describe the system as one dominant resonance structure. As the Fock matrix is not diagonal in terms of the NBOs, coupling between orbitals can be quantified with second order perturbation theory. These couplings represent donation from an occupied NBO to an unoccupied NBO that would stabilize the system. The results are presented in Table 9. In both cases, there is also donation from the halogen lone pairs to C–H and C–C antibonding orbitals, but as these effects were near equivalent in both chair structures, they are omitted.

Conclusion

We described the synthesis and conformational analysis of halogenated pyran analogues of D-talose. All analogues adopt standard $^4C_1$-like conformations both in solution and in the solid-

Table 9: Second order perturbation theory energies of the Fock matrix in the NBO basis for $^4C_1$ and $^1C_4$ structures, from CAM-B3LYP-D3BJ/Def2TZVP results. Only results from $CHCl_3$ solvation (PCM) are reported as gas phase results showed no qualitative difference. Entries marked – are below the 0.50 kcal/mol threshold.

Entry	Donor σ	Acceptor σ*	X = F	X = Cl	X = Br	X = I	X = F	X = Cl	X = Br	X = I
1	C5–H5	C4–X4	5.07	6.58	7.46	7.83	–	–	–	–
2	C4–H4	C4–X4	1.05	0.88	0.97	0.75	1.10	0.80	0.81	0.56
3	C4–H4	C3–F3	–	–	–	–	5.18	5.53	5.67	5.88
4	C3–H3	C4–X4	5.36	6.59	7.46	7.71	0.61	–	–	–
5	C3–H3	C3–F3	1.05	1.03	1.02	1.02	1.00	1.02	1.02	1.05
6	C3–H3	C2–F2	5.00	5.18	5.20	5.22	0.58	0.59	0.59	0.61
7	C2–H2	C3–F3	0.50	0.50	0.50	0.52	4.63	4.61	4.58	4.58
8	C2–H2	C2–F2	1.01	0.99	0.99	0.99	1.01	1.00	1.00	1.01
9	C1–H1	C2–F2	1.10	1.21	1.22	1.26	0.53	0.56	0.57	0.56

state. The conformations were corroborated using DFT calculations by looking at the energy, enthalpy and Gibbs' free energy differences between $^1C_4$ and $^4C_1$ chair structures. Crystallographic data of halogenated analogues shows intra-annular torsion angles demonstrated with the increasing distance between F2···X4 in relation with the nature of the halogen at C4: F (d = 2.82 Å) < Cl (d = 3.06 Å) < Br (d = 3.14 Å) < I (d = 3.23 Å). Moreover, the Cremer–Pople ring puckering parameters show suitable differences in the distortion of the chair conformations. Crystal packing arrangements showed that the halogen at C4 contributed in the nonbonding (along the σ-hole) and hydrogen bond (perpendicular to the C–X bond) interactions. Finally, this study should be of general interest in the understanding of weak interactions that are now important to so many areas of chemistry, such as crystal engineering and supramolecular chemistry.

Supporting Information

Supporting Information File 1

Experimental and analytical data, crystal structure determination and NMR spectra.
[https://www.beilstein-journals.org/bjoc/content/supplementary/1860-5397-20-208-S1.pdf]

Funding

This work was supported by the Natural Sciences and Engineering Research Council of Canada (NSERC) and Universiteé Laval. O. L. thanks NSERC for a postgraduate fellowship. P. A. J. acknowledges funding from NSERC. This research was enabled by the Digital Research Alliance of Canada.

Author Contributions

Olivier Lessard: conceptualization; data curation; formal analysis; investigation; visualization; writing – original draft; writing – review & editing. Mathilde Grosset-Magagne: data curation; investigation; validation. Paul A. Johnson: resources; software; writing – original draft; writing – review & editing. Denis Giguère: conceptualization; funding acquisition; project administration; resources; supervision; visualization; writing – original draft; writing – review & editing.

ORCID® iDs

Paul A. Johnson - https://orcid.org/0000-0003-1133-6880
Denis Giguère - https://orcid.org/0000-0003-2209-1428

Data Availability Statement

All data that supports the findings of this study is available in the published article and/or the supporting information to this article.

Preprint

A non-peer-reviewed version of this article has been previously published as a preprint: https://doi.org/10.3762/bxiv.2024.37.v1

References

1. Zhou, Y.; Wang, J.; Gu, Z.; Wang, S.; Zhu, W.; Aceña, J. L.; Soloshonok, V. A.; Izawa, K.; Liu, H. *Chem. Rev.* **2016,** *116,* 422–518. doi:10.1021/acs.chemrev.5b00392
2. Wang, J.; Sánchez-Roselló, M.; Aceña, J. L.; del Pozo, C.; Sorochinsky, A. E.; Fustero, S.; Soloshonok, V. A.; Liu, H. *Chem. Rev.* **2014,** *114,* 2432–2506. doi:10.1021/cr4002879
3. O'Hagan, D. *J. Fluorine Chem.* **2010,** *131,* 1071–1081. doi:10.1016/j.jfluchem.2010.03.003
4. Gillis, E. P.; Eastman, K. J.; Hill, M. D.; Donnelly, D. J.; Meanwell, N. A. *J. Med. Chem.* **2015,** *58,* 8315–8359. doi:10.1021/acs.jmedchem.5b00258
5. Meanwell, N. A. *J. Med. Chem.* **2018,** *61,* 5822–5880. doi:10.1021/acs.jmedchem.7b01788
6. Linclau, B.; Ardá, A.; Reichardt, N.-C.; Sollogoub, M.; Unione, L.; Vincent, S. P.; Jiménez-Barbero, J. *Chem. Soc. Rev.* **2020,** *49,* 3863–3888. doi:10.1039/c9cs00099b
7. Huonnic, K.; Linclau, B. *Chem. Rev.* **2022,** *122,* 15503–15602. doi:10.1021/acs.chemrev.2c00086
8. Lessard, O.; Lainé, D.; Giguère, D. *Eur. J. Org. Chem.* **2024,** *27,* e202400120. doi:10.1002/ejoc.202400120
9. Govindaraj, V.; Ungati, H.; Jakka, S. R.; Bose, S.; Mugesh, G. *Chem. – Eur. J.* **2019,** *25,* 11180–11192. doi:10.1002/chem.201902243
10. Ungati, H.; Govindaraj, V.; Nair, C. R.; Mugesh, G. *Chem. – Eur. J.* **2019,** *25,* 3391–3399. doi:10.1002/chem.201806122
11. Gerebtzoff, G.; Li-Blatter, X.; Fischer, H.; Frentzel, A.; Seelig, A. *ChemBioChem* **2004,** *5,* 676–684. doi:10.1002/cbic.200400017
12. Nunes, R. S.; Vila-Viçosa, D.; Costa, P. J. *J. Am. Chem. Soc.* **2021,** *143,* 4253–4267. doi:10.1021/jacs.0c12470
13. Heidrich, J.; Sperl, L. E.; Boeckler, F. M. *Front. Chem. (Lausanne, Switz.)* **2019,** *7,* 9. doi:10.3389/fchem.2019.00009
14. Xu, Z.; Yang, Z.; Liu, Y.; Lu, Y.; Chen, K.; Zhu, W. *J. Chem. Inf. Model.* **2014,** *54,* 69–78. doi:10.1021/ci400539q
15. Mendez, L.; Henriquez, G.; Sirimulla, S.; Narayan, M. *Molecules* **2017,** *22,* 1397. doi:10.3390/molecules22091397
16. Hernandes, M. Z.; Cavalcanti, S. M. T.; Moreira, D. R. M.; de Azevedo Junior, W. F.; Leite, A. C. L. *Curr. Drug Targets* **2010,** *11,* 303–314. doi:10.2174/138945010790711996
17. Wilcken, R.; Zimmermann, M. O.; Lange, A.; Joerger, A. C.; Boeckler, F. M. *J. Med. Chem.* **2013,** *56,* 1363–1388. doi:10.1021/jm3012068
18. Chiodi, D.; Ishihara, Y. *J. Med. Chem.* **2023,** *66,* 5305–5331. doi:10.1021/acs.jmedchem.2c02015
19. Tan, Y.; Luo, S.; Li, D.; Zhang, N.; Jia, S.; Liu, Y.; Qin, W.; Song, C. E.; Yan, H. *J. Am. Chem. Soc.* **2017,** *139,* 6431–6436. doi:10.1021/jacs.7b02076
20. Bucher, C.; Deans, R. M.; Burns, N. Z. *J. Am. Chem. Soc.* **2015,** *137,* 12784–12787. doi:10.1021/jacs.5b08398
21. Gribble, G. W. *Mar. Drugs* **2015,** *13,* 4044–4136. doi:10.3390/md13074044
22. Gál, B.; Bucher, C.; Burns, N. Z. *Mar. Drugs* **2016,** *14,* 206. doi:10.3390/md14110206
23. Lessard, O.; Lainé, D.; Fecteau, C.-É.; Johnson, P. A.; Giguère, D. *Org. Chem. Front.* **2022,** *9,* 6566–6572. doi:10.1039/d2qo01433e

24. Denavit, V.; Lainé, D.; St-Gelais, J.; Johnson, P. A.; Giguère, D. *Nat. Commun.* **2018,** *9,* 4721. doi:10.1038/s41467-018-06901-y
25. Denavit, V.; St-Gelais, J.; Tremblay, T.; Giguère, D. *Chem. – Eur. J.* **2019,** *25,* 9272–9279. doi:10.1002/chem.201901346
26. Denavit, V.; Lainé, D.; Bouzriba, C.; Shanina, E.; Gillon, É.; Fortin, S.; Rademacher, C.; Imberty, A.; Giguère, D. *Chem. – Eur. J.* **2019,** *25,* 4478–4490. doi:10.1002/chem.201806197
27. St-Gelais, J.; Bouchard, M.; Denavit, V.; Giguère, D. *J. Org. Chem.* **2019,** *84,* 8509–8522. doi:10.1021/acs.joc.9b00795
28. Lainé, D.; Denavit, V.; Lessard, O.; Carrier, L.; Fecteau, C.-É.; Johnson, P. A.; Giguère, D. *Beilstein J. Org. Chem.* **2020,** *16,* 2880–2887. doi:10.3762/bjoc.16.237
29. St-Gelais, J.; Côté, É.; Lainé, D.; Johnson, P. A.; Giguère, D. *Chem. – Eur. J.* **2020,** *26,* 13499–13506. doi:10.1002/chem.202002825
30. Leclerc, C.; St-Gelais, J.; Cecioni, S.; Giguère, D. *J. Fluorine Chem.* **2024,** *273,* 110232. doi:10.1016/j.jfluchem.2023.110232
31. Lainé, D.; Lessard, O.; St-Gelais, J.; Giguère, D. *Chem. – Eur. J.* **2021,** *27,* 3799–3805. doi:10.1002/chem.202004646
32. Passaglia, L.; Zanardi, M. M.; Sarotti, A. M. *Org. Biomol. Chem.* **2024,** *22,* 2435–2442. doi:10.1039/d3ob02077k
33. Deposition number 2344127 (for **13**), 2344124 (for **14**), and 2344126 (for **15**) contains the supplementary crystallographic data for this paper. These data are provided free of charge by the joint Cambridge Crystallographic Data Centre and Fachinformationszentrum Karlsruhe Access Structures service.
34. Deposition number 1824902 (for **17**) contains the supplementary crystallographic data for this paper. These data are provided free of charge by the joint Cambridge Crystallographic Data Centre and Fachinformationszentrum Karlsruhe Access Structures service.
35. Hansen, L. K.; Hordvik, A. *Acta Chem. Scand., Ser. A* **1977,** *31,* 187–191. doi:10.3891/acta.chem.scand.31a-0187
36. Hunter, L.; Slawin, A. M. Z.; Kirsch, P.; O'Hagan, D. *Angew. Chem., Int. Ed.* **2007,** *46,* 7887–7890. doi:10.1002/anie.200701988
37. Hunter, L.; O'Hagan, D.; Slawin, A. M. Z. *J. Am. Chem. Soc.* **2006,** *128,* 16422–16423. doi:10.1021/ja066188p
38. Bentler, P.; Erdeljac, N.; Bussmann, K.; Ahlqvist, M.; Knerr, L.; Bergander, K.; Daniliuc, C. G.; Gilmour, R. *Org. Lett.* **2019,** *21,* 7741–7745. doi:10.1021/acs.orglett.9b02662
39. O'Hagan, D. *Chem. – Eur. J.* **2020,** *26,* 7981–7997. doi:10.1002/chem.202000178
40. Marchand, A. P.; Sorokin, V. D.; Rajagopal, D.; Bott, S. G. *Tetrahedron* **1994,** *50,* 9933–9942. doi:10.1016/s0040-4020(01)89608-3
41. Rodríguez-Vázquez, N.; Salzinger, S.; Silva, L. F.; Amorín, M.; Granja, J. R. *Eur. J. Org. Chem.* **2013,** 3477–3493. doi:10.1002/ejoc.201201565
42. Jeffrey, G. A. *Acta Crystallogr., Sect. B: Struct. Sci.* **1990,** *46,* 89–103. doi:10.1107/s0108768189012449
43. Bock, K.; Duus, J. Ø. *J. Carbohydr. Chem.* **1994,** *13,* 513–543. doi:10.1080/07328309408011662
44. Linclau, B.; Golten, S.; Light, M.; Sebban, M.; Oulyadi, H. *Carbohydr. Res.* **2011,** *346,* 1129–1139. doi:10.1016/j.carres.2011.04.007
45. Kim, H. W.; Rossi, P.; Shoemaker, R. K.; DiMagno, S. G. *J. Am. Chem. Soc.* **1998,** *120,* 9082–9083. doi:10.1021/ja9803714
46. Allen, F. H.; Kennard, O.; Watson, D. G.; Brammer, L.; Orpen, A. G.; Taylor, R. *J. Chem. Soc., Perkin Trans. 2* **1987,** S1–S19. doi:10.1039/p298700000s1
47. Jeffrey, G. A.; Pople, J. A.; Radom, L. *Carbohydr. Res.* **1972,** *25,* 117–131. doi:10.1016/s0008-6215(00)82752-4
48. O'Hagan, D. *Chem. Soc. Rev.* **2008,** *37,* 308–319. doi:10.1039/b711844a
49. Bondi, A. *J. Phys. Chem.* **1964,** *68,* 441–451. doi:10.1021/j100785a001
50. Cremer, D.; Pople, J. A. *J. Am. Chem. Soc.* **1975,** *97,* 1354–1358. doi:10.1021/ja00839a011
51. Jeffrey, G. A.; Yates, J. H. *Carbohydr. Res.* **1979,** *74,* 319–322. doi:10.1016/s0008-6215(00)84786-2
52. Steiner, T. *Angew. Chem., Int. Ed.* **2002,** *41,* 48–76. doi:10.1002/1521-3773(20020104)41:1<48::aid-anie48>3.0.co;2-u
53. Bresciani, S.; Lebl, T.; Slawin, A. M. Z.; O'Hagan, D. *Chem. Commun.* **2010,** *46,* 5434–5436. doi:10.1039/c0cc01128b
54. O'Hagan, D. *Chem. Rec.* **2023,** *23,* e202300027. doi:10.1002/tcr.202300027
55. Clark, T.; Hennemann, M.; Murray, J. S.; Politzer, P. *J. Mol. Model.* **2007,** *13,* 291–296. doi:10.1007/s00894-006-0130-2
56. Politzer, P.; Murray, J. S.; Clark, T. *Phys. Chem. Chem. Phys.* **2013,** *15,* 11178–11189. doi:10.1039/c3cp00054k
57. Scholfield, M. R.; Zanden, C. M. V.; Carter, M.; Ho, P. S. *Protein Sci.* **2013,** *22,* 139–152. doi:10.1002/pro.2201
58. Nelyubina, Y. V.; Antipin, M. Y.; Dunin, D. S.; Kotov, V. Y.; Lyssenko, K. A. *Chem. Commun.* **2010,** *46,* 5325–5327. doi:10.1039/c0cc01094d
59. Brammer, L.; Bruton, E. A.; Sherwood, P. *Cryst. Growth Des.* **2001,** *1,* 277–290. doi:10.1021/cg015522k
60. Aakeröy, C. B.; Desper, J.; Helfrich, B. A.; Metrangolo, P.; Pilati, T.; Resnati, G.; Stevenazzi, A. *Chem. Commun.* **2007,** *43,* 4236–4238. doi:10.1039/b707458a
61. Scholfield, M. R.; Ford, M. C.; Carlsson, A.-C. C.; Butta, H.; Mehl, R. A.; Ho, P. S. *Biochemistry* **2017,** *56,* 2794–2802. doi:10.1021/acs.biochem.7b00022
62. Lu, Y.; Wang, Y.; Zhu, W. *Phys. Chem. Chem. Phys.* **2010,** *12,* 4543–4551. doi:10.1039/b926326h
63. Auffinger, P.; Hays, F. A.; Westhof, E.; Ho, P. S. *Proc. Natl. Acad. Sci. U. S. A.* **2004,** *101,* 16789–16794. doi:10.1073/pnas.0407607101
64. Lin, F.-Y.; MacKerell, A. D., Jr. *J. Phys. Chem. B* **2017,** *121,* 6813–6821. doi:10.1021/acs.jpcb.7b04198
65. Lu, Y.; Wang, Y.; Xu, Z.; Yan, X.; Luo, X.; Jiang, H.; Zhu, W. *J. Phys. Chem. B* **2009,** *113,* 12615–12621. doi:10.1021/jp906352e
66. Decato, D. A.; Sun, J.; Boller, M. R.; Berryman, O. B. *Chem. Sci.* **2022,** *13,* 11156–11162. doi:10.1039/d2sc03792k
67. *Gaussian 16,* Revision B.01; Gaussian, Inc.: Wallingford CT, 2016.
68. Becke, A. D. *J. Chem. Phys.* **1993,** *98,* 5648–5652. doi:10.1063/1.464913
69. Lee, C.; Yang, W.; Parr, R. G. *Phys. Rev. B* **1988,** *37,* 785–789. doi:10.1103/physrevb.37.785
70. Yanai, T.; Tew, D. P.; Handy, N. C. *Chem. Phys. Lett.* **2004,** *393,* 51–57. doi:10.1016/j.cplett.2004.06.011
71. Weigend, F.; Ahlrichs, R. *Phys. Chem. Chem. Phys.* **2005,** *7,* 3297–3305. doi:10.1039/b508541a
72. Grimme, S.; Antony, J.; Ehrlich, S.; Krieg, H. *J. Chem. Phys.* **2010,** *132,* 154104. doi:10.1063/1.3382344
73. Grimme, S.; Ehrlich, S.; Goerigk, L. *J. Comput. Chem.* **2011,** *32,* 1456–1465. doi:10.1002/jcc.21759
74. Becke, A. D.; Johnson, E. R. *J. Chem. Phys.* **2006,** *124,* 014104. doi:10.1063/1.2139668
75. Tomasi, J.; Mennucci, B.; Cammi, R. *Chem. Rev.* **2005,** *105,* 2999–3094. doi:10.1021/cr9904009
76. Foster, J. P.; Weinhold, F. *J. Am. Chem. Soc.* **1980,** *102,* 7211–7218. doi:10.1021/ja00544a007

BEILSTEIN JOURNAL OF ORGANIC CHEMISTRY

Photoluminescence color-tuning with polymer-dispersed fluorescent films containing two fluorinated diphenylacetylene-type fluorophores

Kazuki Kobayashi, Shigeyuki Yamada*, Motohiro Yasui and Tsutomu Konno

Full Research Paper

Open Access

Address:
Faculty of Molecular Chemistry and Engineering, Kyoto Institute of Technology, Matsugasaki, Sakyo-ku, Kyoto 606-8585, Japan

Email:
Shigeyuki Yamada* - syamada@kit.ac.jp

* Corresponding author

Keywords:
energy transfer; fluorinated diphenylacetylenes; photoluminescence; polymer-dispersed films; white luminescence

Beilstein J. Org. Chem. **2024,** *20,* 2682–2690.
https://doi.org/10.3762/bjoc.20.225

Received: 29 July 2024
Accepted: 08 October 2024
Published: 23 October 2024

This article is part of the thematic issue "Organofluorine chemistry VI".

Associate Editor: P. J. Skabara

Abstract

The development of organic light-emitting devices has driven demand for new luminescent materials, particularly after the 2001 discovery of aggregation-induced emission. This study focuses on fluorinated diphenylacetylene-based luminescent molecules, revealing that specific molecular modifications can enhance fluorescence and achieve a wide range of photoluminescence colors. A simple and effective luminescence color-tuning method is proposed to investigate the photoluminescence behavior of two-component polymer dispersion films blended with two types of fluorinated diphenylacetylenes, namely blue- and yellow- or red-fluorescent fluorinated diphenylacetylenes. It is confirmed that if blue and green–yellow or yellow fluorophores are blended in appropriate ratios, a binary blend with color coordinates (0.20, 0.32) can be achieved, which approaches the white point of pure white emission. These findings contribute to the development of effective lighting and display devices as new white-light-emitting materials.

Introduction

Luminescent materials in lighting and display devices have become indispensable in daily life [1-3]. In recent years, organic electroluminescent devices have attracted significant attention as lightweight and energy-saving optical devices, and there has been a strong demand for the development of luminescent materials. Until now, the design of solid-state light-emitting materials has not been established, and therefore, their development has been severely delayed [4-6]. However, since Tang et al. first reported the aggregation-induced emission phenomenon in 2001 [7], the development of solid-state light-emitting materials has accelerated significantly [8-10].

Many photoluminescent materials that emit blue, green, and yellow photoluminescence (PL) have been developed, whereas red PL with PL wavelengths in the long wavelength region is considered difficult to achieve owing to the energy gap law [11-

13]. Over the past few decades, our group has been vigorously pursuing the exploration of functional molecules with a linear diphenylacetylene structure as the π-conjugated core. As a part of our research projects, we have begun to explore diphenylacetylene-based luminescent molecules despite diphenylacetylene not exhibiting fluorescence at room temperature because it undergoes a πσ* excited state that rapidly forms a *trans*-bend structure (Figure 1a) [14-16].

Our extensive efforts have revealed that introducing electron-donating alkoxy and electron-withdrawing cyano groups at both ends of the diphenylacetylene scaffold slows the internal conversion to the πσ* excited state. Further incorporating four fluoro substituents in the short-axis direction of the electron-deficient aromatic ring significantly retards the internal conversion via the formation of H···F hydrogen bonds, leading to a marked blue fluorescence in the crystalline state (Figure 1b) [17-20]. Recently, the introduction of *N*,*N*-disubstituted amino groups as electron-donating groups was shown to promote intramolecular charge transfer (ICT) and shifted the PL wavelength to longer wavelengths, resulting in yellow or orange fluorescence in the solid state [21,22]. In addition, cross-linking between the amino group and attached benzene ring effectively suppresses the formation of the twisted ICT state, resulting in red fluorescence even in the solid state (Figure 2) [23].

The precise tuning of molecular and electronic structures has made it possible to produce a wide range of PL colors. However, the development of white-light-emitting materials, which are especially indispensable for our affluent life, is more difficult

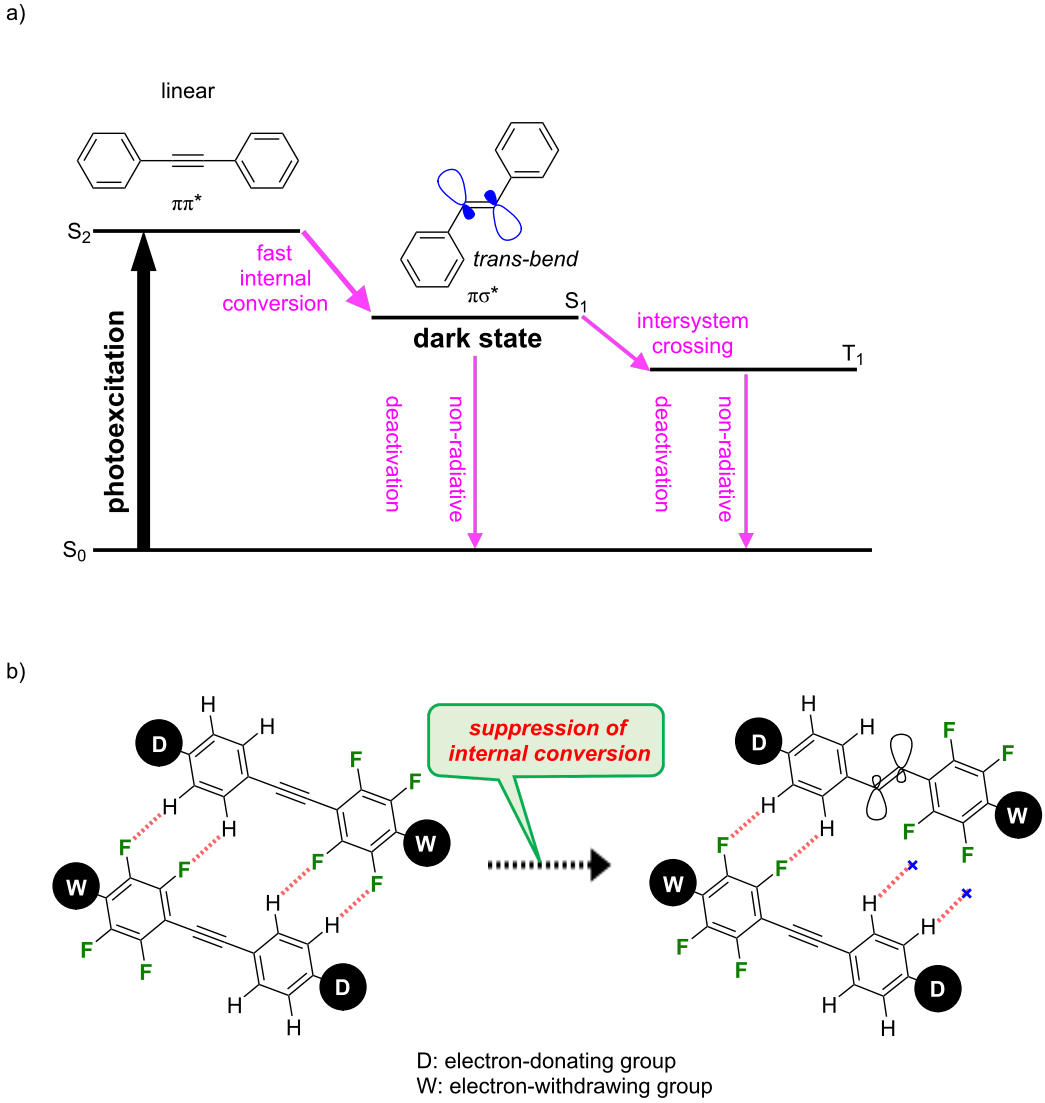

Figure 1: (a) Reported photophysics of diphenylacetylene after photoexcitation. (b) Our molecular design to suppress internal conversion.

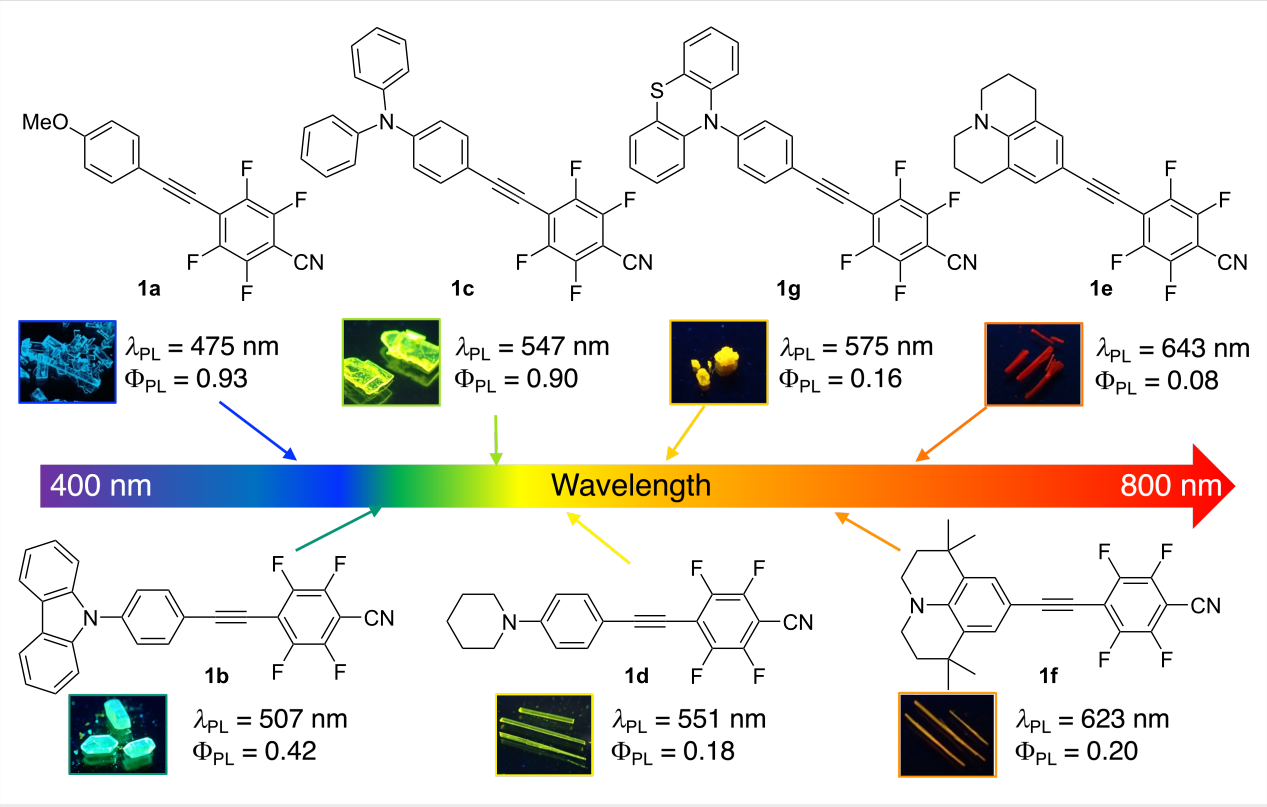

Figure 2: Relationship between the molecular structure of fluorinated diphenylacetylenes and photoluminescence (PL) color in their crystalline states.

than the development of the blue-, yellow-, and red-light-emitting molecules mentioned above [24-26]. Therefore, to achieve white luminescence covering the entire spectral range of the visible light region, two or more colors of fluorescence or phosphorescence from different luminescent centers in the polymer matrix should be combined, and the PL color can be precisely tuned by controlling the ratio of the PL luminescent materials [27-29]. In this study, we prepared polymer dispersion fluorescent films containing two compounds from our fluorinated diphenylacetylene library that exhibit different PL characteristics from blue to red in the solid state, as shown in Figure 2, and investigated their PL behavior and PL color-tuning potential.

Results and Discussion

Photoluminescence behavior of poly(methyl methacrylate) (PMMA) films

Initially, we tested the PL behavior of polymer dispersion films containing fluorinated diphenylacetylenes **1a**–**g** as a single component, as shown in Figure 3, because the PL behavior of fluorescent molecules dispersed in a polymer matrix generally differs from that in a dilute solution or the crystalline state. The PL wavelengths (λ_{PL}), fluorescence quantum yields (Φ_{PL}), fluorescence lifetimes (τ_{PL}), and Commission Internationale de l'Eclairage (CIE) chromaticity coordinates of the PMMA dispersion films containing 1 wt % of compounds **1a**–**g** are summarized in Table 1.

The PMMA dispersion films containing 1 wt % of compounds **1a**–**g** all exhibited a single PL band with λ_{PL}s in the range of 415–544 nm, and their PL colors varied from dark blue to yellow with (*x*, *y*) coordinates of (0.16, 0.09) and (0.41, 0.54), respectively (Figure 3). A blueshift in the λ_{PL} ranging from 28 nm to a maximum of 126 nm was observed for all compounds contained in a PMMA film, based on a comparison with the λ_{PL} of the crystalline state shown in Figure 2. A decrease in the Φ_{PL} was observed for the PMMA dispersion films containing **1a** with a methoxy substituent, **1c** with a diphenylamino group, or **1g** with a phenothiazine unit. Judging from the fact that compounds **1a** and **1c** form a tight molecular packing via intermolecular H···F hydrogen bonds which suppress non-radiative deactivation in the crystalline state [20,21], we speculated that the polymer dispersion state had lost the intermolecular interactions, which accelerated the non-radiative deactivation process. On the other hand, the other derivatives, namely **1b** and **1d**–**f**, showed increased Φ_{PL} values in the PMMA films compared with those in the crystalline state, presumably due to a suppression of the formation of non-fluorescent twisted intramolecular charge transfer (TICT) states caused by the large ICT characteristics.

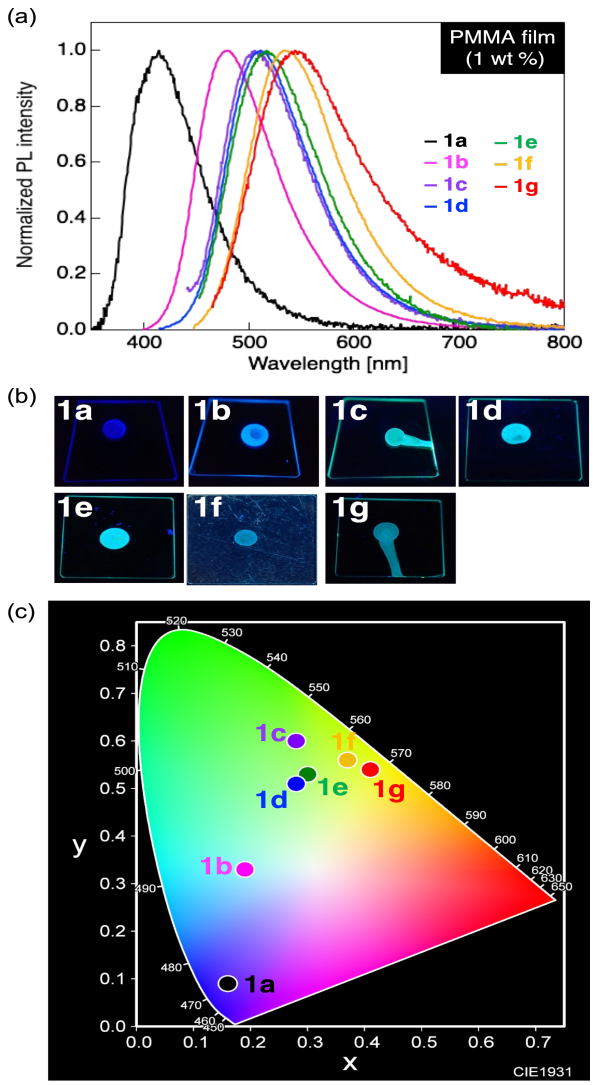

Figure 3: (a) PL spectra of the donor–π–acceptor (D–π–A)-type diphenylacetylene compounds **1a–g** contained in a poly(methyl methacrylate) (PMMA) dispersion film. (b) Photographs of the PMMA dispersion films under ultraviolet (UV) irradiation (λ_{ex} = 365 nm). (c) A PL color diagram defined by the Commission Internationale de l'Eclairage (CIE).

Photoluminescence behavior of PMMA dispersion fluorescent films containing two fluorinated diphenylacetylenes

Based on the solid-state fluorescent molecule library **1a–g** developed by our group [20-23], we expected that white photoluminescent devices could be developed by precisely controlling the two-component mixture system of blue- and yellow-fluorescent molecules. From the perspective of both the PL color and Φ_{PL}, we selected the methoxy-substituted compound **1a** as an effective blue-fluorescent molecule for use in a two-component mixing system. Among diphenylamino-substituted **1c** with chromaticity (*x, y*) coordinates of (0.28, 0.60), **1f** containing a tetramethyljulolidine unit with (*x, y*) coordinates of (0.37, 0.56), and **1g** containing a phenothiazine unit with (*x, y*) coordinates of (0.41, 0.54), **1c** and **1f** were finally selected as candidates for yellow-fluorescent molecules from the viewpoint of their Φ_{PL}. Therefore, we investigated the PL behavior of PMMA dispersion films containing blue-fluorescent **1a**, green–yellow fluorescent **1c**, and yellow-fluorescent **1f**.

Photoluminescence behavior of PMMA dispersion films containing a mixture of blue fluorophore **1a** and green–yellow fluorophore **1c**

PMMA dispersion films containing 1 wt % of blue fluorophore **1a** and green–yellow fluorophore **1c** in various weight ratios were prepared. Their PL spectra and photophysical data are depicted in Figure 4 and Table 2 summarizes the collected photophysical data.

As mentioned above, the PMMA film containing 1 wt % of fluorophore **1a** with a methoxy group exhibited a single PL band with a λ_{PL} at approximately 415 nm and dark blue PL with chromaticity coordinates of (0.16, 0.09). In contrast, the PMMA film containing 1 wt % of fluorophore **1c** with a diphenylamino group showed green–yellow PL with a λ_{PL} at approximately 506 nm and chromaticity coordinates of (0.28, 0.60). The PL behavior of the 1 wt % PMMA film blended with blue fluorophore **1a** and green–yellow fluorophore **1c** in a 50:50 ratio was

Table 1: Photophysical data of compounds **1a–g** contained in a PMMA dispersion film.

	λ_{ex} [nm]	λ_{PL} [nm] (Φ_{PL})[a]	τ_{PL} [ns]	coordinate (*x*, *y*)[b]
1a	310	415 (0.76)	4.68	(0.16, 0.09)
1b	300	479 (1.00)	3.21	(0.19, 0.33)
1c	300	506 (0.84)	3.19	(0.28, 0.60)
1d	400	512 (0.66)	3.89	(0.28, 0.51)
1e	440	517 (0.54)	2.26	(0.30, 0.53)
1f	440	534 (0.66)	3.73	(0.37, 0.56)
1g	450	544 (0.03)	4.84	(0.41, 0.54)

[a]Measured using an integrating sphere; [b]chromaticity coordinates defined by the CIE.

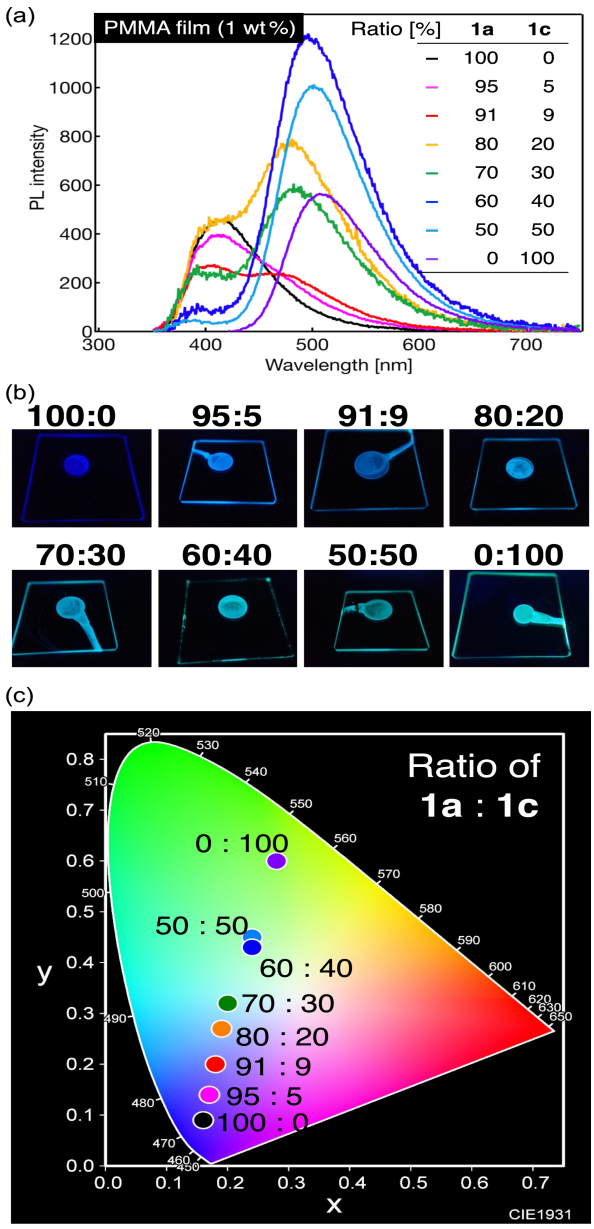

Figure 4: (a) PL spectra of PMMA dispersion films containing 1 wt % of blue fluorophore **1a** and green–yellow fluorophore **1c** in various weight ratios. (b) Photographs of the PMMA dispersion films under UV irradiation (λ_{ex} = 365 nm). (c) A CIE color diagram of the PL color of the PMMA dispersion films containing **1a** and **1c** in various ratios.

evaluated, and two PL bands appeared, namely major and minor PL bands with λ_{PL}s at approximately 504 and 390 nm, respectively. The fluorescent color of the PMMA film mixed in a 50:50 ratio showed light green–yellow PL with chromaticity coordinates of (0.24, 0.45), which suggests a rapid energy transfer of the excitation energy from blue fluorophore **1a** to green–yellow fluorophore **1c**. The absorption wavelengths and spectral shapes in the ultraviolet (UV)–visible absorption spectra of the PMMA films containing 1 wt % of **1a** and **1c** or **1f** as representative examples (Figure S2 in Supporting Information File 1) were similar to those in the corresponding excitation spectra, which clearly indicates that the PL originates from a single fluorophore. Using a 1 wt % PMMA film blended with **1a** and **1c** in an 80:20 ratio (Figure S2g in Supporting Information File 1), the excitation spectrum obtained by monitoring the long PL wavelength derived from **1c** was also in good agreement with the absorption spectrum of **1a** in the two-component film. This result also clearly suggests an energy transfer from **1a** to **1c**.

The fluorescence resonance energy transfer efficiency (E_{FRET}) [30,31] was calculated from the ratio of the fluorescence lifetimes of the two- and high-energy-component films (Equation 1):

$$E_{FRET} = \left(1 - \frac{\tau_{DA}}{\tau_D}\right) \times 100, \quad (1)$$

where τ_{DA} and τ_D are the PL lifetimes of the two- and single-component films, respectively. An E_{FRET} of 40% for the two-component PMMA film blended in a 50:50 ratio indicates that the excitation energy was transferred relatively efficiently from **1a** to **1c**.

Next, the PL behavior of a PMMA film with a higher ratio of **1a** was investigated by mixing **1a**:**1c** in a ratio of 95:5. Contrary to the above result, a single PL band with a λ_{PL} at approximately 404 nm and a shoulder peak in the long-wavelength region were observed. The τ_{PL} of the PMMA film blended in a 95:5 ratio was 2.50 ns with an E_{FRET} of 47%, indicating that the PL band of **1c** was very small because of non-radiative deactivation, in addition to the low PL component of **1c**. The PL color of the PMMA film blended in a 95:5 ratio was dark blue, with color coordinates of (0.17, 0.14).

Based on these results, various mixing ratios of **1a** and **1c** ranging from 50:50 to 95:5 were investigated (91:9, 80:20, 70:30, and 60:40). Thus, a PMMA film mixed with **1a** and **1c** in a ratio of 91:9 exhibited two PL bands with λ_{PL}s at approximately 404 and 473 nm, respectively. The PL bands on the short- and long-wavelength sides were considered to be derived from the emissions of **1a** and **1c**, respectively. For the PL of the PMMA film blended in a 91:9 ratio, the τ_{PL} and E_{FRET} values were 2.52 ns and 46%, respectively. Although the PMMA film blended in a 91:9 ratio was observed to have two distinct PL bands, the PL color turned blue with coordinates of (0.18, 0.20). Furthermore, when the mixing ratio of **1a** to **1c** was changed to 80:20, 70:30, and 60:40, the relative intensity of the long-wavelength PL band originating from the PL of **1c** relative to that of

Table 2: Photophysical data of PMMA dispersion films containing 1 wt % of blue fluorophore **1a** and green–yellow fluorophore **1c** in various weight ratios.

Ratio of **1a**:**1c**	λ_{PL} [nm] (Φ_{PL})[a]	τ_{PL} [ns]	coordinate (x, y)[b]	E_{FRET} [%][c]
100:0	415 (0.76)	4.68	(0.16, 0.09)	–
95:5	404 (0.97)	2.50	(0.17, 0.14)	47
91:9	404, 473 (0.92)	2.52	(0.18, 0.20)	46
80:20	400, 480 (0.93)	1.58	(0.19, 0.27)	66
70:30	392, 482 (0.76)	1.35	(0.20, 0.32)	71
60:40	496 (0.95)	2.73	(0.24, 0.43)	42
50:50	390, 504 (1.0)	2.79	(0.24, 0.45)	40
0:100	506 (0.84)	3.19	(0.28, 0.60)	–

[a]Measured using an integrating sphere; [b]PL color coordinate defined by the CIE; [c]fluorescence resonance energy transfer (FRET) efficiency (E_{FRET}) = 1 – (τ_{DA}/τ_D).

1a increased with the increasing mixing ratio of **1c**. The τ_{PL} values were in the range of 1.35–2.73 ns in these blends and the E_{FRET} values were in the range of 42–71%. These results indicate a good energy transfer for all **1a** and **1c** mixtures. Based on the PL spectra of the PMMA films blended in each mixing ratio, the PL colors of the 80:20 and 70:30 blends were light blue with coordinates of (0.19, 0.27) and (0.20, 0.32), respectively, and the PL color of the 60:40 blend was green–blue with coordinates of (0.24, 0.43). The PL color of the PMMA films containing the **1a**/**1c** mixture prepared in each mixing ratio varied along a straight line connecting the color coordinates of the PMMA films containing the individual component **1a** or **1c**. In other words, tuning the PL color was possible by controlling the mixing ratio. In addition, when the mixing ratio of **1a** to **1c** was 70:30, the chromaticity coordinates were (0.20, 0.32), which are relatively close to the ideal color coordinates of (0.33, 0.33) for white. The results for the PMMA film containing a mixture of **1a** and **1c** indicate that the use of fluorophores with PL bands on the longer-wavelength side is more effective in approaching the ideal white color than green–yellow fluorophore **1c**.

Photoluminescence behavior of PMMA dispersion films containing a mixture of blue fluorophore **1a** and yellow fluorophore **1f**

Based on our investigation of the PL behavior of PMMA dispersion films containing a mixture of **1a** and **1c**, we investigated the PL properties of PMMA dispersion films containing a mixture of blue fluorophore **1a** and yellow fluorophore **1f** (Figure 5). The collected photophysical data are summarized in Table 3.

Unlike the PMMA film containing green–yellow fluorophore **1c**, the 1 wt % PMMA film containing **1f** with a tetramethyljulolidine backbone exhibited yellow PL with a λ_{PL} at approximately 534 nm and chromaticity coordinates of (0.37, 0.56). When blue fluorophore **1a** and yellow fluorophore **1f** were blended in ratios of 50:50 and 80:20, the 1 wt % PMMA films containing this mixture showed a major PL band derived from **1f** with a λ_{PL} at 530–541 nm, along with a minor PL band derived from **1a** at 384–392 nm. The fluorescent color of the PMMA film containing this blend was yellow with chromaticity coordinates of (0.38, 0.54) for the blend in a 50:50 ratio, and green–yellow with chromaticity coordinates of (0.35, 0.53) for the blend in an 80:20 ratio. The τ_{PL} values of the PMMA films containing blends with ratios of 50:50 and 80:20 were 2.12 and 2.53 ns, respectively, and their E_{FRET} values were 55% and 46%. Both mixtures showed a relatively fast energy transfer, which likely caused the PL of **1f** to be the major component. Furthermore, the excitation spectrum obtained by monitoring the long PL wavelength originating from **1f** using a 1 wt % PMMA film blended with **1a** and **1f** in an 80:20 ratio was also consistent with the corresponding absorption spectrum of **1a** (Figure S2h in Supporting Information File 1). This result clearly indicates an energy transfer from **1a** to **1f**. Next, we evaluated the PL properties of the PMMA film blended in a 95:5 ratio, which had a higher weight ratio of **1a**. As a result, two distinct PL bands with λ_{PL}s at approximately 401 and 520 nm appeared, which correspond to the PL derived from blue-fluorescent **1a** and yellow-fluorescent **1f**, respectively. The τ_{PL} was measured to be 2.48 ns, indicating an increase in the short-lived **1a** component. The E_{FRET} was also calculated to be 47%, which indicates that energy transfer occurred smoothly from **1a** to **1f**. The PL color of the PMMA film blended in a 95:5 ratio was pale green–yellow with chromaticity coordinates of (0.26, 0.41).

Further studies were conducted on PMMA films with increased content of **1a** and blends of **1a** and **1f** in ratios of 97:3 and 98:2. Compared with the PL spectrum of the PMMA film blended in

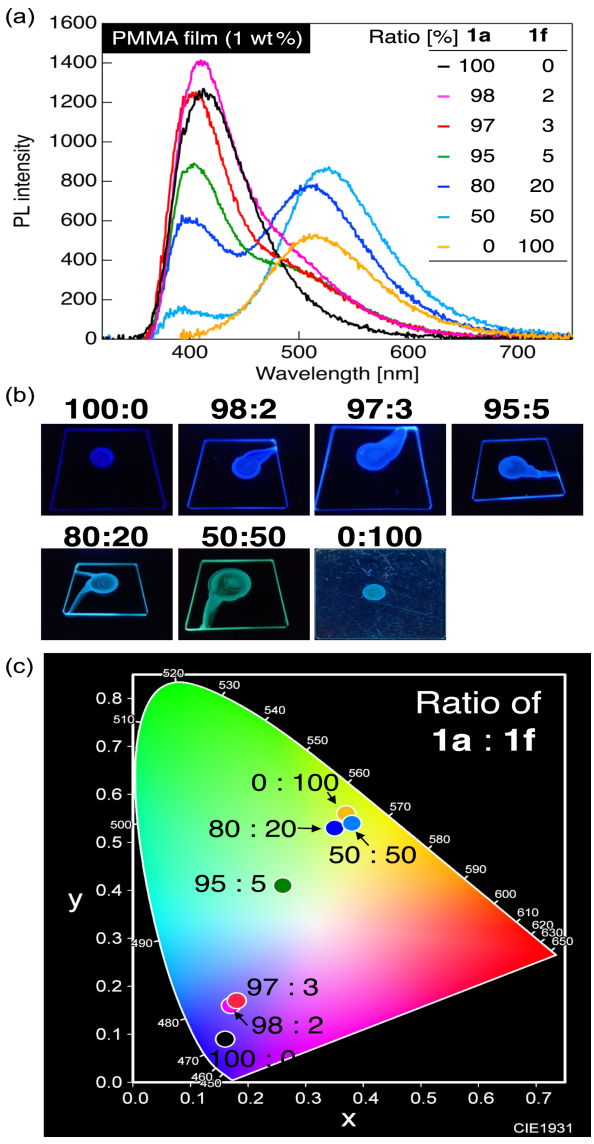

Figure 5: (a) PL spectra of PMMA dispersion films containing 1 wt % of blue fluorophore **1a** and yellow fluorophore **1f** in various weight ratios. (b) Photographs of their PMMA dispersion films under UV irradiation (λ_{ex} = 365 nm). (c) A CIE color diagram of the PL color of PMMA dispersion films containing **1a** and **1f** in various weight ratios.

a 95:5 ratio, the PL intensity of the short-wavelength PL band derived from the emission of **1a** increased with increasing contents of **1a**. The τ_{PL} values of the PMMA films blended in ratios of 97:3 and 98:2 were 2.04 and 1.96 ns, respectively, and their E_{FRET} values were 56% and 58%. These results indicate that a relatively efficient transfer of energy occurred from **1a** to **1f**. However, the PL color of the PMMA films containing the blend was light purple with chromaticity coordinates of (0.18, 0.17) for the 97:3 ratio, and blue with chromaticity coordinates of (0.17, 0.16) for the 98:2 ratio. Similar to the PL color trend in the PMMA films blended with **1a** and **1c**, the PL colors of the PMMA films blended with **1a** and **1f** were located on a line connecting them, suggesting that tuning the PL color from blue to yellow is possible by precisely adjusting the mixing ratios of **1a** and **1f**. When the mixing ratio of **1a** to **1f** was 95:5, the chromaticity coordinates were (0.26, 0.41). The PL of the PMMA films blended with the **1a**/**1f** binary mixture was relatively close to white, although it was slightly different from the ideal white point.

Conclusion

In conclusion, we prepared PMMA dispersion films with a single component of fluorinated diphenylacetylene or a blend of two fluorinated diphenylacetylenes at a concentration of 1 wt % and investigated their PL behavior in detail. Among the fluorinated diphenylacetylene libraries with excellent solid-state luminescent properties, the PMMA dispersion film containing a methoxy-substituted fluorinated diphenylacetylene exhibited dark blue PL, the PMMA film containing a diphenylamino-substituted fluorinated diphenylacetylene exhibited green–yellow PL, and the PMMA film containing a fluorinated diphenylacetylene with a tetramethyljulolidine skeleton exhibited yellow PL. Intensive investigation of the PL behavior of these PMMA films blended as a binary mixture of blue and green–yellow or yellow fluorophores showed smooth energy transfer from the high-energy fluorescent component, that is, the methoxy-substituted fluorinated diphenylacetylene, to the yellow–green or yellow fluorophore, respectively. The PL be-

Table 3: Photophysical data of PMMA dispersion films containing 1 wt % of blue fluorophore **1a** and yellow fluorophore **1f** in various weight ratios.

Ratio of **1a**:**1f**	λ_{PL} [nm] (Φ_{PL})[a]	τ_{PL} [ns]	coordinate (x, y)[b]	E_{FRET} [%][c]
100:0	415 (0.76)	4.68	(0.16, 0.09)	–
98:2	407 (0.76)	1.96	(0.17, 0.16)	58
97:3	417 (0.82)	2.04	(0.18, 0.17)	56
95:5	401, 520 (0.94)	2.48	(0.26, 0.41)	47
80:20	384, 530 (1.0)	2.53	(0.35, 0.53)	46
50:50	392, 541 (1.0)	2.12	(0.38, 0.54)	55
0:100	534 (0.66)	3.73	(0.37, 0.56)	–

[a]Measured using an integrating sphere; [b]PL color coordinates defined by the CIE; [c]$E_{FRET} = 1 - (\tau_{DA}/\tau_D)$.

havior of each PMMA film blended as a binary mixture was investigated by varying the mixing ratio, and a wide range of PL colors, including dark blue, green–yellow, and yellow with chromaticity coordinates of (0.16, 0.09), (0.28, 0.60), and (0.37, 0.56), respectively, were obtained. In addition, both PMMA films containing the binary blends had color coordinates of (0.20, 0.32) and (0.26, 0.41) by precisely controlling the mixing ratio, and an approach to the white point (0.33, 0.33) of pure white emission could be observed. Further fine-tuning of the mixing ratios and PMMA films containing red–green–blue ternary mixtures holds promise for developing white-light-emitting materials with higher color purities and more diverse PL color tunings.

Experimental

Fabrication of PMMA dispersion films

PMMA films containing one of two fluorinated diphenylacetylenes were prepared using an Opticoat MS-B100 spin coater (MIKASA, Japan). The mother liquor for the thin-film deposition was prepared as follows: it was mounted on a thoroughly cleaned glass slide and clamped to the upper rotating plate of the spin coater. PMMA (100 mg) and the fluorophore (1.0 wt %) were dissolved in $CHCl_3$ (3 mL), and a few drops of the solution were dropped onto a glass substrate. The top plate of the spin coater was rotated sequentially at 500 rpm for 5 s, 750 rpm for 5 s, and 1200 rpm for 10 s. For photophysical measurements, thin and smooth films were prepared by spin-coating followed by solvent evaporation.

Photophysical properties

The PL spectra and quantum yields were measured using a Quantaurus-QY C11347-01 absolute PL quantum yield spectrometer (Hamamatsu Photonics, Japan). The PL lifetime was measured using a Quantaurus-Tau C11367-34 fluorescence lifetime spectrometer (Hamamatsu Photonics, Japan).

Supporting Information

Supporting Information File 1

PL spectra and PL decay profiles of PMMA films containing 1 wt % of compounds or binary mixtures.
[https://www.beilstein-journals.org/bjoc/content/supplementary/1860-5397-20-225-S1.pdf]

Funding

This research was partially funded by the Murata Science Foundation and Shorai Foundation for Science and Technology. Research equipment from the MEXT Project was used in this study to promote the public utilization of an advanced research infrastructure, which is a program for supporting the introduction of the new sharing system (grant number: JPMXS0421800223).

Author Contributions

Kazuki Kobayashi: data curation; investigation; methodology; writing – original draft. Shigeyuki Yamada: conceptualization; data curation; funding acquisition; investigation; methodology; project administration; resources; supervision; validation; visualization; writing – original draft. Motohiro Yasui: investigation; resources; writing – original draft. Tsutomu Konno: investigation; resources; writing – original draft.

ORCID® iDs

Shigeyuki Yamada - https://orcid.org/0000-0002-6379-0447
Motohiro Yasui - https://orcid.org/0000-0001-9324-3463
Tsutomu Konno - https://orcid.org/0000-0002-5146-9840

Data Availability Statement

All data that supports the findings of this study is available in the published article and/or the supporting information of this article.

References

1. Bispo-Jr, A. G.; Saraiva, L. F.; Lima, S. A. M.; Pires, A. M.; Davolos, M. R. *J. Lumin.* **2021,** *237,* 118167. doi:10.1016/j.jlumin.2021.118167
2. Zhang, Q.; Wang, X.; Wang, Y. *Inorg. Chem. Front.* **2020,** *7,* 1034–1045. doi:10.1039/c9qi01428d
3. Jüstel, T.; Nikol, H.; Ronda, C. *Angew. Chem., Int. Ed.* **1998,** *37,* 3084–3103. doi:10.1002/(sici)1521-3773(19981204)37:22<3084::aid-anie3084>3.0.co;2-w
4. Birks, J. B. *Photophysics of Aromatic Molecules;* John Wiley & Sons: New York, NY, USA, 1970.
5. Thomas, S. W.; Joly, G. D.; Swager, T. M. *Chem. Rev.* **2007,** *107,* 1339–1386. doi:10.1021/cr0501339
6. Chen, C.-T. *Chem. Mater.* **2004,** *16,* 4389–4400. doi:10.1021/cm049679m
7. Luo, J.; Xie, Z.; Lam, J. W. Y.; Cheng, L.; Chen, H.; Qiu, C.; Kwok, H. S.; Zhan, X.; Liu, Y.; Zhu, D.; Tang, B. Z. *Chem. Commun.* **2001,** 1740–1741. doi:10.1039/b105159h
8. Xu, L. *Coord. Chem. Rev.* **2024,** *506,* 215701. doi:10.1016/j.ccr.2024.215701
9. Xie, Y.; Li, Z.; Zhao, C.; Lv, R.; Li, Y.; Zhang, Z.; Teng, M.; Wan, Q. *Luminescence* **2024,** *39,* e4621. doi:10.1002/bio.4621
10. Huang, G.; Du, X.; Bo, H.; Li, B. S. *Mater. Chem. Front.* **2024,** *8,* 104–132. doi:10.1039/d3qm00621b
11. Yoon, S.; Teets, T. S. *Chem. Commun.* **2021,** *57,* 1975–1988. doi:10.1039/d0cc08067e
12. Englman, R.; Jortner, J. *Mol. Phys.* **1970,** *18,* 145–164. doi:10.1080/00268977000100171
13. Englman, R.; Jortner, J. *J. Lumin.* **1970,** *1–2,* 134–142. doi:10.1016/0022-2313(70)90029-3
14. Saltiel, J.; Kumar, V. K. R. *J. Phys. Chem. A* **2012,** *116,* 10548–10558. doi:10.1021/jp307896c

15. Zgierski, M. Z.; Lim, E. C. *Chem. Phys. Lett.* **2004,** *387,* 352–355. doi:10.1016/j.cplett.2004.02.029
16. Ferrante, C.; Kensy, U.; Dick, B. *J. Phys. Chem.* **1993,** *97,* 13457–13463. doi:10.1021/j100153a008
17. Yamada, S.; Konno, T. *Chem. Rec.* **2023,** *23,* e202300094. doi:10.1002/tcr.202300094
18. Morita, M.; Yamada, S.; Konno, T. *New J. Chem.* **2022,** *46,* 4562–4569. doi:10.1039/d1nj05539a
19. Morita, M.; Yamada, S.; Konno, T. *Molecules* **2021,** *26,* 2274. doi:10.3390/molecules26082274
20. Morita, M.; Yamada, S.; Konno, T. *New J. Chem.* **2020,** *44,* 6704–6708. doi:10.1039/d0nj01268h
21. Yamada, S.; Kobayashi, K.; Morita, M.; Konno, T. *CrystEngComm* **2022,** *24,* 936–941. doi:10.1039/d1ce01671g
22. Yamada, S.; Kobayashi, K.; Konno, T. *Molecules* **2022,** *27,* 5782. doi:10.3390/molecules27185782
23. Kobayashi, K.; Yamada, S.; Sakurai, T.; Yasui, M.; Konno, T. *J. Mater. Chem. C* submitted.
24. Kumari, B.; Dahiwadkar, R.; Kanvah, S. *Aggregate* **2022,** *3,* e191. doi:10.1002/agt2.191
25. Panigrahi, K.; Nag, A. *J. Phys. Chem. C* **2022,** *126,* 8553–8564. doi:10.1021/acs.jpcc.2c01679
26. Chen, Z.; Ho, C.-L.; Wang, L.; Wong, W.-Y. *Adv. Mater. (Weinheim, Ger.)* **2020,** *32,* e1903269. doi:10.1002/adma.201903269
27. Furukawa, S.; Shono, H.; Mutai, T.; Araki, K. *ACS Appl. Mater. Interfaces* **2014,** *6,* 16065–16070. doi:10.1021/am503956t
28. Sato, T.; Pandey, R. K.; Higuchi, M. *Dalton Trans.* **2013,** *42,* 16036–16042. doi:10.1039/c3dt51354h
29. Sun, M.; Li, Y.; Zhao, L.; Zhang, X.; Zhang, C.; Jin, X.; Shan, D.; Li, G. *ACS Appl. Polym. Mater.* **2021,** *3,* 2998–3008. doi:10.1021/acsapm.1c00162
30. Chung, H. S.; Louis, J. M.; Gopich, I. V. *J. Phys. Chem. B* **2016,** *120,* 680–699. doi:10.1021/acs.jpcb.5b11351
31. Becker, W. *J. Microsc. (Oxford, U. K.)* **2012,** *247,* 119–136. doi:10.1111/j.1365-2818.2012.03618.x

License and Terms

BEILSTEIN JOURNAL OF ORGANIC CHEMISTRY

Synthesis of fluoroalkenes and fluoroenynes via cross-coupling reactions using novel multihalogenated vinyl ethers

Yukiko Karuo, Keita Hirata, Atsushi Tarui, Kazuyuki Sato, Kentaro Kawai and Masaaki Omote*

Full Research Paper

Open Access

Address:
Faculty of Pharmaceutical Sciences, Setsunan University, 45-1 Nagaotoge-cho, Hirakata, Osaka 573-0101, Japan

Email:
Masaaki Omote* - omote@pharm.setsunan.ac.jp

* Corresponding author

Keywords:
fluoroalkenes; fluoroenynes; multihalogenated vinyl ethers; Suzuki–Miyaura cross-coupling reactions; Sonogashira cross-coupling reactions

Beilstein J. Org. Chem. **2024,** *20,* 2691–2703.
https://doi.org/10.3762/bjoc.20.226

Received: 29 July 2024
Accepted: 09 October 2024
Published: 24 October 2024

This article is part of the thematic issue "Organofluorine chemistry VI".

Guest Editor: D. O'Hagan

Abstract

In this study, we develop the synthesis methods of fluoroalkenes and fluoroenynes via Suzuki–Miyaura and Sonogashira cross-coupling reactions using novel multihalogenated fluorovinyl ethers, which are easily prepared from the reaction between phenols and 2-bromo-2-chloro-1,1,1-trifluoroethane (halothane). These reactions make use of the unique structure of multihalogenated fluorovinyl ethers, which contains a reactive bromine atom, to afford a series of fluoroalkenes and fluoroenynes in moderate to high yields.

Introduction

Fluoroalkenes are one of the important frameworks for a wide range of industrial fields. For example, they are used as a bioisostere of amide bonds in medicines and agrochemicals, and contribute to the synthesis of peptide medicines that are stable to enzymatic metabolism and possess high lipophilicity [1]. In fact, several inhibitors of the β-site amyloyd β A4 precursor protein cleaving enzyme (BACE1), which is involved in the production of β-amyloid, and fluoroalkene analogs of dipeptidyl peptidase-4 inhibitors have previously been reported [2,3]. These inhibitors possess higher drug efficacies than their parent compounds. Furthermore, fluoroalkenes can be utilized as feedstock for fluoropolymers. Teflon, which is a well-known fluoropolymer with excellent water-repellent and oleophobic properties, is synthesized by polymerizing a monomer called tetrafluoroethylene. As a consequence, convenient and diverse synthetic methods for fluoroalkenes have attracted considerably and become increasingly necessary in pharmaceutical and industrial fields.

Fluoroalkenes have been constructed in a variety of methods [4-14], and one of the methods is to make use of fluorine-containing building blocks. When using them as nucleophilic reagents [15-20], the reaction between anion species, such as fluorine-containing Horner–Wadsworth–Emmons reagents, and carbonyl compounds led to *E*-selective olefination (Scheme 1A) [15]. On the other hand, some reactions with electrophilic fluorine-containing building blocks have been developed [21-25]. Jubault and Poisson et al. reported S_N2' reactions of hydride or alcohols to electrophilic fluorine-containing alkenes gave the corresponding fluoroalkenes (Scheme 1B) [21]. In recent years, many fluorine-containing coupling reagents have been developed. These reagents are easily being converted into multisubstituted fluoroalkenes through cross-coupling using palladium, nickel, copper, ruthenium, and manganese catalysts [26-41]. Hosoya and Niwa et al. published the development of a dual-reactive fluorine-containing C2-unit, which was prepared from trifluoroethanol in two steps in 63% yield, allowed the convergent synthesis of fluoroalkenes (Scheme 1C) [26]. We recently found multihalogenated vinyl ethers **1** could be obtained by the reaction of phenols with 2-bromo-2-chloro-1,1,1-trifluoroethane (halothane) in good yields (Scheme 1D) [42]. Compound **1** has a unique structure possessing three types of halogen atoms, namely bromine, chlorine, and fluorine, and it would be expected to afford multisubstituted fluoroalkenes by installing various substituents to bromine or chlorine atoms as reported by Hosoya and Niwa et al. In this study, we investigated the synthesis of fluoroalkenes **2** or fluoroenynes **3** by Suzuki–Miyaura or Sonogashira cross-couplings with a key building block **1** (Scheme 1D).

Results and Discussion

Optimization of the conditions of cross-coupling reactions

First, we optimized the conditions of the Suzuki–Miyaura cross-coupling in reference to the report by Yang et al. (Table 1) [43]. Upon the treatment of multihalogenated vinyl ether **1a** with phenylboronic acid **4a** (1.3 equiv) and palladium diacetate (10 mol %) as a catalyst at 40 °C, Suzuki–Miyaura cross-coupling proceeded to produce fluoroalkene **2a** in 50% yield (Table 1, entry 1). Increasing the amount of **4a** to 2.0 equiv and

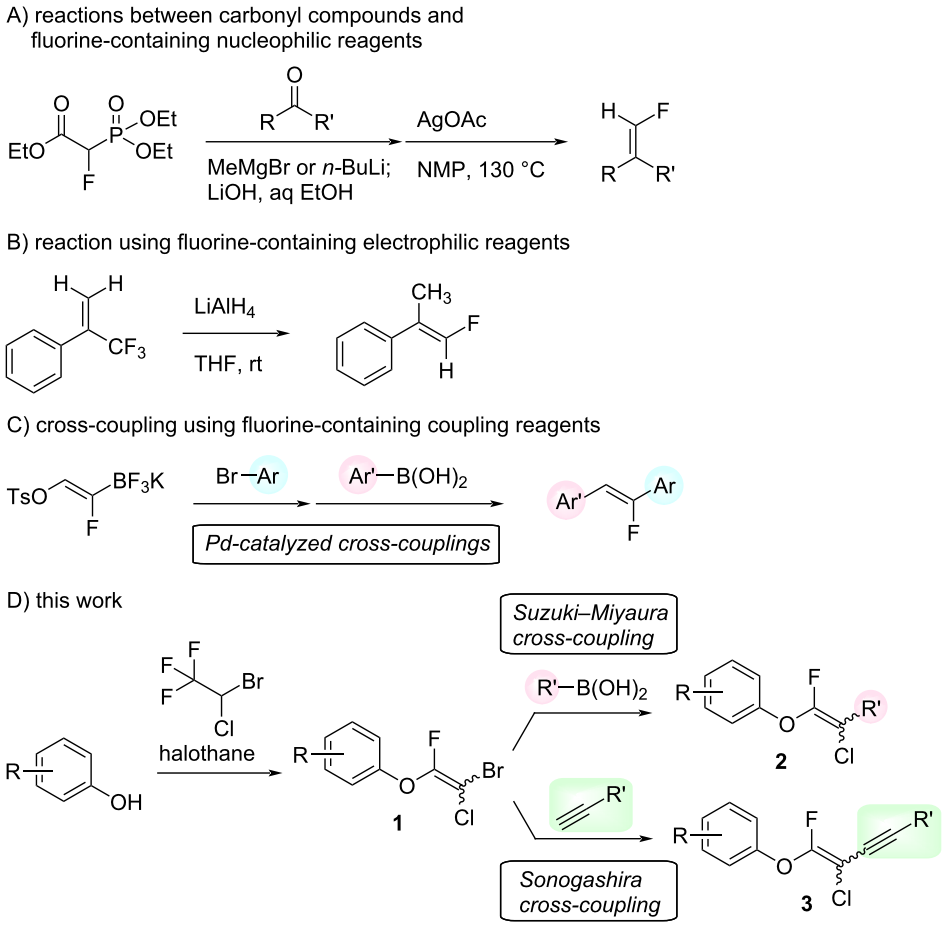

Scheme 1: Synthesis of monofluoroalkenes using fluorine-containing building blocks.

Table 1: Optimization of reaction conditions for Suzuki–Miyaura cross-coupling using multihalogenated vinyl ether **1a**.

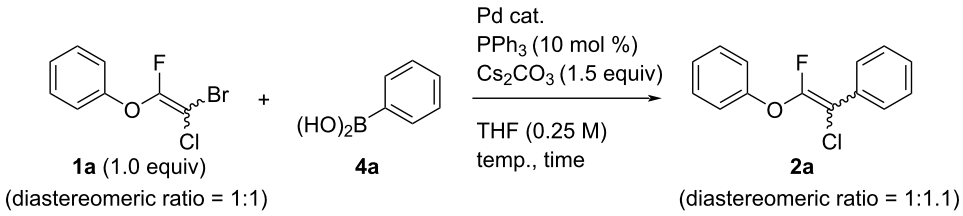

1a (1.0 equiv) (diastereomeric ratio = 1:1) | **4a** | **2a** (diastereomeric ratio = 1:1.1)

Entry	**4a** (equiv)	Pd cat. (mol %)	Temp. (°C)	Time (h)	**2a** (%)[a]
1	1.3	$Pd(OAc)_2$ (10)	40	3.0	50
2	2.0	$Pd(OAc)_2$ (5)	40	2.5	73
3	2.0	$Pd(OAc)_2$ (5)	60	2.5	68
4	2.0	$Pd(OAc)_2$ (5)	reflux	3.5	84
5	2.0	$PdCl_2$ (5)	reflux	3.5	61
6	2.0	$Pd(acac)_2$ (5)	reflux	3.5	12
7	2.0	$[Pd(allyl)Cl]_2$ (5)	reflux	3.5	81
8	2.0	$Pd(PPh_3)_2Cl_2$ (5)	reflux	3.5	84
9	2.0	$Pd[P(o\text{-}Tol)_3]_2Cl_2$ (5)	reflux	3.5	89
10	2.0	$Pd(MeCN)_2Cl_2$ (5)	reflux	3.5	93
11	2.0	$Pd(PhCN)_2Cl_2$ (5)	reflux	3.5	92
12	2.0	$Pd(OCOCF_3)_2$ (5)	reflux	3.5	96
13[b]	2.0	$Pd(OCOCF_3)_2$ (5)	reflux	3.5	12

[a]Isolated yields; [b]no PPh_3.

decreasing the amount of palladium diacetate to 5 mol % improved the reaction yield (Table 1, entry 2). When the reaction mixture was heated to 60 °C or reflux conditions, **2a** could be synthesized in 84% yield under reflux conditions (Table 1, entries 3 and 4). Next, we examined an effective catalyst for the cross-coupling. Reactions using palladium dichloride or bis(2,4-pentanedionato)palladium significantly reduced the yields of **2a** (Table 1, entries 5 and 6, respectively). When an allylpalladium chloride dimer or bis(triphenylphosphine)palladium dichloride were used as catalyst, the reaction proceeded with the same yield as that in Table 1, entry 4 (entries 7 and 8). Utilizing palladium catalyst such as bis(triphenylphosphine)palladium dichloride, all these reactions could convert **1a** into **2a** in good yields (Table 1, entries 9–11). Cross-coupling with palladium bis(trifluoroacetate), which is more reactive than palladium diacetate, gave the corresponding product in high yield of 96% (Table 1, entry 12). Without the addition of triphenylphosphine, the reaction proceeded in only 12% yield (Table 1, entry 13). Thus, it was concluded that triphenylphosphine is necessary for Suzuki–Miyaura cross-coupling of **1** with **4** and that it is involved in the production of palladium(0).

Next, the reaction conditions for the Sonogashira cross-coupling were optimized (Table 2). On the basis of a previous study by Thorand [44], we performed the reaction between fluorine-containing vinyl ether **1a** and 1.05 equiv of trimethylsilylacetylene (**5a**) to afford the corresponding enyne **3a** in 55% yield (Table 2, entry 1). Cross-coupling utilizing a palladium(II) catalysts containing phosphine ligands produced low yields of **3a** (Table 2, entries 2 and 3). In the case of palladium(II), which produced good yields of the Suzuki–Miyaura cross-coupling products, only a small amount of **3a** was obtained (Table 2, entries 4–8). In particular, when the allylpalladium dichloride dimer was used, Sonogashira coupling hardly proceeded at all, and the starting ether **1a** was recovered in an 83% yield (Table 2, entry 6). Zero-valent tetrakis(triphenylphosphine)palladium and tris(dibenzylideneacetone)dipalladium allowed the reaction to undergo in 37% or 23% yields, respectively (Table 2, entries 9 and 10). In entry 11, Table 2, we selected bis(triphenylphosphine)palladium as an effective catalyst, but increase of **5a** to 1.5 equiv did not improve the reaction yield. Diluting the reaction concentration from 0.83 M to 0.2 M achieved to give **3a** in a 63% yield (Table 2, entry 12). Increasing the amount of palladium catalyst to 4 mol % led to the conversion of **1a** into **3a** in 77% yield (Table 2, entry 13). In addition, using 2.0 equiv of **5a** gave **3a** in high 80% yield (Table 2, entry 14).

Based on these results, we determined entry 13 in Table 1 and entry 14 in Table 2 as the optimum reaction conditions. We used **1** as a mixture of diastereomers (diastereomer ratio = 1:1) for cross-coupling, and the corresponding compounds **2** and **3**

Table 2: Optimization of reaction conditions for Sonogashira cross-coupling using multihalogenated vinyl ether **1a**.

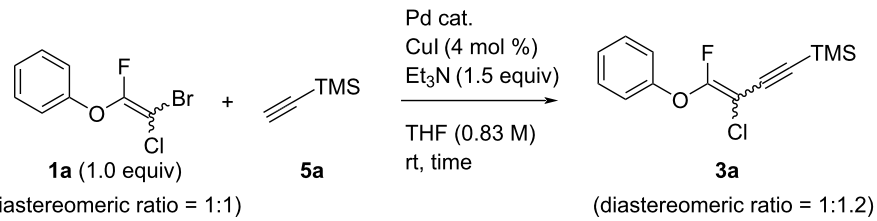

1a (1.0 equiv) (diastereomeric ratio = 1:1) | **5a** | **3a** (diastereomeric ratio = 1:1.2)

Entry	**5a** (equiv)	Pd cat. (mol %)	Time (h)	**3a** (%)[a]
1	1.05	$Pd(PPh_3)_2Cl_2$ (2)	6.5	55
2	1.05	$Pd[P(o\text{-}Tol)_3]_2Cl_2$ (2)	24	14
3	1.05	$Pd(PCy_3)_2Cl_2$ (2)	24	0
4	1.05	$Pd(OAc)_2$ (2)	20	6
5	1.05	$PdCl_2$ (2)	24	13
6[b]	1.05	$[Pd(allyl)Cl]_2$ (2)	18.5	0
7	1.05	$Pd(MeCN)_2Cl_2$ (2)	25.5	13
8	1.05	$Pd(PhCN)_2Cl_2$ (2)	24	10
9	1.05	$Pd(PPh_3)_4$ (2)	21.5	37
10	1.05	$Pd_2(dba)_3$ (2)	24	23
11	1.5	$Pd(PPh_3)_2Cl_2$ (2)	19	53
12[c]	1.5	$Pd(PPh_3)_2Cl_2$ (2)	17	63
13[c]	1.5	$Pd(PPh_3)_2Cl_2$ (4)	18	77
14[c]	2.0	$Pd(PPh_3)_2Cl_2$ (4)	19	80

[a]Isolated yields; [b]Recovery of **1a** was 83% yield; [c]THF (0.2 M) was used.

were obtained as mixtures of diastereomers in a certain ratio as estimated by proton and fluorine NMR spectroscopy.

Substrate scope for cross-coupling reactions

The substrate scope was investigated using various boronic acids **4** and alkynes **5** in cross-coupling reactions using **1** (Table 3 and Table 4). *p*-Tolylboronic acid **4b** provided **2b** quantitatively, whereas *m*- and *o*-tolylboronic acids **4c** and **4d** produced **2c** and **2d** in low yields because the methyl group was positioned near the reaction site (Table 3, entries 1–3). Introduction of 3,4-methylenedioxyphenyl (**4e**) or *p*-fluorophenyl groups (**4f**) to **1a** proceeded in high yields (Table 3, entries 4 and 5). Boronic acids with carbonyl groups such as acetyl, ester or formyl moieties in *para* position (**4g–i**) underwent the cross-coupling in 76, 96 or 77% yields (Table 3, entries 6–8). The reaction between **1a** and **4j**, which contains an electron-withdrawing nitro group, afforded **2j** in 88% yield (Table 3, entry 9). Although *p*-hydroxyphenylboronic acid (**4k**) gave **2k** in only 9% yield, *m*-aminophenylboronic acid (**4l**) provided **2l** in high yield (Table 3, entries 10 and 11). We predicted that the product yield would decrease because **2k** is labile in column chromatography. Utilizing a boronic acid bearing an *n*-butyl group as a primary alkyl group (**4m**), the cross-coupling did not proceed due to β-elimination (Table 3, entry 12). In contrast, the reaction with cyclopropylboronic acid (**4n**) achieved to give **2n** in a 71% yield (Table 3, entry 13). When thiopheneboronic acid **4o** was used as a coupling partner, the thiophene ring could be installed on **1a** in a comparatively low yield of 31% (Table 3, entry 14). In addition, we investigated the substrate scope of **1** in the Suzuki–Miyaura cross-coupling. The reaction of **1b** or **1c**, which had a *m*-methoxy or *p*-nitro group on the benzene ring, with **4a** proceeded smoothly to furnish **2p** or **2q** in good yieds (Table 3, entries 15 and 16). A phenyl group could be introduced into **1d** possessing an ester moiety in moderate yield, whereas the cross-coupling between **1e**, derived from *m*-aminophenol, and **4a** proceeded in only 15% yield (Table 3, entries 17 and 18).

We performed Sonogashira cross-couplings between **1** and a variety of alkynes **5** (Table 4). Arylacetylenes, which have electron-donating substituents on the aromatic ring (**5b–f**), and 2-naphthylacetylene (**5g**) provided the corresponding enynes (**3b–g**) in 43–92% yields (Table 4, entries 1–6). On the contrary, electron-withdrawing substituents such as chloro, trifluoromethyl and nitro groups resulted in low cross-coupling yields (**3h–j**) (Table 4, entries 7–9). *p*-Acetyl or *p*-formylphenylacetylene (**5k** or **5l**) could be introduced into **1a** in 76% or 52% yields, respectively (Table 4, entries 10 and 11). Reac-

Table 3: Cross-coupling reactions between multihalogenated vinyl ethers **1** and various boronic acids **4**.

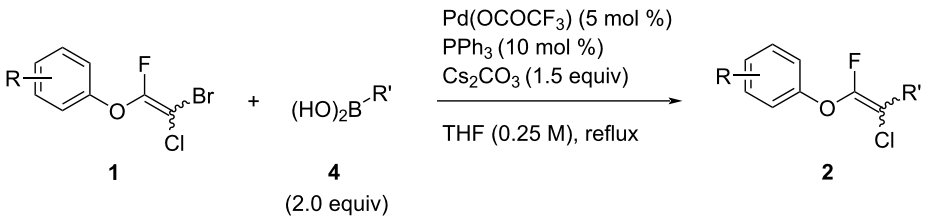

Entry	**1** (diastereomeric ratio)	**4**	**2** (diastereomeric ratio)	Time (h)	Yield (%)[a]
1	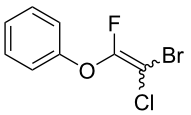 **1a** (1:1)	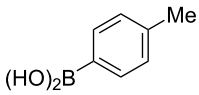 **4b**	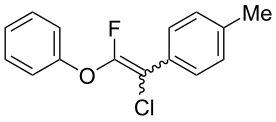 **2b** (1:1)	3.5	98
2[b]	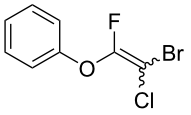 **1a** (1:1)	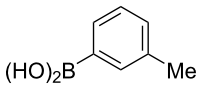 **4c**	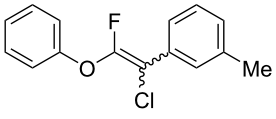 **2c** (1:1)	2.5	26
3	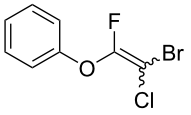 **1a** (1:1)	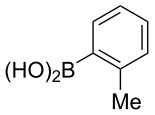 **4d**	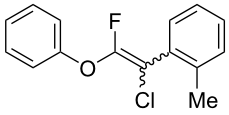 **2d** (1:1)	3.5	16
4	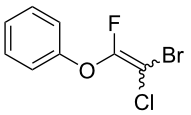 **1a** (1:1)	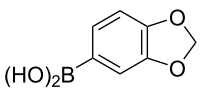 **4e**	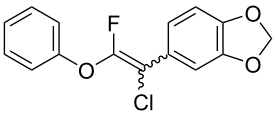 **2e** (1:1)	3.5	85
5	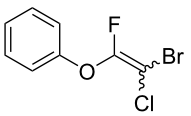 **1a** (1:1)	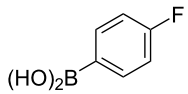 **4f**	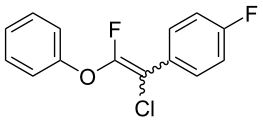 **2f** (1:1)	3.5	94
6	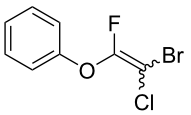 **1a** (1:1)	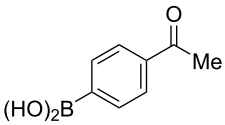 **4g**	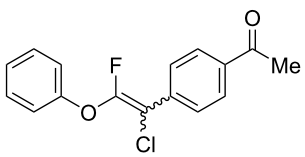 **2g** (1:1)	2.5	76
7	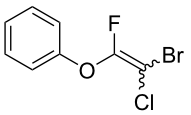 **1a** (1:1)	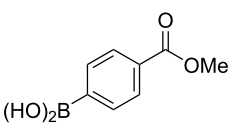 **4h**	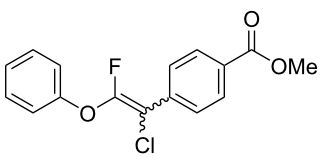 **2h** (1:1)	1.5	96

Table 3: Cross-coupling reactions between multihalogenated vinyl ethers **1** and various boronic acids **4**. (continued)

8	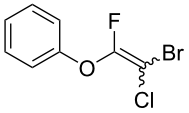 **1a** (1:1)	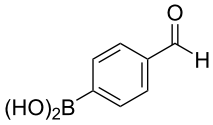 **4i**	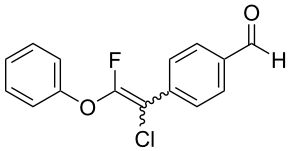 **2i** (1:1)	3.5	77
9	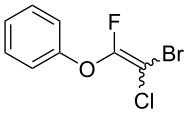 **1a** (1:1)	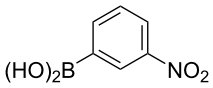 **4j**	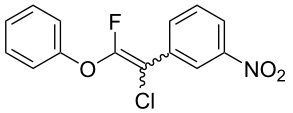 **2j** (1:1:1)	3.0	88
10	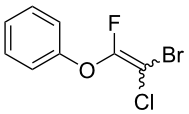 **1a** (1:1)	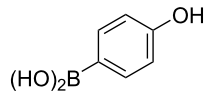 **4k**	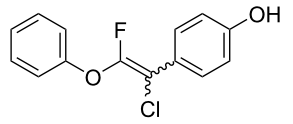 **2k** (1:1.4)	6.5	9
11	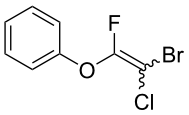 **1a** (1:1)	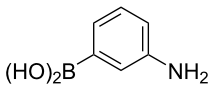 **4l**	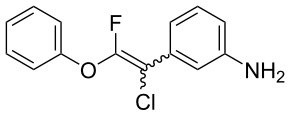 **2l** (1:1)	4.0	92
12	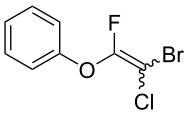 **1a** (1:1)	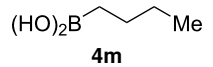 **4m**	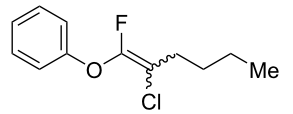 **2m** (1:1)	3.5	trace
13	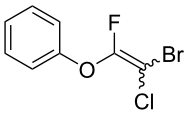 **1a** (1:1)	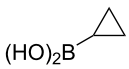 **4n**	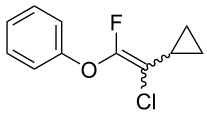 **2n** (1:1)	5.0	71
14	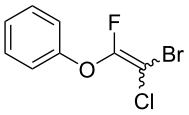 **1a** (1:1)	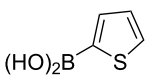 **4o**	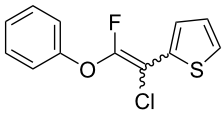 **2o** (1:1.1)	4.0	31
15	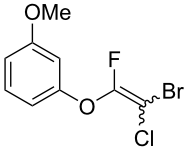 **1b** (1:1)	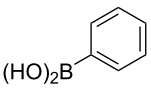 **4a**	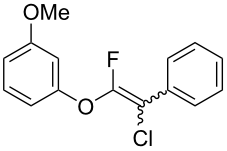 **2p** (1:1)	3.5	62
16	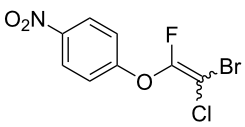 **1c** (1:1)	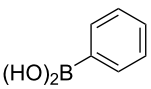 **4a**	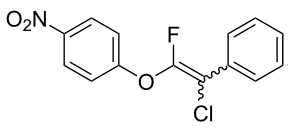 **2q** (1:1)	5.5	85

Table 3: Cross-coupling reactions between multihalogenated vinyl ethers **1** and various boronic acids **4**. (continued)

17	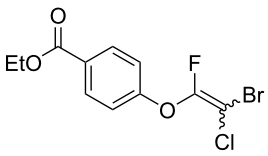 **1d** (1:1)	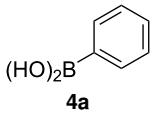 **4a**	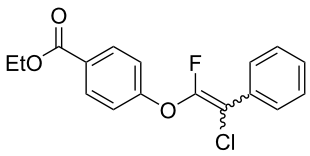 **2r** (1:1.6)	3.5	45
18[c]	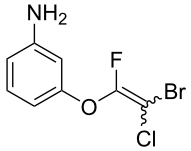 **1e** (1:1)	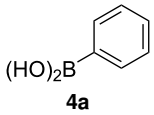 **4a**	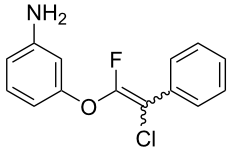 **2s** (1:1.2)	21.5	15

[a]Isolated yields; [b]**1** (1.5 equiv) and **2** (1.0 equiv) were used; [c]DME was used as a solvent.

Table 4: Cross-coupling reactions between multihalogenated vinyl ethers **1** and various alkynes **5**.

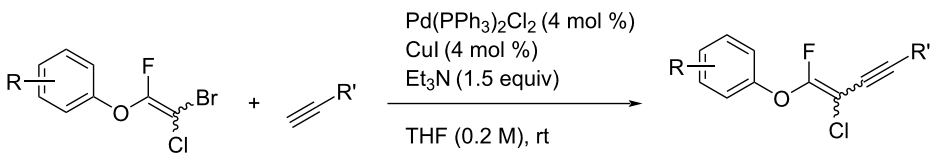

1 **5** **3**

Entry	**1** (diastereomeric ratio)	**5**	**3** (diastereomeric ratio)	Time (h)	Yield (%)[a]
1	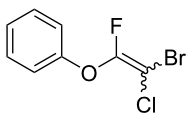 **1a** (1:1)	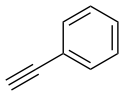 **5b**	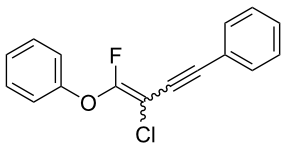 **3b** (1:1.1)	18.5	92
2[b]	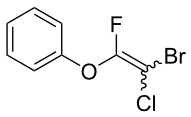 **1a** (1:1)	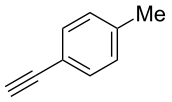 **5c**	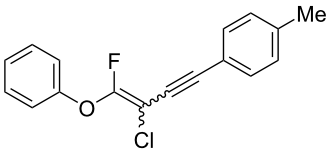 **3c** (1:1.4)	3.5	74
3[b]	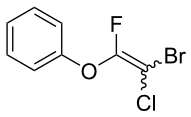 **1a** (1:1)	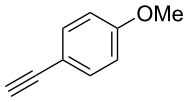 **5d**	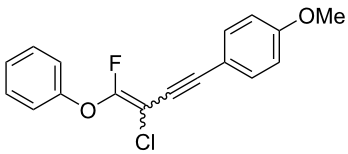 **3d** (1:1.4)	2.5	49

Table 4: Cross-coupling reactions between multihalogenated vinyl ethers **1** and various alkynes **5**. (continued)

4[b]	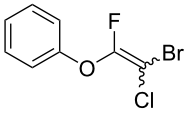 **1a** (1:1)	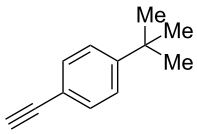 **5e**	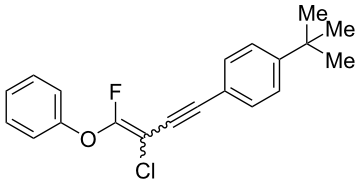 **3e** (1:1.4)	4.5	70
5	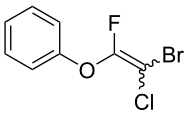 **1a** (1:1)	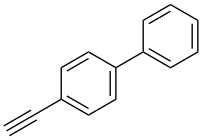 **5f**	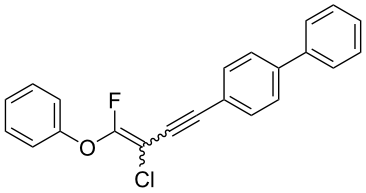 **3f** (1:1.1)	4.5	43
6	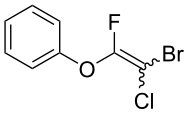 **1a** (1:1)	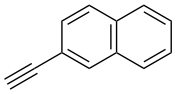 **5g**	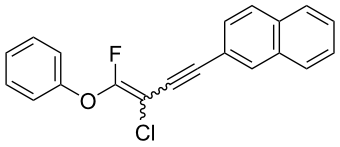 **3g** (1:1.2)	17.5	59
7[c]	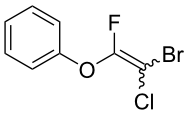 **1a** (1:1)	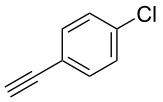 **5h**	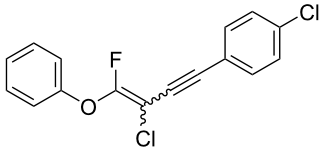 **3h** (1:1)	16	39
8	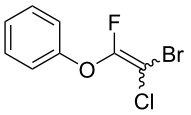 **1a** (1:1)	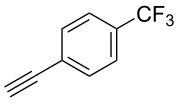 **5i**	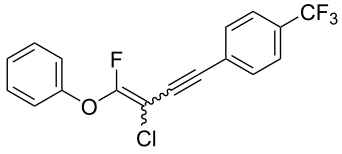 **3i** (1:1.2)	14	49
9	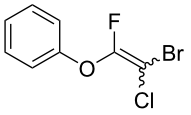 **1a** (1:1)	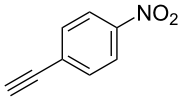 **5j**	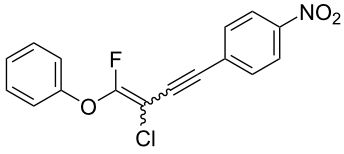 **3j** (1:1.3)	17	42
10	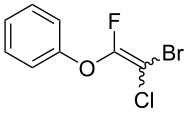 **1a** (1:1)	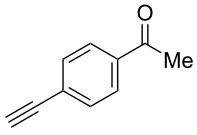 **5k**	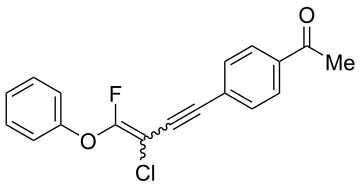 **3k** (1:1.1)	16.5	76

Table 4: Cross-coupling reactions between multihalogenated vinyl ethers **1** and various alkynes **5**. (continued)

11	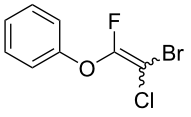 **1a** (1:1)	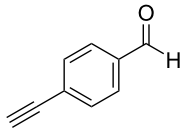 **5l**	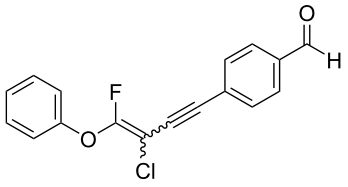 **3l** (1:1.1)	28.5	52
12	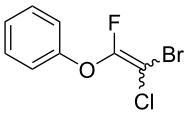 **1a** (1:1)	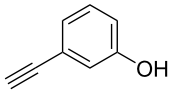 **5m**	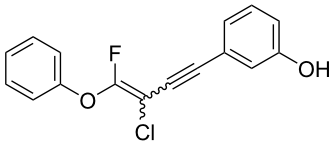 **3m** (1:1)	15.5	38
13	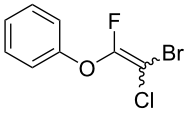 **1a** (1:1)	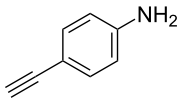 **5n**	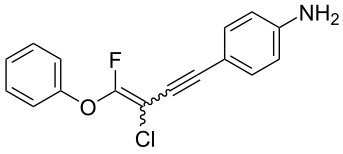 **3n** (1:1.1)	15.5	87
14[b]	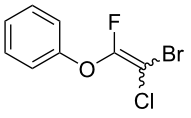 **1a** (1:1)	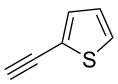 **5o**	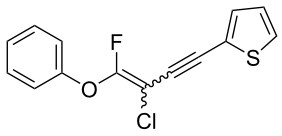 **3o** (1:1)	15	37
15[d]	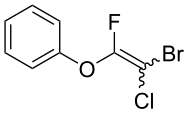 **1a** (1:1)	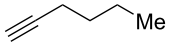 **5p**	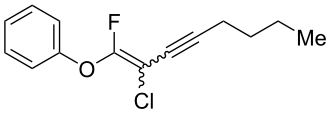 **3p** (1:1.1)	15	89
16	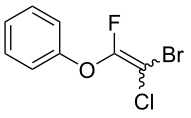 **1a** (1:1)	 **5q**	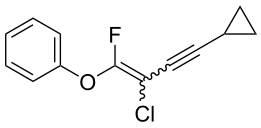 **3q** (1:1.4)	14.5	86
17	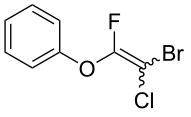 **1a** (1:1)	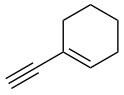 **5r**	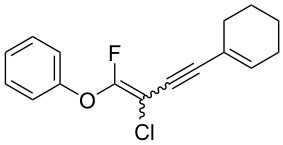 **3r** (1:1.4)	15	52
18	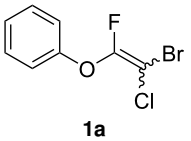 **1a** (1:1)	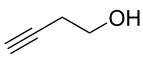 **5s**	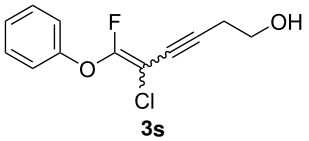 **3s** (1:1)	13.5	53

Table 4: Cross-coupling reactions between multihalogenated vinyl ethers **1** and various alkynes **5**. (continued)

19	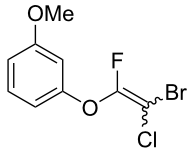 **1b** (1:1)	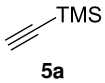 **5a**	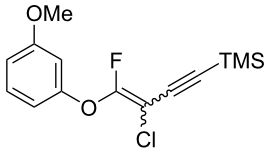 **3t** (1:1.1)	12.5	35
20[e]	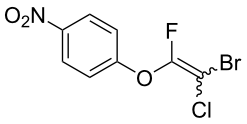 **1c** (1:1)	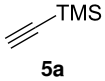 **5a**	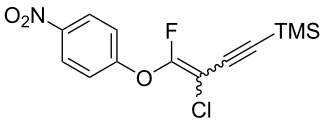 **3u** (1:1.2)	22	29
21	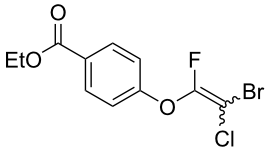 **1d** (1:1.1)	 **5a**	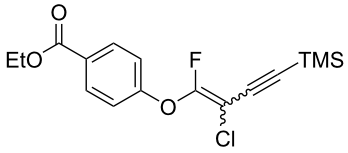 **3v** (1:1.6)	20.5	35
22[f]	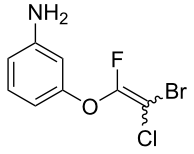 **1e** (1:1.1)	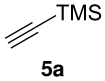 **5a**	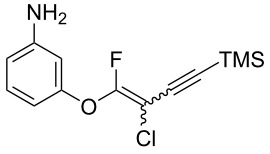 **3w** (1:1.3)	110	7

[a]Isolated yields; [b]**1** (2.0 equiv) and **5** (1.0 equiv) were used; [c]**1** (2.0 equiv) and **5** (1.0 equiv) were used; [d]reaction temperature was 50 °C; [e]**5** (1.3 equiv) was used; [f]reaction temperature was rt to 50 °C.

tions using acetylenes possessing a hydroxy group, amino group and thiophene proceeded well (**3m**–**o**) (Table 4, entries 12–14). Hexa-1-yne **5p** and cyclopropylacetylene (**5q**) afforded **3p** and **3q**, respectively, in high yields without byproduct formation (Table 4, entries 15 and 16). Enyne compound **5r** and 3-butyn-1-ol **5s** also participated in cross-coupling reactions and products **3r** and **3s** could be obtained in moderate yields of 52 and 53% (Table 4, entries 17 and 18). Then, we attempted the cross-coupling between **1** derived from various phenols and **5a**. Vinyl ethers **1b**–**d** were converted into enynes **3t**–**v** in 29–35% yields (Table 4, entries 19–21). The reaction using **1e**, which bears an amino group on the benzene ring, did not complete despite requiring a long reaction time (Table 4, entry 22).

Therefore, Suzuki–Miyaura and Sonogashira cross-coupling with **1** has a broad substrate scope and can be used to synthesize various fluoroalkenes **2** and fluoroenyne **3**. We speculate that these reaction mechanisms were similar to general cross-coupling mechanisms [45,46].

Conclusion

We used Suzuki–Miyaura and Sonogashira cross-coupling to exploit the unique structure of multihalogenated fluorovinyl ethers **1** for the synthesis of many kinds of fluoroalkenes **2** and fluoroenynes **3** in moderate to high yields. The synthesized alkenes **2** still possess reactive chlorine atoms and phenoxy groups. Thus, new multisubstituted fluoroalkenes could be synthesized by applying other cross-couplings to **2**. In addition, enynes **3** could be converted into derivatives, such as fluorine-containing alkynylalcohols [47], allene compounds [48-50], and heterocycles [51,52]. However, further experiments are required to expand the abilities of **2** and **3** as new fluorine-containing building blocks.

Experimental

General information

^{1}H NMR, ^{19}F NMR, and ^{13}C NMR spectra were recorded on JEOL ECZ 400S spectrometers. Chemical shifts of ^{1}H NMR are reported in ppm from tetramethylsilane (TMS) as an internal standard. Chemical shifts of ^{13}C NMR are reported in ppm from

the center line of the triplet at 77.16 ppm for deuteriochloroform. Chemical shifts of ^{19}F NMR are reported in ppm from $CFCl_3$ as an internal standard. All data are reported as follows: chemical shifts, multiplicity (s = singlet, d = doublet, t = triplet, q = quartet, sep = septet, br = broad, brd = broad-doublet, m = multiplet), coupling constants (Hz), relative integration value. Mass spectra were obtained on a JEOL JMS-700T spectrometer (EI). Melting points were measured on a Yanaco MP-500V.

Materials

All commercially available materials were used as received without further purification. All experiments were carried out under argon atmosphere in flame-dried glassware using standard inert techniques for introducing reagents and solvents unless otherwise noted.

Suzuki–Miyaura cross-coupling with multihalogenated vinyl ethers **1**

To a solution of **1** (1.0 equiv), triphenylphosphine (10 mol %), cesium carbonate (1.5 equiv), palladium bis(trifluoroacetate) (5 mol %) in THF (2.0 mL) was added the respective boronic acid derivative **4** (2.0 equiv). The reaction solution was refluxed for 3.5 h. The reaction mixture was quenched by the addition of water (40 mL) at 0 °C and extracted with EtOAc. The organic phase was washed with brine (40 mL), dried over Na_2SO_4 and filtered. Then, the filtrate was concentrated under reduced pressure. The residue was purified by column chromatography and preparative TLC to afford **2**.

2-Chloro-1-fluoro-2-phenylethenyl phenyl ether (2a): Compound **2a** was purified by column chromatography and preparative TLC (hexane only), and obtained in 96% yield (122.0 mg) as a pale yellow oil; ^{1}H NMR (400 MHz, $CDCl_3$) δ 7.04–7.22 (m, 2H), 7.26–7.50 (m, 6H), 7.55–7.69 (m, 2H); ^{13}C NMR (100 MHz, $CDCl_3$) δ 101.4 (d, J = 30.9 Hz), 102.5 (d, J = 48.0 Hz), 116.5 (d, J = 3.8 Hz), 124.8, 127.3, 127.4, 127.9 (d, J = 3.2 Hz), 128.2 (d, J = 5.5 Hz), 128.5 (d, J = 7.2 Hz), 128.6 (d, J = 11.8 Hz), 128.9, 130.1 (d, J = 4.2 Hz), 132.46 (d, J = 5.7 Hz), 132.52, 141.3, 151.2 (d, J = 286.1 Hz), 151.5 (d, J = 287.3 Hz), 154.3 (d, J = 3.4 Hz), 154.4 (d, J = 3.3 Hz); ^{19}F NMR (376 MHz, $CDCl_3$) δ −80.8 (s) and −87.6 (s) (1F, 1:1.1); EIMS (*m*/*z*): 248, 250 $[M]^+$; HREIMS $[M]^+$ (*m*/*z*): calcd. for $C_{14}H_{10}ClFO$, 248.0402; found, 248.0404.

Sonogashira cross-coupling with multihalogenated vinyl ethers **1**

To a solution of **1** (1.0 equiv), copper iodide (4 mol %), bis(triphenylphosphine)palladium dichloride (4 mol %) and triethylamine (1.5 equiv) in THF (2.5 mL) was added the respective alkyne **5** (2.0 equiv). The reaction solution was stirred at room temperature until **1** was disappeared. The reaction mixture was evaporated and concentrated under reduced pressure. The residue was purified by column chromatography and preparative TLC to afford **3**.

(3-Chloro-4-fluoro-4-phenoxybut-3-en-1-yn-1-yl)trimethylsilane (3a): Reaction time was 19 h. **3a** was purified by column chromatography (pentane only), and obtained in 80% yield (107.2 mg) as a yellow oil; ^{1}H NMR (400 MHz, $CDCl_3$) δ 0.13 (s) and 0.24 (s) (9H), 7.08 (d, J = 8.0 Hz, 2H), 7.07–7.15 (m, 2H), 7.16–7.23 (m, 1H) , 7.33–7.42 (m, 1H); ^{13}C NMR (100 MHz, $CDCl_3$) δ −0.36, −0.26, 85.2 (d, J = 44.8 Hz), 85.6 (d, J = 53.3 Hz), 94.5 (d, J = 47.8 Hz), 94.6 (d, J = 43.5 Hz), 103.7 (d, J = 63.4 Hz), 103.8 (d, J = 66.3 Hz), 117.2, 117.3, 125.2, 125.3, 130.0, 130.1, 154.00 (d, J = 75.1 Hz), 154.02 (d, J = 75.8 Hz), 158.2 (d, J = 292.4 Hz), 158.8 (d, J = 290.1 Hz); ^{19}F NMR (376 MHz, $CDCl_3$) δ −73.3 (s) and −78.4 (s) (1F, 1:1.2); EIMS *m*/*z*: 268 (M^+); HREIMS $[M]^+$ (*m*/*z*): calcd. for $C_{13}H_{14}ClFOSi$, 268.0486; found, 268.0490.

Supporting Information

Supporting Information File 1

Characterization data for **2b–s** and **3b–w,** and copies of ^{1}H, ^{13}C, and ^{19}F NMR spectra.
[https://www.beilstein-journals.org/bjoc/content/supplementary/1860-5397-20-226-S1.pdf]

ORCID® iDs

Yukiko Karuo - https://orcid.org/0000-0002-2106-3399
Atsushi Tarui - https://orcid.org/0009-0003-7461-2763
Kazuyuki Sato - https://orcid.org/0000-0001-6572-602X
Masaaki Omote - https://orcid.org/0000-0003-1210-1768

Data Availability Statement

All data that supports the findings of this study is available in the published article and/or the supporting information of this article.

References

1. Drouin, M.; Paquin, J.-F. *Beilstein J. Org. Chem.* **2017,** *13,* 2637–2658. doi:10.3762/bjoc.13.262
2. Frohn, M.; Liu, L.; Siegmund, A. C.; Qian, W.; Amegadzie, A.; Chen, N.; Tan, H.; Hickman, D.; Wood, S.; Wen, P. H.; Bartberger, M. D.; Whittington, D. A.; Allen, J. R.; Bourbeau, M. P. *Bioorg. Med. Chem. Lett.* **2020,** *30,* 127240. doi:10.1016/j.bmcl.2020.127240
3. Van der Veken, P.; Kertèsz, I.; Senten, K.; Haemers, A.; Augustyns, K. *Tetrahedron Lett.* **2003,** *44,* 6231–6234. doi:10.1016/s0040-4039(03)01542-9

4. Lee, S. H.; Schwartz, J. *J. Am. Chem. Soc.* **1986,** *108,* 2445–2447. doi:10.1021/ja00269a052
5. Suga, H.; Hamatani, T.; Guggisberg, Y.; Schlosser, M. *Tetrahedron* **1990,** *46,* 4255–4260. doi:10.1016/s0040-4020(01)86762-4
6. Salim, S. S.; Bellingham, R. K.; Satcharoen, V.; Brown, R. C. D. *Org. Lett.* **2003,** *5,* 3403–3406. doi:10.1021/ol035065w
7. Koh, M. J.; Nguyen, T. T.; Zhang, H.; Schrock, R. R.; Hoveyda, A. H. *Nature* **2016,** *531,* 459–465. doi:10.1038/nature17396
8. Kojima, R.; Kubota, K.; Ito, H. *Chem. Commun.* **2017,** *53,* 10688–10691. doi:10.1039/c7cc05225a
9. Hu, J.; Han, X.; Yuan, Y.; Shi, Z. *Angew. Chem., Int. Ed.* **2017,** *56,* 13342–13346. doi:10.1002/anie.201708224
10. Vandamme, M.; Paquin, J.-F. *Org. Lett.* **2017,** *19,* 3604–3607. doi:10.1021/acs.orglett.7b01581
11. Zhou, Y.; Fan, B.; Chen, J.; He, Z.; Fan, R.; Sun, W.; Li, K. Preparation method of fluorinated olefin and its application in preparation of medical material, pesticide special material and organic chemical material. Chin. Patent CN111170856, May 19, 2020.
12. Du, H.-W.; Sun, J.; Gao, Q.-S.; Wang, J.-Y.; Wang, H.; Xu, Z.; Zhou, M.-D. *Org. Lett.* **2020,** *22,* 1542–1546. doi:10.1021/acs.orglett.0c00134
13. Li, K.; Chen, J.; Yang, C.; Zhang, K.; Pan, C.; Fan, B. *Org. Lett.* **2020,** *22,* 4261–4265. doi:10.1021/acs.orglett.0c01294
14. Yang, H.; Wang, J.; Jin, C.; Li, X.; Xu, X. *J. Org. Chem.* **2023,** *88,* 12074–12078. doi:10.1021/acs.joc.3c00594
15. Volchkov, I.; Powell, B. V.; Zatolochnaya, O. V.; Leung, J. C.; Pennino, S.; Wu, L.; Gonnella, N. C.; Bhaskararao, B.; Kozlowski, M. C.; Reeves, J. T. *J. Org. Chem.* **2023,** *88,* 10881–10904. doi:10.1021/acs.joc.3c00917
16. Schlosser, M.; Zimmermann, M. *Synthesis* **1969,** 75–76. doi:10.1055/s-1969-20377
17. Tsai, H.-J. *Tetrahedron Lett.* **1996,** *37,* 629–632. doi:10.1016/0040-4039(95)02218-x
18. Prakash, G. K. S.; Shakhmin, A.; Zibinsky, M.; Ledneczki, I.; Chacko, S.; Olah, G. A. *J. Fluorine Chem.* **2010,** *131,* 1192–1197. doi:10.1016/j.jfluchem.2010.06.009
19. Liu, Q.; Shen, X.; Ni, C.; Hu, J. *Angew. Chem., Int. Ed.* **2017,** *56,* 619–623. doi:10.1002/anie.201610127
20. Mandal, D.; Gupta, R.; Young, R. D. *J. Am. Chem. Soc.* **2018,** *140,* 10682–10686. doi:10.1021/jacs.8b06770
21. Poutrel, P.; Pannecoucke, X.; Jubault, P.; Poisson, T. *Org. Lett.* **2020,** *22,* 4858–4863. doi:10.1021/acs.orglett.0c01701
22. Debien, L.; Quiclet-Sire, B.; Zard, S. S. *Org. Lett.* **2012,** *14,* 5118–5121. doi:10.1021/ol3023903
23. Hamel, J.-D.; Cloutier, M.; Paquin, J.-F. *Org. Lett.* **2016,** *18,* 1852–1855. doi:10.1021/acs.orglett.6b00590
24. Carreras, V.; Ollevier, T. *J. Org. Chem.* **2021,** *86,* 13160–13168. doi:10.1021/acs.joc.1c01724
25. Li, H.; Zhu, C. *J. Org. Chem.* **2023,** *88,* 4134–4144. doi:10.1021/acs.joc.2c02568
26. Isoda, M.; Uetake, Y.; Takimoto, T.; Tsuda, J.; Hosoya, T.; Niwa, T. *J. Org. Chem.* **2021,** *86,* 1622–1632. doi:10.1021/acs.joc.0c02474
27. Heinze, P. L.; Burton, D. J. *J. Org. Chem.* **1988,** *53,* 2714–2720. doi:10.1021/jo00247a010
28. Matthews, D. P.; Gross, R. S.; McCarthy, J. R. *Tetrahedron Lett.* **1994,** *35,* 1027–1030. doi:10.1016/s0040-4039(00)79956-4
29. Raghavanpillai, A.; Burton, D. J. *J. Org. Chem.* **2004,** *69,* 7083–7091. doi:10.1021/jo049179c
30. Andrei, D.; Wnuk, S. F. *J. Org. Chem.* **2006,** *71,* 405–408. doi:10.1021/jo051980e
31. Ohashi, M.; Kambara, T.; Hatanaka, T.; Saijo, H.; Doi, R.; Ogoshi, S. *J. Am. Chem. Soc.* **2011,** *133,* 3256–3259. doi:10.1021/ja109911p
32. Liu, J.; Ren, Q.; Zhang, X.; Gong, H. *Angew. Chem., Int. Ed.* **2016,** *55,* 15544–15548. doi:10.1002/anie.201607959
33. Cai, S.-H.; Ye, L.; Wang, D.-X.; Wang, Y.-Q.; Lai, L.-J.; Zhu, C.; Feng, C.; Loh, T.-P. *Chem. Commun.* **2017,** *53,* 8731–8734. doi:10.1039/c7cc04131d
34. Sakaguchi, H.; Uetake, Y.; Ohashi, M.; Niwa, T.; Ogoshi, S.; Hosoya, T. *J. Am. Chem. Soc.* **2017,** *139,* 12855–12862. doi:10.1021/jacs.7b08343
35. Sakaguchi, H.; Ohashi, M.; Ogoshi, S. *Angew. Chem., Int. Ed.* **2018,** *57,* 328–332. doi:10.1002/anie.201710866
36. Tian, H.; Yang, S.; Wang, X.; Xu, W.; Liu, Y.; Li, Y.; Wang, Q. *J. Org. Chem.* **2021,** *86,* 12772–12782. doi:10.1021/acs.joc.1c01363
37. Wang, C.; Liu, Y.-C.; Xu, M.-Y.; Xiao, B. *Org. Lett.* **2021,** *23,* 4593–4597. doi:10.1021/acs.orglett.1c01289
38. Wang, Y.; Ma, Q.; Tsui, G. C. *Org. Lett.* **2021,** *23,* 5241–5245. doi:10.1021/acs.orglett.1c01768
39. Wu, X.; Zeng, Y.; Jiang, Z.-T.; Zhu, Y.; Xie, L.; Xia, Y. *Org. Lett.* **2022,** *24,* 8429–8434. doi:10.1021/acs.orglett.2c03544
40. Liu, F.; Zhuang, Z.; Qian, Q.; Zhang, X.; Yang, C. *J. Org. Chem.* **2022,** *87,* 2730–2739. doi:10.1021/acs.joc.1c02662
41. Wang, Y.; Tsui, G. C. *Org. Lett.* **2023,** *25,* 6217–6221. doi:10.1021/acs.orglett.3c02452
42. Karuo, Y.; Tarui, A.; Sato, K.; Kawai, K.; Omote, M. *Beilstein J. Org. Chem.* **2022,** *18,* 1567–1574. doi:10.3762/bjoc.18.167
43. Yang, Z.; Chen, X.; Kong, W.; Xia, S.; Zheng, R.; Luo, F.; Zhu, G. *Org. Biomol. Chem.* **2013,** *11,* 2175–2185. doi:10.1039/c3ob27307e
44. Thorand, S.; Krause, N. *J. Org. Chem.* **1998,** *63,* 8551–8553. doi:10.1021/jo9808021
45. Miyaura, N.; Suzuki, A. *Chem. Rev.* **1995,** *95,* 2457–2483. doi:10.1021/cr00039a007
46. Sonogashira, K.; Tohda, Y.; Hagihara, N. *Tetrahedron Lett.* **1975,** *16,* 4467–4470. doi:10.1016/s0040-4039(00)91094-3
47. Nguyen, K. D.; Herkommer, D.; Krische, M. J. *J. Am. Chem. Soc.* **2016,** *138,* 5238–5241. doi:10.1021/jacs.6b02279
48. Mori, Y.; Onodera, G.; Kimura, M. *Chem. Lett.* **2014,** *43,* 97–99. doi:10.1246/cl.130865
49. Huang, Y.; del Pozo, J.; Torker, S.; Hoveyda, A. H. *J. Am. Chem. Soc.* **2018,** *140,* 2643–2655. doi:10.1021/jacs.7b13296
50. Xu, T.; Wu, S.; Zhang, Q.-N.; Wu, Y.; Hu, M.; Li, J.-H. *Org. Lett.* **2021,** *23,* 8455–8459. doi:10.1021/acs.orglett.1c03179
51. Chun, Y. S.; Lee, J. H.; Kim, J. H.; Ko, Y. O.; Lee, S.-g. *Org. Lett.* **2011,** *13,* 6390–6393. doi:10.1021/ol202691b
52. Wang, Y.-J.; Zhang, Y.; Qiang, Z.; Liang, J.-Y.; Chen, Z. *Chem. Commun.* **2021,** *57,* 12607–12610. doi:10.1039/d1cc05260h

BEILSTEIN JOURNAL OF ORGANIC CHEMISTRY

Access to optically active tetrafluoroethylenated amines based on [1,3]-proton shift reaction

Yuta Kabumoto[1], Eiichiro Yoshimoto[1], Bing Xiaohuan[1], Masato Morita[2], Motohiro Yasui[1], Shigeyuki Yamada[1] and Tsutomu Konno[*1]

Full Research Paper

Open Access

Address:
[1]Faculty of Molecular Chemistry and Engineering, Kyoto Institute of Technology, Matsugasaki, Sakyo-ku, Kyoto 606-8585, Japan and [2]Department of Materials Science and Engineering, Graduate School of Science and Engineering, Ibaraki University, 4-12-1 Nakanarusawa, Hitachi, Ibaraki 316-8511, Japan

Email:
Tsutomu Konno[*] - konno@kit.ac.jp

* Corresponding author

Keywords:
amine; chirality transfer; [1,3]-proton shift reaction; tetrafluoroethylene fragment

Beilstein J. Org. Chem. **2024,** *20,* 2776–2783.
https://doi.org/10.3762/bjoc.20.233

Received: 22 July 2024
Accepted: 25 October 2024
Published: 01 November 2024

This article is part of the thematic issue "Organofluorine chemistry VI".

Guest Editor: D. O'Hagan

Abstract

Treatment of various (*R*)-*N*-(2,2,3,3-tetrafluoropent-4-en-1-ylidene)-1-phenylethylamine derivatives with 2.4 equiv of DBU in toluene at room temperature to 50 °C for 24 h led to a smooth [1,3]-proton shift reaction with a high chirality transfer, affording the corresponding rearranged products in acceptable yields. Without purification, these products were subjected to acid hydrolysis and the subsequent *N*-Cbz protection, providing the optically active tetrafluoroethylenated amides in moderate three-step yields.

Introduction

A fluorine atom has quite peculiar chemical and physical properties compared to others, and hence changes in molecular properties resulting from the introduction of fluorine atom(s) into organic molecules are also significantly unique, and often extremely noticeable even when the number of the atom introduced is small [1-3]. By skillfully utilizing such characteristics, fluorine-containing organic molecules have established themselves as indispensable compounds in various frontlines, such as medicinal, agrochemical, and material fields [4-7].

In particular, tetrafluoroethylenated compounds possessing two fluorine atoms on each of two adjacent carbons, have been attracting an enormous attention these days. This stems from the fact that substances with a tetrafluoroethylene fragment exhibit significantly different molecular properties compared to monofluorinated, difluorinated, or trifluoromethylated molecules [8,9]. Therefore, more and more tetrafluoroethylenated molecules having a variety of applications, such as bioactive substances (Figure 1a, **1**, **2**) [10-12], liquid crystals (Figure 1b, **3**, **4**) [13-17], fluorescence materials (Figure 1c, **5**) [18,19], and so on, have been developed in recent years.

In sharp contrast to the major development of such non-chiral tetrafluoroethylenated compounds, there have been only few

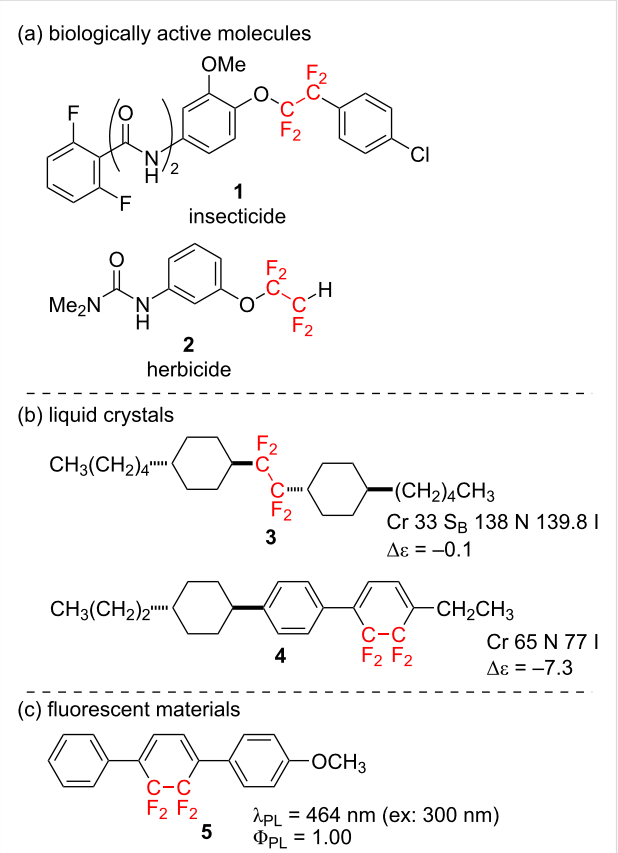

Figure 1: Various applications of tetrafluoroethylenated molecules.

reports on the preparation of chiral molecules possessing a tetrafluoroethylene unit on an asymmetric carbon center in a high optical purity, and to the best of our knowledge, only the following have been published so far (Scheme 1).

As a highly enantioselective synthesis, there has been a pioneering work by Linclau et al. They have reported that the asymmetric Sharpless dihydroxylation of readily available (*E*)-5-bromo-4,4,5,5-tetrafluoro-2-penten-1-ol derivative **6** led to the corresponding chiral diols **7** with an excellent enantiomeric excess, 96% ee (reaction 1 in Scheme 1) [20,21]. It has also been published that the asymmetric conjugate addition of 4-methylphenylboronic acid towards (*E*)-5-bromo-4,4,5,5-tetrafluoro-1-phenyl-2-penten-1-one (**8**) in the presence of a rhodium catalyst coordinated with (*S*)-BINAP gave the corresponding Michael adduct **9** in 94% enantiomeric excess (reaction 2, Scheme 1) [22].

As a diastereoselective synthesis, reductive coupling reactions of commercially available 4-bromo-3,3,4,4-tetrafluoro-1-butene and glyceraldehyde **10a**, its imine derivative **11**, or Garner's aldehyde **10b** have been reported [23,24]. Although the diastereoselectivities were low in some cases, the diastereomers **12** and **13** are often easily separable, and each diastereomer of optically active alcohols or amines can be obtained with an excellent optical purity (reactions 3 and 4 in Scheme 1).

To the best of our knowledge, these are the only four works for the preparation of optically active substances having a tetrafluoroethylene group on an asymmetric carbon center. In order to overcome the current lack of synthetic methods for preparing such molecules, we came up with the idea of utilizing the [1,3]-proton shift reaction reported by Soloshonok et al.

In 1997, Soloshonok et al. reported that fluoroalkylated amines **15** with high optical purity could be easily prepared through [1,3]-proton shift reactions of optically active imines **14** which in turn were readily synthesized by condensation of various perfluoroalkyl ketones with optically active (*R*)-1-phenylethylamine (Scheme 2a) [25-32]. Therefore, we envisioned that optically active tetrafluoroethylenated amines **17** could be synthesized by applying the [1,3]-proton shift to optically active imines **16** derived from readily prepared tetrafluoroethylenated ketones (Scheme 2b).

In this paper, we describe the details of the [1,3]-proton shift reaction of various tetrafluoroethylenated imines.

Results and Discussion

The preparation of substrates used in this study was as outlined in Scheme 3. Namely, the zinc reagent was prepared from commercially available 3,3,4,4-tetrafluoro-1-butene (**18**) [33] and reacted with various acid chlorides in the presence of a copper catalyst to afford the corresponding tetrafluoroethylenated ketones **19**. The ketones were then condensed with (*R*)-1-phenylethylamine under the influence of $TiCl_4$ [34,35] to prepare various optically active imines (*R*)-**16** in high yields (Scheme 3). Based on the result of the NOESY spectrum of the imine (*R*)-**16c,** the stereochemistry of the imines (*R*)-**16** was determined as *E* [36].

Among the imines thus obtained, (*R*)-**16b** was used to investigate the optimum reaction conditions (Table 1). Treatment of (*R*)-**16b** with 1.2 equiv of DBU (1,8-diazabicyclo[5.4.0]undec-7-ene) in THF at room temperature for 24 h gave the corresponding [1,3]-proton shift adduct (*S*)-**20b** in 31% yield (Table 1, entry 1). In this case, the HF-elimination product **21b** was also obtained in 16% [37], and the starting material was recovered in 53%. As shown in entries 2–7 of Table 1, the reactions in various solvents were next examined. When CH_3CN or CH_2Cl_2 was used, 17% or 36% of the target product (*S*)-**20b** were obtained and almost no HF-elimination product **21b** was formed, while about 40% of the azocine derivative **22b** was afforded as a byproduct [38], along with the recovery of (*R*)-

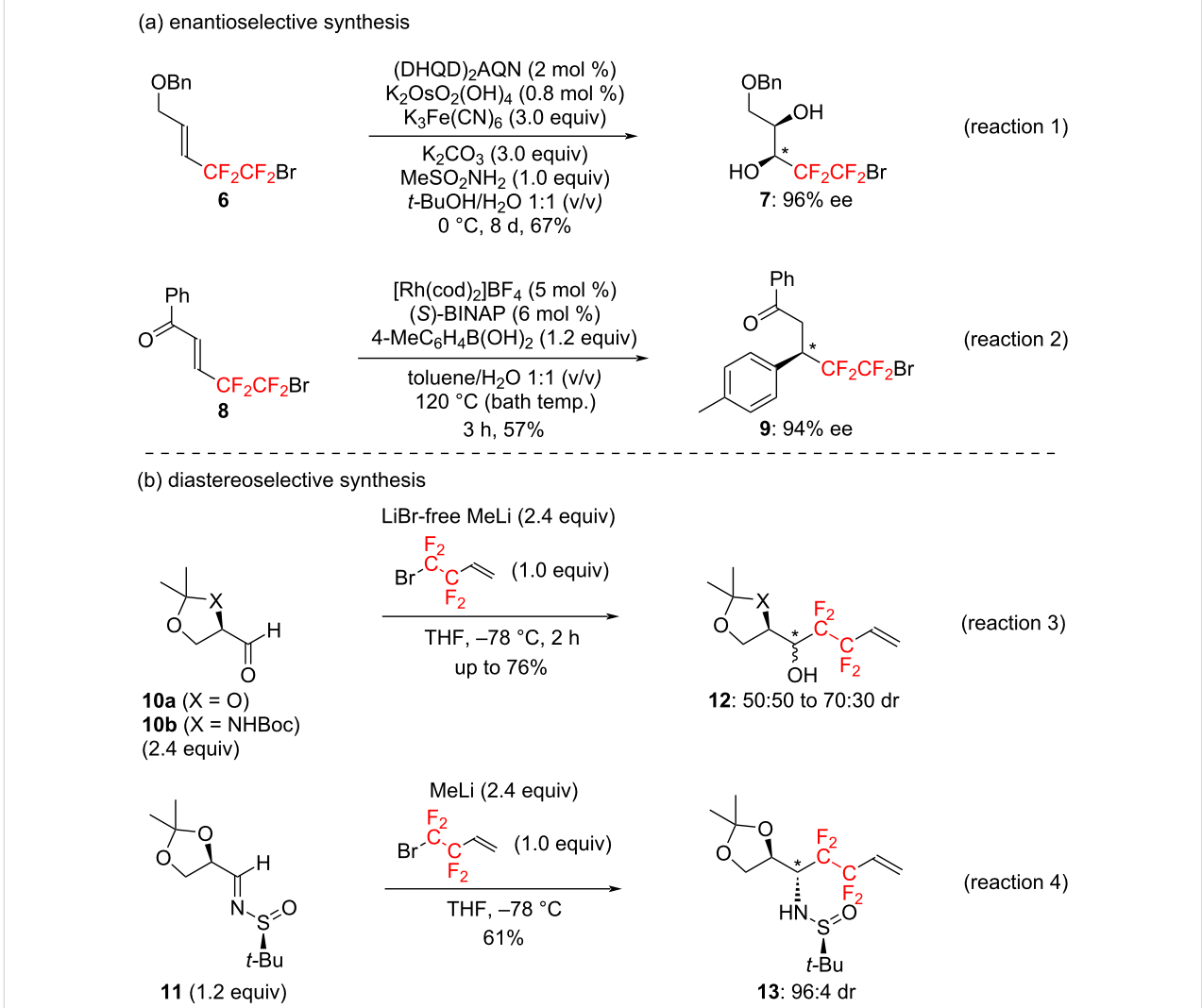

Scheme 1: Precedent synthetic approaches to optically active compounds possessing a tetrafluoroethylene group on an asymmetric carbon center.

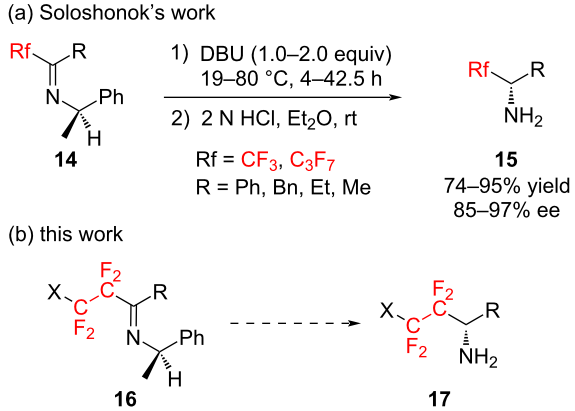

Scheme 2: Synthetic strategy for preparing fluorine-containing amines via [1,3]-proton shift reactions.

16b. In the case of diethyl ether, toluene, hexane, and cyclohexane, (*S*)-**20b** was obtained in 30% to 40% yield and significant amounts of unreacted substrate were still observed, although formation of the byproduct **22b** could be generally suppressed.

We also examined the reaction using other bases instead of DBU. As shown in entries 9 and 10 of Table 1, the reaction did not proceed at all with triethylamine or DABCO, and (*R*)-**16b** was quantitatively recovered. The influence of the amount of DBU upon the reaction was also investigated (Table 1, entries 11–13). The results showed that when 2.4 equiv of DBU were used, the target compound (*S*)-**20b** was obtained in 50% yield, along with byproduct **22b** in 43% yield (Table 1, entry 11), while increasing the number of equivalents of DBU decreased the yield of the target product (*S*)-**20b** and increased the yield of the byproduct **22b** (Table 1, entries 12 and 13). Also carrying

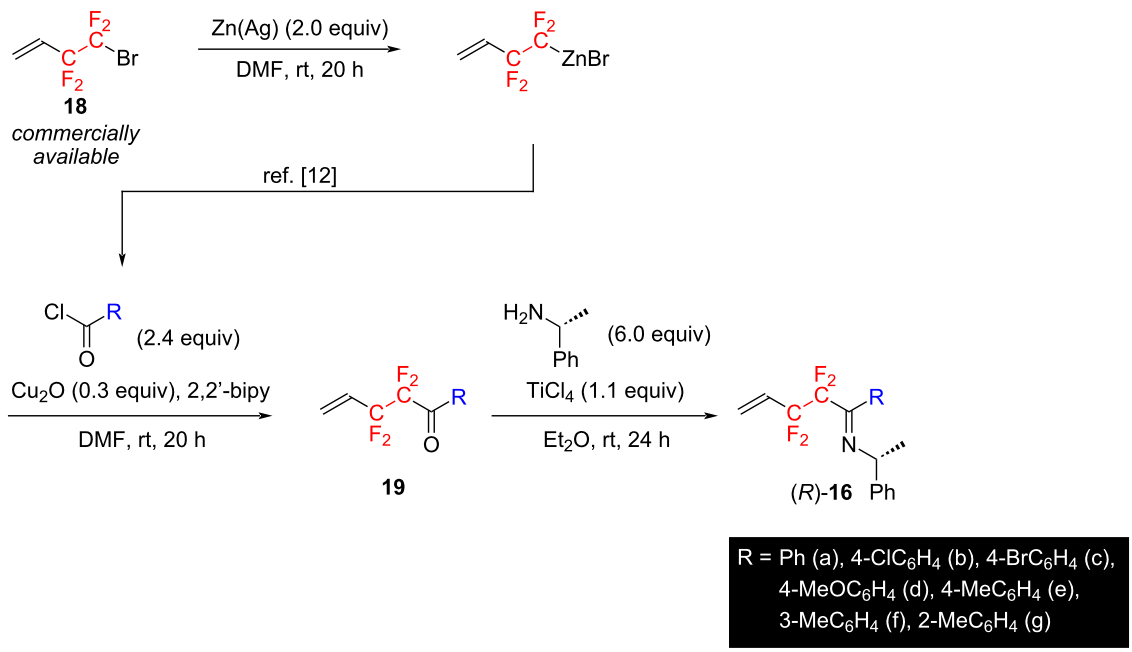

Scheme 3: Preparation of the substrates used in this study.

Table 1: Investigation of the reaction conditions.

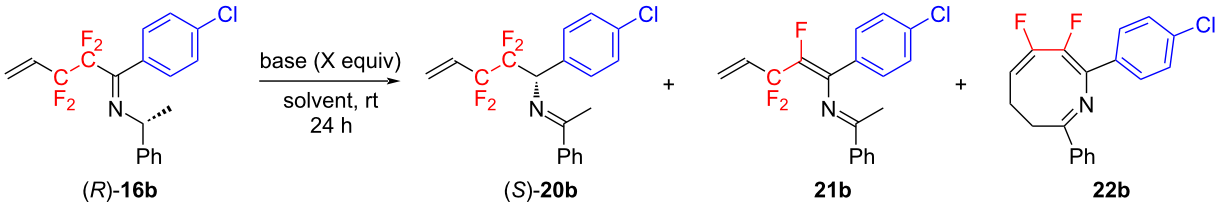

Entry	Base/X equiv	Solvent	Yield[a] [%] of (*S*)-**20b**	Yield[a] [%] of **21b**	Yield[a] [%] of **22b**	Recovery[a] [%] of (*R*)-**16b**
1	DBU/1.2	THF	31	16	0	53
2	DBU/1.2	CH_3CN	17	0	39	44
3	DBU/1.2	Et_2O	38	14	17	31
4	DBU/1.2	toluene	37	13	0	50
5	DBU/1.2	hexane	26	12	0	62
6	DBU/1.2	CH_2Cl_2	36	3	38	23
7	DBU/1.2	cyclohexane	32	17	0	51
8	DBU/1.2	toluene	33	18	0	49
9	Et_3N/1.2	toluene	0	0	0	100
10	DABCO/1.2	toluene	0	0	0	100
11	DBU/2.4	toluene	50	2	43	5
12	DBU/4.8	toluene	29	0	71	0
13	DBU/6.8	toluene	31	0	69	0
14[b]	DBU/2.4	toluene	8	13	0	79

[a]Determined by ^{19}F NMR spectroscopy; [b]the reaction was carried out at 0 °C.

out the reaction at 0 °C gave unsatisfactory results and a large amount of (*R*)-**16b** was recovered (Table 1, entry 14).

Based on these results, the reaction conditions in entry 11 (Table 1) were determined as the optimum ones, which gave the highest yield, although the formation of the byproduct azocine derivative **22b** could not be completely suppressed.

The thus obtained [1,3]-proton shift product (*S*)-**20b** was subjected to 2 N HCl aq in Et_2O for 2 h, and subsequently 2 N NaOH aq, affording the corresponding free amine (*S*)-**17b**. Then, treatment of the amine with CbzCl and pyridine in CH_2Cl_2 gave the corresponding amide (*S*)-**23b** in 27% isolated yield over three-steps. The measurement of HPLC equipped with a chiral column, CHIRALPAK AD-H for (*S*)-**23b**, showed that the amide had an optical purity of 95% ee (Scheme 4).

On the next stage, the substrate scope for the present reaction was explored by using various imines (*R*)-**16** (Scheme 5). When the substituent R is an aromatic ring substituted by a halogen

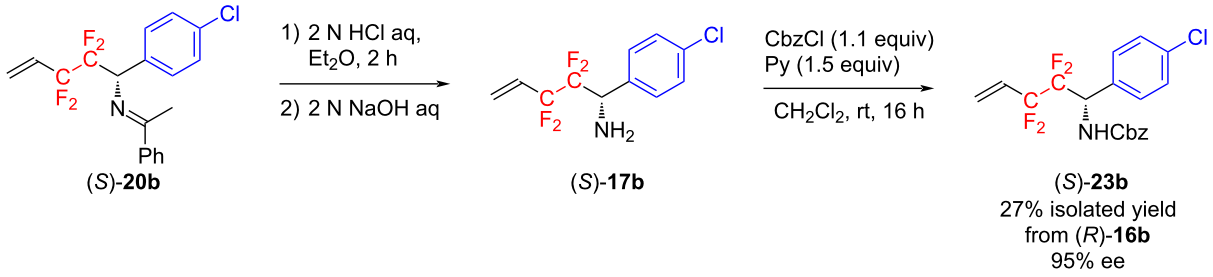

Scheme 4: Derivatization of (*S*)-**20b** to (*S*)-**23b** for determining the optical purity of (*S*)-**20b**.

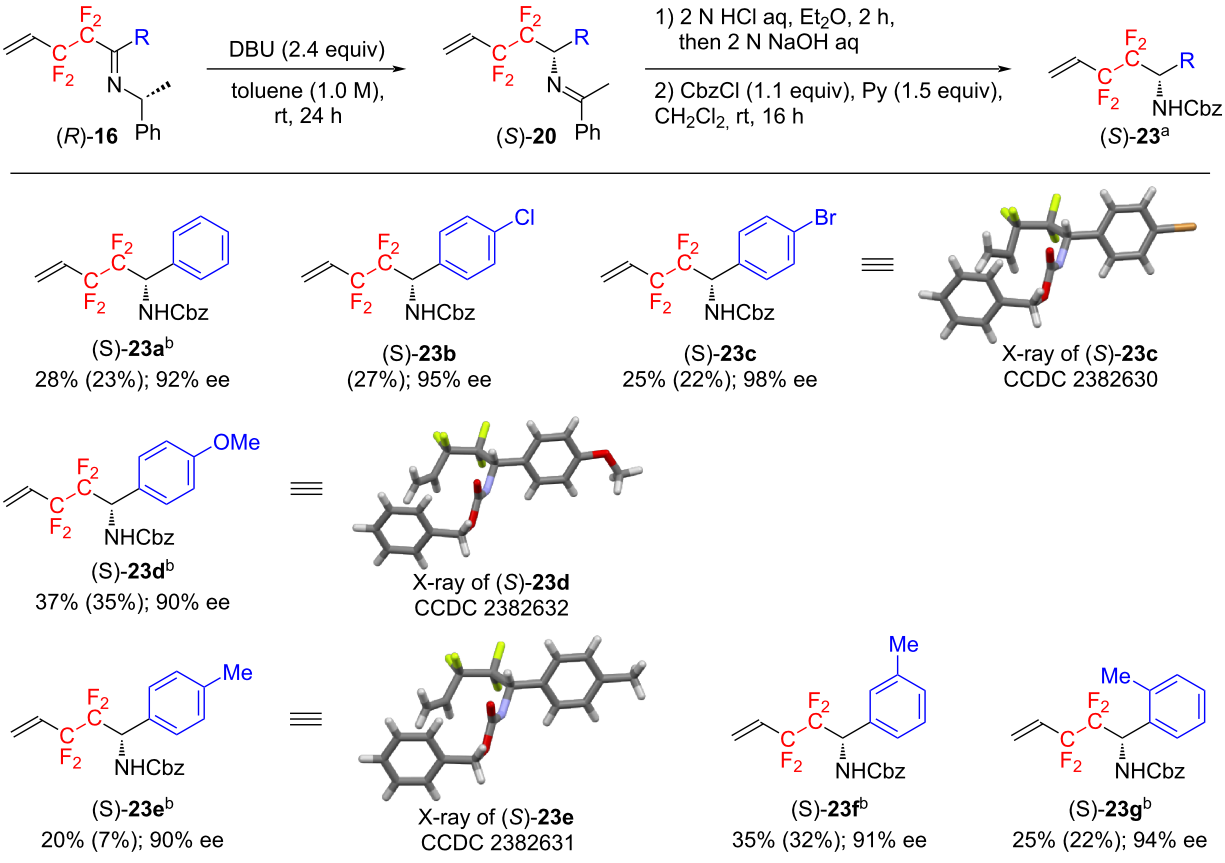

Scheme 5: Substrate scope for the present [1,3]-proton shift reaction. [a]Yields are determined by ^{19}F NMR spectroscopy. Values in parentheses show isolated yields. Enantiomeric excesses are deteremined by HPLC equipped with DAICEL CHIRALPAK AD-H. [b]Carried our at 50 °C in the [1,3]-proton shift reaction step.

such as chlorine and bromine atoms, the amides (*S*)-**23** were obtained in 22–27% yield and with very high optical purity ((*S*)-**23b**, (*S*)-**23c**), although as for (*S*)-**23a**, a satisfactory result (92% ee) could be obtained when the reaction was performed at 50 °C. The substrates with an aromatic ring substituted by not only an electron-withdrawing halogen atom but also an electron-donating group such as methoxy and methyl group also smoothly underwent the [1,3]-proton shift reaction, affording the desired products with high enantiomeric excess (90% ee for (*S*)-**23d** and (*S*)-**23e**). Furthermore, it was found that the substituent position on the aromatic ring did not significantly influence the reaction efficiency as well as optical purity and the reaction proceeded in a highly enantioselective manner (91% ee for (*S*)-**23f** and 94% ee for (*S*)-**23g**). Disappointingly, when R is an alkyl group, the desired rearrangement products were rarely obtained, resulting in unidentified products together with a large amount of starting material. This may be due to the following reasons. Namely, when the substituent R is an aryl group, the negative charge generated on the imine carbon can be delocalized, hence the transition state is stabilized and the reaction proceeds smoothly. On the other hand, when the substituent R is an alkyl group, the negative charge generated on the imine carbon is an unstable factor, and therefore the transition state is not stabilized, leading to the increase of the activation energy of the reaction. As a result, the reaction does not proceed smoothly.

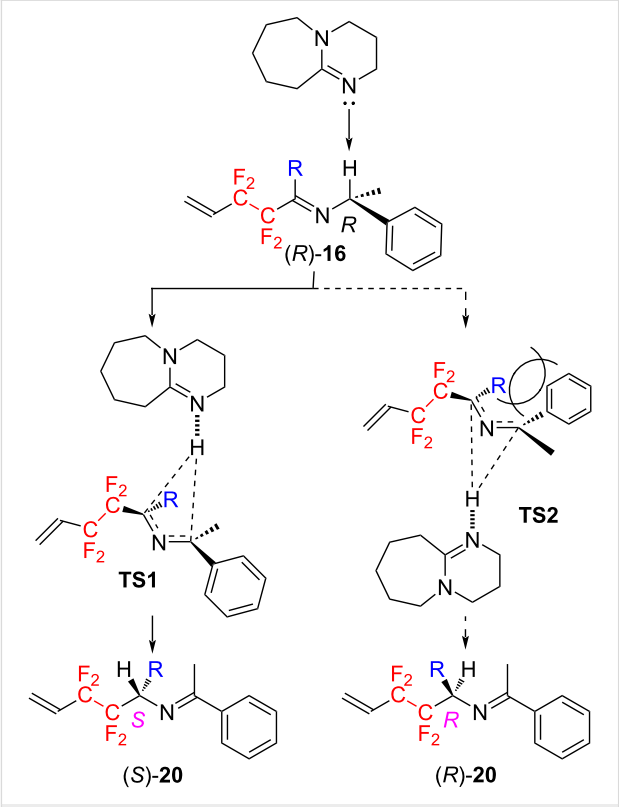

Scheme 6: Proposed reaction mechanism.

The absolute configurations of product (*S*)-**23c**, (*S*)-**23d**, and (*S*)-**23e** were determined on the basis of their X-ray crystallographic analyses. The validity of their absolute configurations was confirmed by the convergence of the Flack parameters of three compounds to values close to 0, i.e. −0.006(12), 0.1(4) and 0.2(4), respectively. As indicated in Scheme 5, therefore, the absolute configurations of all compounds were determined as *S*. Then, the [1,3]-proton shift reaction in this study is expected to proceed via the reaction mechanism reported by Soloshonok [25-32], as shown in Scheme 6.

First, DBU interacts with the benzylic hydrogen of the imine (*R*)-**16**, and this hydrogen is about to be abstracted as a proton. This hydrogen which is being abstracted simultaneously interacts with the carbon possessing the tetrafluoroethylene fragment. At this time, transition states **TS1** or **TS2** are possible, but the reaction proceeds exclusively through the transition state **TS1** to avoid significant steric repulsion between the substituent R and the phenyl group. Therefore, the product (*S*)-**20** with *S* configuration is obtained preferentially.

Conclusion

In summary, we have succeeded in synthesizing optically active amines having a tetrafluoroethylene group on the asymmetric carbon center by applying the [1,3]-proton shift reaction using various optically active imines, which can be easily prepared starting from commercially available 4-bromo-3,3,4,4-tetrafluoro-1-butene. In this reaction, although the formation of azocine derivatives as byproducts could not be completely suppressed, the [1,3]-proton shift reaction proceeded in relatively good yield and a high asymmetric transfer was achieved. As a result, it was found that various optically active amine derivatives could be obtained with high optical purity.

Supporting Information

Supporting Information File 1

Full experimental details, ^{1}H, ^{13}C, ^{19}F NMR spectra of **16a–g** and **23a–g**, and HPLC charts of racemic as well as chiral compounds **23a–g**.
[https://www.beilstein-journals.org/bjoc/content/supplementary/1860-5397-20-233-S1.pdf]

Supporting Information File 2

Crystallographic information files (CIF) for compounds **23c**, **23d**, and **23e**.
[https://www.beilstein-journals.org/bjoc/content/supplementary/1860-5397-20-233-S2.zip]

Acknowledgements

We thank TOSOH FINECHEM for the general gift of 4-bromo-3,3,4,4-tetrafluoro-1-butene (**1**).

Author Contributions

Yuta Kabumoto: investigation. Eiichiro Yoshimoto: investigation. Bing Xiaohuan: investigation. Masato Morita: investigation. Motohiro Yasui: investigation; project administration; writing – review & editing. Shigeyuki Yamada: investigation; project administration; writing – review & editing. Tsutomu Konno: conceptualization; data curation; investigation; methodology; project administration; supervision; writing – original draft; writing – review & editing.

ORCID® iDs

Shigeyuki Yamada - https://orcid.org/0000-0002-6379-0447
Tsutomu Konno - https://orcid.org/0000-0002-5146-9840

Data Availability Statement

All data that supports the findings of this study will be available in the published article and/or the supporting information of this article.

Preprint

A non-peer-reviewed version of this article has been previously published as a preprint: https://doi.org/10.3762/bxiv.2024.51.v1

References

1. Szabó, K. J.; Selander, N., Eds. *Organofluorine Chemistry: Synthesis, Modeling, and Applications;* Wiley-VCH: Weinheim, Germany, 2021. doi:10.1002/9783527825158
2. Haufe, G.; Leroux, F. R., Eds. *Fluorine in Life Sciences: Pharmaceuticals, Medicinal Diagnostics, and Agrochemicals;* Academic Press: London, UK, 2019. doi:10.1016/c2016-0-03808-1
3. Tressaud, A. *Fluorine: A Paradoxical Element;* Elsevier: Amsterdam, Netherlands, 2019. doi:10.1016/c2016-0-02485-3
4. Inoue, M.; Sumii, Y.; Shibata, N. *ACS Omega* **2020,** *5,* 10633–10640. doi:10.1021/acsomega.0c00830
5. Ogawa, Y.; Tokunaga, E.; Kobayashi, O.; Hirai, K.; Shibata, N. *iScience* **2020,** *23,* 101467. doi:10.1016/j.isci.2020.101467
6. Han, J.; Kiss, L.; Mei, H.; Remete, A. M.; Ponikvar-Svet, M.; Sedgwick, D. M.; Roman, R.; Fustero, S.; Moriwaki, H.; Soloshonok, V. A. *Chem. Rev.* **2021,** *121,* 4678–4742. doi:10.1021/acs.chemrev.0c01263
7. Wang, Y.; Yang, X.; Meng, Y.; Wen, Z.; Han, R.; Hu, X.; Sun, B.; Kang, F.; Li, B.; Zhou, D.; Wang, C.; Wang, G. *Chem. Rev.* **2024,** *124,* 3494–3589. doi:10.1021/acs.chemrev.3c00826
8. Václavík, J.; Klimánková, I.; Budinská, A.; Beier, P. *Eur. J. Org. Chem.* **2018,** 3554–3593. doi:10.1002/ejoc.201701590
9. Biffinger, J. C.; Kim, H. W.; DiMagno, S. G. *ChemBioChem* **2004,** *5,* 622–627. doi:10.1002/cbic.200300910
10. Bianchi, D.; Cesti, P.; Spezia, S.; Garavaglia, C.; Mirenna, L. *J. Agric. Food Chem.* **1991,** *39,* 197–201. doi:10.1021/jf00001a040
11. N'Go, I.; Golten, S.; Ardá, A.; Cañada, J.; Jiménez-Barbero, J.; Linclau, B.; Vincent, S. P. *Chem. – Eur. J.* **2014,** *20,* 106–112. doi:10.1002/chem.201303693
12. Sari, O.; Bassit, L.; Gavegnano, C.; McBrayer, T. R.; McCormick, L.; Cox, B.; Coats, S. J.; Amblard, F.; Schinazi, R. F. *Tetrahedron Lett.* **2017,** *58,* 642–644. doi:10.1016/j.tetlet.2017.01.006
13. Kirsch, P.; Bremer, M.; Huber, F.; Lannert, H.; Ruhl, A.; Lieb, M.; Wallmichrath, T. *J. Am. Chem. Soc.* **2001,** *123,* 5414–5417. doi:10.1021/ja010024l
14. Yamada, S.; Tamamoto, K.; Kida, T.; Asai, T.; Ishihara, T.; Konno, T. *Org. Biomol. Chem.* **2017,** *15,* 9442–9454. doi:10.1039/c7ob02399e
15. Yamada, S.; Hashishita, S.; Asai, T.; Ishihara, T.; Konno, T. *Org. Biomol. Chem.* **2017,** *15,* 1495–1509. doi:10.1039/c6ob02431a
16. Yamada, S.; Hashishita, S.; Konishi, H.; Nishi, Y.; Kubota, T.; Asai, T.; Ishihara, T.; Konno, T. *J. Fluorine Chem.* **2017,** *200,* 47–58. doi:10.1016/j.jfluchem.2017.05.013
17. Kumon, T.; Hashishita, S.; Kida, T.; Yamada, S.; Ishihara, T.; Konno, T. *Beilstein J. Org. Chem.* **2018,** *14,* 148–154. doi:10.3762/bjoc.14.10
18. Ohsato, H.; Morita, M.; Yamada, S.; Agou, T.; Fukumoto, H.; Konno, T. *Mol. Syst. Des. Eng.* **2022,** *7,* 1129–1137. doi:10.1039/d2me00055e
19. Ohsato, H.; Kawauchi, K.; Yamada, S.; Konno, T. *Chem. Rec.* **2023,** *23,* e202300080. doi:10.1002/tcr.202300080
20. Boydell, A. J.; Vinader, V.; Linclau, B. *Angew. Chem., Int. Ed.* **2004,** *43,* 5677–5679. doi:10.1002/anie.200460746
21. Linclau, B.; Boydell, A. J.; Timofte, R. S.; Brown, K. J.; Vinader, V.; Weymouth-Wilson, A. C. *Org. Biomol. Chem.* **2009,** *7,* 803–814. doi:10.1039/b817260a
22. Yamashika, K.; Morishitabara, S.; Yamada, S.; Kubota, T.; Konno, T. *J. Fluorine Chem.* **2018,** *207,* 24–37. doi:10.1016/j.jfluchem.2017.12.013
23. Fontenelle, C. Q.; Tizzard, G. J.; Linclau, B. *J. Fluorine Chem.* **2015,** *174,* 95–101. doi:10.1016/j.jfluchem.2014.07.015
24. Konno, T.; Hoshino, T.; Kida, T.; Takano, S.; Ishihara, T. *J. Fluorine Chem.* **2013,** *152,* 106–113. doi:10.1016/j.jfluchem.2013.02.013
25. Soloshonok, V. A.; Catt, H. T.; Ono, T. *J. Fluorine Chem.* **2010,** *131,* 261–265. doi:10.1016/j.jfluchem.2009.10.013
26. Nagy, P.; Ueki, H.; Berbasov, D. O.; Soloshonok, V. A. *J. Fluorine Chem.* **2008,** *129,* 409–415. doi:10.1016/j.jfluchem.2008.02.001
27. Soloshonok, V. A.; Soloshonok, I. V.; Kukhar, V. P.; Svedas, V. K. *J. Org. Chem.* **1998,** *63,* 1878–1884. doi:10.1021/jo971777m
28. Soloshonok, V. A.; Ono, T. *J. Org. Chem.* **1997,** *62,* 3030–3031. doi:10.1021/jo970425c
29. Soloshonok, V. A.; Ono, T.; Soloshonok, I. V. *J. Org. Chem.* **1997,** *62,* 7538–7539. doi:10.1021/jo9710238
30. Ono, T.; Kukhar, V. P.; Soloshonok, V. A. *J. Org. Chem.* **1996,** *61,* 6563–6569. doi:10.1021/jo960503g
31. Soloshonok, V. A.; Kukhar, V. P. *Tetrahedron* **1996,** *52,* 6953–6964. doi:10.1016/0040-4020(96)00300-6
32. Soloshonok, V. A.; Ono, T. *Tetrahedron* **1996,** *52,* 14701–14712. doi:10.1016/0040-4020(96)00920-9
33. Tamamoto, K.; Yamada, S.; Konno, T. *Beilstein J. Org. Chem.* **2018,** *14,* 2375–2383. doi:10.3762/bjoc.14.213
34. Braconi, E.; Cramer, N. *Angew. Chem., Int. Ed.* **2022,** *61,* e202112148. doi:10.1002/anie.202112148
35. Hou, W.; Tang, C.; Liu, G.; Huang, Z. *Organometallics* **2022,** *41,* 3115–3121. doi:10.1021/acs.organomet.2c00321
36. In the NOESY spectrum of (*R*)-**16c**, a cross-peak was observed between the methine or methyl protons and the *ortho* proton of the 4-chlorophenyl group. This indicates that the 4-chlorophenyl and 1-phenylethyl groups are in close proximity, i.e., the stereochemistry of the imine is *E*.

37. The HF elimination product, **21b**, was too unstable in silica gel column chromatography to be isolated in a pure form, and hence its identification by ^{1}H NMR analysis could not be carried out. A similar compound, however, *N*-benzylidene-(1-phenyl)-2,3,3-trifluoro-1,4-pentdienylamine, could be easily isolated, and the structure could be completely identified (see Supporting Information File 1). Accordingly, it was determined unambiguously that **21b** also has an azatriene structure, on the basis of the comparison of the ^{19}F NMR chemical shifts for **21b** and *N*-benzylidene-(1-phenyl)-2,3,3-trifluoro-1,4-pentdienylamine.
38. Electrocyclization of 5,6-difluoro-3-azaocta-1,3,5,7-tetraene derivative which resulted from two HF eliminations of the imine (*R*)-**16b** under the influence of DBU might take place, giving the corresponding azocine derivative **22b**. The details are currently under investigation. See Supporting Information File 1.

BEILSTEIN JOURNAL OF ORGANIC CHEMISTRY

Mechanochemical difluoromethylations of ketones

Jinbo Ke‡, Pit van Bonn‡ and Carsten Bolm*

Letter

Open Access

Address:
Institute of Organic Chemistry, RWTH Aachen University, Landoltweg 1, 52074 Aachen, Germany

Email:
Carsten Bolm* - carsten.bolm@oc.rwth-aachen.de

* Corresponding author ‡ Equal contributors

Keywords:
ball milling; difluorocarbene; difluoromethylations; difluoromethyl enol ether; mechanochemistry

Beilstein J. Org. Chem. **2024,** *20,* 2799–2805.
https://doi.org/10.3762/bjoc.20.235

Received: 06 September 2024
Accepted: 25 October 2024
Published: 04 November 2024

This article is part of the thematic issue "Organofluorine chemistry VI".

Associate Editor: J. G. Hernández

Abstract

We present a mechanochemical synthesis of difluoromethyl enol ethers. Utilizing an in situ generation of difluorocarbenes, ketones are efficiently converted to the target products under solvent-free conditions. The reactions proceed at room temperature and are complete within 90 minutes, demonstrating both efficiency and experimental simplicity.

Introduction

In recent years, mechanochemical organic synthesis has been advanced significantly, prompting organic chemists to reconsider the necessity of solvents in their reactions [1-11]. Eliminating hazardous solvents substantially reduces the ecological footprint of organic reactions [12,13]. Beyond environmental benefits and enhanced human safety, mechanochemical reactions often feature shorter reaction times, eliminate the need for external heating, and offer alternative product selectivity [3,14]. In general, such reactions are characterized by the absorption of mechanical energy and they are influenced by several factors, including the lack of solvation, changes in morphology and rheology of the reaction mixtures during the milling, and variations in concentration and dielectric environment. Consequently, an increased reactivity can be achieved through the formation of novel reactive intermediates [15-18].

Fluorine-containing functional groups are essential structural motifs in the development of new bioactive compounds and functional materials. Compared to their non-fluorinated analogs, the presence of fluorine atoms in molecular structures can improve physicochemical and biological properties [19-27]. Among these groups, the difluoromethyl moiety has gained considerable attention [28-30]. Commonly, it is synthesized by the reaction of a nucleophile with difluorocarbene. However, the generation of difluorocarbene typically requires harsh conditions and involves toxic precursors, alongside with the risk of dimerization to tetrafluoroethylene [31]. Although this dimerization can be mitigated by controlling the concentration and reaction environment, as longer half-lives are observed for difluorocarbenes in the gas phase than in solution [32,33], it has remained a challenge to control such reactions.

Our group has recently reported a mechanochemical difluoromethylation of primary, secondary, and tertiary alcohols [34], yielding products with difluoromethoxy groups, which are promising organofluorine compounds [35-38]. Notably, also

sterically hindered alcohols, which are typically less reactive in solution, could be applied under solvent-free conditions in a ball mill [39], which was attributed to a better accessibility of the difluorocarbene in the mechanochemical environment [40].

Motivated by these findings, we now explored difluoromethylation reactions with compounds bearing less nucleophilic functional groups. Ketones caught our particular attention as they contain a weak nucleophilic carbonyl oxygen adjacent to an electrophilic carbonyl carbon. Previous studies have focused on reactions of difluorocarbene with cyclic and acyclic 1,3-diones (Scheme 1A) [41-45]. Typically, they were conducted with a base to form the corresponding enolate anions which then reacted with difluorocarbene to yield difluoromethyl enol ethers. Those products are of interest because they contain a unique structural motif with potential for further functionalizations into highly diverse secondary or tertiary difluoroalkyl ethers. Dolbier and co-workers investigated reactions of difluorocarbene generated from its precursor trimethylsilyl 2,2-difluoro-2-(fluorosulfonyl)acetate (TFDA) and sodium fluoride catalyst, with simple ketones, which resulted in the formation of difluoromethyl 2,2-difluorocyclopropyl ethers (Scheme 1B). Although the reactions worked well, it is also noteworthy that the use of TFDA as reagent, liberated fluoro(trimethyl)silane (TMSF), carbon dioxide, and ozone-depleting sulfur dioxide as side products [46,47]. Later, Ichikawa and co-workers established the release of difluorocarbene from TFDA with catalytic amounts of an *N*-heterocyclic carbene and a base (Scheme 1C) [29,48,49]. In these reactions, difluoromethyl enol ethers were obtained, which were subsequently oxidized to yield the corresponding aryl difluoromethyl ethers. Noteworthy, however, the latter study focused mostly on cyclic ketones, with only one reported example of a difluoromethylation reaction of an acyclic substrate.

Against this background and seeing new synthetic opportunities, we wondered about reactions of mechanochemically generated difluorocarbene with simple acyclic ketones. The results and observations of this study are summarized here.

Results and Discussion

For the optimization of the reaction conditions, 4-methylacetophenone (**1a**) was chosen as model substrate. Under standard reaction conditions with difluorocarbene precursor $TMSCF_2Br$ (**2**, 2.0 equiv), activator KFHF (4.0 equiv), and grinding auxiliary CsCl (4.0 equiv), difluoromethyl enol ether **3a** was obtained after 90 min reaction time at 25 Hz in 74% yield, determined by quantitative ^1H NMR spectroscopy (Table 1, entry 1). The reaction was conducted in a PTFE milling equipment with two milling balls (diameter: 10 mm). Changing to a heavier

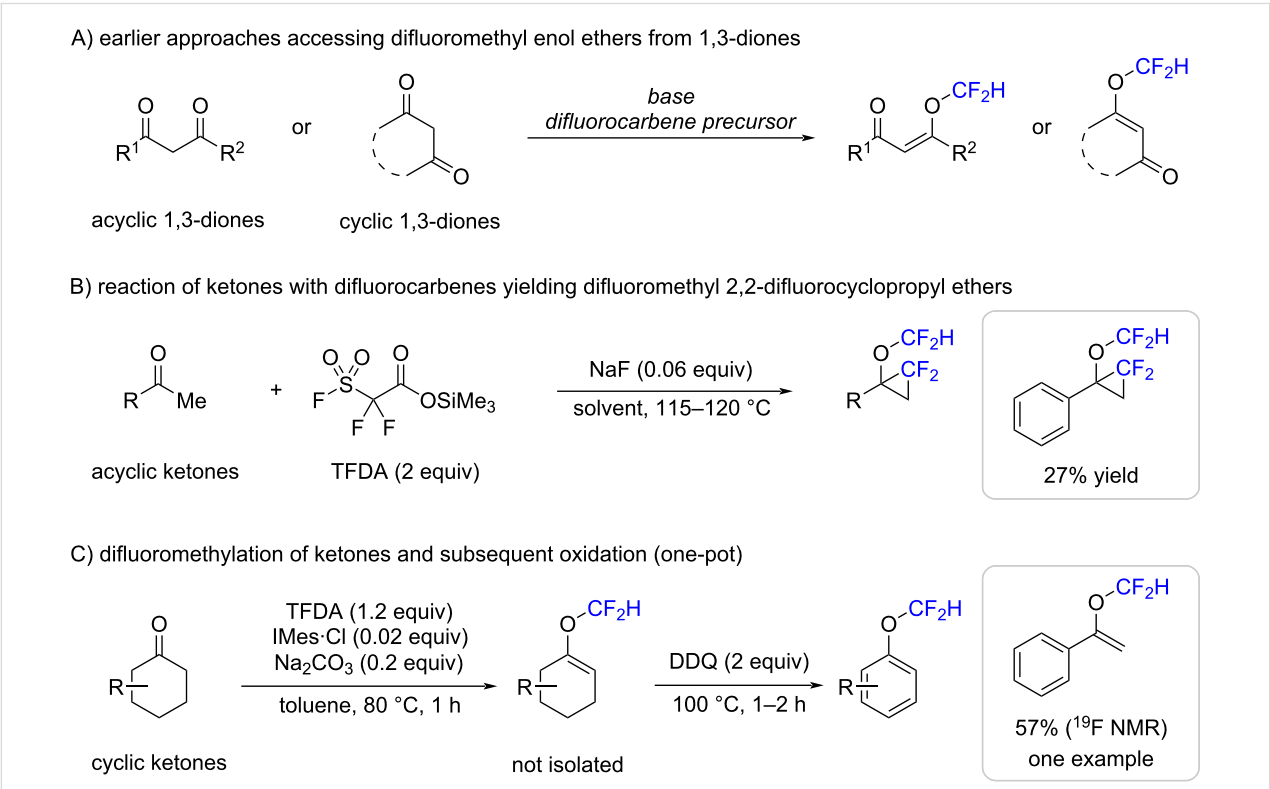

Scheme 1: Overview over difluoromethyl enol ether syntheses from acyclic and cyclic 1,3-diones (A), acyclic ketones (B), and cyclic ketones (C).

Table 1: Optimization of the reaction conditions.[a]

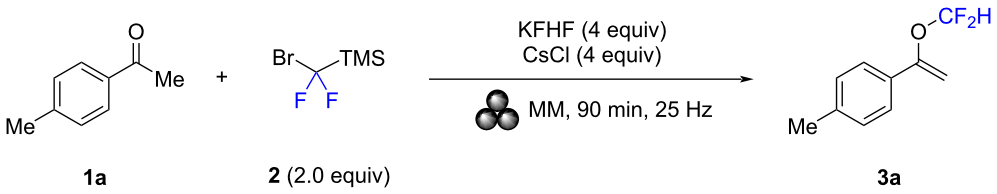

1a **2** (2.0 equiv) **3a**

Entry	Deviation from the reaction conditions	Yield of **3a** (%)[b]
1	none	74[c]
2	with one PTFE milling ball (diameter: 15 mm)	67
3	60 min	72
4	60 min, **2** (1.5 equiv)	61
5	60 min, **2** (3.0 equiv)	60
6	60 min, KCl instead of CsCl	69
7	60 min, KBr instead of CsCl	69
8	60 min, NaCl instead of CsCl	64
9	60 min, SiO_2 instead of CsCl	0
10	LAG (H_2O)	37
11	LAG (1,4-dioxane)	43
12	LAG ($CHCl_3$)	62
13	LAG (toluene)	68

[a]Reaction performed with two PTFE milling balls (diameter: 10 mm) in a PTFE jar (volume: 25 mL). Liquid-assisted grinding (LAG): 0.25 μL·mg^{-1}. [b]Determined by ^{1}H NMR spectroscopy using 1,2-dichloroethane as the internal standard. [c]Repetition of the experiment gave consistent results.

milling ball (diameter: 15 mm) resulted in a yield of 67% of **3a** (Table 1, entry 2). Stopping the reaction after 60 min gave product **3a** in 72% yield (Table 1, entry 3). At a reaction time of 60 min, both reducing and increasing the amount of **2** (from initially used 2.0 equiv to 1.5 equiv and 3.0 equiv, respectively) reduced the yield of **3a** by about 10% (Table 1, entries 3–5). Probably, with less carbene precursor the amount of generated difluorocarbene was insufficient, and with too much of it, side reactions occurred [31-33]. Next, various grinding auxiliaries were investigated at a reaction time of 60 min (Table 1, entries 6–9). A similar yield of **3a** (69%) was obtained with KCl or KBr instead of CsCl (Table 1, entries 6 and 7 versus entry 3). Using NaCl, gave **3a** in 64% yield (Table 1, entry 8). Finally, CsCl was substituted by silica, which, to our surprise, blocked the product formation completely (Table 1, entry 9). Apparently, the presence of an alkali halide salt was beneficial, most likely by stabilizing the consistency of the reaction mixture leading to a sufficient mixing. Silica could not fulfill this role. Lastly, water, 1,4-dioxane, chloroform, and toluene were tested in a liquid-assisted grinding (LAG) protocol (Table 1, entries 10–13). The lowest yields were obtained with water and 1,4-dioxane, providing **3a** in yields of 37% and 43%, respectively (Table 1, entries 10 and 11). With the less polar solvents chloroform and toluene **3a** was obtained in 62% and 68% yield, respectively (Table 1, entries 12 and 13).

For comparison, the difluoromethylation of ketone **1a** with difluorocarbene precursor $TMSCF_2Br$ (**2**) was investigated in solution (Scheme 2). The reaction conditions were chosen based on those reported by Ni, Hu and co-workers for the difluoromethylation of alcohols in solution [39]. The two activators KFHF and KOAc were investigated in a dichloromethane/water mixture at room temperature for 10 h. In both cases, the yield of **3a** was negligible (with KFHF: 3%, with KOAc: nil). Following these initial attempts, the mechanochemical approach appears to be superior. However, it should also be noted that the reaction with difluorocarbene precursor **2** was not further optimized in solution.

Next, various ketones were investigated under the optimized reaction conditions with difluorocarbene precursor **2**, KFHF (4 equiv) as activator, and CsCl or KCl (4 equiv) as grinding auxiliaries in a PTFE milling jar for 90 min at 25 Hz (Scheme 3). To get an initial efficiency estimate, the crude reaction mixtures were first analyzed by quantitative ^{1}H NMR spectroscopy with 1,2-dichloroethane as the internal standard. After these analyses, isolating the products by column chromatography was attempted. Unfortunately, many products were highly volatile and very non-polar, rendering the purification difficult. As a result, in several cases only little or no product was obtained. Furthermore, most isolated products had only purities of

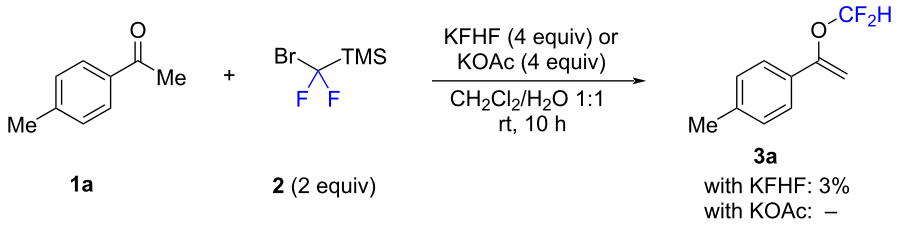

Scheme 2: Attempted difluoromethylation of **1a** in solution. The reactions were performed on a 0.2 mmol scale. Method A: **2** (2.0 equiv), KFHF (4.0 equiv), CH_2Cl_2 (0.2 mL), H_2O (0.2 mL), rt, 10 h; Method B: **2** (2.0 equiv), KOAc (4.0 equiv), CH_2Cl_2 (0.2 mL), H_2O (0.2 mL), rt, 10 h. The yields were determined by ^{19}F NMR spectroscopy using trifluoromethoxybenzene as the internal standard.

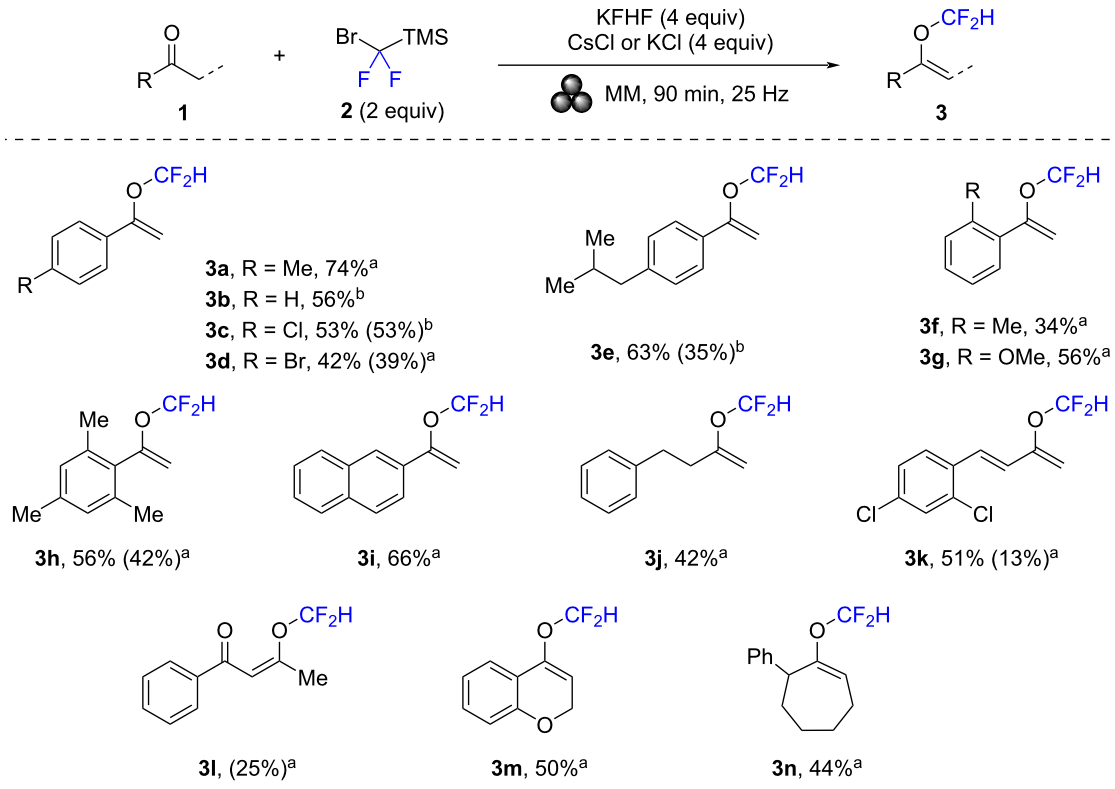

Scheme 3: Scope of ketones. The yields were determined by ^1H NMR spectroscopy using 1,2-dichloroethane as the internal standard. In parentheses: yields after column chromatography (with product purities of ca. 90%). [a]With CsCl. [b]With KCl.

ca. 90% still containing inseparable impurities (as revealed by NMR spectroscopy).

In the first series of substrates, acetophenone derivatives with various *para*-substituents were applied. Similar to methyl tolyl ketone (**1a**), which afforded product **3a** in 74% yield, acetophenone (**1b**) gave **3b** in 56% yield. Substrates **1c** and **1d** bearing a chloro or a bromo group in *para* position of the aryl moiety, gave the corresponding products in yields of 53% (for **3c**) and 42% (for **3d**). These two difluoromethyl enol ethers were also isolated by column chromatography, which afforded the products in 53% and 39% yield, respectively. Product **3e** with an isobutyl group in *para*-position was obtained in 63% yield and isolated in 35% yield. Changing the position of the methyl group to the *ortho*-position led to a decrease in yield (**3f**: 34%). *ortho*-Methoxy-substituted ketone **1g** provided the corresponding product **3g** in 56% yield. Difluoromethyl enol ether **3h** with three methyl groups was obtained in 56% yield and column chromatography allowed to isolate it in 42% yield. 2-Acetonaphthone was successfully converted to **3i** in 66% yield. Besides aryl ketones, arylalkyl ketones reacted well too. Accordingly, **3j** was obtained in 42% yield. Enone **1k** gave **3k** in 51% yield, and after isolation by column chromatography the product was obtained in 13% yield. Difluoromethyl enol ether

3l was formed from diketone **1l** in 25% yield. Finally, conversions of the two cyclic ketones **1m** and **1n** were studied. Both gave the expected products in yields of 50% (for **3m**) and 44% (for **3n**).

Besides these successful transformations several ketones proved unsuitable (Scheme S1 in Supporting Information File 1). Additionally, attempted [4 + 1]-type cycloadditions of three 1-arylprop-2-en-1-ones as heteroconjugated alkenes with difluorocarbene to give 2,2-difluoro-2,3-dihydrofurans [50] remained unsuccessful (Scheme S2 in Supporting Information File 1).

Two mechanisms have been proposed for the difluoromethylation of ketones, as illustrated in Scheme 4A. In both cases, the process begins with the generation of difluorocarbene from $TMSCF_2Br$ and KFHF. This is followed by a nucleophilic attack of the oxygen atom of ketone **1** on the difluorocarbene. Subsequently, a protonation–deprotonation sequence occurs, which can either be intermolecular, involving a molecule of HF, or intramolecular, proceeding through a five-membered transition state.

To clarify the mechanism, two experiments were conducted. In the first one, 2-acetonaphthone with a trideuteromethyl group (**1i-d$_3$**) was subjected to the standard reaction conditions. Two products were obtained: First, **3i-d$_2$** containing a CF_2H group, and second **3i-d$_3$** bearing a CF_2D group. The yields were 57% and 15%, respectively. In the second experiment, the potential for proton exchange in difluoromethyl enol ether **3h** was investigated. The compound was milled with the activator KFHF, CsCl as grinding auxiliary, and D_2O in a liquid-assisted grinding process. As a result, no H/D-exchange was detected. The experimental results of both experiments suggest that the reaction predominantly proceeds through an intermolecular pathway. The occurrence of the CF_2D product may be attributed to a minor intramolecular reaction path or the involvement of DF formed during the reaction.

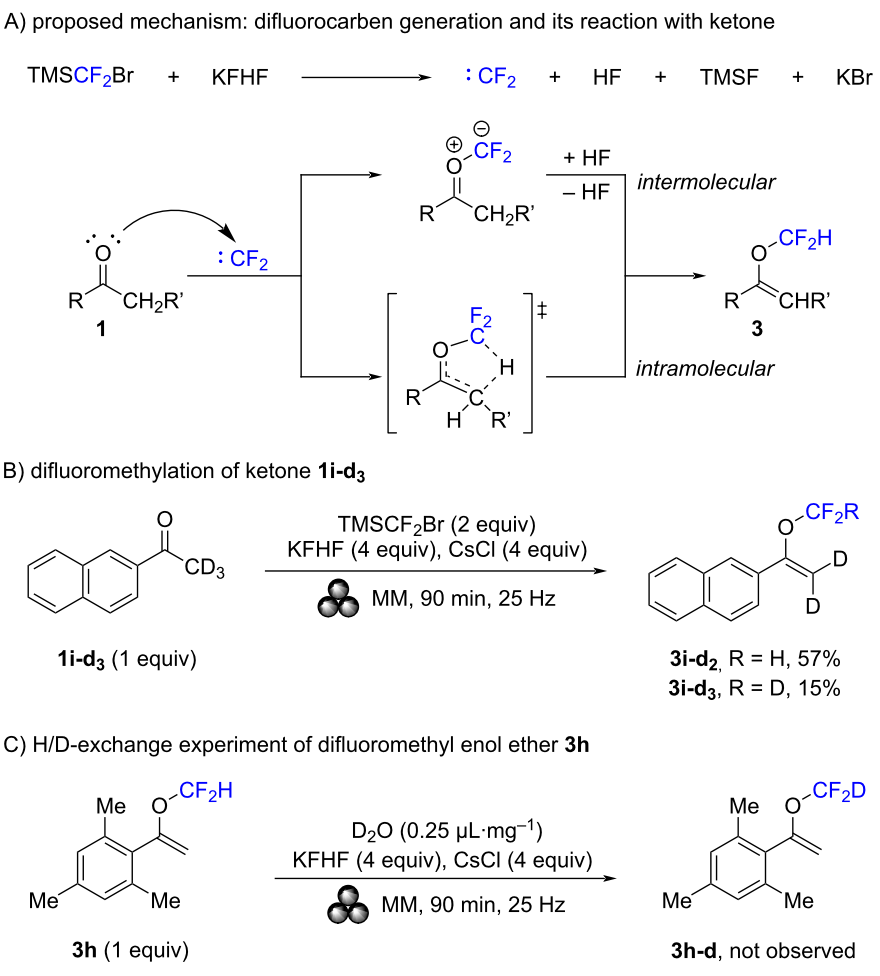

Scheme 4: Proposed mechanism (A) and mechanistic investigations (B and C). The yields were determined by ^{1}H NMR spectroscopy using 1,2-dichloroethane as internal standard.

Conclusion

In conclusion, we discovered a mechanochemical synthesis of difluoromethyl enol ethers. The products were obtained from the corresponding ketones at room temperature after a reaction time of 90 minutes. The investigation of the reaction scope revealed challenges in isolating the low-boiling non-polar products. Mechanistic studies suggested that in situ-generated difluorocarbene reacts with the ketone oxygen, followed by intermolecular protonation/deprotonation. Although the process has still synthetic limitations, also acyclic ketones can now be converted into difluoromethyl enol ethers, which have the potential for further functionalization.

Supporting Information

Supporting Information File 1

Experimental procedures, optimization studies, compound characterization data, NMR spectra, and mechanistic investigations.
[https://www.beilstein-journals.org/bjoc/content/supplementary/1860-5397-20-235-S1.pdf]

Funding

General support by RWTH Aachen University is appreciated.

Author Contributions

Jinbo Ke: investigation; writing – review & editing. Pit van Bonn: conceptualization; investigation; writing – original draft. Carsten Bolm: conceptualization; funding acquisition; methodology; supervision; writing – review & editing.

ORCID® iDs

Pit van Bonn - https://orcid.org/0000-0003-2900-1552
Carsten Bolm - https://orcid.org/0000-0001-9415-9917

Data Availability Statement

All data that supports the findings of this study is available in the published article and/or the supporting information of this article.

References

1. Stolle, A.; Szuppa, T.; Leonhardt, S. E. S.; Ondruschka, B. *Chem. Soc. Rev.* **2011,** *40,* 2317–2329. doi:10.1039/c0cs00195c
2. James, S. L.; Adams, C. J.; Bolm, C.; Braga, D.; Collier, P.; Friščić, T.; Grepioni, F.; Harris, K. D. M.; Hyett, G.; Jones, W.; Krebs, A.; Mack, J.; Maini, L.; Orpen, A. G.; Parkin, I. P.; Shearouse, W. C.; Steed, J. W.; Waddell, D. C. *Chem. Soc. Rev.* **2012,** *41,* 413–447. doi:10.1039/c1cs15171a
3. Howard, J. L.; Cao, Q.; Browne, D. L. *Chem. Sci.* **2018,** *9,* 3080–3094. doi:10.1039/c7sc05371a
4. Andersen, J.; Mack, J. *Green Chem.* **2018,** *20,* 1435–1443. doi:10.1039/c7gc03797j
5. Bolm, C.; Hernández, J. G. *Angew. Chem., Int. Ed.* **2019,** *58,* 3285–3299. doi:10.1002/anie.201810902
6. Friščić, T.; Mottillo, C.; Titi, H. M. *Angew. Chem., Int. Ed.* **2020,** *59,* 1018–1029. doi:10.1002/anie.201906755
7. Egorov, I. N.; Santra, S.; Kopchuk, D. S.; Kovalev, I. S.; Zyryanov, G. V.; Majee, A.; Ranu, B. C.; Rusinov, V. L.; Chupakhin, O. N. *Green Chem.* **2020,** *22,* 302–315. doi:10.1039/c9gc03414e
8. Kubota, K.; Ito, H. *Trends Chem.* **2020,** *2,* 1066–1081. doi:10.1016/j.trechm.2020.09.006
9. Pickhardt, W.; Grätz, S.; Borchardt, L. *Chem. – Eur. J.* **2020,** *26,* 12903–12911. doi:10.1002/chem.202001177
10. Cuccu, F.; De Luca, L.; Delogu, F.; Colacino, E.; Solin, N.; Mocci, R.; Porcheddu, A. *ChemSusChem* **2022,** *15,* e202200362. doi:10.1002/cssc.202200362
11. Colacino, E.; García, F. *Mechanochemistry and Emerging Technologies for Sustainable Chemical Manufacturing;* CRC Press: Boca Raton, FL, USA, 2023. doi:10.1201/9781003178187
12. Ardila-Fierro, K. J.; Hernández, J. G. *ChemSusChem* **2021,** *14,* 2145–2162. doi:10.1002/cssc.202100478
13. Fantozzi, N.; Volle, J.-N.; Porcheddu, A.; Virieux, D.; García, F.; Colacino, E. *Chem. Soc. Rev.* **2023,** *52,* 6680–6714. doi:10.1039/d2cs00997h
14. Hernández, J. G.; Bolm, C. *J. Org. Chem.* **2017,** *82,* 4007–4019. doi:10.1021/acs.joc.6b02887
15. Hutchings, B. P.; Crawford, D. E.; Gao, L.; Hu, P.; James, S. L. *Angew. Chem., Int. Ed.* **2017,** *56,* 15252–15256. doi:10.1002/anie.201706723
16. Pladevall, B. S.; de Aguirre, A.; Maseras, F. *ChemSusChem* **2021,** *14,* 2763–2768. doi:10.1002/cssc.202100497
17. Ardila-Fierro, K. J.; Hernández, J. G. *Angew. Chem., Int. Ed.* **2024,** *63,* e202317638. doi:10.1002/anie.202317638
18. Zholdassov, Y. S.; Kwok, R. W.; Shlain, M. A.; Patel, M.; Marianski, M.; Braunschweig, A. B. *RSC Mechanochem.* **2024,** *1,* 11–32. doi:10.1039/d3mr00018d
19. Müller, K.; Faeh, C.; Diederich, F. *Science* **2007,** *317,* 1881–1886. doi:10.1126/science.1131943
20. O'Hagan, D. *Chem. Soc. Rev.* **2008,** *37,* 308–319. doi:10.1039/b711844a
21. Purser, S.; Moore, P. R.; Swallow, S.; Gouverneur, V. *Chem. Soc. Rev.* **2008,** *37,* 320–330. doi:10.1039/b610213c
22. Liang, T.; Neumann, C. N.; Ritter, T. *Angew. Chem., Int. Ed.* **2013,** *52,* 8214–8264. doi:10.1002/anie.201206566
23. Zhou, Y.; Wang, J.; Gu, Z.; Wang, S.; Zhu, W.; Aceña, J. L.; Soloshonok, V. A.; Izawa, K.; Liu, H. *Chem. Rev.* **2016,** *116,* 422–518. doi:10.1021/acs.chemrev.5b00392
24. Meanwell, N. A. *J. Med. Chem.* **2018,** *61,* 5822–5880. doi:10.1021/acs.jmedchem.7b01788
25. Britton, R.; Gouverneur, V.; Lin, J.-H.; Meanwell, M.; Ni, C.; Pupo, G.; Xiao, J.-C.; Hu, J. *Nat. Rev. Methods Primers* **2021,** *1,* 47. doi:10.1038/s43586-021-00042-1
26. Han, J.; Remete, A. M.; Dobson, L. S.; Kiss, L.; Izawa, K.; Moriwaki, H.; Soloshonok, V. A.; O'Hagan, D. *J. Fluorine Chem.* **2020,** *239,* 109639. doi:10.1016/j.jfluchem.2020.109639
27. Yu, Y.; Liu, A.; Dhawan, G.; Mei, H.; Zhang, W.; Izawa, K.; Soloshonok, V. A.; Han, J. *Chin. Chem. Lett.* **2021,** *32,* 3342–3354. doi:10.1016/j.cclet.2021.05.042

28. Sap, J. B. I.; Meyer, C. F.; Straathof, N. J. W.; Iwumene, N.; am Ende, C. W.; Trabanco, A. A.; Gouverneur, V. *Chem. Soc. Rev.* **2021,** *50,* 8214–8247. doi:10.1039/d1cs00360g
29. Fuchibe, K.; Ichikawa, J. *Chem. Commun.* **2023,** *59,* 2532–2540. doi:10.1039/d2cc03950h
30. Xie, Q.; Hu, J. *Acc. Chem. Res.* **2024,** *57,* 693–713. doi:10.1021/acs.accounts.3c00719
31. Li, L.; Ni, C.; Xie, Q.; Hu, M.; Wang, F.; Hu, J. *Angew. Chem., Int. Ed.* **2017,** *56,* 9971–9975. doi:10.1002/anie.201705734
32. Olsen, D. A.; Osteraas, A. J. *J. Appl. Polym. Sci.* **1969,** *13,* 1523–1535. doi:10.1002/app.1969.070130715
33. Kirmse, W. *Carbene Chemistry;* Academic Press: New York, NY, USA, 1971; Vol. 1, pp 9–84. doi:10.1016/b978-0-12-409956-2.50006-6
34. van Bonn, P.; Ke, J.; Weike, C.; Ward, J. S.; Rissanen, K.; Bolm, C. *CCS Chem.* **2023,** *5,* 1737–1744. doi:10.31635/ccschem.023.202302783
35. Zafrani, Y.; Yeffet, D.; Sod-Moriah, G.; Berliner, A.; Amir, D.; Marciano, D.; Gershonov, E.; Saphier, S. *J. Med. Chem.* **2017,** *60,* 797–804. doi:10.1021/acs.jmedchem.6b01691
36. Zafrani, Y.; Sod-Moriah, G.; Yeffet, D.; Berliner, A.; Amir, D.; Marciano, D.; Elias, S.; Katalan, S.; Ashkenazi, N.; Madmon, M.; Gershonov, E.; Saphier, S. *J. Med. Chem.* **2019,** *62,* 5628–5637. doi:10.1021/acs.jmedchem.9b00604
37. Lin, J.-H.; Xiao, J.-C. Extension to the Construction of ORf Motifs (OCF_2H, $OCFH_2$, OCH_2CF_3, $OCFHCH_3$). In *Emerging Fluorinated Motifs: Synthesis, Properties, and Applications;* Cahard, D.; Ma, J.-A., Eds.; Wiley-VCH: Weinheim, Germany, 2020; Vol. 2, pp 267–288.
38. Loison, A.; Toulgoat, F.; Billard, T.; Hanquet, G.; Panossian, A.; Leroux, F. R. *Tetrahedron* **2021,** *99,* 132458. doi:10.1016/j.tet.2021.132458
39. Xie, Q.; Ni, C.; Zhang, R.; Li, L.; Rong, J.; Hu, J. *Angew. Chem., Int. Ed.* **2017,** *56,* 3206–3210. doi:10.1002/anie.201611823
40. Ford, J.; Hopkin, B.; Sap, J. B. I.; Gouverneur, V. *Isr. J. Chem.* **2023,** *63,* e202300109. doi:10.1002/ijch.202300109
41. Liu, G.; Wang, X.; Xu, X.-H.; Lu, X.; Tokunaga, E.; Tsuzuki, S.; Shibata, N. *Org. Lett.* **2013,** *15,* 1044–1047. doi:10.1021/ol4000313
42. Lin, X.; Weng, Z. *Org. Biomol. Chem.* **2015,** *13,* 3432–3437. doi:10.1039/c5ob00020c
43. Liu, C.; Deng, X.-Y.; Zeng, X.-L.; Zhao, G.; Lin, J.-H.; Wang, H.; Xiao, J.-C. *J. Fluorine Chem.* **2016,** *192,* 27–30. doi:10.1016/j.jfluchem.2016.10.011
44. Yue, C.-B.; Lin, J.-H.; Cai, J.; Zhang, C.-P.; Zhao, G.; Xiao, J.-C.; Li, H. *RSC Adv.* **2016,** *6,* 35705–35708. doi:10.1039/c6ra06338a
45. Liu, G.-K.; Li, X.; Qin, W.-B.; Lin, W.-F.; Lin, L.-T.; Chen, J.-Y.; Liu, J.-J. *Chin. Chem. Lett.* **2019,** *30,* 1515–1518. doi:10.1016/j.cclet.2019.03.036
46. Cai, X.; Zhai, Y.; Ghiviriga, I.; Abboud, K. A.; Dolbier, W. R. *J. Org. Chem.* **2004,** *69,* 4210–4215. doi:10.1021/jo049570y
47. Cai, X.; Wu, K.; Dolbier, W. R., Jr. *J. Fluorine Chem.* **2005,** *126,* 477–480. doi:10.1016/j.jfluchem.2004.11.006
48. Fuchibe, K.; Koseki, Y.; Sasagawa, H.; Ichikawa, J. *Chem. Lett.* **2011,** *40,* 1189–1191. doi:10.1246/cl.2011.1189
49. Fuchibe, K.; Koseki, Y.; Aono, T.; Sasagawa, H.; Ichikawa, J. *J. Fluorine Chem.* **2012,** *133,* 52–60. doi:10.1016/j.jfluchem.2011.09.012
50. Jia, Y.; Yuan, Y.; Huang, J.; Jiang, Z.-X.; Yang, Z. *Org. Lett.* **2021,** *23,* 2670–2675. doi:10.1021/acs.orglett.1c00577

License and Terms

BEILSTEIN JOURNAL OF ORGANIC CHEMISTRY

C–H Trifluoromethylthiolation of aldehyde hydrazones

Victor Levet[1], Balu Ramesh[1], Congyang Wang[*2] and Tatiana Besset[*1]

Full Research Paper

Open Access

Address:
[1]INSA Rouen Normandie, Univ Rouen Normandie, CNRS, Normandie Univ, COBRA UMR 6014, INC3M FR 3038, F-76000 Rouen, France and [2]Beijing National Laboratory for Molecular Sciences CAS key Laboratory of Molecular Recognition and Function CAS Research/Education Center for Excellence in Molecular Sciences Institute of Chemistry, Chinese Academy of Sciences, Beijing 100190, China

Email:
Congyang Wang[*] - wangcy@iccas.ac.cn; Tatiana Besset[*] - tatiana.besset@insa-rouen.fr

* Corresponding author

Keywords:
C–H bond functionalization; C–S bond formation; hydrazones; synthetic method; trifluoromethylthiolation

Beilstein J. Org. Chem. **2024,** *20,* 2883–2890.
https://doi.org/10.3762/bjoc.20.242

Received: 25 July 2024
Accepted: 28 October 2024
Published: 12 November 2024

This article is part of the thematic issue "Organofluorine chemistry VI".

Guest Editor: D. O'Hagan

Abstract

The selective C–H trifluoromethylthiolation of aldehyde hydrazones afforded interesting fluorinated building blocks, which could be used as a synthetic platform. Starting from readily available (hetero)aromatic and aliphatic hydrazones, the formation of a C–SCF_3 bond was achieved under oxidative and mild reaction conditions in the presence of the readily available $AgSCF_3$ salt via a one-pot sequential process (28 examples, up to 91% yield). Mechanistic investigations revealed that $AgSCF_3$ was the active species in the transformation.

Introduction

Fluorinated molecules are of paramount importance [1-12] from industrial applications [13-15] to our daily lives thanks to the specific features [16] of the fluorine atom or the fluorinated groups. Aiming at pushing beyond the frontiers of knowledge in this very active research field, emergent fluorinated groups [17-20] such as the SCF_3 moiety [21-51], an interesting fluorinated moiety with unique electron-withdrawing character and lipophilicity [52,53], have recently garnered interest from the scientific community. Various reagents and chemical transformations have been elaborated in this context over the years [21-51]. Despite these recent advances, the design of highly functionalized trifluoromethylthiolated molecules, which could be used as synthetic handles for synthesizing more complex molecules, is still appealing. In this context, we turned our attention to the trifluoromethylthiolated hydrazones, an interesting building block. Indeed, aldehyde hydrazones have been well studied and used in various transformations [54-64]. In consequence, a large number of transition-metal-catalyzed or radical-mediated processes for C–H functionalization of aldehyde hydrazones has flourished over the years.

An ideal scenario for a direct and sustainable synthetic route towards trifluoromethylthiolated hydrazones will be the direct C–H functionalization of the corresponding aldehyde hydrazone, an uncharted transformation to date. Forging a C–S bond by the direct C–H-bond functionalization of hydrazones is still underdeveloped. Except for transformations leading to the corresponding sulfur-containing heteroarenes, only a few methods have been developed (Scheme 1). In 1988, Lee and co-workers reported the synthesis of SR-containing hydrazones in a two-step process (chlorination [65] then reaction with thiols) from readily available aldehyde-derived hydrazones [66]. Wang et al. developed a method to access thiocyanated derivatives including an aldehyde hydrazone (a unique example) in 70% yield thanks to the in situ generation of SCN-succinimide from NCS and NH_4SCN (Scheme 1) [67]. In the same vein, the group of Monteiro [68], then Hajra [69], independently, reported the synthesis of 5-thioxo-1,2,4-triazolium inner salts by the nucleophilic thiocyanation of *N,N*-dialkylhydrazonoyl bromides, in situ generated from aldehyde-derived hydrazones in the presence of an oxidant (NBS, $(NH_4)_2S_2O_8$), Scheme 1). In 2024, the synthesis of 2-imino-1,3,4-thiadiazoles was achieved by cyclization of aryl hydrazones with aryl isothiocyanates promoted by elemental sulfur [70]. In the course of their studies for the thiocyanation of ketene dithioacetals, Yang, Wang and co-workers developed an electrochemical oxidization-based synthetic strategy to circumvent the need for external oxidants. In this context, a unique example of the thiocyanation of a hydrazone was depicted [71]. A key feature of the approach is to circumvent the need for external oxidants. In the same vein, the group of Hajra [72] and Yang [73], independently, investigated the electrochemical C–H sulfonylation of a library of aldehyde hydrazones using sodium sulfinates.

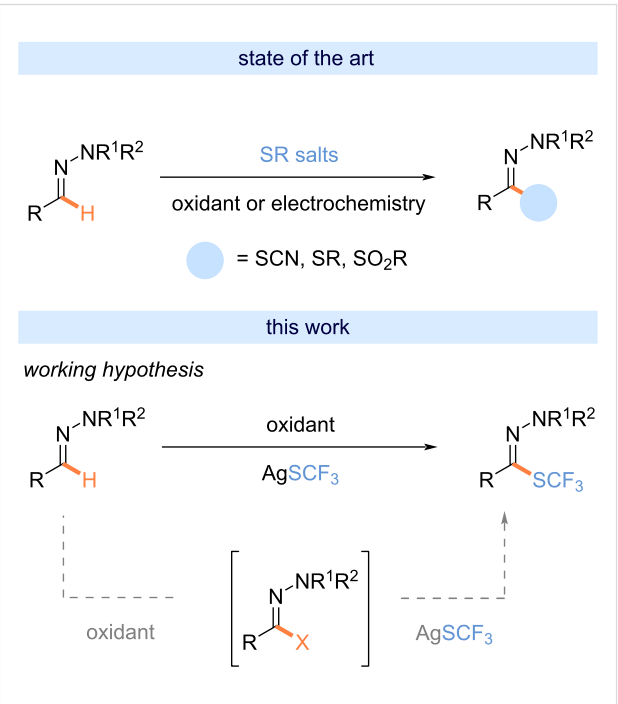

Scheme 1: State of the art and this work.

These seminal works brought interesting proofs of concept for the synthesis of SR-containing hydrazones. Inspired by these previous works and taking benefit from our in-home expertise to forge N–SCF_3 bond (after chlorination/anion metathesis with $AgSCF_3$ from the corresponding R^1R^2NH) [74], we assumed that a one-pot two-step process could be an efficient strategy for the trifluoromethylthiolation of hydrazones. Herein, the synthesis of trifluoromethylthiolated hydrazones from aldehyde hydrazones is depicted.

Results and Discussion

At the outset of the study, the morpholine hydrazone derived from 4-nitrobenzaldehyde was selected as a model substrate (Table 1). The latter was engaged in a two-step process: 1) halogenation to provide the corresponding *N,N*-hydrazonoyl bromide, which will then undergo an anion metathesis upon the addition of $AgSCF_3$ to the reaction mixture. When the reaction was conducted in the presence of NBS in acetonitrile for 10 min, followed by the addition of $AgSCF_3$, the desired product was isolated in 91% yield. A total selectivity for the formation of the *Z* isomer was observed as ascertained by 2D NMR (for more details, see Supporting Information File 1) [75]. Different reagents for the bromination or chlorination were also evaluated (Table 1, entries 1–3) and NBS was the most efficient one (Table 1, entry 1).

With the best reaction conditions in hand, the nature of the hydrazone part was first investigated (Scheme 2). Under standard reaction conditions, electron-enriched hydrazones provided the expected products in high yields (**2a**, **3a**, **4a**). Note, that in the case of the *N*-tosylhydrazone, further optimization reactions were required (for more details, see Supporting Information File 1), and reducing the temperature for the halogenation reaction was beneficial to the outcome of the reaction, affording **5a** in 55% yield. However, some other hydrazones **6a**–**8a** were reluctant (for more details, see Supporting Information File 1) [75].

Then, the scope of the reaction was investigated using the hydrazones derived from morpholine (Scheme 3). Hydrazones derived from aromatic aldehydes (**1a**–**p**) were first investigated. It turned out that *para*-substituted compounds with electron-rich groups (e.g., OMe, OBn), halogens (Cl, Br, I), and electron-withdrawing groups (e.g., CF_3) were smoothly trifluoromethylthiolated. In the same vein, *meta*- and *ortho*-substituted derivatives (**1l**–**o**) were converted into the corresponding fluorinated

Table 1: Optimization of the reaction conditions.[a]

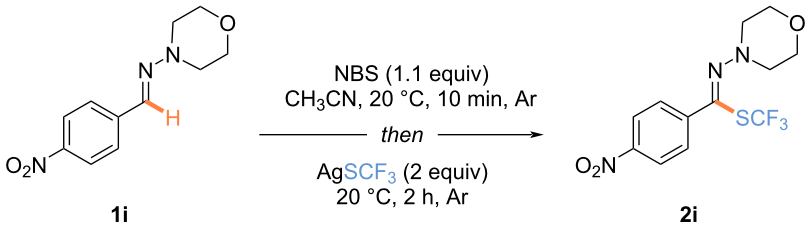

Entry	Deviation from reaction conditions	Yield (%)[b]
1	none	91
2	*N*-bromophthalimide instead of NBS	86[c]
3	NCS instead of NBS	ND

[a]Reaction conditions: hydrazone **1i** (0.15 mmol, 1.0 equiv), oxidant (0.165 mmol, 1.1 equiv), in CH_3CN (0.4 M), 20 °C, 10 min, then $AgSCF_3$ (0.3 mmol, 2.0 equiv), under argon. [b]Isolated yields are given. [c]The product was isolated with an inseparable impurity. ND = not determined.

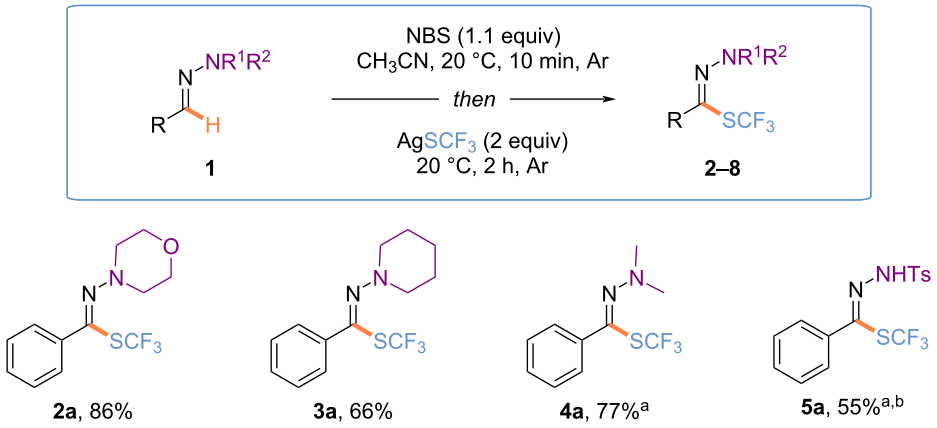

Scheme 2: Reaction conditions: hydrazone (0.3 mmol, 1.0 equiv), NBS (0.33 mmol, 1.1 equiv), in CH_3CN (0.4 M), 20 °C, 10 min; then, $AgSCF_3$ (0.6 mmol, 2.0 equiv), under argon. Isolated yields are given. [a]Products **4a** and **5a** were isolated with an inseparable impurity. [b]Reaction performed at 0 °C for the 1st step, and 20 °C for the 2nd one.

analogs. The functionalization of the 2,4-difluorophenyl derivative (**1p**) and the heteroaromatic compounds such as furan (**1q**) as well as pyridine (**1r**) derivatives went smoothly, with the lower yield obtained in the case of **2r** being explained by a tedious purification. Interestingly, the methodology was successfully applied to the functionalization of aliphatic hydrazones **1s** and **1t** and even the hydrazone derived from citronellal **1u**. The method was functional group-tolerant to various functional groups (nitro, CN, ester, alkenes) and halogens allowing an array of post-functionalization reactions. Finally, the trifluoromethylthiolation of molecules derived from compounds of interest was achieved to illustrate the synthetic utility of the method. Hence, the desired products **2v–x** were efficiently isolated.

To get more insights into the transformation, additional experiments were conducted. First, the reaction was repeated in the presence of radical scavengers, namely 2,2,6,6-tetramethylpiperidin-1-yl)oxyl (TEMPO) or di-*tert*-butylhydroxytoluene (BHT), and no significant impact on the outcome of the reaction was noticed (Scheme 4A). Pleasingly, the scale up of the reaction was smoothly conducted. Under standard reaction conditions, product **2a** (1.2 g) was afforded starting from **1a** (1 g), showcasing the robustness of the transformation (Scheme 4B). Intrigued about the nature of the active source of SCF_3 in the transformation, experiments with different SCF_3 sources were conducted. First, we hypothesized that trifluoromethylthiolated succinimide, which might be in situ generated from NBS and $AgSCF_3$, could be the active species. When the

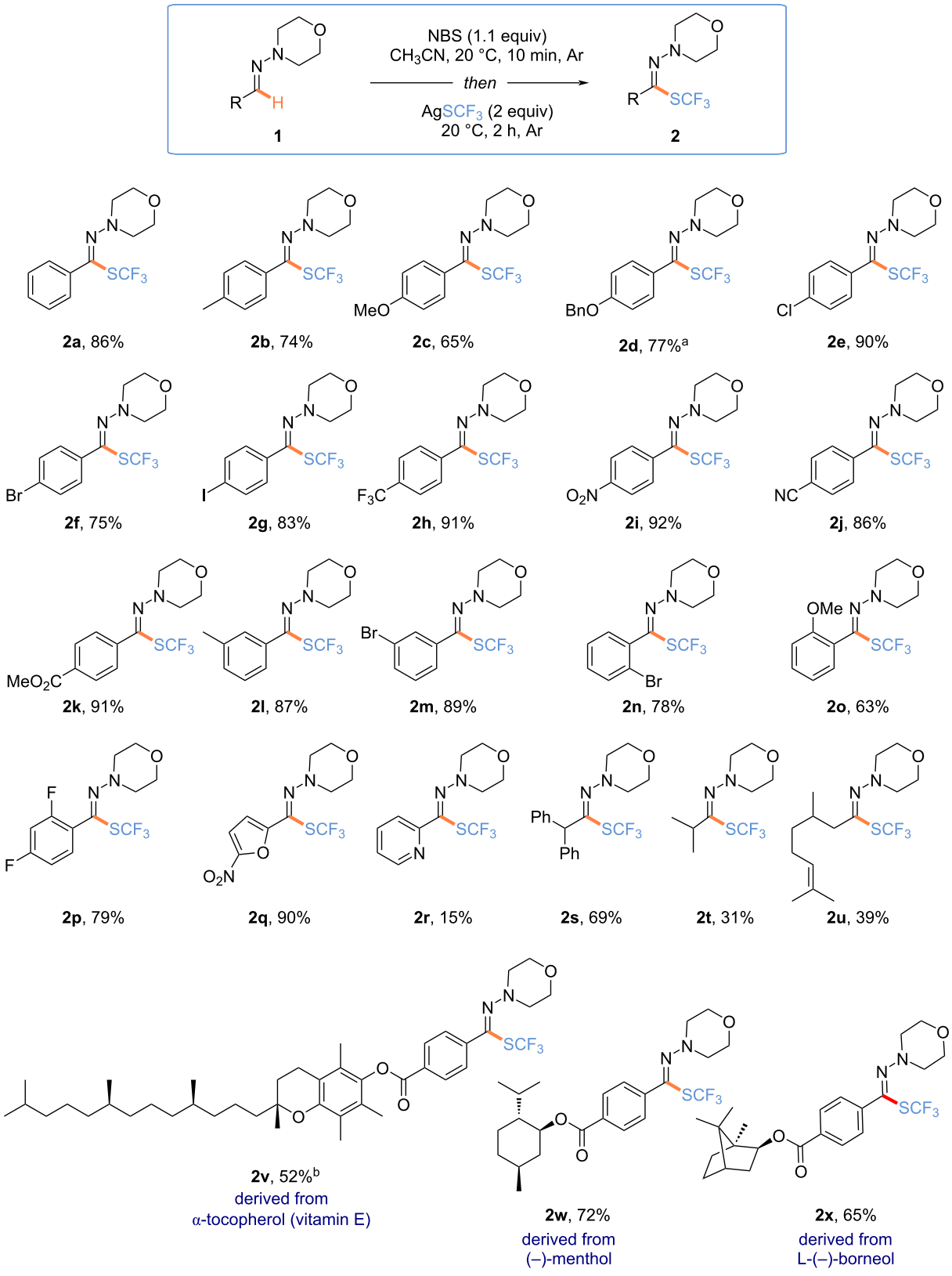

Scheme 3: Scope of the reaction. Reaction conditions: **1** (0.3 mmol, 1.0 equiv), NBS (0.33 mmol, 1.1 equiv) in CH_3CN (0.4 M), 20 °C, 10 min; then, $AgSCF_3$ (0.6 mmol, 2.0 equiv), 2 h, under argon. [a]0.15 mmol reaction scale. [b]Product **2v** was isolated with an inseparable impurity.

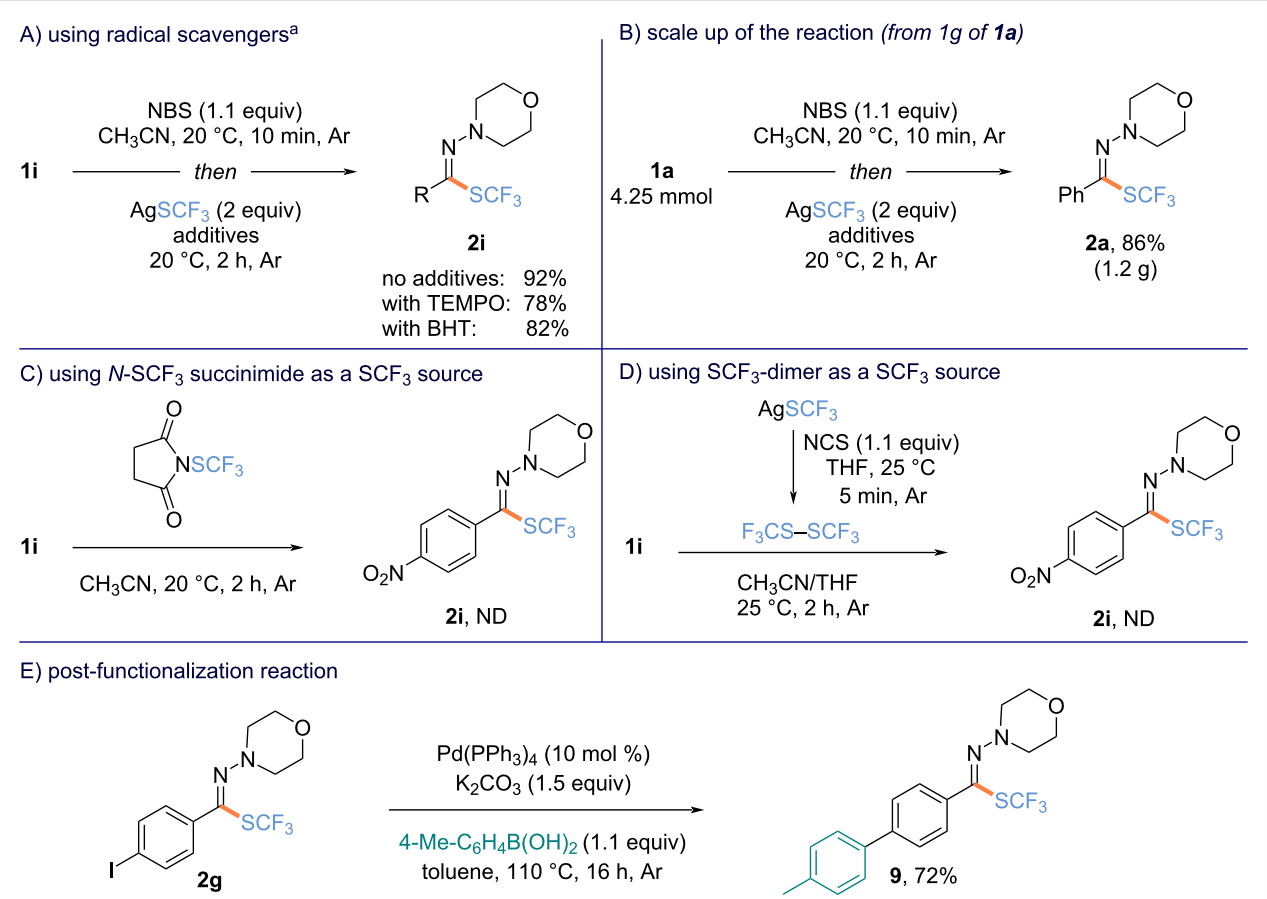

Scheme 4: Mechanistic investigations and post-functionalization reactions. [a]^{19}F NMR yields using α,α,α-trifluoroacetophenone as an internal standard. ND = not detected.

reaction was carried out in the presence of this electrophilic source and **1a**, no expected product was detected (Scheme 4C). Having in mind that in the presence of an oxidant, the SCF_3 dimer $(SCF_3)_2$ might be generated, an additional test was realized. In the presence of NCS in THF, $AgSCF_3$ was converted into the corresponding dimer in 5 min (monitored by ^{19}F NMR). Then, the reaction was conducted in the presence of **1a** in a THF/MeCN mixture (1:1) [75], but no product was detected (Scheme 4D). Based on these experiments and literature data [66], a two-step one-pot process was suggested based on 1) the bromination of the hydrazone **1** followed by 2) the anion metathesis in the presence of $AgSCF_3$. Finally, to further illustrate the synthetic utility of the trifluoromethylthiolated hydrazones, product **2g** was further functionalized. In the presence of 4-methylboronic acid, the arylation of **2g** occurred and the expected product was isolated in 72% yield with the SCF_3-hydrazone motif remaining untouched (Scheme 4E) [42].

Conclusion

In summary, a one-pot two-step process has been developed for the trifluoromethylthiolation of aldehyde hydrazones. A myriad of (hetero)aromatic and aliphatic hydrazones were efficiently functionalized including analogs of compounds of interest (28 examples, up to 91% yield) using readily available reagents, namely NBS and the nucleophilic reagent $AgSCF_3$. This approach provides a straightforward access to an unprecedented class of trifluoromethylthiolated derivatives. This method offers new avenues for synthesizing a plethora of valuable SCF_3-containing molecules using the synthetic potential of hydrazones in organic synthesis.

Experimental

General procedure for the preparation of trifluoromethylthiolated products 2–6: An oven-dried 10 mL reaction tube equipped with a stirring bar was charged with the hydrazone derivative (0.3 mmol, 1.0 equiv) and CH_3CN (0.7 mL). The mixture was stirred until the solubilization of the reagent. Then, recrystallized NBS (58.7 mg, 0.33 mmol, 1.1 equiv) was added, and the reaction mixture was stirred for 5–10 minutes, after which, $AgSCF_3$ (125.0 mg, 0.6 mmol, 2.0 equiv) was added. The reaction was stirred for another 2 hours at room temperature. α,α,α-Trifluoroacetophenone (42 µL, 0.3 mmol, 1.0 equiv)

was added as an internal standard for determining the ^{19}F NMR yield. The mixture was then filtered on a pad of celite and rinsed with CH_2Cl_2. The solution was then washed with brine twice (20 mL) and the organic layers were collected separately, dried over $MgSO_4$, and concentrated in vacuo. The crude was purified by column chromatography on silica gel, flash chromatography to afford the desired product **2**–**6**.

Supporting Information

Supporting Information File 1

Full experimental procedures, characterization of products, details of mechanistic studies, and spectral data.
[https://www.beilstein-journals.org/bjoc/content/supplementary/1860-5397-20-242-S1.pdf]

Funding

This work has been partially supported by University of Rouen Normandy, INSA Rouen Normandy, the Centre National de la Recherche Scientifique (CNRS), European Regional Development Fund (ERDF), Labex SynOrg (ANR-11-LABX-0029), Carnot Institute I2C, the graduate school for research XL-Chem (ANR-18-EURE-0020 XL CHEM), and Region Normandie. V.L. thanks the region Normandie for a doctoral fellowship. The French National Research Agency (ANR-21-CE07-0035-02 and ANR-22-CE92-0083) is gratefully acknowledged for generous financial support. R.B. thanks Normandy Region for a post-doctoral fellowship with the project NextFluoChem under the program «Normandie Recherche—Labels d'excellence» (n°23E02521).

Author Contributions

Victor Levet: investigation; methodology. Balu Ramesh: investigation; methodology. Congyang Wang: writing – review & editing. Tatiana Besset: conceptualization; funding acquisition; methodology; project administration; writing – original draft; writing – review & editing.

ORCID® iDs

Tatiana Besset - https://orcid.org/0000-0003-4877-5270

Data Availability Statement

All data that supports the findings of this study is available in the published article and/or the supporting information of this article.

References

1. Purser, S.; Moore, P. R.; Swallow, S.; Gouverneur, V. *Chem. Soc. Rev.* **2008,** *37,* 320–330. doi:10.1039/b610213c
2. Berger, R.; Resnati, G.; Metrangolo, P.; Weber, E.; Hulliger, J. *Chem. Soc. Rev.* **2011,** *40,* 3496–3508. doi:10.1039/c0cs00221f
3. Fujiwara, T.; O'Hagan, D. *J. Fluorine Chem.* **2014,** *167,* 16–29. doi:10.1016/j.jfluchem.2014.06.014
4. Ilardi, E. A.; Vitaku, E.; Njardarson, J. T. *J. Med. Chem.* **2014,** *57,* 2832–2842. doi:10.1021/jm401375q
5. Gillis, E. P.; Eastman, K. J.; Hill, M. D.; Donnelly, D. J.; Meanwell, N. A. *J. Med. Chem.* **2015,** *58,* 8315–8359. doi:10.1021/acs.jmedchem.5b00258
6. Zhou, Y.; Wang, J.; Gu, Z.; Wang, S.; Zhu, W.; Aceña, J. L.; Soloshonok, V. A.; Izawa, K.; Liu, H. *Chem. Rev.* **2016,** *116,* 422–518. doi:10.1021/acs.chemrev.5b00392
7. Landelle, G.; Panossian, A.; Leroux, F. R. *Curr. Top. Med. Chem.* **2014,** *14,* 941–951. doi:10.2174/1568026614666140202210016
8. Besset, T.; Poisson, T.; Pannecoucke, X. *Chem. – Eur. J.* **2014,** *20,* 16830–16845. doi:10.1002/chem.201404537
9. Champagne, P. A.; Desroches, J.; Hamel, J.-D.; Vandamme, M.; Paquin, J.-F. *Chem. Rev.* **2015,** *115,* 9073–9174. doi:10.1021/cr500706a
10. Ni, C.; Hu, J. *Chem. Soc. Rev.* **2016,** *45,* 5441–5454. doi:10.1039/c6cs00351f
11. Pan, Y. *ACS Med. Chem. Lett.* **2019,** *10,* 1016–1019. doi:10.1021/acsmedchemlett.9b00235
12. Nobile, E.; Castanheiro, T.; Besset, T. *Angew. Chem., Int. Ed.* **2021,** *60,* 12170–12191. doi:10.1002/anie.202009995
13. Inoue, M.; Sumii, Y.; Shibata, N. *ACS Omega* **2020,** *5,* 10633–10640. doi:10.1021/acsomega.0c00830
14. Wang, J.; Sánchez-Roselló, M.; Aceña, J. L.; del Pozo, C.; Sorochinsky, A. E.; Fustero, S.; Soloshonok, V. A.; Liu, H. *Chem. Rev.* **2014,** *114,* 2432–2506. doi:10.1021/cr4002879
15. Landelle, G.; Panossian, A.; Pazenok, S.; Vors, J.-P.; Leroux, F. R. *Beilstein J. Org. Chem.* **2013,** *9,* 2476–2536. doi:10.3762/bjoc.9.287
16. O'Hagan, D. *Chem. Soc. Rev.* **2008,** *37,* 308–319. doi:10.1039/b711844a
17. Xiong, H.-Y.; Pannecoucke, X.; Besset, T. *Chem. – Eur. J.* **2016,** *22,* 16734–16749. doi:10.1002/chem.201603438
18. Xiao, X.; Zheng, Z.-T.; Li, T.; Zheng, J.-L.; Tao, T.; Chen, L.-M.; Gu, J.-Y.; Yao, X.; Lin, J.-H.; Xiao, J.-C. *Synthesis* **2020,** *52,* 197–207. doi:10.1055/s-0039-1690714
19. Pannecoucke, X.; Besset, T. *Org. Biomol. Chem.* **2019,** *17,* 1683–1693. doi:10.1039/c8ob02995d
20. Besset, T.; Poisson, T. Extension to the SCF_2H, SCH_2F, and SCF_2R Motifs (R = $PO(OEt)_2$, CO_2R, R_f). In *Emerging Fluorinated Motifs;* Ma, A.; Cahard, D., Eds.; Wiley-VCH: Weinheim, Germany, 2020; pp 449–475. doi:10.1002/9783527824342.ch16
21. Toulgoat, F.; Alazet, S.; Billard, T. *Eur. J. Org. Chem.* **2014,** 2415–2428. doi:10.1002/ejoc.201301857
22. Boiko, V. N. *Beilstein J. Org. Chem.* **2010,** *6,* 880–921. doi:10.3762/bjoc.6.88
23. Xu, X.-H.; Matsuzaki, K.; Shibata, N. *Chem. Rev.* **2015,** *115,* 731–764. doi:10.1021/cr500193b
24. Barata-Vallejo, S.; Bonesi, S.; Postigo, A. *Org. Biomol. Chem.* **2016,** *14,* 7150–7182. doi:10.1039/c6ob00763e
25. Ye, K.-Y.; Zhang, X.; Dai, L.-X.; You, S.-L. *J. Org. Chem.* **2014,** *79,* 12106–12110. doi:10.1021/jo5019393
26. Lefebvre, Q.; Fava, E.; Nikolaienko, P.; Rueping, M. *Chem. Commun.* **2014,** *50,* 6617–6619. doi:10.1039/c4cc02060j
27. Liu, J.-B.; Xu, X.-H.; Chen, Z.-H.; Qing, F.-L. *Angew. Chem., Int. Ed.* **2015,** *54,* 897–900. doi:10.1002/anie.201409983

28. Jiang, L.; Qian, J.; Yi, W.; Lu, G.; Cai, C.; Zhang, W. *Angew. Chem., Int. Ed.* **2015,** *54,* 14965–14969. doi:10.1002/anie.201508495
29. Zheng, J.; Wang, L.; Lin, J.-H.; Xiao, J.-C.; Liang, S. H. *Angew. Chem., Int. Ed.* **2015,** *54,* 13236–13240. doi:10.1002/anie.201505446
30. Yin, G.; Kalvet, I.; Schoenebeck, F. *Angew. Chem., Int. Ed.* **2015,** *54,* 6809–6813. doi:10.1002/anie.201501617
31. Li, X.; Zhao, J.; Zhang, L.; Hu, M.; Wang, L.; Hu, J. *Org. Lett.* **2015,** *17,* 298–301. doi:10.1021/ol5034018
32. Li, M.; Guo, J.; Xue, X.-S.; Cheng, J.-P. *Org. Lett.* **2016,** *18,* 264–267. doi:10.1021/acs.orglett.5b03433
33. Candish, L.; Pitzer, L.; Gómez-Suárez, A.; Glorius, F. *Chem. – Eur. J.* **2016,** *22,* 4753–4756. doi:10.1002/chem.201600421
34. Zheng, H.; Huang, Y.; Weng, Z. *Tetrahedron Lett.* **2016,** *57,* 1397–1409. doi:10.1016/j.tetlet.2016.02.073
35. Matheis, C.; Wagner, V.; Goossen, L. J. *Chem. – Eur. J.* **2016,** *22,* 79–82. doi:10.1002/chem.201503524
36. Jarrige, L.; Carboni, A.; Dagousset, G.; Levitre, G.; Magnier, E.; Masson, G. *Org. Lett.* **2016,** *18,* 2906–2909. doi:10.1021/acs.orglett.6b01257
37. Liu, X.; An, R.; Zhang, X.; Luo, J.; Zhao, X. *Angew. Chem., Int. Ed.* **2016,** *55,* 5846–5850. doi:10.1002/anie.201601713
38. Yang, Y.; Xu, L.; Yu, S.; Liu, X.; Zhang, Y.; Vicic, D. A. *Chem. – Eur. J.* **2016,** *22,* 858–863. doi:10.1002/chem.201504790
39. Wang, F.; Zhao, L.; You, J.; Wang, M.-X. *Org. Chem. Front.* **2016,** *3,* 880–886. doi:10.1039/c6qo00161k
40. Bu, M.-j.; Lu, G.-p.; Cai, C. *Org. Chem. Front.* **2017,** *4,* 266–270. doi:10.1039/c6qo00622a
41. Lübcke, M.; Yuan, W.; Szabó, K. J. *Org. Lett.* **2017,** *19,* 4548–4551. doi:10.1021/acs.orglett.7b02139
42. Zhao, Q.; Poisson, T.; Pannecoucke, X.; Bouillon, J.-P.; Besset, T. *Org. Lett.* **2017,** *19,* 5106–5109. doi:10.1021/acs.orglett.7b02384
43. Gelat, F.; Poisson, T.; Biju, A. T.; Pannecoucke, X.; Besset, T. *Eur. J. Org. Chem.* **2018,** 3693–3696. doi:10.1002/ejoc.201800418
44. Ghiazza, C.; Khrouz, L.; Monnereau, C.; Billard, T.; Tlili, A. *Chem. Commun.* **2018,** *54,* 9909–9912. doi:10.1039/c8cc05256e
45. Saravanan, P.; Anbarasan, P. *Adv. Synth. Catal.* **2018,** *360,* 2894–2899. doi:10.1002/adsc.201800366
46. Xi, C.-C.; Chen, Z.-M.; Zhang, S.-Y.; Tu, Y.-Q. *Org. Lett.* **2018,** *20,* 4227–4230. doi:10.1021/acs.orglett.8b01627
47. He, J.; Chen, C.; Fu, G. C.; Peters, J. C. *ACS Catal.* **2018,** *8,* 11741–11748. doi:10.1021/acscatal.8b04094
48. Lindberg, E.; Angerani, S.; Anzola, M.; Winssinger, N. *Nat. Commun.* **2018,** *9,* 3539. doi:10.1038/s41467-018-05916-9
49. Zhang, J.; Yang, J.-D.; Zheng, H.; Xue, X.-S.; Mayr, H.; Cheng, J.-P. *Angew. Chem., Int. Ed.* **2018,** *57,* 12690–12695. doi:10.1002/anie.201805859
50. Luo, Z.; Yang, X.; Tsui, G. C. *Org. Lett.* **2020,** *22,* 6155–6159. doi:10.1021/acs.orglett.0c02235
51. Doche, F.; Poisson, T.; Besset, T. *ACS Catal.* **2023,** *13,* 14112–14120. doi:10.1021/acscatal.3c03249
52. Leo, A.; Hansch, C.; Elkins, D. *Chem. Rev.* **1971,** *71,* 525–616. doi:10.1021/cr60274a001
53. Hansch, C.; Leo, A.; Taft, R. W. *Chem. Rev.* **1991,** *91,* 165–195. doi:10.1021/cr00002a004
54. Xu, P.; Li, W.; Xie, J.; Zhu, C. *Acc. Chem. Res.* **2018,** *51,* 484–495. doi:10.1021/acs.accounts.7b00565
55. Xu, X.; Zhang, J.; Xia, H.; Wu, J. *Org. Biomol. Chem.* **2018,** *16,* 1227–1241. doi:10.1039/c8ob00056e
56. Brehme, R.; Enders, D.; Fernandez, R.; Lassaletta, J. M. *Eur. J. Org. Chem.* **2007,** 5629–5660. doi:10.1002/ejoc.200700746
57. Tatum, L. A.; Su, X.; Aprahamian, I. *Acc. Chem. Res.* **2014,** *47,* 2141–2149. doi:10.1021/ar500111f
58. Lazny, R.; Nodzewska, A. *Chem. Rev.* **2010,** *110,* 1386–1434. doi:10.1021/cr900067y
59. Kobayashi, S.; Mori, Y.; Fossey, J. S.; Salter, M. M. *Chem. Rev.* **2011,** *111,* 2626–2704. doi:10.1021/cr100204f
60. Kölmel, D. K.; Kool, E. T. *Chem. Rev.* **2017,** *117,* 10358–10376. doi:10.1021/acs.chemrev.7b00090
61. Cabré, A.; Verdaguer, X.; Riera, A. *Chem. Rev.* **2022,** *122,* 269–339. doi:10.1021/acs.chemrev.1c00496
62. Pair, E.; Monteiro, N.; Bouyssi, D.; Baudoin, O. *Angew. Chem., Int. Ed.* **2013,** *52,* 5346–5349. doi:10.1002/anie.201300782
63. Streit, A. D.; Zoll, A. J.; Hoang, G. L.; Ellman, J. A. *Org. Lett.* **2020,** *22,* 1217–1221. doi:10.1021/acs.orglett.0c00186
64. Zhang, M.; Duan, Y.; Li, W.; Xu, P.; Cheng, J.; Yu, S.; Zhu, C. *Org. Lett.* **2016,** *18,* 5356–5359. doi:10.1021/acs.orglett.6b02711
65. Patel, H. V.; Vyas, K. A.; Pandey, S. P.; Fernandes, P. S. *Tetrahedron* **1996,** *52,* 661–668. doi:10.1016/0040-4020(95)00916-7
66. Lee, V. J.; Curran, W. V.; Fields, T. F.; Learn, K. *J. Heterocycl. Chem.* **1988,** *25,* 1873–1891. doi:10.1002/jhet.5570250651
67. Chen, Q.; Lei, Y.; Wang, Y.; Wang, C.; Wang, Y.; Xu, Z.; Wang, H.; Wang, R. *Org. Chem. Front.* **2017,** *4,* 369–372. doi:10.1039/c6qo00676k
68. Prieto, A.; Uzel, A.; Bouyssi, D.; Monteiro, N. *Eur. J. Org. Chem.* **2017,** 4201–4204. doi:10.1002/ejoc.201700819
69. Mondal, S.; Samanta, S.; Hajra, A. *Eur. J. Org. Chem.* **2018,** 1060–1066. doi:10.1002/ejoc.201701722
70. Huynh, T. N.; Ong, K. T. N.; Dinh, P. T.; Nguyen, A. T.; Nguyen, T. T. *J. Org. Chem.* **2024,** *89,* 3202–3210. doi:10.1021/acs.joc.3c02675
71. Wen, J.; Zhang, L.; Yang, X.; Niu, C.; Wang, S.; Wei, W.; Sun, X.; Yang, J.; Wang, H. *Green Chem.* **2019,** *21,* 3597–3601. doi:10.1039/c9gc01351b
72. Sarkar, B.; Ghosh, P.; Hajra, A. *Org. Lett.* **2023,** *25,* 3440–3444. doi:10.1021/acs.orglett.3c00999
73. Yang, Q.-L.; Lei, P.-P.; Hao, E.-J.; Zhang, B.-N.; Zhou, H.-H.; Li, W.-W.; Guo, H.-M. *SynOpen* **2023,** *7,* 535–547. doi:10.1055/s-0042-1751510
74. Xiong, H.-Y.; Pannecoucke, X.; Besset, T. *Org. Chem. Front.* **2016,** *3,* 620–624. doi:10.1039/c6qo00064a
75. Note that when the standard reaction was conducted in a THF/MeCN mixture (1.3:1), **2a** was isolated in 82% yield.

BEILSTEIN JOURNAL OF ORGANIC CHEMISTRY

4,6-Diaryl-5,5-difluoro-1,3-dioxanes as chiral dopants for liquid crystal compositions

Maurice Médebielle[*1], Peer Kirsch[*2,3], Jérémy Merad[1], Carolina von Essen[‡2], Clemens Kühn[‡2] and Andreas Ruhl[‡2]

Full Research Paper

Open Access

Address:
[1]Universite Claude Bernard Lyon 1, CNRS, INSA Lyon, CPE, ICBMS, UMR 5246, Bâtiment LEDERER, 1 rue Victor Grignard, 69100 Villeurbanne Cedex, France, [2]Merck Electronics KGaA, Frankfurter Str. 250, D-64293 Darmstadt, Germany and [3]Institute of Materials Science, Technical University of Darmstadt, Peter-Grünberg-Str. 2, D-64287 Darmstadt, Germany

Email:
Maurice Médebielle[*] - maurice.medebielle@univ-lyon1.fr;
Peer Kirsch[*] - peer.kirsch@merckgroup.com

* Corresponding author ‡ Equal contributors

Keywords:
chiral dopant; chirality; cholesteric phase; diols; fluorine; helical twisting power; liquid crystal

Beilstein J. Org. Chem. **2024,** *20,* 2940–2945.
https://doi.org/10.3762/bjoc.20.246

Received: 30 July 2024
Accepted: 01 November 2024
Published: 14 November 2024

This article is part of the thematic issue "Organofluorine chemistry VI".

Guest Editor: D. O'Hagan

Abstract

Two racemic *anti*-4,6-diphenyl-5,5-difluoro-1,3-dioxanes were prepared and the corresponding enantiomers were evaluated as potential new chiral dopants for liquid-crystal compositions.

Introduction

Liquid crystals for use in liquid crystal displays (LCDs) have become one of the most prominent application areas of fluoro-organic chemistry [1-3]. In particular, cholesteric, i.e., chiral nematic, liquid crystals (LCs) are attractive for many display applications due to their chiroptical characteristics as well as the selective reflection of light giving rise to Bragg interference colors [4]. Cholesteric LCs can be obtained either from neat chiral mesogens, or through the addition of a chiral dopant to an achiral nematic liquid crystal [5,6]. The ability of the dopant to induce chirality in the nematic phase is defined as the *helical twisting power* [HTP; $\beta = (pc)^{-1}$; with p the helical pitch and c the molar concentration]. The most common type of liquid crystal displays (LCD) is based on the so-called twisted nematic (TN) mode and requires only a quite small HTP (typically around 10–15 μm^{-1}) with a low dopant concentration (around 0.1%) [1,2,7]. However, there are other display modes, such as super-twisted nematic (STN) LCDs which need a higher HTP or increased dopant concentrations [8,9]. TN and STN displays are still based on liquid crystals in the nematic or cholesteric mesophase. Even higher concentrations of chiral dopants with extremely high HTP tend to induce a Blue Phase, which is a cubic mesophase composed of double twist cylinders [10,11]. A

prototype of a polymer-stabilized Blue Phase LCD with ultra-fast switching times has been presented in 2008 by Samsung [12]. Another class of materials including high HTP chiral dopants are cholesteric films prepared by the polymerization of reactive mesogens (RMs). They are used, e.g., for improving the viewing angle-dependency of the image quality of LCD panels or as polarizing reflectors [13,14]. For such applications, new dopants with very high HTP are in constant demand. There have been many reported chiral dopants with relatively high HTPs, including 4,5-diaryl-1,3-dioxolanes [15], TADDOLs [16,17], axially chiral alleno-acetylenes [18] and strained axially chiral 1,1'-binaphthyl derivatives [19-22] to cite a few (Figure 1 for selected examples).

As a general observation, the more elongated the liquid crystal-like shape of a molecule appears, the more efficient is the induction of chirality in a nematic host. Additionally, the location of the chiral substructure within the dopant molecule seems to play a role. A more 'central' location within in the mesogenic core structure corresponds to a higher HTP of the resulting chiral compound. Molecular structures like those depicted in Figure 1 suggest that low conformational flexibility in combination with π-stacking interactions between the aryl moieties of the dopant and those of the LC mixture might be the key parameters for a high HTP. Significant efforts have been made exploring a wide range of chiral, twisted molecules such as binaphthyls [23-25], biphenyls [26,27], TADDOLs [16,17] and 1,2-diphenylethane-1,2-diol [28] to reveal possible relationships between the molecular structure of chiral dopants and their HTP value. However, quantitative structure–property relationships still remain elusive and are not well understood [29].

Recently we have become interested in the preparation of racemic [30] *anti*- and highly enantioenriched 2,2-difluoro-1,3-diols [30-32] through an acylative double catalytic kinetic resolution (DoCKR) process [33]. While the 1,3-diol motif is found in some natural products [34] with some fluorinated analogues [35,36], this motif is rarely found in LCs [37-39].

Based on these observations and literature data, we embarked in the synthesis and evaluation of enantiomerically pure acetals derived from *anti*-2,2-difluoro-1,3-diols as potential chiral dopants. Our long-term goal would be to provide a structure–property relationship of this class of molecules by i) modification of the aryl and ii) and/or acetal moieties (Scheme 1) and to elucidate the possible role of fluorine on their physical properties, with comparison to their non-fluorinated analogs [38]. It is anticipated that the introduction of a CF_2 could eventually stabilize the conformation of the six-membered ring via stereolectronic interactions of the CF σ* orbitals with the neighboring CH σ orbital [40]. The 180° FCCH dihedral would rigidify the six-membered ring.

We present here preliminary results with the diastereoselective synthesis of two 4,6-diphenyl-5,5-difluoro-1,3-dioxanes (*rac*-**3** and *rac*-**4**) and their separation into their corresponding enantio-

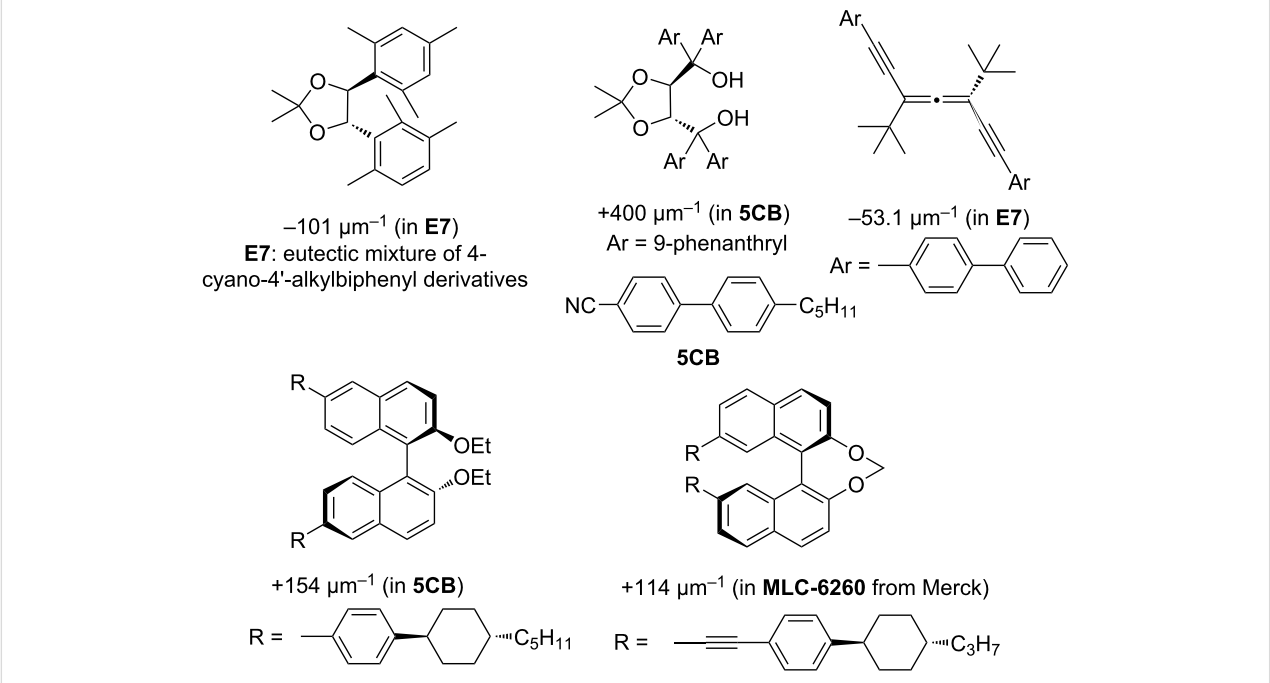

Figure 1: Selected examples of chiral dopants with high HTPs in their nematic host LC mixture.

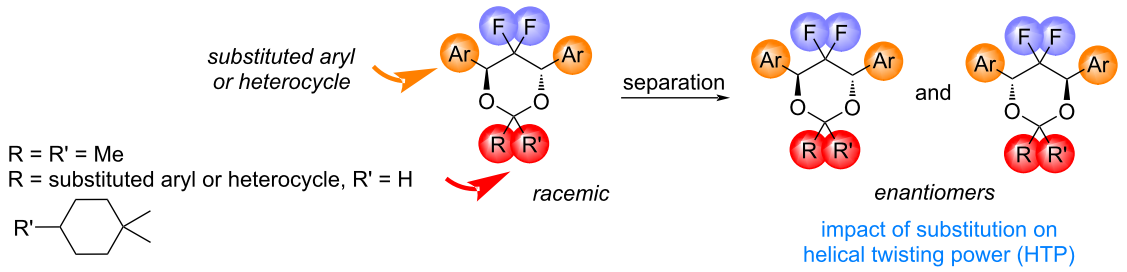

Scheme 1: Structure–property relationship of 4,6-diheteroaryl-5,5-difluoro-1,3-dioxanes as potential chiral dopants.

mers ((*R*,*R*)-**3** and (*S*,*S*)-**3**; (*R*,*R*)-**4** and (*S*,*S*)-**4**). *rac*-**3** and *rac*-**4** are obtained from readily available racemic 2,2-difluoro-1,3-diphenyl-1,3-propanediol (*rac*-**2**). These enantiomers were then evaluated as chiral dopants using two commercially available liquid crystal host mixtures (Host 1 and Host 2 from Merck KGaA) (Scheme 2).

Results and Discussion

Racemic *anti*-2,2-difluoro-1,3-diol *rac*-**2** was easily prepared through a single step by an aldol-Tishchenko reaction [30] starting from commercially available difluoromethyl phenyl ketone [41,42] and an excess of benzaldehyde (4 equiv), under basic conditions (Scheme 3). Diol *rac*-**2** was obtained in a 62% yield after recrystallization from $CHCl_3$ with no need for chromatography purification. Ketalization of *rac*-**2** with liquid crystal-like ketone **1** [43] (in toluene) or 2,2-dimethoxypropane **5** (in THF) provided dioxanes *rac*-**3** and *rac*-**4** in 56% and 62% yields, respectively (Scheme 2).

Samples of *rac*-**3** and *rac*-**4** were separated by preparative HPLC on a chiral phase. Suitable crystals of all enantiomers (*R*,*R*)-**3**/(*S*,*S*)-**3**, (*R*,*R*)-**4**/(*S*,*S*)-**4** were obtained by slow evaporation from *n*-heptane solution and structures were determined by X-ray diffraction, which allowed the correlation of the chiroptical properties with the configuration (Figure 2 and Figure 3).

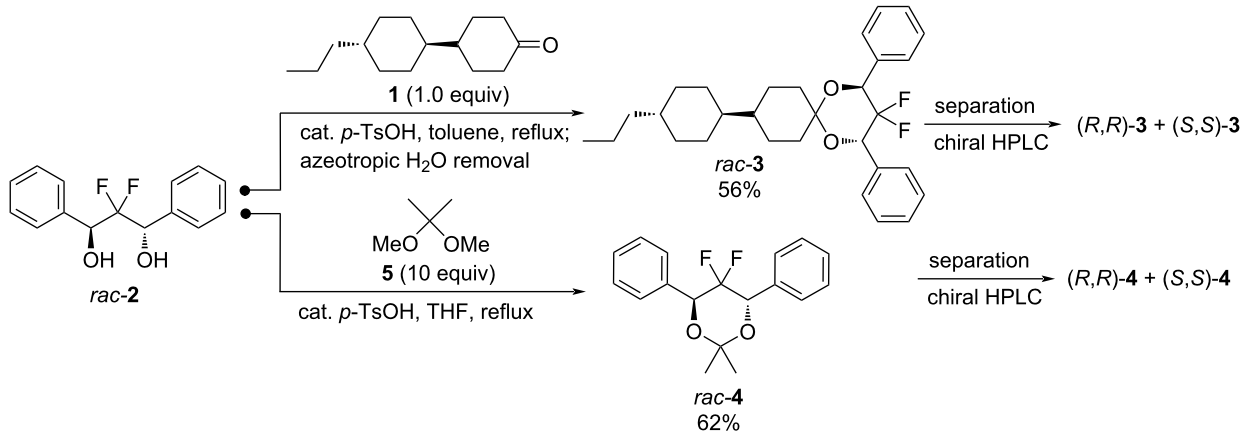

Scheme 2: The syntheses of chiral 4,6-diphenyl-5,5-difluoro-1,3-dioxanes **3** and **4** as dopants for cholesteric liquid crystals.

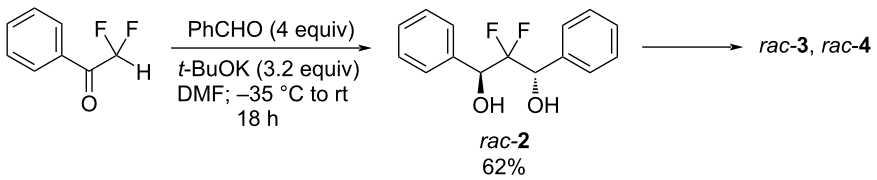

Scheme 3: Synthesis of *rac*-**2** as precursor of *rac*-**3** and *rac*-**4**.

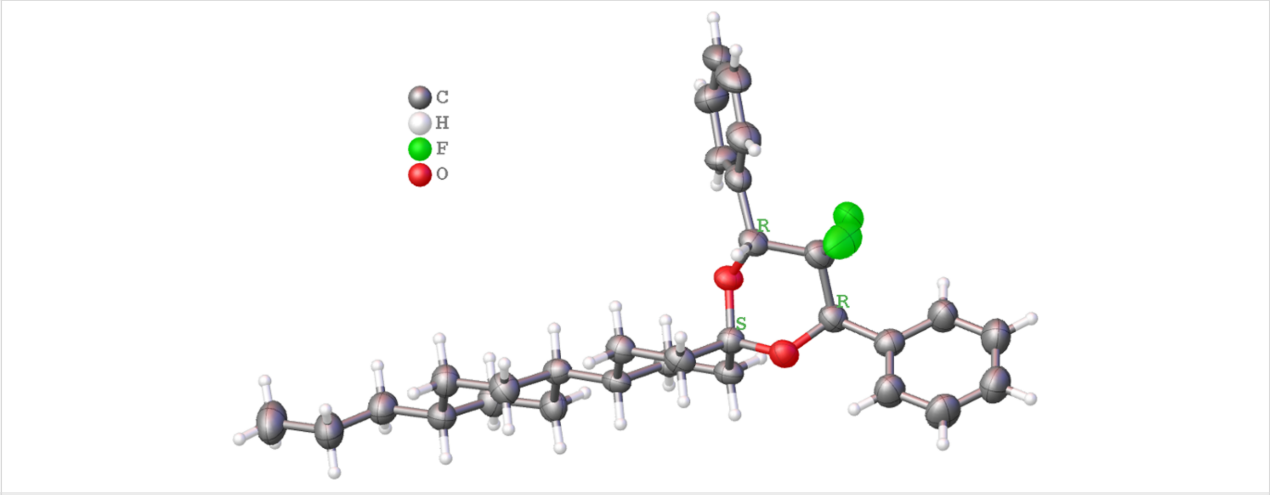

Figure 2: Configuration of (*R*,*R*)-**3** determined by X-ray crystallography.

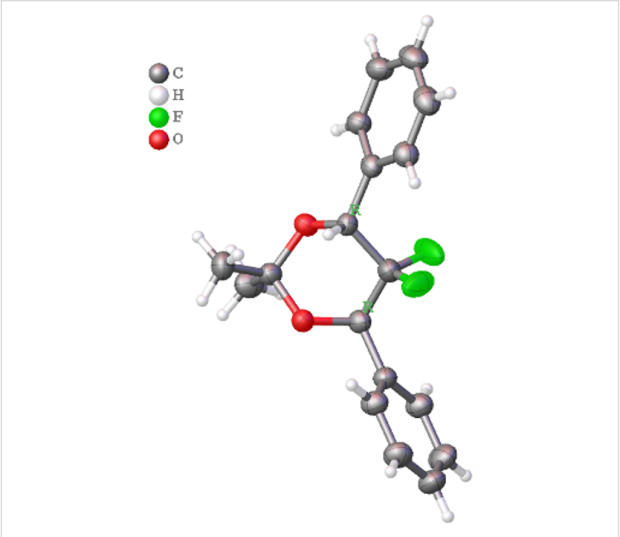

Figure 3: Configuration of (*R*,*R*)-**4** determined by X-ray crystallography.

The HTP of all enantiomers were measured with two achiral nematic host mixtures (Host 1 and Host 2 from Merck) (Table 1). (*R*,*R*)-**3** and (*S*,*S*)-**3** with a more liquid crystal-like shape have higher HTP [16 μm^{-1} (Host 1), 38 μm^{-1} (Host 2)] than the dimethylacetal analogues (*R*,*R*)-**4** and (*S*,*S*)-**4** [8 μm^{-1} (Host 1), 15 μm^{-1} (Host 2)]. The difference between the two nematic host mixtures is their polarity: whereas Host 1 is only moderately polar ($\Delta\varepsilon$ = 4.0), the mixture Host 2 was developed for Blue Mode LCD application and is extremely polar. As compared to chiral dopants depicted in Figure 1, HTPs are lower and closest analogues for comparison could be the 4,5-diaryl-1,3-dioxolanes [15,28]. However, in particular the HTPs obtained for **3** are encouraging, since the values are still equal or higher than those of many commercially used chiral dopants [7]. Both compounds **3** and **4** have good solubilities in LCs hosts, and since their syntheses require few steps and are easily amenable to structural variation (e.g., of the aromatic moieties), there is a clear path towards even higher HTPs values.

Table 1: Comparison of the physical properties of enantiopures (*R*,*R*)-**3**, (*S*,*S*)-**3**, (*R*,*R*)-**4** and (*S*,*S*)-**4**.

No	Phase sequence[a]	ΔH_{Cl}[b]	$T_{NI,virt}$[a,c]	$[\alpha]_D^{20}$[d]	HTP[e]
(*R*,*R*)-**3**	C 148 I	8500	–58.3	–5.20	–16 (Host 1) –38 (Host 2)
(*S*,*S*)-**3**	C 149 I	8500	–61.2	+ 6.80	+16 (Host 1) +38 (Host 2)
(*R*,*R*)-**4**	C 142 I	5100	–	–0.67	–8 (Host 1) –15 (Host 2)
(*S*,*S*)-**4**	C 142 I	5600	–	+ 0.60	+8 (Host 1) +15 (Host 2)

[a]The phase transition and virtual clearing temperatures $T_{NI,virt}$ are given in °C; [b]the melting enthalpies ΔH_{Cl} are given in cal mol^{-1}; [c]the values are extrapolated from a 5% w/w solution in ZLI-4792; [d]the optical rotations are given in °; [e]the helical twisting power (HTP) is given in μm^{-1}; C = crystalline, I = isotropic. The "virtual" clearing temperatures T_{NI} were determined by linear extrapolation from a 5% w/w solution in the Merck mixture ZLI-4792 (T_{NI} = 92.8 °C, $\Delta\varepsilon$ = 5.3, Δn = 0.0964). The extrapolated values are corrected empirically for differences in the order parameter. For the pure substances the phase transitions were identified by optical microscopy, and the corresponding temperatures by differential scanning calorimetry (DSC).

Conclusion

In general, the C_2-symmetric substructure in compounds (*R*,*R*)-/(*S*,*S*)-**3** and (*R*,*R*)-/(*S*,*S*)-**4** is quite efficient in inducing a chiral pitch into the nematic host mixtures Host 1 and Host 2. The extension of the chiral substructure (**4** →**3**) by the liquid crystal building block **1** into a more rod-like shape is further boosting the HTP by roughly a factor of 2. Moreover, the HTP of both compounds **3** and **4** depends strongly on the LC host mixture: for the more polar mixture Host 2 it is twice as high as for less polar Host 1.

Supporting Information

Supporting Information File 1

Experimental procedures, analytical data and copies of NMR spectra.
[https://www.beilstein-journals.org/bjoc/content/supplementary/1860-5397-20-246-S1.pdf]

Acknowledgements

The Centre Commun de Spectrométrie de Masse (CCSM) et de RMN (CCRMN) of the Université Claude Bernard Lyon 1 are thanked for assistance.

Funding

This work was supported by the Université Claude Bernard Lyon 1, Centre National de la Recherche Scientifique (CNRS) and Merck KGaA.

ORCID® iDs

Maurice Médebielle - https://orcid.org/0000-0002-6032-4790
Peer Kirsch - https://orcid.org/0000-0002-9024-7933
Jérémy Merad - https://orcid.org/0000-0003-2364-2535
Carolina von Essen - https://orcid.org/0000-0001-7970-5473
Clemens Kühn - https://orcid.org/0000-0003-2133-5400

Data Availability Statement

All data that supports the findings of this study is available in the published article and/or the supporting information of this article.

References

1. Kirsch, P.; Bremer, M. *Angew. Chem., Int. Ed.* **2000,** *39,* 4216–4235. doi:10.1002/1521-3773(20001201)39:23<4216::aid-anie4216>3.0.co;2-k
2. Bremer, M.; Kirsch, P.; Klasen-Memmer, M.; Tarumi, K. *Angew. Chem., Int. Ed.* **2013,** *52,* 8880–8896. doi:10.1002/anie.201300903
3. Kirsch, P. *J. Fluorine Chem.* **2015,** *177,* 29–36. doi:10.1016/j.jfluchem.2015.01.007
4. Kitzerow, H. S.; Bahr, C., Eds. *Chirality in Liquid Crystals;* Springer: New York, NY, USA, 2001. doi:10.1007/b97374
5. Eelkema, R.; Feringa, B. L. *Org. Biomol. Chem.* **2006,** *4,* 3729–3745. doi:10.1039/b608749c
6. Katsonis, N.; Lacaze, E.; Ferrarini, A. *J. Mater. Chem.* **2012,** *22,* 7088–7097. doi:10.1039/c2jm15962g
7. Pauluth, D.; Wächtler, A. E. F. *Synthesis and Application of Chiral Liquid Crystals*. In *Chirality in Industry II;* Collins, A. N.; Sheldrake, G. N.; Crosby, J., Eds.; John Wiley & Sons: New York, NY, USA, 1997; pp 263–286.
8. Scheffer, T. J.; Nehring, J. *Appl. Phys. Lett.* **1984,** *45,* 1021–1023. doi:10.1063/1.95048
9. Scheffer, T. J.; Nehring, J. *J. Appl. Phys.* **1985,** *58,* 3022–3031. doi:10.1063/1.335851
10. Kikuchi, H.; Yokota, M.; Hisakado, Y.; Yang, H.; Kajiyama, T. *Nat. Mater.* **2002,** *1,* 64–68. doi:10.1038/nmat712
11. Wittek, M.; Tanaka, N.; Bremer, M.; Wilkes, D.; Pauluth, D.; Tarumi, K. Novel materials for polymer-stabilized blue phase. In *Proc. SPIE 8279,* Emerging Liquid Crystal Technologies VII, San Francisco, CA, USA, Feb 10, 2012; 82790W. doi:10.1117/12.908138
12. https://phys.org/news/2008-05-samsung-worlds-blue-phase-technology.html (accessed June 21, 2024).
13. Allen, J. D. W.; Adlem, K.; Heeney, M. *J. Mater. Chem. C* **2021,** *9,* 17419–17426. doi:10.1039/d1tc05068k
14. Thiem, H.; Strohriegl, P.; Shkunov, M.; McCulloch, I. *Macromol. Chem. Phys.* **2005,** *206,* 2153–2159. doi:10.1002/macp.200500272
15. Rosini, C.; Spada, G. P.; Proni, G.; Masiero, S.; Scamuzzi, S. *J. Am. Chem. Soc.* **1997,** *119,* 506–512. doi:10.1021/ja962445m
16. Kuball, H.-G.; Weiß, B.; Beck, A. K.; Seebach, D. *Helv. Chim. Acta* **1997,** *80,* 2507–2514. doi:10.1002/hlca.19970800818
17. Seebach, D.; Beck, A. K.; Heckel, A. *Angew. Chem., Int. Ed.* **2001,** *40,* 92–138. doi:10.1002/1521-3773(20010105)40:1<92::aid-anie92>3.0.co;2-k
18. Wezenberg, S. J.; Ferroni, F.; Pieraccini, S.; Schweizer, W. B.; Ferrarini, A.; Spada, G. P.; Diederich, F. *RSC Adv.* **2013,** *3,* 22845–22848. doi:10.1039/c3ra44883e
19. Kakisaka, K.; Higuchi, H.; Okumura, Y.; Kikuchi, H. *J. Mater. Chem. C* **2014,** *2,* 6467–6470. doi:10.1039/c4tc01049c
20. Goh, M.; Park, J.; Han, Y.; Ahn, S.; Akagi, K. *J. Mater. Chem.* **2012,** *22,* 25011–25018. doi:10.1039/c2jm35282f
21. Taugerbeck, A.; Kirsch, P.; Pauluth, D.; Krause, J.; Suermann, J.; Heckmeier, M. Chiral binaphthol derivatives. WO Patent WO2002034739A1, May 2, 2002.
22. Kühn, C.; Bremer, M.; Schreiner, P. R. *Liq. Cryst.* **2019,** *46,* 1763–1768. doi:10.1080/02678292.2019.1599455
23. Gottarelli, G.; Hibert, M.; Samori, B.; Solladié, G.; Spada, G. P.; Zimmermann, R. *J. Am. Chem. Soc.* **1983,** *105,* 7318–7321. doi:10.1021/ja00363a019
24. Deußen, H.-J.; Shibaev, P. V.; Vinokur, R.; Bjørnholm, T.; Schaumburg, K.; Bechgaard, K.; Shibaev, V. P. *Liq. Cryst.* **1996,** *21,* 327–340. doi:10.1080/02678299608032841
25. Proni, G.; Spada, G. P.; Lustenberger, P.; Welti, R.; Diederich, F. *J. Org. Chem.* **2000,** *65,* 5522–5527. doi:10.1021/jo0001683
26. Williams, V. E.; Lemieux, R. P. *Chem. Commun.* **1996,** 2259–2260. doi:10.1039/cc9960002259
27. di Matteo, A.; Todd, S. M.; Gottarelli, G.; Solladié, G.; Williams, V. E.; Lemieux, R. P.; Ferrarini, A.; Spada, G. P. *J. Am. Chem. Soc.* **2001,** *123,* 7842–7851. doi:10.1021/ja010406r

28. Superchi, S.; Donnoli, M. I.; Proni, G.; Spada, G. P.; Rosini, C. *J. Org. Chem.* **1999,** *64,* 4762–4767. doi:10.1021/jo990038y
29. Pieraccini, S.; Ferrarini, A.; Spada, G. P. *Chirality* **2008,** *20,* 749–759. doi:10.1002/chir.20482
30. Xu, W.; Médebielle, M.; Bellance, M.-H.; Dolbier, W. R., Jr. *Adv. Synth. Catal.* **2010,** *352,* 2787–2790. doi:10.1002/adsc.201000548
31. Shao, N.; Rodriguez, J.; Quintard, A. *Org. Lett.* **2020,** *22,* 7197–7201. doi:10.1021/acs.orglett.0c02536
32. Prakash, G. K. S.; Hu, J.; Mathew, T.; Olah, G. A. *Angew. Chem., Int. Ed.* **2003,** *42,* 5216–5219. doi:10.1002/anie.200352172
33. Desrues, T.; Merad, J.; Andrei, D.; Pons, J.-M.; Parrain, J.-L.; Médebielle, M.; Quintard, A.; Bressy, C. *Angew. Chem., Int. Ed.* **2021,** *60,* 24924–24929. doi:10.1002/anie.202107041
34. Herkommer, D.; Schmalzbauer, B.; Menche, D. *Nat. Prod. Rep.* **2014,** *31,* 456–467. doi:10.1039/c3np70093c
See for a review on polyketide natural products containing the anti-1,3-diol motif.
35. Bentler, P.; Bergander, K.; Daniliuc, C. G.; Mück-Lichtenfeld, C.; Jumde, R. P.; Hirsch, A. K. H.; Gilmour, R. *Angew. Chem., Int. Ed.* **2019,** *58,* 10990–10994. doi:10.1002/anie.201905452
See for the development of fluorinated analogs of natural 1,3-diols.
36. Sperandio, C.; Quintard, G.; Naubron, J.-V.; Giorgi, M.; Yemloul, M.; Parrain, J.-L.; Rodriguez, J.; Quintard, A. *Chem. – Eur. J.* **2019,** *25,* 15098–15105. doi:10.1002/chem.201902983
See for the development of fluorinated analogs of natural 1,3-diols.
37. Kusumoto, T.; Sato, K.-I.; Ogino, K.; Hiyama, T.; Takehara, S.; Osawa, M.; Nakamura, K. *Liq. Cryst.* **1993,** *14,* 727–732. doi:10.1080/02678299308027750
38. Farrand, L. D.; Saxton, P. E.; Patrick, J. Mesogenic compounds, liquid crystal medium and liquid crystal composition. Eur. Pat. Appl. EP1690916A1, March 12, 2008.
39. Yang, S.; Wang, B.; Cui, D.; Kerwood, D.; Wilkens, S.; Han, J.; Luk, Y.-Y. *J. Phys. Chem. B* **2013,** *117,* 7133–7143. doi:10.1021/jp401382h
40. O'Hagan, D. *Chem. – Eur. J.* **2020,** *26,* 7981–7997. doi:10.1002/chem.202000178
41. Amii, H.; Kobayashi, T.; Hatamoto, Y.; Uneyama, K. *Chem. Commun.* **1999,** *14,* 1323–1324. doi:10.1039/a903681d
42. Prakash, G. K. S.; Hu, J.; Olah, G. A. *J. Fluorine Chem.* **2001,** *112,* 355–360. doi:10.1016/s0022-1139(01)00535-8
43. CAS 82832-73-3 for the bicyclohexanone derivative **1** which is a common liquid crystal building block and was obtained from Merck KGaA, Darmstadt.

License and Terms

BEILSTEIN JOURNAL OF ORGANIC CHEMISTRY

gem-Difluorovinyl and trifluorovinyl Michael acceptors in the synthesis of α,β-unsaturated fluorinated and nonfluorinated amides

Monika Bilska-Markowska[*1], Marcin Kaźmierczak[*1,2], Wojciech Jankowski[1] and Marcin Hoffmann[1]

Letter

Open Access

Address:
[1]Faculty of Chemistry, Adam Mickiewicz University in Poznań, Uniwersytetu Poznańskiego 8, 61-614 Poznań, Poland and [2]Center for Advanced Technologies, Adam Mickiewicz University in Poznań, Uniwersytetu Poznańskiego 10, 61-614 Poznań, Poland

Email:
Monika Bilska-Markowska[*] - mbilska@amu.edu.pl;
Marcin Kaźmierczak[*] - marcin.kazmierczak@amu.edu.pl

* Corresponding author

Keywords:
gem-difluorovinyl Michael acceptors; Michael addition; trifluorovinyl Michael acceptors; α,β-unsaturated amides

Beilstein J. Org. Chem. **2024,** *20,* 2946–2953.
https://doi.org/10.3762/bjoc.20.247

Received: 25 September 2024
Accepted: 08 November 2024
Published: 15 November 2024

This article is part of the thematic issue "Organofluorine chemistry VI" and is dedicated to Professor Henryk Koroniak in honor of his 75th birthday.

Guest Editor: D. O'Hagan

Abstract

The incorporation of fluorine atoms within the structure of organic compounds is known to exert a significant impact on their electronic properties, thereby modulating their reactivity in diverse chemical transformations. In the context of our investigation, we observed a striking illustration of this phenomenon. A Michael addition involving *gem*-difluorovinyl and trifluorovinyl acceptors was successfully achieved, demonstrating high stereoselectivity. This selectivity was further elucidated through theoretical calculations. Using this methodology, a series of new α,β-unsaturated amides, both fluorinated and nonfluorinated, were synthesized.

Introduction

The Michael reaction, characterized by the addition of stable carbon nucleophiles to unsaturated compounds with electron-withdrawing groups, is a cornerstone in constructing carbon–carbon and carbon–heteroatom bonds [1]. It is instrumental in synthesizing natural products [2-5] and pharmaceuticals [6], underlining its significance in organic chemistry. Recent advancements have broadened the scope of Michael donors and acceptors to encompass fluorine-containing compounds, enhancing the reaction's utility in synthesizing fluorinated derivatives [7,8]. Shibata and colleagues pioneered the use of fluorinated Michael donors, notably achieving enantioselective addition of 1-fluorobis(phenylsulfonyl)methane (FBSM) to α,β-unsaturated ketones with cinchona alkaloids [9]. Fluorinated Michael acceptors usually contain one fluorine atom or a

trifluoromethyl group in the structure [10-12]. There are also known examples of *gem*-difluoroalkenes being used as Michael acceptors [13-17]. The Michael addition with fluorinated acceptors finds application in the synthesis of, among others, fluorinated amino acids, which can be a structural motif in many biologically active compounds [18]. There are also known studies on the incorporation of highly reactive fluorinated Michael acceptors into peptide structures, which can act as the link between an active molecule and its cellular target [19,20]. Such endeavors hint at the potential of fluorinated acceptors in designing fluorinated peptidomimetics, an area attracting global research interest [21-24].

In our laboratory, we have explored the synthesis of 3,3,3-trifluoro- and 2,3,3,3-tetrafluoro-*N*-substituted propanamides, contributing to the field of fluorinated amides [25]. We have also investigated deprotonation at the α position of other fluorinated carbonyl derivatives as a route to new building blocks [26]. Despite the known instability of trifluoromethylated carbanions [27], their catalytic application has yielded valuable products [28-30]. *gem*-Difluoroalkenes and trifluoroalkenes are excellent acceptors in the Michael addition reactions. There are also known examples of the use of *gem*-difluoroalkenes and trifluoroalkenes in reactions with Grignard reagents [13,31]. Although, similar compounds are reported to be unstable molecules that are prone to decomposition under reaction conditions [32,33].

The goal of this work was the formation of *gem*-difluoro- and trifluorovinyl Michael acceptors by using organolithium reagents (Scheme 1), revealing new avenues in fluorinated unsaturated amide synthesis, which are present in numerous natural products, pharmaceuticals, and polymers [34-38]. The obtained α,β-unsaturated amides may represent promising structural motifs for further synthesis, e.g., via pericyclic reactions or nucleophilic additions.

Results and Discussion

We commenced our research by screening the nature of the base to generate carbanion at *alpha* position. We chose 2,3,3,3-tetrafluoro-*N*-heptylpropanamide, obtained according to the procedure developed earlier in our laboratory [25], for our model reaction. The reactions were carried out under inert gas conditions in anhydrous solvents (THF or DCM) at −78 °C for 3 h, using several bases and electrophiles (Table 1). The use of electrophiles in the first test reactions was to confirm the generation of a carbanion, which was to be evidenced by a substitution reaction at the *alpha* position. We started testing the different bases with lithium bis(trimethylsilyl)amide [39]. The reactions did not take place in the presence of LiHMDS (Table 1, entries 1 and 2), using either benzyl bromide or methyl iodide as electrophiles. Next, $TiCl_4$ as metal enolate mediator was applied. In the presence of both, Et_3N as well as *N,N,N′,N′*-tetramethyl-1,3-propanediamine no reaction was observed (Table 1, entries 3–6) [40]. With titanium chloride and *n*-BuLi, low conversion of the starting material and obtained product *Z*-**9a** was characteristic (Table 1, entry 7). A slightly higher reactivity was achieved when the $BF_3{\cdot}(OEt_2)$ was used instead of $TiCl_4$ (Table 1, entry 8) [28]. The reactions were monitored by ^{19}F NMR of the crude mixtures. The full conversion was reached by applying exclusively *n*-BuLi, but the formed product was not the anticipated α-substituted compound (Table 1, entry 9). The NMR analysis revealed that the obtained compounds were Michael addition products. The formation of the presented compounds (Table 1) was due to the earlier generation of *gem*-difluoroalkenes by the elimination of one of the fluorine atoms from the CF_3 group, proving that both *gem*-difluoroalkenes and the double bond of product *Z*-**9a** were

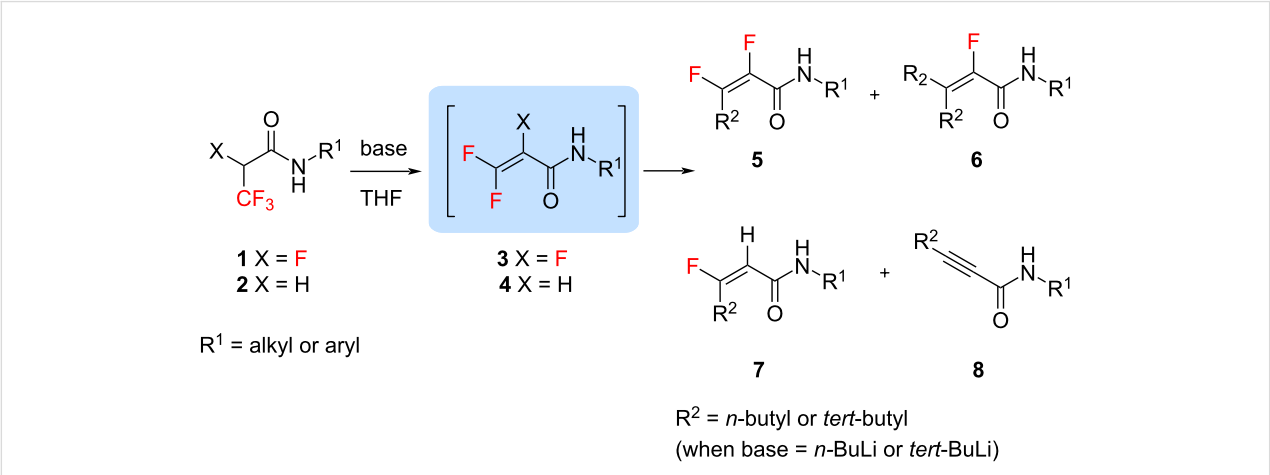

Scheme 1: Generation of *gem*-difluorovinyl and trifluorovinyl Michael acceptors and their use in the synthesis of α,β-unsaturated fluoroamides.

Table 1: Optimization of reaction conditions.

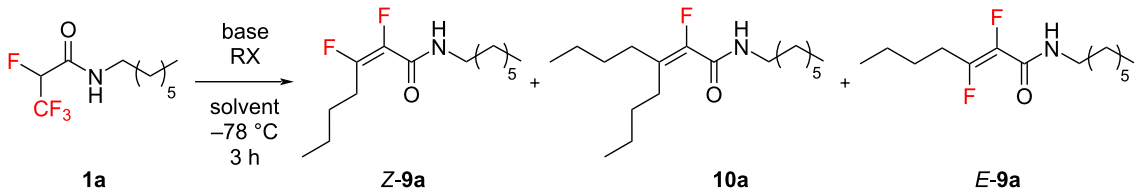

1a *Z*-**9a** **10a** *E*-**9a**

* *Z*-**9a**, **10a**, *E*-**9a** – when base was *n*-BuLi

Entry	Base/Lewis acid, base	Electrophile RX, RCHO	Solvent	Result
1	LiHMDS, 2 equiv	BnBr, 2 equiv	THF	n. r.[a]
2	LiHMDS, 2 equiv	MeI, 2 equiv	THF	n. r.
3	Et_3N, 3 equiv $TiCl_4$, 1.2 equiv	MeI, 2 equiv	DCM	n. r.
4	TMPDA, 1.2 equiv $TiCl_4$, 1.2 equiv	MeI, 2 equiv	DCM	n. r.
5	Et_3N, 3 equiv $TiCl_4$, 1.2 equiv	PhCHO, 2 equiv	DCM	n. r.
6	TMPDA, 1.2 equiv $TiCl_4$, 1.2 equiv	PhCHO, 2 equiv	DCM	n. r.
7	*n*-BuLi, 4 equiv $TiCl_4$, 1.2 equiv	PhCHO, 2 equiv	THF	traces of *Z*-**9a**[b]
8	*n*-BuLi, 4 equiv $BF_3{\cdot}OEt_2$, 1.2 equiv	PhCHO, 2 equiv	THF	1:2.8:0.3:traces (**1a**/*Z*-**9a**/**10a**/*E*-**9a**)[b]
9	*n*-BuLi, 4 equiv	MeI, 2 equiv	THF	0:1:0.15:traces (**1a**/*Z*-**9a**/**10a**/*E*-**9a**)[b]
10	*n*-BuLi, 4 equiv	–	THF	0:1:0.1:0 (**1a**/*Z*-**9a**/**10a**/*E*-**9a**)[b]

[a]No reaction. [b]Determined by ^{19}F NMR spectroscopy of crude reaction mixtures.

excellent Michael acceptors. This confirmed that electrophiles were not involved in the reaction. We therefore focused only on using *n*-BuLi, which, as it turned out, acted as both the base and Michael's donor (Table 1, entry 10).

Having the optimized conditions in hand, we subjected other 2,3,3,3-tetrafluoropropanamides to the same process. Both amides substituted by electron-withdrawing and electron-donating groups proved to be suitable substrates for this reaction, providing the corresponding Michael addition products. These highly stable compounds were isolated after purification on silica gel in good yields (Scheme 2) and characterized by spectroscopic methods. The reaction proceeded with very high *Z*-stereoselectivity (Scheme 2, compounds **9a**–**d**). In the ^{19}F NMR spectra of crude mixtures, only trace amounts of *E*-isomer of products **9** were identified. The fluorine atom signals of **9a**–**d** were located at approximately −112 ppm (triplets, $J \approx 27$ Hz, F_β) and at −155 to −159 ppm (multiplets, F_α). The stereochemistry was determined by $^{19}F\{^1H\}$ NMR spectroscopy. The observed coupling constants $J \approx 2$ Hz between vinylic fluorine atoms were typical and confirmed that the *Z* isomers were obtained predominantly [41]. The vicinal coupling constant between the F_β and H_γ atoms amounted approximately 27 Hz in cases of **9a**–**d**. Based on these findings, we concluded that the dihedral angle between the F_β and H_γ atoms is approximately 150° [42-45]. These data were consistent with DFT calculations (see Supporting Information File 1). The reaction of the amide **1d** with *n*-BuLi resulted in a surprising outcome. In this case, product **9d** and only traces of the expected product **10d** were received, as indicated by the ^{19}F NMR spectrum of the crude reaction mixture. Interestingly, for this reaction we also observed that the *Z*-**9d**/*E*-**9d** products were obtained in a ratio of 1:0.2. However, the main *Z*-isomer was only isolated and fully characterized.

In our subsequent investigation of the 3,3,3-trifluoropropanamides substrate **2a**–**d** scope, we observed that *gem*-difluoroalkenes produced β-fluoro-unsaturated amides **11a**–**d** (Scheme 3). In these reactions, we used conditions previously optimised for derivatives **1a**–**d** (*n*-BuLi 4 equiv, THF, −78 °C, 3 h). The amides **11a**–**d** preferred HF elimination over engaging in another Michael reaction, leading to the formation of products **12a**–**d** as illustrated in Scheme 3. This outcome suggests a significant role of the fluorine atom at the *alpha* position, where

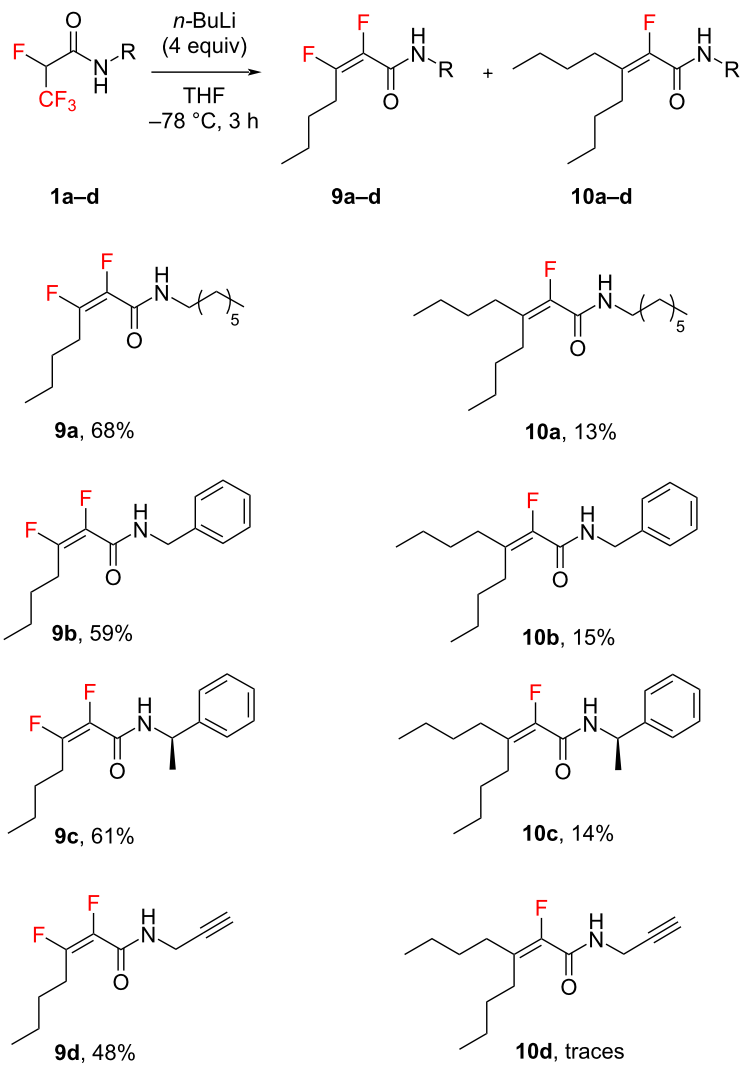

Scheme 2: Formation of α,β-difluorinated and α-fluorinated α,β-unsaturated amides.

its electron-withdrawing effect likely influenced the feasibility of the following Michael addition for compounds **9a–d** (Scheme 2). Interestingly, such a reaction pathway was absent for derivatives **11a–d**, where the *alpha*-positioned proton exhibited a low pK_a, favouring an easy elimination reaction. This is supported by the higher yields of products **12a–d** compared to their **11a–d** counterparts. The exclusive formation of *E* isomers in compounds **11a–d** was confirmed by the observed coupling constants ($J \approx 21$ Hz) between the vinylic proton and the fluorine atom [41]. Moreover, the vicinal coupling constants between the F_β and H_γ atoms ranging from 25–26 Hz for **11a–d** suggest a dihedral angle of approximately 170° between these atoms [42-45]. These findings are in alignment with DFT calculations (see Supporting Information File 1) and corroborate data for compounds **9a–d**.

We further decided to use *tert*-BuLi in our research, considering its role as a stronger base and simultaneously as a weak nucleophile. We first performed the reaction with 2 equiv of *tert*-BuLi, which did not yield the expected results. The substrate was still observed in the reaction mixture. Only the use of 4 equiv of base gave the desired findings. The treatment of compounds **1a–d** and **2a–d**, respectively, with *tert*-BuLi induced the carbanion formation followed by an addition–elimination reaction, affording the corresponding fluorinated **13a–d** (Scheme 4) and nonfluorinated **14a–d** (Scheme 5) unsaturated products. Also this time, for compounds **13a–d**, the formation of only *Z* isomers was observed (Scheme 4). The stereochemistry was determined by $^{19}F\{^1H\}$ NMR spectroscopy methods by the observed coupling constants $J \approx 6$ Hz between vinylic fluorine atoms [41]. Due to the steric hindrance, these

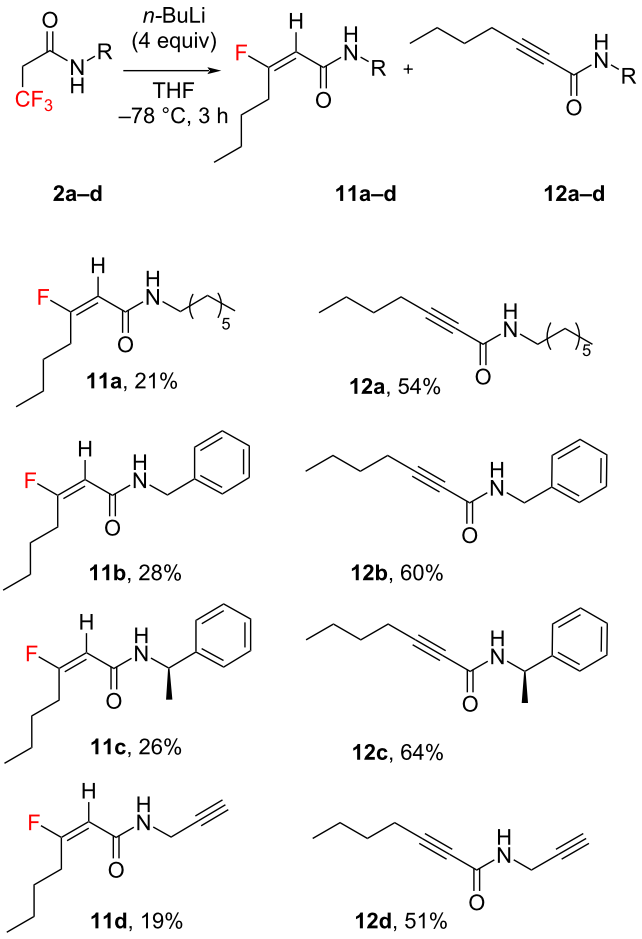

Scheme 3: Formation of β-fluorinated and nonfluorinated α,β-unsaturated amides.

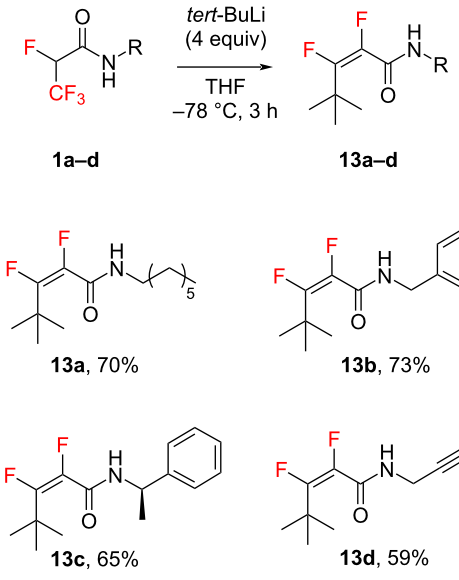

Scheme 4: Michael addition of **1a–d** with *tert*-BuLi.

compounds did not serve as good Michael acceptors for the next step.

Only elimination products **14a–d** were obtained from trifluorinated amides **2a–d**, showing good yields (Scheme 5).

We also tried to perform a substitution reaction by treating compounds **1a** and **2a** with *tert*-BuLi, employing methyl iodide as the electrophile. However, similar to previous reactions, this did not yield substitution products at the *alpha* position, but to the addition–elimination reaction products. More importantly, the application of 8 equiv of *tert*-BuLi induced the formation of *N*-methylation products (Scheme 6).

Compounds **15a** (**15a'**) and **16a** (**16a'**) existed as two rotamers, in ratios of 1:1.15 and 1:1.76, respectively, with the predominant *cisoid* isomer. *Transoid* (*trans* **15a**(**16a**)) isomers contained a larger substituent at nitrogen located in the opposite direction to the carbonyl group, while *cisoid* (*cis* **15a'** (**16a'**)) isomers featured a smaller substituent at nitrogen locat-

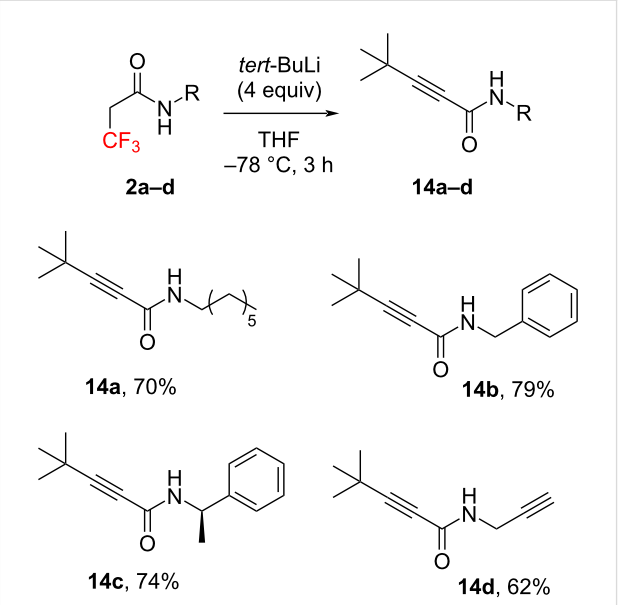

Scheme 5: Michael addition of **2a–d** with *tert*-BuLi.

ed in the opposite direction to the carbonyl group. We determined the quantitative ratio as well as the *cis*/*trans* configuration of isomers by analyzing the differences in the chemical shift values in the ^{1}H NMR spectra for NCH_3 and NCH_2-proton groups, based on our previous studies concerning fluorinated amides [46,47].

Conclusion

In this study, we have established that tri- and tetrafluorinated amides, featuring a CF_3 group at the α position, serve as effective motifs for designing stable *gem*-difluorovinyl and trifluorovinyl Michael acceptors. To our knowledge, this represents the inaugural instance of employing potent bases such as *n*-BuLi and *tert*-BuLi to fulfill dual roles as both base catalysts and Michael donors. The reactions exhibited remarkable stereoselectivity, a finding elucidated by DFT analysis. These results mark significant progress toward the synthesis of novel fluorinated building blocks. Our team is currently exploring the application of this methodology to amino acid substrates, aiming to contribute further to the burgeoning field of fluorinated peptidomimetics.

Experimental

See Supporting Information File 1 for the Experimental section.

Supporting Information

Supporting Information File 1

Detailed experimental procedures, DFT calculations, characterization data, and copies of ^{1}H, ^{13}C, ^{19}F NMR and ^{1}H–^{13}C HSQC spectra.
[https://www.beilstein-journals.org/bjoc/content/supplementary/1860-5397-20-247-S1.pdf]

Acknowledgements

The calculations were performed in the Poznan Supercomputing and Networking Center.

ORCID® iDs

Monika Bilska-Markowska - https://orcid.org/0000-0002-9024-5479
Marcin Kaźmierczak - https://orcid.org/0000-0003-0199-9197
Wojciech Jankowski - https://orcid.org/0000-0003-2058-6945
Marcin Hoffmann - https://orcid.org/0000-0002-1729-977X

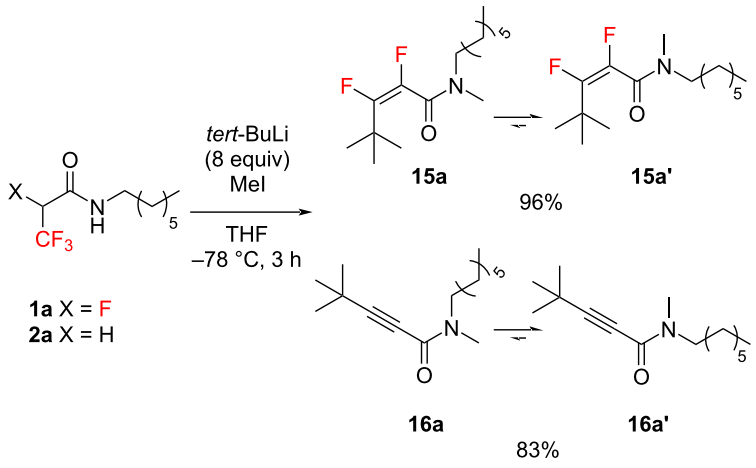

Scheme 6: Formation of *N*-methylation products.

Data Availability Statement

All data that supports the findings of this study is available in the published article and/or the supporting information of this article.

References

1. Reznikov, A. N.; Klimochkin, Y. N. *Synthesis* **2020,** *52,* 781–795. doi:10.1055/s-0039-1690044
2. Kaplan, W.; Khatri, H. R.; Nagorny, P. *J. Am. Chem. Soc.* **2016,** *138,* 7194–7198. doi:10.1021/jacs.6b04029
3. Hui, C.; Pu, F.; Xu, J. *Chem. – Eur. J.* **2017,** *23,* 4023–4036. doi:10.1002/chem.201604110
4. Li, L.; Yang, Q.; Wang, Y.; Jia, Y. *Angew. Chem., Int. Ed.* **2015,** *54,* 6255–6259. doi:10.1002/anie.201411338
5. Zhang, Y.; Wang, W. *Catal. Sci. Technol.* **2012,** *2,* 42–53. doi:10.1039/c1cy00334h
6. Santos, P. P.; Veiros, L. F. *Tetrahedron* **2020,** *76,* 131373. doi:10.1016/j.tet.2020.131373
7. Valero, G.; Companyó, X.; Rios, R. *Chem. – Eur. J.* **2011,** *17,* 2018–2037. doi:10.1002/chem.201001546
8. Barron, B.; Edge, C.; Fenner, S.; Shrives, H.; Sollis, S.; Whiting, M.; Valette, D. *Org. Lett.* **2024,** *26,* 1533–1538. doi:10.1021/acs.orglett.3c03694
9. Furukawa, T.; Shibata, N.; Mizuta, S.; Nakamura, S.; Toru, T.; Shiro, M. *Angew. Chem., Int. Ed.* **2008,** *47,* 8051–8054. doi:10.1002/anie.200802904
10. Huang, X.; Besset, T.; Jubault, P.; Couve-Bonnaire, S. *J. Org. Chem.* **2022,** *87,* 9210–9221. doi:10.1021/acs.joc.2c00937
11. Huang, X.; Besset, T.; Jubault, P.; Couve-Bonnaire, S. *Adv. Synth. Catal.* **2023,** *365,* 2467–2486. doi:10.1002/adsc.202300565
12. Ramb, D. C.; Lerchen, A.; Kischkewitz, M.; Beutel, B.; Fustero, S.; Haufe, G. *Eur. J. Org. Chem.* **2016,** 1751–1759. doi:10.1002/ejoc.201600088
13. Adam, A. T.; Fronczek, F. R.; Colby, D. A. *Org. Lett.* **2020,** *22,* 2630–2633. doi:10.1021/acs.orglett.0c00599
14. Ma, Y.; Mao, K.; Chen, Y.; Lv, L.; Li, Z. *Tetrahedron Lett.* **2022,** *100,* 153902. doi:10.1016/j.tetlet.2022.153902
15. Gao, G.; Li, Z. *New J. Chem.* **2023,** *47,* 6171–6175. doi:10.1039/d2nj06338g
16. Zong, Y.; Tsui, G. C. *Org. Lett.* **2024,** *26,* 1261–1264. doi:10.1021/acs.orglett.4c00095
17. Li, M.; Tsui, G. C. *Org. Lett.* **2024,** *26,* 376–379. doi:10.1021/acs.orglett.3c04037
18. Aparici, I.; Guerola, M.; Dialer, C.; Simón-Fuentes, A.; Sánchez-Roselló, M.; del Pozo, C.; Fustero, S. *Org. Lett.* **2015,** *17,* 5412–5415. doi:10.1021/acs.orglett.5b02759
19. Zhou, H.; Schmidt, D. M. Z.; Gerlt, J. A.; van der Donk, W. A. *ChemBioChem* **2003,** *4,* 1206–1215. doi:10.1002/cbic.200300654
20. Volonterio, A.; Chiva, G.; Fustero, S.; Piera, J.; Sanchez Rosello, M.; Sani, M.; Zanda, M. *Tetrahedron Lett.* **2003,** *44,* 7019–7022. doi:10.1016/s0040-4039(03)01787-8
21. Molteni, M.; Pesenti, C.; Sani, M.; Volonterio, A.; Zanda, M. *J. Fluorine Chem.* **2004,** *125,* 1735–1743. doi:10.1016/j.jfluchem.2004.09.014
22. Altman, R. A.; Sharma, K. K.; Rajewski, L. G.; Toren, P. C.; Baltezor, M. J.; Pal, M.; Karad, S. N. *ACS Chem. Neurosci.* **2018,** *9,* 1735–1742. doi:10.1021/acschemneuro.8b00085
23. Yang, M.-H.; Matikonda, S. S.; Altman, R. A. *Org. Lett.* **2013,** *15,* 3894–3897. doi:10.1021/ol401637n
24. Van der Veken, P.; Senten, K.; Kertèsz, I.; De Meester, I.; Lambeir, A.-M.; Maes, M.-B.; Scharpé, S.; Haemers, A.; Augustyns, K. *J. Med. Chem.* **2005,** *48,* 1768–1780. doi:10.1021/jm0495982
25. Bilska-Markowska, M.; Patyk-Kaźmierczak, E.; Lusina, A. *Eur. J. Org. Chem.* **2022,** e202101378. doi:10.1002/ejoc.202101378
26. Bilska-Markowska, M.; Jankowski, W.; Hoffmann, M.; Kaźmierczak, M. *Molecules* **2022,** *27,* 5404. doi:10.3390/molecules27175404
27. Uneyama, K.; Katagiri, T.; Amii, H. *Acc. Chem. Res.* **2008,** *41,* 817–829. doi:10.1021/ar7002573
28. Shimada, T.; Yoshioka, M.; Konno, T.; Ishihara, T. *Org. Lett.* **2006,** *8,* 1129–1131. doi:10.1021/ol0531435
29. Brewitz, L.; Arteaga, F. A.; Yin, L.; Alagiri, K.; Kumagai, N.; Shibasaki, M. *J. Am. Chem. Soc.* **2015,** *137,* 15929–15939. doi:10.1021/jacs.5b11064
30. Sun, Z.; Sun, B.; Kumagai, N.; Shibasaki, M. *Org. Lett.* **2018,** *20,* 3070–3073. doi:10.1021/acs.orglett.8b01109
31. Watanabe, S.; Fujita, T.; Sakamoto, M.; Hosokawa, O.; Ikeda, N. *Int. J. Mater. Prod. Technol.* **1990,** *5,* 213–219.
32. Yu, J.-S.; Noda, H.; Kumagai, N.; Shibasaki, M. *Synlett* **2019,** *30,* 488–492. doi:10.1055/s-0037-1611642
33. Matsuzawa, A.; Noda, H.; Kumagai, N.; Shibasaki, M. *J. Org. Chem.* **2017,** *82,* 8304–8308. doi:10.1021/acs.joc.7b01381
34. Shi, G.-q.; Cai, W.-l. *J. Org. Chem.* **1995,** *60,* 6289–6295. doi:10.1021/jo00125a013
35. Gaikwad, N.; Nanduri, S.; Madhavi, Y. V. *Eur. J. Med. Chem.* **2019,** *181,* 111561. doi:10.1016/j.ejmech.2019.07.064
36. Li, S.-N.; Li, B.; Yu, Z.-R.; Dai, S.-W.; Shen, S.-C.; Mao, M.; Gong, L.-X.; Feng, Y.; Jia, D.; Zhou, Y.; Tang, L.-C. *ACS Appl. Polym. Mater.* **2020,** *2,* 1874–1885. doi:10.1021/acsapm.0c00106
37. Rozsar, D.; Formica, M.; Yamazaki, K.; Hamlin, T. A.; Dixon, D. J. *J. Am. Chem. Soc.* **2022,** *144,* 1006–1015. doi:10.1021/jacs.1c11898
38. Verma, S.; Singh, V.; Jat, J. L.; Tiwari, B. *J. Org. Chem.* **2024,** *89,* 8201–8207. doi:10.1021/acs.joc.3c02478
39. Skibinska, M.; Warowicka, A.; Koroniak, H.; Cytlak, T.; Crousse, B. *Org. Lett.* **2024,** *26,* 692–696. doi:10.1021/acs.orglett.3c04094
40. Chen, J.-L.; You, Z.-W.; Qing, F.-L. *J. Fluorine Chem.* **2013,** *155,* 143–150. doi:10.1016/j.jfluchem.2013.07.017
41. Dolbier, W. R., Jr. *Guide to Fluorine NMR for Organic Chemists;* John Wiley & Sons: Hoboken, NJ, USA, 2009. doi:10.1002/9780470483404
42. Thibaudeau, C.; Plavec, J.; Chattopadhyaya, J. *J. Org. Chem.* **1998,** *63,* 4967–4984. doi:10.1021/jo980144k
43. San Fabián, J.; Guilleme, J.; Dıez, E. *J. Magn. Reson.* **1998,** *133,* 255–265. doi:10.1006/jmre.1998.1465
44. Kaźmierczak, M.; Kubicki, M.; Koroniak, H. *Eur. J. Org. Chem.* **2018,** 3844–3852. doi:10.1002/ejoc.201800631
45. Govil, G. *Mol. Phys.* **1971,** *21,* 953–957. doi:10.1080/00268977100102111
46. Bilska-Markowska, M.; Rapp, M.; Siodła, T.; Katrusiak, A.; Hoffmann, M.; Koroniak, H. *New J. Chem.* **2014,** *38,* 3819–3830. doi:10.1039/c4nj00317a
47. Bilska-Markowska, M.; Siodla, T.; Patyk-Kaźmierczak, E.; Katrusiak, A.; Koroniak, H. *New J. Chem.* **2017,** *41,* 12631–12644. doi:10.1039/c7nj02986a

BEILSTEIN JOURNAL OF ORGANIC CHEMISTRY

Synthesis of fluorinated acid-functionalized, electron-rich nickel porphyrins

Mike Brockmann, Jonas Lobbel, Lara Unterriker and Rainer Herges*

Full Research Paper

Open Access

Address:
Otto Diels-Institute of Organic Chemistry,
Christian-Albrechts-Universität zu Kiel, Otto-Hahn-Platz 4, 24118 Kiel, Germany

Email:
Rainer Herges* - rherges@oc.uni-kiel.de

* Corresponding author

Keywords:
acid-functionalized porphyrin; electron-rich porphyrin; nickel porphyrin; perfluorinated aliphatic carboxylic acids; porphyrin synthesis

Beilstein J. Org. Chem. **2024,** *20,* 2954–2958.
https://doi.org/10.3762/bjoc.20.248

Received: 17 September 2024
Accepted: 08 November 2024
Published: 15 November 2024

This article is part of the thematic issue "Organofluorine chemistry VI".

Guest Editor: D. O'Hagan

Abstract

In this study, novel fluorinated carboxylic acid esters of the generic structure TfO–CH_2–$(CF_2)_n$–$COOCH_3$ (n = 2,4,6, Tf = triflate) were synthesized. The triflates were reacted with 2-hydroxy-3,4,5-trimethoxybenzaldehyde via Williamson ether syntheses. The resulting electron-rich compounds were used as aldehydes in the Rothemund reaction with pyrrole to form ester-substituted porphyrins. After metalation with $Ni(acac)_2$ and hydrolysis electron-rich porphyrins were obtained, that are equipped with covalently attached long chain acid substituents. The target compounds have potential applications in catalysis, sensing, and materials science. The fluorinated aliphatic carboxylic acids (TfO–CH_2–$(CF_2)_n$–$COOCH_3$) with triflate as leaving group in terminal position are easily accessible and versatile building blocks for attaching long chain acids (pK_a 0–1) to substrates in Williamson ether-type reactions.

Introduction

Metal porphyrins are prosthetic groups in a number of essential biomolecules, including hemoglobin, chlorophyll, and cytochromes, supporting processes such as oxygen transport, photosynthesis, and electron transfer [1-5]. Beyond their essential biological roles, porphyrins and their derivatives are employed in a number of applications, acting as catalysts in numerous reactions, including oxidation, reduction, and cycloaddition [6-10]. Particularly when electron-rich porphyrins act as reducing agents, e.g. in electrocatalytic hydrogen evolution reactions, a proton source is needed [11]. In this context, trifluoroacetic acid is very frequently chosen as the proton source, because it is a strong acid but just not strong enough to destroy (demetallate) the Ni porphyrin [10]. Covalent attachment of acids facilitates proton transfer and increases the efficiency [12]. Three conditions should be met for the target porphyrins of this study. 1. The acid covalently bound to the porphyrin should have an acid strength similar to trifluoroacetic acid. 2. The length of the tether with which the acid group is bound should be sufficient to serve as a proton source for redox reactions at the metal. 3. The electronic properties of the porphyrin,

especially the low oxidation potential, should not be increased. We have chosen four-fold meso-3,4,5-trimethoxyphenyl-substituted Ni porphyrin as the electron-rich system, however, the post-synthetic modification of this porphyrin proved to be difficult. Therefore, we have integrated the acid group into the aldehyde component of the Rothemund reaction to prepare the target porphyrin. In initial tests, we have established that trifluoroacetic acid can be replaced by perfluorinated alkyl carboxylic acids [10]. It was therefore obvious to use a perfluoroalkyl chain as a tether. However, a perfluoroalkyl chain as a substituent on the porphyrin has an electron-withdrawing effect and thus a negative influence on the oxidation potential. We have therefore inserted an O–CH_2 group between the phenyl group of the porphyrin and the perfluoroalkyl chain. The oxygen atom, especially in the 2-position, should even improve the electronic properties of the porphyrin.

Results and Discussion

Our synthesis started with the readily available fluorinated symmetric diols HO–CH_2–$(CF_2)_n$–CH_2–OH (n = 2,4,6, see Scheme 1).

In order to break the symmetry and to generate the acid function only on one side, benzyl protection was performed. From diols **1**, **2**, and **3** statistical mixtures of unprotected, mono-, and di-protected products were obtained, from which the isolation of the desired mono-protected products **4** (65%), **5** (50%), and **6** (40%) by chromatography was straightforward. However, the subsequent oxidation of the alcohol with the usual oxidizing agents (Jones reagent, $KMnO_4$, etc.) was not successful. A radical oxidation with TEMPO, potassium bromide (KBr), sodium hypochlorite (NaOCl), and sodium bicarbonate ($NaHCO_3$) provided acids **7**, **8**, and **9**. A byproduct is obtained during oxidation and it is assumed that this is the molecule oxidized at the benzyl position (see Supporting Information File 1, compounds **35**–**40**). Work-up and isolation proved to be difficult, and therefore, the acids were directly converted into the methyl esters **10** (54%), **11** (52%), and **12** (46%). The benzyl-protecting group was removed hydrogenolytically to give products **13** (85%), **14** (65%), and **15** (99%). The alcohols were then converted to the triflates **16** (28%), **17** (41%), and **18** (63%).

We have chosen 3,4,5-trimethoxybenzaldehyde (**19**) as the aldehyde component due to its commercial availability. A OH group was introduced to serve as the nucleophile in the Williamson ether synthesis with the triflates **16**, **17**, and **18** (Scheme 2).

Towards this end, 3,4,5-trimethoxybenzaldehyde (**19**) was iodinated using *N*-iodosuccinimide (NIS) to give **20** in a yield of 89% [13]. To convert the iodo to an OH group, compound **20** was reacted with Cu_2O, 2-pyridinaldoxime and CsOH to give 2-hydroxy-3,4,5-trimethoxybenzaldehyde (**21**, 65%) [13]. In a subsequent nucleophilic substitution, the fluorinated alkyl chains of **16**, **17**, and **18** were linked via a Williamson ether synthesis to yield **22** (78%), **23** (44%), and **24** (44%).

Compounds **22**, **23**, and **24** were used as aldehyde components in the Rothemund-type synthesis of metal-free porphyrins **26** (9%), **27** (18%), and **28** (21%) (see Scheme 3).

Metalation was achieved with nickel acetylacetonate to obtain the ester-substituted Ni porphyrins **29** (78%), **30** (97%), and **31** (57%). The latter were treated with LiOH and HCl to give the

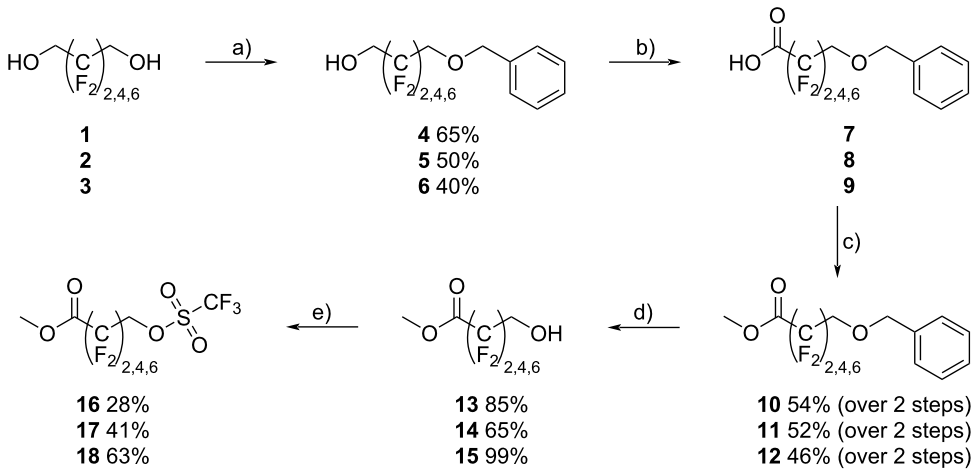

Scheme 1: Synthesis of the starting materials **16**, **17**, and **18** for the subsequent Williamson ether synthesis with 2-hydroxy-3,4,5-trimethoxybenzaldehyde (**21**). Conditions: a) K_2CO_3, benzyl bromide, abs. MeCN, N_2, reflux, 18 h; b) TEMPO, KBr, NaOCl, $NaHCO_3$, MeCN, rt, 76 h; c) MeOH, H_2SO_4, reflux, 18 h; d) Pd/C, H_2, EtOH, rt, 24 h; e) Tf_2O, pyridine, DCM, rt, 18 h.

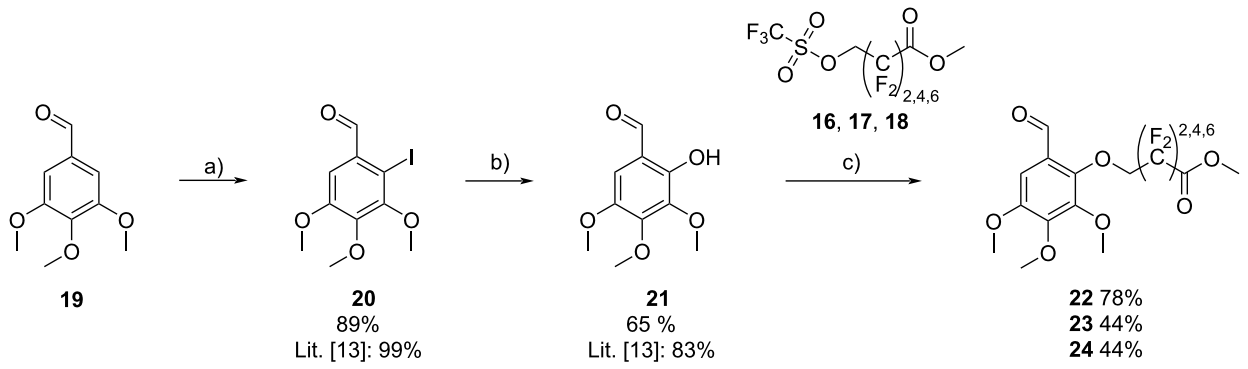

Scheme 2: Synthesis of perfluoroalkyl ester-functionalized aldehydes **22**, **23**, and **24**. Conditions: a) NIS, TFA, Na_2CO_3, MeCN, reflux, 18 h; b) $Cu_2O{\cdot}H_2O$, 2-pyridinaldoxime, TBAB, CsOH, H_2O, N_2, rt, 18 h; c) Cs_2CO_3, DMAc, N_2, rt, 3 h.

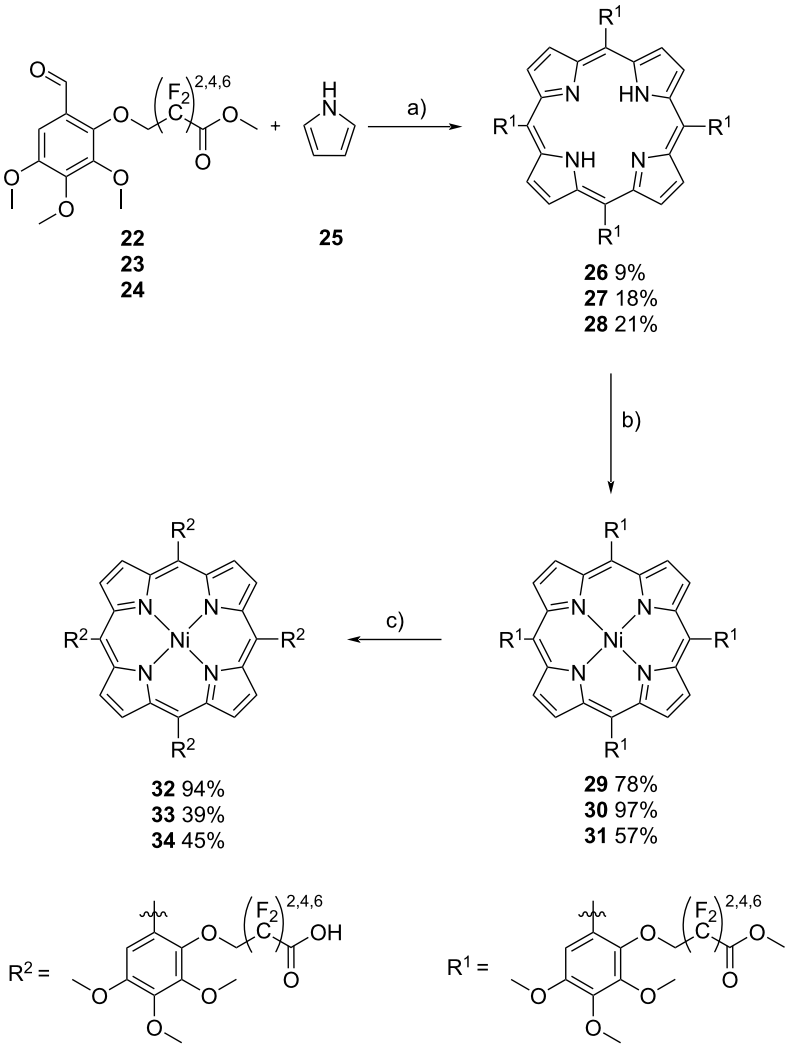

Scheme 3: Porphyrin synthesis. a) Rothemund porphyrin synthesis of metal-free porphyrins **26**, **27**, and **28**; b) metalation of porphyrins with $Ni(acac)_2$; c) ester hydrolysis to generate the free acids **32**, **33**, and **34**. Conditions: a) 1) **22**/**23**/**24**, TFA, abs. DCM, N_2, reflux, 30 min, 2) pyrrole, reflux, 2.5 h, 3) DDQ, reflux, 2 h; b) $Ni(acac)_2$, toluene, reflux, 20 h; c) 1) LiOH, MeOH, rt, 1 h, 2) HCl.

free acids **32** (94%), **33** (39%), and **34** (45%). The HPLC–ESIMS analysis of **32**, **33**, and **34** revealed that two major atropisomers of each porphyrin had formed. In **32** both atropisomers exhibit a roughly 1:1 ratio, in **33** we observed a roughly 1:2 ratio, and in **34** almost only one atropisomer was formed (see Figures S102, S106, and S110 in Supporting Information File 1). We attribute this to the increasing sterical hindrance of the increasing chain lengths in compounds **32**, **33**, and **34**, which should favor an alternating sequence of the chains pointing upward and downward.

Conclusion

This study reports the synthesis of perfluoroalkyl carboxylic esters with CH_2–OTf groups in the ω-position of the type TfO–CH_2–$(CF_2)_n$–$COOCH_3$ (n = 2, 4, 6, Tf = triflate). The latter compounds were used in Williamson ether reactions with 2-hydroxy-3,4,5-trimethoxybenzaldehyde (**21**) to prepare the aldehyde component for a Rothemund-type porphyrin synthesis of acid-functionalized electron-rich porphyrins. The corresponding Ni porphyrins are potential compounds for electrocatalysis and sensor applications. The ω-triflated, perfluoroalkylated carboxylic acids **16**, **17**, and **18** are easily accessible and versatile building blocks for connecting long chain acids (pK_a range between 0 and 1) to substrates in Williamson ether-type reactions.

Supporting Information

Supporting Information File 1

Experimental procedures, characterization data of all products, and copies of ^1H, ^{13}C, and ^{19}F NMR spectra.
[https://www.beilstein-journals.org/bjoc/content/supplementary/1860-5397-20-248-S1.pdf]

Acknowledgements

We thank Dr. Claus Bier for the help with the HPLC–ESIMS measurements.

Author Contributions

Mike Brockmann: conceptualization; data curation; investigation; methodology; project administration; supervision; validation; visualization; writing – original draft. Jonas Lobbel: investigation. Lara Unterriker: investigation. Rainer Herges: project administration; supervision; writing – review & editing.

ORCID® iDs

Rainer Herges - https://orcid.org/0000-0002-6396-6991

Data Availability Statement

All data that supports the findings of this study is available in the published article and/or the supporting information of this article.

Preprint

A non-peer-reviewed version of this article has been previously published as a preprint: https://doi.org/10.3762/bxiv.2024.60.v1

References

1. Droege, D. G.; Parker, A. L.; Milligan, G. M.; Jenkins, R.; Johnstone, T. C. *J. Org. Chem.* **2022,** *87,* 11783–11795. doi:10.1021/acs.joc.2c01538
2. Hopp, M.-T.; Schmalohr, B. F.; Kühl, T.; Detzel, M. S.; Wißbrock, A.; Imhof, D. *Anal. Chem. (Washington, DC, U. S.)* **2020,** *92,* 9429–9440. doi:10.1021/acs.analchem.0c00415
3. Upoma, N. J.; Akter, N.; Ferdousi, F. K.; Sultan, M. Z.; Rahman, S.; Alodhayb, A.; Alibrahim, K. A.; Habib, A. *ACS Omega* **2024,** *9,* 22325–22335. doi:10.1021/acsomega.4c01708
4. Moore, M. R. An Historical Introduction to Porphyrin and Chlorophyll Synthesis. In *Tetrapyrroles: Birth, Life and Death;* Warren, M. J.; Smith, A. G., Eds.; Springer Science & Business Media: New York, NY, USA, 2009; pp 1–28. doi:10.1007/978-0-387-78518-9_1
5. Munro, A. W.; Givran, H. M.; McLean, K. J.; Cheesman, M. R.; Leys, D. Heme and Hemoproteins. In *Tetrapyrroles: Birth, Life and Death;* Warren, M.; Smith, A., Eds.; Springer Science & Business Media: New York, NY, USA, 2009; pp 160–183. doi:10.1007/978-0-387-78518-9_10
6. Peters, M. K.; Röhricht, F.; Näther, C.; Herges, R. *Org. Lett.* **2018,** *20,* 7879–7883. doi:10.1021/acs.orglett.8b03433
7. Shaikh, R. R.; Pornpraprom, S.; D'Elia, V. *ACS Catal.* **2018,** *8,* 419–450. doi:10.1021/acscatal.7b03580
8. Silva, A. M. G.; Tomé, A. C.; Neves, M. G. P. M. S.; Silva, A. M. S.; Cavaleiro, J. A. S. *J. Org. Chem.* **2005,** *70,* 2306–2314. doi:10.1021/jo048349i
9. Zhou, C.-Y.; Yu, W.-Y.; Che, C.-M. *Org. Lett.* **2002,** *4,* 3235–3238. doi:10.1021/ol0201254
10. Brockmann, M.; Glotz, G.; von Glasenapp, J.-S.; Unterriker, L.; Neshchadin, D.; Gescheidt, G.; Herges, R. *J. Am. Chem. Soc.* **2024,** *146,* 13010–13024. doi:10.1021/jacs.3c14118
11. Wu, Z.-Y.; Wang, T.; Meng, Y.-S.; Rao, Y.; Wang, B.-W.; Zheng, J.; Gao, S.; Zhang, J.-L. *Chem. Sci.* **2017,** *8,* 5953–5961. doi:10.1039/c7sc02073b
12. Castro-Cruz, H. M.; Macías-Ruvalcaba, N. A. *Coord. Chem. Rev.* **2022,** *458,* 214430. doi:10.1016/j.ccr.2022.214430
13. Gao, W.; Li, Q.; Chen, J.; Wang, Z.; Hua, C. *Molecules* **2013,** *18,* 15613–15623. doi:10.3390/molecules181215613

BEILSTEIN JOURNAL OF ORGANIC CHEMISTRY

Controlled oligomerization of [1.1.1]propellane through radical polarity matching: selective synthesis of SF_5- and CF_3SF_4-containing [2]staffanes

Jón Atiba Buldt‡, Wang-Yeuk Kong‡, Yannick Kraemer, Masiel M. Belsuzarri, Ansh Hiten Patel, James C. Fettinger, Dean J. Tantillo* and Cody Ross Pitts*

Full Research Paper

Open Access

Address:
Department of Chemistry, University of California, Davis, 1 Shields Avenue, Davis, CA 95616, U.S.A.

Email:
Dean J. Tantillo* - djtantillo@ucdavis.edu; Cody Ross Pitts* - crpitts@ucdavis.edu

* Corresponding author ‡ Equal contributors

Keywords:
pentafluorosulfanylation; [1.1.1]propellane; radical chain oligomerization; staffanes; strain-release

Beilstein J. Org. Chem. **2024,** *20,* 3134–3143.
https://doi.org/10.3762/bjoc.20.259

Received: 11 July 2024
Accepted: 06 November 2024
Published: 29 November 2024

This article is part of the thematic issue "Organofluorine chemistry VI" and is dedicated to Professor Josef Michl who recently passed away.

Guest Editor: D. O'Hagan

Abstract

Selectivity in radical chain oligomerizations involving [1.1.1]propellane – i.e., to make [*n*]staffanes – has been notoriously challenging to control when $n > 1$ is desired. Herein, we report selective syntheses of SF_5- and CF_3SF_4-containing [2]staffanes from SF_5Cl and CF_3SF_4Cl, demonstrating cases whereby oligomerization is preferentially truncated after incorporation of two bicyclopentane (BCP) units. Synthetic and computational studies suggest this phenomenon can be attributed to alternating radical polarity matching. In addition, single-crystal X-ray diffraction (SC-XRD) data reveal structurally interesting features of the CF_3SF_4-containing [2]staffane in the solid state.

Introduction

In various radical additions of X–Y across [1.1.1]propellane (**1**), functionalized oligomers known as [*n*]staffanes – with $n > 1$, where *n* denotes the number of individual [1.1.1]bicyclopentane (BCP) linkers – are often observed and swiftly devalorized as *side-products* [1]. However, targeted synthesis of functionalized [*n*]staffanes as rigid "molecular spacers" as proposed by Kaszynski and Michl [2-4] could facilitate new developments in nanotechnology [5], liquid crystal design [6-10], and the study of energy-transfer [11,12] or electron-transfer [13-17] processes. We also posit that lower-order [*n*]staffanes (i.e., $n = 2$ or 3) are potentially valuable C(sp^3)-rich bioisosteres [18,19] that have been seemingly overlooked in the medicinal chemistry arena, in stark contrast to single BCP units over the past 12 years [20-24].

One plausible explanation for the paucity of applications of [*n*]staffanes in materials or biological settings is a synthetic accessibility issue. For instance, dimerization of substituted BCPs [25-27] or photochemical appendage of **1** onto an extant BCP [28-31] are relatively effective tactics for the selective assembly of certain [*n*]staffanes; the main caveat is that multiple synthetic steps are required. On the other hand, while a one-pot radical chain oligomerization is conceptually appealing, radical additions of X–Y across **1** in practice can be challenging to control and often lead to complex mixtures of functionalized [*n*]staffanes, n = 1–5 (Figure 1, top) [2,31-34]. Even though [*n*]staffanes are often separable by column chromatography, the yields for a single oligomer across a panoply of different transformations typically range from <1% to ≈30% when $n > 1$ is desired [35]. To the best of our knowledge, the assembly of functionalized [*n*]staffanes from **1** in high yield/selectivity and in one step via controlled radical oligomerization remains a synthetic challenge.

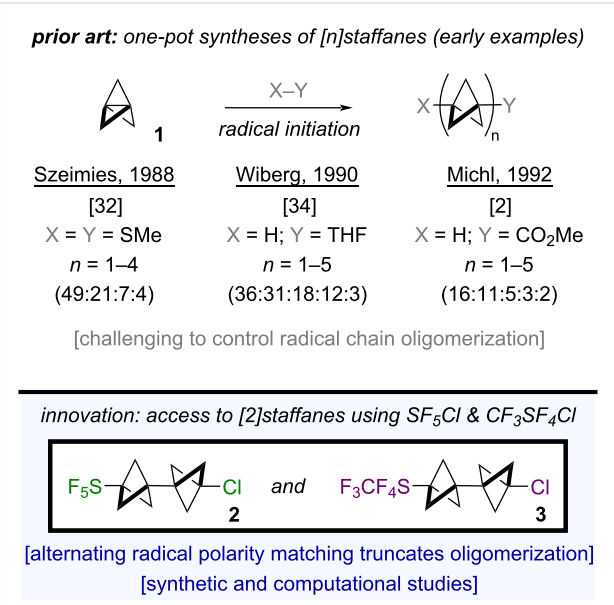

Figure 1: (Top) highlighting selectivity challenges in the synthesis of [*n*]staffanes using excess [1.1.1]propellane (**1**). (Bottom) selective synthesis of [2]staffanes bearing the SF_5 (**2**) and CF_3SF_4 (**3**) groups (this work).

Herein, we report proof-of-concept that our previous work on strain-release pentafluorosulfanylation of **1** [36] using SF_5Cl (prepared in house [37] under mild oxidative fluorination conditions [38-44]) can be extended to the selective synthesis of the associated chloropentafluorosulfanylated [2]staffane (SF_5-BCP-BCP-Cl, **2**), based on alternating radical polarity matching in the chain-propagation steps (Figure 1, bottom) [45-47]. Density functional theory (DFT) calculations provide insight into our observed selectivity, and our hypothesis is bolstered by computation of relative bicyclopentyl radical philicities. In addition, we demonstrate that similar reaction conditions can be applied to the synthesis of the analogous CF_3SF_4-containing [2]staffane (CF_3SF_4-BCP-BCP-Cl, **3**). Finally, we examined compound **3** by SC-XRD and found that it undergoes a phase transition as a function of rate of cooling; this highlights that the [2]staffanes synthesized during this study are also interesting from a fundamental structural standpoint.

Results and Discussion

Over the past few years, our group has begun to establish strain-release pentafluorosulfanylation as a viable strategy for $C(sp^3)$–SF_5 bond formation [35,48]. For instance, in 2022, we reported a method for chloropentafluorosulfanylation of [1.1.1]propellane, i.e., to make SF_5-BCP-Cl (**4**), that ostensibly proceeds through a radical chain propagation mechanism [36]. Under optimized conditions, we obtained product **4** in 86% yield, and the corresponding [2]staffane – SF_5-BCP-BCP-Cl (**2**) – was formed as a minor side-product in 7% yield. While our original goal was to suppress formation of **2**, we later pondered whether preferential synthesis of compound **2** would also be possible. Accordingly, we began our screening process by systematically increasing the equivalents of [1.1.1]propellane (**1**) relative to SF_5Cl and evaluating the impact on selectivity (Table 1).

Table 1: Effect of [1.1.1]propellane (**1**) equivalents relative to SF_5Cl on selectivity[a].

1 4 2

entry	**1** (equiv)	**4** (% yield)[b]	**2** (% yield)[b]	**4**:**2**
1	1.0	49%	4%	12:1.0
2	2.0	74%	22%	3.4:1.0
3	3.0	44%	29%	1.5:1.0
4	4.0	54%	40%	1.3:1.0
5	6.0	48%	45%	1.1:1.0
6	8.0	43%	53%	1.0:1.3
7	10	32%	51%	1.0:1.6
8	20	24%	72%	1.0:3.0
9[c]	**6.0**	**30%**	**63% (51%)**[d]	**1.0:2.1**

[a]A 0.1 M solution of SF_5Cl in *n*-pentane (0.1 mmol) was added to a 0.8 M solution of [1.1.1]propellane in Et_2O under Ar atmosphere and stirred at rt for 3 h. [b]Yield determined by ^{19}F NMR; [c]SF_5Cl was added portion-wise. [d]Isolated yield.

A 0.1 M solution of SF_5Cl in *n*-pentane was added to a 0.8 M solution of **1** in Et_2O at room temperature, and the mixture was stirred for 3 hours prior to ^{19}F NMR analysis. Upon increasing

from 1.0 to 6.0 equiv of **1**, we observed the **4**:**2** product ratio decreased dramatically from 12:1 to 1.1:1. Using 8.0 equiv of **1**, the ratio flipped such that **2** became the major product (i.e., **4**:**2** = 1:1.3) and was formed in 53% yield. Interestingly, even with 8.0 equiv of **1**, 96% of the material balance could be accounted for in the formation of *these two products alone* by ^{19}F NMR. To the best of our knowledge, this is an exceptionally rare instance whereby oligomerization of **1** appears to be stunted beyond formation of the [2]staffane; only trace yields of putative higher-order staffanes (n > 2) were detected in the crude reaction mixture. Remarkably, using 20 equiv of **1**, the observed **4**:**2** product ratio improved to 1:3, with **2** formed in 72% yield. In an even more extreme case, the [2]staffane still remained the major product formed in 66% yield when using 50 equiv of **1** (^{19}F NMR signals of presumed higher-order staffanes became more apparent, though their combined yield still remained ≈18%).

Ultimately, we found adding SF_5Cl portion-wise – to keep the "effective" equiv of **1** higher at any given moment – proved to be a suitable compromise to access **2** in 63% yield by ^{19}F NMR (51% isolated) using 6.0 equiv of **1** (Table 1). We also demonstrated that this procedure can be performed on a 4.0 mmol scale (with respect to SF_5Cl) to provide access to ≈0.5 g of **2** in 43% isolated yield. Additional details on reaction optimization can be found in Supporting Information File 1.

Upon increasing the equivalents of **1** during the screening process, we also found that irradiation with white LEDs was not necessary to boost product yields, as it was in our previously reported synthesis of **4** [36]. Both our laboratory [36] and the Qing laboratory [49] have previously observed that SF_5Cl additions to **1** can proceed in the absence of light. Note that recent work from the laboratories of Cahard and Bizet [50] suggests that autoxidation of the ethereal solvent could serve as one possible explanation for initial formation of SF_5 radicals in the absence of light to initiate a radical chain reaction. It is also well established that [1.1.1]propellane participates in radical-chain reactions (i.e., oligomerization) at room temperature in solution to form unsubstituted [n]staffanes.

The origin of this innately controlled oligomerization was then investigated through density functional theory (DFT) calculations. The free energy profile of the radical chain propagation sequence was computed at the PWPB95-D4/def2-QZVPP//PCM(Et_2O)-ωB97X-D/def2-TZVP level of theory [51-58] (Figure 2). Following addition of an SF_5 radical to **1** to form **INT1**, a Cl atom could be abstracted from SF_5Cl via **TS1** to

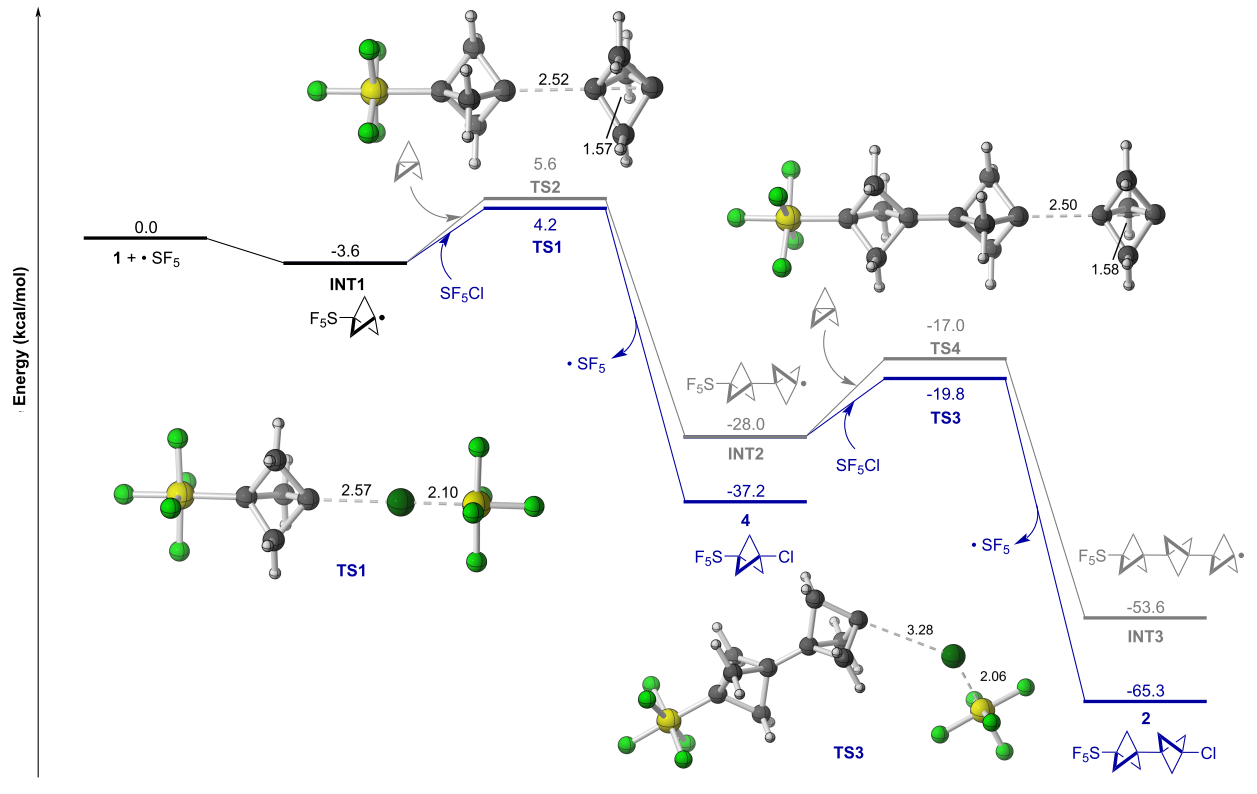

Figure 2: Computed free energy profile for the oligomerization of [1.1.1]propellane (**1**) following SF_5 radical addition at PWPB95-D4/def2-QZVPP//PCM(Et_2O)-ωB97X-D/def2-TZVP level of theory.

form **4** or, alternatively, **INT1** could be added to another equiv of **1** via **TS2** to form **INT2**. Although formation of **4** is notably more thermodynamically favorable than **INT2** ($\Delta\Delta G$ = −9.2 kcal/mol), a small difference in activation free energy is predicted ($\Delta\Delta G^{‡}$ = −1.4 kcal/mol). This, at least in part, provides an explanation as to how favoring the path to **INT2** may be achieved in practice through increasing concentration of **1**.

Subsequently, **INT2** could abstract a Cl atom from SF_5Cl via **TS3** to form **2** or add to a third equiv of **1** through **TS4**, leading to **INT3**. Once again, Cl atom abstraction is thermodynamically ($\Delta\Delta G$ = −11.7 kcal/mol) and kinetically ($\Delta\Delta G^{‡}$ = −2.8 kcal/mol) favored. However, the $\Delta\Delta G^{‡}$ is notably greater in the second product-determining step than the first product-determining step, which is consistent with our experimental observation that **2** forms preferentially over further oligomerization.

For another point of comparison, we examined the reactivity of **1** with CF_3SF_4Cl. This reagent is known to behave comparably to SF_5Cl in radical chain reactions [17,59-61] and can also be prepared conveniently in house [62]. In an analogous equivalents screen, we found that the **5**:**3** product ratio shifts from 7.7:1 using 1.0 equiv of **1** to 1:2.1 using 20 equiv of **1** (Table 2). In the latter scenario, 96% of the material balance could be accounted for in the formation of **5** and **3**, indicating oligomerization is likewise stunted beyond incorporation of two BCP units. Also similar to pentafluorosulfanylation conditions, we found that adding CF_3SF_4Cl portion-wise to 6.0 equiv of **1** enables access to **3** in 60% yield by ^{19}F NMR (53% isolated).

Interestingly, we observed that aryl-SF_4Cl compounds do not follow the same selectivity trend as SF_5Cl and CF_3SF_4Cl additions, suggesting that the controlled oligomerization phenomenon is quite sensitive to changes in the fluorinated sulfur reagent scaffold (see Supporting Information File 1 for more details).

This second instance of controlled oligomerization of **1** using CF_3SF_4Cl was also studied at the PWPB95-D4/def2-QZVPP//PCM(Et_2O)-ωB97X-D/def2-TZVP level of theory (Figure 3). Addition of a CF_3SF_4 radical to **1** affords **INT4**, which can either abstract a Cl atom from CF_3SF_4Cl via **TS5** to make **5** or add to another equiv of **1** via **TS6** to access **INT5**. As anticipated, chlorination of the radical is thermodynamically favored over addition to **1** ($\Delta\Delta G$ = −10.7 kcal/mol). It is also predicted here that the free energy of activation is lower for chlorination, albeit only by 0.4 kcal/mol. This is consistent with the notion that the kinetic preference can be overcome by increasing the concentration of **1** relative to CF_3SF_4Cl. In the second product-determining step, Cl atom abstraction by **INT5** via **TS7** to make **3** is kinetically favorable over addition of a third equiv of **1** via **TS8** to access **INT6**, although the preference is not as large as for formation of **2** ($\Delta\Delta G^{‡}$ = −1.3 kcal/mol).

Thus, the predicted trend for both SF_5Cl and CF_3SF_4Cl additions across **1** indicates a stronger preference for Cl atom abstraction over continued oligomerization in the second product-determining step than in the first – in line with our experimental observations. One possible explanation for this phenomenon is rooted in better radical polarity matching after incorporation of the second BCP unit [37,38]. That is, the carbon-

Table 2: Effect of [1.1.1]propellane (**1**) equivalents relative to CF_3SF_4Cl on selectivity.[a]

1 **5** **3**

entry	**1** (equiv)	**5** (% yield)[b]	**3** (% yield)[b]	**5**:**3**
1	1.0	80%	10%	7.7:1.0
2	2.0	71%	21%	3.4:1.0
3	3.0	65%	31%	2.1:1.0
4	4.0	55%	40%	1.4:1.0
5	6.0	49%	40%	1.2:1.0
6	8.0	39%	46%	1.0:1.2
7	10	33%	62%	1.0:1.9
8	20	31%	65%	1.0:2.1
9[c]	**6.0**	**35%**	**60% (53%)**[d]	**1.0:1.7**

[a]A 0.1 M solution of CF_3SF_4Cl in *n*-pentane (0.03 mmol) was added to a 0.8 M solution of [1.1.1]propellane in Et_2O under Ar atmosphere and stirred at rt for 3 h. [b]Yield determined by ^{19}F NMR. [c]CF_3SF_4Cl was added portion-wise. [d]Isolated yield.

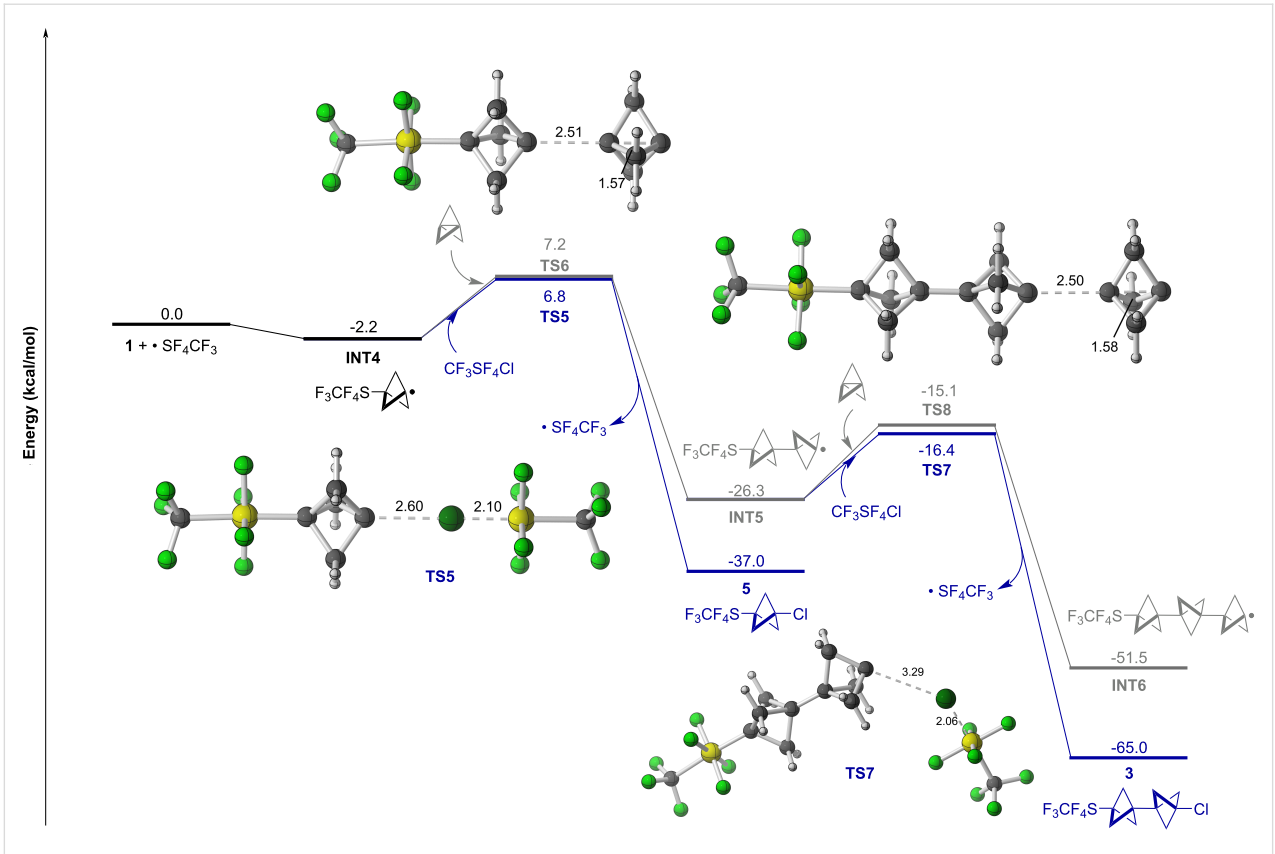

Figure 3: Computed free energy profile for the oligomerization of [1.1.1]propellane (**1**) following CF_3SF_4 radical addition at the PWPB95-D4/def2-QZVPP//PCM(Et_2O)-ωB97X-D/def2-TZVP level of theory.

centered radicals in both **INT1** and **INT4** are closer to strong electron-withdrawing groups than are the radical centers in **INT2** and **INT5**, rendering **INT1** and **INT4** relatively more electrophilic. Inductive effects drop off steeply with distance, and it is also established that a substituent (or, e.g., a radical or cation) on the transannular carbon atom of a bicyclopentyl moiety can interact through space [35,63,64]. The consequence is ostensibly that more "nucleophilic" **INT2** and **INT5** are better matched for Cl atom abstraction from the "electrophilic" reagent (SF_5Cl or CF_3SF_4Cl).

To test this hypothesis, we examined computed trends in various electronic parameters for the **INT1**–**INT3** and the **INT4**–**INT6** series (Table 3). For instance, across several charge models (i.e., Hirshfeld [65], NPA [66-68], and CHELPG [69]), the charge (q) on the carbon atom on which the radical is centered becomes more negative (or less positive) the farther it is from either the SF_5 or CF_3SF_4 substituent, consistent with the notion that it becomes more nucleophilic. Moreover, the Δq is largest between the first two intermediates in both series – **INT1** vs **INT2** and **INT3** vs **INT4** – indicating that the most dramatic change in bicyclopentyl radical philicity would arise after incorporation of the second BCP unit.

In addition to charge models, we evaluated global reactivity indices (ω: electrophilicity index [70] and N: nucleophilicity index [71]) within the conceptual density functional theory (CDFT) framework [72-74]. The data show that BCP has a higher N value – thus stronger nucleophilic tendency – compared to both SF_5Cl and CF_3SF_4Cl. Conversely, comparison of ω values shows significantly higher electrophilicity of SF_5Cl and CF_3SF_4Cl compared to BCP. These results, coupled with decreasing ω and increasing N when more BCP units are incorporated, lend qualitative support to our radical polarity matching hypothesis. Moreover, assessment of radical Fukui functions (f^0) [75] indicates that both SF_5Cl and CF_3SF_4Cl are intrinsically more susceptible to radical attack than **1**, which is consistent with the lower computed barriers for Cl atom abstraction in each case.

These computed trends also potentially account for the fact that selectivity for the [2]staffane (i.e., truncated oligomerization) using aryl-SF_4Cl reagents was not observed. On the basis of CDFT results, a model aryl-SF_4Cl compound (i.e., 5-chloropyrimidyl-SF_4Cl) was determined to be significantly less "electrophilic" than SF_5Cl or CF_3SF_4Cl, consistent with a reduction in the radical polarity matching effect (see Supporting Informa-

Table 3: Key indices computed to compare reactivity. Partial charges (q) and condensed Fukui functions are evaluated at the reacting carbon or chlorine atom and are in units of elementary charge (*e*).[a]

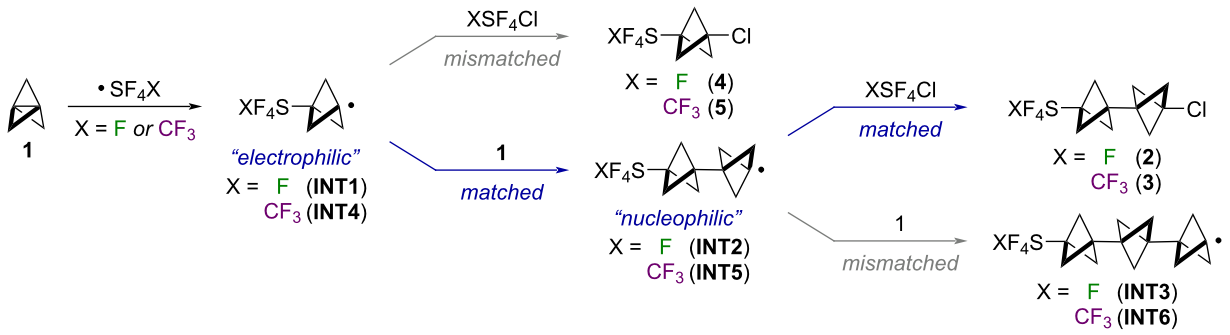

compound	q(Hirshfled) (e)	q(NPA) (e)	q(CHELPG) (e)	f ^{0} (e)[b]	ω (*eV*)[c]	N (*eV*)[d]
1	−0.090	−0.069	−0.255	0.235	0.82	1.70
SF_5Cl	−0.055	−0.160	0.030	0.534	2.48	−0.74
CF_3SF_4Cl	−0.061	−0.150	0.056	0.527	2.52	−0.66
INT1	−0.019	0.092	−0.125	0.307	2.70	2.95
INT2	−0.053	0.073	−0.196	0.347	1.78	3.58
INT3	−0.060	0.065	−0.214	0.345	1.66	3.77
INT4	−0.019	0.092	−0.144	0.301	2.74	2.97
INT5	−0.053	0.073	−0.193	0.346	1.78	3.59
INT6	−0.060	0.064	−0.214	0.345	1.65	3.77

[a]Calculations performed at the PCM(Et_2O)-ωB97X-D/def2-TZVP level of theory. [b]Radical Fukui function. [c]Electrophilicity index. [d]Nucleophilicity index.

tion File 1 for details). This was difficult to predict or rationalize based on calculation of free energies of activation alone. Overall, our results suggest that this alternating polarity matching effect is subtle and subject to mitigation yet can lead to desirable products if employed thoughtfully.

Lastly, following our synthetic and computational studies, accessing a CF_3SF_4-containing [2]staffane in good yield and for the first time created an opportunity for structural analysis. We previously reported and contextualized single-crystal X-ray diffraction (SC-XRD) data on **2** [36]; thus, we proceeded to grow crystals of **3** suitable for X-ray analysis through slow evaporation of ethyl acetate.

To our surprise, an initial measurement of **3** at 90 K revealed an unusually large unit cell (a = 7.14 Å, b = 21.38 Å, and c = 44.04 Å). Following structure solution and refinement [76], we found that **3** crystallizes in an orthorhombic space group $P2_12_12_1$ with five symmetry independent moieties (Z' = 5) and with no solvent present in the unit cell as an inversion twin (Figure 4). After close examination of the model, we noticed that the c-axis was roughly divisible by five with a substructure of Z' = 1. This suggested that the Z' = 5 unit cell may be due to a phase transition caused by anisotropic contraction [77].

In fact, we confirmed that a phase transition had occurred following structure determination at 240 K [78,79]. The X-ray data revealed that **3** crystallizes in the centrosymmetric orthorhombic space group *Pnma* in the high temperature phase (HTP) with cell axes a = 21.56 Å, b = 8.95 Å, and c = 7.28 Å, in contrast to $P2_12_12_1$ in the low temperature phase (LTP). Note that the b-axis is roughly 1/5 of the c-axis observed at 90 K (the axial rearrangement is due to the change in space group). To discern the approximate temperature of the phase transition, the unit cell was measured in 20 K increments upon cooling from 260 K down to 100 K; additional details are reported in Supporting Information File 1. Interestingly, the original LTP unit cell was not detected; instead, only the reduced cell observed in the HTP was found at all temperatures. However, after warming the same crystal of **3** back to room temperature, it was rapidly cooled to 100 K under a stream of N_2 and the larger, disordered cell was observed once more [80]. (These observations also prompted us to measure a structure of **2** at 240 K; in this case, the unit cell is virtually identical at both high and low temperatures, indicating no phase transition had occurred – see Supporting Information File 1 for details.)

Accordingly, we gather that the rate of cooling plays an important role whereby rapid cooling effectively "shocks" the crystal

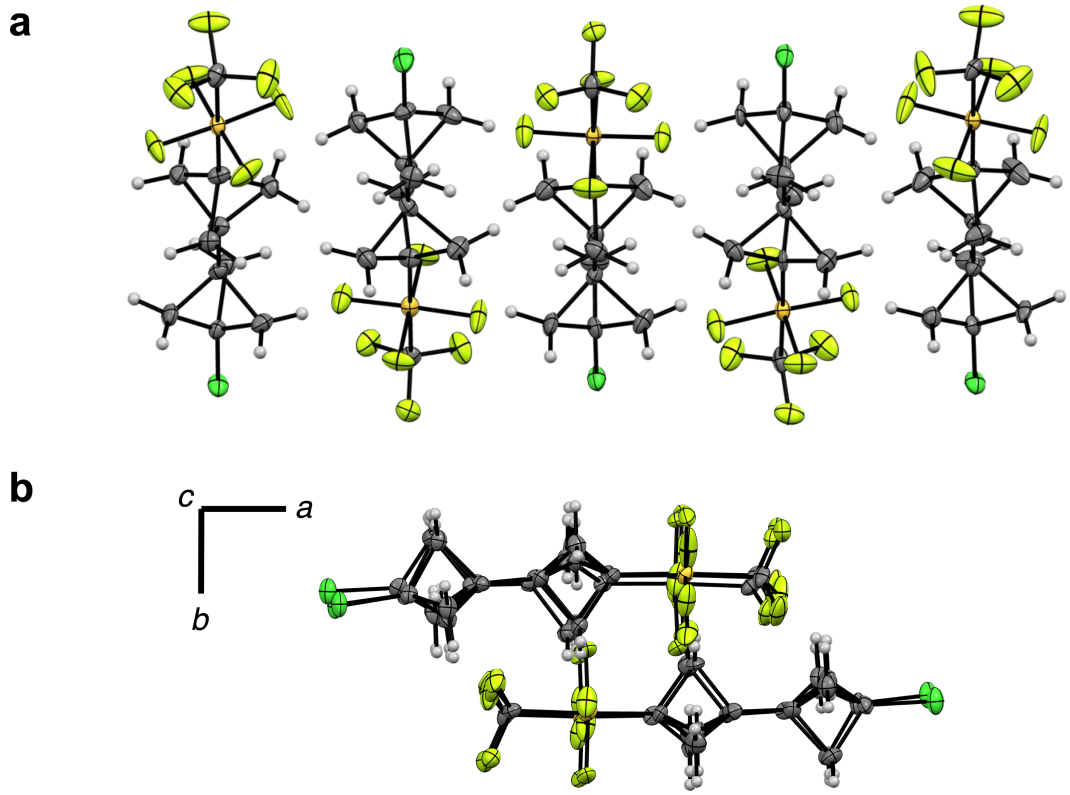

Figure 4: (A) The molecular structure of **3** at 90 K with 5 independent moieties in the asymmetric axis viewed along the *b*-axis. (B) The asymmetric unit of **3** at 90 K viewed along the *c*-axis. Thermal displacement ellipsoids depicted at 50% probability.

of **3**, compressing the unit cell isotropically, and ultimately leads to more disorder in the asymmetric unit [81]. This unexpected observation suggests that CF_3SF_4-containing [2]staffanes, in particular, warrant additional studies and may be of interest, e.g., in liquid crystal design.

Conclusion

Suppressing [*n*]staffane formation beyond $n = 1$ in radical chain reactions involving [1.1.1]propellane (**1**) tends to be more manageable than controlling oligomerization. However, under the right circumstances, alternating radical polarity matching throughout the chain propagation steps could be one way to theoretically "switch off" oligomerization beyond formation of a [2]staffane. Using this logic, our synthetic and computational study demonstrates that selective one-pot syntheses of [2]staffanes can be achieved when employing reagents that serve as radical sources of "extreme" electron-withdrawing groups (e.g., SF_5 or CF_3SF_4), which impact relative philicities of the bicyclopentyl radical intermediates. Over the course of this study, we also found that the SF_5- and CF_3SF_4-containing [2]staffanes reported herein are structurally interesting in their own right. Future work will examine potential applications of **2** and **3** and explore tactics for C–Cl bond functionalization.

Supporting Information

Supporting Information File 1

Experimental procedures, characterization data, NMR spectra, computational details, and X-ray crystallographic experimental details.
[https://www.beilstein-journals.org/bjoc/content/supplementary/1860-5397-20-259-S1.pdf]

Supporting Information File 2

LTP X-ray crystal structure of compound **3** (2357079.cif), HTP X-ray crystal structure of compound **3** (2357080.cif) and X-ray crystal structure of compound **2** at 240 K (238115.cif).
[https://www.beilstein-journals.org/bjoc/content/supplementary/1860-5397-20-259-S2.zip]

Acknowledgements

C.R.P. and Y.K. thank Dr. Nils Trapp (ETH Zürich) for helpful discussions. The authors also thank the UC Davis core NMR facility.

Funding

C.R.P. thanks the NIH/NIGMS (R35GM150861) and the University of California, Davis for financial support. W.Y.K thanks the Croucher Foundation for financial support through a doctoral scholarship. W.Y.K. and D.J.T. thank the NSF ACCESS program (CHE030089) for computational support. The authors also thank the NSF (CHE1531193) for the Dual Source X-ray Diffractometer.

ORCID® iDs

Jón Atiba Buldt - https://orcid.org/0009-0005-4900-0479
Wang-Yeuk Kong - https://orcid.org/0000-0002-4592-0666
Yannick Kraemer - https://orcid.org/0000-0002-2136-7253
Ansh Hiten Patel - https://orcid.org/0009-0006-2278-9227
James C. Fettinger - https://orcid.org/0000-0002-6428-4909
Dean J. Tantillo - https://orcid.org/0000-0002-2992-8844
Cody Ross Pitts - https://orcid.org/0000-0003-1047-8924

Data Availability Statement

All experimental data that supports the findings of this study are available in the published article and/or the supporting information to this article; coordinates for computed structures are openly available in ioChem-BD at https://doi.org/10.19061/iochem-bd-6-384.

References

1. Shire, B. R.; Anderson, E. A. *JACS Au* **2023,** *3,* 1539–1553. doi:10.1021/jacsau.3c00014
2. Kaszynski, P.; Friedli, A. C.; Michl, J. *J. Am. Chem. Soc.* **1992,** *114,* 601–620. doi:10.1021/ja00028a029
3. Levin, M. D.; Kaszynski, P.; Michl, J. *Chem. Rev.* **2000,** *100,* 169–234. doi:10.1021/cr990094z
4. Dilmaç, A. M.; Spuling, E.; de Meijere, A.; Bräse, S. *Angew. Chem., Int. Ed.* **2017,** *56,* 5684–5718. doi:10.1002/anie.201603951
5. Kaszynski, P.; Michl, J. *J. Am. Chem. Soc.* **1988,** *110,* 5225–5226. doi:10.1021/ja00223a070
6. Friedli, A. C.; Lynch, V. M.; Kaszynski, P.; Michl, J. *Acta Crystallogr., Sect. A: Found. Crystallogr.* **1990,** *46,* 377–389. doi:10.1107/s0108768189014096
7. Kaszynski, P.; Friedli, A. C.; McMurdie, N. D.; Michl, J. *Mol. Cryst. Liq. Cryst. (1969-1991)* **1990,** *191,* 193–197. doi:10.1080/00268949008038593
8. Friberg, S. E.; Kayali, I.; Kaszynski, P.; Michl, J. *Langmuir* **1992,** *8,* 996–998. doi:10.1021/la00039a041
9. Janecki, T.; Shi, S.; Kaszynski, P.; Michl, J. *Collect. Czech. Chem. Commun.* **1993,** *58,* 89–104. doi:10.1135/cccc19930089
10. Messner, M.; Kozhushkov, S. I.; de Meijere, A. *Eur. J. Org. Chem.* **2000,** 1137–1155. doi:10.1002/1099-0690(200004)2000:7<1137::aid-ejoc1137>3.0.co;2-2
11. Zimmerman, H. E.; Goldman, T. D.; Hirzel, T. K.; Schmidt, S. P. *J. Org. Chem.* **1980,** *45,* 3933–3951. doi:10.1021/jo01308a001
12. Obeng, Y. S.; Laing, M. E.; Friedli, A. C.; Yang, H. C.; Wang, D.; Thulstrup, E. W.; Bard, A. J.; Michl, J. *J. Am. Chem. Soc.* **1992,** *114,* 9943–9952. doi:10.1021/ja00051a029
13. Joran, A. D.; Leland, B. A.; Geller, G. G.; Hopfield, J. J.; Dervan, P. B. *J. Am. Chem. Soc.* **1984,** *106,* 6090–6092. doi:10.1021/ja00332a062
14. Leland, B. A.; Joran, A. D.; Felker, P. M.; Hopfield, J. J.; Zewail, A. H.; Dervan, P. B. *J. Phys. Chem.* **1985,** *89,* 5571–5573. doi:10.1021/j100272a002
15. Murthy, G. S.; Hassenrück, K.; Lynch, V. M.; Michl, J. *J. Am. Chem. Soc.* **1989,** *111,* 7262–7264. doi:10.1021/ja00200a057
16. Yang, H. C.; Magnera, T. F.; Lee, C.; Bard, A. J.; Michl, J. *Langmuir* **1992,** *8,* 2740–2746. doi:10.1021/la00047a026
17. Mazières, S.; Raymond, M. K.; Raabe, G.; Prodi, A.; Michl, J. *J. Am. Chem. Soc.* **1997,** *119,* 6682–6683. doi:10.1021/ja971059h
18. Lovering, F.; Bikker, J.; Humblet, C. *J. Med. Chem.* **2009,** *52,* 6752–6756. doi:10.1021/jm901241e
19. Tsien, J.; Hu, C.; Merchant, R. R.; Qin, T. *Nat. Rev. Chem.* **2024,** *8,* 605–627. doi:10.1038/s41570-024-00623-0
20. Stepan, A. F.; Subramanyam, C.; Efremov, I. V.; Dutra, J. K.; O'Sullivan, T. J.; DiRico, K. J.; McDonald, W. S.; Won, A.; Dorff, P. H.; Nolan, C. E.; Becker, S. L.; Pustilnik, L. R.; Riddell, D. R.; Kauffman, G. W.; Kormos, B. L.; Zhang, L.; Lu, Y.; Capetta, S. H.; Green, M. E.; Karki, K.; Sibley, E.; Atchison, K. P.; Hallgren, A. J.; Oborski, C. E.; Robshaw, A. E.; Sneed, B.; O'Donnell, C. J. *J. Med. Chem.* **2012,** *55,* 3414–3424. doi:10.1021/jm300094u
21. Locke, G. M.; Bernhard, S. S. R.; Senge, M. O. *Chem. – Eur. J.* **2019,** *25,* 4590–4647. doi:10.1002/chem.201804225
22. Mykhailiuk, P. K. *Org. Biomol. Chem.* **2019,** *17,* 2839–2849. doi:10.1039/c8ob02812e
23. Tse, E. G.; Houston, S. D.; Williams, C. M.; Savage, G. P.; Rendina, L. M.; Hallyburton, I.; Anderson, M.; Sharma, R.; Walker, G. S.; Obach, R. S.; Todd, M. H. *J. Med. Chem.* **2020,** *63,* 11585–11601. doi:10.1021/acs.jmedchem.0c00746
24. Cuadros, S.; Goti, G.; Barison, G.; Raulli, A.; Bortolato, T.; Pelosi, G.; Costa, P.; Dell'Amico, L. *Angew. Chem., Int. Ed.* **2023,** *62,* e202303585. doi:10.1002/anie.202303585
25. Rehm, J. D. D.; Ziemer, B.; Szeimies, G. *Eur. J. Org. Chem.* **2001,** 1049–1052. doi:10.1002/1099-0690(200103)2001:6<1049::aid-ejoc1049>3.0.co;2-v
26. Mazal, C.; Paraskos, A. J.; Michl, J. *J. Org. Chem.* **1998,** *63,* 2116–2119. doi:10.1021/jo971419j
27. Bunz, U.; Szeimies, G. *Tetrahedron Lett.* **1990,** *31,* 651–652. doi:10.1016/s0040-4039(00)94592-1
28. Blokhin, A. V.; Tyurekhodzhaeva, M. A.; Sadovaya, N. K.; Zefirov, N. S. *Russ. Chem. Bull.* **1989,** *38,* 1779. doi:10.1007/bf00956980
29. Sadovaya, N. K.; Blokhin, A. V.; Tyurekhodzhaeva, M. A.; Grishin, Y. K.; Surmina, L. S.; Koz'min, A. S.; Zefirov, N. S. *Russ. Chem. Bull.* **1990,** *39,* 637–638. doi:10.1007/bf00959608
30. Cheng, X.-Y.; Du, F.-S.; Li, Z.-C. *J. Polym. Sci. (Hoboken, NJ, U. S.)* **2023,** *61,* 472–481. doi:10.1002/pol.20220635
31. Bunz, U.; Szeimies, G. *Tetrahedron Lett.* **1989,** *30,* 2087–2088. doi:10.1016/s0040-4039(01)93718-9
32. Bunz, U.; Polborn, K.; Wagner, H.-U.; Szeimies, G. *Chem. Ber.* **1988,** *121,* 1785–1790. doi:10.1002/cber.19881211014
33. Sadovaya, N. K.; Blokhin, A. V.; Surmina, L. S.; Tyurekhodzhaeva, M. A.; Koz'min, A. S.; Zefirov, N. S. *Russ. Chem. Bull.* **1990,** *39,* 2224. doi:10.1007/bf01557749
34. Wiberg, K. B.; Waddell, S. T. *J. Am. Chem. Soc.* **1990,** *112,* 2194–2216. doi:10.1021/ja00162a022
35. Friedli, A. C.; Kaszynski, P.; Michl, J. *Tetrahedron Lett.* **1989,** *30,* 455–458. doi:10.1016/s0040-4039(00)95226-2

36. Kraemer, Y.; Ghiazza, C.; Ragan, A. N.; Ni, S.; Lutz, S.; Neumann, E. K.; Fettinger, J. C.; Nöthling, N.; Goddard, R.; Cornella, J.; Pitts, C. R. *Angew. Chem., Int. Ed.* **2022,** *61,* e202211892. doi:10.1002/anie.202211892
37. Shou, J.-Y.; Xu, X.-H.; Qing, F.-L. *Angew. Chem., Int. Ed.* **2021,** *60,* 15271–15275. doi:10.1002/anie.202103606
38. Pitts, C. R.; Santschi, N.; Togni, A. Method For Preparing a Polyfluorinated Compound. WO Patent WO/2019/229103, Dec 5, 2019.
39. Pitts, C. R.; Bornemann, D.; Liebing, P.; Santschi, N.; Togni, A. *Angew. Chem., Int. Ed.* **2019,** *58,* 1950–1954. doi:10.1002/anie.201812356
40. Häfliger, J.; Pitts, C. R.; Bornemann, D.; Käser, R.; Santschi, N.; Charpentier, J.; Otth, E.; Trapp, N.; Verel, R.; Lüthi, H. P.; Togni, A. *Chem. Sci.* **2019,** *10,* 7251–7259. doi:10.1039/c9sc02162k
41. Bornemann, D.; Pitts, C. R.; Ziegler, C. J.; Pietrasiak, E.; Trapp, N.; Kueng, S.; Santschi, N.; Togni, A. *Angew. Chem., Int. Ed.* **2019,** *58,* 12604–12608. doi:10.1002/anie.201907359
42. Brüning, F.; Pitts, C. R.; Kalim, J.; Bornemann, D.; Ghiazza, C.; de Montmollin, J.; Trapp, N.; Billard, T.; Togni, A. *Angew. Chem., Int. Ed.* **2019,** *58,* 18937–18941. doi:10.1002/anie.201910594
43. Ragan, A. N.; Kraemer, Y.; Kong, W.-Y.; Prasad, S.; Tantillo, D. J.; Pitts, C. R. *Angew. Chem., Int. Ed.* **2022,** *61,* e202208046. doi:10.1002/anie.202208046
44. Kraemer, Y.; Bergman, E. N.; Togni, A.; Pitts, C. R. *Angew. Chem., Int. Ed.* **2022,** *61,* e202205088. doi:10.1002/anie.202205088
45. Tyurekhodzhaeva, M. A.; Bratkova, A. A.; Blokhin, A. V.; Brel, V. K.; Koz'min, A. S.; Zefirov, N. S. *J. Fluorine Chem.* **1991,** *55,* 237–240. doi:10.1016/s0022-1139(00)82351-9
46. De Vleeschouwer, F.; Van Speybroeck, V.; Waroquier, M.; Geerlings, P.; De Proft, F. *Org. Lett.* **2007,** *9,* 2721–2724. doi:10.1021/ol071038k
47. Domingo, L. R.; Pérez, P. *Org. Biomol. Chem.* **2013,** *11,* 4350–4358. doi:10.1039/c3ob40337h
48. Kraemer, Y.; Buldt, J. A.; Kong, W.-Y.; Stephens, A. M.; Ragan, A. N.; Park, S.; Haidar, Z. C.; Patel, A. H.; Shey, R.; Dagan, R.; McLoughlin, C. P.; Fettinger, J. C.; Tantillo, D. J.; Pitts, C. R. *Angew. Chem., Int. Ed.* **2024,** *63,* e202319930. doi:10.1002/anie.202319930
49. Zhao, X.; Shou, J.-Y.; Qing, F.-L. *Sci. China: Chem.* **2023,** *66,* 2871–2877. doi:10.1007/s11426-023-1715-2
50. Nguyen, T. M.; Popek, L.; Matchavariani, D.; Blanchard, N.; Bizet, V.; Cahard, D. *Org. Lett.* **2024,** *26,* 365–369. doi:10.1021/acs.orglett.3c04043
51. Goerigk, L.; Grimme, S. *J. Chem. Theory Comput.* **2011,** *7,* 291–309. doi:10.1021/ct100466k
52. Caldeweyher, E.; Bannwarth, C.; Grimme, S. *J. Chem. Phys.* **2017,** *147,* 034112. doi:10.1063/1.4993215
53. Caldeweyher, E.; Ehlert, S.; Hansen, A.; Neugebauer, H.; Spicher, S.; Bannwarth, C.; Grimme, S. *J. Chem. Phys.* **2019,** *150,* 154122. doi:10.1063/1.5090222
54. Weigend, F.; Ahlrichs, R. *Phys. Chem. Chem. Phys.* **2005,** *7,* 3297–3305. doi:10.1039/b508541a
55. Cancès, E.; Mennucci, B.; Tomasi, J. *J. Chem. Phys.* **1997,** *107,* 3032–3041. doi:10.1063/1.474659
56. Chai, J.-D.; Head-Gordon, M. *Phys. Chem. Chem. Phys.* **2008,** *10,* 6615–6620. doi:10.1039/b810189b
57. Neese, F. *Wiley Interdiscip. Rev.: Comput. Mol. Sci.* **2022,** *12,* e1606. doi:10.1002/wcms.1606
58. *Gaussian 16,* Revision. C.01; Gaussian, Inc.: Wallingford, CT, 2016.
59. Ikeda, A.; Zhong, L.; Savoie, P. R.; von Hahmann, C. N.; Zheng, W.; Welch, J. T. *Eur. J. Org. Chem.* **2018,** 772–780. doi:10.1002/ejoc.201701568
60. Ikeda, A.; Capellan, A.; Welch, J. T. *Org. Biomol. Chem.* **2019,** *17,* 8079–8082. doi:10.1039/c9ob01797f
61. Deng, M.; Wilde, M.; Welch, J. T. *J. Org. Chem.* **2023,** *88,* 11363–11366. doi:10.1021/acs.joc.3c01177
62. Zhao, X.; Shou, J.-Y.; Newton, J. J.; Qing, F.-L. *Org. Lett.* **2022,** *24,* 8412–8416. doi:10.1021/acs.orglett.2c03540
63. Wu, J. I.-C.; Schleyer, P. v. R. *Pure Appl. Chem.* **2013,** *85,* 921–940. doi:10.1351/pac-con-13-01-03
64. Sterling, A. J.; Smith, R. C.; Anderson, E. A.; Duarte, F. *J. Org. Chem.* **2024,** *89,* 9979–9989. doi:10.1021/acs.joc.4c00857
65. Hirshfeld, F. L. *Theor. Chim. Acta* **1977,** *44,* 129–138. doi:10.1007/bf00549096
66. Reed, A. E.; Weinstock, R. B.; Weinhold, F. *J. Chem. Phys.* **1985,** *83,* 735–746. doi:10.1063/1.449486
67. *NBO 7.0;* Theoretical Chemistry Institute, University of Wisconsin: Madison, WI, USA, 2018.
68. Glendening, E. D.; Landis, C. R.; Weinhold, F. *J. Comput. Chem.* **2019,** *40,* 2234–2241. doi:10.1002/jcc.25873
69. Breneman, C. M.; Wiberg, K. B. *J. Comput. Chem.* **1990,** *11,* 361–373. doi:10.1002/jcc.540110311
70. Parr, R. G.; Szentpály, L. v.; Liu, S. *J. Am. Chem. Soc.* **1999,** *121,* 1922–1924. doi:10.1021/ja983494x
71. Domingo, L. R.; Chamorro, E.; Pérez, P. *J. Org. Chem.* **2008,** *73,* 4615–4624. doi:10.1021/jo800572a
72. Lu, T.; Chen, Q. Realization of Conceptual Density Functional Theory and Information-Theoretic Approach in Multiwfn Program. In *Conceptual Density Functional Theory;* Liu, S., Ed.; Wiley-VCH: Weinheim, Germany, 2022; Vol. 2, pp 631–647. doi:10.1002/9783527829941.ch31
73. Geerlings, P.; De Proft, F.; Langenaeker, W. *Chem. Rev.* **2003,** *103,* 1793–1874. doi:10.1021/cr990029p
74. Lu, T.; Chen, F. *J. Comput. Chem.* **2012,** *33,* 580–592. doi:10.1002/jcc.22885
75. Parr, R. G.; Yang, W. *J. Am. Chem. Soc.* **1984,** *106,* 4049–4050. doi:10.1021/ja00326a036
76. Sheldrick, G. M. *Acta Crystallogr., Sect. C: Struct. Chem.* **2015,** *71,* 3–8. doi:10.1107/s2053229614024218
77. Stephenson, G. A. *J. Pharm. Sci.* **2006,** *95,* 821–827. doi:10.1002/jps.20442
78. Chen, L.-Z.; Huang, D.-D.; Pan, Q.-J.; Ge, J.-Z. *RSC Adv.* **2015,** *5,* 13488–13494. doi:10.1039/c4ra12690d
79. Tello, M. J.; Lopez-Echarri, A.; Zubillaga, J.; Ruiz-Larrea, I.; Zuniga, F. J.; Madariaga, G.; Gomez-Cuevas, A. *J. Phys.: Condens. Matter* **1994,** *6,* 6751–6760. doi:10.1088/0953-8984/6/34/007
80. Izyumov, Y. A.; Syromyatnikov, V. N. *Phase Transitions and Crystal Symmetry;* Kluwer Academic Publishers: Dordrecht, Netherlands, 1990. doi:10.1007/978-94-009-1920-4
81. Chattoraj, S.; Sun, C. C. *Crystals* **2023,** *13,* 270. doi:10.3390/cryst13020270

BEILSTEIN JOURNAL OF ORGANIC CHEMISTRY

Synthesis of extended fluorinated tripeptides based on the tetrahydropyridazine scaffold

Thierry Milcent*[1], Pascal Retailleau[2], Benoit Crousse[1] and Sandrine Ongeri[1]

Full Research Paper

Open Access

Address:
[1]UMR 8076, BioCIS, CNRS, Université Paris-Saclay, avenue des sciences, 91400 Orsay, France and [2]Université Paris-Saclay, CNRS, Institut de Chimie des Substances Naturelles, 91198 Gif-sur-Yvette, France

Email:
Thierry Milcent* - thierry.milcent@universite-paris-saclay.fr

* Corresponding author

Keywords:
fluoroalkyl groups; heterocycles; hydrazino acids; peptides; tetrahydropyridazines

Beilstein J. Org. Chem. **2024,** *20,* 3174–3181.
https://doi.org/10.3762/bjoc.20.262

Received: 05 August 2024
Accepted: 20 November 2024
Published: 04 December 2024

This article is part of the thematic issue "Organofluorine chemistry VI".

Guest Editor: D. O'Hagan

Abstract

The synthesis of tripeptides incorporating new fluorinated heterocyclic hydrazino acids, based on the tetrahydropyridazine scaffold is described. Starting from simple fluorinated hydrazones, these non-proteinogenic cyclic β-amino acids were easily prepared by a zinc-catalyzed aza-Barbier reaction followed by an intramolecular Michael addition. Preliminary conformational studies on tripeptides including this scaffold in the central position show an extended conformation in solution (NMR) and in the solid state (X-ray).

Introduction

The synthesis of molecules capable of mimicking the various secondary structures and key functions of proteins is a major challenge in medicinal chemistry, especially in the fields of protein–protein interactions [1,2]. Accordingly, the incorporation of heterocyclic amino acids into peptides stabilizes their secondary structure and their metabolic stability, which is useful for numerous applications [3-5]. Indeed, the cyclic structure considerably reduces the number of possible rotational conformers, allowing a rational control of the 3D conformational space. Among these cyclic structures, the tetrahydropyridazines, six-atom nitrogenous heterocycles, are found in various bioactive molecules such as influenza virus neuraminidase inhibitors, GABA type A receptor modulators, and regulators of progesterone receptor or cannabinoid CB1 receptor antagonists (Figure 1) [6-9].

This tetrahydropyridazine scaffold is also found in numerous natural linear or cyclic peptides such as svetamycins or antrimycins as dehydropiperazic acid (Figure 2) [10].

Whereas many publications have been devoted to the synthesis and structure of piperazic acid derivatives (dehydro, chloro, hydroxy, …) [11,12], nothing is known about its β-analog (Figure 3), although β-amino acids have been shown to strongly modulate the structural, metabolic, and biological characteristics of peptides [13].

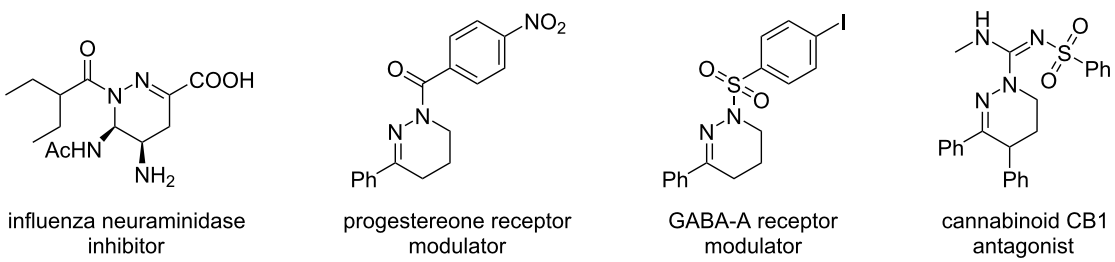

Figure 1: Examples of bioactive tetrahydropyridazine derivatives.

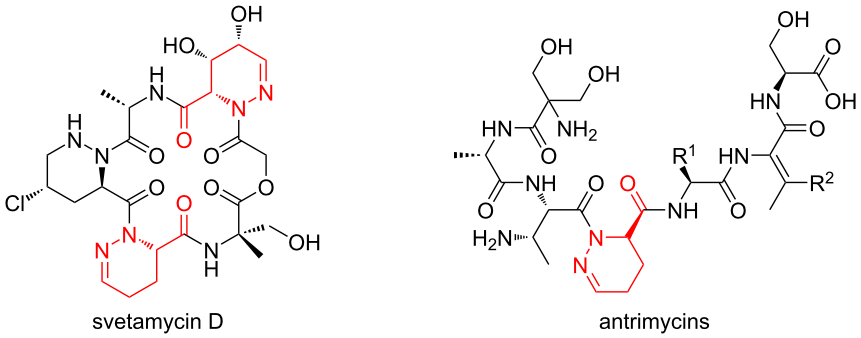

Figure 2: Linear and cyclic peptides incorporating the dehydropiperazic acid moiety.

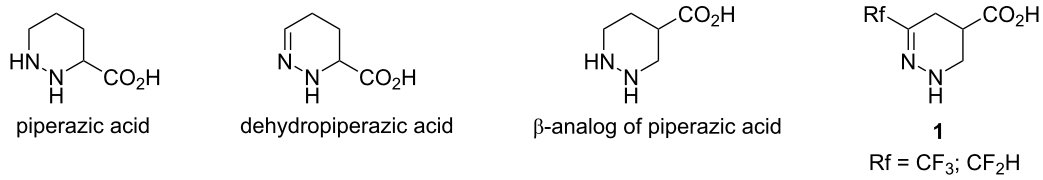

Figure 3: Piperazic acid and analogues and target trifluoro/difluoromethylated tetrahydropyridazine acids.

Finally, it is well known that fluorine is a very useful tool in medicinal chemistry as the incorporation of fluorinated groups (CF_3 or CF_2H) in organic molecules can modulate their physicochemical (pK_a, lipophilicity), structural (additional hydrophobic and hydrogen-bond interactions), and biological properties (metabolic stability, membrane permeability) [14,15]. Alongside the very well-known CF_3 group, the CF_2H group has become an essential structural motif in medicinal chemistry due to its hydrogen-bond donor capacity, its lipophilic character, and as a bioisostere for alcohol, thiol, or amine groups [16-19]. Thus, the contribution of fluorinated compounds to pharmaceuticals has been crucial for more than half a century [20].

In this context and in our ongoing effort to synthesize fluorinated non-proteinogenic linear or cyclic β-amino acids [21,22], it appeared attractive to build fluorinated β-analogs of dehydropiperazic acid (Figure 3). This novel fluorinated amino acid **1** will combine the electronic and structural properties of the fluorinated groups (CF_3 or CF_2H) and the geometric constraints due to its partially unsaturated cycle, which could help in the design of peptidomimetics.

To our knowledge, only a few publications report the synthesis of tetrahydropyridazines with a carboxylic acid or ester substituent. Firstly, the group of Haupt reported the synthesis of ethyl esters of tetrahydromethylpyridazine in 20% yield in a mixture of methanol and water by the reaction of methylhydrazine with acetylene dicarboxylic esters through the formation of enhydrazine (Scheme 1a), [23]. Later, Tomilov et al. described the formation of tetrahydropyridazine 3,4,5,6-tetracarboxylic esters in 42% yield upon the decomposition in chloroform at 60 °C of methyl diazoacetate in the presence of pyridine and catalyzed by rhodium(II) acetate (Scheme 1b) [24,25]. More recently, an unusual [4 + 2]-cycloaddition reaction between electron-poor

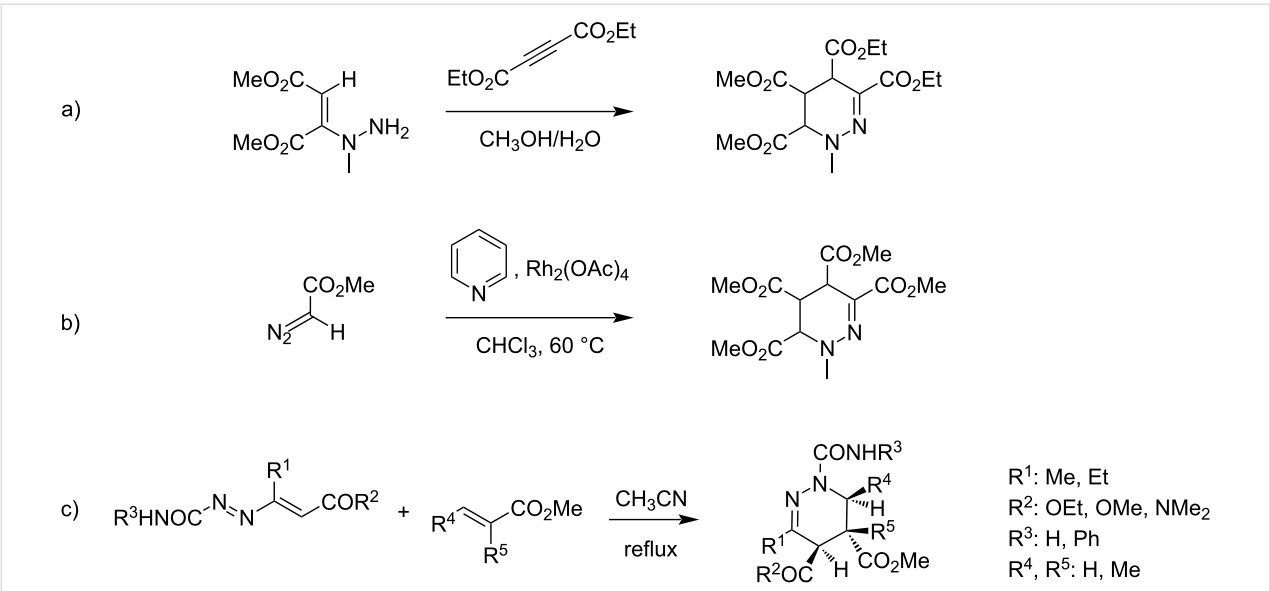

Scheme 1: Reported syntheses of tetrahydropyridazine ester derivatives.

1,2-diaza-1,3-dienes and electron-poor alkenes in refluxing acetonitrile was reported leading to various substituted tetrahydropyridazines in 17–78% yields (Scheme 1c) [26,27].

Nevertheless, these methods are neither relevant for the synthesis of **1** nor appropriate for peptide synthesis. Consequently, developing a simple and efficient methodology is still challenging. Our new strategy to synthesize these compounds is based on an aza-Barbier reaction on difluoro- or trifluoromethylated hydrazones. The thus obtained compounds will then be oxidized and cyclized in order to lead to the expected fluorinated tetrahydropyridazines (Figure 4).

Results and Discussion

First, the difluoro- and trifluoromethylated hydrazones **3a**–**f** were synthesized by condensing the corresponding hydrazide with the fluorinated aldehyde hemiacetal **2a** or **2b** (Scheme 2). Benzyl and *tert*-butyl carbazate (NH_2-NHCbz/NH_2-NHBoc) were chosen as starting materials in order to obtain final building blocks suitable for peptide synthesis. While the synthesis of compound **3a** was already reported [28], compounds **3b**–**f** are not described in the literature. All the fluorinated hydrazones were obtained in good yields and used directly in the next step without further purification (Scheme 2). In the case of Boc-protected hydrazones, the reaction must be carefully followed and reacted less than 2 hours in order to avoid the cleavage of the Boc group. The hydrazones **3e** and **3f** substituted by *N*-Cbz-L-phenylalanine could easily be synthesized under the same reaction conditions starting from the corresponding hydrazide amino acid. Compounds **3e** and **3f** were obtained as a mixture of conformers (1:1 ratio) which is often observed with *N*-acylhydrazones [29-31]. Indeed, in theory, *N*-acylhydrazones can exhibit four isomers, two due to the *E* and *Z* isomers of the imine group (–N=CH–) and two due to the *syn/anti*-conformers of the amide bond (–NH-CO–). Experimentally, the *E* isomer is often more stable and so, predominant. The strong correlation between the NH and CH of the imine observed in 2D ^{1}H-^{1}H NOE experiments for the two conformers of hydrazones **3e** and **3f** (see Supporting Information File 1) is in accordance with the *E* stereoisomers. Furthermore, another correlation is observed for one conformer involving the NH of the imine on one side and the α-proton and the CH_2 of the Cbz of the phenylalanine on the other. This correlation is present for one conformer (*anti*) and not for the other (*syn*), and this observation is similar for hydrazones **3e** and **3f** (see Supporting Information File 1). Based on these experimental data we can hypothesize the geometry of the two conformers of hydrazones **3e** and **3f** is *E,syn* and *E,anti*.

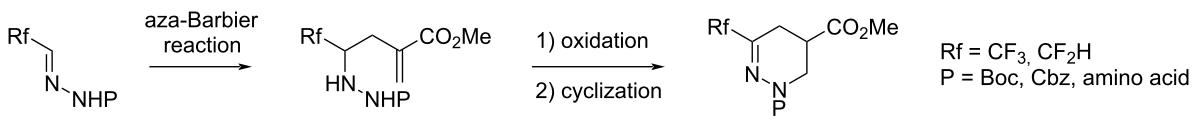

Figure 4: Synthetic strategy to obtain fluorinated tetrahydropyridazines from difluoro- or trifluoromethylated hydrazones.

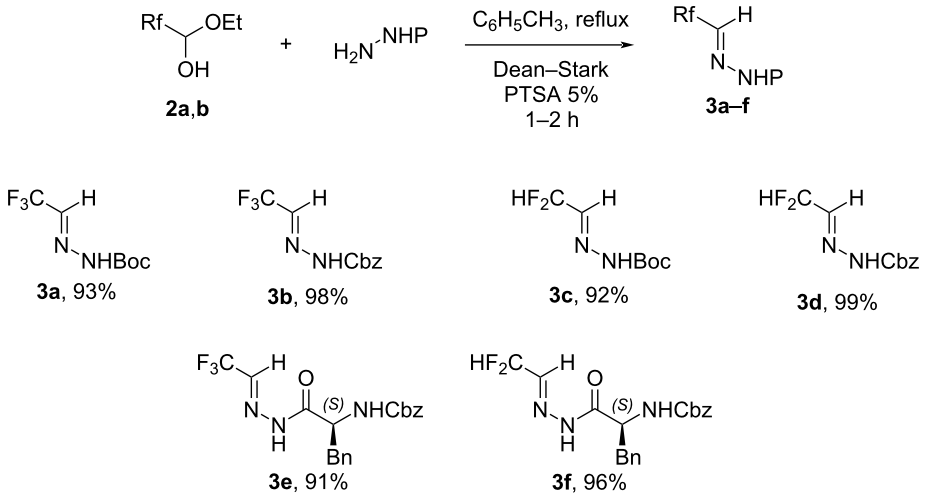

Scheme 2: Synthesis of fluorinated hydrazones **3a–f**.

Then, hydrazones **3** were reacted with zinc and methyl 2-(bromomethyl)acrylate (**4**). This aza-Barbier reaction was performed in a biphasic medium (THF/aqueous solution of saturated NH_4Cl) to avoid the formation of the α-methylene-γ-lactam obtained by intramolecular cyclization of the zinc amide on the ester function, as previously reported [32-35]. The corresponding adducts **5a–f** were isolated with good yields from 66 to 88%. In the case of hydrazides **5e** and **5f**, the mixture of diastereomers (1:1 ratio) could not be separated at this stage. Although no stereoselectivity is observed, it can be noticed that the presence of an amino acid is compatible with the conditions of the reaction and did not interfere or significantly decrease the yield of the reaction (Scheme 3).

Then, the *N*-carboxylate hydrazides **5a–d** were firstly oxidized with iodine in the presence of potassium carbonate to lead to the corresponding hydrazones **6a–d** in good yields (69–80%). Surprisingly, these conditions were unsuitable for compounds **5e** and **5f** and led to the formation of numerous byproducts. Fortunately, the replacement of iodine with *N*-bromosuccinimide (NBS), previously reported for the oxidation of hydrazine [36], allowed the expected compounds **6e** and **6f** to be obtained in good yields. This methodology was applied to the previous hydrazides **5a–d** giving the corresponding compounds **6a–d** in similar yields. As expected, no isomerization occurred during the oxidation, leading exclusively to the imine and not the enamine. As for the hydrazones **3e** and **3f**, we assumed that the

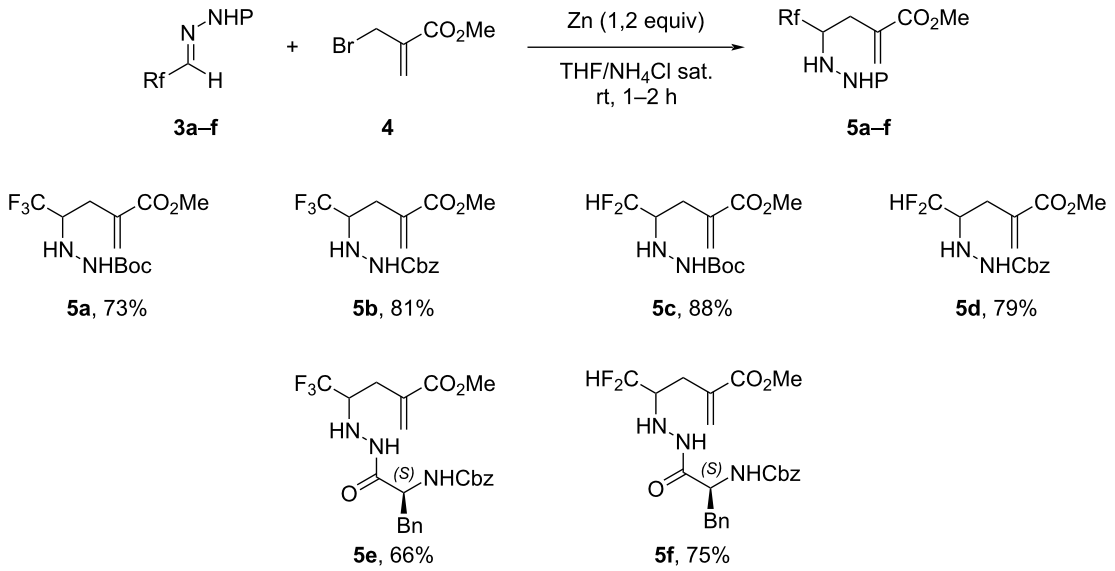

Scheme 3: Allylation of fluorinated hydrazones **3a–f** to obtain **5a–f**.

hydrazones **6e** and **6f** were obtained as a mixture of conformers, *E,syn* and *E,anti* (Scheme 4). Surprisingly, the ratio of each conformer differs for hydrazones **6e** (ratio 77:23) and **6f** (ratio 52:48).

The last cyclization step was based on an intramolecular Michael addition carried out in DMF and catalyzed by 10% of potassium carbonate. As previously observed [37], under these conditions, the 5-*endo-trig* cyclization was selective and the lactam resulting from the 5-*exo-trig* cyclization was not observed. Furthermore, in the case of compounds **7e** and **7f**, no competition with the NH of the phenylalanine was observed. The corresponding tetrahydropyridazines **7a–f** were obtained in moderate to good yields (Scheme 5).

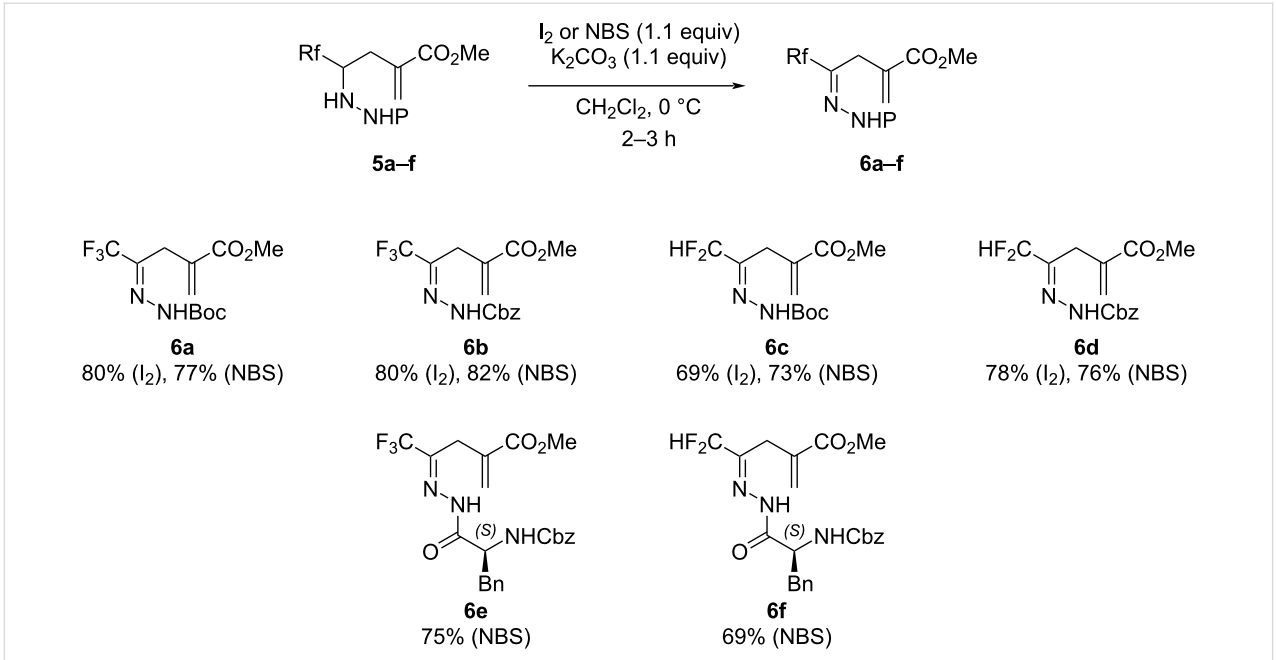

Scheme 4: Oxidation of hydrazines **5a–f** to obtain hydrazones **6a–f**.

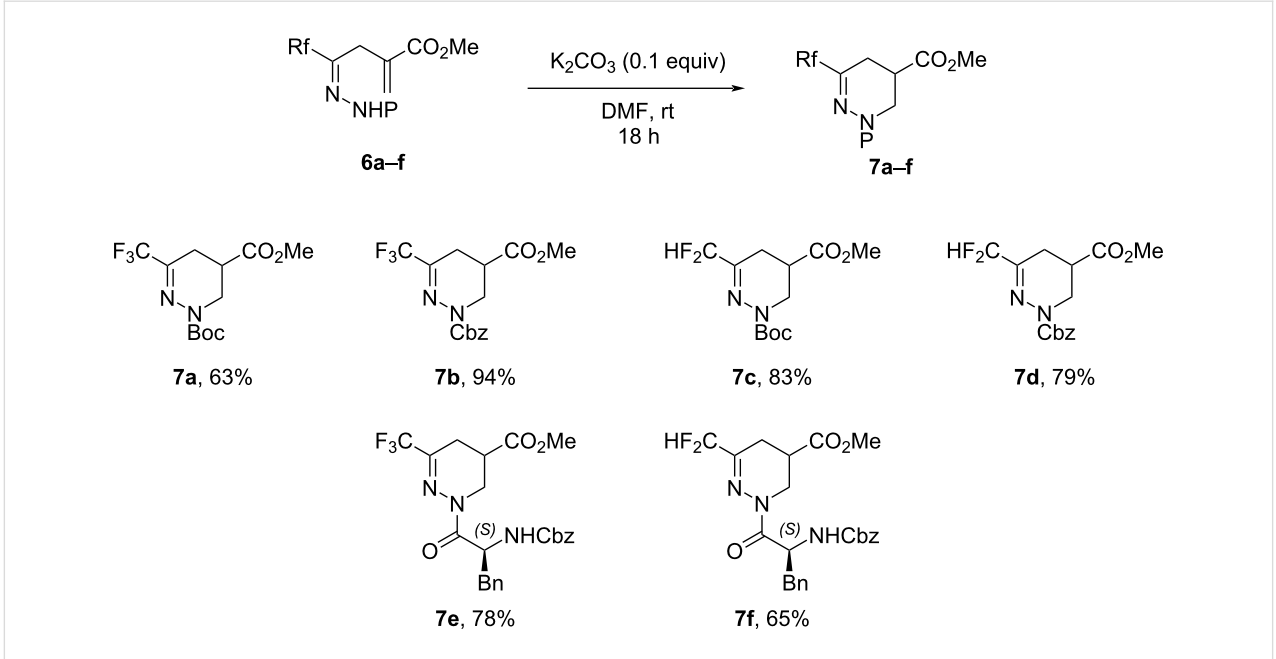

Scheme 5: Intramolecular cyclization of compounds **6a–f** to obtain tetrahydropyridazines **7a–f**.

Concerning compounds **7e** and **7f**, each diastereomer of the 1:1 ratio mixture could be isolated after purification by flash silica chromatography.

With dipeptides **7e** and **7f** stereoisomerically pure, we next focused our attention on the preparation of novel peptidic structures to perform some conformational analyses. Starting from the methyl ester **7**, each diastereomer was engaged in a classical sequence of saponification in the presence of LiOH, followed by a coupling reaction with L-valine methyl ester hydrochloride, to give the corresponding four enantiomerically pure tripeptides **8** with satisfactory yields over two steps (Scheme 6).

The absolute configuration (*S,S,S*) of the isomer **8f** was unambiguously assigned by X-ray crystallographic analysis (Figure 5).

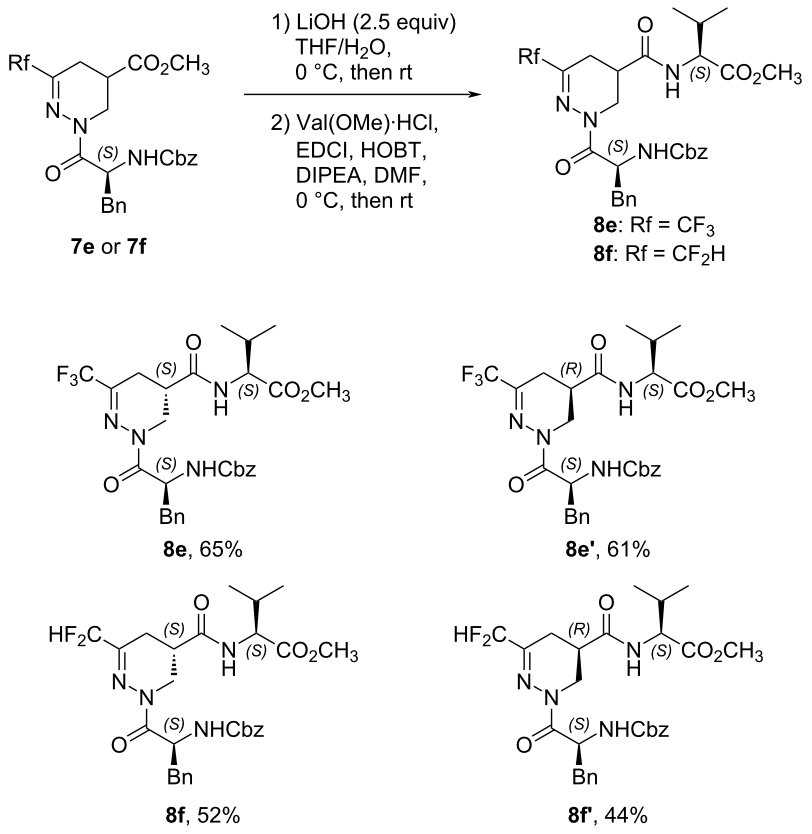

Scheme 6: Preparation of tripeptides **8e**, **8e'**, **8f**, and **8f'**. Yields refer to the yield over 2 steps.

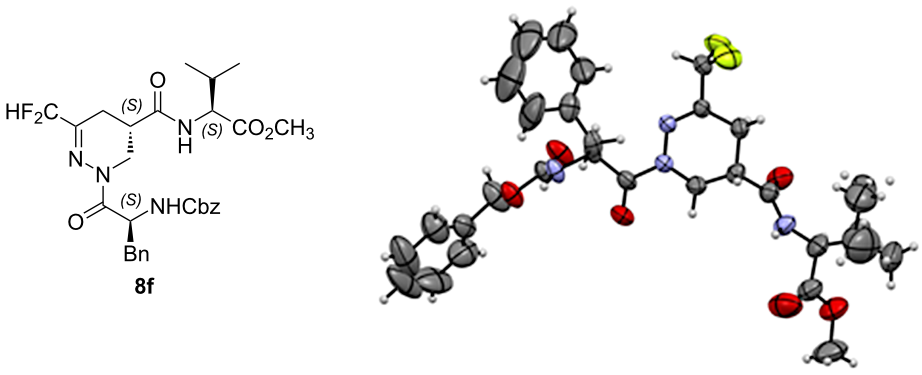

Figure 5: X-ray diffraction of compound **8f**.

Consequently, it was possible to assess the stereochemistry of the other diastereoisomer **8f'** and their precursors **7f** and **7f'**. On the other hand, considering the similarities of the ^{1}H NMR spectra of the CF_2H and CF_3 analogs, by comparison, we could hypothesize the absolute configuration of compounds **7e** and **7e'** and consequently of tripeptides **8e** and **8e'** (see Supporting Information File 1).

Next, some preliminary conformational studies were performed. Firstly, the X-ray crystallographic analysis of compound **8f** did not show any hydrogen-bond pattern and the global structure of the tripeptide is extended. Secondly, 2D ^{1}H-^{1}H NOE experiments of compound **8f** confirmed this result. Indeed, no correlation was observed between the protons of the side chain of the phenylalanine and those of the valine, suggesting an extended structure in accordance with the X-ray structure. Furthermore, the 2D ^{19}F,^{1}H NOE experiments of compound **8f** did not show any specific correlation between fluorine atoms and the protons of the amino acids (see Supporting Information File 1). Finally, the low chemical shifts of the amide and carbamate protons (6.4 ppm for NH of valine and 5.5 ppm for the NH of phenylalanine) indicate that they are not involved in hydrogen bonds. Furthermore, the 2D ^{1}H-^{1}H NOE NMR spectra and the chemical shifts of the NH protons of compounds **8f'**, **8e**, and **8e'** did not show any significant differences compared to **8f**. Overall, the ability of the new fluorinated β-analogs of dehydropiperazic acid to act as β or γ-turn is excluded. Interestingly, this novel scaffold rather promotes extended structures.

Conclusion

To conclude, we have developed a new methodology to synthesize β-analogs of dehydropiperazic acid incorporating fluorinated groups. In order to improve the efficiency of this strategy, the control of the stereoselectivity of the intramolecular aza-Michael addition could be envisaged with various chiral catalysts in further studies. These heterocyclic hydrazino acids, when incorporated into the peptidic structure, appear to confer an extended conformation. These interesting feature results will be further confirmed by the insertion of these cyclic β-dehydropiperazic acids in longer peptide sequences.

Supporting Information

Supporting Information File 1

Experimental procedures, product characterization, X-ray analysis and copies of NMR spectra.
[https://www.beilstein-journals.org/bjoc/content/supplementary/1860-5397-20-262-S1.pdf]

Acknowledgements

The authors gratefully acknowledge Central Glass Co. for the gift of trifluoro- and difluoroacetaldehyde hemiacetal.

Author Contributions

Thierry Milcent: conceptualization; methodology; writing – original draft. Pascal Retailleau: investigation; resources. Benoit Crousse: project administration; supervision; writing – review & editing. Sandrine Ongeri: funding acquisition; project administration; supervision; writing – review & editing.

ORCID® iDs

Thierry Milcent - https://orcid.org/0000-0002-2197-3843

Data Availability Statement

Additional research data generated and analyzed during this study is not shared.

References

1. Groß, A.; Hashimoto, C.; Sticht, H.; Eichler, J. *Front. Bioeng. Biotechnol.* **2016,** *3,* 211. doi:10.3389/fbioe.2015.00211
2. Li Petri, G.; Di Martino, S.; De Rosa, M. *J. Med. Chem.* **2022,** *65,* 7438–7475. doi:10.1021/acs.jmedchem.2c00123
3. Bąchor, U.; Mączyński, M. *Molecules* **2021,** *26,* 438. doi:10.3390/molecules26020438
4. Miura, T.; Malla, T. R.; Brewitz, L.; Tumber, A.; Salah, E.; Lee, K. J.; Terasaka, N.; Owen, C. D.; Strain-Damerell, C.; Lukacik, P.; Walsh, M. A.; Kawamura, A.; Schofield, C. J.; Katoh, T.; Suga, H. *Bull. Chem. Soc. Jpn.* **2024,** *97,* uoae018. doi:10.1093/bulcsj/uoae018
5. Liu, J.; Han, J.; Izawa, K.; Sato, T.; White, S.; Meanwell, N. A.; Soloshonok, V. A. *Eur. J. Med. Chem.* **2020,** *208,* 112736. doi:10.1016/j.ejmech.2020.112736
6. Zhang, L.; Williams, M. A.; Mendel, D. B.; Escarpe, P. A.; Chen, X.; Wang, K.-Y.; Graves, B. J.; Lawton, G.; Kim, C. U. *Bioorg. Med. Chem. Lett.* **1999,** *9,* 1751–1756. doi:10.1016/s0960-894x(99)00280-2
7. Rybczynski, P. J.; Combs, D. W.; Jacobs, K.; Shank, R. P.; Dubinsky, B. *J. Med. Chem.* **1999,** *42,* 2403–2408. doi:10.1021/jm9805889
8. Combs, D. W.; Reese, K.; Phillips, A. *J. Med. Chem.* **1995,** *38,* 4878–4879. doi:10.1021/jm00025a003
9. Lange, J. H. M.; den Hartog, A. P.; van der Neut, M. A. W.; van Vliet, B. J.; Kruse, C. G. *Bioorg. Med. Chem. Lett.* **2009,** *19,* 5675–5678. doi:10.1016/j.bmcl.2009.08.007
10. Morgan, K. D.; Andersen, R. J.; Ryan, K. S. *Nat. Prod. Rep.* **2019,** *36,* 1628–1653. doi:10.1039/c8np00076j
11. Handy, E. L.; Sello, J. K. *Top. Heterocycl. Chem.* **2015,** *48,* 97–124. doi:10.1007/7081_2015_185
12. Ciufolini, M. A.; Xi, N. *Chem. Soc. Rev.* **1998,** *27,* 437–445. doi:10.1039/a827437z
13. Cabrele, C.; Martinek, T. A.; Reiser, O.; Berlicki, Ł. *J. Med. Chem.* **2014,** *57,* 9718–9739. doi:10.1021/jm5010896
14. Gillis, E. P.; Eastman, K. J.; Hill, M. D.; Donnelly, D. J.; Meanwell, N. A. *J. Med. Chem.* **2015,** *58,* 8315–8359. doi:10.1021/acs.jmedchem.5b00258

15. Hagmann, W. K. *J. Med. Chem.* **2008,** *51,* 4359–4369. doi:10.1021/jm800219f
16. Zafrani, Y.; Yeffet, D.; Sod-Moriah, G.; Berliner, A.; Amir, D.; Marciano, D.; Gershonov, E.; Saphier, S. *J. Med. Chem.* **2017,** *60,* 797–804. doi:10.1021/acs.jmedchem.6b01691
17. Purser, S.; Moore, P. R.; Swallow, S.; Gouverneur, V. *Chem. Soc. Rev.* **2008,** *37,* 320–330. doi:10.1039/b610213c
18. Zafrani, Y.; Sod-Moriah, G.; Yeffet, D.; Berliner, A.; Amir, D.; Marciano, D.; Elias, S.; Katalan, S.; Ashkenazi, N.; Madmon, M.; Gershonov, E.; Saphier, S. *J. Med. Chem.* **2019,** *62,* 5628–5637. doi:10.1021/acs.jmedchem.9b00604
19. Sessler, C. D.; Rahm, M.; Becker, S.; Goldberg, J. M.; Wang, F.; Lippard, S. J. *J. Am. Chem. Soc.* **2017,** *139,* 9325–9332. doi:10.1021/jacs.7b04457
20. Inoue, M.; Sumii, Y.; Shibata, N. *ACS Omega* **2020,** *5,* 10633–10640. doi:10.1021/acsomega.0c00830
21. Hao, J.; Milcent, T.; Retailleau, P.; Soloshonok, V. A.; Ongeri, S.; Crousse, B. *Eur. J. Org. Chem.* **2018,** 3688–3692. doi:10.1002/ejoc.201800255
22. Milcent, T.; Hao, J.; Kawada, K.; Soloshonok, V. A.; Ongeri, S.; Crousse, B. *Eur. J. Org. Chem.* **2014,** 3072–3075. doi:10.1002/ejoc.201402078
23. Sucrow, W.; Ellermann, K.-H.; Flörke, U.; Haupt, H.-J. *Chem. Ber.* **1988,** *121,* 2007–2012. doi:10.1002/cber.19881211117
24. Tomilov, Y. V.; Platonov, D. N.; Averkiev, B. B.; Shulishov, E. V.; Nefedov, O. M. *Russ. Chem. Bull.* **2003,** *52,* 187–191. doi:10.1023/a:1022421020644
25. Tomilov, Y. V.; Platonov, D. N.; Dorokhov, D. V.; Nefedov, O. M. *Russ. Chem. Bull.* **2005,** *54,* 1008–1012. doi:10.1007/s11172-005-0349-6
26. D'Auria, M.; Racioppi, R.; Attanasi, O. A.; Mantellini, F. *Synlett* **2010,** 1363–1366. doi:10.1055/s-0029-1219834
27. Attanasi, O.; Bianchi, L.; D'Auria, M.; Mantellini, F.; Racioppi, R. *Curr. Org. Synth.* **2013,** *10,* 631–639. doi:10.2174/1570179411310040006
28. Wang, J.; Shang, Y.; Zhao, X.; Cui, Z.; Li, Y.; Wang, K.-H.; Huang, D.; Hu, Y.; Wang, N.; Feng, L. *Chem. Commun.* **2023,** *59,* 14293–14296. doi:10.1039/d3cc03854h
29. Munir, R.; Javid, N.; Zia-ur-Rehman, M.; Zaheer, M.; Huma, R.; Roohi, A.; Athar, M. M. *Molecules* **2021,** *26,* 4908. doi:10.3390/molecules26164908
30. Socea, L.-I.; Barbuceanu, S.-F.; Pahontu, E. M.; Dumitru, A.-C.; Nitulescu, G. M.; Sfetea, R. C.; Apostol, T.-V. *Molecules* **2022,** *27,* 8719. doi:10.3390/molecules27248719
31. Palla, G.; Predieri, G.; Domiano, P.; Vignali, C.; Turner, W. *Tetrahedron* **1986,** *42,* 3649–3654. doi:10.1016/s0040-4020(01)87332-4
32. Xu, Y.; Huang, D.; Wang, K.-H.; Ma, J.; Su, Y.; Fu, Y.; Hu, Y. *J. Org. Chem.* **2015,** *80,* 12224–12233. doi:10.1021/acs.joc.5b02154
33. Elaas, N. A.; Huang, D.; Wang, K.-H.; Su, Y.; Hu, Y. *Heterocycl. Commun.* **2018,** *24,* 159–163. doi:10.1515/hc-2017-0249
34. Wang, J.; Huang, D.; Wang, K.-H.; Peng, X.; Su, Y.; Hu, Y.; Fu, Y. *Org. Biomol. Chem.* **2016,** *14,* 9533–9542. doi:10.1039/c6ob01487a
35. Du, G.; Huang, D.; Wang, K.-H.; Chen, X.; Xu, Y.; Ma, J.; Su, Y.; Fu, Y.; Hu, Y. *Org. Biomol. Chem.* **2016,** *14,* 1492–1500. doi:10.1039/c5ob02260f
36. Wang, Y.; Wang, K.-H.; Su, Y.; Yang, Z.; Wen, L.; Liu, L.; Wang, J.; Huang, D.; Hu, Y. *J. Org. Chem.* **2018,** *83,* 939–950. doi:10.1021/acs.joc.7b02934
37. Ichikawa, J.; Lapointe, G.; Iwai, Y. *Chem. Commun.* **2007,** 2698–2700. doi:10.1039/b618251h

License and Terms

BEILSTEIN JOURNAL OF ORGANIC CHEMISTRY

Efficient synthesis of fluorinated triphenylenes with enhanced arene–perfluoroarene interactions in columnar mesophases

Yang Chen[‡1], Jiao He[‡1], Hang Lin[‡1], Hai-Feng Wang[‡1], Ping Hu[1], Bi-Qin Wang[1], Ke-Qing Zhao[*1] and Bertrand Donnio[*2]

Full Research Paper

Open Access

Address:
[1]College of Chemistry and Materials Science, Sichuan Normal University, Chengdu 610066, China and [2]Institut de Physique et Chimie des Matériaux de Strasbourg (IPCMS), CNRS-Université de Strasbourg (UMR 7504), F-67034 Strasbourg, France

Email:
Ke-Qing Zhao[*] - kqzhao@sicnu.edu.cn; Bertrand Donnio[*] - bertrand.donnio@ipcms.unistra.fr

* Corresponding author ‡ Equal contributors

Keywords:
arene–perfluoroarene interaction; decafluorobiphenyl; fluorinated triphenylene; fluoroarene nucleophilic substitution; organolithium

Beilstein J. Org. Chem. **2024,** *20,* 3263–3273.
https://doi.org/10.3762/bjoc.20.270

Received: 21 October 2024
Accepted: 03 December 2024
Published: 16 December 2024

This article is part of the thematic issue "Organofluorine chemistry VI".

Guest Editor: D. O'Hagan

Abstract

The high potential of non-covalent arene–fluoroarene intermolecular interactions in the design of liquid crystals lies in their ability to strongly promote self-assembly, improve the order and stability of the supramolecular mesophases, and enable tuneability of the optical and electronic properties, which can potentially be exploited for advanced applications in display technologies, photonic devices, sensors, and organic electronics. We recently successfully reported the straightforward synthesis of several mesogens containing four lateral aliphatic chains and derived from the classical triphenylene core self-assembling in columnar mesophases based on this paradigm. These mesogenic compounds were simply obtained in good yields by the nucleophilic substitution (S_NFAr) of various types of commercially available fluoroarenes with the electrophilic organolithium derivatives 2,2'-dilithio-4,4',5,5'-tetraalkoxy-1,1'-biphenyl (2Li-**BP***n*). In a continuation of this study, aiming at testing the limits of the reaction and providing a large diversity of structures, a structurally related series of compounds is reported here, namely 1,2,4-trifluoro-6,7,10,11-tetraalkoxy-3-(perfluorophenyl)triphenylenes (**F***n*). They were obtained by reacting the above mentioned 2,2'-dilithiobiphenyl derivatives with decafluorobiphenyl, C_6F_5–C_6F_5. These compounds differ from the previously reported series, 1,2,4-trifluoro-6,7,10,11-tetraalkoxy-3-aryltriphenylenes (**PH***n*), solely by the substitution of the terminal phenyl ring with a pentafluorophenyl ring. Thus, as expected, they display a Col_{hex} mesophase over large temperature ranges, with only small differences in the mesophase stability and transition temperatures. Furthermore, the presence of the terminal fluorophenyl group enables a subsequent second annulation, yielding a new series of extended polyaromatic mesomorphic compounds, i.e., 1,1',3,3',4,4'-hexafluoro-6,6',7,7',10,10',11,11'-octaalkoxy-2,2'-bitriphenylene (**G***nm*) which were found to display a Col_{rec} mesophase. The specific nucleo-

philic substitution patterns of the **F***n* derivatives and the antiparallel stacking mode into columnar structures stabilized by arene–perfluoroarene intermolecular interactions were confirmed by the single-crystal structure of the alkoxy-free side chain analog, i.e., 1,2,4-trifluoro-3-(perfluorophenyl)triphenylene (**F**). UV–vis absorption and fluorescence emission spectroscopies reveal green photoluminescence with fluorescence quantum yields of up to 33% for the **F***n* derivatives. The *J*-aggregation for the inner fluorine-substituted dimers **G***nm* is energetically and stereoelectronically more favorable and **G**66 exhibits thin-film fluorescence with a large red-shift of the emission peak.

Introduction

Non-covalent arene–fluoroarene intermolecular interactions [1,2] are drawing increasing attention due to their critical role in the engineering of functional and complex supramolecular assemblies [3-11], ranging from rigid crystalline architectures [3-8] to soft liquid crystalline materials [9-11]. Their unique properties originate from the high electronegativity of the fluorine atoms, inserted in the aromatic rings, which considerably modifies the dipole moment of the corresponding fluorinated aromatic rings with respect to their hydrogenated homologs, thus influencing their behavior, binding affinities, and optoelectronic properties. These interactions already represent an effective tool for the design of liquid crystalline materials [3-8]. Rod-like liquid crystalline molecules with fluorine-substituted arenes are ubiquitous in the displays industry [12]. They are also gaining importance in the design of π-conjugated polycyclic aromatic discotic liquid crystals (*F*-DLCs) [13-17] of interest for organic electronics and optical advanced materials, as they tend to promote more efficient molecular stacking into columns than their purely hydrogenated counterparts [18,19], thereby improving one-dimensional charge transport properties [20-22] in combination with tunable absorption and emission of visible light. Polar nematic phase [23] and chiral columnar phase materials [24] based on polar fluorobenzene rings have also recently emerged as interesting new classes of fluorous materials, revealing their enormous potential in the high-tech fields.

Although, F-DLCs seem to show unique and advantageous physical properties, their numbers and structural variation types are very limited due partially to several synthetic challenges [25-34]. Their syntheses usually are based on the direct transformation of commercial perfluoroarene chemical blocks and reagents, involving catalyzed C–F-bond activation and cross-coupling reactions, usually requiring precious transition-metal catalysts and tedious synthetic routes [28-34]. Therefore, low-cost and facile synthetic strategies are desired to increase their structural and functional diversity. In the modern organic synthetic tool-box, the fluoroarene nucleophilc substitution (S_NFAr) reaction possesses many outstanding advantages in the synthesis of π-conjugated functional molecules: the electrophiles are plentiful and include cheaply available perfluorobenzene, perfluoropyridine, perfluoronaphthalene, decafluorobiphenyl, and many other synthesized perfluoroarenes, and the nucleophiles are also abundant and contain aryllithium, conjugated organic dilithium reagents, phenols and benzenethiols, etc. [35-43].

We recently reported the high versatility of these intermolecular interactions in the design of several Janus-like discotic mesogens (Figure 1) [44-47]. A first study dealt with the synthesis of two sets of compounds, namely 1,2,3,4-tetrafluoro-6,7,10,11-tetraalkxoytriphenylenes (4*F*-**TP***n*) and 9,10,11,12,13,14-hexafluoro-2,3,6,7-tetraalkoxybenzo[*f*]tetraphenes (6*F*-**BTP***n*) [44], obtained by the straightforward nucleophilic substitution of fluoroarenes (S_NFAr) between 2,2'-dilithio-4,4',5,5'-tetraalkoxy-1,1'-biphenyl (2Li-**BP***n*) derivatives and hexafluorobenzene, C_6F_6 (4*F*-**TP***n*), on the one hand, and octafluoronaphthalene, $C_{10}F_8$ (6*F*-**BTP***n*), on the other. With only four alkoxy chains, these polar "Janus" mesogens [33,44] display a columnar hexagonal mesophase over broader temperature ranges and higher mesophase stability than the archetypical 2,3,6,7,10,11-hexa(alkoxy)triphenylene counterparts [48], whereas the corresponding hydrogenated 2,3,6,7-tetraalkoxytriphenylene counterparts (**TP***n*) were not mesomorphic. Testing further this approach to evaluate the persistence of mesomorphism in this family of compounds, another set of related compounds but with inhomogeneous chain substitution patterns, namely 7,10-dialkoxy-1,2,3,4-tetrafluoro-6,11-dimethoxytriphenylene (*p*-**TPF***n*) and 6,11-dialkoxy-1,2,3,4-tetrafluoro-7,10-dimethoxytriphenylene (*m*-**TPF***n*), were synthesized by this method [46]. Both isomers also displayed liquid crystalline properties, despite an even larger deficit of alkyl chains, although the inhomogeneous chain distribution had a net impact on both stability and nature of the mesophases. The versatility of this synthetic approach allows us to synthesize another set of mesomorphic compounds, based on a triphenylene core, 1,2,4-trifluoro-6,7,10,11-tetra(alkyloxy)-3-phenyltriphenylenes (**PH***n*, and extended to other aryl derivatives) by reacting lipophilic 2,2'-dilithiobiphenyl derivatives with the bulkier pentafluorobiphenyl, C_6F_5–C_6H_5. All these compounds display large mesomorphic ranges again, with the final phenyl ring being immersed with both the aliphatic continuum and the columns of stacked aromatic cores [45]. All these structural investigations revealed the great resilience of such a molecular

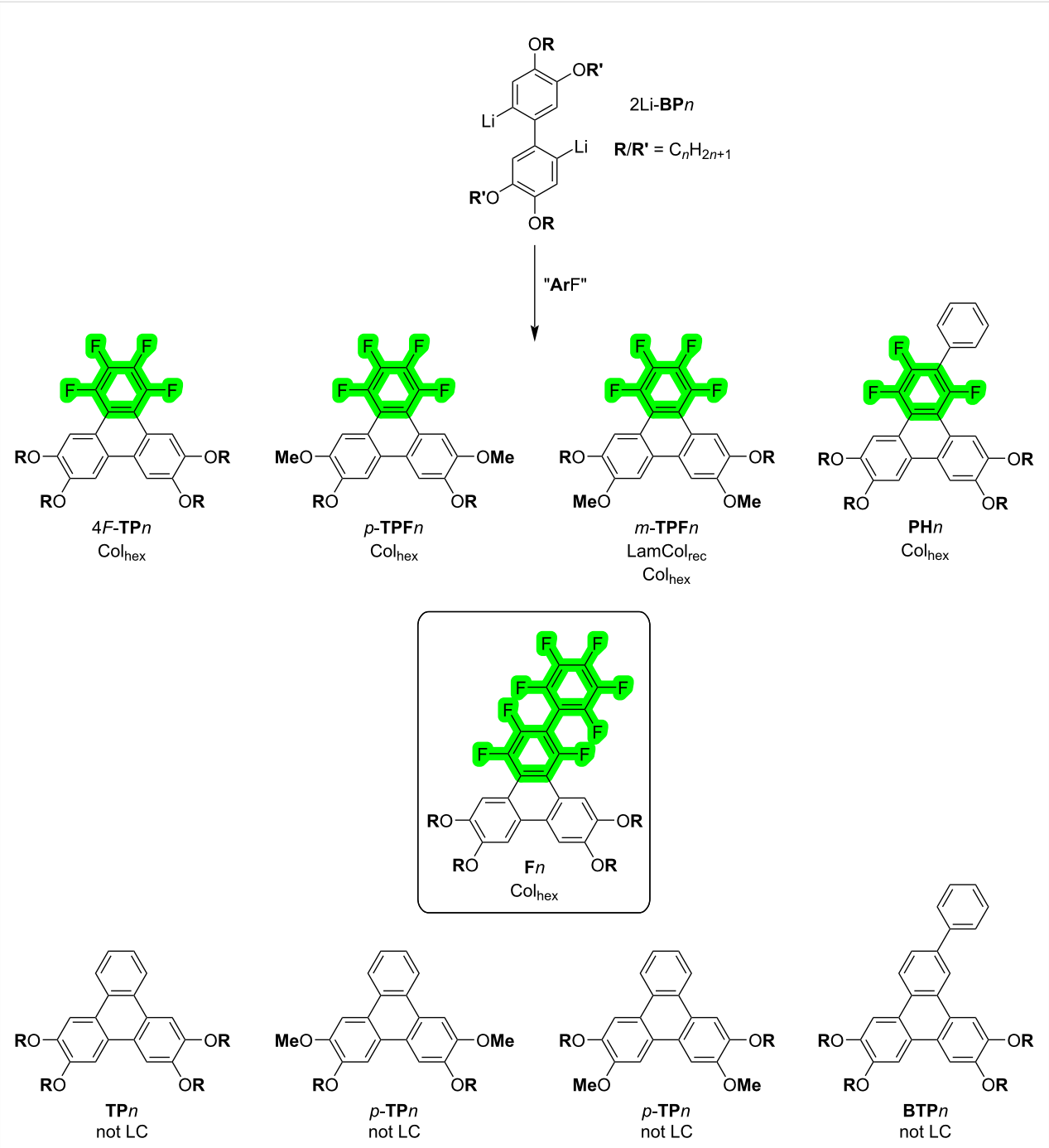

Figure 1: Fluorotriphenylene derivatives and their nonfluorinated homologs obtained by S_NFAr from 2,2'-dilithio-4,4',5,5'-tetraalkoxy-1,1'-biphenyl (2Br-**BP***n* → 2Li-**BP***n*) e.g., 4*F*-**TP***n* [44], *p*-**TPF***n* [46], *m*-**TPF***n* [46], **PH***n* [45], and **F***n* (this work); **BTP***n* was synthesized by a Suzuki–Scholl reaction sequence (Scheme S3, Supporting Information File 1).

system to important structural changes, and the essential role of the fluorinated phenyl moieties in the induction and stability of liquid crystalline mesophases.

The present study focuses on synthesizing new, structurally-related series of π-conjugated aromatic compounds (Figure 1) based on a simple triphenylene core and evaluating the mesomorphic and optical properties. Specifically 1,2,4-trifluoro-6,7,10,11-tetraalkoxy-3-(perfluorophenyl)triphenylenes (**F***n*, Figure 1), bearing a terminal fluoroarene ring was obtained using the same reaction as previously reported for **PH***n* (Figure 1) [45], between 2,2'-dilithiobiphenyl derivatives but

this time with the electrophile decafluorobiphenyl C_6F_5–C_6F_5 instead of C_6H_5–C_6F_5 (**F***n*, *n* = 3–12, Scheme 1). The presence of the terminal fluoroarene group in **F***n* enables to exploit further the S_NFAr procedure, as demonstrated for 4*F*-**TP***n* and 6*F*-**BTP***n* [44], through a subsequent second annulation reaction. This results in a second series of extended π-conjugated aromatic mesomorphic compounds, 1,1',3,3',4,4'-hexafluoro-6,6',7,7',10,10',11,11'-octaalkoxy-2,2'-bitriphenylene (**G***nm*, *n,m* = 4, 5, 6, Scheme 1), with the possibility to synthesize molecules with dissymmetrical chain substitution patterns. The investigation has two main objectives. First, it seeks to explore and understand the impact of the fluorination of the pendant ring on both the self-organization and optical properties of these compounds by comparing the properties of **F***n* with those of partially fluorinated **PH***n* and non-fluorinated **BTP***n*. Such comparison is critical for optimizing materials for specific applications. Second, the presence of this terminal fluoroarene group provides a basic platform to expand this chemistry, enabling access to new π-extended molecular systems that might be challenging to synthesize through conventional synthetic routes. This dual focus highlights the study's potential to advance both the design of functional materials and the development of innovative synthetic methodologies.

The mesomorphous properties of these two sets of compounds were investigated by polarized optical microscopy (POM), differential scanning calorimetry (DSC), and small-and wide-angle X-ray scattering (S/WAXS) and compared to related fluorinated and non-fluorinated homologs. The results showed that the Janus **F***n* derivatives exhibit a hexagonal columnar liquid crystal phase (Col_{hex}), with clearing temperatures decreasing gradually with the elongation of the alkoxy side-chains, from nearly 200 °C for the shortest homologs down to ca. 100 °C for the dodecyloxy derivative. The larger lath-like compounds, **G***nm*, exhibit a rectangular columnar phase (Col_{rec}) also over large temperature ranges from ambient up to 183 and 164 °C, respectively. The unsymmetrically alkoxy-substituted derivative, **G**48, also displays a Col_{rec} over a similar temperature range. The compounds' photophysical properties have also been studied in various solutions and thin film: **G**66 emitted green light in solution with an absolute photoluminescent quantum yield of ca. 33%.

Results and Discussion

Synthesis and characterization

We have recently generalized a very efficient "palladium-free" synthesis for the preparation of a variety of triphenylene derivatives (Figure 1) [44-47] based on the nucleophilic substitution of various electrophilic perfluoroarenes, including $C_6F_2H_4$, C_6F_6, $C_{10}F_8$, and C_6F_5-Ph, by nucleophilic organolithium reagents. e.g., 2,2'-dilithio-4,4',5,5'-tetrakis(alkoxy)-1,1'-biphenyls, 2Li-**BP***n*, prepared in situ from the reaction between 3,3',4,4'-tetra(alkoxy)-2,2'-dibromo-1,1'-biphenyl, 2Br-**BP***n*, and *n*-BuLi at low temperature. All new **F***n* compounds were prepared as previously described by reaction of 2Li-**BP***n* with decafluorobiphenyl, C_6F_5-C_6F_5 (Scheme 1). The starting materials 2Br-**BP***n* were prepared in high yield via $FeCl_3$-oxidative coupling of 1,2-dialkoxy-4-bromobenzene (Scholl reaction). The new triphenylene derivatives, **F**3–**F**12, were prepared in moderate to high yields (51–73%). In addition, three bitripheny-

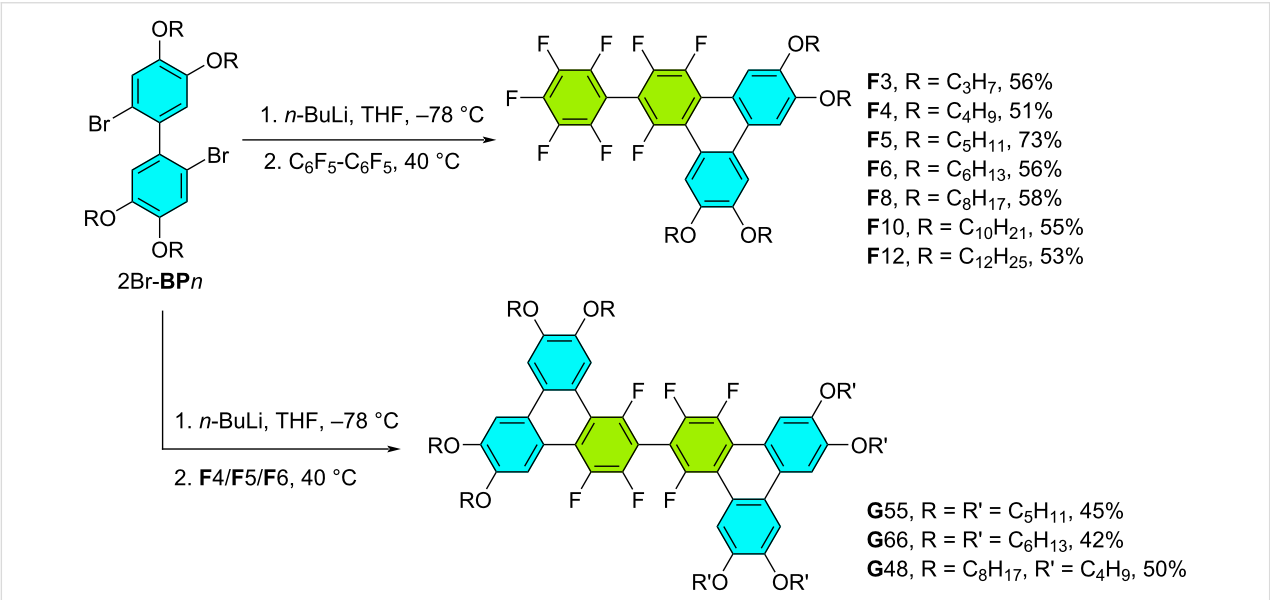

Scheme 1: Synthesis, yields, and nomenclature of 1,2,4-trifluoro-6,7,10,11-tetraalkoxy-3-(perfluorophenyl)triphenylene (**F***n*, *n* = 3–12) and corresponding 1,1',3,3',4,4'-hexafluoro-6,6',7,7',10,10',11,11'-octakisalkoxy-2,2'-bitriphenylene dimers (**G**55, **G**66 and **G**48).

lene derivatives were synthesized in a subsequent annulation step from **F***n* derivatives: the in situ prepared 2Li-**BP**5/6 was reacted with **F**5/6 to yield the symmetrical discotic dimers, **G**55/**G**66 respectively, in an average yield of 42–45% (Scheme 1). The reaction of 2Li-**BP**8 with **F**4 was also successfully tested, and allowed the preparation of the unsymmetrical discotic dimer **G**48, obtained in 50% yield, opening great possibilities in structural variations. The facile synthesis of **G**55, **G**66, and **G**48 demonstrates again the versatility of this synthetic method. The synthesis and detailed characterization of compounds **F**6 and **G**66 have been the subject of a preliminary patent description. This documentation describes the methodologies employed for their preparation, the analytical techniques used to confirm their structures, and the data obtained confirming their identities [49].

Two additional compounds were synthesized to complete this study: the derivative with no alkoxy chains (**F**) was prepared to grow single crystals suitable for X-ray analysis (Scheme S2 in Supporting Information File 1) in order to confirm the annulation reaction pattern, and 2,3,6,7-tetrakishexyloxy-10-phenyltriphenylene (**BTP**6, Scheme S3), the non-fluorinated isomer of **F**6 and **PH**6 (Figure 1), for probing the effect of fluorinated rings and the decisive role of arene–fluoroarene interactions in both mesomorphism induction and stabilization. Thus, 2Li-**BP** was reacted with C_6F_5–C_6F_5 to produce 2-perfluorophenyl-1,3,4-trifluorotriphenylene (**F**), in 37% yield and 2,3,6,7-tetrakishexyloxy-10-phenyltriphenylene (**BTP**6) was synthesized via consecutive Suzuki coupling and Scholl reaction in a total yield of 77%.

The synthesis, molecular structures, nomenclature, and synthetic yields of all compounds are shown in general Scheme 1. All prepared molecules were fully characterized by NMR (^{1}H, ^{19}F and ^{13}C), HRMS, and CHN analysis (Figures S1–S32, Supporting Information File 1), and all the results agree with the proposed molecular structures.

Single-crystal structure of F

Suitable single crystals of compound **F** for X-ray analysis were obtained by slow evaporation of an ethyl acetate/ethanol solution (Figure 2, and Supporting Information File 1, Figures S33, S34 and Tables S1–S3). The crystal structure unequivocally confirms that the reaction pattern between 2Li-**BP** and perfluorobiphenyl, effectively yielded the desired 1,2,4-trifluoro-3-(perfluorophenyl)triphenylene and that the annulation occurred at the expected positions. The similarity of the ^{19}F NMR spectra of **F** and alkoxy-substituted derivatives, **F***n*, showing 6 single peaks, corresponding to the 8 different fluorine atoms at almost identical positions (Figures S8–S14 and S21 in Supporting Information File 1), confirms that the pattern of the annulation reaction is the same for all triphenylene derivatives. Thus, compound **F** crystallizes in an orthorhombic crystallographic system (*Pccn* space group, no. 56) [50] with unit cell dimensions a = 13.2645(2) Å, b = 5.5284(1) Å, and c = 22.7571(3) Å; the unit cell contains 8 molecules, which gives a calculated molecular density of 1.688 g cm^{-3}.

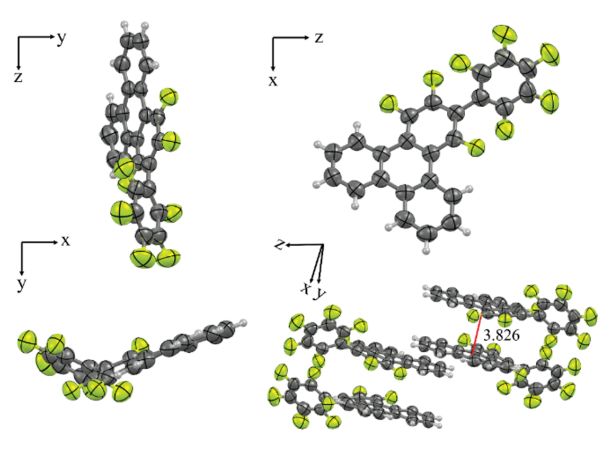

Figure 2: Single crystal structure of 1,2,4-trifluoro-3-(perfluorophenyl)triphenylene (**F**) viewed along the main axes: ORTEP diagram showing 50% thermal ellipsoid probability: carbon (gray), fluorine (green), and hydrogen (white).

In more details, the crystal structure reveals two short intramolecular F···H hydrogen contacts in the triphenylene core part with lengths of 2.047 Å and 2.114 Å, respectively (see Figure S33 in Supporting Information File 1). The triphenylene part of the molecule is rather flat, with, however, a substantial planar deviation of the pending perfluorophenyl group, forming a large tilt of ca. 45°. From the view along the *b*-axis, it can be seen that the flat triphenylene cores stack perfectly on top of each other, but with the pending fluoroarene group being alternately distributed from one side to the other, likely for steric hindrance, thus maximizing the fluoro–arene interactions by superimposing hydrogenated phenyl segments with fluoroarene ones (Figure S34 in Supporting Information File 1). Consequently, the triphenylene core–core distance is 3.83 Å and almost identical to the stacking distance in the columnar mesophase as measured by wide-angle X-ray scattering. Due to the efficient space filling and fluoroarene polar π-interaction, neighboring **F** molecules stack in an antiparallel way with a slippering distance of 1.697 Å from each other. Of course, with the presence of the lateral aliphatic chains, the cores rotate in order to maximize aliphatic–aromatic segregation whilst preserving fluoro–arene interactions.

Liquid crystal properties

Prior to investigating the mesomorphism of **F***n* and **G***nm* compounds, their thermal stability was first examined by thermal

gravimetric analysis (TGA) under a N_2 atmosphere in the dynamic mode. The TGA curves (Figure S35 and Table S4 in Supporting Information File 1) show that all compounds undergo two thermal decomposition processes; an initial thermal event with a decomposition temperature (T_{dec}, at weight loss 5%) between 283–332 °C for **F***n* and above 340 °C for **G***nm*, probing their excellent thermal stability.

All **F***n* and **G***nm* compounds display mesophases at room temperature. Their optical textures and phase-transition behaviors were observed via hot stage polarizing optical microscopy (POM). POM images were systematically captured during the cooling process at a cooling rate of 1 °C/min after the compounds were heated into the isotropic liquid (Figure 3 and Figure S36 in Supporting Information File 1). The liquid crystalline phases of the Janus triphenylenes, **F**3 to **F**12, all showed optical textures of a hexagonal columnar mesophase. Slowly cooled from its isotropic liquid state, **F**6 grew up into broken, fan-shaped color plates among a large dark area, with straight line defects, characteristic of the hexagonal columnar mesophase. The discotic dimers **G***nm* displayed a dense optical texture with dendritic- and flower-like features, with small fraction of dark area, which could be possibly attributed to a reduction of the mesophase symmetry.

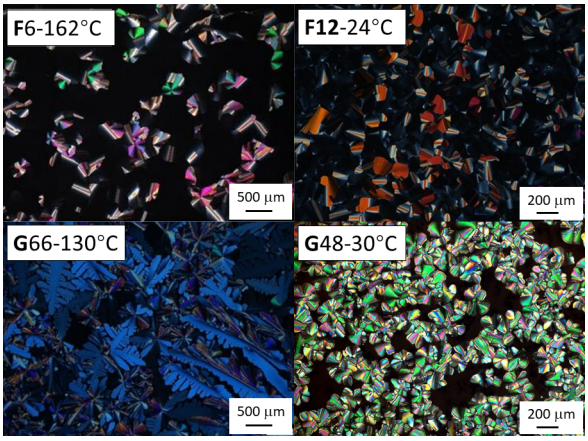

Figure 3: POM textures, observed between crossed polarizers of Janus and dimer, **F**6, **F**12, **G**66, and **G**48, respectively, as representative examples. More images can be seen in Supporting Information File 1 (Figure S36).

The results of the differential scanning calorimetry (DSC) are summarized in Figure 4 (see also Supporting Information File 1, Figures S37, S38 and Table S5 for details), confirming the POM observations and their room temperature behaviors (no crystallization is observed even at low temperature, except for **F**12). Compounds with shorter alkyl chains, **F**3, **F**4, and **F**5, possess almost the same clearing temperatures near 190 °C, whereas from **F**6 to **F**12, the clearing temperature gradually lowers from 176 down to 112 °C. When comparing **F***n* and **PH***n* (Figure 4) [45], both types of compounds show a high-range columnar mesophase at high temperature with almost identical clearing temperatures, which decrease gradually with the elongation of the alkoxy side-chains. The only difference is the emergence of a more ordered, 3D phase for some **PH***n* derivatives observed on cooling at lower temperature. As expected, neither **F** or **BTP**6 are mesomorphic.

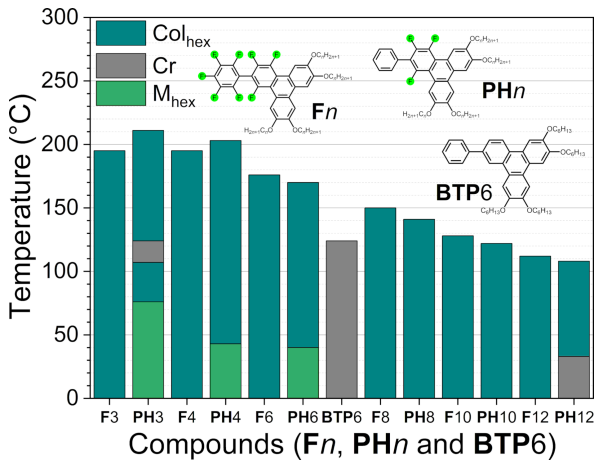

Figure 4: Comparative bar graph summarizing the thermal behavior of **F***n*, **BTP**6, and **PH***n* derivatives (2nd heating DSC data).

As for the larger fluorine derivatives **G***nm* (**G**55, **G**66, and **G**48), they all possess enantiotropic columnar mesophases right from room temperature up to 183 (**G**55), 164 (**G**66), and ca. 120 °C (**G**48). Compared to the previously synthesized non-fluorous pentyloxy homolog, showing a monotropic Col_{rec} phase [51,52], core fluorination surely plays a positive role in the induction of mesomorphism.

The mesophases of **F***n* and **G***nm* compounds were fully characterized by small- and wide-angle X-ray scattering (S/WAXS) at several temperatures (Figure 5, Figures S39–S41 and Table S6 in Supporting Information File 1). The X-ray patterns of the **F***n* compounds exhibit one main, sharp, and intense reflection in the small-angle range, and an additional small peak indexed as (20) for **F**3 and **F**4, or two peaks indexed as (11) and (20), respectively, for **F**10 and **F**12, confirming unambiguously the hexagonal symmetry (**F**5, **F**6, and **F**8 only show the intense small-angle reflection). In addition, they all show a broad diffuse scattering and a sharp and intense diffraction peak in the wide-angle region, assigned respectively to as h_{ch}, for the disordered chains, and h_{π}, for the long-range core–core stacking resulting from strong polar–π interactions. The correlation length of the stacking was calculated by the Debye–Scherrer formula,

which correspond to ca. 15–25 stacked molecules (Table 1). This coincides with the high clearing temperatures and high stability of the columnar mesophase of **F***n*. Overall, the behaviors of **F***n* and **PH***n* compounds are very similar, with only minor deviations of the isotropic temperatures.

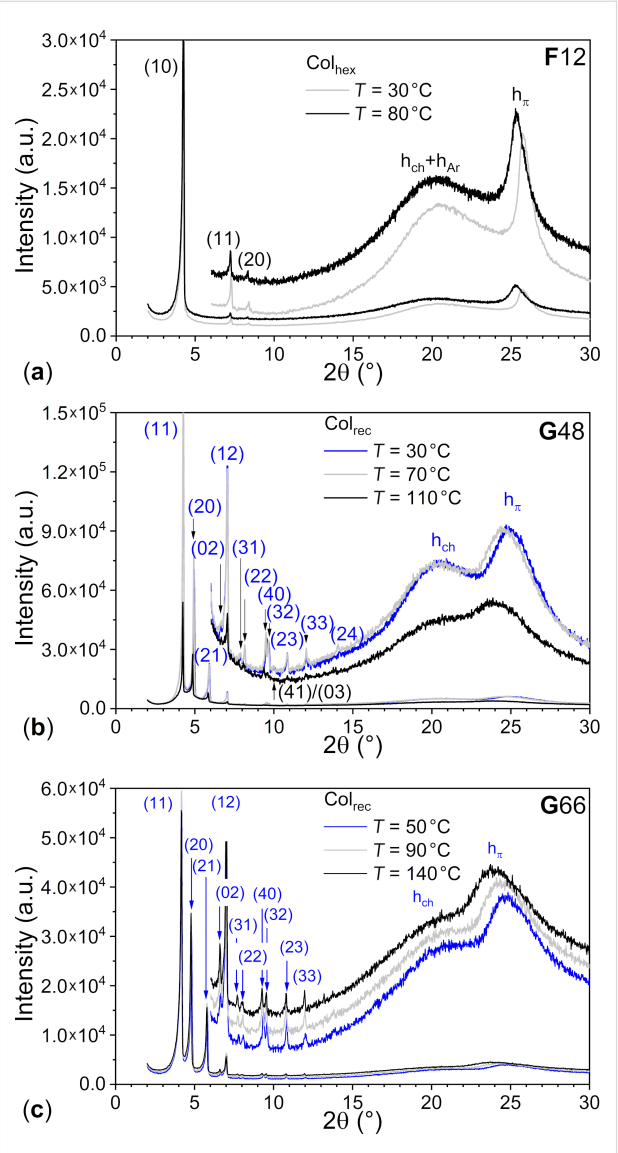

Figure 5: Representative S/WAXS patterns of **F***n* and **G***nm* compounds.

The single structure shows that the flat triphenylene cores almost stack perfectly on top of each other, with an alternation of the pending fluorinated phenyl groups by superimposition of one of the hydrogenated rings of the triphenylene segment above the trifluoroarene one, in order to maximize fluoro–arene intermolecular interactions between the molecules (Figure S34 in Supporting Information File 1). It also shows that the pending fluorophenyl makes an angle of ca. 45° with the triphenylene plane (see also DFT below). Despite this conformational distortion, the molecular thickness, h_{mol}, obtained by dividing the molecular volume with the columnar cross section, is not drastically increased (Table 1); h_{mol} ranges between 3.62 and 3.73 Å, very close to the stacking distance between consecutive cores measured by S/WAXS (3.42 Å ≤ h_π ≤ 3.62 Å), confirming that the triphenylene mesogens pile up in the columns with no or little tilt, reminiscent of the stacking observed in the crystal structure. It would thus consist of the piling of the triphenylene cores with the protruding fluorophenyl segments partly mixed with the aliphatic medium, with specific orientations of the triphenylenes (multiple of 120° orientations which contribute to the average circular cross-section of the columns) in order to maximize both the intermolecular interactions through the superimposition of fluoroarene segments and (alkylated) arene ones, partly similar to the crystal structure, and the homogeneous distribution of the chains around the columns, in agreement with the hexagonal symmetry. Both sets **F***n* and **PH***n* show rather similar variation of the cross-sectional area, increasing homogeneously with *n*, as well as similar molecular thickness throughout (*A* and h_{mol}, Figure S41 in Supporting Information File 1). Consequently, both the packing of **F***n* and of **PH***n* in the Col$_{hex}$ phase must be very similar, with no effect of the pending group nature (C_6H_5 vs C_6F_5) on the mesophase stability. A proposed model for the supramolecular organization of **F***n* in the Col$_{hex}$ phase is shown in Figure S42 of Supporting Information File 1.

The bitriphenylene **G***nm* materials exhibit different X-ray patterns, with a multitude of sharp peaks, that could be indexed according to a rectangular lattice (*p2gg* symmetry) [50], confirming the reduction of the phase symmetry and well-defined interfaces between aliphatic continuum, hydrogenated aromatics, and fluorinated arenes. The S/WAXS patterns of the three compounds are also identical, independently of the chain length or the chain distribution, and the lattice expansion with temperature is not significative. However, the stacking appears to be less effective than for the Janus derivatives as the signal corresponding to core–core stacking is not as sharp and intense, corresponding to a decrease of fluoroarene–arene interactions. This agrees with an increase of the molecular thickness (see h_{mol} values, Table 1), likely due to some electrostatic and steric repulsion between fluorine atoms within the inner core. DFT shows that both triphenylene segments do not lie in the same plane and that the overall molecule is slightly twisted. Nevertheless, the molecules still stack on top of each other in columns, maintaining the segregation between the various regions as in polyphilic molecules [9,10,54] and, since the molecules have a more anisotropic shape, the columnar cross-section cannot adopt a circular shape but rather an elliptical one, hence their arrangement into a rectangular lattice (Figure S43 in

Table 1: Mesophases' parameters.

Cpds	Phase	Temp.[a]	a^b/b^b	A^b	$h_\pi(\xi)/h_{ch}{}^c$	$V_{mol}{}^d/\rho^d$	$h_{mol}{}^e$
F3	Col_{hex}	120	16.73	242.44	3.53 (67)/4.41	895/1.26	3.69
F3	Col_{hex}	180	16.71	241.77	3.64 (56)/4.40	938/1.20	3.88
F4	Col_{hex}	50	17.57	267.38	3.45 (64)/4.42	968/1.26	3.62
F4	Col_{hex}	120	17.74	272.60	3.55 (65)/4.31	1010/1.21	3.71
F5	Col_{hex}	40	18.46	295.14	3.44 (79)/4.44	1074/1.22	3.64
F5	Col_{hex}	100	18.52	297.08	3.52 (83)/4.38	1111/1.18	3.74
F5	Col_{hex}	160	18.57	298.57	3.62 (59)/4.37	1161/1.13	3.89
F6	Col_{hex}	70	19.31	322.78	3.48 (72)/4.47	1203/1.17	3.73
F6	Col_{hex}	150	19.56	331.25	3.60 (47)/4.58	1270/1.11	3.83
F8	Col_{hex}	50	21.43	397.59	3.46 (79)/4.30	1410/1.13	3.55
F8	Col_{hex}	130	21.46	398.76	3.58 (42)/4.40	1485/1.07	3.72
F10	Col_{hex}	30	22.79	450.03 Å^2	3.45 (78)/4.37	1612/1.10	3.58
F10	Col_{hex}	100	23.09	461.88 Å^2	3.54 (42)/4.36	1629/1.09	3.64
F12	Col_{hex}	30	24.30	511.40 Å^2	3.45 (75)/4.38	1829/1.08	3.58
F12	Col_{hex}	80	24.47	518.53 Å^2	3.51 (47)/4.40	1886/1.04	3.64
G55	Col_{rec}	40	35.20/25.46	896.19 Å^2	3.57 (–)/4.28	1778/1.17	4.04
G55	Col_{rec}	100	35.26/25.55	900.89 Å^2	3.68 (–)/4.45	1853/1.12	4.11
G55	Col_{rec}	160	35.32/25.74	909.00 Å^2	3.72 (–)/4.51	1952/1.06	4.31
G66	Col_{rec}	50	37.18/26.80	996.42 Å^2	3.56 (–)/4.36	2009/1.13	4.03
G66	Col_{rec}	90	37.32/26.65	994.58 Å^2	3.66 (–)/4.48	2066/1.10	4.15
G66	Col_{rec}	140	37.46/26.53	993.81 Å^2	3.75 (–)/4.50	2152/1.05	4.33
G48	Col_{rec}	30	36.78/26.61	978.71 Å^2	3.54 (67)/4.39	1985/1.14	4.06
G48	Col_{rec}	70	36.98/26.54	981.45 Å^2	3.59 (–)/4.45	2036/1.11	4.15
G48	Col_{rec}	110	37.14/26.31	977.15 Å^2	3.66 (–)/4.39	2098/1.08	4.29

[a]Temperature of experiment (°C); [b]lattice parameter, *a*/*b* (Å) and area, *A* (Å^2), $A = a^2\sqrt{3}/2$ (for Col_{hex}) = $a \times b$ (for Col_{rec}), N_{col}: number of columns per lattice: N_{col} = 1 for Col_{hex}, N_{col} = 2 for Col_{rec}; [c]average face-to-face stacking distance (Å) between consecutive mesogens, h_π, determined from scattering maximum from SWAXS pattern, and ξ, correlation length (Å) calculated by Debye–Scherrer formula; h_{ch}, average distance (Å) between molten chains; [d]molecular volume (Å^3) and density (g·cm^{-3}) calculated from partial volumes of reference substances: $V_{mol} = V_{ar} + V_{ch}$, the sum of the volume of the aromatic part, V_{ar} (from reference compounds) and the volume of the chains, V_{ch} [53], $\rho = MW/(N_A \cdot V_{mol})$; [e]columnar slice thickness (Å), $h_{mol} = N_{col}V_{mol}/A$ (Å).

Supporting Information File 1). For **G***nm*, the mesomorphism is thus essentially driven by microsegregation between the various molecular constituents.

Photophysical properties: UV–vis absorption and photoluminescence

UV–vis absorption and fluorescence spectra of the synthesized fluorine polycyclic aromatic hydrocarbons **F***n* and **G***nm* were measured in solution (in various solvents) and thin film and the results are summarized in Figure 6 and Table S7 in Supporting Information File 1; **F**6 and **G**66 were chosen as representative examples.

F6 and **G**66 show almost identical UV–vis absorption spectra, both of them possessing a very broad absorption band below 400 nm with two maxima at ca. 380 nm for the strongest peak, and at ca. 360 nm for the smaller one (λ_{abs} = 284 nm for **PH**8), with no or little influence of the solvent polarity (Figure 6a). This may suggest that the sigma-bonded **F**6 and **G**66 have no conjugation in their ground states, the electron density being located on one triphenylene moiety (see DFT). **G**66 shows a stronger absorption band than **F**6, with expected ε values in the range of 10^4 and 10^5 L·mol^{-1}·cm^{-1}, respectively, as **G**66 possesses two triphenylene units whereas **F**6 only one.

Both compounds, however, display substantially different photoluminescent behavior. Both **F**6 and **G**66 show a single, broad emission band with a peak maximum around 410–430 nm for **F**6 (λ_{em} = 402 nm for **PH**8) and 460–500 nm for **G**66, with absolute quantum yields of 30% and 32%, respectively. Further, their fluorescence spectra in solutions show some solvent polarity influence, with a substantial red shift as the solvent polarity is increased. In thin film, the single luminescence maximum is shifted to 450 nm (518 nm) and 610 nm for **F**6

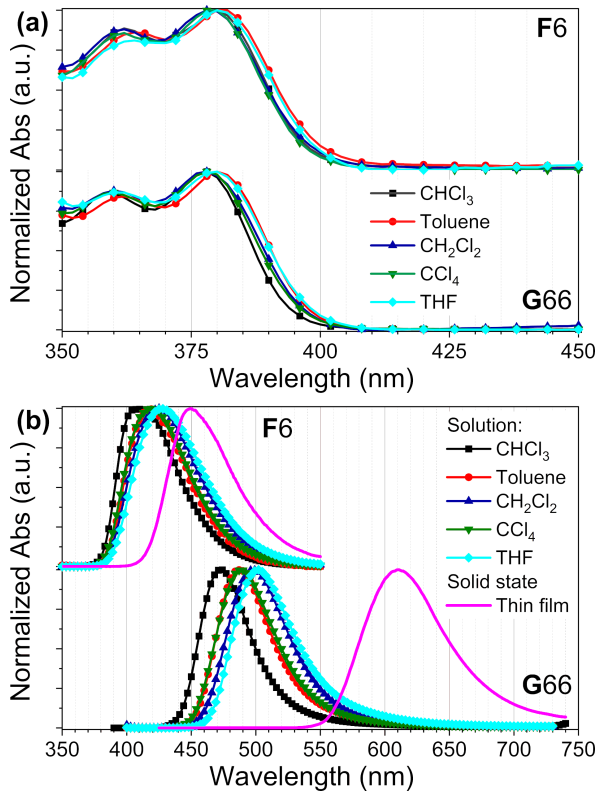

Figure 6: Absorption (a) and emission (b) spectra of **F**6 and **G**66, measured in different solvents at a concentration of 1×10^{-5} mol/L and in solid-state thin film.

(**PH**8) and **G**66, respectively. The thin film emission of **G**66 is red-shifted by about 120 nm compared with its solution, while the one of **F**6 is red-shifted only by 30 nm. This huge difference in thin film emission can be explained via their intermolecular slipped *J*-type aggregation, supported by S/WAXS and proposed the model of Col_{rec} mesophase [55-57].

DFT computation

For a deeper understanding of the electronic properties of these fluorine triphenylenes, we performed some DFT computation of **F**1 and **G**11 with the shortest methyl chain, and the results are summarized in Figure 7 and Figure S44 in Supporting Information File 1. First, the theoretically optimized molecular structure of **F**1 agrees well with the single crystal structure of **F**: the triphenylene core is planar and the side arm perfluorophenyl group is rotated by a few degrees due to the F···F repulsion on different rings. **G**11 exhibits a similar twist between the two triphenylene cores. Further, the calculated HOMO electron cloud of **F**1 (−5.8 eV; −5.89 eV for **PH**1) and **G**11 (−5.60 eV) both are located on a triphenylene core, which explains the similarity of their UV–vis absorption spectra. Their LUMO electron density maps distribute across to the side arm for **F**1 (−1.88 eV; −1.78 eV for **PH**1) and to the other triphenylene core for the dimer **G**11 (−1.78 eV). The π-conjugation of excited states results in a difference of their HOMO and LUMO energy levels: the fluorine dimer **G**11 possesses higher HOMO and LUMO energy levels than that of the monomer **F**1, with a smaller HOMO–LUMO energy gap (3.92 eV for **F**1 versus 4.11 eV for **PH**1). The DFT results thus agree pretty well with the fluorescence spectra in solution: **G**66 shows a fluorescence peak at 470–500 nm, while **F**6 has peaks located between 410–430 nm. It is noted that **G**66 shows deeper red-shifted fluorescence than **F**6, with peaks of 610 nm and 450 nm, respectively. The *J*-type aggregation for **G**66 in thin film and liquid crystalline state is energetically favorable for the arene–perfluo-

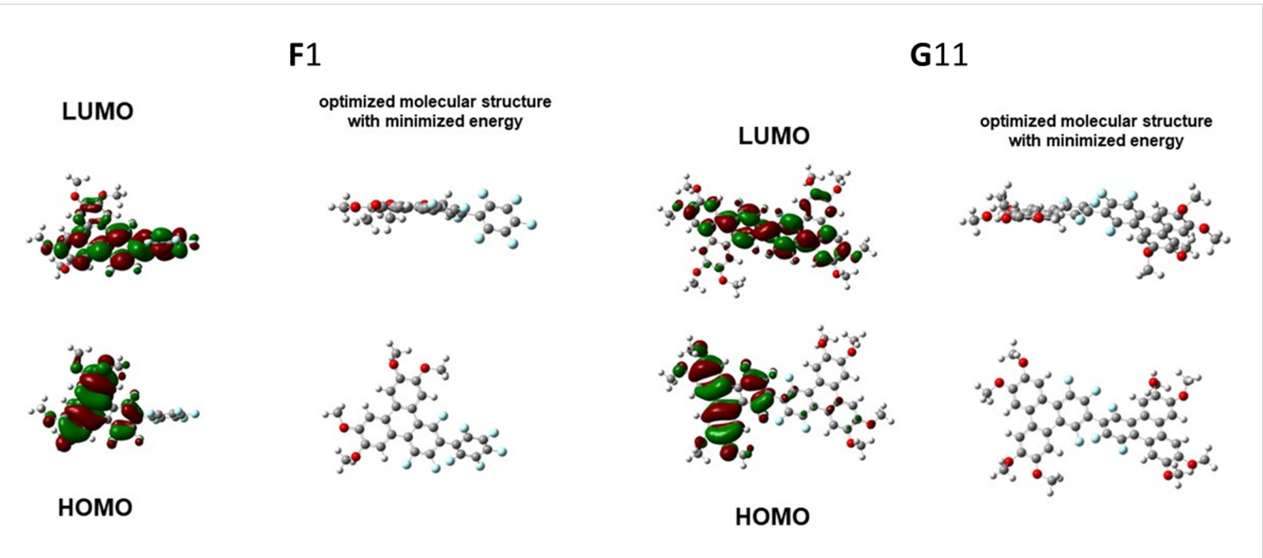

Figure 7: DFT calculated frontier molecular orbitals and optimized molecular structures for **F**1 and **G**11.

roarene overlap stacking and related stereoelectronic effects, which results in more than 100 nm red-shift of the fluorescence peak.

Conclusion

We have successfully prepared seven fluorine triphenylenes (**F**3 to **F**12) with various alkyl chain lengths and three bitriphenylene dimers (**G**55, **G**66, and **G**48) with different molecular symmetry by the S_NAr reaction. This "palladium-free" reaction between 2Li-**BP***n* and C_6F_5–C_6F_5 possesses several advantages: easily available starting chemicals, low cost, efficient, and versatile, displaying the potential to synthesize more complicated fluoroarene molecules and polymers. These fluorine-containing triphenylenes **F***n* and dimers **G***nm* display Col_{hex} and Col_{rec} mesophases, respectively, with high stability of the columnar mesophases due to strong arene–perfluoroarene polar π-interactions and related stereoelectronic effects. These Janus-type **F***n* compounds exhibit high clearing temperatures, and no crystalline phase, thus a very broad columnar mesophase range. Further, the sigma-bonded triphenylene dimers **G***nm* display an enantiotropic Col_{rec} mesophase including room temperature. These π-conjugated materials are advantageous for further investigation in device applications. The aromatic core fluorination changes the electronic structures of the triphenylenes, and their supramolecular arene–perfluoroarene slipped stacks (*J*-aggregate) result in **G**66 with orange-yellow color fluorescence in the solid state.

Supporting Information

Synthesis (Schemes S1–S3) and characterization, ^1H, ^{13}C, and ^{19}F NMR (Figures S1–S21), HRMS (Figures S22–S32), EA, single crystal X-ray structures (Figures S33, S34, Tables S1–S3), TGA (Figure S35, Table S4), POM (Figure S36), DSC (Figures S37, S38, Table S5), S/WAXS (Figures S39–S43, Table S6), optical properties (Table S7), and DFT (Figure S44, Table S8).

Supporting Information File 1

Experimental part.
[https://www.beilstein-journals.org/bjoc/content/supplementary/1860-5397-20-270-S1.pdf]

Acknowledgements

B.D. thanks the CNRS and the University of Strasbourg for constant support.

Funding

The authors thank the National Natural Science Foundation of China for funding (51773140, 51973143 and 21772135).

ORCID® iDs

Hai-Feng Wang - https://orcid.org/0009-0005-1979-0086
Ke-Qing Zhao - https://orcid.org/0000-0001-5703-3768
Bertrand Donnio - https://orcid.org/0000-0001-5907-7705

Data Availability Statement

All data that supports the findings of this study is available in the published article and/or the supporting information of this article.

References

1. Wang, W.; Wu, W. X.; Zhang, Y.; Jin, W. J. *Chem. Phys. Rev.* **2024,** *5,* 031303. doi:10.1063/5.0205540
2. Pace, C. J.; Gao, J. *Acc. Chem. Res.* **2013,** *46,* 907–915. doi:10.1021/ar300086n
3. Roesner, E. K.; Asheghali, D.; Kirillova, A.; Strauss, M. J.; Evans, A. M.; Becker, M. L.; Dichtel, W. R. *Chem. Sci.* **2022,** *13,* 2475–2480. doi:10.1039/d1sc05932g
4. Braunecker, W. A.; Hurst, K. E.; Ray, K. G.; Owczarczyk, Z. R.; Martinez, M. B.; Leick, N.; Keuhlen, A.; Sellinger, A.; Johnson, J. C. *Cryst. Growth Des.* **2018,** *18,* 4160–4166. doi:10.1021/acs.cgd.8b00630
5. Neitz, H.; Bessi, I.; Kachler, V.; Michel, M.; Höbartner, C. *Angew. Chem., Int. Ed.* **2023,** *62,* e202214456. doi:10.1002/anie.202214456
6. Liu, B.; Gao, J.; Hao, A.; Xing, P. *Angew. Chem., Int. Ed.* **2023,** *62,* e202305135. doi:10.1002/anie.202305135
7. Zhang, H.; Han, J.; Jin, X.; Duan, P. *Angew. Chem., Int. Ed.* **2021,** *60,* 4575–4580. doi:10.1002/anie.202014891
8. Cheng, Q.; Hao, A.; Xing, P. *Chem. Sci.* **2024,** *15,* 618–628. doi:10.1039/d3sc05212e
9. Tschierske, C. *Top. Curr. Chem.* **2011,** *318,* 1–108. doi:10.1007/128_2011_267
10. Hird, M. *Chem. Soc. Rev.* **2007,** *36,* 2070–2095. doi:10.1039/b610738a
11. Kishikawa, K. *Isr. J. Chem.* **2012,** *52,* 800–808. doi:10.1002/ijch.201200028
12. Kirsch, P.; Bremer, M. *Angew. Chem., Int. Ed.* **2000,** *39,* 4216–4235. doi:10.1002/1521-3773(20001201)39:23<4216::aid-anie4216>3.0.co;2-k
13. Wöhrle, T.; Wurzbach, I.; Kirres, J.; Kostidou, A.; Kapernaum, N.; Litterscheidt, J.; Haenle, J. C.; Staffeld, P.; Baro, A.; Giesselmann, F.; Laschat, S. *Chem. Rev.* **2016,** *116,* 1139–1241. doi:10.1021/acs.chemrev.5b00190
14. O'Neill, M.; Kelly, S. M. *Adv. Mater. (Weinheim, Ger.)* **2011,** *23,* 566–584. doi:10.1002/adma.201002884
15. Sergeyev, S.; Pisula, W.; Geerts, Y. H. *Chem. Soc. Rev.* **2007,** *36,* 1902–1929. doi:10.1039/b417320c
16. Kaafarani, B. R. *Chem. Mater.* **2011,** *23,* 378–396. doi:10.1021/cm102117c
17. Kumar, S. *Chemistry of discotic liquid crystals: from monomer to polymers;* CRC Press: Boca Raton, FL, 2011. doi:10.1201/b10457
18. Boden, N.; Bushby, R. J.; Cammidge, A. N.; Duckworth, S.; Headdock, G. *J. Mater. Chem.* **1997,** *7,* 601–605. doi:10.1039/a606447g
19. Yardley, R. E.; Paquette, J. A.; Taing, H.; Gaebler, H. M.; Eichhorn, S. H.; Hamilton, I. P.; Maly, K. E. *Org. Lett.* **2019,** *21,* 10102–10105. doi:10.1021/acs.orglett.9b04091
20. Bushby, R. J.; Donovan, K. J.; Kreouzis, T.; Lozman, O. R. *Opto-Electron. Rev.* **2005,** *13,* 269–279.

21. Sasada, Y.; Monobe, H.; Ueda, Y.; Shimizu, Y. *Mol. Cryst. Liq. Cryst.* **2010,** *525,* 153–157. doi:10.1080/15421401003799060
22. Zhao, K.-Q.; Du, J.-Q.; Long, X.-H.; Jing, M.; Wang, B.-Q.; Hu, P.; Monobe, H.; Henrich, B.; Donnio, B. *Dyes Pigm.* **2017,** *143,* 252–260. doi:10.1016/j.dyepig.2017.04.048
23. Cruickshank, E. *ChemPlusChem* **2024,** *89,* e202300726. doi:10.1002/cplu.202300726
24. Concellón, A.; Lu, R.-Q.; Yoshinaga, K.; Hsu, H.-F.; Swager, T. M. *J. Am. Chem. Soc.* **2021,** *143,* 9260–9266. doi:10.1021/jacs.1c05268
25. Weck, M.; Dunn, A. R.; Matsumoto, K.; Coates, G. W.; Lobkovsky, E. B.; Grubbs, R. H. *Angew. Chem., Int. Ed.* **1999,** *38,* 2741–2745. doi:10.1002/(sici)1521-3773(19990917)38:18<2741::aid-anie2741>3.0.co;2-1
26. Kishikawa, K.; Oda, K.; Aikyo, S.; Kohmoto, S. *Angew. Chem., Int. Ed.* **2007,** *46,* 764–768. doi:10.1002/anie.200603594
27. Sasada, Y.; Monobe, H.; Ueda, Y.; Shimizu, Y. *Chem. Commun.* **2008,** 1452–1454. doi:10.1039/b716920e
28. Zhao, K.-Q.; Gao, Y.; Yu, W.-H.; Hu, P.; Wang, B.-Q.; Heinrich, B.; Donnio, B. *Eur. J. Org. Chem.* **2016,** 2802–2814. doi:10.1002/ejoc.201600270
29. Zhao, K.-Q.; Jing, M.; An, L.-L.; Du, J.-Q.; Wang, Y.-H.; Hu, P.; Wang, B.-Q.; Monobe, H.; Heinrich, B.; Donnio, B. *J. Mater. Chem. C* **2017,** *5,* 669–682. doi:10.1039/c6tc04530h
30. Zhang, Q.; Prins, P.; Jones, S. C.; Barlow, S.; Kondo, T.; An, Z.; Siebbeles, L. D. A.; Marder, S. R. *Org. Lett.* **2005,** *7,* 5019–5022. doi:10.1021/ol051972k
31. Ahmida, M.; Larocque, R.; Ahmed, M. S.; Vacaru, A.; Donnio, B.; Guillon, D.; Eichhorn, S. H. *J. Mater. Chem.* **2010,** *20,* 1292–1303. doi:10.1039/b917169j
32. Vieira, A. A.; Farias, G.; Costa, W. C.; Eccher, J.; Bechtold, I. H.; Durola, F.; Bock, H. *Chem. – Eur. J.* **2021,** *27,* 9003–9010. doi:10.1002/chem.202005456
33. Li, Z.; Powers, M.; Ivey, K.; Adas, S.; Ellman, B.; Bunge, S. D.; Twieg, R. J. *Mater. Adv.* **2022,** *3,* 534–546. doi:10.1039/d1ma00606a
34. Guragain, P.; Powers, M.; Portman, J.; Ellman, B.; Twieg, R. J. *Mater. Adv.* **2023,** *4,* 4129–4137. doi:10.1039/d3ma00281k
35. Górski, K.; Ostojić, T.; Banasiewicz, M.; Ouellette, E. T.; Grisanti, L.; Gryko, D. T. *Chem. – Eur. J.* **2023,** *29,* e202203464. doi:10.1002/chem.202203464
36. See, Y. Y.; Morales-Colón, M. T.; Bland, D. C.; Sanford, M. S. *Acc. Chem. Res.* **2020,** *53,* 2372–2383. doi:10.1021/acs.accounts.0c00471
37. Wang, Z.; Wang, C.; Xi, Z. *Tetrahedron Lett.* **2006,** *47,* 4157–4160. doi:10.1016/j.tetlet.2006.04.035
38. Cho, D. M.; Parkin, S. R.; Watson, M. D. *Org. Lett.* **2005,** *7,* 1067–1068. doi:10.1021/ol050019c
39. Wang, Y.; Parkin, S. R.; Gierschner, J.; Watson, M. D. *Org. Lett.* **2008,** *10,* 3307–3310. doi:10.1021/ol8003468
40. Morrison, D. J.; Trefz, T. K.; Piers, W. E.; McDonald, R.; Parvez, M. *J. Org. Chem.* **2005,** *70,* 5309–5312. doi:10.1021/jo0506231
41. Leroux, F.; Mangano, G.; Schlosser, M. *Eur. J. Org. Chem.* **2005,** 5049–5054. doi:10.1002/ejoc.200500514
42. Kaga, A.; Iida, H.; Tsuchiya, S.; Saito, H.; Nakano, K.; Yorimitsu, H. *Chem. – Eur. J.* **2021,** *27,* 4567–4572. doi:10.1002/chem.202005223
43. Li, H.; Wang, X.-Y.; Wei, B.; Xu, L.; Zhang, W.-X.; Pei, J.; Xi, Z. *Nat. Commun.* **2014,** *5,* 4508. doi:10.1038/ncomms5508
44. Zhou, M.-M.; He, J.; Pan, H.-M.; Zeng, Q.; Lin, H.; Zhao, K.-Q.; Hu, P.; Wang, B.-Q.; Donnio, B. *Chem. – Eur. J.* **2023,** *29,* e202301829. doi:10.1002/chem.202301829
45. Pan, H.-M.; He, J.; Yu, W.-H.; Hu, P.; Wang, B.-Q.; Zhao, K.-Q.; Donnio, B. *J. Mater. Chem. C* **2023,** *11,* 14695–14704. doi:10.1039/d3tc02569a
46. Zhang, K.-L.; Yu, W.-H.; Zhao, K.-Q.; Hu, P.; Wang, B.-Q.; Donnio, B. *Chem. – Asian J.* **2024,** *19,* e202301080. doi:10.1002/asia.202301080
47. He, J.; Chen, Y.; Hu, P.; Wang, B.-Q.; Zhao, K.-Q.; Donnio, B. *J. Mol. Liq.* **2024,** *414,* 126218. doi:10.1016/j.molliq.2024.126218
48. Monobe, H.; Shimizu, Y.; Okamoto, S.; Enomoto, H. *Mol. Cryst. Liq. Cryst.* **2007,** *476,* 31/[277]–41/[287]. doi:10.1080/15421400701732324
49. Zhao, K.-Q.; He, J.; Zhao, K.-X.; Hu, P.; Wang, B.-Q. Synthesis of discotic perfluorophenyl-trifluorotriphenylene and hexafluorobitriphenylene. Chin. Pat. Appl. CN115477573 A, Nov 16, 2022.
50. Aroyo, M. I., Ed. *International Tables for Crystallography Volume A: Space-group symmetry,* 2nd ed.; John Wiley & Sons, 2016. doi:10.1107/9780955360206000114
51. Zhao, K.-C.; Du, J.-Q.; Wang, H.-F.; Zhao, K.-Q.; Hu, P.; Wang, B.-Q.; Monobe, H.; Heinrich, B.; Donnio, B. *Chem. – Asian J.* **2019,** *14,* 462–470. doi:10.1002/asia.201801483
52. Lin, H.; Zhao, K.-X.; Jing, M.; Long, X.-H.; Zhao, K.-Q.; Hu, P.; Wang, B.-Q.; Lei, P.; Zeng, Q.-D.; Donnio, B. *J. Mater. Chem. C* **2022,** *10,* 14453–14470. doi:10.1039/d2tc02441a
53. Donnio, B.; Heinrich, B.; Allouchi, H.; Kain, J.; Diele, S.; Guillon, D.; Bruce, D. W. *J. Am. Chem. Soc.* **2004,** *126,* 15258–15268. doi:10.1021/ja0471673
54. Kishikawa, K.; Aikyo, S.; Akiyama, S.; Inoue, T.; Takahashi, M.; Yagai, S.; Aonuma, H.; Kohmoto, S. *Soft Matter* **2011,** *7,* 5176–5187. doi:10.1039/c0sm01459a
55. Milián-Medina, B.; Gierschner, J. *J. Phys. Chem. Lett.* **2017,** *8,* 91–101. doi:10.1021/acs.jpclett.6b02495
56. Hayashi, S.; Asano, A.; Kamiya, N.; Yokomori, Y.; Maeda, T.; Koizumi, T. *Sci. Rep.* **2017,** *7,* 9453. doi:10.1038/s41598-017-09848-0
57. Bischof, D.; Tripp, M. W.; Hofmann, P. E.; Ip, C.-H.; Ivlev, S. I.; Gerhard, M.; Koert, U.; Witte, G. *Chem. – Eur. J.* **2022,** *28,* e202103653. doi:10.1002/chem.202103653

License and Terms

BEILSTEIN JOURNAL OF ORGANIC CHEMISTRY

Nickel-catalyzed cross-coupling of 2-fluorobenzofurans with arylboronic acids via aromatic C–F bond activation

Takeshi Fujita*[1], Haruna Yabuki[2], Ryutaro Morioka[2], Kohei Fuchibe[2] and Junji Ichikawa[3]

Full Research Paper

Open Access

Address:
[1]The Institute for Solid State Physics, The University of Tokyo, 5-1-5 Kashiwanoha, Kashiwa, Chiba 277-8581, Japan, [2]Division of Chemistry, Faculty of Pure and Applied Sciences, University of Tsukuba, 1-1-1 Tennodai, Tsukuba, Ibaraki 305-8571, Japan and [3]Sagami Chemical Research Institute, 2743-1 Hayakawa, Ayase, Kanagawa 252-1193, Japan

Email:
Takeshi Fujita* - tfujita@issp.u-tokyo.ac.jp

* Corresponding author

Keywords:
arylboronic acid; benzofuran; C–F bond activation; cross-coupling; nickel

Beilstein J. Org. Chem. **2025,** *21,* 146–154.
https://doi.org/10.3762/bjoc.21.8

Received: 02 November 2024
Accepted: 23 December 2024
Published: 15 January 2025

This article is part of the thematic issue "Organofluorine chemistry VI".

Guest Editor: D. O'Hagan

Abstract

2-Fluorobenzofurans underwent efficient nickel-catalyzed coupling with arylboronic acids through the activation of aromatic C–F bonds. This method allowed us to successfully synthesize a range of 2-arylbenzofurans with various substituents. The reaction, which proceeded under mild conditions, involved β-fluorine elimination from nickelacyclopropanes formed by the interaction of 2-fluorobenzofurans with zero-valent nickel species. This protocol facilitates orthogonal coupling reactions of aromatic C–F and C–Br bonds with arylboronic acids.

Introduction

The metal-catalyzed activation of aromatic carbon–fluorine (C–F) bonds is widely recognized as a challenging task in synthetic organic chemistry owing to their high bond dissociation energy compared to other aromatic C–X (X = Cl, Br, I) bonds [1-7]. This activation is essential for the late-stage functionalization of stable C–F bonds in complex molecules with reactive functional groups, providing an orthogonal approach to complex molecule synthesis. Despite considerable efforts to develop various catalytic systems, the activation of aromatic C–F bonds often requires high temperatures [1-7]. Therefore, methods for activating aromatic C–F bonds at ambient temperature remain underdeveloped.

We have developed efficient metal-mediated methods for activating (i) vinylic [8-13] and (ii) allylic C–F bonds [14-18] using β-fluorine elimination under mild conditions. In these studies, (i) we discovered zirconium-mediated β-fluorine elimination from zirconacyclopropanes **A**, which are generated by treating 1,1-difluoroethylenes with a zirconocene equivalent ($ZrCp_2$, Scheme 1a) [8]. The resulting 1-fluorovinylzirconocenes **B** then

undergo palladium-catalyzed coupling with aryl iodides to produce arylated fluoroethylenes. Additionally, (ii) we observed that electron-deficient 2-(trifluoromethyl)-1-alkenes strongly interact with electron-rich zero-valent nickel species to form nickelacyclopropanes **C** [15-17]. These intermediates enable C–F bond activation through the formation of nickelacyclopentenes **D** with alkynes, followed by β-fluorine elimination, leading to defluorinative coupling between these components (Scheme 1b).

Among aromatic fluorides, we have targeted 2-fluorobenzofurans **1** for C–F bond activation [19]. These compounds, which we prepared efficiently via 5-*endo*-*trig* cyclization of β,β-difluoro-*o*-hydroxystyrenes [20,21], possess a C–C double bond with an electron-deficient carbon atom owing to the nearby fluorine and oxygen atoms. We expected that 2-fluorobenzofurans **1** could form nickelacyclopropanes **E** upon treatment with zero-valent nickel species. Subsequent β-fluorine elimination from these intermediates **E** would facilitate the activation of aromatic C–F bonds (Scheme 1c). In this study, we demonstrate nickel-catalyzed defluorinative cross-coupling [22-37] of 2-fluorobenzofurans **1** with arylboronic acids **2** at ambient temperature, with nickelacyclopropanes **E** serving as crucial intermediates for the activation of aromatic C–F bonds.

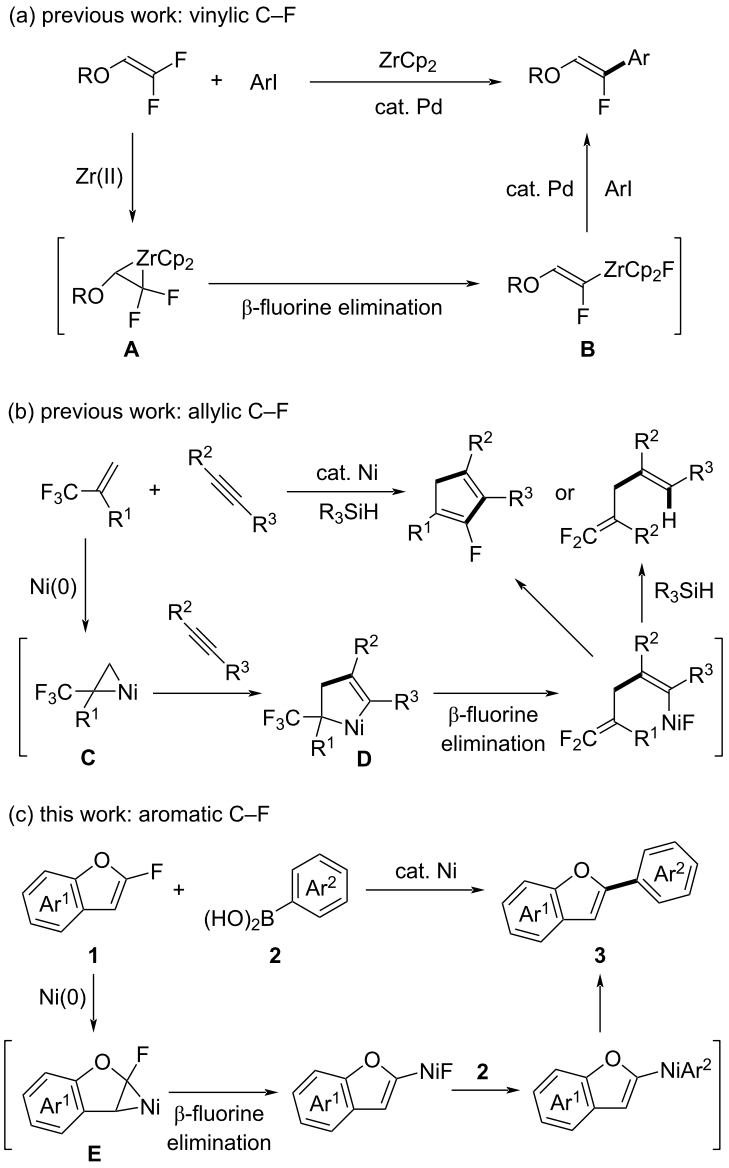

Scheme 1: C–F bond activation through β-fluorine elimination via metalacyclopropanes.

Results and Discussion

First, we explored optimal conditions for nickel-catalyzed defluorinative coupling using 2-fluoronaphtho[2,1-*b*]furan (**1b**) and *m*-tolylboronic acid (**2b**) as model substrates (Table 1). When **1b** was reacted with **2b** at 80 °C using $Ni(cod)_2$ (10 mol %) as a catalyst, PCy_3 (20 mol %) as a ligand, and K_2CO_3 (2.0 equiv) as a base, the desired arylated naphthofuran **3bb** was obtained in 75% yield (Table 1, entry 1). Reducing the reaction temperature improved the yield of **3bb**, reaching a quantitative yield when the reaction was performed at room temperature (Table 1, entry 3). Reducing the catalyst loading to 5 mol % slightly affected the yield of **3bb**, which was 90% (Table 1, entry 4). Next, we evaluated various additives with 5 mol % of $Ni(cod)_2$ to stabilize regenerated zero-valent nickel species (Table 1, entries 5–8). While phosphine ligands such as triphenyl phosphite were ineffective (Table 1, entry 5), the inclusion of chelating dienes improved the yield of **3bb** (Table 1, entries 6–8). Among these, 5 mol % of 1,5-cyclooctadiene (cod) proved to be the most effective additive, affording **3bb** in 95% yield (Table 1, entry 8). Additionally, by reducing the equivalents of **2b** to 1.0 equiv and K_2CO_3 to 1.2 equiv, we achieved the highest yield of 98% for **3bb** (Table 1, entry 9).

Under the optimized conditions, we investigated the substrate scope using 2-fluorobenzofurans **1** and arylboronic acids **2** (Scheme 2). The coupling reaction was efficient with 2-fluorobenzofuran (**1a**) when reacted with phenylboronic acid (**2a**) as well as arylboronic acids containing electron-donating groups, such as a methyl group at the 3-position (**2b**), two methyl groups at the 2- and 5-positions (**2c**), and a *tert*-butyl group at the 4-position (**2d**). The reaction with 3,5-dimethoxyphenylboronic acid (**2e**), which has electron-withdrawing groups on the aromatic ring, also yielded a satisfactory result of 73%. Additionally, using 2-fluoronaphtho[2,1-*b*]furan (**1b**), the reaction with phenylboronic acid (**2a**) and arylboronic acids with a methyl group at the 3-position (**2b**) or a *tert*-butyl group at the 4-position (**2d**) also produced high yields (94–98%). For arylboronic acid **2f**, which has a methoxy group at the 4-position, the use of potassium phosphate as a base resulted in a 94% yield of **3bf**. For arylboronic acid **2g**, which features a strongly electron-withdrawing trifluoromethyl group, we optimized the coupling reaction using potassium phosphate as a base and increasing the nickel catalyst loading to 20 mol %, achieving a yield of 78% for the desired product **3bg**. When 2-naphthylboronic acid (**2i**) was employed, its solubility was enhanced using a mixed solvent system of toluene, methanol, and water, which effectively promoted the reaction and resulted in a 70% yield of **3bi**. Furthermore, when methoxy- and ethoxy-substituted benzofurans **1c** and **1d** were used, the corresponding coupling products **3ca** and **3da** were obtained with yields of 67% and 65%, respectively.

Additionally, in the coupling reaction of 2-fluorobenzothiophene (**4**) with **2a**, increasing the amount of $Ni(cod)_2$ to

Table 1: Screening of conditions for coupling of **1b** with **2b**.

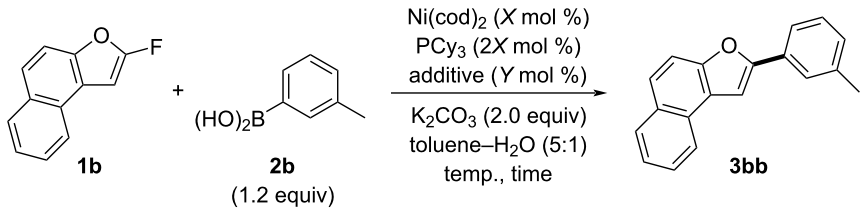

Entry	*X*	Additive	*Y*	Temp.	Time (h)	**3bb** (%)
1	10	–	–	80 °C	24	75[a]
2	10	–	–	40 °C	72	91[a]
3	10	–	–	rt	72	quant.[a]
4	5	–	–	rt	28	90[b]
5	5	$P(OPh)_3$	5	rt	58	12[b]
6	5	nbd[c]	5	rt	58	93[b]
7	5	chd[d]	5	rt	58	93[b]
8	5	cod[e]	5	rt	52	95[b]
9[f]	5	cod[e]	5	rt	14	98[b]

[a]Yield was determined by ^1H NMR spectroscopy using CH_2Br_2 as an internal standard. [b]Isolated yield. [c]nbd = 2,5-norbornadiene. [d]chd = 1,4-cyclohexadiene. [e]cod = 1,5-cyclooctadiene. [f]**2b** (1.0 equiv) and K_2CO_3 (1.2 equiv).

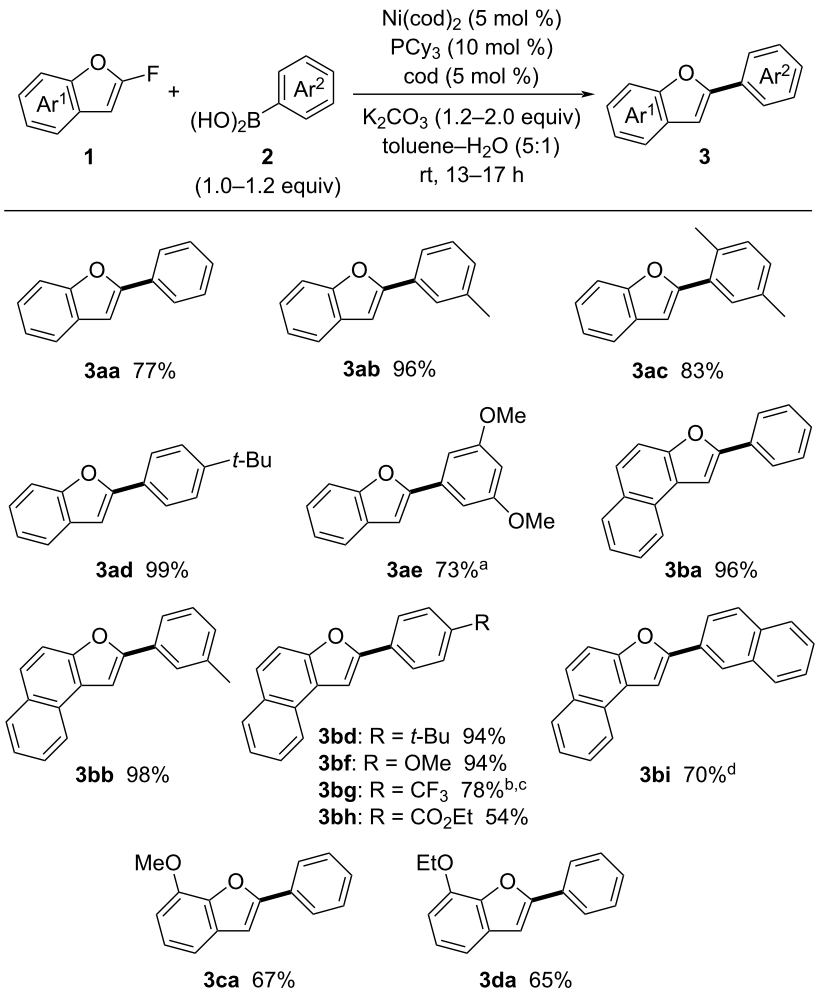

Scheme 2: Synthesis of 2-arylbenzofurans **3** via the coupling of **1** with **2**. Isolated yields are given. [a]$Ni(cod)_2$ (10 mol %), PCy_3 (20 mol %), and cod (10 mol %). [b]$Ni(cod)_2$ (20 mol %), PCy_3 (40 mol %), and cod (20 mol %). [c]K_3PO_4 (1.2 equiv) was used as a base. [d]Toluene–MeOH–H_2O (5:1:1) was used as a solvent.

20 mol % without adding extra cod yielded 48% of the desired product **5** (Scheme 3). This result indicates that the reaction is applicable to benzothiophenes as well as benzofurans.

Moreover, we successfully introduced two distinct aryl groups onto a benzofuran ring through orthogonal coupling reactions, exploiting the reactivity difference between C–F and C–Br bonds (Scheme 4). Using a palladium catalyst, 5-bromo-2-fluorobenzofuran (**1e**) was coupled with [4-(trifluoromethyl)phenyl]boronic acid (**2g**). In this reaction, only the C–Br bond was transformed while the C–F bond remained intact, yielding 2-fluoro-5-[4-(trifluoromethyl)phenyl]benzofuran (**1f**) in 95% yield. Subsequently, nickel-catalyzed defluorinative arylation of **1f** with phenylboronic acid (**2a**) efficiently produced 2-phenyl-5-[4-(trifluoromethyl)phenyl]benzofuran (**3fa**) in 81% yield.

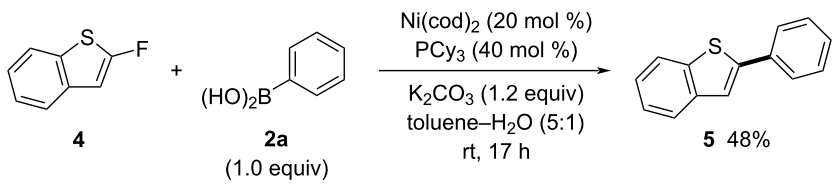

Scheme 3: Synthesis of 2-phenylbenzothiophene (**5**).

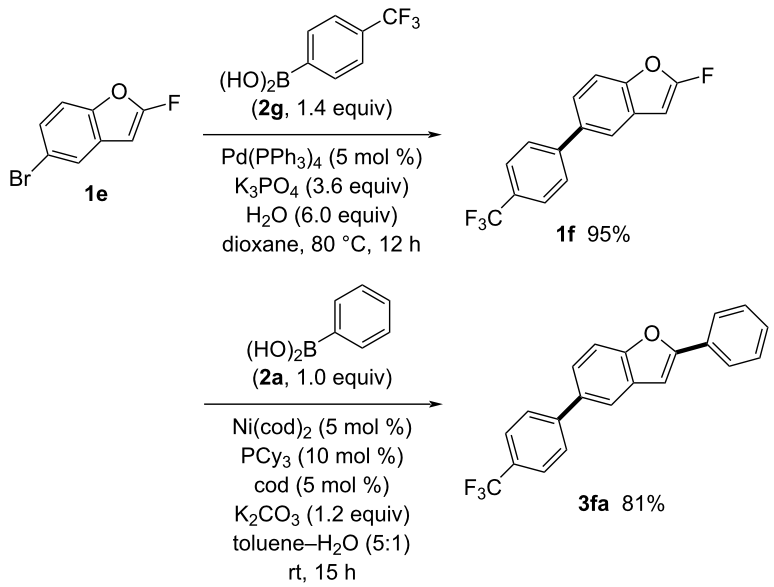

Scheme 4: Orthogonal approach to 2,5-diarylbenzofuran **3fa**.

Next, we explored the mechanism of the coupling reactions between 2-fluorobenzofurans **1** and arylboronic acids **2**. Because these reactions proceed under mild conditions despite involving aromatic C–F bond activation [19], direct oxidative addition of C–F bonds is unlikely (Scheme 5, path a). Instead, the reactions are thought to proceed through a formal oxidative addition involving nickelacyclopropane intermediates **E** [15-17,38,39], which are generated from 2-fluorobenzofurans **1** and zerovalent nickel species (Scheme 5). Following β-fluorine elimination, this results in a formal oxidative addition to form benzofuranylnickel(II) fluorides **F**, which then undergo transmetallation with arylboronic acids **2** to produce intermediates **G** (Scheme 5, path b). Alternatively, a direct transition from **E** to **G** via transition state **H** is also possible (Scheme 5, path c). Ultimately, reductive elimination from **G** yields the coupling products **3**.

The following experiments were performed to elucidate the mechanism. Under the same conditions as the coupling reaction, stoichiometric amounts of $Ni(cod)_2$, PCy_3, and cod were treated with fluoronaphthofuran **1b** at room temperature for 13 h, excluding boronic acid **2a** (Scheme 6). The reaction was monitored using ^{19}F and ^{31}P NMR spectroscopy. The ^{19}F NMR analysis showed that 79% of **1b** remained and revealed a new

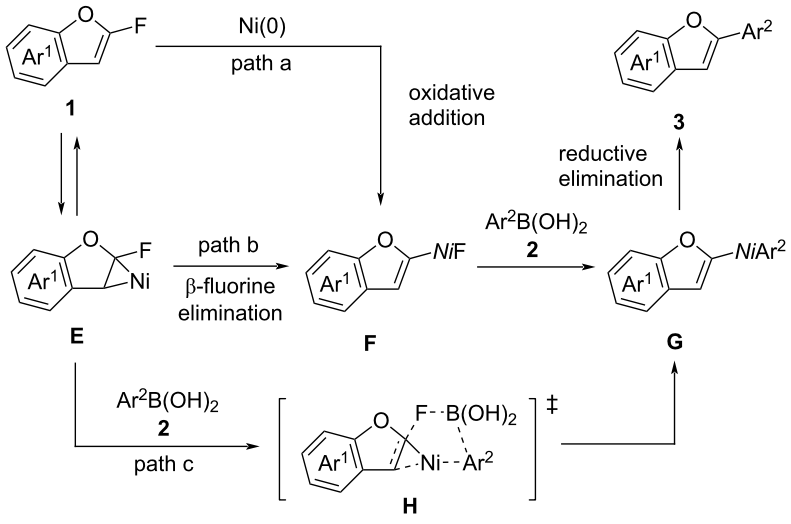

Scheme 5: Possible mechanisms.

broad double doublet peak at 55.0 ppm (J_{FP} = 53, 42 Hz) relative to internal C_6F_6 (δ = 0.0 ppm). The ^{31}P NMR spectrum depicted broad singlet peaks at 32.0–33.4 ppm and 38.6–40.5 ppm, appearing in a 1:1 ratio. These new peaks were attributed to nickelacyclopropane $\mathbf{E_b}$, which was formed in 19% yield. No peaks corresponding to benzofuranylnickel(II) fluoride $\mathbf{F_b}$, which would arise from the oxidative addition of **1b** to nickel(0), were detected [40]. High-resolution mass spectrometry (HRMS) analysis of the reaction mixture also supported the formation of $\mathbf{E_b}$ (calcd, 804.4474; found, 804.4449). Additionally, 79% of **1b** remained, while the catalytic reaction between **1b** and **2a** was completed in 13 h, yielding **3ba** in 96% (Scheme 2). These findings suggest that nickelacyclopropanes **E** and 2-fluorobenzofurans **1** are in equilibrium (see Scheme 5). Consequently, in the absence of arylboronic acids **2**, the consumption of **1** was suppressed. Upon adding phenylboronic acid (**2a**, 1.0 equiv) to the above reaction mixture, the coupling proceeded, producing **3ba** in 70% yield, with neither complex $\mathbf{E_b}$ nor $\mathbf{F_b}$ observed (Scheme 6). These results suggest that nickelacyclopropanes **E** are initially formed and facilitate a formal oxidative addition. Notably, the absence of **F** in the reaction mixture indicates that fluorine elimination and transmetallation occur simultaneously between **E** and the arylboronic acids **2**, leading to the formation of **G** (Scheme 5, path c). The intermediates **G** then undergo reductive elimination to yield **3**.

To assess the impact of halogen substituents, we also examined reactions of 2-halogenated benzofurans **1a-X** (**1a-Cl**: X = Cl; **1a-Br**: X = Br; **1a-I**: X = I) with (3-methylphenyl)boronic acid (**2b**) (Table 2). Both 2-chlorobenzofuran (**1a-Cl**) and 2-bromobenzofuran (**1a-Br**) hardly yielded **3ab** under the optimized conditions for **1a** (Table 2, entries 2 and 3), while the reaction of 2-iodobenzofuran (**1a-I**) resulted in a much lower yield (32%) of 2-arylbenzofuran **3ab** (Table 2, entry 4) compared to that of **1a** (X = F, quant.). The strong interaction between fluorine and boron in **H** likely facilitates β-fluorine elimi-

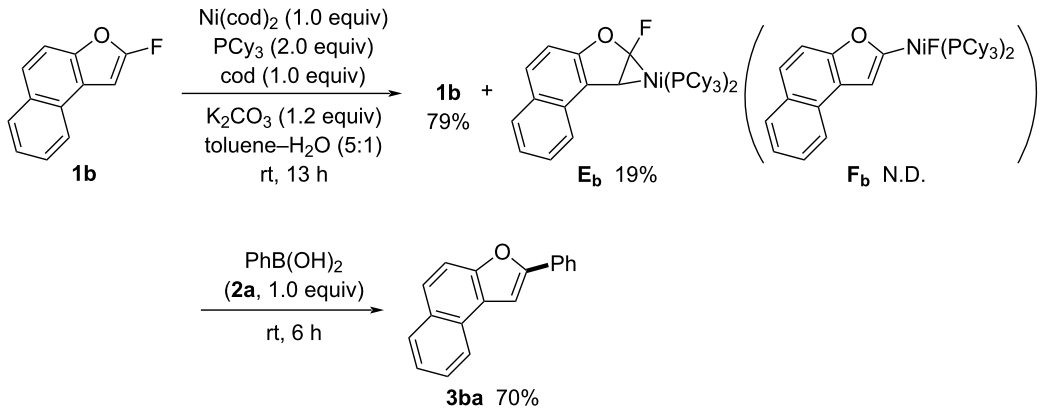

Scheme 6: Formation of nickelacyclopropane $\mathbf{E_b}$ in a stoichiometric reaction.

Table 2: Effect of halogen substituents.

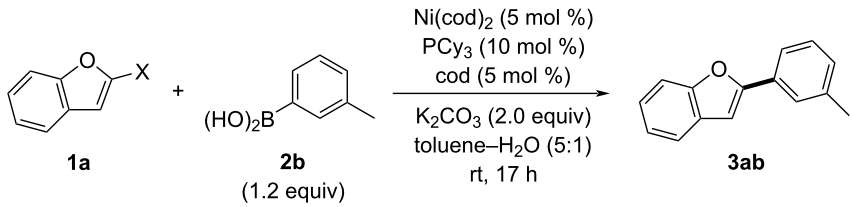

Entry	1a-X	X	3ab (%)[a]
1	**1a**	F	quant.
2	**1a-Cl**	Cl	trace
3	**1a-Br**	Br	1
4	**1a-I**	I	32

[a]Yield was determined by ^1H NMR spectroscopy using CH_2Br_2 as an internal standard.

nation and transmetallation. Thus, the considerably different result observed with **1a** is attributed to the distinct mechanistic aspects of the metalacyclopropanation/β-fluorine elimination sequence influenced by the fluorine substituent.

Conclusion

In summary, we have presented a nickel-catalyzed method for synthesizing 2-arylbenzofurans through aromatic C–F bond activation, with the formation of metallacyclopropanes as an essential step. This protocol allows for the late-stage transformation of C–F bonds, as demonstrated by the orthogonal activation of both aromatic C–F and C–Br bonds, thereby facilitating the synthesis of complex 2-arylbenzofurans. Given that natural and synthetic 2-arylbenzofurans often exhibit considerable biological activities and are important in pharmaceuticals and agrochemicals [41-47], we expect that this method will provide a novel and efficient approach for producing these valuable compounds.

Experimental

General: ^{1}H NMR, ^{13}C NMR, ^{19}F NMR, and ^{31}P NMR were recorded on a Bruker Avance 500 or a JEOL ECS-400 spectrometer. Chemical shift values are given in ppm relative to internal Me_4Si (for ^{1}H NMR: δ = 0.00 ppm), $CDCl_3$ (for ^{13}C NMR: δ = 77.0 ppm), C_6F_6 (for ^{19}F NMR: δ = 0.0 ppm), and H_3PO_4 (for ^{31}P NMR: δ = 0.0 ppm). IR spectra were recorded on a Horiba FT-730 spectrometer. Mass spectra were measured on a JEOL JMS-T100GCV or a JEOL JMS-T200GC spectrometer. All the reactions were conducted under argon or nitrogen.

Materials: Column chromatography was conducted on silica gel (Silica Gel 60 N, Kanto Chemical Co., Inc.). Toluene and *N*,*N*-dimethylformamide (DMF) were purified by a solvent-purification system (GlassContour) equipped with columns of activated alumina and supported-copper catalyst (Q-5) before use. 1,4-Dioxane and methanol were distilled from sodium, and stored over 4 Å molecular sieves. Unless otherwise noted, materials were obtained from commercial sources and used directly without further purifications.

Typical procedure for coupling of 2-fluorobenzofurans 1 with arylboronic acids 2: To the mixture of 2-fluoronaphtho[2,1-*b*]furan (**1b**, 56 mg, 0.30 mmol), (3-methylphenyl)boronic acid (**2b**, 41 mg, 0.30 mmol), $Ni(cod)_2$ (4.2 mg, 0.015 mmol), PCy_3 (8.2 mg, 0.029 mmol), 1,5-cyclooctadiene (1.8 μL, 0.015 mmol), and K_2CO_3 (50 mg, 0.36 mmol) were added toluene (3.0 mL) and H_2O (0.6 mL). After stirring at room temperature for 13 h, the reaction mixture was diluted with H_2O. Organic materials were extracted with diethyl ether three times. The combined extracts were washed with brine and dried over Na_2SO_4. After removal of the solvent under reduced pressure, the residue was purified by silica gel column chromatography (hexane/EtOAc = 10:1) to give **3bb** (76 mg, 98%) as a white solid. ^{1}H NMR (500 MHz, $CDCl_3$) δ 8.15 (d, *J* = 8.2 Hz, 1H), 7.93 (d, *J* = 8.2 Hz, 1H), 7.75–7.67 (m, 4H), 7.58 (ddd, *J* = 8.2, 6.9, 1.2 Hz, 1H), 7.49–7.46 (m, 2H), 7.35 (dd, *J* = 7.7, 7.6 Hz, 1H), 7.16 (d, *J* = 7.6 Hz, 1H), 2.44 (s, 3H); ^{13}C NMR (126 MHz, $CDCl_3$) δ 155.6, 152.3, 138.5, 130.5, 130.4, 129.1, 128.8, 128.7, 127.6, 126.2, 125.3, 125.1, 124.6, 124.5, 123.4, 121.9, 112.3, 100.3, 21.5; IR (KBr): 3051, 1606, 1487, 1387, 1280, 1255, 1163, 1053, 991, 935, 789, 690 cm^{-1}; HREIMS *m*/*z*: $[M]^+$ calcd for $C_{19}H_{14}O$, 258.1045; found, 258.1035.

Supporting Information

Supporting Information File 1

Detailed experimental procedures and spectral data.
[https://www.beilstein-journals.org/bjoc/content/supplementary/1860-5397-21-8-S1.pdf]

Acknowledgements

This work was partially performed using facilities of the Institute for Solid State Physics, the University of Tokyo (^{1}H, ^{13}C, and ^{19}F NMR spectrometer, mass spectroscopy system, and IR spectroscopy system in Mori Laboratory).

Funding

This work was financially supported by JSPS KAKENHI Grant Number JP21K05066 in Grant-in-Aid for Scientific Research (C) (T.F.) and JSPS KAKENHI Grant Number JP22H02071 in Grant-in-Aid for Scientific Research (B) (J.I.).

ORCID® iDs

Takeshi Fujita - https://orcid.org/0000-0001-9666-022X
Kohei Fuchibe - https://orcid.org/0000-0002-6759-7003
Junji Ichikawa - https://orcid.org/0000-0001-6498-326X

Data Availability Statement

All data that supports the findings of this study is available in the published article and/or the supporting information of this article.

Preprint

A non-peer-reviewed version of this article has been previously published as a preprint: https://doi.org/10.3762/bxiv.2024.63.v1

References

1. Amii, H.; Uneyama, K. *Chem. Rev.* **2009,** *109,* 2119–2183. doi:10.1021/cr800388c

2. Sun, A. D.; Love, J. A. *Dalton Trans.* **2010,** *39,* 10362–10374. doi:10.1039/c0dt00540a
3. Ahrens, T.; Kohlmann, J.; Ahrens, M.; Braun, T. *Chem. Rev.* **2015,** *115,* 931–972. doi:10.1021/cr500257c
4. Chen, W.; Bakewell, C.; Crimmin, M. R. *Synthesis* **2017,** *49,* 810–821. doi:10.1055/s-0036-1588663
5. Wang, M.; Shi, Z. *Chem. Rev.* **2020,** *120,* 7348–7398. doi:10.1021/acs.chemrev.9b00384
6. Zhao, B.; Rogge, T.; Ackermann, L.; Shi, Z. *Chem. Soc. Rev.* **2021,** *50,* 8903–8953. doi:10.1039/c9cs00571d
7. Zhang, J.; Geng, S.; Feng, Z. *Chem. Commun.* **2021,** *57,* 11922–11934. doi:10.1039/d1cc04729a
8. Fujiwara, M.; Ichikawa, J.; Okauchi, T.; Minami, T. *Tetrahedron Lett.* **1999,** *40,* 7261–7265. doi:10.1016/s0040-4039(99)01491-4
9. Sakoda, K.; Mihara, J.; Ichikawa, J. *Chem. Commun.* **2005,** 4684–4686. doi:10.1039/b510039a
10. Fuchibe, K.; Morikawa, T.; Shigeno, K.; Fujita, T.; Ichikawa, J. *Org. Lett.* **2015,** *17,* 1126–1129. doi:10.1021/ol503759d
11. Fujita, T.; Watabe, Y.; Yamashita, S.; Tanabe, H.; Nojima, T.; Ichikawa, J. *Chem. Lett.* **2016,** *45,* 964–966. doi:10.1246/cl.160427
12. Watabe, Y.; Kanazawa, K.; Fujita, T.; Ichikawa, J. *Synthesis* **2017,** *49,* 3569–3575. doi:10.1055/s-0036-1588842
13. Fujita, T.; Takeishi, M.; Ichikawa, J. *Org. Lett.* **2020,** *22,* 9253–9257. doi:10.1021/acs.orglett.0c03476
14. Ichikawa, J.; Nadano, R.; Ito, N. *Chem. Commun.* **2006,** 4425–4427. doi:10.1039/b610690k
15. Ichitsuka, T.; Fujita, T.; Arita, T.; Ichikawa, J. *Angew. Chem., Int. Ed.* **2014,** *53,* 7564–7568. doi:10.1002/anie.201402695
16. Ichitsuka, T.; Fujita, T.; Ichikawa, J. *ACS Catal.* **2015,** *5,* 5947–5950. doi:10.1021/acscatal.5b01463
17. Fujita, T.; Arita, T.; Ichitsuka, T.; Ichikawa, J. *Dalton Trans.* **2015,** *44,* 19460–19463. doi:10.1039/c5dt02160j
18. Fujita, T.; Kobayashi, Y.; Takahashi, I.; Morioka, R.; Ichitsuka, T.; Ichikawa, J. *Chem. – Eur. J.* **2022,** *28,* e202103643. doi:10.1002/chem.202103643
19. Li, Y. *Monatsh. Chem.* **2022,** *153,* 193–199. doi:10.1007/s00706-021-02881-w
20. Ichikawa, J.; Wada, Y.; Okauchi, T.; Minami, T. *Chem. Commun.* **1997,** 1537–1538. doi:10.1039/a703110f
21. Morioka, R.; Fujita, T.; Ichikawa, J. *Helv. Chim. Acta* **2020,** *103,* e2000159. doi:10.1002/hlca.202000159
22. Tamao, K.; Sumitani, K.; Kiso, Y.; Zembayashi, M.; Fujioka, A.; Kodama, S.-i.; Nakajima, I.; Minato, A.; Kumada, M. *Bull. Chem. Soc. Jpn.* **1976,** *49,* 1958–1969. doi:10.1246/bcsj.49.1958
23. Mongin, F.; Mojovic, L.; Guillamet, B.; Trécourt, F.; Quéguiner, G. *J. Org. Chem.* **2002,** *67,* 8991–8994. doi:10.1021/jo026136s
24. Böhm, V. P. W.; Gstöttmayr, C. W. K.; Weskamp, T.; Herrmann, W. A. *Angew. Chem., Int. Ed.* **2001,** *40,* 3387–3389. doi:10.1002/1521-3773(20010917)40:18<3387::aid-anie3387>3.0.co;2-6
25. Dankwardt, J. W. *J. Organomet. Chem.* **2005,** *690,* 932–938. doi:10.1016/j.jorganchem.2004.10.037
26. Yoshikai, N.; Mashima, H.; Nakamura, E. *J. Am. Chem. Soc.* **2005,** *127,* 17978–17979. doi:10.1021/ja056327n
27. Lu, Y.; Plocher, E.; Hu, Q.-S. *Adv. Synth. Catal.* **2006,** *348,* 841–845. doi:10.1002/adsc.200606002
28. Schaub, T.; Backes, M.; Radius, U. *J. Am. Chem. Soc.* **2006,** *128,* 15964–15965. doi:10.1021/ja064068b
29. Ackermann, L.; Wechsler, C.; Kapdi, A. R.; Althammer, A. *Synlett* **2010,** 294–298. doi:10.1055/s-0029-1219166
30. Xie, L.-G.; Wang, Z.-X. *Chem. – Eur. J.* **2010,** *16,* 10332–10336. doi:10.1002/chem.201001022
31. Sun, A. D.; Love, J. A. *Org. Lett.* **2011,** *13,* 2750–2753. doi:10.1021/ol200860t
32. Tobisu, M.; Xu, T.; Shimasaki, T.; Chatani, N. *J. Am. Chem. Soc.* **2011,** *133,* 19505–19511. doi:10.1021/ja207759e
33. Zhang, J.; Xu, J.; Xu, Y.; Sun, H.; Shen, Q.; Zhang, Y. *Organometallics* **2015,** *34,* 5792–5800. doi:10.1021/acs.organomet.5b00874
34. Malineni, J.; Jezorek, R. L.; Zhang, N.; Percec, V. *Synthesis* **2016,** *48,* 2795–2807. doi:10.1055/s-0035-1562342
35. Ogawa, H.; Yang, Z.-K.; Minami, H.; Kojima, K.; Saito, T.; Wang, C.; Uchiyama, M. *ACS Catal.* **2017,** *7,* 3988–3994. doi:10.1021/acscatal.7b01058
36. Kurisu, N.; Asano, E.; Hatayama, Y.; Kurihara, Y.; Hashimoto, T.; Funatsu, K.; Ueda, K.; Yamaguchi, Y. *Eur. J. Inorg. Chem.* **2019,** 126–133. doi:10.1002/ejic.201801179
37. Jacobs, E.; Keaveney, S. T. *ChemCatChem* **2021,** *13,* 637–645. doi:10.1002/cctc.202001462
38. Zhang, X.; Huang, X.; Chen, Y.; Chen, B.; Ma, Y. *Org. Lett.* **2023,** *25,* 1748–1753. doi:10.1021/acs.orglett.3c00444
39. Yang, P.; Yu, H.; Zhai, R.; Zhou, J. S.; Tang, B. *Chem. Commun.* **2024,** *60,* 6548–6551. doi:10.1039/d4cc00918e
40. Johnson, S. A.; Huff, C. W.; Mustafa, F.; Saliba, M. *J. Am. Chem. Soc.* **2008,** *130,* 17278–17280. doi:10.1021/ja8081395
41. Shi, Y.-Q.; Fukai, T.; Sakagami, H.; Chang, W.-J.; Yang, P.-Q.; Wang, F.-P.; Nomura, T. *J. Nat. Prod.* **2001,** *64,* 181–188. doi:10.1021/np000317c
42. Ni, G.; Zhang, Q.-J.; Zheng, Z.-F.; Chen, R.-Y.; Yu, D.-Q. *J. Nat. Prod.* **2009,** *72,* 966–968. doi:10.1021/np800789y
43. Tan, Y.-X.; Yang, Y.; Zhang, T.; Chen, R.-Y.; Yu, D.-Q. *Fitoterapia* **2010,** *81,* 742–746. doi:10.1016/j.fitote.2010.03.017
44. Artini, M.; Papa, R.; Barbato, G.; Scoarughi, G. L.; Cellini, A.; Morazzoni, P.; Bombardelli, E.; Selan, L. *Bioorg. Med. Chem.* **2012,** *20,* 920–926. doi:10.1016/j.bmc.2011.11.052
45. Morelli, L.; Bernardi, A.; Sattin, S. *Carbohydr. Res.* **2014,** *390,* 33–41. doi:10.1016/j.carres.2014.03.006
46. Tjahjandarie, T. S.; Tanjung, M.; Saputri, R. D.; Rahayu, D. O.; Gunawan, A. N. I.; Aldin, M. F. *Nat. Prod. Res.* **2021,** *35,* 5637–5642. doi:10.1080/14786419.2020.1821016
47. Heravi, M. M.; Zadsirjan, V.; Hamidi, H.; Tabar Amiri, P. H. *RSC Adv.* **2017,** *7,* 24470–24521. doi:10.1039/c7ra03551a
And references cited therein.

License and Terms

BEILSTEIN JOURNAL OF ORGANIC CHEMISTRY

Quantifying the ability of the CF_2H group as a hydrogen bond donor

Matthew E. Paolella[1], Daniel S. Honeycutt[1], Bradley M. Lipka[1], Jacob M. Goldberg[*2] and Fang Wang[*1]

Full Research Paper

Open Access

Address:
[1]Department of Chemistry, University of Rhode Island, 140 Flagg Rd, Kingston, RI 02881, USA and [2]Department of Chemistry, Colgate University, 13 Oak Drive, Hamilton, NY 13346, USA

Email:
Jacob M. Goldberg[*] - jgoldberg@colgate.edu; Fang Wang[*] - fangwang@uri.edu

* Corresponding author

Keywords:
bioisostere; difluoromethyl (CF_2H); fluorine; hydrogen bond donors; hydrogen bond strength

Beilstein J. Org. Chem. **2025,** *21,* 189–199.
https://doi.org/10.3762/bjoc.21.11

Received: 01 November 2024
Accepted: 09 January 2025
Published: 20 January 2025

This article is part of the thematic issue "Organofluorine chemistry VI".

Guest Editor: D. O'Hagan

Abstract

The CF_2H group can act as a hydrogen bond donor, serving as a potential surrogate for OH or SH groups but with a weaker hydrogen bond donation ability. Here, we describe a series of CF_2H group-containing moieties that facilitate hydrogen bond interactions. We survey hydrogen bond donation ability using several established methods, including ^{1}H NMR-based hydrogen bond acidity determination, UV–vis spectroscopy titration with Reichardt's dye, and ^{1}H NMR titration using tri-*n*-butylphosphine oxide as a hydrogen bond acceptor. Our experiments reveal that the direct attachment of the CF_2H group to cationic aromatic systems significantly enhances its hydrogen bond donation ability, a result consistent with theoretical calculations. We anticipate that this chemistry will be valuable for designing functional molecules for chemical biology and medicinal chemistry applications.

Introduction

Hydrogen bonding interactions are ubiquitous non-covalent forces in chemistry and biology [1-4]. In canonical hydrogen bond (HB) donor–acceptor pairs, the donor typically comprises an electronegative heteroatom, such as oxygen, nitrogen, or sulfur, and a positively charged hydrogen atom, which interacts with a lone pair on the acceptor. Apart from these common heteroatom-containing hydrogen bond donors, certain carbon–hydrogen moieties can also act in this way, although in a substantially weaker capacity [5-14]. Of particular interest is the difluoromethyl group, CF_2H, which exhibits hydrogen bond donating character due to the highly polarized F_2C–H bond (Figure 1) [14-24]. This functional group is often used to mimic hydroxy or thiol groups but exhibits slower acid dissociation [25] and different lipophilicity [19,20,26-28]. For these reasons, it is an attractive synthetic target [29-43] and an important bioisostere in drug design and biochemical studies [30,44-46]. Despite the value of these applications, few experimental studies have been conducted to quantify the thermodynamics of

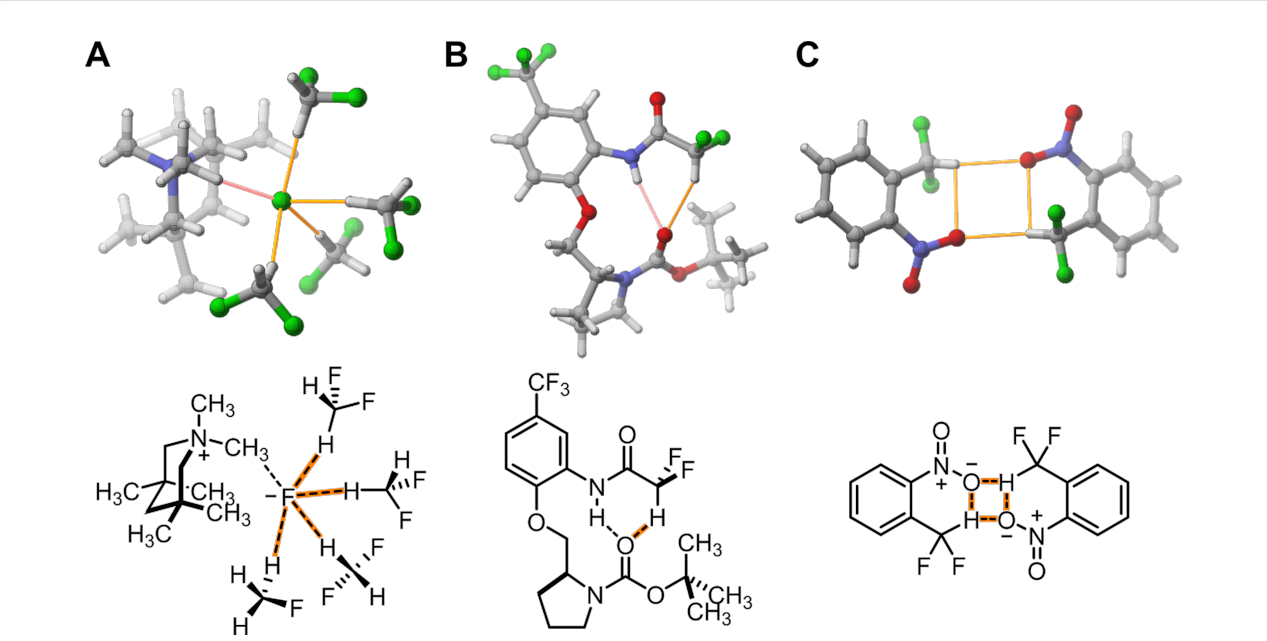

Figure 1: Examples of solid state structures exhibiting CF_2H group-mediated hydrogen bond interactions [16,18,21]. Hydrogen bonding interactions involving the CF_2H group are highlighted in orange.

CF_2H group-mediated hydrogen bond interactions [19,20]. Here, we present a series of CF_2H-containing constructs and a detailed assessment of the corresponding hydrogen bond donation energetics. We expect this information to be useful for the rational application of the CF_2H group in drug development and molecular design.

Previous quantum mechanical calculations revealed that the $CF_2H\cdots O$ binding energy (ΔE) ranges from 1.0 kcal/mol to 5.5 kcal/mol [14,15,18,21]. In addition, as measured by hydrogen bond acidity [47,48] which is derived from the ^1H NMR chemical shift difference of a given proton in DMSO-d_6 and $CDCl_3$, the CF_2H group is generally a stronger donor than the methyl group but substantially weaker than the OH or amide NH groups [19,20]. These results collectively indicate that, although the CF_2H group mimics hydroxy or thiol groups, it is a generally less effective hydrogen bond donor. Given that the HB donation ability of a particular functional group usually increases with increasing Brønsted acidity [49] we chose to incorporate the CF_2H group into the backbone of *N*-methylpyridinium cations and related analogs (Figure 2). We anticipated that such cationic constructs would enhance the Brønsted acidity of the CF_2–H bond by stabilizing the conjugate base of the CF_2H group, in turn, increasing the hydrogen bond donation ability. Additionally, to minimize the effects of counterions, such as the bromide and fluoride anions [50], on HB interactions, all ionic compounds were synthesized with tetrafluoroborate, a classical weakly coordinating anion.

Results and Discussion

We first assessed the hydrogen bond acidity, *A*, of these CF_2H-containing compounds using an established method [19,20,47,48]. This convenient approach relies on comparing the ^1H NMR chemical shift of a hydrogen bond donor in DMSO-d_6 to that of it in $CDCl_3$. The HB donor presumably interacts strongly with hydrogen-accepting DMSO [51], but barely with $CDCl_3$, which has a weak hydrogen bond acceptance ability [51], so the magnitude of the solvent-induced chemical shift difference, $\Delta\delta_{DMSO-CDCl3} = \delta_{DMSO} - \delta_{CDCl3}$ should positively correlate with the HB donation ability. Accordingly, the *A* value can be defined as $A = 0.0065 + 0.133\Delta\delta_{DMSO-CDCl3}$. We determined the $\Delta\delta_{DMSO-CDCl3}$ values for a series of hydrogen bond donors. Our experiment with neutral HB donors reproduced literature results (Table 1, compounds **10**, **11**, and **12**) [20,22,47] and revealed an expected trend in HB donation ability; for example, compound **1a** is a weaker HB donor than **3a**. However, due to limited solubility, the ^1H NMR spectroscopic studies of organic salts in $CDCl_3$, including **1b** and **3b**, did not produce observable signals. To solubilize the salts better, we substituted deuterated nitromethane (CD_3NO_2) for $CDCl_3$. Because of the nearly identical hydrogen donation and acceptance abilities of nitromethane ($\alpha = 0.22$ and $\beta = 0.06$, respectively) and chloroform ($\alpha = 0.20$ and $\beta = 0.10$) [51], $\Delta\delta_{DMSO-CD3NO2}$ and $\Delta\delta_{DMSO-CDCl3}$ should follow a similar trend. Our ^1H NMR experiments showed a strong linear correlation between $\Delta\delta_{DMSO-CD3NO2}$ and $\Delta\delta_{DMSO-CDCl3}$ for neutral HB donors ($R^2 = 0.985$, Figure S15

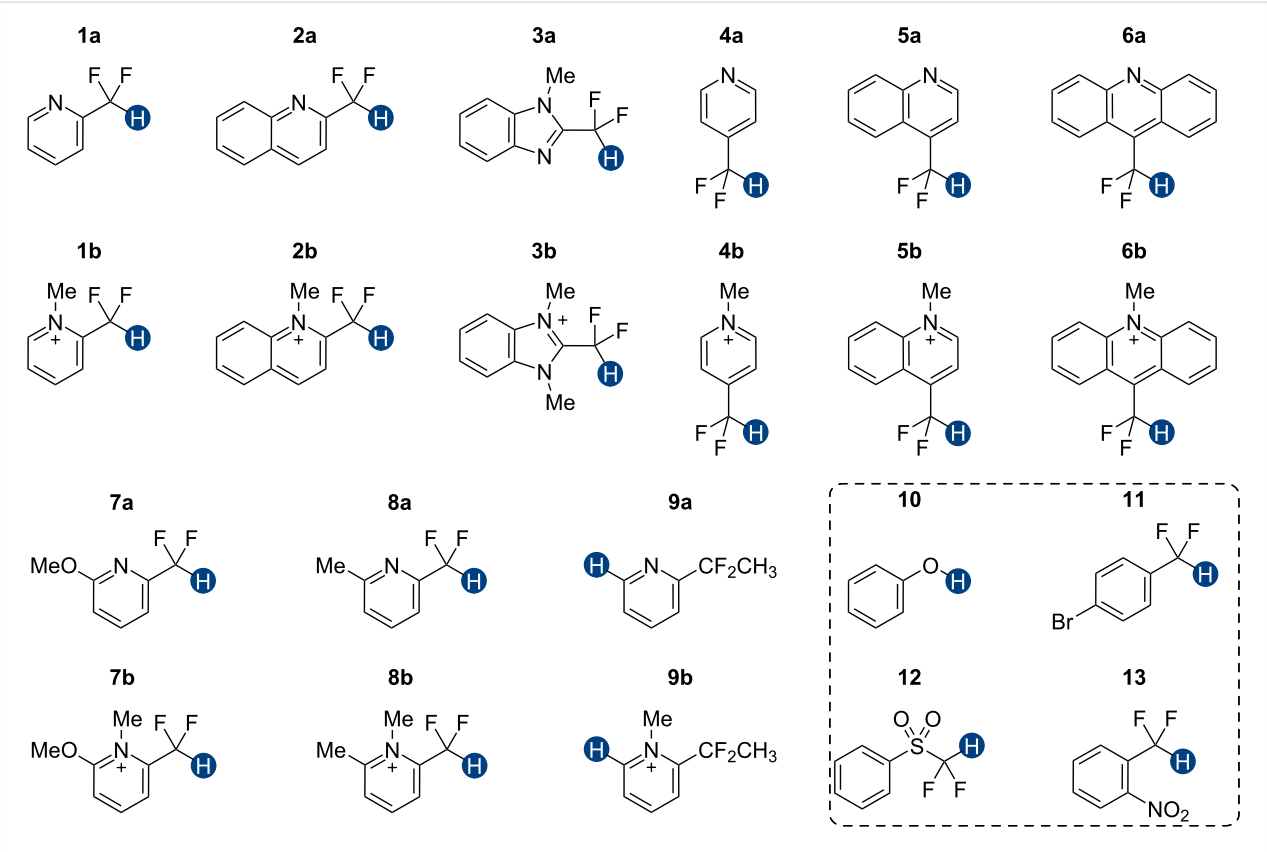

Figure 2: Hydrogen bond donors investigated in this study. For all cationic species, the counteranion is BF_4^-. The reference HB donors are in the dashed line box.

Table 1: Summary of $\Delta\delta_{DMSO-CDCl3}$, $\Delta\delta_{DMSO-CD3NO2}$, and *A* values of select HB donors.[a]

		$\Delta\delta_{DMSO-CDCl3}$ (ppm)	*A*	$\Delta\delta_{DMSO-MeNO2}$ (ppm)
1a	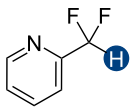	0.31	0.047	0.26
1b	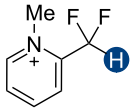	–	–	0.32
2a	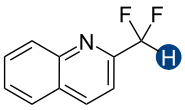	0.31	0.048	–
3a	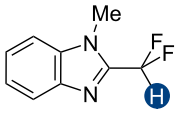	0.47	0.069	0.39
3b	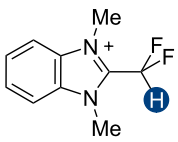	–	–	0.37

Table 1: Summary of $\Delta\delta_{DMSO-CDCl3}$, $\Delta\delta_{DMSO-CD3NO2}$, and *A* values of select HB donors.[a] (continued)

4a	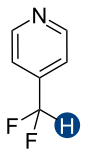	0.30	0.046	–
4b	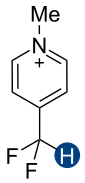	–	–	0.27
5a	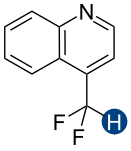	0.53	0.077	–
6a	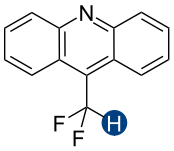	0.54	0.078	0.35
10	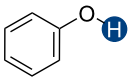	4.66 (4.69)[b]	0.63 (0.63)[b]	3.90
11	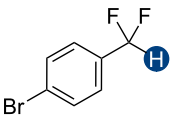	0.44 (0.43)[b]	0.065 (0.064)[b]	0.29
12	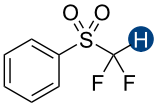	1.13	0.16 (0.16)[b]	0.84
13	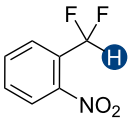	0.08	0.017	0.09

[a]For all cationic species, the counteranion is BF_4^-. [b]Literature values are shown in parentheses.

in Supporting Information File 1), confirming that CD_3NO_2 can be used to determine HB acidity (Table 1 and Figures S1–S13 in Supporting Information File 1). Based on the $\Delta\delta_{DMSO-CD3NO2}$ values, we can rank the relative HB donation ability of the CF_2H-containing salts as **3b** > **1b** > **4b**, a result consistent with the expected Brønsted acidity. Even so, the $\Delta\delta_{DMSO-CD3NO2}$ values of *N*-methylated CF_2H-containing organic salts are generally smaller than those of the corresponding neutral precursors. This observation contradicts our initial prediction that introducing a quaternary nitrogen would enhance the HB donation ability of the CF_2H group. It is also at odds with the experimental and theoretical results described below. We tentatively attributed the discrepancies to the involvement of other possible solute–solvent interactions, such as solute dipolarity, polarizability, and dispersion [47]. Ostensibly, these interactions can vary significantly as the charge of the solute changes, complicating the Δδ-based direct assessment of HB acidity.

To quantify the HB donation ability of both neutral and cationic species on a single scale, we chose an alternative strategy based on an established UV–vis spectroscopy titration method [52] with Reichardt's dye [53-55] as an indicator. These experiments measure the blue shift of Reichardt's dye upon complexation

with an HB donor (Figure 3A, and Figures S13–S18 in Supporting Information File 1), from which the dissociation constant (K_d) of the HB complex can be determined. A smaller K_d value corresponds to a more stable complex, indicating a stronger HB donor. We employed this protocol to investigate a series of HB donors in anhydrous acetonitrile (Figure 3B). Acetonitrile is weakly HB accepting ($\alpha = 0.19$) [51] and was thus chosen to attenuate the competition between the solvent and the dye with the HB donor. As shown in Figure 3B, in our hands, the K_d of the phenol–Reichardt's dye HB adduct determined is consistent with the reported value [52]. Some of our other results, however, were puzzling. For example, according to our titration data, **1a** is a better HB donor than **12**. This observation is inconsistent with the corresponding *A* values (Table 1), which typically provide reliable measurements of the HB donation ability of neutral compounds. We attribute the inconsistency to several factors. First, because the binding affinity is determined solely by the absorbance change of Reichardt's dye, the apparent K_d value only represents the overall ability of a compound to serve as an HB donor. For compounds bearing multiple HB donating sites, such as **1b**, the HB interactions involving individual functional groups cannot be quantified separately, leading to potentially ambiguous results (Figure 3C). Reports in the literature show that the UV–vis absorption of the Lewis basic Reichardt's dye disappears in the presence of some cationic HB donors [52]. We found similar results with **3b** and likewise ascribe the unexpectedly small K_d to such limitations of this assay (Figure 3C and Figure S19 in Supporting Information File 1). Overall, despite the convenience, this UV–vis titration method may not be broadly applicable for quantifying the HB donation ability of some CF_2H group-containing substrates.

To quantify better the thermodynamics of CF_2H group-mediated hydrogen bond interactions, we investigated the HB donation ability of the CF_2H group by ^1H NMR titration with tri-*n*-butylphosphine oxide (*n*-Bu_3PO) as a reference HB acceptor (Figure 4A and Figures S20–S40 in Supporting Information File 1). Unlike a previous method that relied on ^{31}P NMR spectroscopy [52], our titration monitors the HB complex formation by ^1H NMR chemical shift change, thereby allowing the interactions of individual HB donating moieties with *n*-Bu_3PO to be probed (Figure 4B and C). Moreover, we used anhydrous deuterated acetonitrile (CD_3CN) as the solvent, in which both neutral and ionic compounds exhibited appreciable solubility. In this way, we were able to determine the HB donation ability of CF_2H-containing compounds on a single scale.

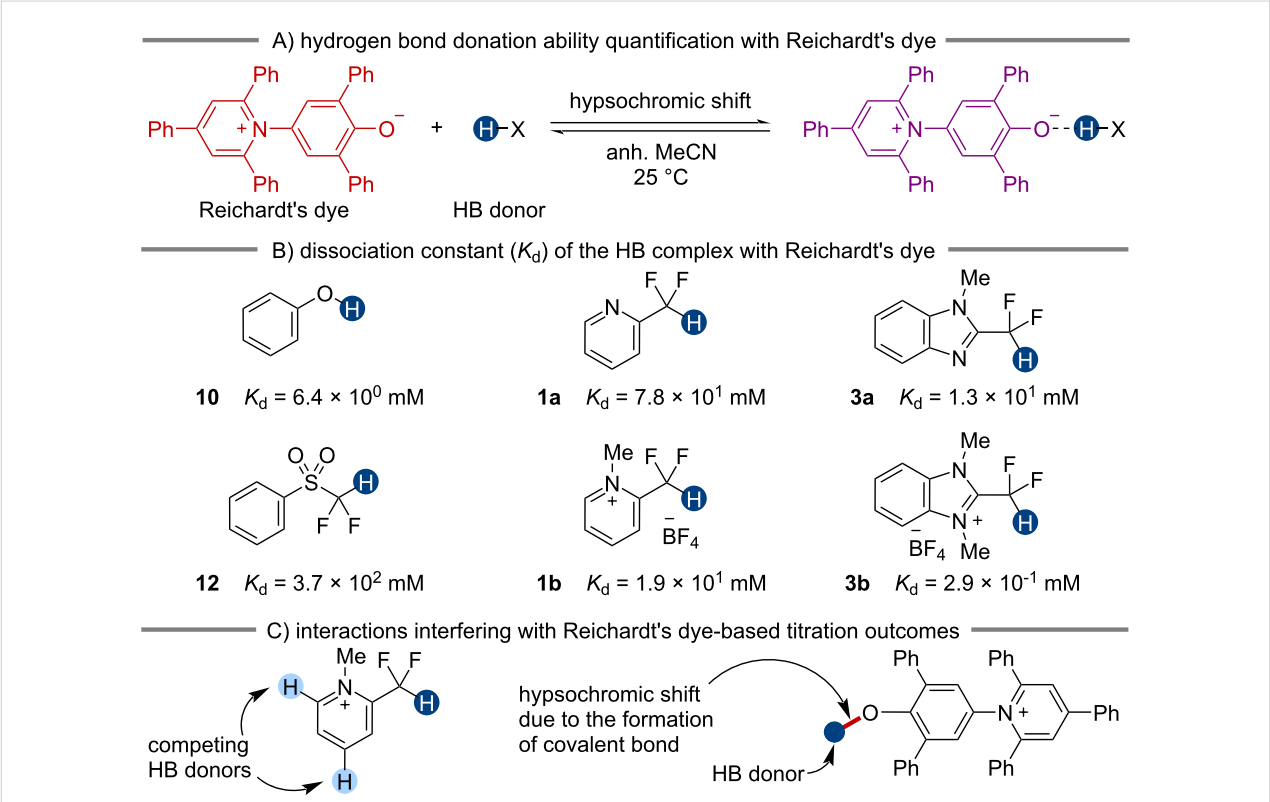

Figure 3: Hydrogen bond donation ability determined by UV–vis spectroscopy titration. A) Formation of HB complexes of Reichardt's dye and HB donors. B) K_d values of Reichardt's dye–hydrogen bond donor complexes. For all cationic species, the counteranion is BF_4^-. C) Possible interactions that interfere with the titration outcomes.

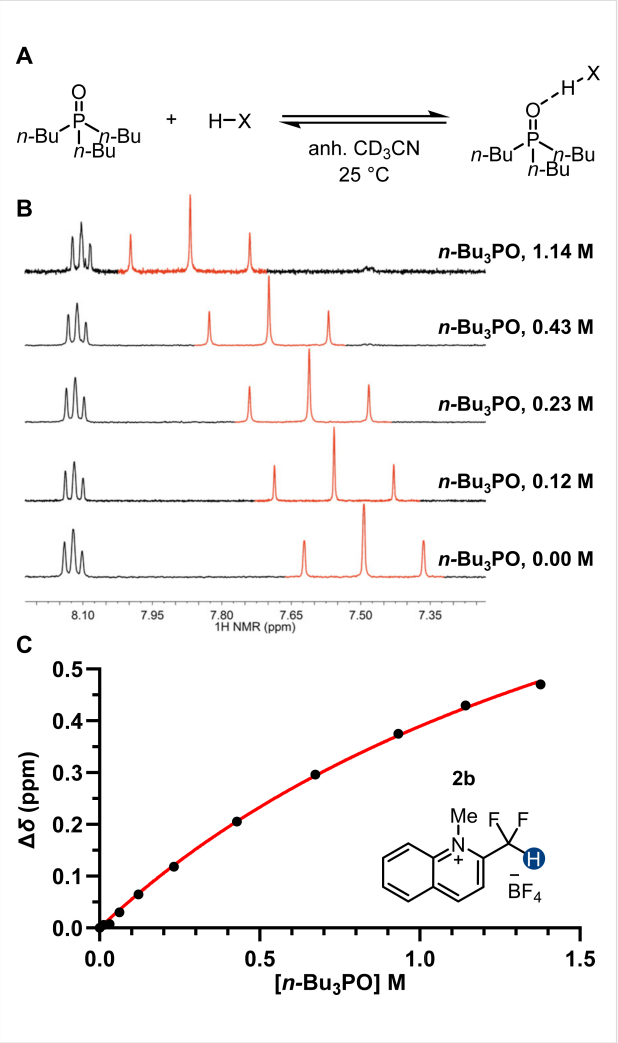

Figure 4: A) HB complex formation between a donor and tri-*n*-butylphosphine oxide. B) ^{1}H NMR spectra of **2b** (5.0 mM) in the presence of different concentrations of tri-*n*-butylphosphine oxide in anhydrous CD_3CN at 298 K. The ^{1}H NMR signals of the CF_2H group are indicated in red. C) Determination of the dissociation constant (K_d) of the *n*-Bu_3PO···**2b** HB complex by fitting the data to a single-site binding model.

As shown in Figure 5, we determined dissociation constants (K_d) of *n*-Bu_3PO···HB donor complexes, revealing several general trends. First, we found that CF_2H groups attached to an extended aromatic system are stronger HB donors (**2a** > **1a**, **2b** > **1b**, and **6a** > **5a** > **4a**), likely due to the increased Brønsted acidity of the CF_2–H bond. Similarly, cationic donors generally exhibited substantially higher HB donation ability than the neutral precursors, as indicated by ten to thirty-fold decreases in K_d values (Figure 5, **1**–**4**). These two enhancing effects are, however, not strictly additive. For example, comparing **1a** and **2a**, a two-fold decrease in the K_d value was observed. Between **1a** and **1b**, there is a 31-fold change; between **2a** and **2b**, the difference is 17-fold. In contrast, the HB interactions involving **2b** are marginally stronger than those involving **1b**. Similar trends were also seen with **4** and **5**. These observations suggest that the delocalization of the positive charge in an extended π system reduces its ability to facilitate CF_2H-mediated HB interactions. Analogously, cationic CF_2H-containing molecules bearing electron-donating methoxy groups are also weak HB donors (**7b** vs **1b**). Furthermore, the cationic activation of HB donors is negligible when the quaternary nitrogen is *para* rather than *ortho* to the CF_2H group (**4** vs **5**). These findings indicate that the presence of either a quaternary nitrogen or an extended aromatic system can enhance the HB donation ability of the CF_2H group, but the effects are more pronounced when they are close to the CF_2H group.

We also compared the HB donation ability of different classes of compounds. In neutral CF_2H-containing HB donors, the phenylsulfonyl group (**12**) is generally a stronger activator than heteroaryl (**1a**–**6a**) or electron-deficient aryl groups (**13**). In contrast, pyridinium and benzimidazolium (**1b**–**5b**) systems show substantially higher capacities to enhance the HB donation ability of the CF_2H group, underscoring the distinct nature of these constructs. Although many of the CF_2H HB donors studied here can promote relatively strong hydrogen bonding interactions with *n*-Bu_3PO, even the strongest CF_2H HB donor (**3b**) is still 30 times weaker than phenol (**10**), corresponding to about a 2 kcal/mol reduction in binding energy at 25 °C. These results reveal the fundamental differences between the C–H bond and the O–H bond as HB donors and provide important quantitative information for applying the CF_2H group as an OH group mimic.

We next attempted to establish correlations of experimentally determined HB donation ability, in terms of K_d or ΔG_{exp}, with other easily accessible parameters. We first calculated the Gibbs free energy of formation (ΔG_{calc}) of the HB complexes of HB donors with trimethylphosphine oxide (Me_3PO), which models *n*-Bu_3PO as a hydrogen bond acceptor, and compared these values with experimental data. We realized that such an analysis oversimplified the system by neglecting to account for potential contributions from different conformers possibly involved in HB interactions. To rectify this problem, we searched for two possible structures for each Me_3PO–HB donor pair, where the HB donor adopts a different conformation in each HB complex. Values for ΔG_{calc} were then calculated as the weighted average of the free energy of each HB complex as

$$\Delta G_{calc} = -RT\ ln\left[\left(P_{Me_3PO\cdots HB,a} + P_{Me_3PO\cdots HB,b}\right)/\left(P_{Me_3PO\,|\,HB,a} + P_{Me_3PO\,|\,HB,b}\right)\right] \quad (1)$$

	1a	2a	3a	4a	5a	6a
	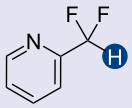	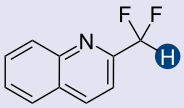	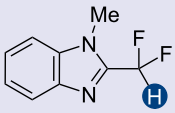	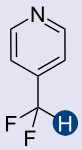	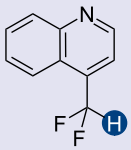	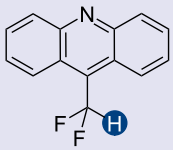
K_d (M)	81	40	20	19	12	7.2
ΔG_{exp} (kcal/mol)	2.6	2.2	1.8	1.8	1.3	1.2
ΔG_{calc} (kcal/mol)	4.5	4.7	3.4	4.1	3.6	3.3
	1b	**2b**	**3b**	**4b**	**5b**	**6b**
	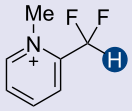	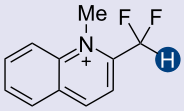	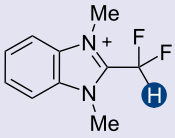	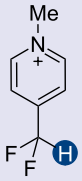	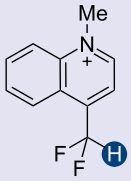	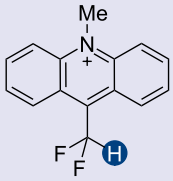
K_d (M)	2.6	2.1	1.5	9.1	11	–
ΔG_{exp} (kcal/mol)	0.56	0.50	0.25	1.3	1.4	–
ΔG_{calc} (kcal/mol)	1.3	1.9	0.6	3.4	2.6	–
	7b	**8b**	**10**	**12**	**13**	
	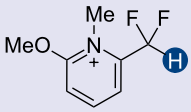	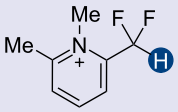	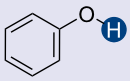	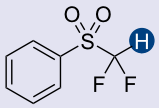		
K_d (M)	6.1	4.0	0.047	7.9	66	
ΔG_{exp} (kcal/mol)	1.1	0.82	–1.8	1.2	2.5	
ΔG_{calc} (kcal/mol)	2.7	0.4	–2.5	2.3	4.0	
	1b	**4b**	**5b**	**9b**		
	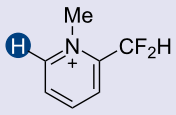	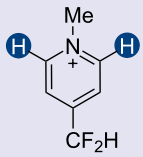	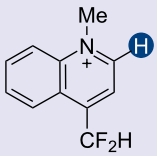	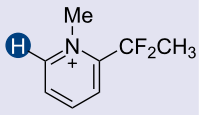		
K_d (M)	4.1	6.6	2.9	5.5		
ΔG_{exp} (kcal/mol)	0.8	1.1	0.63	1.0		
ΔG_{calc} (kcal/mol)	–	–	–	1.8		

Figure 5: Hydrogen bond donation ability of various donors as quantified by the dissociation constant (K_d) of the HB complex with tri-*n*-butylphosphine oxide at 298 K in anhydrous CD_3CN. The K_d for **6b** was not determined due to the formation of non-HB-mediated adducts (Figure S34 in Supporting Information File 1). The corresponding experimental Gibbs free energy of binding (ΔG_{exp}) is calculated based on the K_d values. The predicted Gibbs free energy of binding (ΔG_{calc}) was calculated at the PCM(MeCN)-M06-2X/6-31+G(d,p) level of theory. The counteranion for all cationic species is BF_4^-.

in which $P_{Me3PO\cdots HB,a}$ and $P_{Me3PO\cdots HB,b}$ are the percent populations of the HB complex of Me_3PO with the donor conformer a and b, respectively; $P_{Me3PO\ |\ HB,a}$ and $P_{Me3PO\ |\ HB,b}$ are the percent populations of Me_3PO and the corresponding HB donor conformer as two non-interacting molecules (see Supporting Information File 1 for details). We found a strong linear correlation between ΔG_{exp} and ΔG_{calc} obtained at the PCM(MeCN)-M06-2X/6-31+G(d,p) level of theory

(Figure 5 and Figure 6A). These results demonstrate the reliability of this relatively efficient computational approach for predicting the HB donation ability of CF_2H-containing molecules.

We further conducted natural bond orbital (NBO) [56] second-order perturbation analysis [57] to estimate the interaction energies ($E_{LP\rightarrow\sigma^*}$) of the oxygen lone pairs (LPs) of Me_3PO with the H–CF_2Ar antibonding orbital (σ*). Such hyperconjugative interactions indicate the magnitudes of the charge transfer from the LPs to the σ* orbitals and are considered the major contributors to hydrogen bonding [57]. Using this analysis, strong linear correlations were found between $E_{LP\rightarrow\sigma^*}$ and $\Delta\delta_{DMSO-CDCl3}$ or $\Delta\delta_{DMSO-CD3NO2}$ values (Figure 6B,C and Supporting Information File 1, Figures S44 and S45), implicating specific orbital interactions between the HB donating and accepting motifs that are responsible for chemical shift differences. In contrast, a relatively weak inverse association was observed between ΔG_{exp} and $\Delta\delta_{DMSO-CDCl3}$ values for neutral hydrogen bond donors (Figure 6D). This result suggests that the $CF_2H\cdots O$ interactions are likely to be a predominant contributor to the binding between HB donating and accepting molecules but other weak intermolecular forces, collectively, may also play a role. This proposal is further supported by the weaker linear relationship between ΔG_{exp} and $E_{LP\rightarrow\sigma^*}$ (Figure 6E and Figure S46 in Supporting Information File 1).

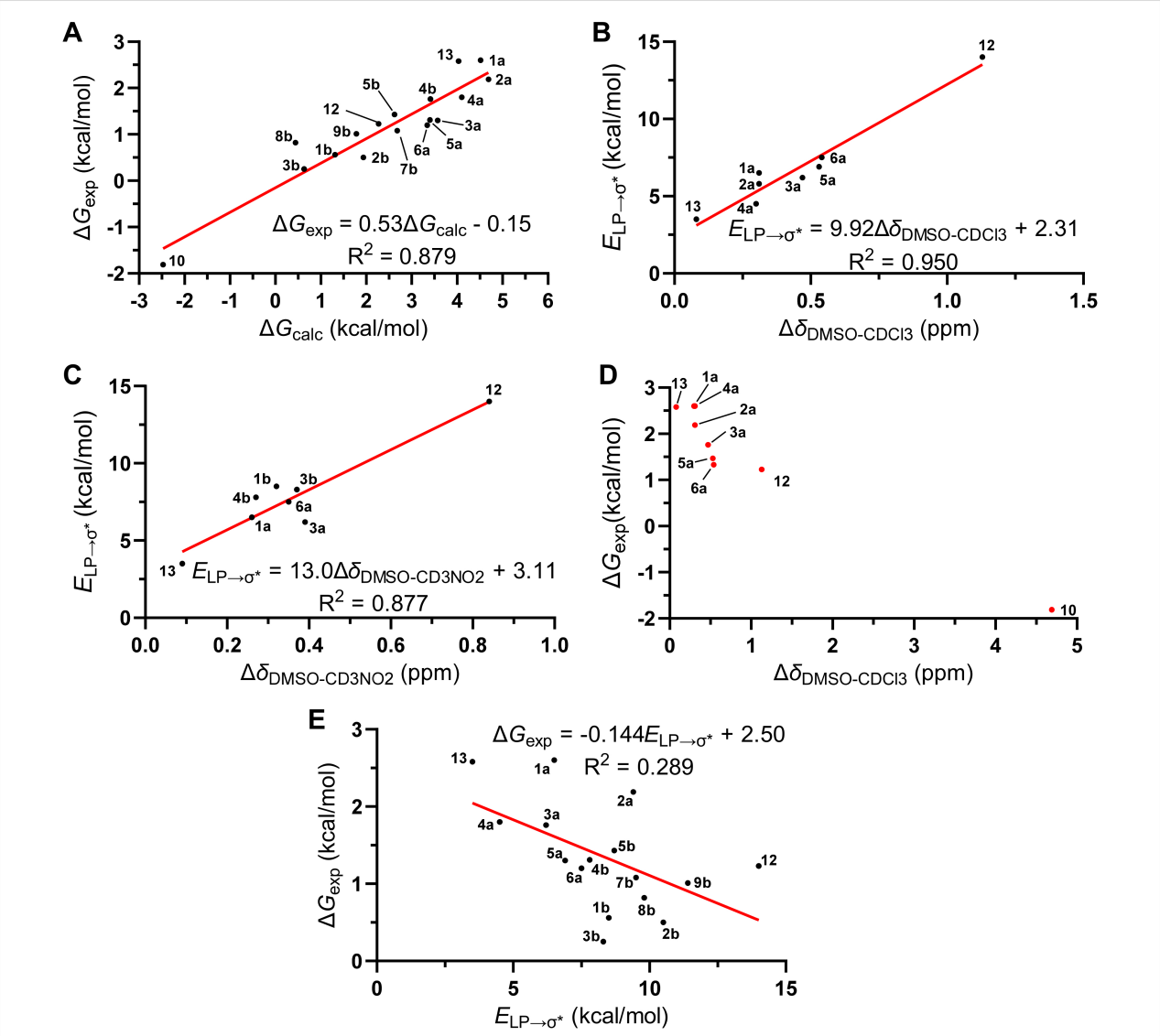

Figure 6: A) Linear correlation between ΔG_{exp} and ΔG_{calc}. ΔG_{exp} and ΔG_{calc} values are shown in Figure 5. B) Linear correlation between $E_{LP\rightarrow\sigma^*}$ and $\Delta\delta_{DMSO-CDCl3}$. $E_{LP\rightarrow\sigma^*}$ values can be found in Supporting Information File 1. $\Delta\delta_{DMSO-CDCl3}$ values are listed in Table 1. C) Linear correlation between $E_{LP\rightarrow\sigma^*}$ and $\Delta\delta_{DMSO-CD3NO2}$. $\Delta\delta_{DMSO-CDCl3}$ values are listed in Table 1. D) Inverse relationship between ΔG_{exp} and $\Delta\delta_{DMSO-CDCl3}$. E) Weak correlation between ΔG_{exp} and $E_{LP\rightarrow\sigma^*}$.

Collectively, these results indicate that the $\Delta\delta_{DMSO-CDCl3}$ or $\Delta\delta_{DMSO-CD3NO2}$ measurement can discriminate CF_2H HB interactions from other non-covalent forces. In this way, it is possible to parse the HB donating contribution of the CF_2H functional group within a given class of compounds, such as neutral or cationic donors, as shown here. One limitation of this approach is that it does not directly provide information about binding affinity or energy, particularly between HB donors and acceptors as molecular entities rather than as a collection of separate functional groups. In contrast, NMR titration experiments quantify the binding affinities and energies between CF_2H-containing molecules and *n*-Bu_3PO as the concatenation of many non-covalent forces. For example, our experiments showed that some C_{Ar}–H bonds, such as those of the pyridinium ring, can serve as good HB donors (Figure 5). Because C_{Ar}–H bonds and the CF_2H group have comparable HB donation abilities, care needs to be taken when assigning specific contributions of each to the observed binding affinities. Even so, ^{1}H NMR titration experiments with phosphine oxides still allow us to partially resolve these two forces by monitoring the proton of the CF_2H group. Such issues are particularly salient when quantification methods that rely only on acceptor readouts, such as the Reichardt's dye-based UV–vis titration, rendering results that are difficult to interpret (Figure 3). Overall, to survey the HB donating ability of the CF_2H-containing molecules systematically, a combination of NMR titration and $\Delta\delta_{DMSO-CDCl3}$ or $\Delta\delta_{DMSO-CD3NO2}$ measurements is desirable.

Conclusion

In conclusion, we have identified a series of CF_2H-containing compounds that can serve as HB donors. We employed several experimental methods to quantify HB donation ability, including (i) ^{1}H NMR chemical shift-based hydrogen bond acidity, *A* value, measurements, (ii) UV–vis spectroscopic titrations with Reichardt's dye, and (iii) ^{1}H NMR titrations using *n*-Bu_3PO as a reference HB acceptor. Our studies revealed that the ^{1}H NMR titrations, although tedious, offered reliable binding affinity data for HB complexes involving neutral and cationic donor molecules. This technique can be employed as a general approach for quantifying the energetics of HB interaction-enabled binding processes. Additionally, the free energies of HB complexation calculated at the PCM(MeCN)-M06-2X/6-31+G(d,p) level correlate well with our experimental data, allowing for binding affinity predictions. Lastly, we found a linear relationship between $\Delta\delta_{DMSO-CDCl3}$ or $\Delta\delta_{DMSO-CD3NO2}$ and hyperconjugative $Me_3PO(LP)\rightarrow\sigma^*_{H-CF2Ar}$ interaction energies, providing a quick and feasible estimation of the intrinsic HB donation ability of the CF_2H moiety. Further studies of the nature of hydrogen bonding interactions involving the CF_2H group are underway.

Supporting Information

Supporting Information File 1

Supplementary figures and schemes, materials, experimental procedures; characterization data (1D and 2D NMR, MS, HRMS) for all compounds; titration studies; DFT calculations.
[https://www.beilstein-journals.org/bjoc/content/supplementary/1860-5397-21-11-S1.pdf]

Acknowledgements

High-Performance Computing at the University of Rhode Island and the Massachusetts Green High-Performance Computing Center (MGHPCC) are gratefully acknowledged.

Funding

This research was made possible by the use of equipment available through the Rhode Island Institutional Development Award (IDeA) Network of Biomedical Research Excellence from the National Institute of General Medical Sciences of the National Institutes of Health under Grant No. P20GM103430 through the Centralized Research Core facility. M.E.P. was a Moissan Summer Undergraduate Research Fellow supported by the ACS Division of Fluorine Chemistry. M.E.P. acknowledges support from the Office of Undergraduate Research and Innovation at the University of Rhode Island and the CAREERS Cyberteam Program funded by the National Science Foundation (Award No. 2018873). J.M.G. acknowledges the Colgate University Research Council.

ORCID® iDs

Matthew E. Paolella - https://orcid.org/0009-0009-7431-4049
Daniel S. Honeycutt - https://orcid.org/0000-0001-6143-4492
Bradley M. Lipka - https://orcid.org/0000-0002-4700-4813
Jacob M. Goldberg - https://orcid.org/0000-0002-8004-3769
Fang Wang - https://orcid.org/0000-0002-9192-6858

Data Availability Statement

All data that supports the findings of this study is available in the published article and/or the supporting information of this article.

References

1. Wittkopp, A.; Schreiner, P. R. *Chem. – Eur. J.* **2003,** *9,* 407–414. doi:10.1002/chem.200390042
2. Doyle, A. G.; Jacobsen, E. N. *Chem. Rev.* **2007,** *107,* 5713–5743. doi:10.1021/cr068373r
3. Jeffrey, G. A. *An Introduction to Hydrogen Bonding;* Oxford University Press: Oxford, UK, 1997.
4. Anslyn, E. V.; Dougherty, D. A. *Modern Physical Organic Chemistry;* University Science Books: Sausalito, CA, USA, 2006.

5. Nepal, B.; Scheiner, S. *Chem. – Eur. J.* **2015,** *21,* 1474–1481. doi:10.1002/chem.201404970
6. Struble, M. D.; Strull, J.; Patel, K.; Siegler, M. A.; Lectka, T. *J. Org. Chem.* **2014,** *79,* 1–6. doi:10.1021/jo4018205
7. Hobza, P.; Havlas, Z. *Chem. Rev.* **2000,** *100,* 4253–4264. doi:10.1021/cr990050q
8. Castellano, R. K. *Curr. Org. Chem.* **2004,** *8,* 845–865. doi:10.2174/1385272043370384
9. Ammer, J.; Nolte, C.; Karaghiosoff, K.; Thallmair, S.; Mayer, P.; de Vivie-Riedle, R.; Mayr, H. *Chem. – Eur. J.* **2013,** *19,* 14612–14630. doi:10.1002/chem.201204561
10. Thalladi, V. R.; Weiss, H.-C.; Bläser, D.; Boese, R.; Nangia, A.; Desiraju, G. R. *J. Am. Chem. Soc.* **1998,** *120,* 8702–8710. doi:10.1021/ja981198e
11. Cai, J.; Sessler, J. L. *Chem. Soc. Rev.* **2014,** *43,* 6198–6213. doi:10.1039/c4cs00115j
12. Allerhand, A.; Von Rague Schleyer, P. *J. Am. Chem. Soc.* **1963,** *85,* 1715–1723. doi:10.1021/ja00895a002
13. Desiraju, G. R. *Acc. Chem. Res.* **1996,** *29,* 441–449. doi:10.1021/ar950135n
14. Kryachko, E.; Scheiner, S. *J. Phys. Chem. A* **2004,** *108,* 2527–2535. doi:10.1021/jp0365108
15. Erickson, J. A.; McLoughlin, J. I. *J. Org. Chem.* **1995,** *60,* 1626–1631. doi:10.1021/jo00111a021
16. Mahjoub, A. R.; Zhang, X.; Seppelt, K. *Chem. – Eur. J.* **1995,** *1,* 261–265. doi:10.1002/chem.19950010410
17. Caminati, W.; Melandri, S.; Moreschini, P.; Favero, P. G. *Angew. Chem., Int. Ed.* **1999,** *38,* 2924–2925. doi:10.1002/(sici)1521-3773(19991004)38:19<2924::aid-anie2924>3.0.co;2-n
18. Jones, C. R.; Baruah, P. K.; Thompson, A. L.; Scheiner, S.; Smith, M. D. *J. Am. Chem. Soc.* **2012,** *134,* 12064–12071. doi:10.1021/ja301318a
19. Zafrani, Y.; Yeffet, D.; Sod-Moriah, G.; Berliner, A.; Amir, D.; Marciano, D.; Gershonov, E.; Saphier, S. *J. Med. Chem.* **2017,** *60,* 797–804. doi:10.1021/acs.jmedchem.6b01691
20. Zafrani, Y.; Sod-Moriah, G.; Yeffet, D.; Berliner, A.; Amir, D.; Marciano, D.; Elias, S.; Katalan, S.; Ashkenazi, N.; Madmon, M.; Gershonov, E.; Saphier, S. *J. Med. Chem.* **2019,** *62,* 5628–5637. doi:10.1021/acs.jmedchem.9b00604
21. Sessler, C. D.; Rahm, M.; Becker, S.; Goldberg, J. M.; Wang, F.; Lippard, S. J. *J. Am. Chem. Soc.* **2017,** *139,* 9325–9332. doi:10.1021/jacs.7b04457
22. Zafrani, Y.; Parvari, G.; Amir, D.; Ghindes-Azaria, L.; Elias, S.; Pevzner, A.; Fridkin, G.; Berliner, A.; Gershonov, E.; Eichen, Y.; Saphier, S.; Katalan, S. *J. Med. Chem.* **2021,** *64,* 4516–4531. doi:10.1021/acs.jmedchem.0c01868
23. Saphier, S.; Zafrani, Y. *Future Med. Chem.* **2024,** *16,* 1181–1184. doi:10.1080/17568919.2024.2359358
24. Columbus, I.; Ghindes-Azaria, L.; Chen, R.; Yehezkel, L.; Redy-Keisar, O.; Fridkin, G.; Amir, D.; Marciano, D.; Drug, E.; Gershonov, E.; Klausner, Z.; Saphier, S.; Elias, S.; Pevzner, A.; Eichen, Y.; Parvari, G.; Smolkin, B.; Zafrani, Y. *J. Med. Chem.* **2022,** *65,* 8511–8524. doi:10.1021/acs.jmedchem.2c00658
25. Streitwieser, A., Jr.; Mares, F. *J. Am. Chem. Soc.* **1968,** *90,* 2444–2445. doi:10.1021/ja01011a056
26. Linclau, B.; Wang, Z.; Compain, G.; Paumelle, V.; Fontenelle, C. Q.; Wells, N.; Weymouth-Wilson, A. *Angew. Chem., Int. Ed.* **2016,** *55,* 674–678. doi:10.1002/anie.201509460
27. O'Hagan, D.; Young, R. J. *Angew. Chem., Int. Ed.* **2016,** *55,* 3858–3860. doi:10.1002/anie.201511055
28. Jeffries, B.; Wang, Z.; Felstead, H. R.; Le Questel, J.-Y.; Scott, J. S.; Chiarparin, E.; Graton, J.; Linclau, B. *J. Med. Chem.* **2020,** *63,* 1002–1031. doi:10.1021/acs.jmedchem.9b01172
29. Josephson, B.; Fehl, C.; Isenegger, P. G.; Nadal, S.; Wright, T. H.; Poh, A. W. J.; Bower, B. J.; Giltrap, A. M.; Chen, L.; Batchelor-McAuley, C.; Roper, G.; Arisa, O.; Sap, J. B. I.; Kawamura, A.; Baldwin, A. J.; Mohammed, S.; Compton, R. G.; Gouverneur, V.; Davis, B. G. *Nature* **2020,** *585,* 530–537. doi:10.1038/s41586-020-2733-7
30. Meanwell, N. A. *J. Med. Chem.* **2018,** *61,* 5822–5880. doi:10.1021/acs.jmedchem.7b01788
31. Trifonov, A. L.; Levin, V. V.; Struchkova, M. I.; Dilman, A. D. *Org. Lett.* **2017,** *19,* 5304–5307. doi:10.1021/acs.orglett.7b02601
32. Prakash, G. K. S.; Ganesh, S. K.; Jones, J.-P.; Kulkarni, A.; Masood, K.; Swabeck, J. K.; Olah, G. A. *Angew. Chem., Int. Ed.* **2012,** *51,* 12090–12094. doi:10.1002/anie.201205850
33. Fujikawa, K.; Fujioka, Y.; Kobayashi, A.; Amii, H. *Org. Lett.* **2011,** *13,* 5560–5563. doi:10.1021/ol202289z
34. O'Hagan, D. *Chem. Soc. Rev.* **2008,** *37,* 308–319. doi:10.1039/b711844a
35. Okusu, S.; Tokunaga, E.; Shibata, N. *Org. Lett.* **2015,** *17,* 3802–3805. doi:10.1021/acs.orglett.5b01778
36. Zhang, X.-Y.; Sun, S.-P.; Sang, Y.-Q.; Xue, X.-S.; Min, Q.-Q.; Zhang, X. *Angew. Chem., Int. Ed.* **2023,** *62,* e202306501. doi:10.1002/anie.202306501
37. Lin, D.; de los Rios, J. P.; Surya Prakash, G. K. *Angew. Chem., Int. Ed.* **2023,** *62,* e202304294. doi:10.1002/anie.202304294
38. Jia, R.; Wang, X.; Hu, J. *Tetrahedron Lett.* **2021,** *75,* 153182. doi:10.1016/j.tetlet.2021.153182
39. Sap, J. B. I.; Meyer, C. F.; Straathof, N. J. W.; Iwumene, N.; am Ende, C. W.; Trabanco, A. A.; Gouverneur, V. *Chem. Soc. Rev.* **2021,** *50,* 8214–8247. doi:10.1039/d1cs00360g
40. Wei, Z.; Miao, W.; Ni, C.; Hu, J. *Angew. Chem., Int. Ed.* **2021,** *60,* 13597–13602. doi:10.1002/anie.202102597
41. Fujiwara, Y.; Dixon, J. A.; Rodriguez, R. A.; Baxter, R. D.; Dixon, D. D.; Collins, M. R.; Blackmond, D. G.; Baran, P. S. *J. Am. Chem. Soc.* **2012,** *134,* 1494–1497. doi:10.1021/ja211422g
42. Fier, P. S.; Hartwig, J. F. *J. Am. Chem. Soc.* **2012,** *134,* 5524–5527. doi:10.1021/ja301013h
43. Surya Prakash, G. K.; Hu, J.; Olah, G. A. *J. Fluorine Chem.* **2001,** *112,* 355–360. doi:10.1016/s0022-1139(01)00535-8
44. Thompson, S.; McMahon, S. A.; Naismith, J. H.; O'Hagan, D. *Bioorg. Chem.* **2016,** *64,* 37–41. doi:10.1016/j.bioorg.2015.11.003
45. Flick, A. C.; Leverett, C. A.; Ding, H. X.; McInturff, E.; Fink, S. J.; Helal, C. J.; O'Donnell, C. J. *J. Med. Chem.* **2019,** *62,* 7340–7382. doi:10.1021/acs.jmedchem.9b00196
46. Gillis, E. P.; Eastman, K. J.; Hill, M. D.; Donnelly, D. J.; Meanwell, N. A. *J. Med. Chem.* **2015,** *58,* 8315–8359. doi:10.1021/acs.jmedchem.5b00258
47. Abraham, M. H.; Abraham, R. J.; Byrne, J.; Griffiths, L. *J. Org. Chem.* **2006,** *71,* 3389–3394. doi:10.1021/jo052631n
48. Abraham, M. H.; Abraham, R. J.; Acree, W. E., Jr.; Aliev, A. E.; Leo, A. J.; Whaley, W. L. *J. Org. Chem.* **2014,** *79,* 11075–11083. doi:10.1021/jo502080p
49. Gilli, P.; Pretto, L.; Bertolasi, V.; Gilli, G. *Acc. Chem. Res.* **2009,** *42,* 33–44. doi:10.1021/ar800001k

50. Zafrani, Y.; Amir, D.; Yehezkel, L.; Madmon, M.; Saphier, S.; Karton-Lifshin, N.; Gershonov, E. *J. Org. Chem.* **2016,** *81,* 9180–9187. doi:10.1021/acs.joc.6b01728
51. Marcus, Y. *Chem. Soc. Rev.* **1993,** *22,* 409–416. doi:10.1039/cs9932200409
52. Pike, S. J.; Lavagnini, E.; Varley, L. M.; Cook, J. L.; Hunter, C. A. *Chem. Sci.* **2019,** *10,* 5943–5951. doi:10.1039/c9sc00721k
53. Machado, V. G.; Stock, R. I.; Reichardt, C. *Chem. Rev.* **2014,** *114,* 10429–10475. doi:10.1021/cr5001157
54. Reichardt, C. *Chem. Rev.* **1994,** *94,* 2319–2358. doi:10.1021/cr00032a005
55. Reichardt, C.; Welton, T. *Solvents and Solvent Effects in Organic Chemistry;* Wiley-VCH: Weinheim, Germany, 2010. doi:10.1002/9783527632220
56. *NBO,* Version 3.1; Gaussian, Inc.: Wallingford, CT, 2001.
57. Reed, A. E.; Curtiss, L. A.; Weinhold, F. *Chem. Rev.* **1988,** *88,* 899–926. doi:10.1021/cr00088a005

License and Terms

BEILSTEIN JOURNAL OF ORGANIC CHEMISTRY

Visible-light-promoted radical cyclisation of unactivated alkenes in benzimidazoles: synthesis of difluoromethyl- and aryldifluoromethyl-substituted polycyclic imidazoles

Yujun Pang[1], Jinglan Yan[1], Nawaf Al-Maharik[2], Qian Zhang[1], Zeguo Fang[*1] and Dong Li[*1]

Letter

Open Access

Address:
[1]New Materials and Green Manufacturing Talent Introduction and Innovation Demonstration Base, Hubei University of Technology, 430068 Wuhan, China and [2]Department of chemistry, Faculty of Science, An Najah National University, Nablus, Palestine

Email:
Zeguo Fang[*] - fangzeguo@hbut.edu.cn; Dong Li[*] - dongli@hbut.edu.cn

* Corresponding author

Keywords:
cyclization; difluoromethylation; hypervalent iodine; polycyclic imidazole; visible light

Beilstein J. Org. Chem. **2025,** *21,* 234–241.
https://doi.org/10.3762/bjoc.21.15

Received: 28 October 2024
Accepted: 13 January 2025
Published: 30 January 2025

This article is part of the thematic issue "Organofluorine chemistry VI".

Guest Editor: D. O'Hagan

Abstract

An efficient and eco-friendly approach for synthesizing difluoromethyl- and aryldifluoromethyl-substituted polycyclic imidazoles was established via a visible-light-promoted radical cyclization reaction. This method employed the readily accessible and inexpensive CF_2HCO_2H or $PhCF_2COOH$, along with benzimidazoles bearing unactivated alkenes and $PhI(OAc)_2$ as substrates, and proceeded without the need of any base, metal catalyst, photocatalyst or additive. In total, 24 examples were examined, and all of them successfully underwent cyclization reaction to produce the target products in good to excellent yields. Mechanistic studies revealed that the reaction proceeds via a radical pathway.

Introduction

Organofluorine compounds continue to play important roles in pharmaceuticals and agrochemicals nowadays, largely due to the unique ability of fluorinated groups to influence the physicochemical and biochemical properties of molecules [1-3]. Among the various fluorinated functionalities, the difluoromethyl (CF_2H) group and its aryl-substituted derivative, the benzylic difluoromethylene ($PhCF_2$) group, stand out as particularly valuable in drug design. The CF_2H group can serve as a lipophilic isostere for hydroxy (OH), amino (NH_2), and thiol (SH) groups, thereby enhancing the efficacy and selectivity of therapeutic agents [4-6]. Similarly, the $PhCF_2$ group offers unique properties that can modify the activity and pharmacokinetic profiles of drugs [7]. Prominent examples include pantoprazole, a widely used proton-pump inhibitor (PPI) featuring a

CF_2H group; deracoxib, another drug that also incorporates a CF_2H moiety in its structure; and a MET inhibitor specifically designed with a $PhCF_2$ group (Figure 1a) [8-10]. As a result, there is a pressing need for the development of efficient methods for incorporating both the CF_2H and $PhCF_2$ groups into diverse molecular frameworks, particularly those with bioactivity properties.

The benzimidazole core is widely recognized as a vital pharmacophore in medicinal chemistry due to its special biological activity [11-13]. In particular, the tricyclic benzimidazole skeleton is ubiquitous in many bioactive compounds and therapeutic agents (Figure 1b) [14-16]. Recent studies have shown that fluorinated benzimidazole derivatives exhibit improved pharmacokinetic properties [17], which has further sparked interest in their development. Consequently, constructing benzimidazoles bearing the CF_2H and $PhCF_2$ groups has garnered significant attention. However, despite this growing interest, only a limited number of research groups have reported the direct difluoromethylation/cyclization reaction of benzimidazoles with alkenes for the syntheses of difluoromethylated tricyclic benzimidazoles to date. For example, in 2023, Chen and co-workers pioneered an electrochemical approach for the difluoromethylation and cyclization reaction of unactivated alkenes within benzimidazole molecules using CF_2HSO_2Na [18]. Subsequently, in 2024, Jin [19] and Yang [20] developed visible light-induced difluoromethylation strategies for unactivated alkenes within benzimidazoles using different CF_2H sources (CF_2HSO_2Na and $([Ph_3PCF_2H]^+Br^-)$, respectively (Scheme 1a). Despite these advances, the above methods still suffer from several limitations, including a narrow substrate scope, the reliance on expensive metal catalysts and excess additives, and the need for multistep synthesis of difluoromethylating reagents. These drawbacks restrict their broader applicability in drug design to some extent. Besides, the incorporation of the $PhCF_2$ group into tricyclic imidazoles has never been reported according to our best knowledge. Therefore, it is essential to explore environmentally friendly, cost-effective synthetic approaches for the construction of both difluoromethylated and aryldifluoromethylated benzimidazoles.

Inspired by previous work in radical chemistry, we turned our attention to difluoroacetic acid (CF_2HCOOH) and α,α-difluorobenzeneacetic acid ($PhCF_2COOH$), both of which are inexpensive and readily available industrial raw materials. In 2019, Gouverneur and co-workers reported a hydrodifluoromethylation of unactivated alkenes, wherein a CF_2H radical was generated from CF_2HCOOH using (diacetoxyiodo)benzene (PIDA) and light [21]. This CF_2H radical then added to the double bond to form a new alkyl radical, which underwent hydrogen atom abstraction to yield the hydrodifluoromethylation product. Building upon this work, we hypothesized that if the newly formed alkyl radical could undergo intramolecular cyclization with an aromatic ring, instead of hydrogen abstraction, it could enable the construction of polycyclic structures. Thus, as part of our ongoing interest in radical cyclization reactions [22-26], we

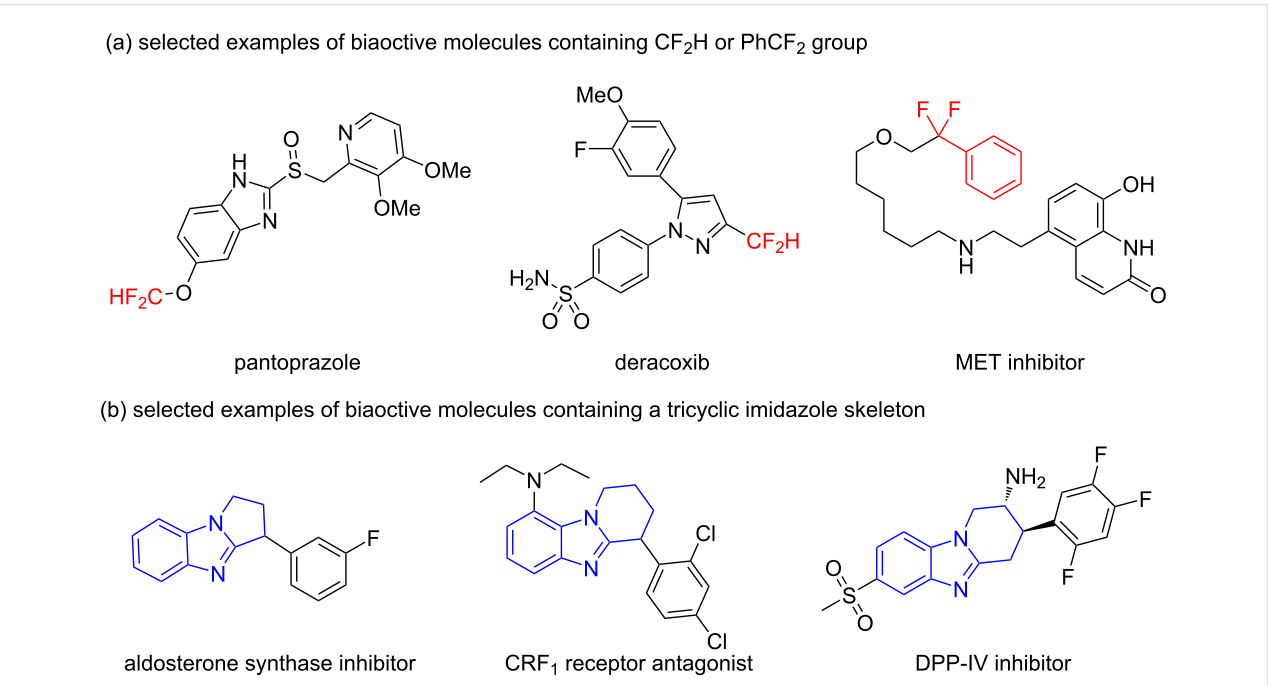

Figure 1: Selected examples containing tricyclic imidazole, CF_2H or $PhCF_2$ group.

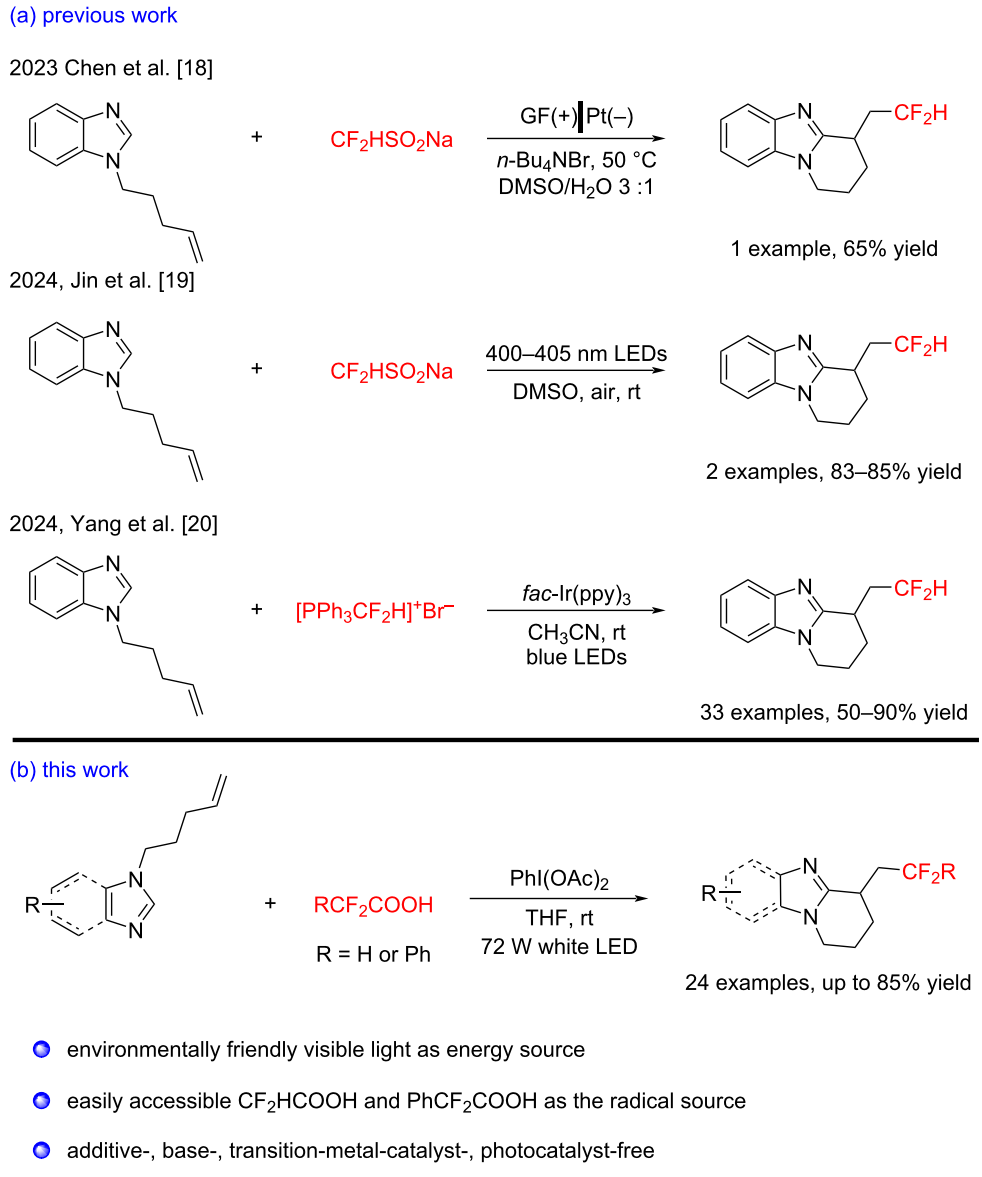

Scheme 1: Strategies for the synthesis of difluoromethylated and difluoroarylmethylated tricyclic imidazoles.

report here a sustainable and efficient protocol for synthesizing difluoromethylated and aryldifluoromethylated polycyclic imidazoles via visible-light-promoted cyclization of unactivated alkene-containing imidazoles with CF_2HCOOH or $PhCF_2COOH$, and PIDA under additive-, base-, and metal catalyst-free conditions (Scheme 1b).

Results and Discussion

Initially, 1-(pent-4-en-1-yl)-1*H*-benzo[*d*]imidazole (**1a**), CF_2HCOOH, and PIDA were chosen as the template substrates for this radical difluoromethylation and cyclization reaction (Table 1). Employing PIDA as the promoter, THF as the solvent, and 72 W white LED as the light source, the desired product **3a** formed in 85% isolated yield at room temperature (Table 1, entry 1). We found that the hypervalent iodine reagent was of significant importance for the present transformation (Table 1, entries 2 and 3), and PIDA was the most efficient promoter. Changing THF to other solvents, such as DCM, EtOH, DMF, CH_3CN, EtOAc, or DMSO, resulted in a lower yield (Table 1, entries 4–9). Furthermore, variations in the amounts of PIDA or CF_2HCOOH led to diminished yields (Table 1, entries 10–13), and conducting the reaction under air instead of nitrogen significantly lowered the yield (Table 1, entry 14). Control experiments showed that the absence of

Table 1: Optimization of reaction conditions.[a]

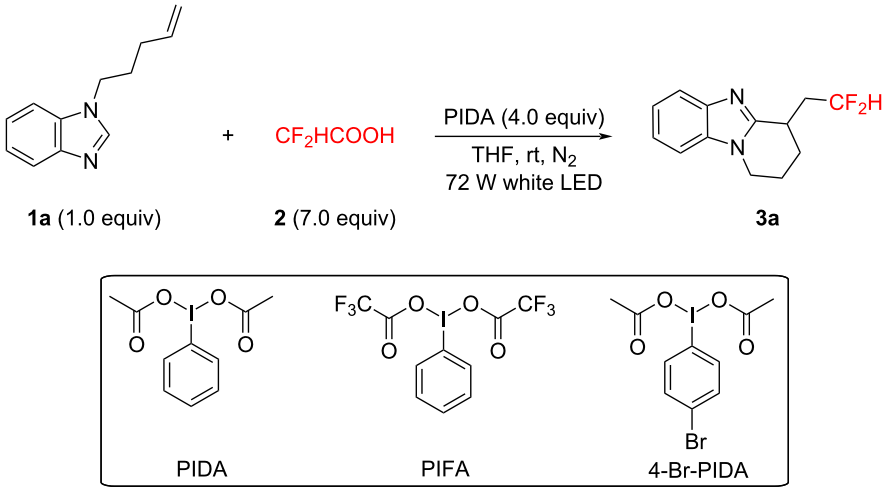

Entry	Variation from the standard conditions	Yield (%)[b]
1	none	85
2	PIFA	37
3	4-Br-PIDA	trace
4	DCM instead of THF	trace
5	EtOH instead of THF	NR
6	DMF instead of THF	13
7	CH_3CN instead of THF	17
8	EtOAc instead of THF	12
9	DMSO instead of THF	12
10	PIDA (3.0 equiv) instead of PIDA (4.0 equiv)	62
11	PIDA (5.0 equiv) instead of PIDA (4.0 equiv)	80
12	**2** (6 equiv) instead of **2** (7.0 equiv)	78
13	**2** (8 equiv) instead of **2** (7.0 equiv)	83
14	air instead of N_2	55
15	without PIDA	NR
16	40 W white LED instead of 72 W white LED	42
17	dark	40

[a]Reaction conditions: **1a** (0.2 mmol), **2** (1.4 mmol), and PIDA (0.8 mmol) in solvent (2 mL) irradiated with 72 W white LEDs at room temperature for 12 h under a N_2 atmosphere. NR no reaction. [b]Isolated yield.

PIDA resulted in no reaction (Table 1, entry 15), while the use of a 40 W light source or the absence of visible light also reduced the product yield (Table 1, entries 16 and 17).

With the optimized conditions in hand (Table 1, entry 1), the generality of the visible-light-promoted radical difluoromethlation/cyclization reaction was first investigated (Scheme 2). We were delighted to observe that the benzimidazole ring exhibited good tolerance for both electron-withdrawing groups such as fluorine (–F), bromine (–Br), and chlorine (–Cl), as well as electron-donating substituents like methoxy (–OMe) and methyl (–Me), yielding the corresponding 6-membered tricyclic imidazoles in moderate to good yields (**3b**–**h**). Benzene rings substituted with halogen atoms (–F, –Cl, –Br) were also suitable for this transformation, efficiently giving the desired products in yields of 65–80% (**3b**, **3e**–**g**), thus facilitating further functionalization possibilities. Notably, substrates with substituents at the sterically hindered 7-position of the benzimidazole ring also successfully underwent smooth cyclization, leading to the formation of products **3c** and **3d**. Furthermore, the methodology was compatible with 5,6-disubstituted *N*-alkenylbenzimidazoles, including those with -difluoro, -dichloro, -dibromo, and -dimethyl substitutions, resulting in the production of the anticipated products in yields ranging from moderate to good (**3e**–**h**).

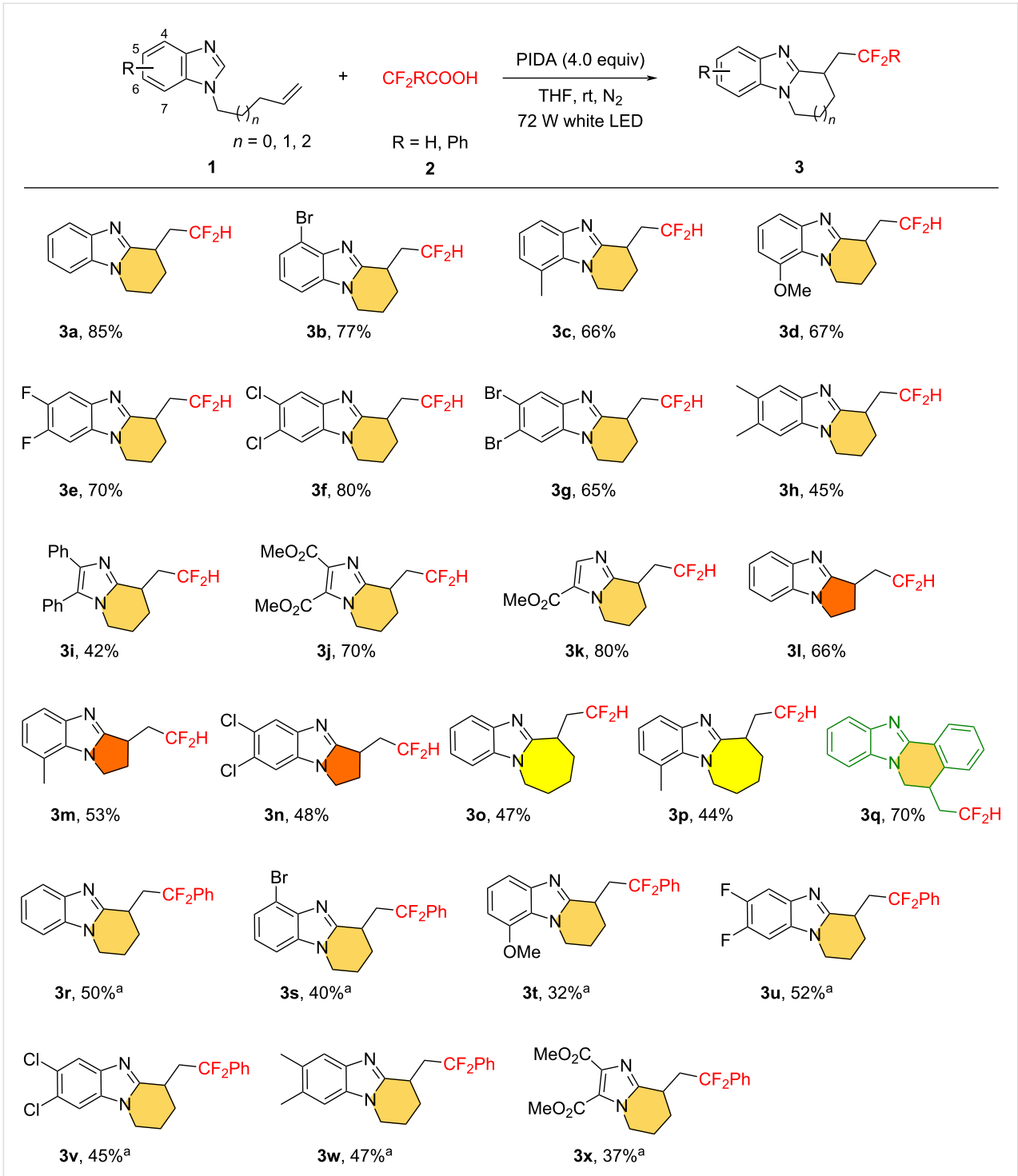

Scheme 2: Substrate scope of the protocol. Reaction conditions: **1** (0.2 mmol), **2** (1.4 mmol), and PIDA (0.8 mmol) in solvent (2 mL) irradiated with 72 W white LEDs at room temperature for 12 h under a N_2 atmosphere. Yields refer to isolated yield. [a]α,α-Difluorobenzeneacetic acid (2 equiv) was used.

Afterwards, we shifted our focus to substrates containing a single imidazole ring and discovered that the radical difluoromethylation and subsequent cyclization of unactivated olefin-containing imidazoles proceeded efficiently, generating the CF_2H-substituted bicyclic imidazoles with yields ranging from moderate to high (specifically, **3i** yielded 42%, **3j** yielded 70%, and **3k** yielded 80%). The relatively lower yield of **3i** can be attributed to the formation of side products due to the presence of

the phenyl ring. Furthermore, terminal olefins with varying chain lengths also reacted successfully, resulting in 5-membered and 7-membered cyclized products (**3l**–**p**) with yields between 44% and 66%. The lower yields in these cases might be due to the low reactivity of the intermediate **C** (Scheme 3), which may have made it less likely to undergo the desired transformation. To broaden application of this strategy, we tested other substrates as well. For instance, we successfully converted the *N*-alkenyl 2-arylbenzimidazole substrate into the desired product (**3q**). Finally, we examined the substrates for the radical aryldifluoromethylation/cyclization reaction (for details about optimization conditions, please see Supporting Information File 1). We were delighted to find that when 2-fluorophenylacetic acid was employed as the fluorine source, a wide range of benzimidazole substrates were also compatible with this reaction. For example, substrates with a bromine atom occupying the 4-position and a methoxy group at the 7-position could be successfully converted into the target products (**3s** and **3t**). In addition, doubly substituted benzimidazoles (**3u**–**w**), as well as the single imidazole (**3x**), were also found to be applicable. This demonstrates the versatility of our methodology and its potential for further exploration in diverse chemical spaces.

To gain a deeper understanding of the mechanism behind the observed reaction, we conducted a series of control experiments as outlined in Scheme 3a. Initially, we performed the model reaction with **1a** and $PhI(OCOCF_2H)_2$, which resulted in

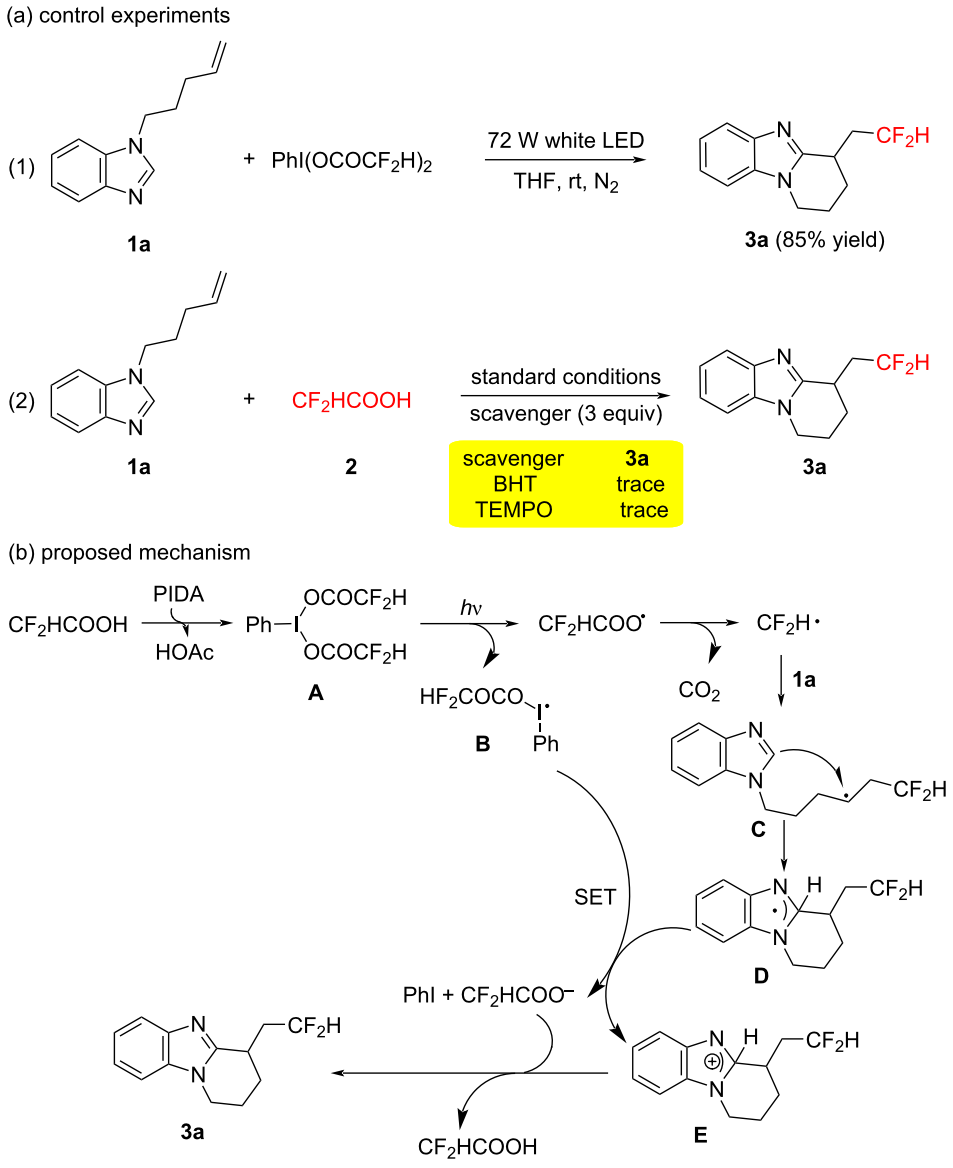

Scheme 3: Control experiments and plausible mechanism.

the formation of product **3a** with an 85% yield. This finding indicated that $PhI(OCOCF_2H)_2$ played a crucial role as an intermediate in the reaction. Subsequently, we introduced 3 equivalents of a radical scavenger (either TEMPO or BHT) into the reaction mixture, which significantly impeded the progress of the desired reaction. Therefore, on the basis of the above experimental results and previous reports [21,27-30], we proposed a possible reaction mechanism (Scheme 3b), taking CF_2HCOOH as the illustrative example. Initially, a double ligand exchange between PIDA and CF_2HCOOH would generate $PhI(OCOCF_2H)_2$ **A**. Homolysis of **A** under visible light (72 W white light) produced an iodanyl radical **B** and a CF_2H radical. The CF_2H radical regioselectively added to **1a** to form intermediate **C**. Subsequently, intermediate **C** could be converted into the radical intermediate **D** via intramolecular radical cyclization. A single-electron-transfer (SET) process then occurred between the radical **B** and the radical **D**, resulting in the generation of cationic intermediate **E**, difluoroacetate anion and PhI. Finally, the product **3a** was obtained after the deprotonation by difluoroacetate anion.

Conclusion

In summary, we have successfully developed a sustainable and efficient method for synthesizing difluoromethylated and aryldifluoromethylated polycyclic imidazoles through visible-light-promoted radical reactions. In contrast to previous reports, we achieved high yields of tricyclic and bicyclic imidazoles under additive-, base-, and metal catalyst-free conditions utilizing difluoroacetic acid and α,α-difluorobenzeneacetic acid as the readily available fluorine sources. The significant advantages of this approach, including its environmental friendliness and cost-effectiveness, position it as a valuable strategy in drug design and the synthesis of fluorinated compounds.

Supporting Information

Supporting Information File 1

Experimental procedures, product characterization, and copies of NMR spectra.
[https://www.beilstein-journals.org/bjoc/content/supplementary/1860-5397-21-15-S1.pdf]

Funding

We are grateful to the Scientific Research Project of Hubei Education Department (T2020023 and Q20211402) and the open project of Hubei Provincial Key Laboratory of Green Materials for Light Industry (202107B06) and the Doctoral Research Start-up Fund of Hubei University of Technology (XJKY20220023) for financial support.

ORCID® iDs

Nawaf Al-Maharik - https://orcid.org/0000-0002-7014-6190
Zeguo Fang - https://orcid.org/0000-0002-4844-1476
Dong Li - https://orcid.org/0000-0002-1246-1926

Data Availability Statement

All data that supports the findings of this study is available in the published article and/or the supporting information of this article.

References

1. Isanbor, C.; O'Hagan, D. *J. Fluorine Chem.* **2006,** *127,* 303–319. doi:10.1016/j.jfluchem.2006.01.011
2. Purser, S.; Moore, P. R.; Swallow, S.; Gouverneur, V. *Chem. Soc. Rev.* **2008,** *37,* 320–330. doi:10.1039/b610213c
3. Meanwell, N. A. *J. Med. Chem.* **2011,** *54,* 2529–2591. doi:10.1021/jm1013693
4. Zafrani, Y.; Sod-Moriah, G.; Yeffet, D.; Berliner, A.; Amir, D.; Marciano, D.; Elias, S.; Katalan, S.; Ashkenazi, N.; Madmon, M.; Gershonov, E.; Saphier, S. *J. Med. Chem.* **2019,** *62,* 5628–5637. doi:10.1021/acs.jmedchem.9b00604
5. Sessler, C. D.; Rahm, M.; Becker, S.; Goldberg, J. M.; Wang, F.; Lippard, S. J. *J. Am. Chem. Soc.* **2017,** *139,* 9325–9332. doi:10.1021/jacs.7b04457
6. Zafrani, Y.; Yeffet, D.; Sod-Moriah, G.; Berliner, A.; Amir, D.; Marciano, D.; Gershonov, E.; Saphier, S. *J. Med. Chem.* **2017,** *60,* 797–804. doi:10.1021/acs.jmedchem.6b01691
7. Geri, J. B.; Wade Wolfe, M. M.; Szymczak, N. K. *J. Am. Chem. Soc.* **2018,** *140,* 9404–9408. doi:10.1021/jacs.8b06093
8. Jungnickel, P. W. *Clin. Ther.* **2000,** *22,* 1268–1293. doi:10.1016/s0149-2918(00)83025-8
9. Bienhoff, S. E.; Smith, E. S.; Roycroft, L. M.; Roberts, E. S.; Baker, L. D. *Int. Scholarly Res. Not.* **2011,** 593015. doi:10.5402/2011/593015
10. Wade Wolfe, M. M.; Guo, S.; Yu, L. S.; Vogel, T. R.; Tucker, J. W.; Szymczak, N. K. *Chem. Commun.* **2022,** *58,* 11705–11708. doi:10.1039/d2cc01938h
11. Venugopal, S.; Kaur, B.; Verma, A.; Wadhwa, P.; Magan, M.; Hudda, S.; Kakoty, V. *Chem. Biol. Drug Des.* **2023,** *102,* 357–376. doi:10.1111/cbdd.14236
12. Guo, Y.; Hou, X.; Fang, H. *Mini-Rev. Med. Chem.* **2021,** *21,* 1367–1379. doi:10.2174/1389557520666200804124924
13. Beltran-Hortelano, I.; Alcolea, V.; Font, M.; Pérez-Silanes, S. *Eur. J. Med. Chem.* **2020,** *206,* 112692. doi:10.1016/j.ejmech.2020.112692
14. Kojima, T.; Mochizuki, M.; Takai, T.; Hoashi, Y.; Morimoto, S.; Seto, M.; Nakamura, M.; Kobayashi, K.; Sako, Y.; Tanaka, M.; Kanzaki, N.; Kosugi, Y.; Yano, T.; Aso, K. *Bioorg. Med. Chem.* **2018,** *26,* 2229–2250. doi:10.1016/j.bmc.2018.01.020
15. Edmondson, S. D.; Mastracchio, A.; Cox, J. M.; Eiermann, G. J.; He, H.; Lyons, K. A.; Patel, R. A.; Patel, S. B.; Petrov, A.; Scapin, G.; Wu, J. K.; Xu, S.; Zhu, B.; Thornberry, N. A.; Roy, R. S.; Weber, A. E. *Bioorg. Med. Chem. Lett.* **2009,** *19,* 4097–4101. doi:10.1016/j.bmcl.2009.06.011
16. Guo, Z.; Chen, X.; Xue, Y.; Li, J.; Zou, D.; Wu, Y.; Wu, Y. *Adv. Synth. Catal.* **2022,** *364,* 4231–4236. doi:10.1002/adsc.202200854

17. Randolph, J. T.; Flentge, C. A.; Donner, P.; Rockway, T. W.; Patel, S. V.; Nelson, L.; Hutchinson, D. K.; Mondal, R.; Mistry, N.; Reisch, T.; Dekhtyar, T.; Krishnan, P.; Pilot-Matias, T.; Stolarik, D. F.; Beno, D. W. A.; Wagner, R.; Maring, C.; Kati, W. M. *Bioorg. Med. Chem. Lett.* **2016,** *26,* 5462–5467. doi:10.1016/j.bmcl.2016.10.030
18. Chen, Z.; Li, Z.; Li, S.; Qian, G.; Sun, Y. *New J. Chem.* **2023,** *47,* 11465–11469. doi:10.1039/d3nj01759a
19. Huang, P.; Lv, C.; Song, H.; Wang, C.; Du, J.; Li, J.; Sun, B.; Jin, C. *Green Chem.* **2024,** *26,* 7198–7205. doi:10.1039/d4gc00728j
20. Lin, S.-N.; Deng, Y.; Zhong, H.; Mao, L.-L.; Ji, C.-B.; Zhu, X.-H.; Zhang, X.; Yang, B.-M. *ACS Omega* **2024,** *9,* 28129–28143. doi:10.1021/acsomega.4c01177
21. Meyer, C. F.; Hell, S. M.; Misale, A.; Trabanco, A. A.; Gouverneur, V. *Angew. Chem., Int. Ed.* **2019,** *58,* 8829–8833. doi:10.1002/anie.201903801
22. Xie, L.; Cao, R.; Huang, Y.; Zhang, Q.; Fang, Z.; Li, D. *Org. Chem. Front.* **2022,** *9,* 5929–5934. doi:10.1039/d2qo01175a
23. Fang, Z.; Liu, W.; Al-Maharik, N.; Cao, R.; Huang, Y.; Yuan, Y.; Zhang, Q.; Li, D. *J. Org. Chem.* **2023,** *88,* 15428–15436. doi:10.1021/acs.joc.3c01964
24. Fang, Z.; Xie, L.; Wang, L.; Zhang, Q.; Li, D. *RSC Adv.* **2022,** *12,* 26776–26780. doi:10.1039/d2ra05283k
25. Liu, W.; Wang, L.; Mu, H.; Zhang, Q.; Fang, Z.; Li, D. *Org. Biomol. Chem.* **2023,** *21,* 1168–1171. doi:10.1039/d2ob02086f
26. Wang, L.; Xie, L.; Fang, Z.; Zhang, Q.; Li, D. *Org. Chem. Front.* **2022,** *9,* 3061–3067. doi:10.1039/d2qo00207h
27. Sakamoto, R.; Kashiwagi, H.; Maruoka, K. *Org. Lett.* **2017,** *19,* 5126–5129. doi:10.1021/acs.orglett.7b02416
28. Mei, Y.; Zhao, L.; Liu, Q.; Ruan, S.; Wang, L.; Li, P. *Green Chem.* **2020,** *22,* 2270–2278. doi:10.1039/d0gc00009d
29. Yoshimura, A.; Zhdankin, V. V. *Chem. Rev.* **2024,** *124,* 11108–11186. doi:10.1021/acs.chemrev.4c00303
30. Gui, Q.-W.; Teng, F.; Li, Z.-C.; Xiong, Z.-Y.; Jin, X.-F.; Lin, Y.-W.; Cao, Z.; He, W.-M. *Chin. Chem. Lett.* **2021,** *32,* 1907–1910. doi:10.1016/j.cclet.2021.01.021

License and Terms

BEILSTEIN JOURNAL OF ORGANIC CHEMISTRY

Asymmetric synthesis of fluorinated derivatives of aromatic and γ-branched amino acids via a chiral Ni(II) complex

Maurizio Iannuzzi*, Thomas Hohmann*, Michael Dyrks, Kilian Haoues, Katarzyna Salamon-Krokosz and Beate Koksch*

Full Research Paper

Open Access

Address:
Institute of Chemistry and Biochemistry, Freie Universität Berlin, Arnimallee 20, 14195 Berlin, Germany

Email:
Maurizio Iannuzzi* - maurizio.iannuzzi@fu-berlin.de;
Thomas Hohmann* - thomas.hohmann@chem.ox.ac.uk;
Beate Koksch* - beate.koksch@fu-berlin.de

* Corresponding author

Keywords:
chiral nickel complexes; fluorinated amino acids; gram-scale amino acid synthesis; stereoselective synthesis

Beilstein J. Org. Chem. **2025,** *21,* 659–669.
https://doi.org/10.3762/bjoc.21.52

Received: 06 January 2025
Accepted: 18 February 2025
Published: 21 March 2025

This article is part of the thematic issue "Organofluorine chemistry VI".

Guest Editor: D. O'Hagan

Abstract

Fluorinated amino acids are essential building blocks in the spheres of protein engineering and medicinal chemistry. In the last decades, a large number of different synthetic strategies have been developed to produce a large variety of fluorinated amino acids. Still, obtaining fluorinated amino acids in great quantities can be challenging, or the corresponding pathways are heavily time-consuming and synthetically challenging. In this context, chiral Ni(II) complexes can be powerful tools to obtain tailor-made non-canonical amino acids. In this work, we wanted to take advantage of this strategy and extend the range of this method to include additional fluorinated amino acids. We synthesized two fluorinated analogs of phenylalanine, which are still unexplored in the context of peptide and protein chemistry. Furthermore, both diastereomers of trifluoroleucine were synthesized, demonstrating that the described strategy can also be applied to synthesize enantio- and diastereomerically pure γ-branched fluorinated amino acids. This work further underlines the importance of chiral Ni(II) complexes in the synthesis of fluorinated amino acids.

Introduction

Non-natural amino acids are pivotal in protein engineering and drug development. Over 30% of approved small-molecule drugs today contain non-canonical amino acid building blocks [1,2]. In peptide and protein engineering, non-natural amino acids significantly increase the respective range of tools used to modify a series of peptide and protein-related properties such as stability, specificity, and folding. In this regard, fluorinated amino acids are particularly important. Incorporation of fluorinated groups into the sequence of peptides and proteins can, for instance, regulate the respective hydrophobicity, alter the folding properties, and improve cell permeability [3-5].

Despite the evidence that unnatural amino acids play a significant role in the mentioned areas, synthesizing these building

blocks can still be a major challenge [6]. A potent strategy in this regard is the utilization of chiral nickel complexes. In recent years, the Soloshonok working group demonstrated the synthesis of non-natural amino acids using the corresponding chiral Ni(II) complex [7]. In addition to the high enantiomeric purity of the corresponding products, the scale of the reaction, which extends into the hectogram range, is a major strength of this method. In this context, Han et al. could show that the trifluorinated variant of α-aminobutyric acid, trifluoroethylglycine (TfeGly), can be synthesized on a 100 g scale with great enantiomeric purity [8]. The critical step here is the alkylation of the Ni(II) complex with the corresponding fluorinated alkyl iodide. The aryl moiety of the Ni(II) complex blocks the top face of the complex, ensuring the high diastereoselectivity of this transformation. In principle, synthesis on a gram-scale permits the study of highly fluorinated systems. Recently, we introduced fluoropeptides consisting nearly exclusively of fluorinated building blocks, which could only be accomplished by having the corresponding fluorinated amino acids in gram quantities [9,10]. In the last decades, others have also demonstrated that chiral Ni(II) complexes can be used to synthesize fluorinated amino acids [11,12]. Recently, our working group presented the synthesis of a broad range of fluorinated derivatives of different canonical and non-canonical amino acids (Scheme 1) [13]. Besides the linear fluorinated versions of α-aminobutyric acid and norvaline, the β-branched fluorinated amino acids such as trifluorovaline and trifluoroisoleucine were synthesized on a gram-scale with excellent enantiomeric purities.

In this work, we increase the scope of this methodology even further. First, we present the synthesis of two fluorinated, aromatic amino acids: (2,3,5,6)-tetrafluoro-4-trifluoromethylphenylalanine ([2.3.5.6F]TfMePhe, **2**) and bis(trifluoro-

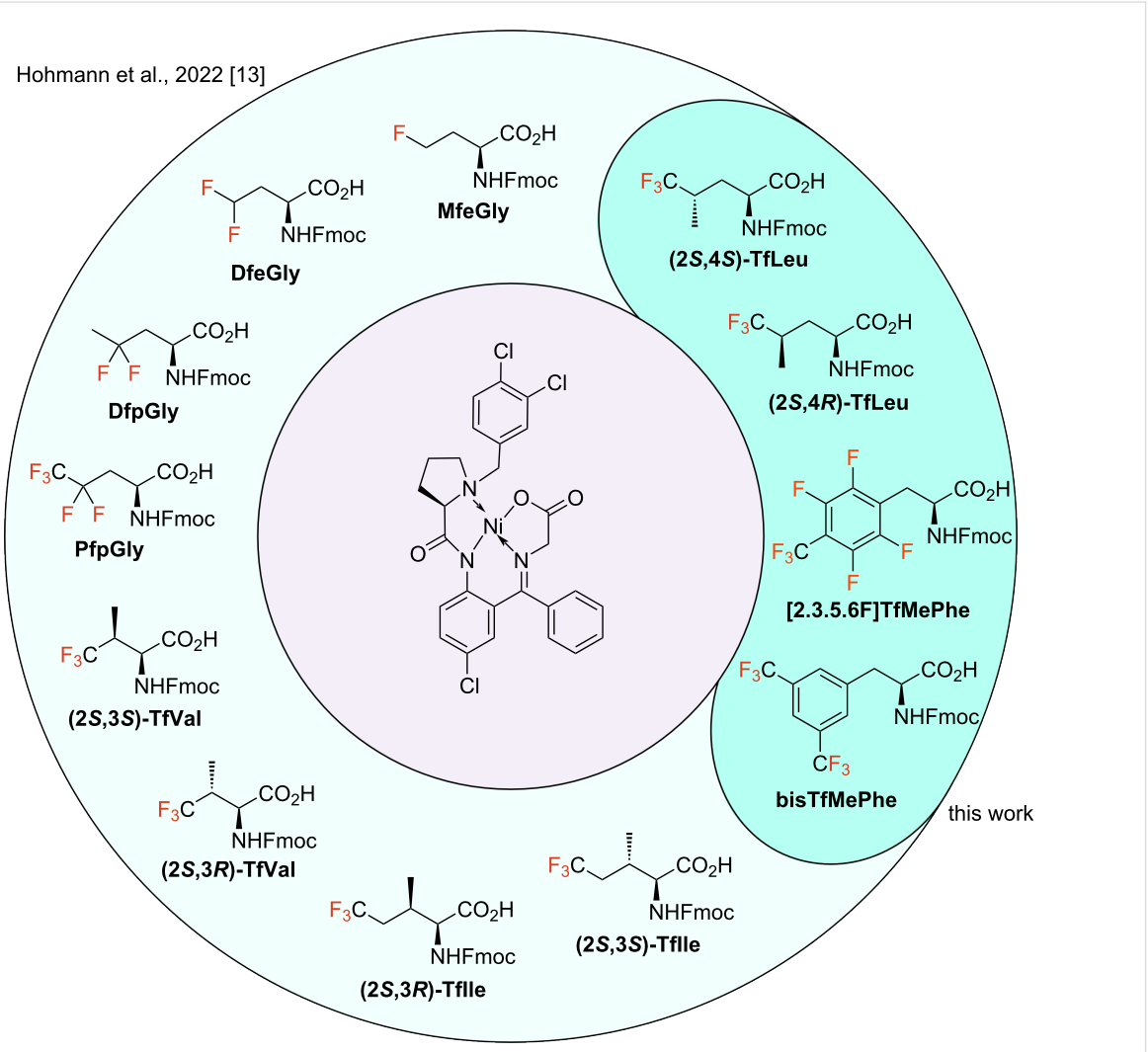

Scheme 1: Previous work for obtaining different fluorinated amino acids and target fluorinated amino acids described in the context of this work.

methyl)phenylalanine (bisTfMePhe, **3**) (Scheme 1). Neither amino acid has, to our knowledge, been described in the context of peptide chemistry yet. In general, fluorinated aromatic amino acids are essential building blocks that allow a modification of aromatic–aromatic interactions. For example, our group highlighted the influence of different fluorinated phenylalanine analogs on the aggregation rate of amyloid-forming NFGAIL peptides [14]. Amino acids **2** and **3**, with their respective fluorination pattern, might be fascinating compounds in this context. As already stated, chiral Ni(II) complexes can be used to synthesize fluorinated analogs of aliphatic canonical amino acids. Recently Naulet et al. presented a strategy for the synthesis of hexafluoroleucine (HfLeu) using a slightly modified version of the respective Ni(II) complex [12]. Furthermore, we introduce our attempts to synthesize the trifluorinated derivatives of leucine: (2*S*,4*S*)-trifluoroleucine ((2*S*,4*S*)-TfLeu) and (2*S*,4*R*)-trifluoroleucine ((2*S*,4*R*)-TfLeu) (Scheme 1). Here, we were especially interested in exploring the applicability of the Ni-based strategy to the synthesis of γ-branched amino acids.

Results and Discussion

Aromatic amino acids

First, we concentrated our efforts on synthesizing the aromatic, fluorinated amino acids (Scheme 2). The corresponding alkyl bromide precursors were commercially available. We screened a broad range of reaction conditions such as temperature, base, solvent, and reagent equivalents to optimize the alkylation reaction for both bromides **4** and **5** (Table 1 and Table 2). For Ni(II) complex of [2.3.5.6F]TfMePhe (**6**), firstly we screened different inorganic and organic bases (Table 1, entries 1–3) and 1,8-diazabicyclo[5.4.0]undec-7-ene (DBU) was identified as optimal delivering a yield of alkylated complex of 60% (Table 1, entry 4). With DBU as base different solvents differing in polarity have been tested. At room temperature, acetonitrile proved best and increased the yield to 88% (Table 1, entry 11). Lowering the temperature to 0 °C led to a final yield of 94%. At these conditions (DBU, MeCN and 0 °C) the base and bromide equivalents were further modified but no further increase in yield could be achieved. Thus, 1.5 equiv DBU with 1.05 equiv alkyl bromide in MeCN at 0 °C have been identified as optimal conditions for the Ni complex formation (Table 1, entry 12). By employing these conditions, the reaction was carried out on a decagram-scale, and the respective alkylated Ni(II) complex **6** was isolated with an excellent yield of 95% and high diastereomeric purity of 90% de (Scheme 2).

In contrast, the optimal conditions to obtain the Ni(II) complex of bisTfMePhe have differed significantly. Here, sodium hydride (NaH) was identified as optimal base leading to a yield of 85% when using DMF as solvent at 0 °C to room temperature (Table 2, entry 4). Testing different base equivalents, solvents, solvent mixtures and temperatures didn't lead to any

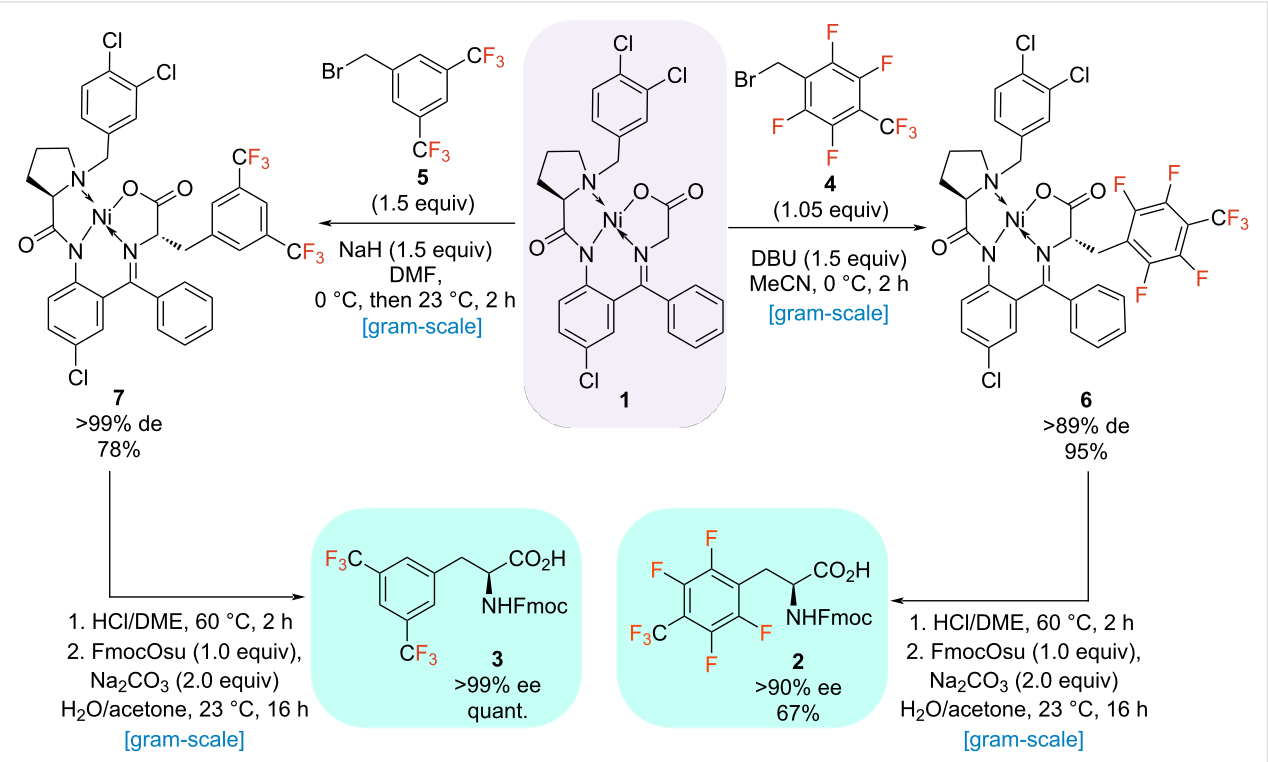

Scheme 2: Synthesis of fluorinated aromatic amino acids **2** and **3**.

Table 1: Optimization of the reaction conditions for the alkylation step using bromide **4**.

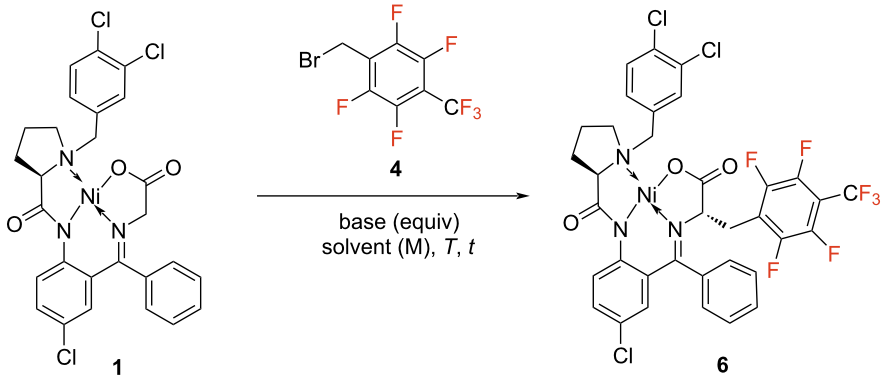

Entry	Base	Base [equiv]	Alkyl bromide [equiv]	*T* [°C]	Solvent	Solvent [M]	Yield [%][a]
1	NaH	1.50	1.05	0–rt	DMF	0.50	56
2	KOH/MeOH	1.50	1.05	0–rt	DMF	0.50	51
3	KO*t*-Bu	1.50	1.05	0–rt	DMF	0.50	41
4	DBU	1.50	1.05	0–rt	DMF	0.50	60
5	DBU	1.50	1.05	0–rt	NMP	0.50	60
6	DBU	1.50	1.05	0–rt	THF	0.50	57
7	DBU	1.50	1.05	0–rt	DMI	0.50	64
8	DBU	1.50	1.05	0–rt	MeCN	0.50	70
9	DBU	1.50	1.05	0–rt	MeCN	0.30	63
10	DBU	1.50	1.05	0–rt	MeCN	0.70	69
11	DBU	1.50	1.05	rt	MeCN	0.50	88
12	**DBU**	**1.50**	**1.05**	**0**	**MeCN**	**0.50**	**94**
13	DBU	1.10	1.05	0	MeCN	0.50	90
14	DBU	2.00	1.05	0	MeCN	0.50	77
15	DBU	1.50	1.50	0	MeCN	0.50	72
16	DBU	1.50	2.00	0	MeCN	0.50	47

[a]Determined by ^{19}F NMR using 2-chloro-4-fluorotoluene as an internal standard.

yield improvement (Table 2, entries 7–13). Herein, using dimethylformamide (DMF), different equiv of alkyl bromide were further screened resulting in a yield of 93%. Thus, 1.5 equiv NaH with 1.5 equiv alkyl bromide in DMF at 0 °C to room temperature have been identified as optimal conditions (Table 2, entry 16). With optimized conditions in hand, the respective alkylated Ni(II) complex was isolated in a good yield of 78% and with excellent diastereomeric purity of >99% de (Scheme 2). Both alkylated Ni(II) complexes (**6** and **7**) were hydrolyzed under standard conditions (HCl/DME 60 °C, 2 h), and the subsequent fluorenylmethoxycarbonyl (Fmoc) protection with FmocOsu led to the formation of the desired fluorinated amino acids. Here, Fmoc-[2.3.5.6F]TfMePhe (**2**) was isolated in a yield of 67% and a good enantiomeric purity of 90% ee. Fmoc-bisTfMePhe (**3**) was obtained even in a quantitative yield and with a great enantiomeric excess of >99% ee (Scheme 2).

Trifluorinated derivatives of leucine

The fluorinated alkyl iodide is commercially available but costly. Thus, we aimed at establishing an appropriate synthesis for this iodide. Our previous work showed that fluorinated alkyl iodides can be efficiently synthesized in gram-scale from the respective fluorinated alcohols using alkyl nonaflates as a key intermediate [13]. Based on these results, 3,3,3-trifluoro-2-methylpropan-1-ol (**8**) was selected as the starting material. We started our efforts by screening the reaction conditions to obtain the corresponding nonaflate. To our surprise, the corresponding yields of this transformation were rather unsatisfying (data not shown). Unfortunately, the yield could not be significantly improved by varying all essential reaction parameters. Therefore, a different strategy for the synthesis of alkyl iodides was investigated. A tosylate functionality was employed as a leaving group in the iodination reaction. Finally, the desired fluorinated tosylate **9** could be isolated on a gram-scale in a moderate yield of

Table 2: Optimization of the reaction conditions for the alkylation step using bromide **5**.

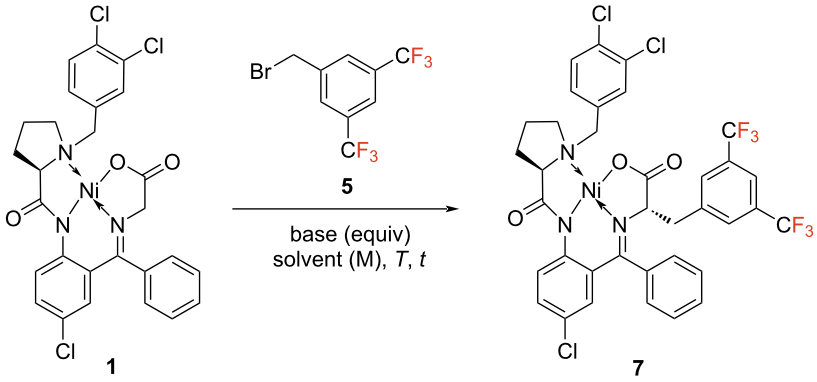

Entry	Base	Base [equiv]	Alkyl bromide [equiv]	*T* [°C]	Solvent	Solvent [M]	Yield [%][a]
1	DBU	1.50	1.05	0–rt	DMF	0.50	79
2	KOH/MeOH	1.50	1.05	0-rt	DMF	0.50	51
3	KO*t*-Bu	1.50	1.05	0–rt	DMF	0.50	59
4	NaH	1.50	1.05	0–rt	DMF	0.50	85
5	NaH	1.10	1.05	0–rt	DMF	0.50	70
6	NaH	2.00	1.05	0–rt	DMF	0.50	50
7	NaH	1.50	1.05	0	DMF	0.50	70
8	NaH	1.50	1.05	rt	DMF	0.50	55
9	NaH	1.50	1.05	0–rt	NMP	0.50	53
10	NaH	1.50	1.05	0–rt	THF	0.50	65
11	NaH	1.50	1.05	0–rt	THF/DMF	0.50	57
12	NaH	1.50	1.05	0–rt	MeCN	0.50	56
13	NaH	1.50	1.05	0–rt	DMI	0.50	61
14	NaH	1.50	1.05	0–rt	DMF	0.30	30
15	NaH	1.50	1.05	0–rt	DMF	0.70	48
16	**NaH**	**1.50**	**1.50**	**0–rt**	**DMF**	**0.50**	**93**
17	NaH	1.50	2.00	0–rt	DMF	0.50	27

[a]Determined by ^{19}F NMR using 2-chloro-4-fluorotoluene as an internal standard.

27% (Scheme 3a). Subsequently, the iodination of the tosylate has been optimized regarding temperature and time and optimized conditions at 80 °C for 24 h (Table 3, entry 3) resulted in the synthesis of the desired fluorinated alkyl iodide **10** with a great yield of 87%. However, scaling up on gram-scale, a slightly decreased yield of 70% was achieved (Scheme 3a).

With the fluorinated alkyl iodide precursor **10**, the corresponding alkylation reaction with the Ni(II) complex **1** was conducted under previously optimized conditions for the synthesis of Fmoc-TfIle [13] in terms of base (NaH) and solvent (DMF) and thoroughly screened in terms of base equivalents, concentration and temperature (Table 4).

By adjusting the base to 1.3 equivalents and carrying the reaction at 0 °C, the yield of the transformation could be improved from 30% to 62% (Table 4, entry 1). By applying the respective conditions, both Ni(II) complexes of TfLeu were synthesized with an excellent overall total alkylation yield of 68%. Since two desired diastereomers are formed in this case, they had to be subsequently separated from one another. This was accomplished using flash column chromatography. The respective Ni(II) complexes of TfLeu (**11a**, **11b**) could be isolated with excellent diastereomeric purities of 95 and 97% de. Both alkylated Ni(II) complexes were then hydrolyzed under standard conditions (HCl/DME 60 °C, 2 h), and the subsequent fluorenylmethoxycarbonyl (Fmoc) protection with FmocOsu led to the formation of the desired fluorinated amino acids. However, only one isomer could be isolated, requiring several chromatographic purification steps (EtOAc/*n*-pentane, 2% AcOH). Hence, in the here described case, the final hydrolysis and Fmoc protection resulted the enantiomerically pure isomer Fmoc-(2*S*,4*R*)-TfLeu (**12a**), isolated in a good yield of 40% and

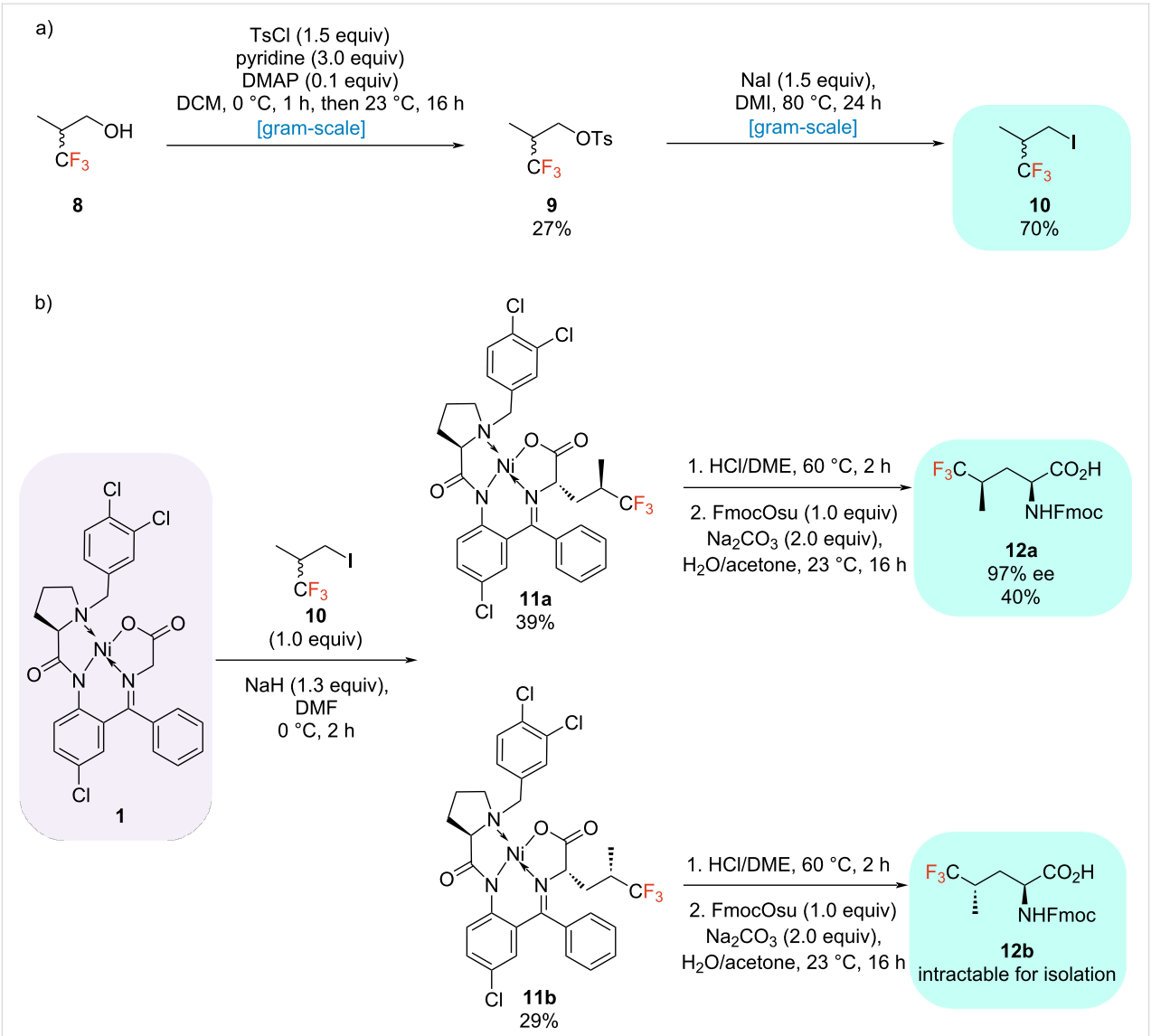

Scheme 3: a) Gram-scale synthesis of fluorinated alkyl iodide precursor **10**; b) Synthesis of trifluorinated leucine analogs **12a** and **12b**.

Table 3: Optimization of the reaction conditions for the synthesis of the alkyl iodide **10**.

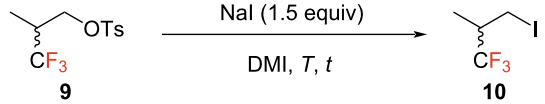

Entry	*T* [°C]	Time [h]	Yield [%][a]
1	100	24	0
2	60	24	40
3	**80**	**24**	**87**
4	80	72	87
5	80	3	31

[a]Determined by ^{19}F NMR using 2-chloro-4-fluorotoluene as an internal standard.

with excellent enantiomeric purity of 97% ee. The configuration was determined by analyzing the ^{1}H NMR spectrum in the δ = 2.8–1.7 ppm region, which displayed the characteristic diastereotopic hydrogen atoms of this compound, as previously reported by Biava et al. [15]. Unfortunately, the corresponding (2*S*,4*S*)-isomer **12b** was intractable for isolation (yield < 5%) despite numerous attempts.

Conclusion

This work described the stereoselective and gram-scale synthesis of a highly attractive palette of fluorinated amino acids prepared for application in solid-phase peptide synthesis. First, two different fluorinated variants of phenylalanine were synthesized, which have yet to be described in the context of peptide chemistry. The several CF_3 groups employ a strong inductive

Table 4: Optimization of the reaction conditions for the synthesis of alkylated complexes **11a** and **11b**.

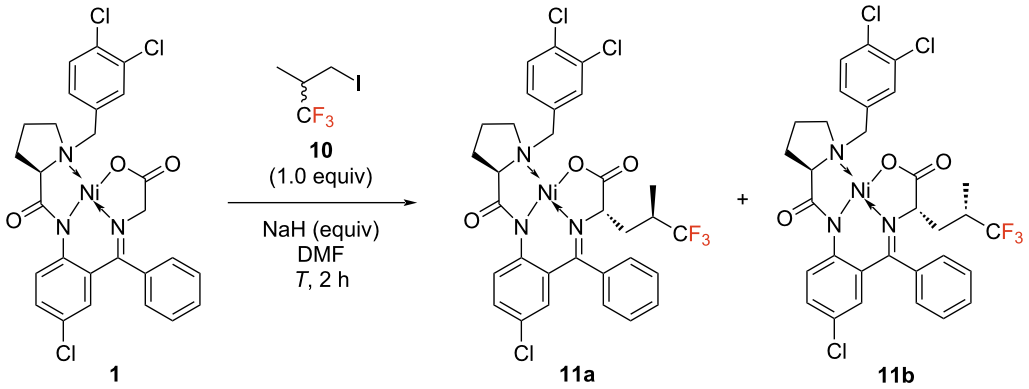

Entry	NaH [equiv]	DMF [mL/mmol of complex]	*T* [°C]	Yield [%][a]
1	**1.3**	**5**	**0**	**62**
2	1.3	5	rt	31
3	1.3	5	–10	20
4	1.3	2.50	rt	7
5	1.3	2.50	0	41
6	3	5	rt	24
7	3	5	0	33
8	3	2.50	rt	36
9	3	2.50	0	31

[a]Determined by ^{19}F NMR using 2-chloro-4-fluorotoluene as an internal standard.

effect on the aromatic ring structure, making these amino acids highly interesting building blocks for modification of aromatic–aromatic interactions in the context of protein folding, interaction and function. Furthermore, the synthesis of both isomers of trifluoroleucine was described. (2*S*,4*R*)-Trifluoroleucine could be isolated on a milligram-scale in good yields and excellent enantiomeric purities, representing a viable synthetic route for these building blocks adding another strategy to the repertoire of published syntheses for this fluorinated derivative of natural leucine. Further attempts to the isolation of the second isomer will be made. Overall, this work further underlines the potential of chiral nickel complexes in synthesizing fluorinated amino acids. The diverse range of fluorinated amino acids that can be synthesized from a single starting material is a unique feature of this method, making it an important cornerstone of fluoropeptide chemistry.

Experimental

General information

Air- and hydrolysis-sensitive reactions were carried out under exclusion of air and water in Schlenk vessels at a Schlenk unit/oil pump vacuum under nitrogen atmosphere. The stated reaction temperatures are the respective values of the silicone oil heating bath. All reactions were stirred with an electric magnetic stirrer. ^{1}H, ^{13}C, and ^{19}F NMR spectra were measured at room temperature with a JEOL ECP 600 (JEOL, Tokyo, Japan) device. MestReNova Version 10.0.0 (Mestrelab Research S. L., Santiago de Compostela, Spain) was used to analyze the respective spectra. The chemical shifts are given in parts per million (ppm). The ^{1}H and ^{13}C NMR chemical shifts were referenced against the specific internal solvent residual peaks ($CDCl_3$, CD_3OD) and given to tetramethylsilane as internal standard (δ = 0.00 ppm). High-resolution mass spectra (HRMS) of the obtained compounds were measured on an Agilent 6220 ESI-TOF MS instrument (Agilent Technologies, Santa Clara, CA, USA) using a spray voltage of 4 kV. The prepared samples were injected into the spray chamber using a syringe pump with flow rates of 10 to 40 µL/min. The desolvation gas was adjusted to 15 psi. Other parameters were optimized for maximal abundance of $[M + H]^+$, $[M + Na]^+$, or $[M + K]^+$. High-resolution electron ionization mass spectra (HREIMS) were measured on a MAT 711 (Varian MAT, Bremen, Germany). Electron energy for EI was set to 70 eV. Infrared spectra (IR) were measured on an ALPHA II (Bruker, Billerica, USA) spectrometer. Characteristic absorption bands are given in wave numbers (cm^{-1}). Qualitative thin-layer chromatography (TLC) was carried out on aluminum plates coated with silica gel 60 F254 (Merck, Darmstadt, Germany). The TLC plates were analyzed using UV light

at 254 nm. Flash chromatography was performed on silica gel 60 M from Macherey-Nagel (grain size of 40–63 μm). The conditions are given in the form "(A/B = a:b)", where A/B refers to the solvents used as mobile phase and a:b to their volume ratio. Analytical high-performance liquid chromatography (HPLC) was used to determine the purity of the obtained Fmoc-protected amino acids. The respective HPLC runs were carried out on a Primaide DAD system (VWR/Hitachi, Germany). The system works with a low-pressure gradient containing a HPLC pump (1110) with a 6-channel solvent degaser, an organizer, an autosampler (1210) with a 100 μL sample loop, a column oven (1310) and a diode array detector (1430). A Kinetex C18 (2) column (5 μm, 250 Å × 4.6 mm, Phenomenex, Torrance, CA, USA) was used. H_2O and MeCN, both containing 0.1% (v/v) TFA, served as eluents. Fmoc-protected amino acids were detected at 220 nm. For a chiral analysis, a CHIRALPAK ZWIX(−) column ((R,R)-ACHSA immobilized on 3 μm silica gel, 250 × 4 mm, Chiral Technologies Europe, Illkirch Cedex, France) was used. MeCN/MeOH/H_2O mixture with 50 mM formic acid and 25 mM diethylamine was used as eluent. A flow rate of 0.5 mL/min was applied and the detection of the respective compounds occurred at 280 nm. Data analysis was carried out with the EZChrom ELITE software (version 3.3.2 SP2, Agilent). Ni(II) complex **1** was synthesized according the procedure described by Romoff et al. [16]. Sodium hydride was used as a 60% dispersion in mineral oil. Triethylamine was dried over CaH_2 and distilled freshly before use. Perfluorobutanesulfonyl fluoride was dried over $CaCl_2$ and freshly distilled before use. Other chemicals were used without further purification and obtained from commercial sources.

Synthesized compounds

3,3,3-Trifluoro-2-methylpropyl 4-methylbenzene-1-sulfonate (9): 8 (5.00 g, 39.0 mmol, 1.0 equiv), was dissolved in DCM (48.8 mL). *p*-Toluenesulfonyl chloride (11.15 g, 58.5 mmol, 1.5 equiv) and DMAP (0.48 g, 3.9 mmol, 0.1 equiv) were added and the mixture was cooled to 0 °C before pyridine (9.41 mL, 117.0 mmol, 3.0 equiv) was added. After 1 h of stirring, the reaction was warmed to room temperature and further stirred for 16 h. Subsequently, the mixture was diluted with H_2O (25 mL) and extracted with DCM (2 × 40 mL). The combined organic phases were then washed with aq HCl (2 M, 12 mL), saturated aqueous $NaHCO_3$ solution (12 mL), and brine (12 mL). Afterward, the combined organic phases were dried over Na_2SO_4, filtered, and dried in vacuo for 16 h. The crude product was purified via flash-column chromatography (*n*-Pen/EtOAc, 10:1). The product **9** was obtained as a colorless oil (2.99 g, 10.6 mmol, 27%). ^{1}H NMR (600 MHz, $CDCl_3$) δ 7.81–7.76 (m, 2H), 7.39–7.34 (m, 2H), 4.16 (dd, *J* = 10.3, 5.3 Hz, 1H), 3.97 (dd, *J* = 10.3, 6.8 Hz, 1H), 2.62–2.54 (m, 1H), 2.46 (s, 3H), 1.23–1.15 (m, 3H) ppm; ^{19}F NMR (565 MHz, $CDCl_3$) δ −71.53 (d, J = 9.4 Hz, 3F) ppm.

1,1,1-Trifluoro-3-iodo-2-methylpropane (10): A mixture of **9** (7.44 g, 26.4 mmol, 1.0 equiv) and 1,3-dimethyl-2-imidazolinone (DMI) (8.8 mL) was heated to 80 °C before NaI (5.94 g, 39.6 mmol, 1.5 equiv) was added and the reaction mixture was stirred for 24 h. The crude product was purified by vacuum distillation (4×10^{-2} mbar). The product **10** was obtained as colorless liquid (4.41 g, 18.5 mmol, 70%). ^{1}H NMR (600 MHz, $CDCl_3$) δ 3.44 (dd, *J* = 10.3, 3.5 Hz, 1H), 2.97 (t, *J* = 10.1 Hz, 1H), 2.53–2.43 (m, 1H), 1.29 (d, *J* = 6.9 Hz, 3H) ppm; ^{19}F NMR (565 MHz, $CDCl_3$) δ −72.74 (d, *J* = 7.9 Hz) ppm.

Ni(II)-Schiff base complex of [2.3.5.6F]TfMePhe 6: Under inert conditions and at 0 °C, DBU (2.23 mL, 15.0 mmol, 1.5 equiv) was added dropwise to a mixture of **1** (6.0 g, 9.97 mmol, 1.0 equiv) and **4** (1.77 mL, 10.5 mmol, 1.05 equiv) in dry, vented MeCN (20 mL). After 2 h of stirring at 0 °C, H_2O (30 mL) was added. After 1 h of stirring, the precipitated product was filtered, washed with H_2O (15 mL), and dried in vacuo at 60 °C to give **6** (7.81 g, 9.39 mmol, 95%, 91% purity determined by analytical HPLC) as an orange solid. The crude was used without further purification. ^{1}H NMR (600 MHz, $CDCl_3$) δ 8.88 (d, *J* = 2.2 Hz, 1H), 8.07 (d, *J* = 9.3 Hz, 1H), 7.79 (dd, *J* = 8.2, 2.2 Hz, 1H), 7.62 (p, *J* = 5.7 Hz, 2H), 7.49 (dt, *J* = 9.0, 4.4 Hz, 1H), 7.37 (d, *J* = 8.1 Hz, 1H), 7.33 (dt, *J* = 6.3, 2.0 Hz, 1H), 7.15 (dd, *J* = 9.3, 2.8 Hz, 1H), 6.88 (d, *J* = 7.7 Hz, 1H), 6.63 (d, *J* = 2.8 Hz, 1H), 4.30 (d, *J* = 12.7 Hz, 1H), 4.13 (dd, *J* = 10.1, 5.9 Hz, 1H), 3.83 (dd, *J* = 13.4, 10.0 Hz, 1H), 3.58 (dt, *J* = 12.7, 3.4 Hz, 1H), 3.55–3.49 (m, 1H), 3.39 (dt, *J* = 11.0, 6.1 Hz, 1H), 3.22 (d, *J* = 12.7 Hz, 1H), 3.08 (dd, *J* = 13.4, 6.0 Hz, 1H), 2.78–2.58 (m, 1H), 2.37–2.24 (m, 1H), 2.08 (td, *J* = 11.0, 5.9 Hz, 1H), 1.65 (m, 1H); ^{13}C NMR (151 MHz, $CDCl_3$) δ 180.1, 176.4, 171.6, 144.7, 141.1, 134.9 (2C), 133.8, 133.7 (2C), 133.6, 133.1, 132.5, 132.2 (2C), 131.3, 130.9, 130.1, 129.8, 129.6, 127.5 (2C), 127.3 (2C), 127.3, 126.1, 124.4 (2C), 71.5, 68.3, 63.2, 58.7, 31.0, 29.1, 23.9; ^{19}F NMR (565 MHz, $CDCl_3$) δ −56.23 (t, *J* = 20.7 Hz), −140.45 (dq, *J* = 28.6, 11.9, 11.1 Hz); ATR-FTIR (neat): 3587, 2975, 2868, 1634, 1500, 1333, 1249, 1137, 870, 820, 709 cm^{-1}; HRMS (ESI-TOF) *m/z*: $[M + Na]^+$ calcd for $C_{35}H_{23}Cl_3F_7N_3NiO_3$, 853.9916; found, 853.9958.

Ni(II)-Schiff base complex of bisTfMePhe 7: Under inert conditions and at 0 °C, NaH (1.0 g, 24.9 mmol, 1.5 equiv) was added slowly to a mixture of **1** (10.0 g, 16.6 mmol, 1.0 equiv) and **5** (4.64 mL, 24.9 mmol, 1.5 equiv) in dry, vented DMF (19.9 mL). The reaction was stirred at room temperature for 2 h. Afterwards, H_2O (50 mL) was added. After 1 h of stirring, the precipitated product was filtered, washed with H_2O (20 mL),

and dried in vacuo at 60 °C. The crude material was purified by flash column chromatography (SiO_2, 10 → 100% EtOAc in diethyl ether) to yield **7** as a red solid (10.7 g, 12.9 mmol, 78%, 99% purity determined by analytical HPLC). ^{1}H NMR (600 MHz, $CDCl_3$) δ 8.90 (d, *J* = 2.2 Hz, 1H), 8.18 (d, *J* = 9.3 Hz, 1H), 7.81 (s, 1H), 7.66 (dd, *J* = 8.2, 2.2 Hz, 1H), 7.67–7.59 (m, 2H), 7.55–7.47 (m, 1H), 7.37 (dt, *J* = 6.6, 1.8 Hz, 1H), 7.34 (d, *J* = 8.2 Hz, 1H), 7.26 (d, *J* = 1.5 Hz, 2H), 7.15 (dd, *J* = 9.3, 2.6 Hz, 1H), 6.89 (dt, *J* = 7.7, 1.0 Hz, 1H), 6.64 (d, *J* = 2.6 Hz, 1H), 4.25 (d, *J* = 12.7 Hz, 1H), 4.20 (dd, *J* = 7.8, 4.0 Hz, 1H), 3.41–3.32 (m, 1H), 3.30 (dd, *J* = 11.1, 5.9 Hz, 1H), 3.18 (dd, *J* = 13.8, 7.8 Hz, 1H), 3.17 (d, *J* = 12.7 Hz, 1H), 3.10 (dd, *J* = 13.7, 3.9 Hz, 1H), 2.86 (dddd, *J* = 19.2, 14.0, 6.6, 3.8 Hz, 1H), 2.49 (dddd, *J* = 13.7, 11.0, 9.6, 8.3 Hz, 1H), 2.45–2.34 (m, 1H), 2.07–2.01 (m, 1H), 1.99 (dt, *J* = 11.1, 5.4 Hz, 1H); ^{13}C NMR (151 MHz, $CDCl_3$) δ 180.1, 177.4, 171.4, 141.3, 138.3, 134.9, 133.8, 133.7, 133.5, 133.1, 133.1, 132.4, 132.1, 131.9, 131.2, 130.9, 130.1, 130.0, 129.9, 129.6, 127.5, 127.3, 126.9, 126.0, 124.3 (2C), 124.1, 122.3, 121.5, 71.2, 70.9, 63.3, 58.6, 40.7, 30.8, 23.7; ^{19}F NMR (565 MHz, $CDCl_3$) δ −62.57 (s); ATR-FTIR (neat): 3062, 2982, 2868, 1638, 1463, 1278, 1133, 894, 820, 705 cm^{-1}; HRMS (ESI-TOF) *m/z*: $[M + Na]^+$ calcd for $C_{36}H_{26}Cl_3F_6N_3NiO_3$, 850.0167; found, 850.0181.

Ni(II)-Schiff base complexes of (2*S*,4*R*)-TfLeu 11a, (2*S*,4*S*)-TfLeu 11b: Under inert conditions and at 0 °C, NaH (0.13 g, 5.4 mmol, 1.3 equiv) was added slowly to a mixture of **1** (2.0 g, 4.16 mmol, 1.0 equiv), and **10** (1.0 g, 4.16 mmol, 1.0 equiv) in dry, vented DMF (5 mL). The reaction was stirred at 0 °C for 2 h. Afterwards, H_2O (10 mL) was added. After 1 h of stirring, an additional amount of H_2O (5 mL) was added, and the reaction mixture was stirred for further 1 h. Afterwards, the precipitated solid was filtered and washed with H_2O/DMF (1:2, 20 mL). The resulting diastereomeric crude products were purified and separated via flash-column chromatography (chloroform/acetone, 3:1) to yield to **11a** (2*S*,4*R*) (1.18 g, 1.7 mmol, 39%) and **11b** (2*S*,4*S*) (0.87 g, 1.22 mmol, 29%) as red solids. **11a**: ^{1}H NMR (600 MHz, $CDCl_3$) δ 8.86 (s, 1H), 8.00 (d, *J* = 9.2 Hz, 1H), 7.75 (d, *J* = 8.2 Hz, 1H), 7.62–7.46 (m, 3H), 7.35 (d, *J* = 8.1 Hz, 1H), 7.30 (d, *J* = 7.4 Hz, 1H), 7.13–7.08 (m, 1H), 6.90 (d, *J* = 7.6 Hz, 1H), 6.59–6.56 (m, 1H), 4.32–4.25 (m, 1H), 3.80 (dd, *J* = 12.0, 3.9 Hz, 1H), 3.64 (dt, *J* = 19.7, 10.5 Hz, 1H), 3.52 (dt, *J* = 10.6, 5.9 Hz, 1H), 3.35 (dd, *J* = 11.4, 5.7 Hz, 1H), 3.19 (d, *J* = 12.6 Hz, 1H), 2.84 (t, *J* = 12.6 Hz, 1H), 2.72–2.50 (m, 3H), 2.27 (dt, *J* = 13.9, 7.1 Hz, 1H), 2.14 (s, 1H), 2.06 (dt, *J* = 11.6, 5.8 Hz, 1H), 1.41 (td, *J* = 12.6, 3.9 Hz, 1H), 0.44 (d, *J* = 6.8 Hz, 2H) ppm; ^{13}C NMR (151 MHz, $CDCl_3$) δ 180.07, 177.89, 170.35, 140.69, 134.95, 133.69, 133.51, 132.66, 132.46, 132.11, 131.17, 130.58, 130.01, 129.52, 128.74, 127.49, 127.29 (d, *J* = 4.4 Hz), 125.97, 124.48, 71.36, 67.22, 63.04, 58.61, 35.99, 34.58, 34.40, 30.96 (d, *J* = 15.8 Hz), 24.03, 23.17, 11.07 ppm; ^{19}F NMR (565 MHz, $CDCl_3$) δ −73.96 (d, *J* = 9.2 Hz) ppm.

11b: ^{1}H NMR (600 MHz, $CDCl_3$) δ 8.84 (s, 1H), 8.01 (d, *J* = 9.4 Hz, 1H), 7.76 (d, *J* = 8.2 Hz, 1H), 7.54 (q, *J* = 9.2 Hz, 2H), 7.47 (t, *J* = 7.6 Hz, 1H), 7.34 (d, *J* = 8.1 Hz, 1H), 7.26 (d, *J* = 6.9 Hz, 1H), 7.10 (d, *J* = 9.3 Hz, 1H), 6.85 (d, *J* = 7.6 Hz, 1H), 6.57 (s, 1H), 4.30 (d, *J* = 12.6 Hz, 1H), 3.92 (dd, *J* = 10.8, 4.8 Hz, 1H), 3.61 (q, *J* = 10.2 Hz, 1H), 3.52 (t, *J* = 8.4 Hz, 1H), 3.36 (dd, *J* = 11.5, 5.6 Hz, 1H), 3.19 (d, *J* = 12.6 Hz, 1H), 2.75–2.48 (m, 3H), 2.36–2.24 (m, 2H), 2.15 (s, 1H), 2.07–2.02 (m, 2H), 1.07 (d, *J* = 7.0 Hz, 3H) ppm; ^{13}C NMR (151 MHz, $CDCl_3$) δ 179.95, 178.16, 170.72, 140.60, 134.92, 133.80–133.43 (m), 132.63, 132.34 (d, *J* = 9.3 Hz), 131.18, 130.53, 130.00, 129.59 (d, *J* = 8.7 Hz), 128.50, 127.43, 127.22 (d, *J* = 19.1 Hz), 125.98, 124.25, 71.38, 68.54, 63.06, 58.50, 37.65, 34.44 (d, *J* = 27.1 Hz), 34.08 (d, *J* = 26.7 Hz), 30.90, 24.12, 14.86 ppm; ^{19}F NMR (565 MHz, $CDCl_3$) δ −73.28 (d, *J* = 9.0 Hz) ppm.

(*S*)-2-((((9*H*-Fluoren-9-yl)methoxy)carbonyl)amino)-3-(2,3,5,6-tetrafluoro-4-(trifluoromethyl)phenyl)propanoic acid [tetrafluoro(trifluoromethyl)phenylalanine, [2.3.5.6F]TfMePhe] (2): At room temperature, aq HCl (3 M, 15.4 mL, 46.3 mmol, 5.0 equiv) was added to a stirring solution of **6** (7.70 g, 9.26 mmol, 1.0 equiv) in DME (30.9 mL). The resulting mixture was stirred at 60 °C for 2 h. After cooling to room temperature, the precipitated ligand was filtered and washed with H_2O (15 mL). The filtrate was concentrated under reduced pressure to a volume of 30 mL. Again, the precipitated ligand was filtered and washed with H_2O (15 mL). Both fractions of the ligand were united and dried in vacuo at 40 °C. To the filtrate, MeCN (18.5 mL) and EDTA-Na_2 (3.45 g, 9.26 mmol, 1.0 equiv) were added and the reaction mixture was stirred at room temperature for 2 h. Subsequently, the solution was treated with aq NaOH (18 M) to pH 7 and Na_2CO_3 (1.96 g, 18.5 mmol, 2.0 equiv) was added. FmocOSu (3.12 g, 9.26 mmol, 1.0 equiv) was dissolved in acetone (37.0 mL) and added dropwise to the reaction mixture. After 17 h of stirring at room temperature, MeCN and acetone were removed under reduced pressure, H_2O (40 mL) was added, and the mixture was treated with aq HCl (6 M) to pH 2. The resulting solution was extracted with EtOAc (4 × 40 mL), dried over Na_2SO_4, filtered, and concentrated in vacuo. The crude material was purified by flash column chromatography (SiO_2, 0 → 10% MeOH in DCM) to yield **2** as a yellow solid (3.36 g, 9.26 mmol, 67%, 91% purity determined by analytical HPLC). ^{1}H NMR (600 MHz, $CDCl_3$) δ 7.77 (d, *J* = 7.6 Hz, 2H), 7.64–7.55 (m, 2H), 7.37 (tt, *J* = 7.6, 0.9 Hz, 2H), 7.28 (td, *J* = 7.4, 1.2 Hz, 2H), 4.65 (d, *J* = 4.7 Hz, 1H), 4.51 (dd, *J* = 9.3, 5.5 Hz, 1H), 4.34–4.20 (m, 2H), 4.14 (t, *J* = 7.0 Hz, 1H), 3.42 (dd, *J* = 14.0,

5.5 Hz, 1H), 3.33–3.23 (m, 1H); ^{13}C NMR (151 MHz, $CDCl_3$) δ 173.3, 158.4, 148.0 (2C), 146.2 (2C), 145.1 (2C), 142.6 (2C), 128.8 (2C), 128.1 (2C), 126.1 (2C), 123.3, 120.9 (3C), 108.9, 68.2, 54.1, 48.2, 26.9; ^{19}F NMR (565 MHz, $CDCl_3$) δ −57.00 (t), −141.58 (td), −142.21 to −144.04 (m); ATR-FTIR (neat): 3313, 3066, 2945, 1698, 1492, 1263, 1146, 966, 738 cm^{-1}; HRMS (ESI-TOF) *m/z*: $[M - H]^-$ calcd for $C_{25}H_{15}F_7NO_4$, 526.0894; found, 526.0871.

(*S*)-2-((((9*H*-Fluoren-9-yl)methoxy)carbonyl)amino)-3-(3,5-bis(trifluoromethyl)phenyl)propanoic acid [bis(trifluoromethyl)phenylalanine, bisTfMePhe] (3): At room temperature, aq HCl (3 M, 21.4 mL, 64.0 mmol, 5.0 equiv) was added to a stirred solution of **7** (10.6 g, 12.8 mmol, 1.0 equiv) in DME (42.7 mL). The resulting mixture was stirred at 60 °C for 2 h. After cooling to room temperature, the precipitated ligand was filtered and washed with H_2O (20 mL). The filtrate was concentrated under reduced pressure to a volume of 40 mL. Again, the precipitated ligand was filtered and washed with H_2O (20 mL). Both fractions of the ligand were united and dried in vacuo at 40 °C. To the filtrate, MeCN (25.6 mL) and EDTA-Na_2 (4.77 g, 12.8 mmol, 1.0 equiv) were added and the reaction mixture was stirred at room temperature for 2 h. Subsequently, the solution was treated with aq NaOH (18 M) to pH 7 and Na_2CO_3 (2.71 g, 25.6 mmol, 2.0 equiv) was added. FmocOSu (4.32 g, 12.8 mmol, 1.0 equiv) was dissolved in acetone (51.2 mL) and added dropwise to the reaction mixture. After 17 h of stirring at room temperature, MeCN and acetone were removed under reduced pressure, H_2O (50 mL) was added, and the mixture was treated with aq HCl (6 M) to pH 2. The resulting solution was extracted with EtOAc (4 × 50 mL), dried over Na_2SO_4, filtered, and concentrated in vacuo. The crude material was purified by flash column chromatography (SiO_2, 20 → 100% EtOAc in diethyl ether) to yield **3** as an off-white solid (6.90 g, 12.8 mmol, 100%, 84% purity determined by analytical HPLC). ^{1}H NMR (600 MHz, $CDCl_3$) δ 7.91–7.85 (m, 2H), 7.82 (s, 1H), 7.76 (ddd, *J* = 7.7, 2.4, 1.5 Hz, 2H), 7.61–7.52 (m, 2H), 7.36 (td, *J* = 7.5, 4.0 Hz, 2H), 7.25 (tdd, *J* = 7.4, 2.8, 1.1 Hz, 2H), 4.48 (dd, *J* = 9.7, 4.9 Hz, 1H), 4.33–4.19 (m, 2H), 4.14 (t, *J* = 7.4 Hz, 1H), 3.41 (dd, *J* = 14.2, 4.9 Hz, 1H), 3.12 (dd, *J* = 14.0, 9.7 Hz, 1H); ^{13}C NMR (151 MHz, $CDCl_3$) δ 174.7, 158.4, 145.2 (2C), 142.5 (2C), 142.5, 132.6 (2C), 131.0 (2C), 128.7 (2C), 128.1 (2C), 126.2 (2C), 125.8, 124.0, 121.5, 120.9 (2C), 68.1, 56.4, 48.3, 38.12; ^{19}F NMR (565 MHz, $CDCl_3$) δ −63.42 (s): ATR-FTIR (neat): 3305, 3066, 2971, 1681, 1451, 1278, 1119, 983, 734 cm^{-1}; HRMS (ESI-TOF) *m/z*: $[M + Na]^+$ calcd for $C_{26}H_{19}F_6NO_4$, 546.1116; found, 546.1080.

(2*S*,4*R*)-2-((((9*H*-Fluoren-9-yl)methoxy)carbonyl)amino)-5,5,5-trifluoro-4-methylpentanoic acid [Trifluoroleucine, TfLeu] (12a): At room temperature aq HCl (3 M, 2.70 mL, 8 mmol, 5 equiv) was added to a stirring solution of **11a** (1.21 g, 1.60 mmol, 1.0 equiv) in DME (5.33 mL). The resulting mixture was stirred at 60 °C for 2 h. After cooling at room temperature, the precipitated ligand was filtered and washed with H_2O (10 mL) leading to further precipitation of ligand. Again, the precipitated was filtered and washed with H_2O (5 mL). Both fractions of the ligand were combined and dried in vacuo at 40 °C. To the filtrate, MeCN (3.20 mL) and EDTA-Na_2 (0.54 g, 1.60 mmol, 1.0 equiv) were added and the reaction mixture was stirred at room temperature for 2 h. Subsequently, the solution was treated with aq NaOH (48%) to pH 8 and Na_2CO_3 (0.34 g, 3.20 mmol, 2.0 equiv) was added. FmocOSu (0.54 g, 1.60 mmol, 1.00 equiv) was dissolved in acetone (6.40 mL) and added dropwise to the reaction mixture. After 17 h of stirring at room temperature, MeCN and acetone were removed under reduced pressure. The mixture was treated with aq HCl (2 M) to pH 2. The resulting solution was extracted with EtOAc (6 × 40 mL), dried over Na_2SO_4, filtered, and concentrated in vacuo. The crude material undergone two purification steps by flash column chromatography (SiO_2, EtOAc/*n*-Pen, 2% AcOH) to yield **12 a** as a white solid (0.26 g, 0.64 mmol, 40%) according to literature [15]. ^{1}H NMR (600 MHz, CD_3OD): δ 7.78–7.73 (m, 2H), 7.67–7.61 (m, 2H), 7.35 (tq, *J* = 7.5, 1.0 Hz, 2H), 7.27 (td, *J* = 7.5, 1.2 Hz, 2H), 4.85 (s, 2H), 4.38–4.33 (m, 2H), 4.26–4.16 (m, 2H), 2.44–2.36 (m, 1H), 2.19 (dt, *J* = 14.3, 6.2 Hz, 1H), 1.64 (ddd, *J* = 14.3, 8.6, 7.1 Hz, 1H), 1.13 (d, *J* = 7.0 Hz, 2H) ppm; ^{13}C NMR (151 MHz, CD_3OD) δ 173.65, 157.23, 144.00, 143.81, 141.29, 129.28, 127.45, 126.82 (d, *J* = 4.3 Hz), 124.90, 119.58 (d, *J* = 3.1 Hz), 66.58, 52.13, 47.10, 35.12 (q, *J* = 26.5 Hz), 31.73, 12.43 (d, *J* = 3.7 Hz) ppm; ^{19}F NMR (565 MHz, CD_3OD) δ −74.50 (d, *J* = 8.2 Hz) ppm; ATR-FTIR (neat): 3392, 3022, 2920, 1698, 1522, 1446, 1262, 1170, 1050, 740 cm^{-1}; HRMS (ESI-TOF) *m/z*: $[M + Na]^+$ calcd for $C_{24}H_{20}F_3NO_4$, 430.1236; found, 430.1288.

Supporting Information

Supporting Information File 1

NMR spectra and HPLC chromatograms.
[https://www.beilstein-journals.org/bjoc/content/supplementary/1860-5397-21-52-S1.pdf]

Author Contributions

Maurizio Iannuzzi: conceptualization; data curation; formal analysis; funding acquisition; investigation; methodology; project administration; resources; supervision; validation; visualization; writing – original draft; writing – review & editing. Thomas Hohmann: conceptualization; data curation; formal analysis; funding acquisition; investigation; methodology; proj-

ect administration; resources; supervision; validation; visualization; writing – original draft; writing – review & editing. Michael Dyrks: data curation. Kilian Haoues: data curation. Katarzyna Salamon-Krokosz: data curation. Beate Koksch: conceptualization; data curation; formal analysis; funding acquisition; investigation; methodology; project administration; resources; supervision; validation; visualization; writing – original draft; writing – review & editing.

ORCID® iDs

Maurizio Iannuzzi - https://orcid.org/0009-0002-8183-2150
Michael Dyrks - https://orcid.org/0000-0001-6432-6905

Data Availability Statement

Data generated and analyzed during this study is available from the corresponding author upon reasonable request.

References

1. Wang, N.; Mei, H.; Dhawan, G.; Zhang, W.; Han, J.; Soloshonok, V. A. *Molecules* **2023,** *28,* 3651. doi:10.3390/molecules28093651
2. Almhjell, P. J.; Boville, C. E.; Arnold, F. H. *Chem. Soc. Rev.* **2018,** *47,* 8980–8997. doi:10.1039/c8cs00665b
3. Mei, H.; Han, J.; White, S.; Graham, D. J.; Izawa, K.; Sato, T.; Fustero, S.; Meanwell, N. A.; Soloshonok, V. A. *Chem. – Eur. J.* **2020,** *26,* 11349–11390. doi:10.1002/chem.202000617
4. Berger, A. A.; Völler, J.-S.; Budisa, N.; Koksch, B. *Acc. Chem. Res.* **2017,** *50,* 2093–2103. doi:10.1021/acs.accounts.7b00226
5. Buer, B. C.; Marsh, E. N. G. *Protein Sci.* **2012,** *21,* 453–462. doi:10.1002/pro.2030
6. Moschner, J.; Stulberg, V.; Fernandes, R.; Huhmann, S.; Leppkes, J.; Koksch, B. *Chem. Rev.* **2019,** *119,* 10718–10801. doi:10.1021/acs.chemrev.9b00024
7. Zou, Y.; Han, J.; Saghyan, A. S.; Mkrtchyan, A. F.; Konno, H.; Moriwaki, H.; Izawa, K.; Soloshonok, V. A. *Molecules* **2020,** *25,* 2739. doi:10.3390/molecules25122739
8. Han, J.; Takeda, R.; Liu, X.; Konno, H.; Abe, H.; Hiramatsu, T.; Moriwaki, H.; Soloshonok, V. A. *Molecules* **2019,** *24,* 4521. doi:10.3390/molecules24244521
9. Chowdhary, S.; Schmidt, R. F.; Sahoo, A. K.; tom Dieck, T.; Hohmann, T.; Schade, B.; Brademann-Jock, K.; Thünemann, A. F.; Netz, R. R.; Gradzielski, M.; Koksch, B. *Nanoscale* **2022,** *14,* 10176–10189. doi:10.1039/d2nr01648f
10. Hohmann, T.; Chowdhary, S.; Ataka, K.; Er, J.; Dreyhsig, G. H.; Heberle, J.; Koksch, B. *Chem. – Eur. J.* **2023,** *29,* e202203860. doi:10.1002/chem.202203860
11. Delamare, A.; Naulet, G.; Kauffmann, B.; Guichard, G.; Compain, G. *Chem. Sci.* **2022,** *13,* 9507–9514. doi:10.1039/d2sc02871a
12. Naulet, G.; Delamare, A.; Guichard, G.; Compain, G. *Eur. J. Org. Chem.* **2023,** *26,* e202201148. doi:10.1002/ejoc.202201148
13. Hohmann, T.; Dyrks, M.; Chowdhary, S.; Weber, M.; Nguyen, D.; Moschner, J.; Koksch, B. *J. Org. Chem.* **2022,** *87,* 10592–10604. doi:10.1021/acs.joc.2c00522
14. Chowdhary, S.; Moschner, J.; Mikolajczak, D. J.; Becker, M.; Thünemann, A. F.; Kästner, C.; Klemczak, D.; Stegemann, A.-K.; Böttcher, C.; Metrangolo, P.; Netz, R. R.; Koksch, B. *ChemBioChem* **2020,** *21,* 3544–3554. doi:10.1002/cbic.202000373
15. Biava, H.; Budisa, N. *Tetrahedron Lett.* **2013,** *54,* 3662–3665. doi:10.1016/j.tetlet.2013.04.128
16. Romoff, T. T.; Ignacio, B. G.; Mansour, N.; Palmer, A. B.; Creighton, C. J.; Abe, H.; Moriwaki, H.; Han, J.; Konno, H.; Soloshonok, V. A. *Org. Process Res. Dev.* **2020,** *24,* 294–300. doi:10.1021/acs.oprd.9b00399

License and Terms

BEILSTEIN JOURNAL OF ORGANIC CHEMISTRY

Origami with small molecules: exploiting the C–F bond as a conformational tool

Patrick Ryan, Ramsha Iftikhar and Luke Hunter*

Review

Open Access

Address:
School of Chemistry, The University of New South Wales (UNSW), Sydney 2052, Australia

Email:
Luke Hunter* - l.hunter@unsw.edu.au

* Corresponding author

Keywords:
conformational analysis; medicinal chemistry; organofluorine chemistry; stereoselective fluorination

Beilstein J. Org. Chem. **2025,** *21,* 680–716.
https://doi.org/10.3762/bjoc.21.54

Received: 10 December 2024
Accepted: 21 March 2025
Published: 02 April 2025

This article is part of the thematic issue "Organofluorine chemistry VI".

Guest Editor: D. O'Hagan

Abstract

When present within an organic molecule, the C–F bond tends to align in predictable ways with neighbouring functional groups, due to stereoelectronic effects such as hyperconjugation and electrostatic attraction/repulsion. These fluorine-derived conformational effects have been exploited to control the shapes, and thereby enhance the properties, of a wide variety of functional molecules including pharmaceutical agents, liquid crystals, fragrance chemicals, organocatalysts, and peptides. This comprehensive review summarises developments in this field during the period 2010–2024.

Introduction

In the art of origami, a practitioner takes a piece of paper and imposes a series of folds in order to transform it into an object that has an intricate three-dimensional shape. This concept can also be applied in the molecular world. Starting with a flexible small molecule, a practitioner can impose certain changes to its chemical composition such that the new molecule has a better-defined three-dimensional shape. Such "small molecule origami" can offer practical benefits. For example, if a drug molecule is pre-organised into the target-binding conformation, it should exhibit the desirable twin characteristics of high potency (since target binding will incur little entropic cost) and high selectivity (since off-target interactions will be minimised) [1].

There are several methods by which the conformations of small molecules can be controlled, but in this review we will focus upon one particular method, which is the installation of fluorine atoms into the structure.

The C–F bond has certain fundamental characteristics that enable it to serve as an effective conformational tool (Figure 1) [2-4]. First, the C–F bond is quite short at only ≈1.35 Å (cf. ≈1.09 Å for C–H, or ≈1.43 Å for C–O). The short length of the C–F bond, and the compact size of the fluorine atom itself, means that fluorine can be incorporated into an organic molecule as a replacement for hydrogen without drastically altering

the molecular volume. Second, the C–F bond is highly polarised. This means that any molecular conformation in which the C–F dipole is oriented antiparallel to another dipole within the molecule, or in which the fluorine atom is located close to a positively charged atom, will be stabilised. Third, the C–F bond has a low-lying σ* antibonding orbital, the larger lobe of which is located behind the carbon atom. This empty orbital is available to mix with any nearby filled orbital in a process known as hyperconjugation, and any molecular conformation in which such mixing can occur, will be stabilised [5-7].

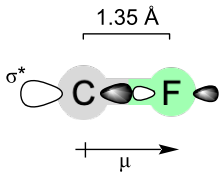

Figure 1: Fundamental characteristics of the C–F bond.

Putting all these concepts together, it is possible to conceive of a process whereby a conformationally flexible lead compound is rigidified in a predictable and desired way, by decorating it with an appropriate pattern of fluorine substituents.

The purpose of this review is to examine cases where this idea has been put into practice. This topic has previously been reviewed [8], but in the time that has elapsed since that prior publication the field has expanded considerably and so we believe that an updated account is warranted. In the present review, we have chosen to organise the material according to the functional group near to which the fluorine substituent can be introduced. We will start with the simplest scaffolds – alkanes – then we will progress to ethers, alcohols, sugars, amines (and their derivatives), carbonyl compounds, peptides, and finally sulfur-containing compounds. By arranging the material in this way, we hope that newcomers to the field might be able to readily envisage ways to apply these concepts to their own scaffolds of interest.

Review

1 Alkanes

The simplest organic scaffolds are the alkanes. In such molecules, C–C bond rotations often have low energy barriers, and they often deliver conformers that are similar in energy, and this means that many alkanes have considerable conformational flexibility. In this section, we will investigate the conformational outcomes that follow from replacing one or more hydrogens of an alkane with fluorine. Depending upon the precise fluorination pattern, different conformational outcomes will follow; usually, but not always, greater rigidity is seen. This section will commence by examining linear alkanes, then it will move on to examine cycloalkanes.

In the case of linear alkanes, we will first consider what happens if fluorine is introduced at the end of the chain. The installation of fluorine converts the alkyl chain from a non-polar into a polar motif (**I**, Figure 2). This has several implications. For example, if the C–C(F) bond rotates, the orientation of the terminal C–F bond dipole changes, and this can alter the overall dipole moment of the molecule. Indoles **1**–**3** illustrate this point (Figure 2) [9]. The non-fluorinated indole **1** has an unvarying molecular dipole moment of 1.90 D. In contrast, the monofluorinated analogue **2** can access three different staggered rotamers **2a**–**c** about the C–C(F) bond; all three of these rotamers have similar energies, but their molecular dipole moments vary considerably depending on whether the C–F dipole is aligned with or against the dipole of the indole moiety. A similar phenomenon occurs with the difluorinated analogue **3**. The fluorinated molecules **2** and **3** can be said to have a "chameleonic" character [9-14]: they have the ability to change polarity to suit their environment. This is a potentially valuable property in the context of drug design, because chameleonic fluorinated molecules such as compounds **2** and **3** might be expected to pass more easily through cell membranes, a manoeuvre which requires some level of solubility in both aqueous and organic environments.

Another consequence of introducing polar C–F bonds at the end of an alkyl chain, is that the terminal C–H bond also becomes polarised. In the case of the difluoromethyl group, the terminal hydrogen bears a partial positive charge and is able to act as a H-bond donor (**II**, Figure 2). This can influence the conformation of the molecule if there is a H-bond acceptor suitably positioned elsewhere in the molecule (e.g., **4** vs **5**, Figure 2) [15-17]. The ability of the difluoromethyl group to serve as a H-bond donor has also proven to be useful for optimising drug–target interactions [18-20], but since that application does not involve conformational control it is outside the scope of this review.

Another way to fluorinate the end of an alkyl chain is with a 1,2-difluoro pattern. The vicinal difluoro motif is able to sample different rotamers (e.g., with the C–F bonds aligned either *gauche* or *anti*). Crucially however, such rotamers have different energies. When the C–F bonds are aligned *gauche*, the vacant σ* orbital of each C–F bond is able to mix with the filled σ orbital of an adjacent C–H bond, and this hyperconjugative interaction stabilises the *gauche* conformer (**III**, Figure 2). The *anti* conformer does not benefit from this hyperconjugative stabilisation, and it is ≈1 kcal·mol^{-1} higher in energy. Thus, we now have a situation where the fluorinated structural motif is not a passive chameleon as was seen above for the 1,1-difluoro

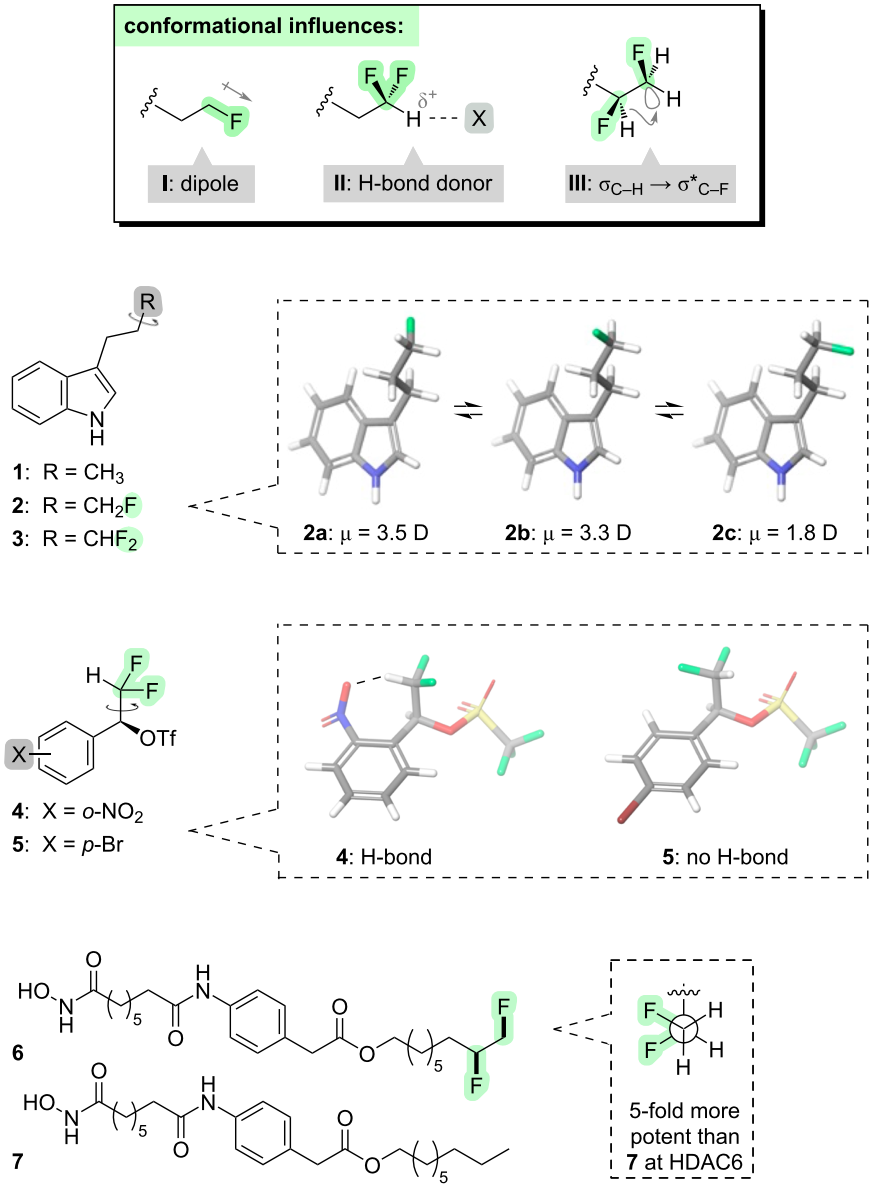

Figure 2: Incorporation of fluorine at the end of an alkyl chain.

pattern, but rather it exerts its own conformational character [21]. The 1,2-difluoro motif has been exploited in the design of bioactive molecules [22,23] such as the histone deacetylase (HDAC) inhibitors **6** and **7** (Figure 2). The presence of the 1,2-difluoro moiety in **6** leads to greater potency and selectivity for certain HDAC isoforms, attributable to the higher polarity of the fluorinated motif with its *gauche*-aligned C–F bonds [22].

We will now consider what happens when fluorine is introduced into the middle of an alkyl chain. If two fluorines are attached to the same carbon (i.e., a 1,1-difluoro pattern), a subtle but important perturbation occurs to the shape of the alkyl chain: the C–C(F_2)–C angle widens to ≈117° (**I**, Figure 3). This can be attributed to the electron-withdrawing character of the fluorine atoms, which accumulates high electron density within a small volume and allows the C–C bonds to spread further apart from one another [2]. An alternative explanation for this phenomenon is provided by Bent's rule [24], which predicts that the C–F bonds will have greater p character and the C(F_2)–C bonds will have greater s character, with an accompanying deviation of the central carbon atom away from a perfectly tetrahedral shape. A functional outcome of C–C(F_2)–C angle widening in *gem*-difluoroalkanes is seen in the rates of the ring-closing methathesis reactions of the dienes **8** and **9**

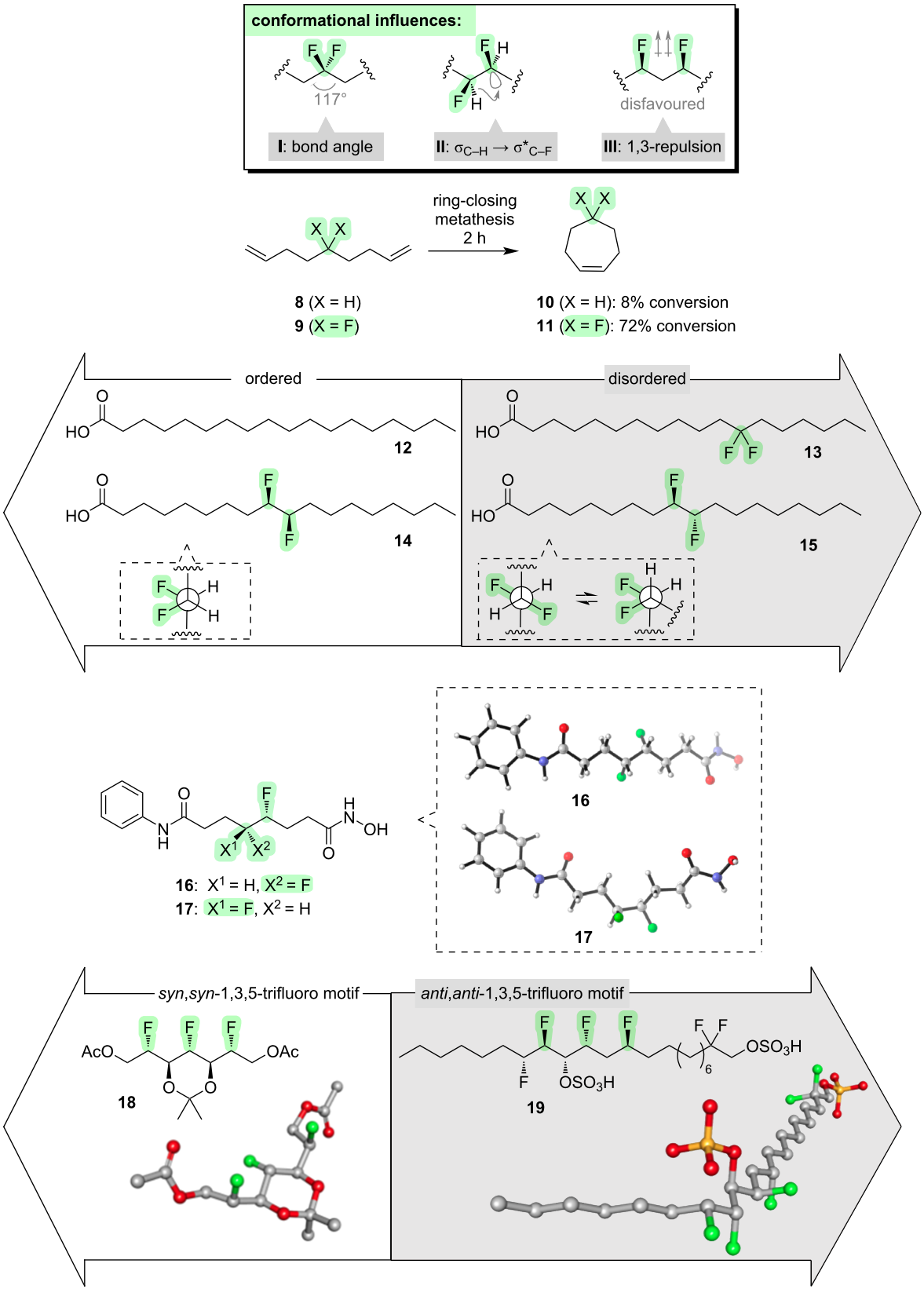

Figure 3: Incorporation of fluorine into the middle of a linear alkyl chain.

(Figure 3) [25]. The fluorinated substrate **9** cyclises much more efficiently than the non-fluorinated substrate **8**, and this was attributed to a thermodynamic effect, i.e., a more favourable accommodation of a wider C–C(F_2)–C angle within the cyclic product **11**. Another illustration of the geometric perturbation caused by the wider C–C(F_2)–C angle comes from the stearic acids **12** and **13** (Figure 3); the *gem*-difluorinated analogue **13** has substantially greater conformational disorder compared to the non-fluorinated stearic acid **12** (Figure 3) [26].

If two fluorines are introduced into the middle of an alkyl chain in a 1,2-pattern, several competing factors arise that can influence the molecular conformation [27]. One factor is hyperconjugation: conformations in which the $\sigma^*_{C–F}$ orbitals are aligned with either $\sigma_{C–H}$ orbitals (**II**, Figure 3), or, to a lesser extent, $\sigma_{C–C}$ orbitals, will be favoured. Another factor is simple sterics: conformations in which the flanking alkyl moieties are further apart from one another will be favoured. A third factor is polarity: for example, conformations in which the two C–F bonds are aligned *gauche* will be favoured in water due to their high molecular dipole moment. A final layer of complexity is afforded by the stereochemistry of the 1,2-difluoroalkane motif: the various conformational factors described above will aggregate differently depending upon whether the 1,2-difluoro stereochemistry is *threo* or *erythro*. For example, the diastereoisomeric difluorinated stearic acids **14** and **15** (Figure 3) are found to have very different physical properties [28]. When deposited into a monolayer above a water phase, the *threo*-isomer **14** occupies a small molecular area and packs efficiently, and this was attributed to the ready ability of this stereoisomer to adopt an extended alkyl chain in which the C–F bonds are aligned *gauche*. In contrast, the *erythro*-isomer **15** occupies a larger molecular area and requires a higher pressure to achieve a monoloayer, and this was attributed to the partial tendency of this stereoisomer to adopt a bent alkyl chain. Another example of the use of the 1,2-difluoro moiety to influence the shape of an alkyl chain is seen in the HDAC inhibitors **16** and **17** (Figure 3) [29]. The *threo*-isomer **16** is found to be consistently more potent across a panel of HDAC isoforms than the *erythro*-isomer **17**, and this was taken as evidence that an extended zigzag conformation of the alkyl chain is required for binding to HDAC.

If two fluorines are introduced into the middle of an alkyl chain in a 1,3-pattern, a new conformational effect emerges. The 1,3-C–F bonds tend to avoid a parallel alignment, due to dipolar repulsion (**III**, Figure 3) [30-32]. This phenomenon can be harnessed to control molecular conformations in a predictable way, and once again the stereochemistry is important. For example, compare the natural product analogues **18** and **19** (Figure 3) [30,33]. Compound **18** contains a 1,3,5-trifluoroalkane moiety with *syn*,*syn*-stereochemistry, and it is found to adopt a bent alkyl chain which is necessary for the avoidance of parallel 1,3-difluoro alignments [30]. Compound **19** also contains a 1,3,5-trifluoroalkane moiety, but it has *anti*,*anti*-stereochemistry and now this portion of the alkyl chain is able to adopt an extended zigzag conformation without incurring any parallel 1,3-difluoro alignments [33].

Other fluorine patterns have been shown to control molecular conformation when embedded in the middle of an alkyl chain [34], for example the 1,1,3-trifluoro motif [35], the 1,1,3,3,-tetrafluoro motif [36] and the 1,1,4,4-tetrafluoro motif [36]. In general, the conformational outcomes in such systems can be understood in terms of an aggregate of the various conformational influences already described (i.e., **I**–**III**, Figure 3).

We will now consider what happens when fluorine is introduced across much, or all, of an alkyl chain. The extreme case is a perfluoroalkane, in which every hydrogen is replaced with a fluorine (e.g., **I**, Figure 4). Perfluoroalkanes are not usually thought of in terms of controllable molecular conformations, but there is one aspect of their conformational behaviour that merits discussion here. The carbon chain in perfluoroalkanes deviates in a precise way from an ideal zigzag conformation: each C–C–C–C dihedral angle is ≈165°, and when propagated along the chain this slight deviation from antiperiplanarity leads to a gradual helical twist (**20**, Figure 4) [37]. The enantiomeric helix is also possible. Various explanations have been offered for this helical propensity, but the current understanding is that the slight twist enables better $\sigma_{C–C} \rightarrow \sigma^*_{C–F}$ hyperconjugation [38].

If just one fluorine atom is attached to every carbon of an alkyl chain (e.g., **II**, Figure 4), then a structure results that is conceptually intermediate between alkanes and perfluoroalkanes. Such structures, dubbed “multivicinal fluoroalkanes”, have interesting conformational properties that are dependent upon the stereochemistry [39-42]. For example, the diastereoisomeric 1,2,3-trifluoroalkanes **21**–**24** (Figure 4) adopt distinct conformations, governed in each case by the avoidance of parallel 1,3-C–F bonds and the maximisation of $\sigma_{C–H} \rightarrow \sigma^*_{C–F}$ hyperconjugation [43]. Notably, the overall shape of diastereoisomer **22** closely mimics that of 2-benzyl-2,3-dihydrobenzofuran (overlaid in Figure 4), a structural motif that is commonly found within bioactive natural products.

Having seen that the conformations of multivicinal fluoroalkanes can be altered by changing the stereochemistry, it follows that other physical properties can be altered, too [44]. For example, consider compounds **26** and **27** (Figure 4), which are fluorinated analogues of the multiple sclerosis drug gilenya

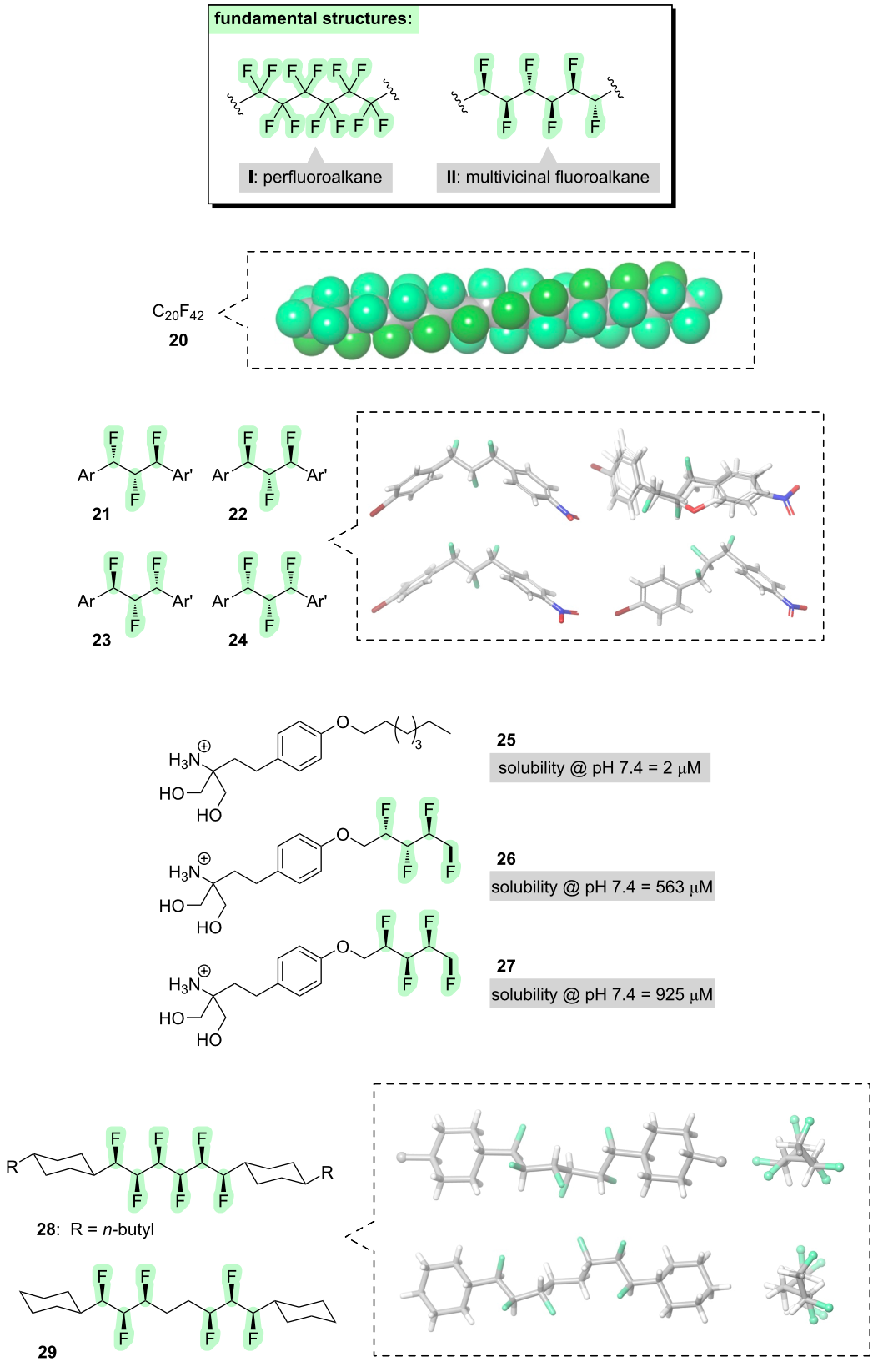

Figure 4: Incorporation of fluorine across much, or all, of a linear alkyl chain.

(**25**) [45]. The *syn*,*anti*-fluorinated stereoisomer **26** has a much higher water solubility than gilenya (**25**), attributable to the presence of new polar bonds in **26** (although the different alkyl chain lengths in **25** and **26** should also be acknowledged). Notably, the all-*syn* fluorinated stereoisomer **27** displays a further increase in water solubility, even compared to the *syn*,*anti*-stereoisomer **26**, highlighting the dramatic impact that a seemingly minor stereochemical change can have upon physical properties.

Another functional context in which multivicinal fluoroalkanes have been explored is in liquid crystals [8,40]. Liquid crystalline materials require the molecules to be rod-shaped, and to have a dipole moment that is oriented perpendicular to the long axis of the molecule. The strategic incorporation of multi-fluorine patterns has been investigated as a method for simultaneously modulating both of these molecular characteristics, i.e., the molecular shape and the dipole moment. For example, compound **28** (Figure 4) contains six vicinal fluorines with all-*syn* stereochemistry [46]. This molecule adopts a helical conformation which maximises 1,2-difluoro *gauche* alignments and minimises 1,3-difluoro parallel alignments. (Note that the helix in this case is much "tighter" than the perfluoroalkane helix described above.) The helical conformation of **28** leads to a low molecular dipole moment, because every C–F bond can be paired with another that has the opposite orientation. In contrast, compound **29** (Figure 4) divides the six fluorines into two groups of three, separated by an ethylene spacer [47]. The same helical conformation is maintained, but the interruption of the fluorine pattern means that the C–F dipoles no longer all cancel each other out, and this results in a very high calculated molecular dipole (μ = 7.15 D).

Having concluded our survey of linear alkanes, we will now focus on cyclic systems [48].

When fluorine is introduced into a small cycloalkane (Figure 5), the preferred pucker is determined through a competition between hyperconjugation (e.g., $\sigma_{C–H} \rightarrow \sigma^*_{C–F}$) and steric effects. For fluorocyclobutane (**30**) and fluorocyclohexane (**32**), the preferred conformation is the one in which fluorine is equatorial [48], with sterics playing the dominant role. In fluorocyclopentane (**31**), the preferred conformation has historically been difficult to conclusively pin down, with different studies identifying different candidates for the global minimum including an envelope with fluorine axial (**31a**); an envelope with fluorine equatorial (**31c**); or, most recently, an intermediate twist conformation (**31b**) [48]. Multiple fluorines can sometimes provide better control. For example, all-*syn*-1,2,3,4-tetrafluorocyclopentane (**33**) appears to prefer an envelope conformation with fluorine in the axial position [49]. Another example of conformational control via multiple fluorines is seen with the trifluorinated cyclohexene **34**: this molecule prefers the half-chair conformation in which $\sigma_{C–H} \rightarrow \sigma^*_{C–F}$ hyperconjugation with the flanking methylene groups is maximised (Figure 5) [50].

When discussing small-ring cycloalkanes, it is impossible to ignore a substantial research effort that has focused upon multifluorinated cyclohexanes [40,48,51]. Notable examples that have been synthesised and studied include all-*syn* 1,3,4-trifluorohexane [52], 1,1,3,3-tetrafluorocyclohexane [53], all-*syn*-1,2,3,4-tetrafluorocyclohexane [54], all-*syn*-1,2,4,5-tetrafluorocyclohexane [55-61], and various stereoisomers of 1,2,3,4,5,6-hexafluorocyclohexane [62] including the iconic all-*syn*-isomer [63-71]. These molecules have been shown to have a variety of fascinating properties and applications, mostly associated with their very high molecular dipoles. However, since the fluorination patterns in these cases do not really control or alter the ring pucker, they are outside the scope of this review.

Finally, we will examine larger-ring cycloalkanes. Large rings have more degrees of freedom than small rings, and hence they offer interesting opportunities and challenges in terms of conformational control. For example, consider cyclododecane (**35**, Figure 5). This molecule has a global minimum energy conformation that features a square shape, but this conformation suffers from steric clashes between 1,4-pairs of hydrogen atoms on the inside of the macrocycle, and so it is only slightly preferred over multiple other possible conformations. Fluorine has the ability to stabilise the square conformation. The key consideration is that 1,1-difluoroalkanes have a wide C–C(F_2)–C angle, as previously discussed; this wide angle is favourably accommodated at the corner positions of the square shape (e.g., **36**, Figure 5) because it alleviates the transannular hydrogen clashes [72]. This effect proves to be quite general: it can be harnessed to force the cyclododecane macrocycle into different shapes by positioning two CF_2 groups in different relative locations around the macrocycle (e.g., **37**, Figure 5), and it can be applied to larger macrocycles too [73]. Most strikingly, this effect has been exploited to modulate the aromas of fragrance compounds (e.g., compounds **38** and **39**, Figure 5) by fine-tuning the shape of the macrocycle [74,75].

2 Ethers

We now turn our attention from alkanes to what is arguably the simplest heteroatom-containing functional group: the ether. The presence of oxygen within a carbon chain offers several new opportunities for engagement by an introduced fluorine atom.

First, we will consider what happens if fluorine is introduced onto one of the carbons that is directly attached to oxygen

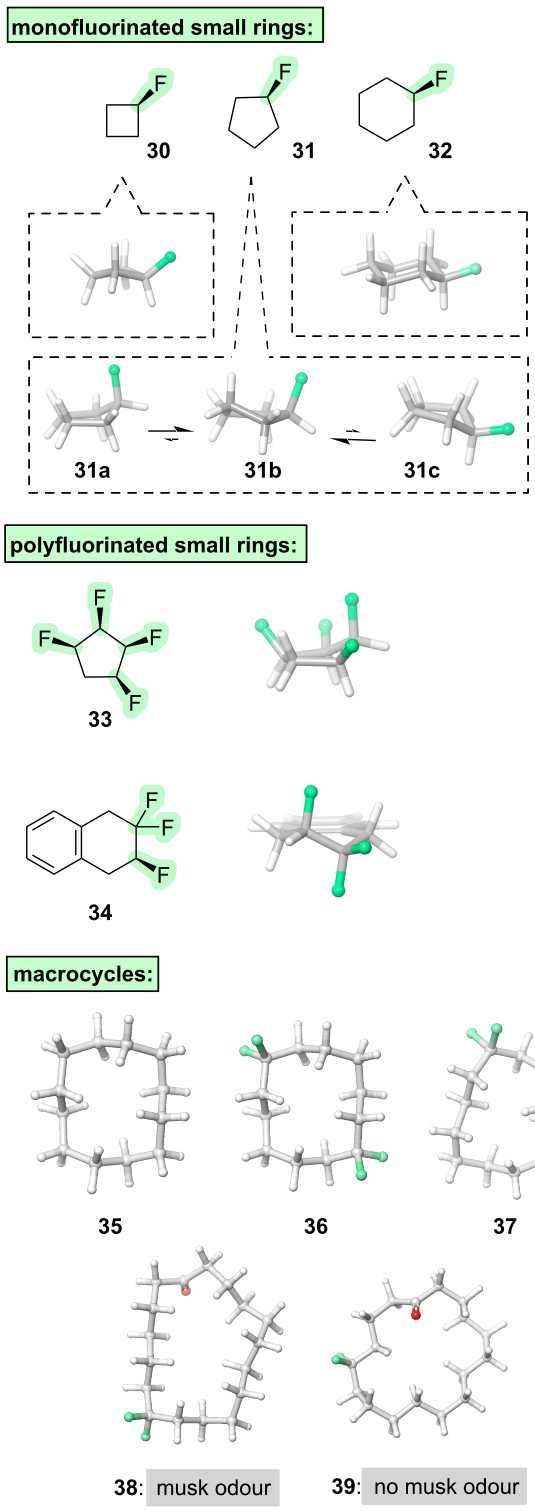

Figure 5: Incorporation of fluorine into cycloalkanes.

(Figure 6). This makes possible a hyperconjugative interaction between a lone pair on oxygen and the σ* orbital of the C–F bond (**I**, Figure 6) [76]. This interaction biases the rotational profile about the O–C(F) bond, such that the *endo* orientation of the C–F bond (as depicted in **I**, Figure 6) is lower in energy than the *exo* conformer (not shown). This is an example of the anomeric effect [77].

The anomeric effect can be visualised perhaps most clearly when the ether moiety is embedded within a small ring [78,79]. For example, consider the diastereoisomeric BACE-1 inhibitors **40** and **41** (Figure 6). The preferred ring pucker for each of **40**, **41** positions the C–F bond in an axial position, allowing $n_O \rightarrow \sigma^*_{C–F}$ hyperconjugation. The shape adopted by diastereoisomer **41**, with a pseudoaxial orientation of the pendant aryl moiety, is better for target-binding and hence **41** is a ≈10-fold more potent inhibitor of BACE-1 than **40**.

Several further examples of cyclic ethers will be examined in section 5 (sugars).

The anomeric effect applies in acyclic ethers, too. Consider the non-fluorinated scaffold, Ph–O–CH_3 (**42**, Figure 6). This molecule preferentially adopts a planar conformation [80]. The planar conformation suffers slightly from a steric clash between the methyl group and an aryl hydrogen, but this is outweighed by the favourable conjugation of the π-system with the lone pair in the 2p orbital of the sp^2-hybridised oxygen atom. When one fluorine is introduced into this scaffold in the form of a fluoromethyl group (**43**, Figure 6), the gross conformation is little changed, but notably the fluorine preferentially resides at an *endo* position (oriented back towards the aryl moiety) which enables $n_O \rightarrow \sigma^*_{C–F}$ hyperconjugation [81].

Progressing to the difluoromethyl system (**44**, Figure 6): now there is a very different situation because the molecule is quite disordered [81,82]. Rotamers about both Ar–O and (Ar)O–C bonds are now observed with similar energies; this notably includes conformations in which the difluoromethyl group is orthogonal to the aryl plane (as depicted in Figure 6). The accessibility of the orthogonoal conformation of **44** can be rationalised by a new effect, namely, hyperconjugation between the π-system and the σ* orbital of the O–C(F) bond (**II**, Figure 6). Overall, **44** is a disordered molecule which has potentially useful chameleonic polarity (and also lipophilic H-bond-donor ability).

Progressing to the trifluoromethyl system (**45**, Figure 6): now there is an even stronger tendency for the fluorinated group to be oriented orthogonal to the aryl plane [80]. This can be explained by two factors. First, $\pi \rightarrow \sigma^*_{O–C(F)}$ hyperconjugation is stronger in the trifluoromethyl case. Second, the steric demand of the trifluoromethyl group would cause a significant clash with the aryl moiety in the planar conformation.

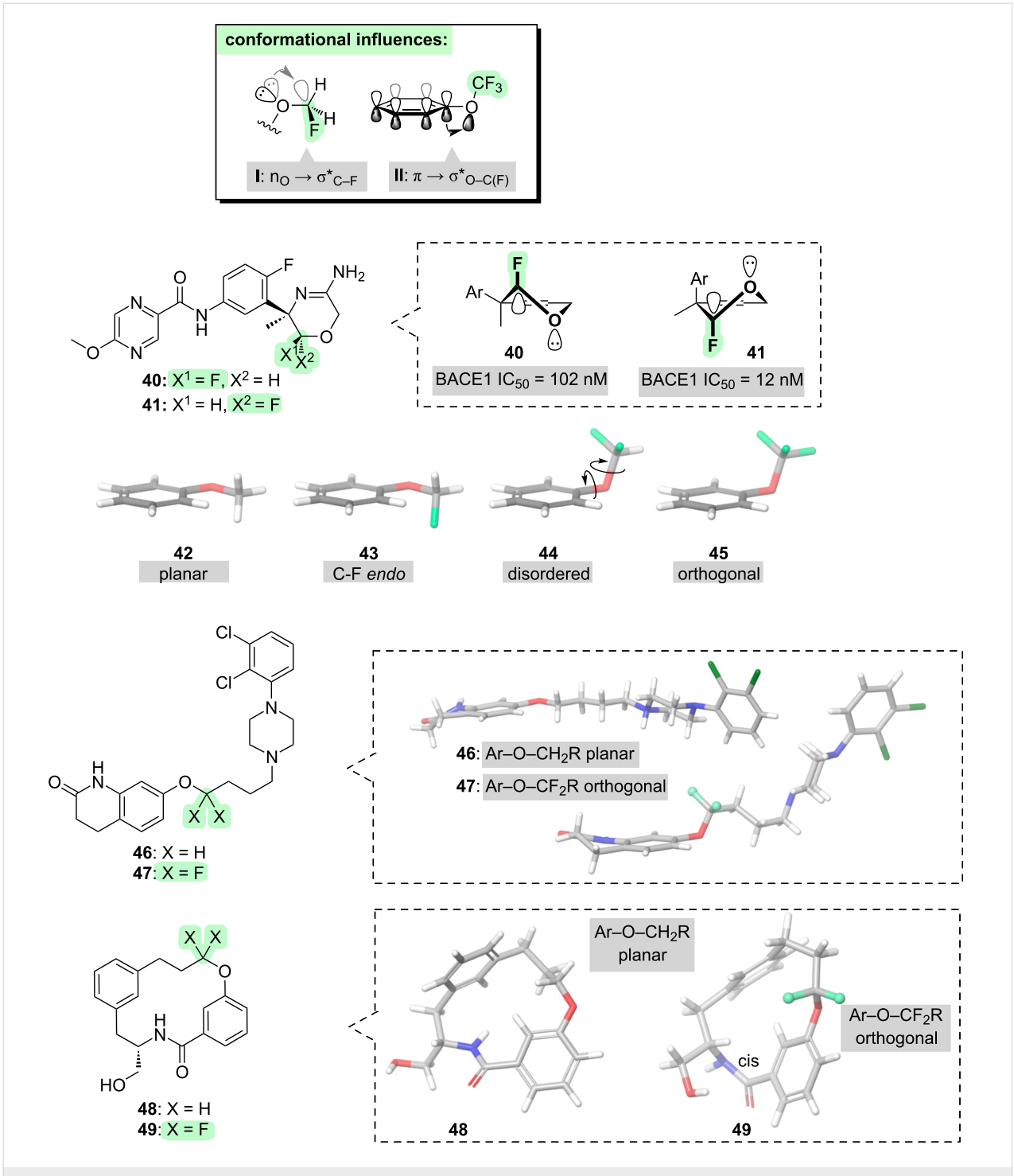

Figure 6: Conformational effects of introducing fluorine into an ether (geminal to oxygen).

The increased accessibility of the orthogonal conformation of highly fluorinated ethers is also seen when Ar–O–CF_2- is a linker moiety. For example, consider compound **47** (Figure 6), which is a fluorinated analogue of the antipsychotic drug, aripiprazole (**46**). The presence of the fluorine atoms in **47** causes a change in the conformation of the aryl ether moiety from planar in **46** [83] to orthogonal in **47** [84], leading to different overall molecular shapes for compounds **46** and **47**. Another illustration of this phenomenon is seen with the macrocycles **48** and **49**, which are simplified analogues of a known BACE-1 inhibitor [85]. In the non-fluorinated macrocycle **48**, the aryl ether moiety features a planar conformation, whereas in the fluori-

nated macrocycle **49**, the aryl ether moiety adopts an orthogonal conformation which necessitates substantial reorganisation elsewhere in the macrocycle including a *cis*-amide on the opposite side of the molecule.

We now consider what happens if fluorine is introduced onto a carbon that is one atom further away from the ether oxygen (Figure 7). So doing introduces the opportunity for a new stereoelectronic phenomenon: a *gauche* effect for the O–C–C–F moiety (**I**, Figure 7). If the vicinal C–O and C–F bonds align *gauche* to one another, two stabilising hyperconjugative interactions can take place (i.e., $\sigma_{C-H} \rightarrow \sigma^*_{C-F}$ and $\sigma_{C-H} \rightarrow \sigma^*_{C-O}$, with the former likely to be stronger). This is only a subtle effect, with the *gauche* conformer just ≈0.3 kcal·mol^{-1} lower in energy than the *anti* conformer (not shown) [86], but it can nevertheless have a significant impact upon molecular properties.

The fluorine–oxygen *gauche* effect has been exploited to influence the properties of liquid crystals [86,87]. For example, the vicinal fluoroether **50** (Figure 7) can adopt a low-energy conformation in which the terminal C–F bond aligns *gauche* to the vicinal C–O bond. This orientation of the C–F bond enlarges the overall molecular dipole moment which is oriented perpendicular to the long axis of the molecule; as described earlier, this an important feature in liquid crystalline materials.

Now consider the case where two fluorine atoms are introduced onto the same carbon (e.g., **51**, Figure 7) [88,89]. This situation is more complex. The *gg* conformer, in which both fluorines are *gauche* to oxygen, benefits from multiple hyperconjugative interactions (i.e., $\sigma_{C-H} \rightarrow \sigma^*_{C-F}$ and $\sigma_{C-H} \rightarrow \sigma^*_{C-O}$) and it is also the most polar conformation, so it is favoured in water. However, the *gg* conformer suffers from Lewis F···O repulsion. In contrast, the *ga* and *ag* conformers have less hyperconjugation but also less F···O repulsion, and are less polar. Since all three conformers are close in energy, the difluoroethyl ether moiety in **51** can be considered to have chameleonic polarity.

3 Alcohols

We now progress from ethers (section 2) to a closely related class of molecules, namely, the alcohols. The focus here in section 3 will be mostly on simple examples; more complex poly-ol examples will be discussed in section 4 (sugars).

Taking the example of a simple alcohol such as ethanol, consider what happens when a fluorine atom is introduced vicinal to the hydroxy group (Figure 8). As was seen with ethers (**I**, Figure 7), there is again a subtle preference for the O–C–C–F motif to adopt a *gauche* conformation [44]. This is attributable in part to the hyperconjugation phenomenon (**I**, Figure 8). In several published crystal structures of vicinal fluorohydrins, the F–C–C–O motif adopts a *gauche* conforma-

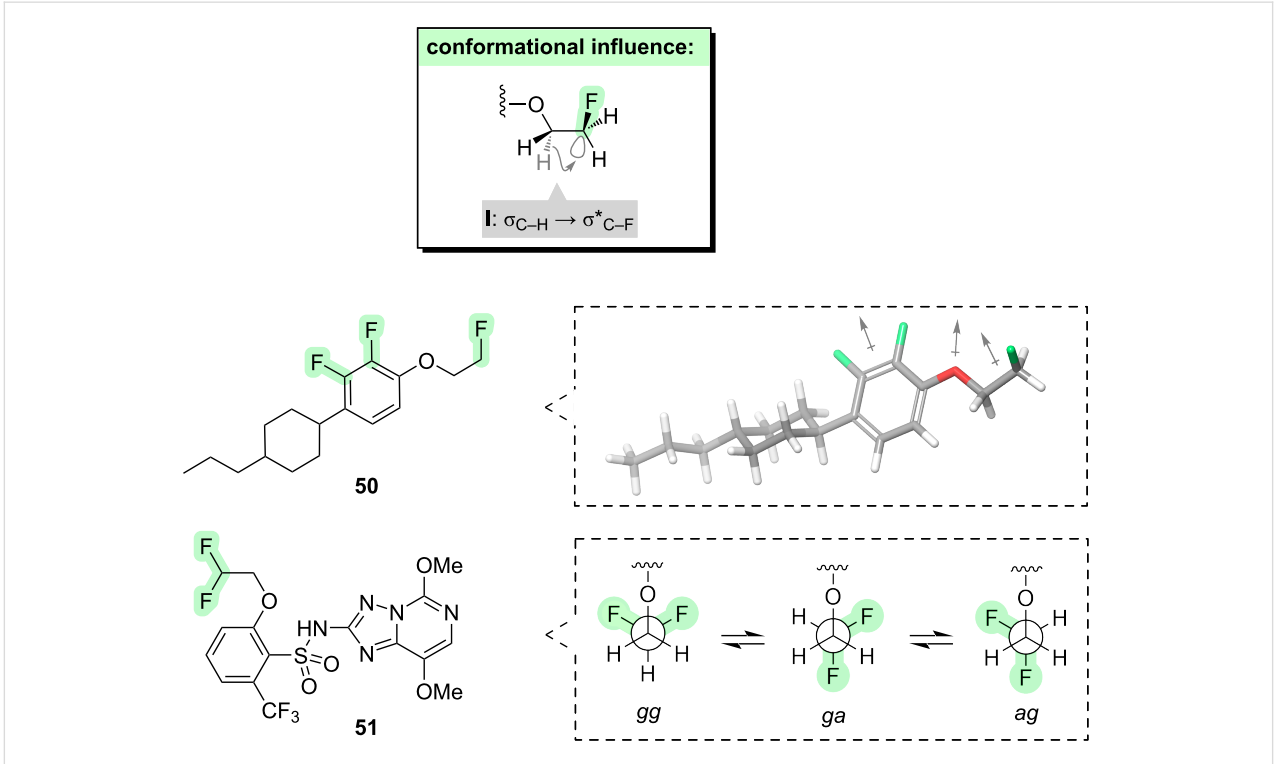

Figure 7: Conformational effects of introducing fluorine into an ether (vicinal to oxygen).

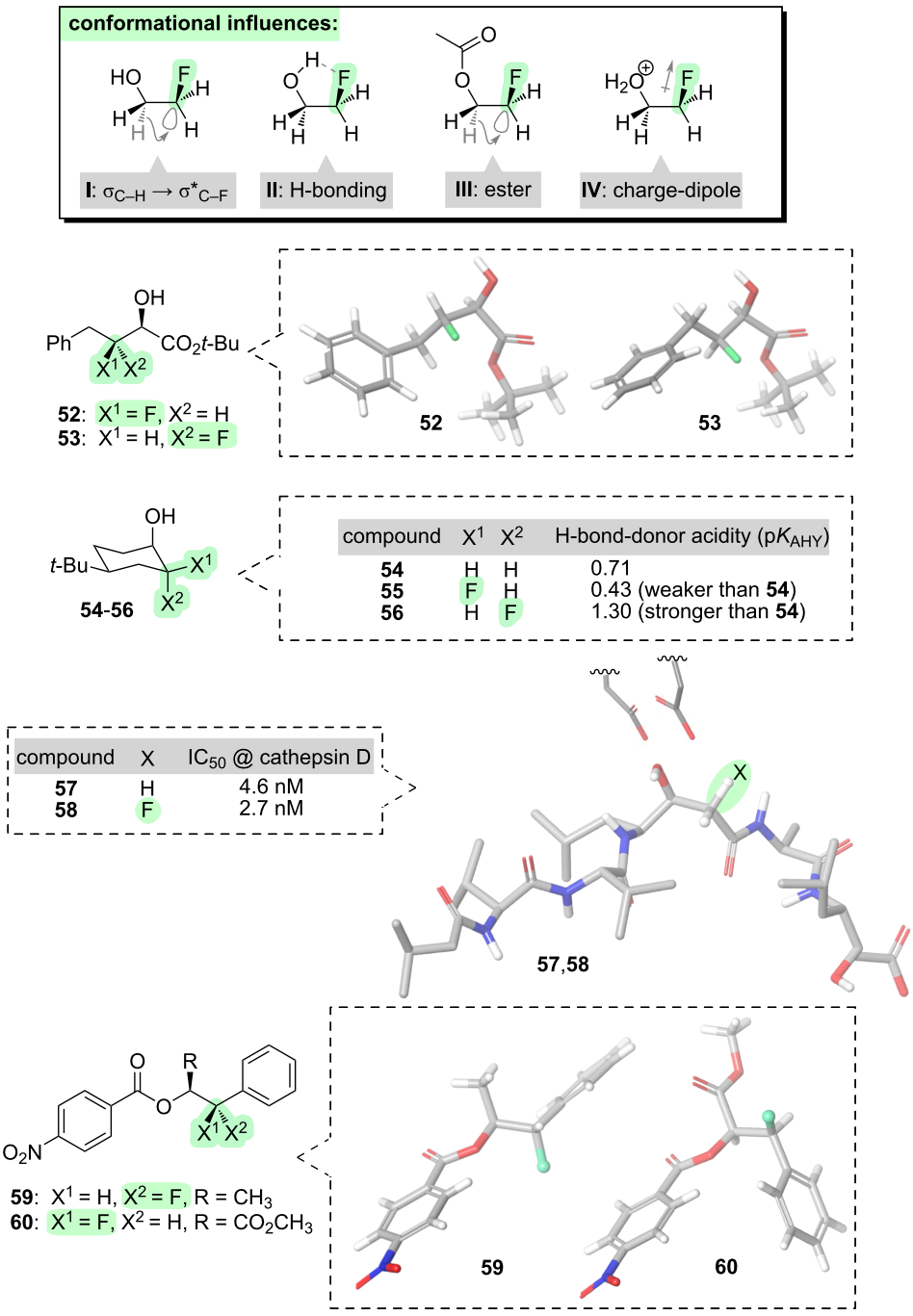

Figure 8: Effects of introducing fluorine into alcohols (and their derivatives).

tion as expected [90-93]. This *gauche* preference can induce different overall shapes to be adopted by diastereoisomeric vicinal fluorohydrins (e.g., **52** and **53**, Figure 8) [94,95], marking this motif as a potentially valuable tool for molecular design.

Additional stabilisation of the *gauche* conformation of vicinal fluorohydrins can also be afforded by an intramolecular H-bond (**II**, Figure 8) [96-98]. Fluorine is a weaker H-bond acceptor than oxygen or nitrogen [99-101], but F···H attraction can still be significant in some contexts [102,103] and the intramolecular H-bond depicted in **II** (Figure 8) can have a significant impact upon the properties of vicinal fluorohydrins [97].

The possibility of intramolecular H-bonding in vicinal fluorohydrins has important consequences for the molecules' intermo-

lecular interactions too. The intramolecular H-bond makes the hydroxy group a weaker intermolecular H-bond donor [104] (e.g., **55** vs **54**, Figure 8). This runs counter to a longstanding assumption [105] that the inductive effect of fluorine should always make the hydroxy group a stronger H-bond donor. For non-rigid molecules, the greater the population of intramolecularly H-bonded conformers, the worse the hydroxy group will be as an intermolecular H-bond donor [106]. To be clear, fluorine can make the hydroxy group a stronger intermolecular H-bond donor in certain circumstances, for instance in highly-fluorinated alcohols (e.g., hexafluoroisopropanol) [107], or in rigid molecules where intramolecular H-bonding is not possible [104] (e.g., **56**, Figure 8); but it is not a universal phenomenon.

The issue of intra- vs intermolecular H-bonding of vicinal fluorohydrins can complicate matters if the hydroxy group is required for target binding. A series of (fluorinated) protease inhibitors illustrates this point (**57** and **58**, Figure 8) [108]. The non-fluorinated lead compound **57** is a natural product known as pepstatin; the backbone of **57** adopts a bent conformation when bound to the protease enzyme, and the hydroxy group of **57** interacts with catalytic aspartate residues in the active site. The fluorinated pepstatin analogue **58** was predicted to be pre-organised into the bent conformation and hence be a more potent inhibitor than **57**. Compound **58** was indeed found to be more potent than **57** (Figure 8), but the magnitude of the improvement was very small. This might be because fluorine delivered competing outcomes: on one hand, fluorine-derived conformational pre-organisation may have delivered an entropic benefit for target binding, but on the other hand, fluorine also may have caused a reduction of the H-bond-donor acidity of the hydroxy group of **58**. (See section 6, which focuses on carbonyl compounds, for a further explanation of the predicted conformation of **58**.)

Finally, two structural variations on the hydroxy group should be mentioned. First, if the hydroxy group is acylated (i.e., to generate an ester), the *gauche* O–C–C–F conformation is favoured over *anti* more strongly than was seen for the parent alcohol (e.g., energy difference between *gauche* and *anti* = 1.0 kcal·mol^{-1} for esters; 0.3 kcal·mol^{-1} for alcohols) [109]. This is likely due to enhanced hyperconjugation effects in the ester case (i.e., $\sigma_{C–H} \rightarrow \sigma^*_{C–F}$ and $\sigma_{C–H} \rightarrow \sigma^*_{C–O}$, **III**, Figure 8). Examples of this phenomenon are seen in the crystal structures of compounds **59** and **60** (Figure 8), which are synthetic precursors of β-fluorinated amphetamines; both of **59** and **60** feature a *gauche* O–C–C–F alignment regardless of other nearby functionality [110].

Second, if the hydroxy group becomes protonated under acidic conditions, the *gauche* $^+$O–C–C–F conformation becomes dramatically more favoured over *anti* (e.g., energy difference between *gauche* and *anti* = 7.2 kcal·mol^{-1}). This is due to a new charge-dipole phenomenon (**IV**, Figure 8) that adds to the hyperconjugation and intramolecular H-bonding phenomena [96].

The conformational effects of fluorination in these two derivatives (i.e., esters and protonated alcohols) have been little exploited to date in the design of functional molecules [111]. However, one standout example that features both an ester moiety and an amino group will be discussed later, in section 5 of this review [112].

4 Sugars

We have examined several classes of molecules of gradually increasing complexity, progressing from alkanes (section 1) to ethers (section 2) and then alcohols (section 3). Throughout, we have seen that the introduction of fluorine can influence the molecular conformations in useful ways. We will now consider a more complex class of molecules in which the fluorine-derived conformational effects seen in all three of the preceding sections are united: namely, sugars.

Sugars are ubiquitous molecules in biology. Their functions permeate every aspect of life, including as essential components of oligonucleotide structure; as principal players in metabolism and energy storage; as motifs for the post-translational modification of proteins; and as partners in myriad supramolecular recognition processes. Therefore, methods for controlling the conformations of sugars are likely to have diverse and valuable applications in biotechnology and medicine.

The structure of a sugar molecule offers several potential locations where fluorine can be introduced. Typical patterns include the introduction of –CHF– or –CF_2– as a replacement for the ring oxygen, or for one (or more) of the –CH(OH)– groups, or for the anomeric oxygen. The various conformational outcomes that flow from making such modifications are discussed below. It should be noted that introducing fluorine into sugars has many other effects, too, e.g., modulating lipophilicity [44,113-115], enabling target-binding interactions to be elucidated [116,117], or providing the opportunity for ^{19}F and ^{18}F imaging. Other reviews have covered many of these aspects [118,119], but here we will focus exclusively on the conformational aspects.

We will first consider how fluorination can affect the ring pucker (Figure 9).

For pyranoses (i.e., six-membered ring sugars), the classic $^4C_1$ chair conformation is usually strongly preferred. This confor-

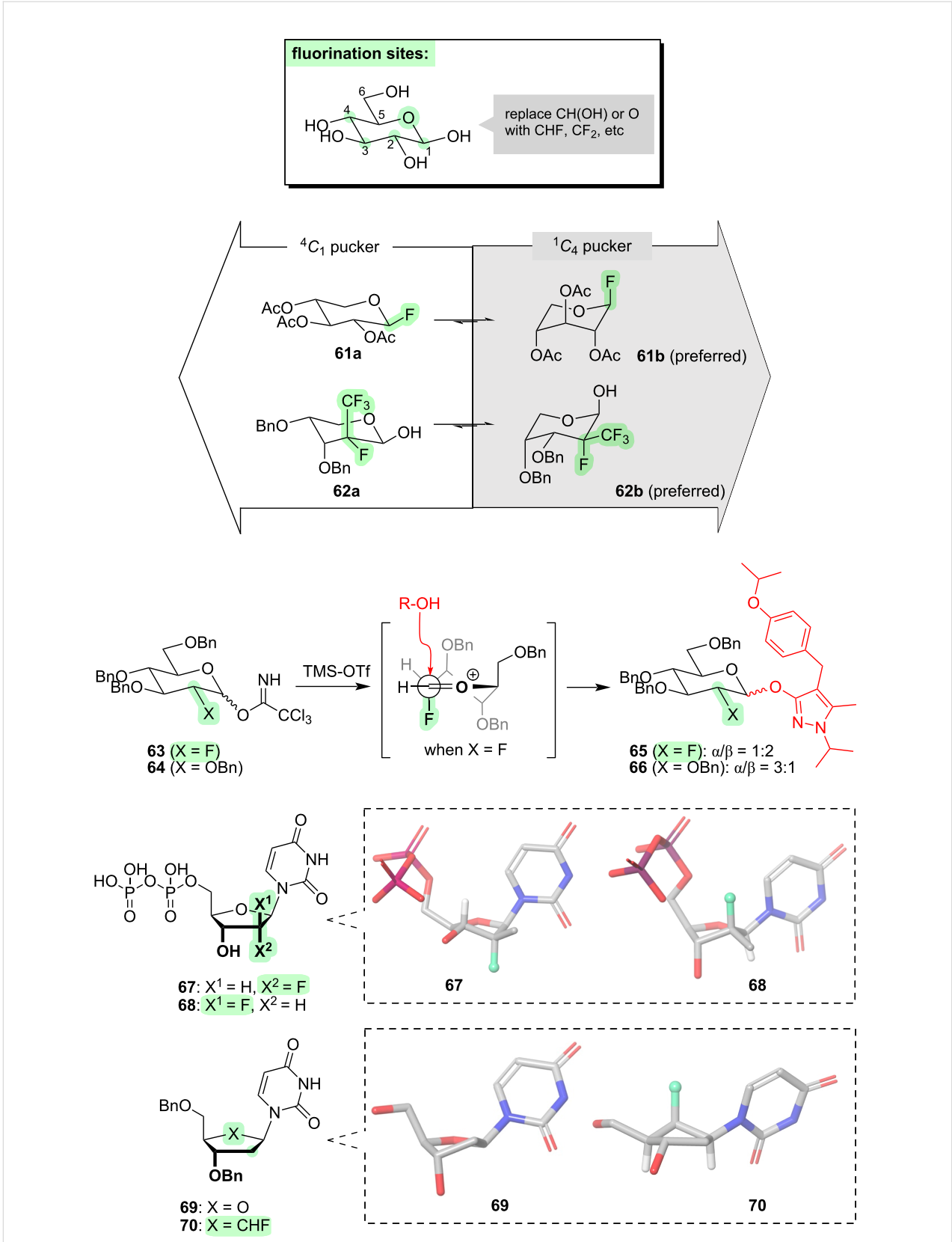

Figure 9: Controlling the ring pucker of sugars through fluorination.

mation tends to be maintained even if one or several fluorines are introduced as replacements for hydroxy groups at positions C-1 and/or C-2 and/or C-3 and/or C-4, regardless of stereochemistry and even if 1,3-difluoro repulsion is incurred [44,117,120-122]. However, there are certain special circumstances where fluorination can invert the pucker. For example, in pentopyranoses (i.e., sugars lacking an exocyclic carbon), the ring pucker can be inverted by placing fluorine at C-1 with appropriate stereochemistry, due to a strong anomeric effect (**61**, Figure 9) [123]. In another example, the ring pucker of a pentopyranose was observed to be inverted when the –CH(OH)– moiety at C-2 was replaced with a –C(F)(CF_3)– moiety with appropriate stereochemistry (i.e., **62**, Figure 9) [124]; in this case, the bulky CF_3 group presumably has a strong tendency to occupy the equatorial position.

Up to now, we have seen that fluorine has a rather limited ability to influence the pucker of the six-membered ring of pyranoses. However, it must be remembered that pyranoses are reactive molecules that can undergo, e.g., glycosylation, and it emerges that fluorine can play a much more significant conformational role during the dynamics of such chemical reactions [125-130]. Glycosylation reactions (e.g., **63** → **65** and **64** → **66**, Figure 9) proceed via an oxocarbenium intermediate. If fluorine is located at C-2, an electrostatic attraction might be expected between the partially negative fluorine and the positively charged C=O^+ moiety, and this interaction would favour one of the half-chair conformations of the oxocarbenium intermediate (Figure 9) [131,132]. Also, in the preferred pucker, the C–F bond is oriented orthogonal to the C=O group, which makes the carbonyl more electrophilic through mixing of the $\pi^*_{C=O}$ orbital with the $\sigma^*_{C–F}$ orbital. These combined effects enhance both the rate and the β-stereoselectivity of the glycosylation reaction (e.g., **63** → **65** vs **64** → **66**, Figure 9) [129]. Of course, the fluorine substituent remains in the product, which may or may not be advantageous depending on the particular biological context.

Let us now consider furanoses (i.e., five-membered ring sugars). Five-membered rings are inherently more flexible than six-membered rings, so there is more scope for fluorine to influence the pucker. When fluorine is introduced anywhere across C-1–C-3 as a replacement for a hydroxy group (e.g., **67** and **68**, Figure 9), the preferred ring pucker is dictated by the maximisation of $\sigma_{C–H} \rightarrow \sigma^*_{C–F}$ hyperconjugative interactions, and this affords different puckers depending on the fluorine stereochemistry [133]. In this sense, the fluorine substituents are performing a similar role to a hydroxy group, so this is a "conformationally conservative" situation. It should be noted that one of the reasons why C-2 fluorinated nucleosides (e.g., **67** and **68**) have become especially popular in the field of medicinal chemistry [133-137], is that the presence of fluorine at C-2 confers enhanced stability towards hydrolysis, through destabilising the oxocarbenium intermediate [136].

Another way that fluorine can alter the shapes of furanoses, is by replacing the ring oxygen. For example, compare the nucleotide derivatives **69** and **70** (Figure 9). When the ring oxygen of **69** is replaced with a fluoromethylene group in **70**, the latter molecule adopts an unusual envelope conformation in which the fluorinated carbon is projected above the ring plane, stabilised by dual $\sigma_{C–H} \rightarrow \sigma^*_{C–F}$ hyperconjugation [138].

Let us now consider ways in which fluorine can influence bond rotations outside the sugar ring (Figure 10). We will focus initially on the C-5–C-6 bond. In natural sugars, rotation about the C-5–C-6 bond is influenced by the stereochemistry at C-4, because a parallel alignment of the 1,3-hydroxy groups at C-4 and C-6 is unfavourable. Fluorine can achieve the same effect whether located at C-4, or C-6, or both (e.g., **71** and **72**, Figure 10) [119]. Another way in which fluorine can control the rotation of the C-5–C-6 bond is seen when a C-6-fluorinated sugar is converted into an oxocarbenium ion (e.g., **73**, Figure 10). The C-6–F bond of **73** preferentially orients over the sugar ring, due to a combination of electrostatic attraction between the partially negative fluorine atom and the positively charged C=O^+ moiety, and $\sigma_{C–H} \rightarrow \sigma^*_{C–F}$ hyperconjugation. The fluorine atom thus shields the top face of the oxocarbenium ion, and this has flow-on effects on the rate and stereoselectivity of subsequent glycosylation reactions [139].

Another important rotatable bond that lies outside the sugar ring, is the C-1–O anomeric bond in glycosides (highlighted in **74**, Figure 10). This anomeric bond serves as a linker between the sugar and the rest of the glycoside; rotation about this bond can dramatically change the overall shape of the molecule, which in turn can affect its target-binding ability [140]. Fluorine can be used to control the rotation of the anomeric bond, through several means as described below.

"Carbasugars" are sugar analogues in which the ring oxygen is replaced with carbon. We have already seen an example of such a structure (i.e., **70**, Figure 9). Carbasugars are of broad interest because they can be used to create non-hydrolysable glycoside mimics; however, they are poor mimics of genuine glycosides in terms of the rotational profile about the anomeric bond. In true glycosides (e.g., **74**, Figure 10), the anomeric bond typically does not rotate freely; instead, it is biased towards one particular rotamer due to $n_O \rightarrow \sigma^*_{C1–O5}$ hyperconjugation. This opportunity for hyperconjugation is lost with the carbasugar glycosides, and hence the anomeric bond in **75** tends to rotate more freely and this can compromise supramolecular binding interactions. However, the natural rotameric profile can be

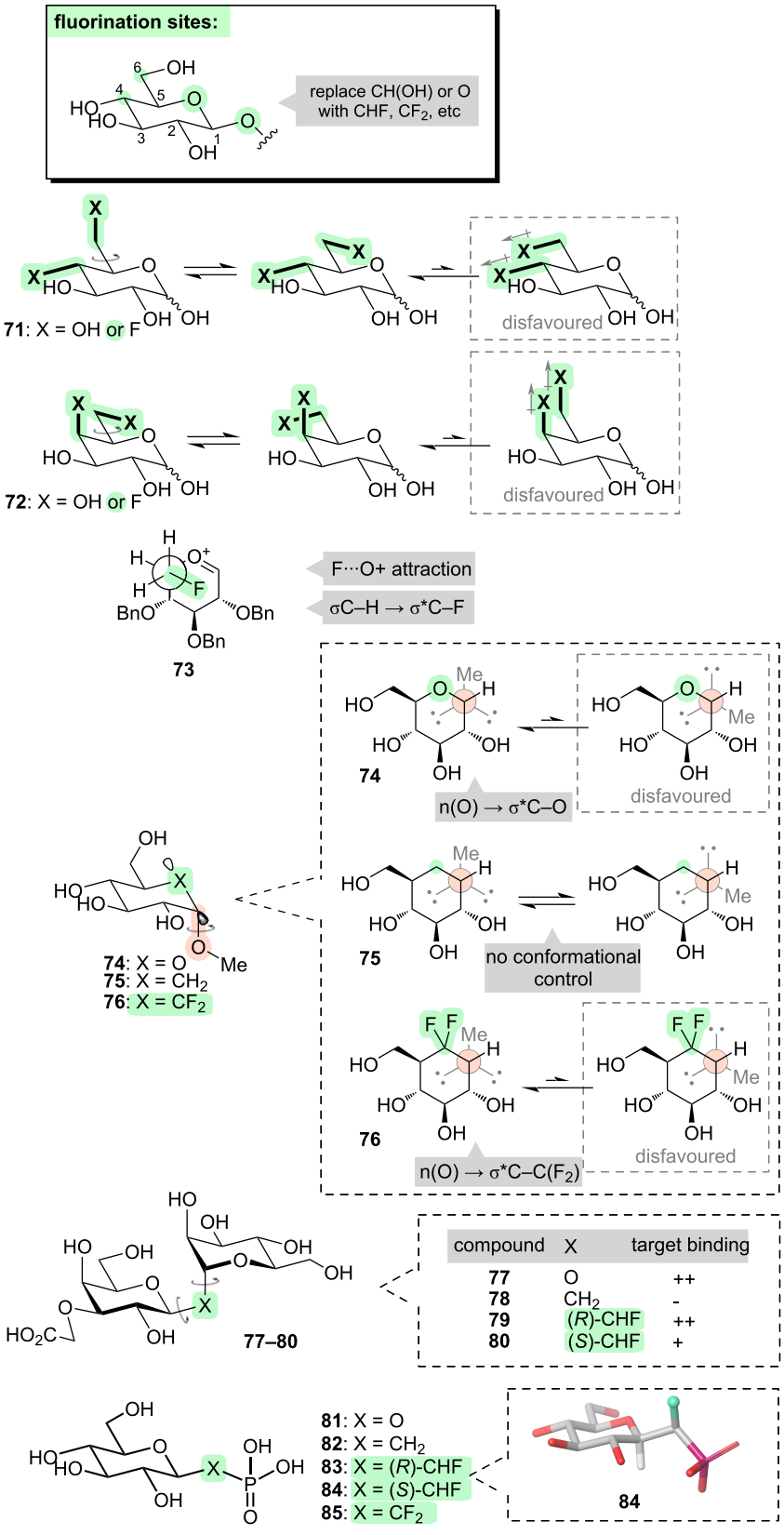

Figure 10: Controlling bond rotations outside the sugar ring through fluorination.

restored by replacing the $–CH_2–$ moiety of the carbasugar with a $–CF_2–$ moiety (e.g., **76**, Figure 10), because the electron-withdrawing character of the fluorine substituents enables reasonably effective $n_O \rightarrow \sigma^*_{C1–C(F)}$ hyperconjugation to occur [141].

Another way to influence the rotameric profile of the anomeric bond in glycosides, is to replace the anomeric oxygen with a (fluorinated) carbon. For disaccharides (e.g., **77**, Figure 10), we have already seen that the lone pairs on the anomeric oxygen play a role in restricting rotation about the anomeric bond, due to $n_O \rightarrow \sigma^*_{C1–O5}$ hyperconjugation. Therefore, if the anomeric oxygen is replaced with CH_2 (e.g., **78**, Figure 10), the anomeric bonds are able to rotate more freely, and this manifests in a reduced binding affinity for the protein target by **78** compared to **77**. However, upon progressing to a CHF linkage (e.g., **79** and **80**, Figure 10), the molecule becomes more rigid again, this time due to dual $\sigma_{C–H} \rightarrow \sigma^*_{C–F}$ hyperconjugation. Notably, different conformations are preferred by the epimeric fluorinated analogues **79** and **80**: analogue **79** is a good match for the parent disaccharide and retains its protein-binding affinity, whereas **80** loses some affinity [142].

A related class of compounds are the phosophosugars (e.g., **81**, Figure 10). Phosphosugars play important roles in a variety of metabolic processes, as well as constituting the backbone of oligonucleotides. Sugar phosphonates (i.e., with a CH_2 linkage between sugar and phosphorus, e.g., **82**, Figure 10) are of interest as non-hydrolysable isosteres, but a better match in terms of pK_a and C–C–P angle is achieved with mono- or difluorophosphonates (e.g., **83**–**85**, Figure 10) [143,144]. In the case of the monofluorophosphonates, conformational effects can also be important [145-147]. For example, the diastereoisomeric monofluorophosphonates **83** and **84** were compared in their ability to bind to a phosphosugar-processing enzyme. Epimer **84** was found to bind with 100-fold higher affinity than epimer **83**, and this was attributed to a lower-energy binding conformation in the case of **84** which benefited from $\sigma_{C1–H} \rightarrow \sigma^*_{C–F}$ hyperconjugation [146,147].

5 Amines

We now turn to a very important and diverse class of molecules: the amines. Nitrogen-containing compounds are highly represented in many fields, including the pharmaceutical and agrochemical industries. It transpires that incorporating fluorine atoms nearby to nitrogen can affect the molecular properties of amines in several useful ways, notably including their conformations. In this section we will commence by examining fluorine-derived conformational control in simple linear amines, then we will move on to cyclic amines. Next, we will examine some important derivatives of amines, such as amides and sulfonamides. Throughout, the emphasis will mostly be on bioactive molecules, but finally this section will conclude by examining a different type of molecular function, namely, organocatalysis.

When fluorine is positioned beta to nitrogen, the fundamental stereoelectronic interactions that arise (**I**–**III**, Figure 11) are conceptually similar to those that we have already seen with oxygen-containing molecules. The dominant interaction is an electrostatic attraction between the amine, which is typically protonated at neutral pH, and the partially negative fluorine atom (**I**, Figure 11) [96]. This attraction has the outcome of favouring a *gauche* $F–C–C–N^+$ alignment. This *gauche* alignment can be further stabilised by two additional interactions: hyperconjugation (**II**, Figure 11) [148], and intramolecular hydrogen bonding (**III**, Figure 11) [149].

These effects have been exploited to control the conformations of simple bioactive amines such as γ-aminobutyric acid (GABA, **86**, Figure 11) [150-155]. GABA is a neurotransmitter that binds to a variety of different GABA receptors, and information about the target-binding conformations of GABA at these various receptors can be gleaned by investigating fluorinated GABA analogues (e.g., **87**–**90**). For example, the enantiomeric analogues **87** and **88** have similar activity at the $GABA_A$ receptor, and this suggests that the binding conformation of GABA has an extended $N^+–C–C–C$ segment, since both fluorinated analogues **87** and **88** have a favourable *gauche* alignment of the C–N and C–F bonds in this conformation [150]. Further information can be obtained by incorporating a second fluorine atom. The difluorinated analogue **89** is found to have no activity at $GABA_A$ whereas the difluorinated analogue **90** has some activity, and this suggests that the binding conformation of GABA has a bent C–C–C–C(O) segment since this conformation is disfavoured for **89** and favoured for **90** [151].

The β-fluoroamine *gauche* preference has been exploited to control the shapes, and hence to elucidate the bioactive conformations, of other simple linear amines too. A *gauche* alignment of the vicinal C–N and C–F bonds is consistently seen [156], whether the scaffold is a primary amine (e.g., tetrafluorovaline, **91** [157]), a secondary amine (e.g., *N*-methyl-D-aspartate(**92**) [158,159]), or a tertiary amine (e.g., a fluorinated analogue of the antidepressant drug, citalopram **93** [160]).

We now turn our attention to cyclic amines. Fluorine has been shown to be capable of modifing the conformations of a variety of *N*-heterocycles, ranging in size from four- to eight-membered rings [48,161-163]. In each case, the conformational outcome is determined by an interplay between electrostatic effects (**I**, Figure 11), hyperconjugation (**II**, Figure 11), intramolecular H-bonding (**III**, Figure 11), and sterics. For example,

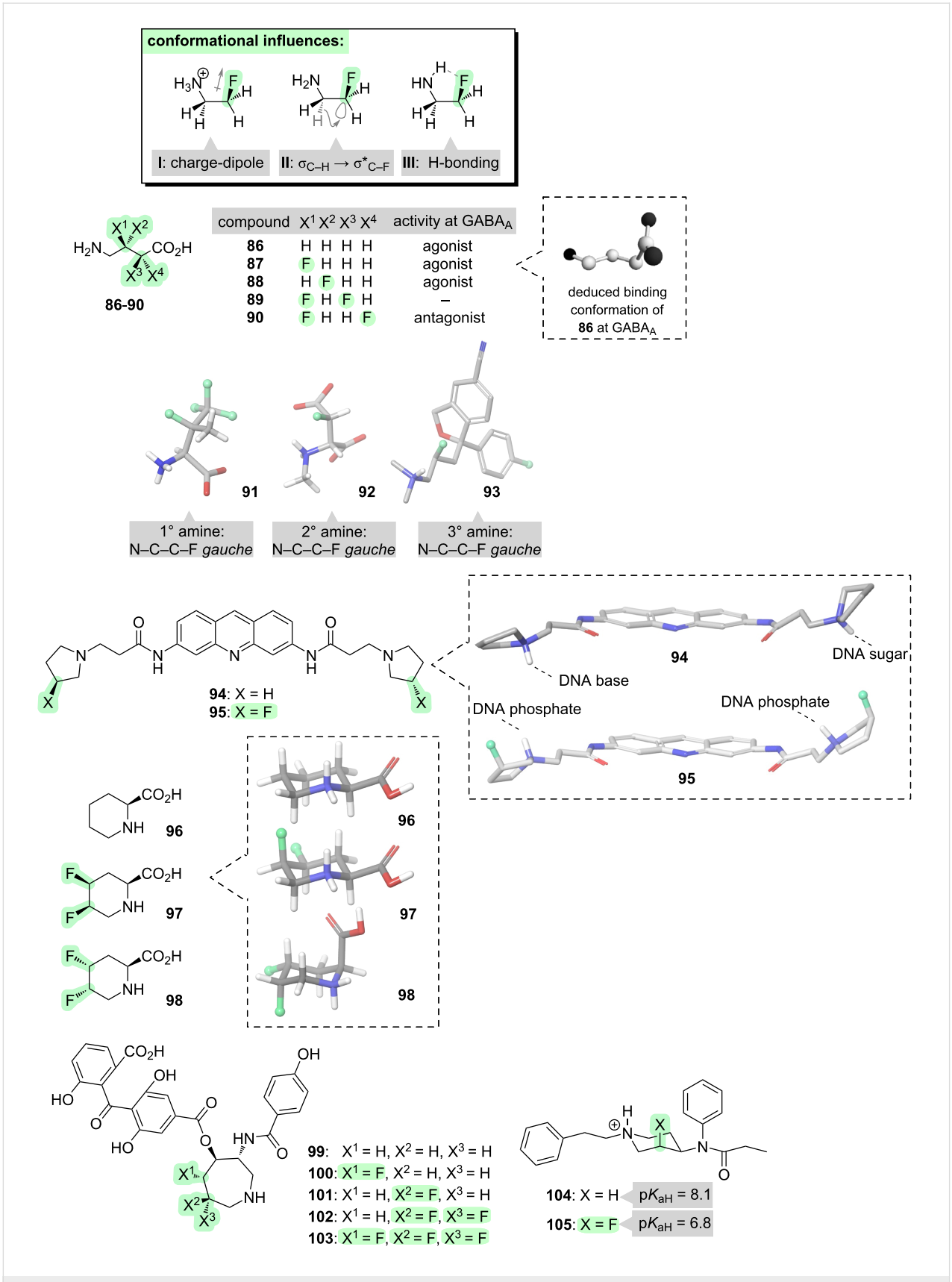

Figure 11: Effects of incorporating fluorine into amines.

consider the G-quadruplex ligand **94** (Figure 11). This molecule contains two pyrrolidine moieties, the NH groups of which interact with the DNA bases and sugars, respectively. When fluorine is incorporated beta to each of the pyrrolidine nitrogens (i.e., **95**, Figure 11), the pucker of each ring changes due to electrostatic attraction between the partially negative fluorine and the protonated amine. These conformational changes alter the DNA-binding mode, such that the pyrrolidine NH groups of **95** now interact with the DNA phosphates rather than the bases or the sugars [164].

Progressing now to a six-membered ring system, consider the scaffold, pipecolic acid (**96**, Figure 11) [165,166]. This molecule is a ring-expanded analogue of proline, and derivatives of it are found within several natural products and drugs. The pucker of the six-membered ring of **96** is quite important for bioactivity, because different puckers project the carboxyl substituent in different orientations (equatorial vs axial). Normally, the pucker with an equatorial carboxyl group is favoured. This pucker is maintained in the difluorinated analogue **97** (Figure 11); in this conformation, in addition to the favourable equatorial placement of the carboxyl group, all of the interactions **I**–**III** (Figure 11) are satisfied. In contrast, the diastereoisomeric difluorinated analogue **98** favours the opposite pucker; in this case, the electrostatic attraction between the partially negative fluorine and the protonated amine (**I**, Figure 11) outweighs the equatorial preference of the carboxyl group.

Another cyclic amine in which the conformation can be controlled by fluorine, is the natural product balanol (**99**, Figure 11) [112,167-172]. Balanol is an ATP mimic that inhibits protein kinase Cε (PKCε), an enzyme that is implicated in cancer. However, compound **99** also inhibits off-target kinases including protein kinase A (PKA). Fluorination was investigated as a strategy for altering the conformation of the central seven-membered nitrogen heterocycle, and hence possibly improving the selectivity for PKCε. A variety of fluorination patterns were investigated (**100**–**103**, Figure 11), which were found to induce subtly different conformations of the seven-membered ring through an interplay of the conformational influences **I**–**III** (Figure 11) and sterics. Promisingly, these different shapes were found to successfully alter the PKCε/PKA selectivity, with one analogue (**100**) displaying higher potency and selectivity for PKCε than balanol itself [112]. This key result was alluded to earlier (in section 3 of this review, during the discussion of acylated alcohols), since compound **100** also features a F–C–C–O(acyl) moiety.

We conclude our examination of amines by considering a final impact of fluorination, which is that the amino group becomes less basic when an inductively electron-withdrawing fluorine atom is nearby. This effect can be exploited to adjust the charge-state of a drug molecule, which can help in optimising the drug's target-binding and/or bioavailability [154,173-181]. For example, consider the analgesic drug fentanyl (**104**, Figure 11). This drug contains a piperidine moiety, which is protonated at physiological pH and forms a salt bridge with an aspartate residue in the binding site of the μ-opioid receptor. One of the drawbacks of fentanyl (**104**) is that it is not selective towards injured tissue: it also binds to μ-opioid receptors in healthy tissue, causing side-effects. To overcome this drawback, a fluorinated analogue of fentanyl ((±)-**105**) was developed [177]. The electron-withdrawing fluorine substituent of **105** lowers the pK_{aH} of the piperidine moiety to 6.8, such that it is only protonated at acidic pH. Since low pH is a hallmark of injured tissue, compound **105** maintains analgesic activity at the site of injury while offering fewer side-effects.

The magnitude of the pK_{aH}-lowering effect varies with the number of fluorines, and with their proximity to the amino group. But there is another aspect to the modulation of pK_{aH} of amines by fluorine: conformation matters, too [182]. If the F–C–C–N alignment is *gauche* (as in **105**, Figure 11), the pK_{aH} will be lowered by ≈1 log unit compared to the non-fluorinated amine. However, if the F–C–C–N alignment is *anti*, the effect is stronger and the pK_{aH} will be lowered by ≈2 log units. Clearly it is important to bear this in mind when utilising fluorine to optimise the properties of nitrogen-containing drugs.

Having concluded our examination of fluorinated amines, let us now focus upon some important derivatives of amines, namely amides and sulfonamides.

Model studies with simple β-fluoroamides (e.g., **106** and **107**, Figure 12) reveal that such molecules consistently adopt conformations in which the F–C–C–N dihedral angle is *gauche* [183-185]. This situation is reminiscent of that already seen with β-fluoroamines, although the predominant driving force with β-fluoroamides is now hyperconjugation (**I**, Figure 12). For secondary amides, i.e., those that contain an NH group, the nitrogen-bound hydrogen sometimes makes a close contact with the fluorine (e.g., **106**), but this not always the case (e.g., **107**), suggesting that the NH···F interaction (i.e., **II**, Figure 12) is not a dominant one.

The *gauche* preference of β-fluoroamides has been exploited to control the conformations of a variety of bioactive molecules [186]. For example, the activity of the GPR119 receptor agonist **108** (Figure 12) can be modulated through fluorination [187]: either an increase or a decrease in potency is seen dependent on the fluorine stereochemistry, suggesting that the bioactive con-

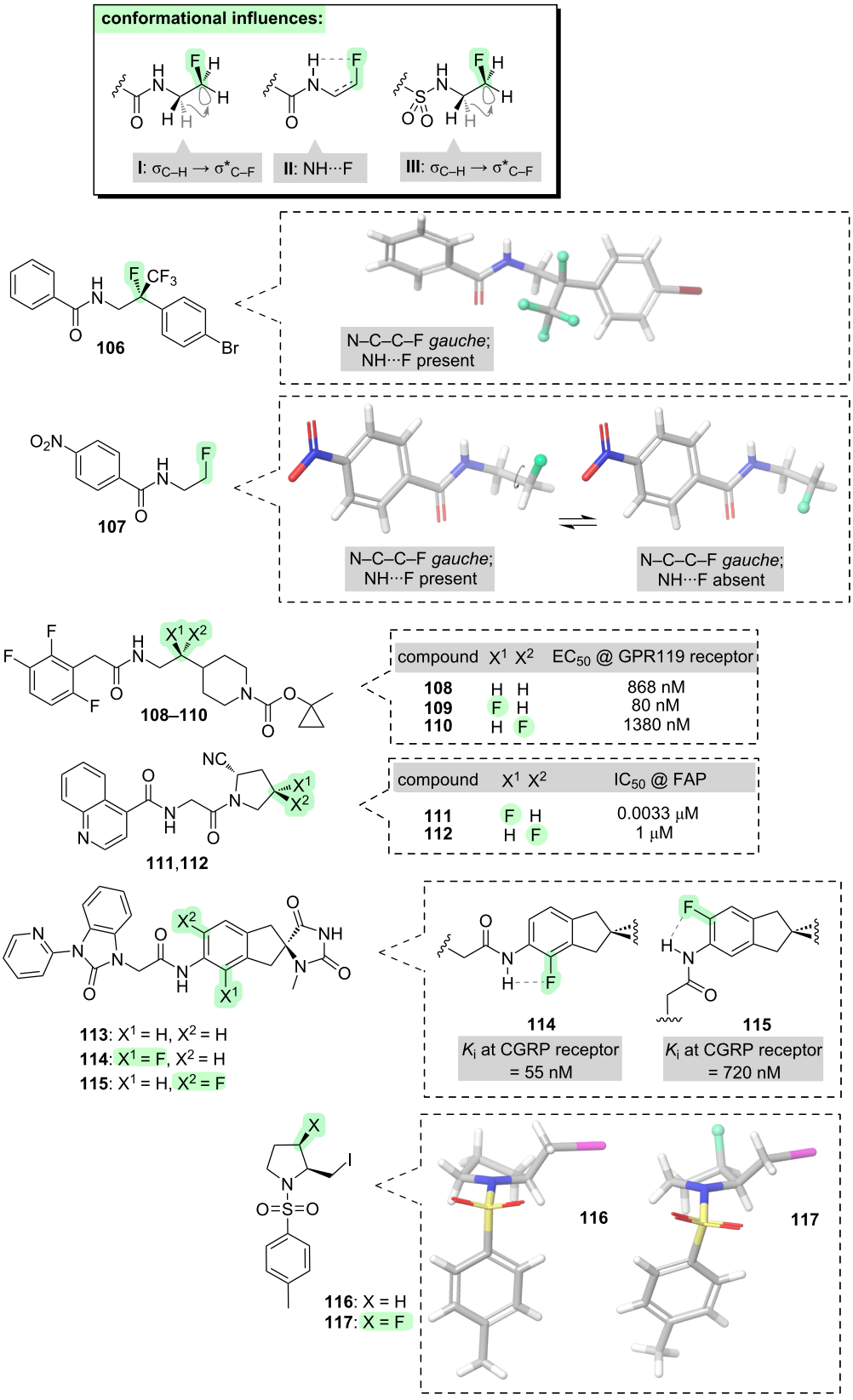

Figure 12: Effects of incorporating fluorine into amine derivatives, such as amides and sulfonamides.

formation is favoured for one stereoisomer (**109**) and disfavoured in the other (**110**). Another context in which the β-fluoroamide *gauche* effect has frequently been exploited is *N*-acylpyrrolidines, a structural motif found within many bioactive molecules (e.g., the fibroblast activation protein (FAP) inhibitors **111** and **112**, Figure 12) [188-192]. When fluorinated analogues of *N*-acylpyrrolidines are prepared, dramatic differences in biological activity are sometimes seen between the fluorinated stereoisomers (e.g., **111** and **112**) [189]. This difference can be attributed to a conformational effect, whereby fluorine controls the pucker of the 5-membered ring through $\sigma_{C–H} \rightarrow \sigma^*_{C–F}$ hyperconjugation. Further examples of this phenomenon will be presented in section 7 (peptides).

It was stated above that the NH···F interaction (i.e., **II**, Figure 12) is not dominant. However, this interaction has been successfully exploited within the slightly different structural context of anilides (e.g., **113**–**115**, Figure 12) [193]. Anilide **113** is a GPCR receptor antagonist. The fluorinated analogues **114** and **115** were found to have very different levels of potency, attributed to different conformations due to the NH···F interaction. This information was subsequently applied to generate next-generation antagonists with even higher potency than **114** (not shown), by building a new ring structure onto the molecule to reinforce the optimal conformation suggested by **114**.

Related to amides are the sulfonamides (e.g., **III**, Figure 12). The sulfonamide functional group is found within a wide variety of important bioactive compounds. There is emerging evidence that the conformations of sulfonamides can be productively influenced through fluorination in a similar manner to that seen with amides. For example, the pucker of an *N*-tosylpyrrolidine **116** can be altered through fluorination (**117**), due to a preference of the F–C–C–N moiety to adopt a *gauche* conformation [194]. Suprisingly, this "fluorine-sulfonamide *gauche* effect" appears to have been exploited only very rarely in molecular design [194-198], suggesting that there may be considerable scope for this under-utilised conformational tool to be applied more widely in the future.

Throughout this section focusing on amines and their derivatives, most of the applications of fluorine-derived conformational control have been in the bioactives space. To conclude this section, a different application will be examined, namely organocatalysis.

Some important examples of organocatalysts are shown in Figure 13, including proline (**118**), an *N*-heterocyclic carbene (NHC, **119**), a proline derivative **120**, an imidazolidinone **121**, and a cinchona alkaloid **122**. These structures are quite diverse, and they operate via different catalytic mechanisms, but they are all *N*-heterocycles and they all offer the opportunity for conformational modulation through fluorination (see green highlights in **118**–**122**) [199,200].

The first general strategy is to employ fluorine to control the ring pucker of the organocatalyst [36,201-205]. For example, incorporating fluorine at the 4-position of proline increases the enantioselectivity of a proline-catalysed transannular aldol reaction (**123** → **124**, Figure 13) [206]. The improved selectivity of the fluorinated catalyst compared to proline itself can be attributed to conformational organisation of the activated intermediate (**I**, Figure 13), due to $\sigma_{C–H} \rightarrow \sigma^*_{C–F}$ hyperconjugation and electrostatic attraction between the partially negative fluorine and the $C{=}N^+$ moiety. In another example, incorporation of fluorine into a NHC catalyst enhances the enantioselectivity of an intermolecular Stetter reaction (**125** → **127**, Figure 13). The improved selectivity can again be attributed to $\sigma_{C–H} \rightarrow \sigma^*_{C–F}$ hyperconjugation, which imposes a curvature onto the Breslow intermediate (**II**, Figure 13).

The second general strategy is to employ fluorine to control rotation of the organocatalyst's exocyclic bonds [202,207-216]. For example, a fluorinated proline-derived catalyst delivers high enantioselectivity in an epoxidation reaction (**128** → **129**, Figure 13). The high selectivity can be attributed to rigidification of the activated intermediate through the "fluorine–iminium *gauche* effect" (**III**, Figure 13), with one of the aryl groups effectively shielding the front face of the molecule [208]. A similar concept is seen with imidazolidone-type catalysts in the context of a Michael reaction (**130** → **131**, Figure 13) [214]. Fluorine can be used to bias the rotation about an exocyclic C–C bond of the catalyst, due to electrostatic attraction between the partially negative fluorine and the $C{=}N^+$ moiety, and comparing the performance of the fluorinated catalysts then provides information about which rotamer is optimal for enantioselectivity (**IV**, Figure 13). A final example of the control of exocyclic bond rotations of an organocatalyst is seen with the cinchona alkaloids, operating as phase-transfer agents in the fluorination reaction of a β-ketoester (**132** → **133**, Figure 13) [212]. The presence of fluorine within the catalyst restricts the rotation of an exocyclic bond, due to electrostatic attraction between the partially negative fluorine and the $C{=}N^+$ moiety (**V**, Figure 13), and this delivers superior enantiocontrol compared to the non-fluorinated catalyst.

6 Carbonyl compounds

We will now turn our attention towards molecules that contain a C=O double bond. We previously saw examples of such molecules when we were considering acylated derivatives of alcohols (section 3) and amines (section 5); however, in those cases we were considering the effect of fluorination on the "oxygen

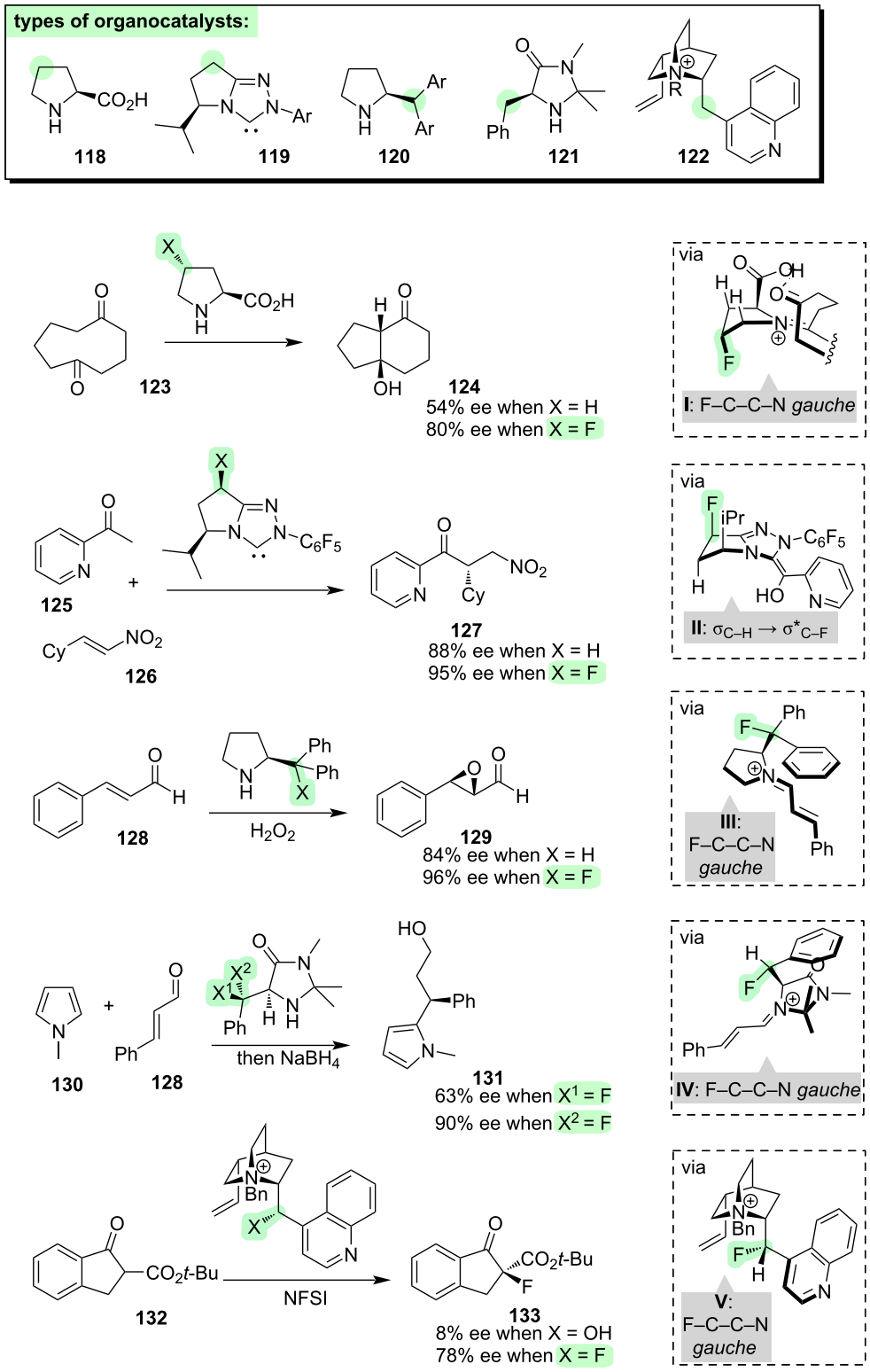

Figure 13: Effects of incorporating fluorine into organocatalysts.

side" or the "nitrogen side" of the carbonyl group, whereas in this section we will consider the effect of fluorination on the "carbon side" (Figure 14).

If a fluorine atom is positioned at the α-position of a secondary amide (i.e., **I**, Figure 14), there is a strong tendency for the C–F and C=O bonds to align antiparallel. This tendency can be ratio-

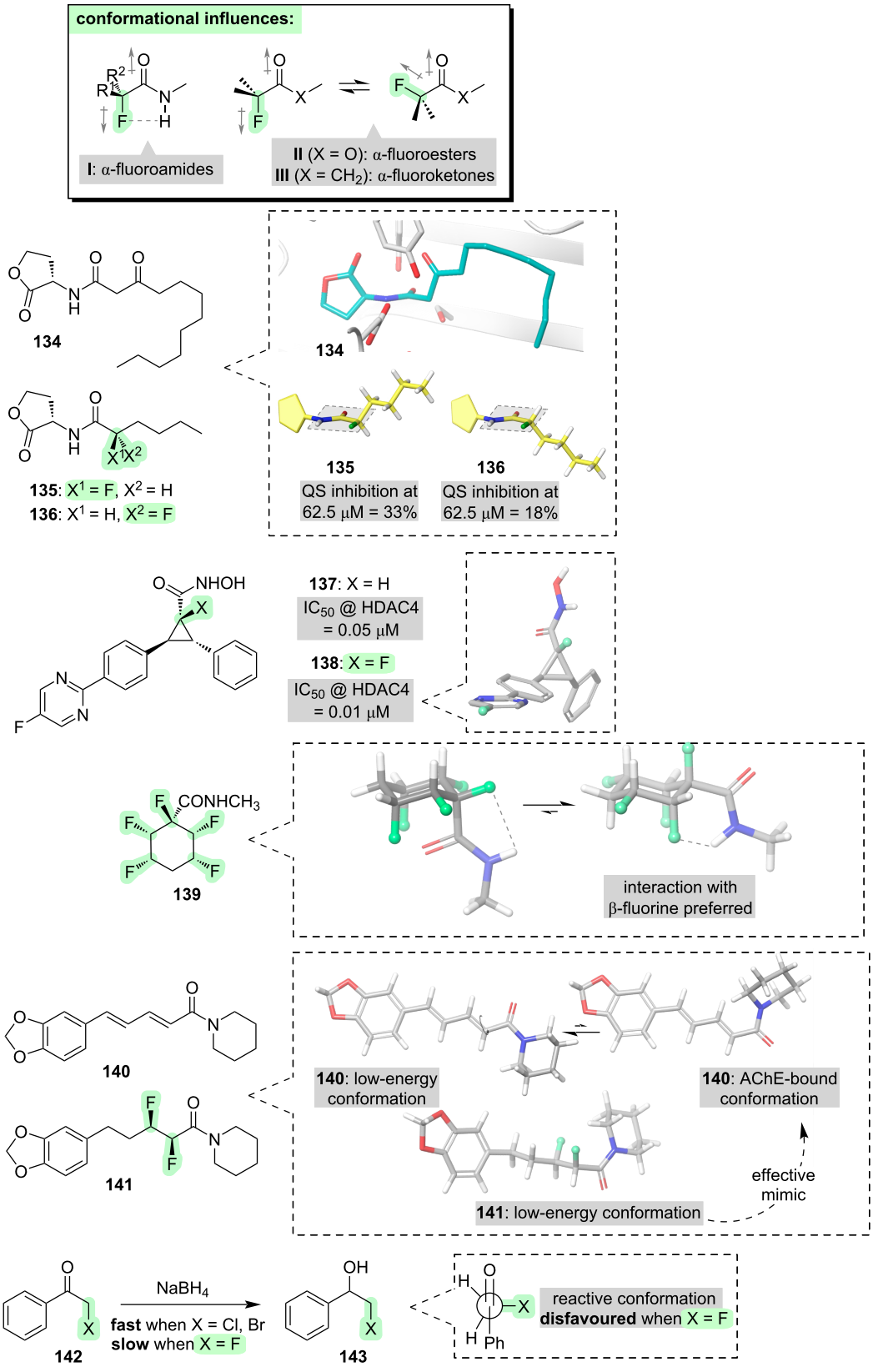

Figure 14: Effects of incorporating fluorine into carbonyl compounds, focusing on the "carbon side."

nalised through a combination of dipole minimisation, and attraction between the fluorine and the nitrogen-bound hydrogen [217-220]. Notably, the conformation depicted in **I** (Figure 14) causes the carbon chain of the amide to deviate from the usual zigzag shape: the substituents R^1 and R^2 are projected in front of, and behind, the amide plane, respectively. This phenomenon has been exploited to control the conformations of bioactive molecules. For example, amide **134** (Figure 14) is an autoinducer involved in the bacterial quorum sensing (QS) response. The fluorinated analogues **135** and **136** were designed as QS inhibitors [221]. In analogue **135**, the fluorine substituent causes the carbon chain to be projected above the amide plane, successfully mimicking the receptor-bound conformation of the natural ligand **134**, and it emerges that analogue **135** is a more potent QS inhibitor than the stereoisomeric analogue **136**. Another illustration of this conformational phenomenon is seen with the HDAC inhibitors **137** and **138** (Figure 14) [222]. The fluorinated analogue **138** is more potent, and this can be attributed to fluorine-derived conformational preorganisation of the key hydroxamic acid moiety in **138**.

Further examples of the "α-fluoroamide effect" will be seen in section 7 (peptides).

It was stated above that the preferred conformation of an α-fluoroamide can be attributed to two separate phenomena, i.e., dipolar minimisation and F···HN attraction (**I**, Figure 14). It is possible to dissect these two phenomena through the study of structural variations. For example, in compound **139** (Figure 14) there are additional fluorine substituents one carbon further away from the carbonyl group [223]. The lowest-energy conformation of **139** features a close contact between one of the β-fluorines and the NH group, speaking to the generality of the F···HN interaction. On the other hand, consider tertiary amides (e.g., **140** and **141**, Figure 14), in which there is no NH group. α-Fluorinated tertiary amides typically do not have a single, dominant conformation: instead, a variety of rotamers about F–C–C=O are accessible, governed by an interplay between dipolar effects and the avoidance of steric repulsion [224-228]. Compound **140** is the natural acetylcholinesterase (AChE) inhibitor, piperine [229]. At first glance, the fluorinated analogue **141** is a poor mimic of the low-energy conformation of **140**. Intriguingly, however, compound **141** retains or even exceeds the AChE inhibitory activity of **140**. This can be explained by considering that piperine (**140**) adopts a higher-energy conformation when bound to AChE [230], and this higher-energy conformation is successfully mimicked by **141**.

We now turn our attention towards other types of carbonyl compounds, namely esters and ketones (e.g., **II** and **III**, Figure 14). As was seen above for α-fluorinated tertiary amides, in α-fluorinated esters and ketones there is no possibility for any F···HN interaction. As might therefore be expected, no single dominant conformation of **II** and **III** is typically observed; instead, rotation about the F–C–C=O dihedral leads to twin minima at ≈0° and ≈180° [231-233]. These two conformations usually have quite similar energies but different dipole moments, and hence the polarity of the surrounding medium can influence which conformation predominates. The lack of a strong inherent conformational preference of α-fluorinated esters and ketones perhaps explains why biological applications of such molecules are quite rare [234]. There is, however, a notable effect in terms of chemical reactivity. α-Halogenated ketones are generally regarded as being good substrates for nucleophilic addition and substitution reactions (e.g., **142** → **143**, Figure 14), but perhaps surprisingly, α-fluorinated ketones are an exception and they display low reactivity. This can be explained by considering that the most reactive conformation of α-haloketones features an orthogonal alignment of the C–X and C=O bonds (Figure 14), in which mixing of the $\sigma^*_{C–X}$ and $\pi^*_{C=O}$ orbitals can occur; this conformation is disfavoured for α-fluoroketones due to a clash between the fluorine lone pairs and the π-orbital [233].

7 Peptides

In previous sections of this review, we examined the conformational effects of fluorination upon amides, either on the "nitrogen side" (section 5) or the "carbon side" (section 6). Now we will go further and examine some more complex oligoamide scaffolds, namely, peptides and proteins. These are archetypal systems in which the 3D structure determines function; hence, methods for controlling the conformations of peptides and proteins are likely to have valuable applications in biotechnology and medicine.

The amino acid upon which most attention has been focused by the fluorine chemistry community to date, is proline (Figure 15).

Fluorination at the 4-position of the proline ring (**144** and **145**, Figure 15) has several conformational outcomes [235-239]. First, the pucker of the ring system can be biased towards either the C^4-*endo* or the C^4-*exo* conformation, depending on the fluorine stereochemistry (**I** and **II**, Figure 15): this can be attributed to $\sigma_{C–H} \rightarrow \sigma^*_{C–F}$ hyperconjugation in each case. Second, the *cis*/*trans* ratio of the amide bond preceding the fluoroproline residue is affected: while *cis*-4-fluoroproline can accommodate a *cis*-amide configuration relatively easily (**III**, Figure 15), *trans*-4-fluoroproline strongly favours the *trans*-amide configuration due to $n_O \rightarrow \pi^*_{C=O}$ hyperconjugation (**IV**, Figure 15). Third, the barrier to *cis*/*trans* isomerisation of the preceding amide bond is affected: *cis*-4-fluoroproline has a higher barrier to rotation while *trans*-4-fluoroproline has a

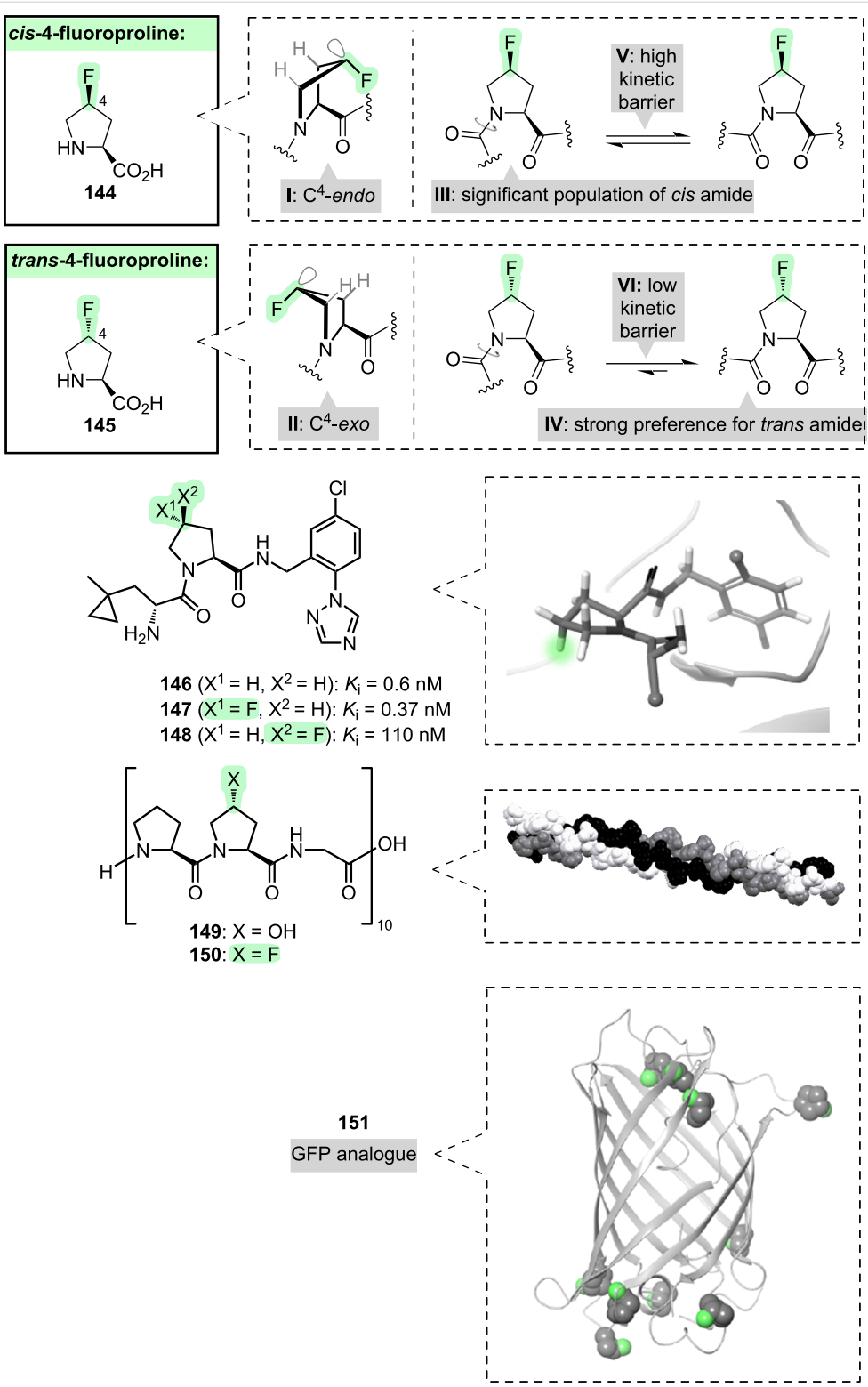

Figure 15: Fluoroproline-containing peptides and proteins.

lower barrier (**V** and **VI**, Figure 15), and this is consistent with the transition state of the isomerisation reaction having a C^4-*exo* ring pucker.

These various conformational effects have been widely exploited to modulate the properties of proline-containing peptides and proteins [238-240].

The first example that we will consider involves a small peptide, and we will focus on the ring pucker. Peptide **146** is a thrombin inhibitor (Figure 15); its target-binding conformation features a C^4-*exo* pucker of the proline ring [241]. Analogue **147**, which contains a *trans*-4-fluoroproline residue, is more potent than **146** because the proline ring of **147** is pre-organised into the required C^4-*exo* pucker. By contrast, analogue **148**, which contains a *cis*-4-fluoroproline residue, is less potent.

The second example involves a larger peptide, and we will consider not just the ring pucker, but the thermodynamics and kinetics of *cis*/*trans* amide isomerisation, too. Peptide **149** (Figure 15) is a simplified and truncated model of the protein collagen. Like collagen, peptide **149** self-assembles into a triple helix in which all of the amide bonds are *trans* and all of the hydroxyproline residues have the C^4-*exo* pucker. If the hydroxyproline residues of **149** are replaced with *trans*-4-fluoroproline (**150**, Figure 15), the resulting triple helix forms more quickly and is more stable [242]. The accelerated self-assembly of **150** can be attributed to a lowering of the *cis*/*trans* amide isomerisation barrier by fluorine (**VI**, Figure 15), while the greater thermodynamic stability of the self-assembled structure of **150** can be attributed, in part, to a stabilisation of both the *trans*-amide (**IV**, Figure 15) and the C^4-*exo* pucker (**II**, Figure 15) by fluorine.

The third example illustrates how fluoroprolines can be used as tools for interrogating the structures and functions of entire proteins [243-254]. Green fluorescent protein (GFP, Figure 15) folds into a barrel shape, with the majority of its proline residues (nine out of ten) adopting the C^4-*endo* pucker. When all of these prolines are replaced with *cis*-4-fluoroproline (**151**, Figure 15), the resulting protein maintains fluorescence properties and is a "superfolder": it exhibits faster folding kinetics, and its folded state has enhanced stability [255]. This is consistent with the C^4-*endo* pucker being favoured by *cis*-4-fluoroproline. In contrast, when all of the proline residues are replaced with *trans*-4-fluoroproline (not shown in Figure 15), the resulting protein fails to fold correctly and lacks fluorescence.

It is also possible to fluorinate at other positions of the proline ring. For example, in 3-fluoroprolines (not shown in Figure 15), analogous conformational effects are observed to those already described for 4-fluoroprolines, as would be expected since both series of molecules contain an N–C–C–F motif [256,257].

Let us now turn our attention away from fluoroprolines, and towards other types of fluorinated peptides.

The fluoroalkene motif has frequently been employed within peptidomimetic structures, where it can serve as an effective isostere of the amide bond [258-261]. For example, a peptide known as Leu-enkephalin (**152**, Figure 16) is a potent ligand of the delta opioid receptor, but it has a poor pharmacokinetic profile due, in part, to its low lipophilicity. Replacement of one of the amide bonds of **152** with a fluoroalkene **153** increases the lipophilicity while retaining much of the receptor-binding activity [262]. In contrast, the non-fluorinated alkene analogue **154** loses receptor-binding activity, and this suggests that the fluorine in **153** serves the important function of mimicking the H-bond-accepting character of the carbonyl group of **152**. The fluoroalkene moiety of **153** is rigid, of course, so at first glance this example might appear to be outside the scope of this review, focusing as we are upon controlling molecular conformation. However, the fluoroalkene moiety of **153** does affect the conformation of a flanking segment of the peptidomimetic: in the synthetic precursor **155** (Figure 16), X-ray crystallography reveals a *gauche* alignment of the F–C–C–N moiety, as would be expected due to hyperconjugative stabilisation ($\sigma_{C-H} \rightarrow \sigma^*_{C-F}$).

Another way to install fluorine on the backbone of a peptide, is to do so between the amino and carboxyl groups of one of the amino acids. This is difficult in the case of α-amino acids, because geminal fluoroamines are typically unstable [263]; but richer opportunities arise with backbone-extended amino acids such as β-, γ-, and δ-amino acids [264-270]. We have already seen an example of a backbone-fluorinated γ-amino acid (i.e., **58**, Figure 8, section 3); previously, compound **58** was considered as an example of a vicinal fluoro-alcohol, but now we can view the structure more holistically as a peptide that contains a backbone-fluorinated γ-amino acid, in which conformational control is exerted not just within the HO–C–C–F segment as discussed in section 3, but also within the F–C–C=O segment.

Another application of fluorinated backbone-extended amino acids is in the conformational control of helical peptide foldamers (Figure 16). For example, consider the β-peptides **156** and **157** [271]. These peptides differ only in the configuration of a single fluorinated stereocentre, yet they have dramatically different conformations: β-peptide **156** adopts a 14-helical shape, stabilised by favourable N–C–C–F and F–C–C=O alignments, whereas β-peptide **157** is forced out of the helical shape (not shown). Next, consider the γ-peptides **158** and **159** [272]. The *erythro*-difluorinated γ-peptide **158** adopts a 9-helical shape (Figure 16), due to favourable N–C–C–F and F–C–C–F and F–C–C=O alignments, whereas the *threo*-difluorinated γ-peptide **159** is disrupted away from this helical shape (not shown). A similar contrast between *erythro*- and *threo*-difluori-

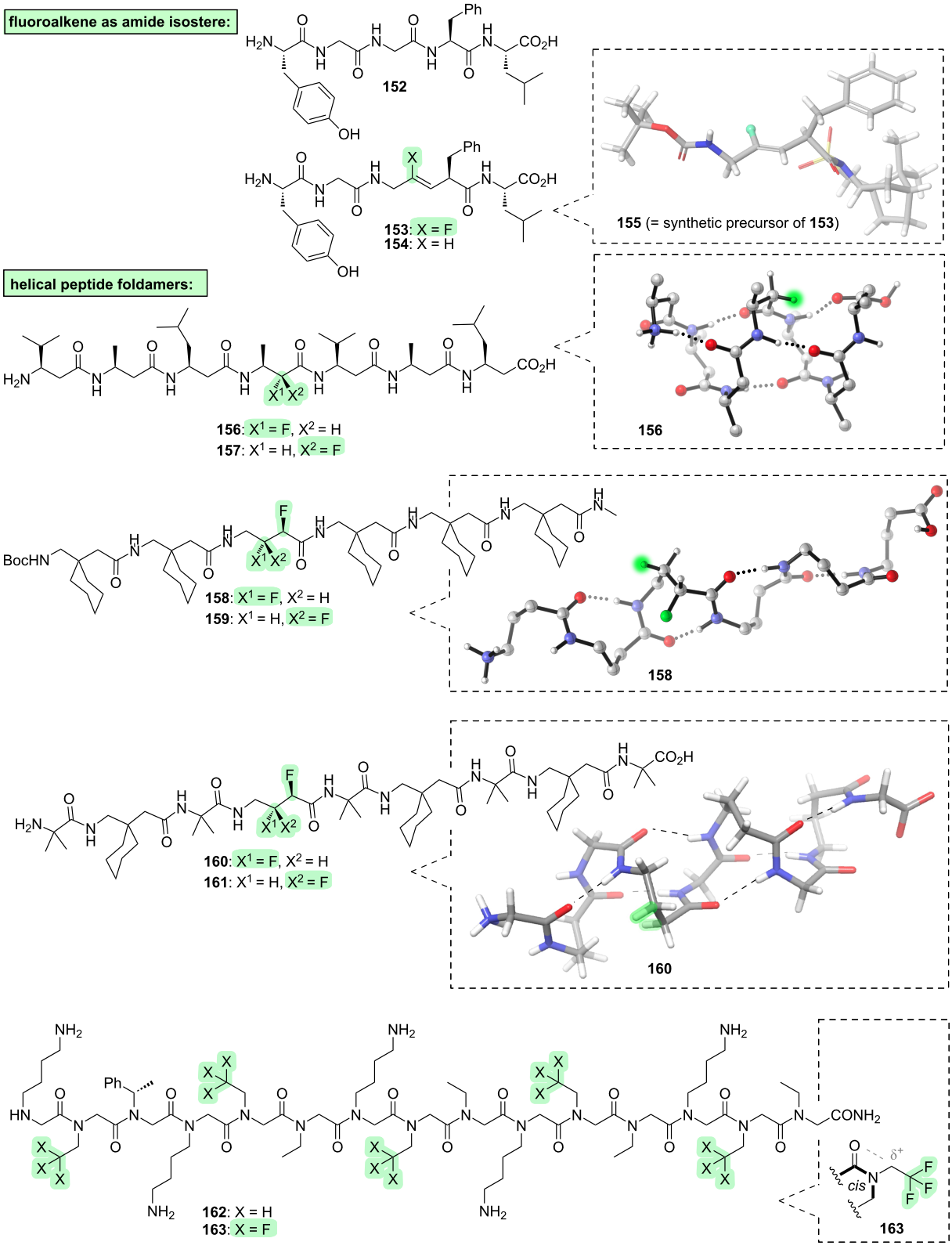

Figure 16: Further examples of fluorinated linear peptides (besides fluoroprolines). For clarity, sidechains are omitted from the 3D structures of **156**/**158**/**160**.

nated stereoisomers is seen within the α,γ-hybrid peptide scaffold **160** and **161** [273]. Notably, the fluorines are the sole source of chirality in peptides **158**–**161**. Finally, consider the peptoids **162** and **163** [274]. The non-fluorinated peptoid **162** has the ability to adopt a helical conformation in which all of the amides are *cis*; but this helix is only a minor fraction of the total population of **162** in solution. The helical propensity is increased in the fluorinated analogue **163**, because the *cis*-amides are stabilised by a dipolar interaction between the carbonyl oxygen and the δ^+ first carbon of the sidechain.

To conclude our survey of fluorinated peptides, we will focus upon cyclic examples.

An attractive feature of the cyclic peptide architecture, is that it becomes possible to control the shape of a bioactive epitope by altering a distant part of the macrocycle [275]. This concept has been explored with the cyclic RGD-containing peptides **164**–**167** (Figure 17) [276]. In these molecules, the shape of the integrin-binding RGD motif can be varied by changing the fluorination pattern within the γ-amino acid at the opposite side of the macrocycle. This alteration in the shape of the RGD motif translates into significant differences in the effects that **164**–**167** have upon cell adhesion and cell spreading. For example, cyclic peptides **164** and **165** inhibit the spreading ability of cells on a fibronectin-enriched extracellular matrix, while peptides **166** and **167** are less active; this suggests that a bent-shaped γ-turn about the glycine residue, as seen in **164** and **165**, is optimal for binding to fibronectin-recognising integrins such as $\alpha_V\beta_3$ integrin.

Another cyclic peptide scaffold in which conformation has been altered by fluorination, is the natural product unguisin A (**168**, Figure 17). Incorporation of different 1,2-difluoro patterns within the γ-amino acid residue leads to different overall molecular shapes **169**–**172** [277,278], and these shape changes affect the ability of the cyclic peptide scaffold to act as a supramolecular host for binding a chloride anion guest [279].

The anion binding concept is taken further with the macrocycle **173** (Figure 17) [280]. This is a rather exotic cyclic hexapeptide comprising an alternating sequence of α- and γ-amino acids, and in which the γ-amino acids contain an embedded fluorosugar moiety. Peptide **173** adopts a "bracelet"-type conformation in which the macrocycle is quite flat and several of the amide bonds are oriented perpendicular to it, stabilised by an antiparallel alignment of each F–C–C=O moiety. This conformation enables supramolecular aggregation to form nanopores that are capable of transporting several different types of anions (e.g., NO_3^-, Cl^-, SCN^-, Br^-) across a membrane.

8 Sulfur-containing compounds

For this final section, we will consider a class of compounds that is only just beginning to be explored in the context of fluorine-derived conformational control. Sulfur-containing compounds are found in a variety of important arenas, including as bioactives, as metal ligands, and as light-harvesting materials. Evidence is beginning to emerge that the conformations of sulfur-containing compounds can be controlled in valuable ways through fluorination.

In some instances, the conformational effects are similar to those that we have already seen elsewhere in this review. For example, consider the aryl thioethers **174** and **175** (Figure 18). By analogy with the oxygen ethers presented in section 2, fluorinated thioethers such as **174** and **175** tend to favour conformations in which the (Ar)C–S bond is orthogonal to the aryl system [281,282]. In the thioether case, this tendency can be attributed primarily to a steric effect rather than the hyperconjugation phenomenon that was discussed in the context of oxygen ethers.

Another fluorinated sulfur-containing compound in which the conformational properties should be somewhat familiar in light of previous discussions in this review, is the vicinal fluorothioether **176** (Figure 18). In compound **176**, there is a preference for the vicinal C–F and C–S bonds to align *gauche*, and this can be attributed to $\sigma_{C-H} \rightarrow \sigma^*_{C-F}$ hyperconjugation [283]. Now, however, a new point of interest arises: the partial charge on sulfur can be manipulated in several different ways, and this can affect the conformation. For example, oxidation of **176** furnishes sulfoxide **177** or sulfone **178**, and in these oxidised analogues the "fluorine–sulfur *gauche* effect" is strengthened [283,284]. The stronger *gauche* effect in **177** and **178** is mostly attributable to a greater electrostatic attraction between fluorine and sulfur. Another way in which the partial charge on sulfur can be increased, and the *gauche* effect thereby strengthened, is through metal complexation (e.g., **176**·Ag^+ and **176**·Au^+, Figure 18) [285].

Another unique feature of sulfur-containing compounds is their ability to engage in attractive 1,5-F···S interactions. For example, compound **179** favours a planar conformation in which a lone pair on fluorine can mix with the σ* orbital of the S–C bond (Figure 18) [286]. This new type of hyperconjugation [287] enables compound **179** to successfully mimic the shape of a previously developed splicing modulator drug **180** while offering superior potency and pharmacokinetic properties. The 1,5-F···S interaction has also been exploited to control the conformations of oligothiophenes (e.g., **181**–**183**) [288], an important class of materials that have light-harvesting and semiconductor applications [289].

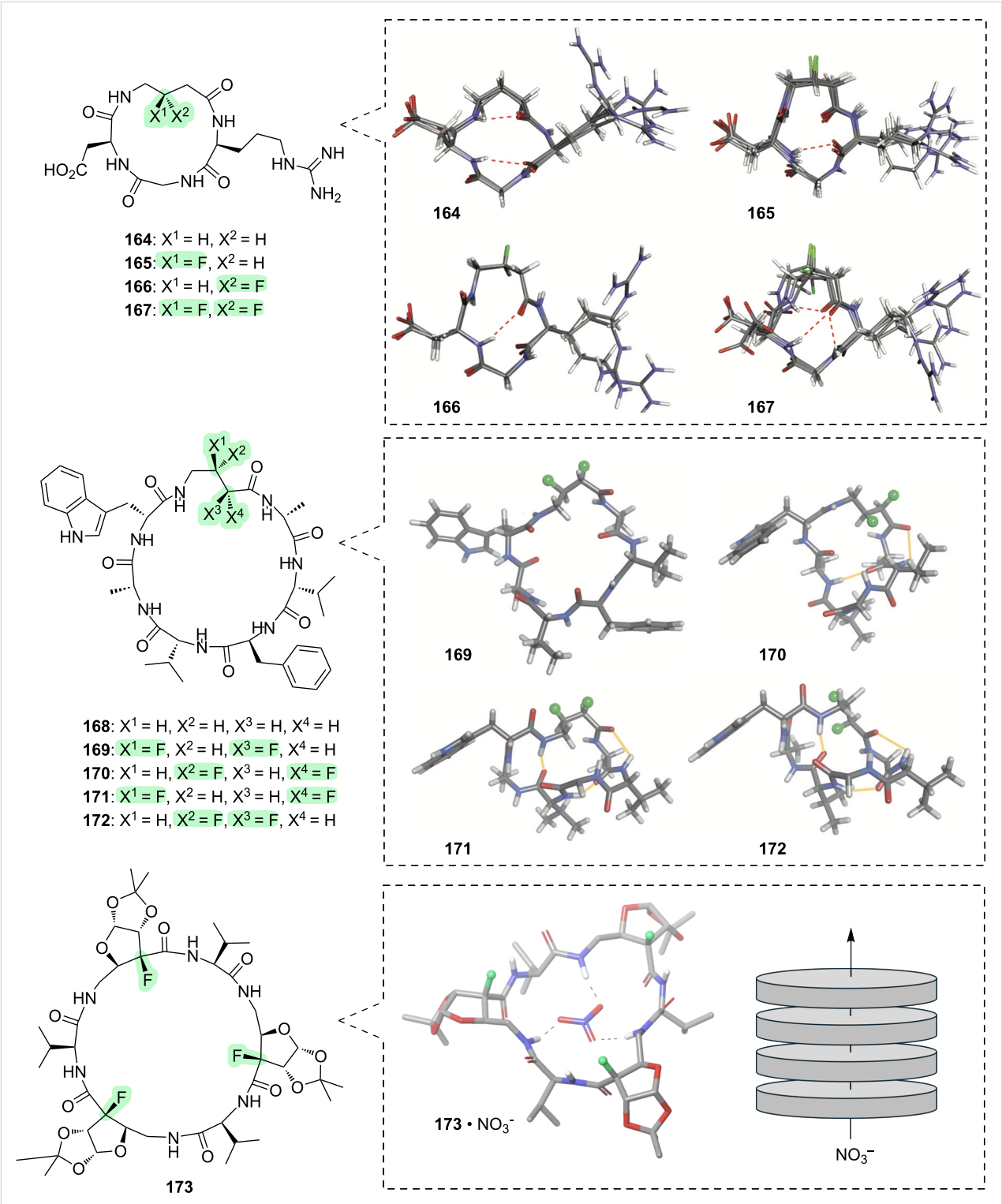

Figure 17: Fluorinated cyclic peptides.

Conclusion

We have seen that the C–F bond tends to align in predictable ways with neighbouring functional groups such as ethers, alcohols, amines, amine derivatives, carbonyl groups, and sulfur-containing moieties. In all cases, the favoured bond alignments can be understood in terms of simple stereoelectronic phenomena such as hyperconjugation and electrostatic attraction/repulsion.

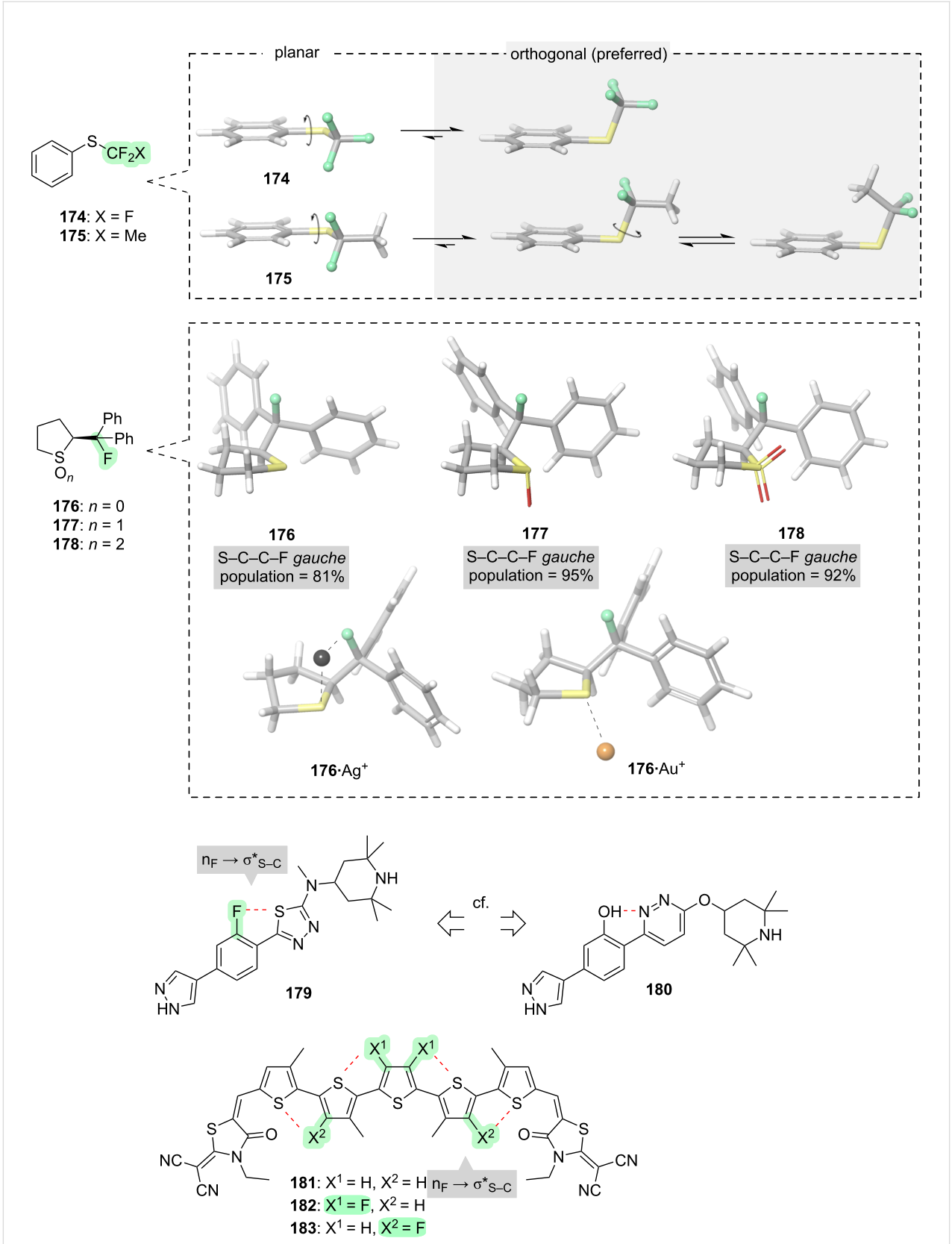

Figure 18: Fluorine-derived conformational control in sulfur-containing compounds.

These conformational effects can deliver several different types of advantages in functional molecules. In some instances, the C–F bond endows a molecule with the ability to change its polarity to suit its environment (a "conformational chameleon"). In other instances, the C–F bond allows a molecule to conservatively mimic the shape of a different molecule such as a natural product, while simultaneously offering some other kind of benefit (e.g., enhanced pharmacokinetic properties). In other instances, the C–F bond causes an otherwise flexible molecule to be rigidified, such that out of an ensemble of previously accessible conformations, a single conformation becomes dominant (application to entropy-driven enhancement of target-binding). Finally, in some instances the introduction of a C–F bond can cause a molecule to adopt an entirely novel shape.

Throughout this review, we have seen how such advantages have been expressed across a wide variety of molecular scaffolds, encompassing bioactive agents, functional materials, organocatalysts, peptide foldamers, supramolecular hosts, and even fragrance chemicals.

In the future, it seems likely that creative new expressions of these ideas will continue to arise, fuelled by ever-evolving synthetic fluorination methods [290]. It is the authors' hope that our review article might contribute in a small way to this expansion, by inspiring readers to consider applying the principles of fluorine-derived conformational control to their own molecular scaffolds of interest.

Author Contributions

Patrick Ryan: conceptualization; data curation; writing – review & editing. Ramsha Iftikhar: conceptualization; data curation; writing – review & editing. Luke Hunter: conceptualization; data curation; writing – original draft; writing – review & editing.

ORCID® iDs

Ramsha Iftikhar - https://orcid.org/0000-0002-6575-110X
Luke Hunter - https://orcid.org/0000-0002-8678-3602

Data Availability Statement

Data sharing is not applicable as no new data was generated or analyzed in this study.

References

1. Kessler, H. *Angew. Chem., Int. Ed. Engl.* **1982,** *21,* 512–523. doi:10.1002/anie.198205121
2. O'Hagan, D. *Chem. Soc. Rev.* **2008,** *37,* 308–319. doi:10.1039/b711844a
3. Meanwell, N. A. *J. Med. Chem.* **2018,** *61,* 5822–5880. doi:10.1021/acs.jmedchem.7b01788
4. Díaz, N.; Jiménez-Grávalos, F.; Suárez, D.; Francisco, E.; Martín-Pendás, Á. *Phys. Chem. Chem. Phys.* **2019,** *21,* 25258–25275. doi:10.1039/c9cp05009d
5. Buissonneaud, D. Y.; van Mourik, T.; O'Hagan, D. *Tetrahedron* **2010,** *66,* 2196–2202. doi:10.1016/j.tet.2010.01.049
6. Thiehoff, C.; Rey, Y. P.; Gilmour, R. *Isr. J. Chem.* **2017,** *57,* 92–100. doi:10.1002/ijch.201600038
7. Rodrigues Silva, D.; de Azevedo Santos, L.; Hamlin, T. A.; Fonseca Guerra, C.; Freitas, M. P.; Bickelhaupt, F. M. *ChemPhysChem* **2021,** *22,* 641–648. doi:10.1002/cphc.202100090
8. Hunter, L. *Beilstein J. Org. Chem.* **2010,** *6,* 38. doi:10.3762/bjoc.6.38
9. Huchet, Q. A.; Kuhn, B.; Wagner, B.; Fischer, H.; Kansy, M.; Zimmerli, D.; Carreira, E. M.; Müller, K. *J. Fluorine Chem.* **2013,** *152,* 119–128. doi:10.1016/j.jfluchem.2013.02.023
10. Müller, K. *Chimia* **2014,** *68,* 356–362. doi:10.2533/chimia.2014.356
11. Huchet, Q. A.; Kuhn, B.; Wagner, B.; Kratochwil, N. A.; Fischer, H.; Kansy, M.; Zimmerli, D.; Carreira, E. M.; Müller, K. *J. Med. Chem.* **2015,** *58,* 9041–9060. doi:10.1021/acs.jmedchem.5b01455
12. Huchet, Q. A.; Schweizer, W. B.; Kuhn, B.; Carreira, E. M.; Müller, K. *Chem. – Eur. J.* **2016,** *22,* 16920–16928. doi:10.1002/chem.201602643
13. Zafrani, Y.; Sod-Moriah, G.; Yeffet, D.; Berliner, A.; Amir, D.; Marciano, D.; Elias, S.; Katalan, S.; Ashkenazi, N.; Madmon, M.; Gershonov, E.; Saphier, S. *J. Med. Chem.* **2019,** *62,* 5628–5637. doi:10.1021/acs.jmedchem.9b00604
14. Jeffries, B.; Wang, Z.; Graton, J.; Holland, S. D.; Brind, T.; Greenwood, R. D. R.; Le Questel, J.-Y.; Scott, J. S.; Chiarparin, E.; Linclau, B. *J. Med. Chem.* **2018,** *61,* 10602–10618. doi:10.1021/acs.jmedchem.8b01222
15. Erickson, J. A.; McLoughlin, J. I. *J. Org. Chem.* **1995,** *60,* 1626–1631. doi:10.1021/jo00111a021
16. Jones, C. R.; Baruah, P. K.; Thompson, A. L.; Scheiner, S.; Smith, M. D. *J. Am. Chem. Soc.* **2012,** *134,* 12064–12071. doi:10.1021/ja301318a
17. Sessler, C. D.; Rahm, M.; Becker, S.; Goldberg, J. M.; Wang, F.; Lippard, S. J. *J. Am. Chem. Soc.* **2017,** *139,* 9325–9332. doi:10.1021/jacs.7b04457
18. Zheng, B.; D'Andrea, S. V.; Sun, L.-Q.; Wang, A. X.; Chen, Y.; Hrnciar, P.; Friborg, J.; Falk, P.; Hernandez, D.; Yu, F.; Sheaffer, A. K.; Knipe, J. O.; Mosure, K.; Rajamani, R.; Good, A. C.; Kish, K.; Tredup, J.; Klei, H. E.; Paruchuri, M.; Ng, A.; Gao, Q.; Rampulla, R. A.; Mathur, A.; Meanwell, N. A.; McPhee, F.; Scola, P. M. *ACS Med. Chem. Lett.* **2018,** *9,* 143–148. doi:10.1021/acsmedchemlett.7b00503
19. Richardson, P. *Expert Opin. Drug Discovery* **2021,** *16,* 1261–1286. doi:10.1080/17460441.2021.1933427
20. König, B.; Watson, P. R.; Reßing, N.; Cragin, A. D.; Schäker-Hübner, L.; Christianson, D. W.; Hansen, F. K. *J. Med. Chem.* **2023,** *66,* 13821–13837. doi:10.1021/acs.jmedchem.3c01345
21. Jeffries, B.; Wang, Z.; Felstead, H. R.; Le Questel, J.-Y.; Scott, J. S.; Chiarparin, E.; Graton, J.; Linclau, B. *J. Med. Chem.* **2020,** *63,* 1002–1031. doi:10.1021/acs.jmedchem.9b01172
22. Erdeljac, N.; Bussmann, K.; Schöler, A.; Hansen, F. K.; Gilmour, R. *ACS Med. Chem. Lett.* **2019,** *10,* 1336–1340. doi:10.1021/acsmedchemlett.9b00287
23. Erdeljac, N.; Thiehoff, C.; Jumde, R. P.; Daniliuc, C. G.; Höppner, S.; Faust, A.; Hirsch, A. K. H.; Gilmour, R. *J. Med. Chem.* **2020,** *63,* 6225–6237. doi:10.1021/acs.jmedchem.0c00648
24. Bent, H. A. *Chem. Rev.* **1961,** *61,* 275–311. doi:10.1021/cr60211a005

25. Urbina-Blanco, C. A.; Skibiński, M.; O'Hagan, D.; Nolan, S. P. *Chem. Commun.* **2013,** *49,* 7201–7203. doi:10.1039/c3cc44312d
26. Dasaradhi, L.; O'Hagan, D.; Petty, M. C.; Pearson, C. *J. Chem. Soc., Perkin Trans. 2* **1995,** 221–225. doi:10.1039/p29950000221
27. Fox, S. J.; Gourdain, S.; Coulthurst, A.; Fox, C.; Kuprov, I.; Essex, J. W.; Skylaris, C.-K.; Linclau, B. *Chem. – Eur. J.* **2015,** *21,* 1682–1691. doi:10.1002/chem.201405317
28. Tavasli, M.; O'Hagan, D.; Pearson, C.; Petty, M. C. *Chem. Commun.* **2002,** 1226–1227. doi:10.1039/b202891c
29. Ariawan, A. D.; Mansour, F.; Richardson, N.; Bhadbhade, M.; Ho, J.; Hunter, L. *Molecules* **2021,** *26,* 3974. doi:10.3390/molecules26133974
30. Bentler, P.; Bergander, K.; Daniliuc, C. G.; Mück-Lichtenfeld, C.; Jumde, R. P.; Hirsch, A. K. H.; Gilmour, R. *Angew. Chem., Int. Ed.* **2019,** *58,* 10990–10994. doi:10.1002/anie.201905452
31. Sharma, H. A.; Mennie, K. M.; Kwan, E. E.; Jacobsen, E. N. *J. Am. Chem. Soc.* **2020,** *142,* 16090–16096. doi:10.1021/jacs.0c08150
32. Poole, W. G.; Peron, F.; Fox, S. J.; Wells, N.; Skylaris, C.-K.; Essex, J. W.; Kuprov, I.; Linclau, B. *J. Org. Chem.* **2024,** *89,* 8789–8803. doi:10.1021/acs.joc.4c00670
33. Fischer, S.; Huwyler, N.; Wolfrum, S.; Carreira, E. M. *Angew. Chem., Int. Ed.* **2016,** *55,* 2555–2558. doi:10.1002/anie.201510608
34. Troup, R. I.; Jeffries, B.; Saudain, R. E.-B.; Georgiou, E.; Fish, J.; Scott, J. S.; Chiarparin, E.; Fallan, C.; Linclau, B. *J. Org. Chem.* **2021,** *86,* 1882–1900. doi:10.1021/acs.joc.0c02810
35. Häfliger, J.; Ruyet, L.; Stübke, N.; Daniliuc, C. G.; Gilmour, R. *Nat. Commun.* **2023,** *14,* 3207. doi:10.1038/s41467-023-38957-w
36. Wang, Y.; Callejo, R.; Slawin, A. M. Z.; O'Hagan, D. *Beilstein J. Org. Chem.* **2014,** *10,* 18–25. doi:10.3762/bjoc.10.4
37. Jang, S. S.; Blanco, M.; Goddard, W. A.; Caldwell, G.; Ross, R. B. *Macromolecules* **2003,** *36,* 5331–5341. doi:10.1021/ma025645t
38. Cormanich, R. A.; O'Hagan, D.; Bühl, M. *Angew. Chem., Int. Ed.* **2017,** *56,* 7867–7870. doi:10.1002/anie.201704112
39. O'Hagan, D. *J. Org. Chem.* **2012,** *77,* 3689–3699. doi:10.1021/jo300044q
40. O'Hagan, D. *Chem. – Eur. J.* **2020,** *26,* 7981–7997. doi:10.1002/chem.202000178
41. Simões, L. H.; Cormanich, R. A. *Eur. J. Org. Chem.* **2020,** 501–505. doi:10.1002/ejoc.201901780
42. Lessard, O.; Lainé, D.; Fecteau, C.-É.; Johnson, P. A.; Giguère, D. *Org. Chem. Front.* **2022,** *9,* 6566–6572. doi:10.1039/d2qo01433e
43. Scheidt, F.; Selter, P.; Santschi, N.; Holland, M. C.; Dudenko, D. V.; Daniliuc, C.; Mück-Lichtenfeld, C.; Hansen, M. R.; Gilmour, R. *Chem. – Eur. J.* **2017,** *23,* 6142–6149. doi:10.1002/chem.201604632
44. Lainé, D.; Lessard, O.; St-Gelais, J.; Giguère, D. *Chem. – Eur. J.* **2021,** *27,* 3799–3805. doi:10.1002/chem.202004646
45. Bentler, P.; Erdeljac, N.; Bussmann, K.; Ahlqvist, M.; Knerr, L.; Bergander, K.; Daniliuc, C. G.; Gilmour, R. *Org. Lett.* **2019,** *21,* 7741–7745. doi:10.1021/acs.orglett.9b02662
46. Hunter, L.; Kirsch, P.; Slawin, A. M. Z.; O'Hagan, D. *Angew. Chem., Int. Ed.* **2009,** *48,* 5457–5460. doi:10.1002/anie.200901956
47. Al-Maharik, N.; Cordes, D. B.; Slawin, A. M. Z.; Bühl, M.; O'Hagan, D. *Org. Biomol. Chem.* **2020,** *18,* 878–887. doi:10.1039/c9ob02647a
48. Mondal, R.; Agbaria, M.; Nairoukh, Z. *Chem. – Eur. J.* **2021,** *27,* 7193–7213. doi:10.1002/chem.202005425
49. Fang, Z.; Al-Maharik, N.; Slawin, A. M. Z.; Bühl, M.; O'Hagan, D. *Chem. Commun.* **2016,** *52,* 5116–5119. doi:10.1039/c6cc01348a
50. Neufeld, J.; Stünkel, T.; Mück-Lichtenfeld, C.; Daniliuc, C. G.; Gilmour, R. *Angew. Chem., Int. Ed.* **2021,** *60,* 13647–13651. doi:10.1002/anie.202102222
51. Luo, Q.; Randall, K. R.; Schaefer, H. F. *RSC Adv.* **2013,** *3,* 6572–6585. doi:10.1039/c3ra40538a
52. Durie, A. J.; Fujiwara, T.; Al-Maharik, N.; Slawin, A. M. Z.; O'Hagan, D. *J. Org. Chem.* **2014,** *79,* 8228–8233. doi:10.1021/jo501432x
53. Jones, M. J.; Callejo, R.; Slawin, A. M. Z.; Bühl, M.; O'Hagan, D. *Beilstein J. Org. Chem.* **2016,** *12,* 2823–2827. doi:10.3762/bjoc.12.281
54. Durie, A. J.; Slawin, A. M. Z.; Lebl, T.; Kirsch, P.; O'Hagan, D. *Chem. Commun.* **2011,** *47,* 8265–8267. doi:10.1039/c1cc13016a
55. Durie, A. J.; Slawin, A. M. Z.; Lebl, T.; Kirsch, P.; O'Hagan, D. *Chem. Commun.* **2012,** *48,* 9643–9645. doi:10.1039/c2cc34679f
56. Durie, A. J.; Fujiwara, T.; Cormanich, R.; Bühl, M.; Slawin, A. M. Z.; O'Hagan, D. *Chem. – Eur. J.* **2014,** *20,* 6259–6263. doi:10.1002/chem.201400354
57. Ayoup, M. S.; Cordes, D. B.; Slawin, A. M. Z.; O'Hagan, D. *Org. Biomol. Chem.* **2015,** *13,* 5621–5624. doi:10.1039/c5ob00650c
58. Ayoup, M. S.; Cordes, D. B.; Slawin, A. M. Z.; O'Hagan, D. *Beilstein J. Org. Chem.* **2015,** *11,* 2671–2676. doi:10.3762/bjoc.11.287
59. Bykova, T.; Al-Maharik, N.; Slawin, A. M. Z.; O'Hagan, D. *Org. Biomol. Chem.* **2016,** *14,* 1117–1123. doi:10.1039/c5ob02334c
60. Bykova, T.; Al-Maharik, N.; Slawin, A. M. Z.; O'Hagan, D. *Beilstein J. Org. Chem.* **2017,** *13,* 728–733. doi:10.3762/bjoc.13.72
61. Rodil, A.; Bosisio, S.; Ayoup, M. S.; Quinn, L.; Cordes, D. B.; Slawin, A. M. Z.; Murphy, C. D.; Michel, J.; O'Hagan, D. *Chem. Sci.* **2018,** *9,* 3023–3028. doi:10.1039/c8sc00299a
62. Durie, A. J.; Slawin, A. M. Z.; Lebl, T.; O'Hagan, D. *Angew. Chem., Int. Ed.* **2012,** *51,* 10086–10088. doi:10.1002/anie.201205577
63. Keddie, N. S.; Slawin, A. M. Z.; Lebl, T.; Philp, D.; O'Hagan, D. *Nat. Chem.* **2015,** *7,* 483–488. doi:10.1038/nchem.2232
64. Cormanich, R. A.; Keddie, N. S.; Rittner, R.; O'Hagan, D.; Bühl, M. *Phys. Chem. Chem. Phys.* **2015,** *17,* 29475–29478. doi:10.1039/c5cp04537a
65. Pratik, S. M.; Nijamudheen, A.; Datta, A. *ChemPhysChem* **2016,** *17,* 2373–2381. doi:10.1002/cphc.201600262
66. Lecours, M. J.; Marta, R. A.; Steinmetz, V.; Keddie, N.; Fillion, E.; O'Hagan, D.; McMahon, T. B.; Hopkins, W. S. *J. Phys. Chem. Lett.* **2017,** *8,* 109–113. doi:10.1021/acs.jpclett.6b02629
67. Ziegler, B. E.; Lecours, M.; Marta, R. A.; Featherstone, J.; Fillion, E.; Hopkins, W. S.; Steinmetz, V.; Keddie, N. S.; O'Hagan, D.; McMahon, T. B. *J. Am. Chem. Soc.* **2016,** *138,* 7460–7463. doi:10.1021/jacs.6b02856
68. Naumkin, F. Y. *J. Phys. Chem. A* **2017,** *121,* 4545–4551. doi:10.1021/acs.jpca.7b02576
69. Sun, W.-M.; Ni, B.-L.; Wu, D.; Lan, J.-M.; Li, C.-Y.; Li, Y.; Li, Z.-R. *Organometallics* **2017,** *36,* 3352–3359. doi:10.1021/acs.organomet.7b00491
70. Shyshov, O.; Siewerth, K. A.; von Delius, M. *Chem. Commun.* **2018,** *54,* 4353–4355. doi:10.1039/c8cc01797b
71. Wang, Y.-F.; Li, J.; Huang, J.; Qin, T.; Liu, Y.-M.; Zhong, F.; Zhang, W.; Li, Z.-R. *J. Phys. Chem. C* **2019,** *123,* 23610–23619. doi:10.1021/acs.jpcc.9b06200
72. Skibinski, M.; Wang, Y.; Slawin, A. M. Z.; Lebl, T.; Kirsch, P.; O'Hagan, D. *Angew. Chem., Int. Ed.* **2011,** *50,* 10581–10584. doi:10.1002/anie.201105060

73. Skibiński, M.; Urbina-Blanco, C. A.; Slawin, A. M. Z.; Nolan, S. P.; O'Hagan, D. *Org. Biomol. Chem.* **2013,** *11,* 8209–8213. doi:10.1039/c3ob42062k
74. Callejo, R.; Corr, M. J.; Yang, M.; Wang, M.; Cordes, D. B.; Slawin, A. M. Z.; O'Hagan, D. *Chem. – Eur. J.* **2016,** *22,* 8137–8151. doi:10.1002/chem.201600519
75. Corr, M. J.; Cormanich, R. A.; von Hahmann, C. N.; Bühl, M.; Cordes, D. B.; Slawin, A. M. Z.; O'Hagan, D. *Org. Biomol. Chem.* **2016,** *14,* 211–219. doi:10.1039/c5ob02023a
76. Kirsch, P.; Bremer, M. *ChemPhysChem* **2010,** *11,* 357–360. doi:10.1002/cphc.200900745
77. Juaristi, E.; Cuevas, G. *Tetrahedron* **1992,** *48,* 5019–5087. doi:10.1016/s0040-4020(01)90118-8
78. Miao, Z.; Zhu, L.; Dong, G.; Zhuang, C.; Wu, Y.; Wang, S.; Guo, Z.; Liu, Y.; Wu, S.; Zhu, S.; Fang, K.; Yao, J.; Li, J.; Sheng, C.; Zhang, W. *J. Med. Chem.* **2013,** *56,* 7902–7910. doi:10.1021/jm400906z
79. Rombouts, F. J. R.; Tresadern, G.; Delgado, O.; Martínez-Lamenca, C.; Van Gool, M.; García-Molina, A.; Alonso de Diego, S. A.; Oehlrich, D.; Prokopcova, H.; Alonso, J. M.; Austin, N.; Borghys, H.; Van Brandt, S.; Surkyn, M.; De Cleyn, M.; Vos, A.; Alexander, R.; Macdonald, G.; Moechars, D.; Gijsen, H.; Trabanco, A. A. *J. Med. Chem.* **2015,** *58,* 8216–8235. doi:10.1021/acs.jmedchem.5b01101
80. Xing, L.; Blakemore, D. C.; Narayanan, A.; Unwalla, R.; Lovering, F.; Denny, R. A.; Zhou, H.; Bunnage, M. E. *ChemMedChem* **2015,** *10,* 715–726. doi:10.1002/cmdc.201402555
81. Huchet, Q. A.; Trapp, N.; Kuhn, B.; Wagner, B.; Fischer, H.; Kratochwil, N. A.; Carreira, E. M.; Müller, K. *J. Fluorine Chem.* **2017,** *198,* 34–46. doi:10.1016/j.jfluchem.2017.02.003
82. Zafrani, Y.; Yeffet, D.; Sod-Moriah, G.; Berliner, A.; Amir, D.; Marciano, D.; Gershonov, E.; Saphier, S. *J. Med. Chem.* **2017,** *60,* 797–804. doi:10.1021/acs.jmedchem.6b01691
83. Zhou, Q.; Tan, Z.; Yang, D.; Tu, J.; Wang, Y.; Zhang, Y.; Liu, Y.; Gan, G. *Crystals* **2021,** *11,* 343. doi:10.3390/cryst11040343
84. Ye, F.; Ge, Y.; Spannenberg, A.; Neumann, H.; Xu, L.-W.; Beller, M. *Nat. Commun.* **2021,** *12,* 3257. doi:10.1038/s41467-021-23504-2
85. Cogswell, T. J.; Lewis, R. J.; Sköld, C.; Nordqvist, A.; Ahlqvist, M.; Knerr, L. *Chem. Sci.* **2024,** *15,* 19770–19776. doi:10.1039/d4sc05424e
86. Li, J.; Yang, X.; Wan, D.; Hu, M.; Yang, C.; Mo, L.; Li, J.; Che, Z.; An, Z.; Gao, A.; Du, W.; Deng, D. *Liq. Cryst.* **2020,** *47,* 2268–2275. doi:10.1080/02678292.2020.1769755
87. Al-Maharik, N.; Kirsch, P.; Slawin, A. M. Z.; O'Hagan, D. *Tetrahedron* **2014,** *70,* 4626–4630. doi:10.1016/j.tet.2014.05.027
88. Selnick, H. G.; Hess, J. F.; Tang, C.; Liu, K.; Schachter, J. B.; Ballard, J. E.; Marcus, J.; Klein, D. J.; Wang, X.; Pearson, M.; Savage, M. J.; Kaul, R.; Li, T.-S.; Vocadlo, D. J.; Zhou, Y.; Zhu, Y.; Mu, C.; Wang, Y.; Wei, Z.; Bai, C.; Duffy, J. L.; McEachern, E. J. *J. Med. Chem.* **2019,** *62,* 10062–10097. doi:10.1021/acs.jmedchem.9b01090
89. Silva, D. R.; Daré, J. K.; Freitas, M. P. *Beilstein J. Org. Chem.* **2020,** *16,* 2469–2476. doi:10.3762/bjoc.16.200
90. Wang, Q.; Eriksson, L.; Szabó, K. J. *Angew. Chem., Int. Ed.* **2023,** *62,* e202301481. doi:10.1002/anie.202301481
91. Liao, F.-M.; Liu, Y.-L.; Yu, J.-S.; Zhou, F.; Zhou, J. *Org. Biomol. Chem.* **2015,** *13,* 8906–8911. doi:10.1039/c5ob01125f
92. Naveen, N.; Balamurugan, R. *Org. Biomol. Chem.* **2017,** *15,* 2063–2072. doi:10.1039/c7ob00140a
93. Liu, Y.-L.; Liao, F.-M.; Niu, Y.-F.; Zhao, X.-L.; Zhou, J. *Org. Chem. Front.* **2014,** *1,* 742–747. doi:10.1039/c4qo00126e
94. Suzuki, S.; Kitamura, Y.; Lectard, S.; Hamashima, Y.; Sodeoka, M. *Angew. Chem., Int. Ed.* **2012,** *51,* 4581–4585. doi:10.1002/anie.201201303
95. Hu, X.-G.; Lawer, A.; Peterson, M. B.; Iranmanesh, H.; Ball, G. E.; Hunter, L. *Org. Lett.* **2016,** *18,* 662–665. doi:10.1021/acs.orglett.5b03592
96. Briggs, C. R. S.; Allen, M. J.; O'Hagan, D.; Tozer, D. J.; Slawin, A. M. Z.; Goeta, A. E.; Howard, J. A. K. *Org. Biomol. Chem.* **2004,** *2,* 732–740. doi:10.1039/b312188g
97. Linclau, B.; Peron, F.; Bogdan, E.; Wells, N.; Wang, Z.; Compain, G.; Fontenelle, C. Q.; Galland, N.; Le Questel, J.-Y.; Graton, J. *Chem. – Eur. J.* **2015,** *21,* 17808–17816. doi:10.1002/chem.201503253
98. Martins, F. A.; Freitas, M. P. *Eur. J. Org. Chem.* **2019,** 6401–6406. doi:10.1002/ejoc.201901234
99. Quiquempoix, L.; Bogdan, E.; Wells, N. J.; Le Questel, J.-Y.; Graton, J.; Linclau, B. *Molecules* **2017,** *22,* 518. doi:10.3390/molecules22040518
100. Abraham, M. H.; Grellier, P. L.; Prior, D. V.; Morris, J. J.; Taylor, P. J. *J. Chem. Soc., Perkin Trans. 2* **1990,** 521–529. doi:10.1039/p29900000521
101. Abraham, M. H. *Chem. Soc. Rev.* **1993,** *22,* 73–83. doi:10.1039/cs9932200073
102. Dugovic, B.; Leumann, C. J. *J. Org. Chem.* **2014,** *79,* 1271–1279. doi:10.1021/jo402690j
103. Piscelli, B. A.; Sanders, W.; Yu, C.; Al Maharik, N.; Lebl, T.; Cormanich, R. A.; O'Hagan, D. *Chem. – Eur. J.* **2020,** *26,* 11989–11994. doi:10.1002/chem.202003058
104. Graton, J.; Wang, Z.; Brossard, A.-M.; Gonçalves Monteiro, D.; Le Questel, J.-Y.; Linclau, B. *Angew. Chem., Int. Ed.* **2012,** *51,* 6176–6180. doi:10.1002/anie.201202059
105. Smart, B. E. *J. Fluorine Chem.* **2001,** *109,* 3–11. doi:10.1016/s0022-1139(01)00375-x
106. Graton, J.; Compain, G.; Besseau, F.; Bogdan, E.; Watts, J. M.; Mtashobya, L.; Wang, Z.; Weymouth-Wilson, A.; Galland, N.; Le Questel, J.-Y.; Linclau, B. *Chem. – Eur. J.* **2017,** *23,* 2811–2819. doi:10.1002/chem.201604940
107. Jones, D. H.; Bresciani, S.; Tellam, J. P.; Wojno, J.; Cooper, A. W. J.; Kennedy, A. R.; Tomkinson, N. C. O. *Org. Biomol. Chem.* **2016,** *14,* 172–182. doi:10.1039/c5ob01924a
108. Lawer, A.; Nesvaderani, J.; Marcolin, G. M.; Hunter, L. *Tetrahedron* **2018,** *74,* 1278–1287. doi:10.1016/j.tet.2017.12.033
109. Briggs, C. R. S.; O'Hagan, D.; Rzepa, H. S.; Slawin, A. M. Z. *J. Fluorine Chem.* **2004,** *125,* 19–25. doi:10.1016/j.jfluchem.2003.08.011
110. Cresswell, A. J.; Davies, S. G.; Lee, J. A.; Roberts, P. M.; Russell, A. J.; Thomson, J. E.; Tyte, M. J. *Org. Lett.* **2010,** *12,* 2936–2939. doi:10.1021/ol100862s
111. Lingier, S.; Szpera, R.; Goderis, B.; Linclau, B.; Du Prez, F. E. *Polymer* **2019,** *164,* 134–141. doi:10.1016/j.polymer.2019.01.014
112. Patel, A. R.; Hardianto, A.; Ranganathan, S.; Liu, F. *Org. Biomol. Chem.* **2017,** *15,* 1570–1574. doi:10.1039/c7ob00129k
113. St-Gelais, J.; Bouchard, M.; Denavit, V.; Giguère, D. *J. Org. Chem.* **2019,** *84,* 8509–8522. doi:10.1021/acs.joc.9b00795
114. St-Gelais, J.; Côté, É.; Lainé, D.; Johnson, P. A.; Giguère, D. *Chem. – Eur. J.* **2020,** *26,* 13499–13506. doi:10.1002/chem.202002825
115. Linclau, B.; Wang, Z.; Compain, G.; Paumelle, V.; Fontenelle, C. Q.; Wells, N.; Weymouth-Wilson, A. *Angew. Chem., Int. Ed.* **2016,** *55,* 674–678. doi:10.1002/anie.201509460

116. Golten, S.; Patinec, A.; Akoumany, K.; Rocher, J.; Graton, J.; Jacquemin, D.; Le Questel, J.-Y.; Tessier, A.; Lebreton, J.; Blot, V.; Pipelier, M.; Douillard, J.-Y.; Le Pendu, J.; Linclau, B.; Dubreuil, D. *Eur. J. Med. Chem.* **2019,** *178,* 195–213. doi:10.1016/j.ejmech.2019.05.069
117. Denavit, V.; Lainé, D.; Bouzriba, C.; Shanina, E.; Gillon, É.; Fortin, S.; Rademacher, C.; Imberty, A.; Giguère, D. *Chem. – Eur. J.* **2019,** *25,* 4478–4490. doi:10.1002/chem.201806197
118. Leclerc, E.; Pannecoucke, X.; Ethève-Quelquejeu, M.; Sollogoub, M. *Chem. Soc. Rev.* **2013,** *42,* 4270–4283. doi:10.1039/c2cs35403a
119. Linclau, B.; Ardá, A.; Reichardt, N.-C.; Sollogoub, M.; Unione, L.; Vincent, S. P.; Jiménez-Barbero, J. *Chem. Soc. Rev.* **2020,** *49,* 3863–3888. doi:10.1039/c9cs00099b
120. Bresciani, S.; Lebl, T.; Slawin, A. M. Z.; O'Hagan, D. *Chem. Commun.* **2010,** *46,* 5434–5436. doi:10.1039/c0cc01128b
121. Denavit, V.; Lainé, D.; St-Gelais, J.; Johnson, P. A.; Giguère, D. *Nat. Commun.* **2018,** *9,* 4721. doi:10.1038/s41467-018-06901-y
122. Wheatley, D. E.; Fontenelle, C. Q.; Kuppala, R.; Szpera, R.; Briggs, E. L.; Vendeville, J.-B.; Wells, N. J.; Light, M. E.; Linclau, B. *J. Org. Chem.* **2021,** *86,* 7725–7756. doi:10.1021/acs.joc.1c00796
123. Hall, L. D.; Manville, J. F. *Can. J. Chem.* **1969,** *47,* 19–30. doi:10.1139/v69-002
124. Xu, S.; del Pozo, J.; Romiti, F.; Fu, Y.; Mai, B. K.; Morrison, R. J.; Lee, K.; Hu, S.; Koh, M. J.; Lee, J.; Li, X.; Liu, P.; Hoveyda, A. H. *Nat. Chem.* **2022,** *14,* 1459–1469. doi:10.1038/s41557-022-01054-4
125. Bucher, C.; Gilmour, R. *Angew. Chem., Int. Ed.* **2010,** *49,* 8724–8728. doi:10.1002/anie.201004467
126. Bucher, C.; Gilmour, R. *Synlett* **2011,** 1043–1046. doi:10.1055/s-0030-1259934
127. Durantie, E.; Bucher, C.; Gilmour, R. *Chem. – Eur. J.* **2012,** *18,* 8208–8215. doi:10.1002/chem.201200468
128. Santschi, N.; Gilmour, R. *Eur. J. Org. Chem.* **2015,** 6983–6987. doi:10.1002/ejoc.201501081
129. Sadurní, A.; Kehr, G.; Ahlqvist, M.; Wernevik, J.; Sjögren, H. P.; Kankkonen, C.; Knerr, L.; Gilmour, R. *Chem. – Eur. J.* **2018,** *24,* 2832–2836. doi:10.1002/chem.201705373
130. Teschers, C. S.; Gilmour, R. *Angew. Chem., Int. Ed.* **2023,** *62,* e202213304. doi:10.1002/anie.202213304
131. Lebedel, L.; Ardá, A.; Martin, A.; Désiré, J.; Mingot, A.; Aufiero, M.; Aiguabella Font, N.; Gilmour, R.; Jiménez-Barbero, J.; Blériot, Y.; Thibaudeau, S. *Angew. Chem., Int. Ed.* **2019,** *58,* 13758–13762. doi:10.1002/anie.201907001
132. Franconetti, A.; Ardá, A.; Asensio, J. L.; Blériot, Y.; Thibaudeau, S.; Jiménez-Barbero, J. *Acc. Chem. Res.* **2021,** *54,* 2552–2564. doi:10.1021/acs.accounts.1c00021
133. Zeng, D.; Zhang, R.; Nie, Q.; Cao, L.; Shang, L.; Yin, Z. *ACS Med. Chem. Lett.* **2016,** *7,* 1197–1201. doi:10.1021/acsmedchemlett.6b00270
134. Sofia, M. J.; Bao, D.; Chang, W.; Du, J.; Nagarathnam, D.; Rachakonda, S.; Reddy, P. G.; Ross, B. S.; Wang, P.; Zhang, H.-R.; Bansal, S.; Espiritu, C.; Keilman, M.; Lam, A. M.; Steuer, H. M. M.; Niu, C.; Otto, M. J.; Furman, P. A. *J. Med. Chem.* **2010,** *53,* 7202–7218. doi:10.1021/jm100863x
135. Gore, K. R.; Harikrishna, S.; Pradeepkumar, P. I. *J. Org. Chem.* **2013,** *78,* 9956–9962. doi:10.1021/jo4012333
136. Fateev, I. V.; Antonov, K. V.; Konstantinova, I. D.; Muravyova, T. I.; Seela, F.; Esipov, R. S.; Miroshnikov, A. I.; Mikhailopulo, I. A. *Beilstein J. Org. Chem.* **2014,** *10,* 1657–1669. doi:10.3762/bjoc.10.173
137. Appleby, T. C.; Perry, J. K.; Murakami, E.; Barauskas, O.; Feng, J.; Cho, A.; Fox, D., III; Wetmore, D. R.; McGrath, M. E.; Ray, A. S.; Sofia, M. J.; Swaminathan, S.; Edwards, T. E. *Science* **2015,** *347,* 771–775. doi:10.1126/science.1259210
138. Borthwick, A. D.; Evans, D. N.; Kirk, B. E.; Biggadike, K.; Exall, A. M.; Youds, P.; Roberts, S. M.; Knight, D. J.; Coates, J. A. V. *J. Med. Chem.* **1990,** *33,* 179–186. doi:10.1021/jm00163a030
139. Santschi, N.; Aiguabella, N.; Lewe, V.; Gilmour, R. *J. Fluorine Chem.* **2015,** *179,* 96–101. doi:10.1016/j.jfluchem.2015.06.004
140. Glaudemans, C. P. J.; Lerner, L.; Daves, G. D., Jr.; Kováč, P.; Venable, R.; Bax, A. *Biochemistry* **1990,** *29,* 10906–10911. doi:10.1021/bi00501a007
141. Xu, B.; Unione, L.; Sardinha, J.; Wu, S.; Ethève-Quelquejeu, M.; Pilar Rauter, A.; Blériot, Y.; Zhang, Y.; Martín-Santamaría, S.; Díaz, D.; Jiménez-Barbero, J.; Sollogoub, M. *Angew. Chem., Int. Ed.* **2014,** *53,* 9597–9602. doi:10.1002/anie.201405008
142. Pérez-Castells, J.; Hernández-Gay, J. J.; Denton, R. W.; Tony, K. A.; Mootoo, D. R.; Jiménez-Barbero, J. *Org. Biomol. Chem.* **2007,** *5,* 1087–1092. doi:10.1039/b615752a
143. Ramos-Figueroa, J. S.; Palmer, D. R. J. *Biochemistry* **2022,** *61,* 868–878. doi:10.1021/acs.biochem.2c00064
144. Cao, J.; Veytia-Bucheli, J. I.; Liang, L.; Wouters, J.; Silva-Rosero, I.; Bussmann, J.; Gauthier, C.; De Bolle, X.; Groleau, M.-C.; Déziel, E.; Vincent, S. P. *Bioorg. Chem.* **2024,** *153,* 107767. doi:10.1016/j.bioorg.2024.107767
145. Forget, S. M.; Bhattasali, D.; Hart, V. C.; Cameron, T. S.; Syvitski, R. T.; Jakeman, D. L. *Chem. Sci.* **2012,** *3,* 1866–1878. doi:10.1039/c2sc01077a
146. Jin, Y.; Bhattasali, D.; Pellegrini, E.; Forget, S. M.; Baxter, N. J.; Cliff, M. J.; Bowler, M. W.; Jakeman, D. L.; Blackburn, G. M.; Waltho, J. P. *Proc. Natl. Acad. Sci. U. S. A.* **2014,** *111,* 12384–12389. doi:10.1073/pnas.1402850111
147. Forget, S. M.; Bushnell, E. A. C.; Boyd, R. J.; Jakeman, D. L. *Can. J. Chem.* **2016,** *94,* 902–908. doi:10.1139/cjc-2015-0477
148. Erxleben, N. D.; Kedziora, G. S.; Urban, J. J. *Theor. Chem. Acc.* **2014,** *133,* 1491. doi:10.1007/s00214-014-1491-8
149. Koshizawa, T.; Morimoto, T.; Watanabe, G.; Watanabe, T.; Yamasaki, N.; Sawada, Y.; Fukuda, T.; Okuda, A.; Shibuya, K.; Ohgiya, T. *Bioorg. Med. Chem. Lett.* **2017,** *27,* 3249–3253. doi:10.1016/j.bmcl.2017.06.034
150. Deniau, G.; Slawin, A. M. Z.; Lebl, T.; Chorki, F.; Issberner, J. P.; van Mourik, T.; Heygate, J. M.; Lambert, J. J.; Etherington, L.-A.; Sillar, K. T.; O'Hagan, D. *ChemBioChem* **2007,** *8,* 2265–2274. doi:10.1002/cbic.200700371
151. Yamamoto, I.; Jordan, M. J. T.; Gavande, N.; Doddareddy, M. R.; Chebib, M.; Hunter, L. *Chem. Commun.* **2012,** *48,* 829–831. doi:10.1039/c1cc15816c
152. Gökcan, H.; Konuklar, F. A. S. *J. Mol. Graphics Modell.* **2014,** *51,* 173–183. doi:10.1016/j.jmgm.2014.05.006
153. Absalom, N.; Yamamoto, I.; O'Hagan, D.; Hunter, L.; Chebib, M. *Aust. J. Chem.* **2015,** *68,* 23–30. doi:10.1071/ch14456
154. Kondratov, I. S.; Bugera, M. Y.; Tolmachova, N. A.; Posternak, G. G.; Daniliuc, C. G.; Haufe, G. *J. Org. Chem.* **2015,** *80,* 12258–12264. doi:10.1021/acs.joc.5b02171
155. Cheerlavancha, R.; Ahmed, A.; Leung, Y. C.; Lawer, A.; Liu, Q.-Q.; Cagnes, M.; Jang, H.-C.; Hu, X.-G.; Hunter, L. *Beilstein J. Org. Chem.* **2017,** *13,* 2316–2325. doi:10.3762/bjoc.13.228
156. Chia, P. W.; Brennan, S. C.; Slawin, A. M. Z.; Riccardi, D.; O'Hagan, D. *Org. Biomol. Chem.* **2012,** *10,* 7922–7927. doi:10.1039/c2ob26402a

157. Brewitz, L.; Noda, H.; Kumagai, N.; Shibasaki, M. *Eur. J. Org. Chem.* **2020,** 1745–1752. doi:10.1002/ejoc.202000109
158. de Villiers, J.; Koekemoer, L.; Strauss, E. *Chem. – Eur. J.* **2010,** *16,* 10030–10041. doi:10.1002/chem.201000622
159. Chia, P. W.; Livesey, M. R.; Slawin, A. M. Z.; van Mourik, T.; Wyllie, D. J. A.; O'Hagan, D. *Chem. – Eur. J.* **2012,** *18,* 8813–8819. doi:10.1002/chem.201200071
160. Adler, P.; Teskey, C. J.; Kaiser, D.; Holy, M.; Sitte, H. H.; Maulide, N. *Nat. Chem.* **2019,** *11,* 329–334. doi:10.1038/s41557-019-0215-z
161. Lam, Y.-h.; Houk, K. N.; Cossy, J.; Gomez Pardo, D.; Cochi, A. *Helv. Chim. Acta* **2012,** *95,* 2265–2277. doi:10.1002/hlca.201200461
162. Hu, X.-G.; Hunter, L. *Beilstein J. Org. Chem.* **2013,** *9,* 2696–2708. doi:10.3762/bjoc.9.306
163. Nairoukh, Z.; Wollenburg, M.; Schlepphorst, C.; Bergander, K.; Glorius, F. *Nat. Chem.* **2019,** *11,* 264–270. doi:10.1038/s41557-018-0197-2
164. Campbell, N. H.; Smith, D. L.; Reszka, A. P.; Neidle, S.; O'Hagan, D. *Org. Biomol. Chem.* **2011,** *9,* 1328–1331. doi:10.1039/c0ob00886a
165. Yan, N.; Fang, Z.; Liu, Q.-Q.; Guo, X.-H.; Hu, X.-G. *Org. Biomol. Chem.* **2016,** *14,* 3469–3475. doi:10.1039/c6ob00063k
166. Chen, S.; Ruan, Y.; Lu, J.-L.; Hunter, L.; Hu, X.-G. *Org. Biomol. Chem.* **2020,** *18,* 8192–8198. doi:10.1039/d0ob01811b
167. Patel, A. R.; Ball, G.; Hunter, L.; Liu, F. *Org. Biomol. Chem.* **2013,** *11,* 3781–3785. doi:10.1039/c3ob40391b
168. Patel, A. R.; Hunter, L.; Bhadbhade, M. M.; Liu, F. *Eur. J. Org. Chem.* **2014,** 2584–2593. doi:10.1002/ejoc.201301811
169. Hardianto, A.; Yusuf, M.; Liu, F.; Ranganathan, S. *BMC Bioinf.* **2017,** *18* (Suppl. 16), 572. doi:10.1186/s12859-017-1955-7
170. Hardianto, A.; Liu, F.; Ranganathan, S. *J. Chem. Inf. Model.* **2018,** *58,* 511–519. doi:10.1021/acs.jcim.7b00504
171. Moore, A. F.; Newman, D. J.; Ranganathan, S.; Liu, F. *Aust. J. Chem.* **2018,** *71,* 917–930. doi:10.1071/ch18416
172. Hardianto, A.; Khanna, V.; Liu, F.; Ranganathan, S. *BMC Bioinf.* **2019,** *19* (Suppl. 13), 342. doi:10.1186/s12859-018-2373-1
173. Grunewald, G. L.; Seim, M. R.; Lu, J.; Makboul, M.; Criscione, K. R. *J. Med. Chem.* **2006,** *49,* 2939–2952. doi:10.1021/jm051262k
174. Xue, F.; Fang, J.; Lewis, W. W.; Martásek, P.; Roman, L. J.; Silverman, R. B. *Bioorg. Med. Chem. Lett.* **2010,** *20,* 554–557. doi:10.1016/j.bmcl.2009.11.086
175. Nakajima, Y.; Inoue, T.; Nakai, K.; Mukoyoshi, K.; Hamaguchi, H.; Hatanaka, K.; Sasaki, H.; Tanaka, A.; Takahashi, F.; Kunikawa, S.; Usuda, H.; Moritomo, A.; Higashi, Y.; Inami, M.; Shirakami, S. *Bioorg. Med. Chem.* **2015,** *23,* 4871–4883. doi:10.1016/j.bmc.2015.05.034
176. Vorberg, R.; Trapp, N.; Zimmerli, D.; Wagner, B.; Fischer, H.; Kratochwil, N. A.; Kansy, M.; Carreira, E. M.; Müller, K. *ChemMedChem* **2016,** *11,* 2216–2239. doi:10.1002/cmdc.201600325
177. Spahn, V.; Del Vecchio, G.; Labuz, D.; Rodriguez-Gaztelumendi, A.; Massaly, N.; Temp, J.; Durmaz, V.; Sabri, P.; Reidelbach, M.; Machelska, H.; Weber, M.; Stein, C. *Science* **2017,** *355,* 966–969. doi:10.1126/science.aai8636
178. Telfer, T. J.; Richardson-Sanchez, T.; Gotsbacher, M. P.; Nolan, K. P.; Tieu, W.; Codd, R. *BioMetals* **2019,** *32,* 395–408. doi:10.1007/s10534-019-00175-7
179. Thum, S.; Schepmann, D.; Ayet, E.; Pujol, M.; Nieto, F. R.; Ametamey, S. M.; Wünsch, B. *Eur. J. Med. Chem.* **2019,** *177,* 47–62. doi:10.1016/j.ejmech.2019.05.034
180. Scott, J. S.; Moss, T. A.; Balazs, A.; Barlaam, B.; Breed, J.; Carbajo, R. J.; Chiarparin, E.; Davey, P. R. J.; Delpuech, O.; Fawell, S.; Fisher, D. I.; Gagrica, S.; Gangl, E. T.; Grebe, T.; Greenwood, R. D.; Hande, S.; Hatoum-Mokdad, H.; Herlihy, K.; Hughes, S.; Hunt, T. A.; Huynh, H.; Janbon, S. L. M.; Johnson, T.; Kavanagh, S.; Klinowska, T.; Lawson, M.; Lister, A. S.; Marden, S.; McGinnity, D. F.; Morrow, C. J.; Nissink, J. W. M.; O'Donovan, D. H.; Peng, B.; Polanski, R.; Stead, D. S.; Stokes, S.; Thakur, K.; Throner, S. R.; Tucker, M. J.; Varnes, J.; Wang, H.; Wilson, D. M.; Wu, D.; Wu, Y.; Yang, B.; Yang, W. *J. Med. Chem.* **2020,** *63,* 14530–14559. doi:10.1021/acs.jmedchem.0c01163
181. Marych, D.; Bilenko, V.; Ilchuk, Y. V.; Kinakh, S.; Soloviov, V.; Yatsymyrskiy, A.; Liashuk, O.; Shishkina, S.; Komarov, I. V.; Grygorenko, O. O. *J. Fluorine Chem.* **2024,** *277,* 110307. doi:10.1016/j.jfluchem.2024.110307
182. Cox, C. D.; Coleman, P. J.; Breslin, M. J.; Whitman, D. B.; Garbaccio, R. M.; Fraley, M. E.; Buser, C. A.; Walsh, E. S.; Hamilton, K.; Schaber, M. D.; Lobell, R. B.; Tao, W.; Davide, J. P.; Diehl, R. E.; Abrams, M. T.; South, V. J.; Huber, H. E.; Torrent, M.; Prueksaritanont, T.; Li, C.; Slaughter, D. E.; Mahan, E.; Fernandez-Metzler, C.; Yan, Y.; Kuo, L. C.; Kohl, N. E.; Hartman, G. D. *J. Med. Chem.* **2008,** *51,* 4239–4252. doi:10.1021/jm800386y
183. O'Hagan, D.; Bilton, C.; Howard, J. A. K.; Knight, L.; Tozer, D. J. *J. Chem. Soc., Perkin Trans. 2* **2000,** 605–607. doi:10.1039/b000205o
184. Schäfer, M.; Stünkel, T.; Daniliuc, C. G.; Gilmour, R. *Angew. Chem., Int. Ed.* **2022,** *61,* e202205508. doi:10.1002/anie.202205508
185. Peddie, V.; Pietsch, M.; Bromfield, K.; Pike, R.; Duggan, P.; Abell, A. *Synthesis* **2010,** 1845–1859. doi:10.1055/s-0029-1218743
186. Hunault, J.; Diswall, M.; Frison, J.-C.; Blot, V.; Rocher, J.; Marionneau-Lambot, S.; Oullier, T.; Douillard, J.-Y.; Guillarme, S.; Saluzzo, C.; Dujardin, G.; Jacquemin, D.; Graton, J.; Le Questel, J.-Y.; Evain, M.; Lebreton, J.; Dubreuil, D.; Le Pendu, J.; Pipelier, M. *J. Med. Chem.* **2012,** *55,* 1227–1241. doi:10.1021/jm201368m
187. Mascitti, V.; Stevens, B. D.; Choi, C.; McClure, K. F.; Guimarães, C. R. W.; Farley, K. A.; Munchhof, M. J.; Robinson, R. P.; Futatsugi, K.; Lavergne, S. Y.; Lefker, B. A.; Cornelius, P.; Bonin, P. D.; Kalgutkar, A. S.; Sharma, R.; Chen, Y. *Bioorg. Med. Chem. Lett.* **2011,** *21,* 1306–1309. doi:10.1016/j.bmcl.2011.01.088
188. Fukushima, H.; Hiratate, A.; Takahashi, M.; Saito, M.; Munetomo, E.; Kitano, K.; Saito, H.; Takaoka, Y.; Yamamoto, K. *Bioorg. Med. Chem.* **2004,** *12,* 6053–6061. doi:10.1016/j.bmc.2004.09.010
189. Jansen, K.; Heirbaut, L.; Verkerk, R.; Cheng, J. D.; Joossens, J.; Cos, P.; Maes, L.; Lambeir, A.-M.; De Meester, I.; Augustyns, K.; Van der Veken, P. *J. Med. Chem.* **2014,** *57,* 3053–3074. doi:10.1021/jm500031w
190. Patrick, D. A.; Gillespie, J. R.; McQueen, J.; Hulverson, M. A.; Ranade, R. M.; Creason, S. A.; Herbst, Z. M.; Gelb, M. H.; Buckner, F. S.; Tidwell, R. R. *J. Med. Chem.* **2017,** *60,* 957–971. doi:10.1021/acs.jmedchem.6b01163

191. Planken, S.; Behenna, D. C.; Nair, S. K.; Johnson, T. O.; Nagata, A.; Almaden, C.; Bailey, S.; Ballard, T. E.; Bernier, L.; Cheng, H.; Cho-Schultz, S.; Dalvie, D.; Deal, J. G.; Dinh, D. M.; Edwards, M. P.; Ferre, R. A.; Gajiwala, K. S.; Hemkens, M.; Kania, R. S.; Kath, J. C.; Matthews, J.; Murray, B. W.; Niessen, S.; Orr, S. T. M.; Pairish, M.; Sach, N. W.; Shen, H.; Shi, M.; Solowiej, J.; Tran, K.; Tseng, E.; Vicini, P.; Wang, Y.; Weinrich, S. L.; Zhou, R.; Zientek, M.; Liu, L.; Luo, Y.; Xin, S.; Zhang, C.; Lafontaine, J. *J. Med. Chem.* **2017,** *60,* 3002–3019. doi:10.1021/acs.jmedchem.6b01894
192. Gabellieri, E.; Capotosti, F.; Molette, J.; Sreenivasachary, N.; Mueller, A.; Berndt, M.; Schieferstein, H.; Juergens, T.; Varisco, Y.; Oden, F.; Schmitt-Willich, H.; Hickman, D.; Dinkelborg, L.; Stephens, A.; Pfeifer, A.; Kroth, H. *Eur. J. Med. Chem.* **2020,** *204,* 112615. doi:10.1016/j.ejmech.2020.112615
193. Stump, C. A.; Bell, I. M.; Bednar, R. A.; Fay, J. F.; Gallicchio, S. N.; Hershey, J. C.; Jelley, R.; Kreatsoulas, C.; Moore, E. L.; Mosser, S. D.; Quigley, A. G.; Roller, S. A.; Salvatore, C. A.; Sharik, S. S.; Theberge, C. R.; Zartman, C. B.; Kane, S. A.; Graham, S. L.; Selnick, H. G.; Vacca, J. P.; Williams, T. M. *Bioorg. Med. Chem. Lett.* **2010,** *20,* 2572–2576. doi:10.1016/j.bmcl.2010.02.086
194. Combettes, L. E.; Clausen-Thue, P.; King, M. A.; Odell, B.; Thompson, A. L.; Gouverneur, V.; Claridge, T. D. W. *Chem. – Eur. J.* **2012,** *18,* 13133–13141. doi:10.1002/chem.201201577
195. Compain, G.; Martin-Mingot, A.; Maresca, A.; Thibaudeau, S.; Supuran, C. T. *Bioorg. Med. Chem.* **2013,** *21,* 1555–1563. doi:10.1016/j.bmc.2012.05.037
196. Le Darz, A.; Mingot, A.; Bouazza, F.; Castelli, U.; Karam, O.; Tanc, M.; Supuran, C. T.; Thibaudeau, S. *J. Enzyme Inhib. Med. Chem.* **2015,** *30,* 737–745. doi:10.3109/14756366.2014.963072
197. Chen, H.; Volgraf, M.; Do, S.; Kolesnikov, A.; Shore, D. G.; Verma, V. A.; Villemure, E.; Wang, L.; Chen, Y.; Hu, B.; Lu, A.-J.; Wu, G.; Xu, X.; Yuen, P.-w.; Zhang, Y.; Erickson, S. D.; Dahl, M.; Brotherton-Pleiss, C.; Tay, S.; Ly, J. Q.; Murray, L. J.; Chen, J.; Amm, D.; Lange, W.; Hackos, D. H.; Reese, R. M.; Shields, S. D.; Lyssikatos, J. P.; Safina, B. S.; Estrada, A. A. *J. Med. Chem.* **2018,** *61,* 3641–3659. doi:10.1021/acs.jmedchem.8b00117
198. Berrino, E.; Michelet, B.; Martin-Mingot, A.; Carta, F.; Supuran, C. T.; Thibaudeau, S. *Angew. Chem., Int. Ed.* **2021,** *60,* 23068–23082. doi:10.1002/anie.202103211
199. Zimmer, L. E.; Sparr, C.; Gilmour, R. *Angew. Chem., Int. Ed.* **2011,** *50,* 11860–11871. doi:10.1002/anie.201102027
200. Cahard, D.; Bizet, V. *Chem. Soc. Rev.* **2014,** *43,* 135–147. doi:10.1039/c3cs60193e
201. DiRocco, D. A.; Rovis, T. *J. Am. Chem. Soc.* **2011,** *133,* 10402–10405. doi:10.1021/ja203810b
202. Quintard, A.; Langlois, J.-B.; Emery, D.; Mareda, J.; Guénée, L.; Alexakis, A. *Chem. – Eur. J.* **2011,** *17,* 13433–13437. doi:10.1002/chem.201102757
203. DiRocco, D. A.; Noey, E. L.; Houk, K. N.; Rovis, T. *Angew. Chem., Int. Ed.* **2012,** *51,* 2391–2394. doi:10.1002/anie.201107597
204. Yap, D. Q. J.; Cheerlavancha, R.; Lowe, R.; Wang, S.; Hunter, L. *Aust. J. Chem.* **2015,** *68,* 44–49. doi:10.1071/ch14129
205. Myers, E. L.; Palte, M. J.; Raines, R. T. *J. Org. Chem.* **2019,** *84,* 1247–1256. doi:10.1021/acs.joc.8b02644
206. Chandler, C. L.; List, B. *J. Am. Chem. Soc.* **2008,** *130,* 6737–6739. doi:10.1021/ja8024164
207. Ho, C.-Y.; Chen, Y.-C.; Wong, M.-K.; Yang, D. *J. Org. Chem.* **2005,** *70,* 898–906. doi:10.1021/jo048378t
208. Sparr, C.; Schweizer, W. B.; Senn, H. M.; Gilmour, R. *Angew. Chem., Int. Ed.* **2009,** *48,* 3065–3068. doi:10.1002/anie.200900405
209. Sparr, C.; Gilmour, R. *Angew. Chem., Int. Ed.* **2010,** *49,* 6520–6523. doi:10.1002/anie.201003734
210. Paul, S.; Schweizer, W. B.; Ebert, M.-O.; Gilmour, R. *Organometallics* **2010,** *29,* 4424–4427. doi:10.1021/om100789n
211. Tanzer, E.-M.; Zimmer, L. E.; Schweizer, W. B.; Gilmour, R. *Chem. – Eur. J.* **2012,** *18,* 11334–11342. doi:10.1002/chem.201201316
212. Tanzer, E.-M.; Schweizer, W. B.; Ebert, M.-O.; Gilmour, R. *Chem. – Eur. J.* **2012,** *18,* 2006–2013. doi:10.1002/chem.201102859
213. Paul, S.; Schweizer, W. B.; Rugg, G.; Senn, H. M.; Gilmour, R. *Tetrahedron* **2013,** *69,* 5647–5659. doi:10.1016/j.tet.2013.02.071
214. Holland, M. C.; Berden, G.; Oomens, J.; Meijer, A. J. H. M.; Schäfer, M.; Gilmour, R. *Eur. J. Org. Chem.* **2014,** 5675–5680. doi:10.1002/ejoc.201402845
215. Molnár, I. G.; Tanzer, E.-M.; Daniliuc, C.; Gilmour, R. *Chem. – Eur. J.* **2014,** *20,* 794–800. doi:10.1002/chem.201303586
216. Sagamanova, I.; Rodríguez-Escrich, C.; Molnár, I. G.; Sayalero, S.; Gilmour, R.; Pericàs, M. A. *ACS Catal.* **2015,** *5,* 6241–6248. doi:10.1021/acscatal.5b01746
217. Yarmolchuk, V. S.; Mykhalchuk, V. L.; Mykhailiuk, P. K. *Tetrahedron* **2014,** *70,* 3011–3017. doi:10.1016/j.tet.2014.03.002
218. Koeller, S.; Thomas, C.; Peruch, F.; Deffieux, A.; Massip, S.; Léger, J.-M.; Desvergne, J.-P.; Milet, A.; Bibal, B. *Chem. – Eur. J.* **2014,** *20,* 2849–2859. doi:10.1002/chem.201303662
219. Mamone, M.; Gonçalves, R. S. B.; Blanchard, F.; Bernadat, G.; Ongeri, S.; Milcent, T.; Crousse, B. *Chem. Commun.* **2017,** *53,* 5024–5027. doi:10.1039/c7cc01298e
220. Cosimi, E.; Trapp, N.; Ebert, M.-O.; Wennemers, H. *Chem. Commun.* **2019,** *55,* 2253–2256. doi:10.1039/c8cc09987a
221. Lizarme-Salas, Y.; Yu, T. T.; de Bruin-Dickason, C.; Kumar, N.; Hunter, L. *Org. Biomol. Chem.* **2021,** *19,* 9629–9636. doi:10.1039/d1ob01649k
222. Luckhurst, C. A.; Breccia, P.; Stott, A. J.; Aziz, O.; Birch, H. L.; Bürli, R. W.; Hughes, S. J.; Jarvis, R. E.; Lamers, M.; Leonard, P. M.; Matthews, K. L.; McAllister, G.; Pollack, S.; Saville-Stones, E.; Wishart, G.; Yates, D.; Dominguez, C. *ACS Med. Chem. Lett.* **2016,** *7,* 34–39. doi:10.1021/acsmedchemlett.5b00302
223. Bykova, T.; Al-Maharik, N.; Slawin, A. M. Z.; Bühl, M.; Lebl, T.; O'Hagan, D. *Chem. – Eur. J.* **2018,** *24,* 13290–13296. doi:10.1002/chem.201802166
224. Olivato, P. R.; Guerrero, S. A.; Yreijo, M. H.; Rittner, R.; Tormena, C. F. *J. Mol. Struct.* **2002,** *607,* 87–99. doi:10.1016/s0022-2860(01)00761-x
225. Bilska-Markowska, M.; Rapp, M.; Siodła, T.; Katrusiak, A.; Hoffmann, M.; Koroniak, H. *New J. Chem.* **2014,** *38,* 3819–3830. doi:10.1039/c4nj00317a
226. Maeno, M.; Tokunaga, E.; Yamamoto, T.; Suzuki, T.; Ogino, Y.; Ito, E.; Shiro, M.; Asahi, T.; Shibata, N. *Chem. Sci.* **2015,** *6,* 1043–1048. doi:10.1039/c4sc03047h
227. Bilska-Markowska, M.; Siodla, T.; Patyk-Kaźmierczak, E.; Katrusiak, A.; Koroniak, H. *New J. Chem.* **2017,** *41,* 12631–12644. doi:10.1039/c7nj02986a
228. Brewitz, L.; Noda, H.; Kumagai, N.; Shibasaki, M. *Eur. J. Org. Chem.* **2018,** 714–722. doi:10.1002/ejoc.201701083
229. Lizarme-Salas, Y.; Ariawan, A. D.; Ratnayake, R.; Luesch, H.; Finch, A.; Hunter, L. *Beilstein J. Org. Chem.* **2020,** *16,* 2663–2670. doi:10.3762/bjoc.16.216

230. Saravanan, K.; Sivanandam, M.; Hunday, G.; Pavan, M. S.; Kumaradhas, P. *J. Mol. Graphics Modell.* **2019,** *92,* 280–295. doi:10.1016/j.jmgm.2019.07.019
231. Tormena, C. F.; Freitas, M. P.; Rittner, R.; Abraham, R. J. *Phys. Chem. Chem. Phys.* **2004,** *6,* 1152–1156. doi:10.1039/b311570d
232. Ellipilli, S.; Palvai, S.; Ganesh, K. N. *J. Org. Chem.* **2016,** *81,* 6364–6373. doi:10.1021/acs.joc.6b01009
233. Pattison, G. *Beilstein J. Org. Chem.* **2017,** *13,* 2915–2921. doi:10.3762/bjoc.13.284
234. Silla, J. M.; Silva, D. R.; Freitas, M. P. *Mol. Inf.* **2017,** *36,* 1700084. doi:10.1002/minf.201700084
235. Kim, W.; Hardcastle, K. I.; Conticello, V. P. *Angew. Chem., Int. Ed.* **2006,** *45,* 8141–8145. doi:10.1002/anie.200603227
236. Pandey, A. K.; Naduthambi, D.; Thomas, K. M.; Zondlo, N. J. *J. Am. Chem. Soc.* **2013,** *135,* 4333–4363. doi:10.1021/ja3109664
237. Kubyshkin, V. *Beilstein J. Org. Chem.* **2020,** *16,* 1837–1852. doi:10.3762/bjoc.16.151
238. Kubyshkin, V.; Davis, R.; Budisa, N. *Beilstein J. Org. Chem.* **2021,** *17,* 439–460. doi:10.3762/bjoc.17.40
239. Miles, S. A.; Nillama, J. A.; Hunter, L. *Molecules* **2023,** *28,* 6192. doi:10.3390/molecules28176192
240. Salwiczek, M.; Nyakatura, E. K.; Gerling, U. I. M.; Ye, S.; Koksch, B. *Chem. Soc. Rev.* **2012,** *41,* 2135–2171. doi:10.1039/c1cs15241f
241. Staas, D. D.; Savage, K. L.; Sherman, V. L.; Shimp, H. L.; Lyle, T. A.; Tran, L. O.; Wiscount, C. M.; McMasters, D. R.; Sanderson, P. E. J.; Williams, P. D.; Lucas, B. J., Jr.; Krueger, J. A.; Dale Lewis, S.; White, R. B.; Yu, S.; Wong, B. K.; Kochansky, C. J.; Reza Anari, M.; Yan, Y.; Vacca, J. P. *Bioorg. Med. Chem.* **2006,** *14,* 6900–6916. doi:10.1016/j.bmc.2006.06.040
242. Holmgren, S. K.; Taylor, K. M.; Bretscher, L. E.; Raines, R. T. *Nature* **1998,** *392,* 666–667. doi:10.1038/33573
243. Lummis, S. C. R.; Beene, D. L.; Lee, L. W.; Lester, H. A.; Broadhurst, R. W.; Dougherty, D. A. *Nature* **2005,** *438,* 248–252. doi:10.1038/nature04130
244. Shoulders, M. D.; Satyshur, K. A.; Forest, K. T.; Raines, R. T. *Proc. Natl. Acad. Sci. U. S. A.* **2010,** *107,* 559–564. doi:10.1073/pnas.0909592107
245. Holzberger, B.; Obeid, S.; Welte, W.; Diederichs, K.; Marx, A. *Chem. Sci.* **2012,** *3,* 2924–2931. doi:10.1039/c2sc20545a
246. Borgogno, A.; Ruzza, P. *Amino Acids* **2013,** *44,* 607–614. doi:10.1007/s00726-012-1383-y
247. Lin, Y.-J.; Horng, J.-C. *Amino Acids* **2014,** *46,* 2317–2324. doi:10.1007/s00726-014-1783-2
248. Catherine, C.; Oh, S. J.; Lee, K.-H.; Min, S.-E.; Won, J.-I.; Yun, H.; Kim, D.-M. *Biotechnol. Bioprocess Eng.* **2015,** *20,* 417–422. doi:10.1007/s12257-015-0190-1
249. Doerfel, L. K.; Wohlgemuth, I.; Kubyshkin, V.; Starosta, A. L.; Wilson, D. N.; Budisa, N.; Rodnina, M. V. *J. Am. Chem. Soc.* **2015,** *137,* 12997–13006. doi:10.1021/jacs.5b07427
250. Huang, K.-Y.; Horng, J.-C. *Biochemistry* **2015,** *54,* 6186–6194. doi:10.1021/acs.biochem.5b00880
251. Dietz, D.; Kubyshkin, V.; Budisa, N. *ChemBioChem* **2015,** *16,* 403–406. doi:10.1002/cbic.201402654
252. Rienzo, M.; Rocchi, A. R.; Threatt, S. D.; Dougherty, D. A.; Lummis, S. C. R. *J. Biol. Chem.* **2016,** *291,* 6272–6280. doi:10.1074/jbc.m115.694372
253. Mosesso, R.; Dougherty, D. A.; Lummis, S. C. R. *Biochemistry* **2018,** *57,* 4036–4043. doi:10.1021/acs.biochem.8b00379
254. Mosesso, R.; Dougherty, D. A.; Lummis, S. C. R. *ACS Chem. Neurosci.* **2019,** *10,* 3327–3333. doi:10.1021/acschemneuro.9b00315
255. Steiner, T.; Hess, P.; Bae, J. H.; Wiltschi, B.; Moroder, L.; Budisa, N. *PLoS One* **2008,** *3,* e1680. doi:10.1371/journal.pone.0001680
256. Hofman, G.-J.; Ottoy, E.; Light, M. E.; Kieffer, B.; Kuprov, I.; Martins, J. C.; Sinnaeve, D.; Linclau, B. *Chem. Commun.* **2018,** *54,* 5118–5121. doi:10.1039/c8cc01493k
257. Hofman, G.-J.; Ottoy, E.; Light, M. E.; Kieffer, B.; Martins, J. C.; Kuprov, I.; Sinnaeve, D.; Linclau, B. *J. Org. Chem.* **2019,** *84,* 3100–3120. doi:10.1021/acs.joc.8b02920
258. Edmondson, S. D.; Wei, L.; Xu, J.; Shang, J.; Xu, S.; Pang, J.; Chaudhary, A.; Dean, D. C.; He, H.; Leiting, B.; Lyons, K. A.; Patel, R. A.; Patel, S. B.; Scapin, G.; Wu, J. K.; Beconi, M. G.; Thornberry, N. A.; Weber, A. E. *Bioorg. Med. Chem. Lett.* **2008,** *18,* 2409–2413. doi:10.1016/j.bmcl.2008.02.050
259. Jakobsche, C. E.; Choudhary, A.; Miller, S. J.; Raines, R. T. *J. Am. Chem. Soc.* **2010,** *132,* 6651–6653. doi:10.1021/ja100931y
260. Chang, W.; Mosley, R. T.; Bansal, S.; Keilman, M.; Lam, A. M.; Furman, P. A.; Otto, M. J.; Sofia, M. J. *Bioorg. Med. Chem. Lett.* **2012,** *22,* 2938–2942. doi:10.1016/j.bmcl.2012.02.051
261. Arcoria, P. J.; Ware, R. I.; Makwana, S. V.; Troya, D.; Etzkorn, F. A. *J. Phys. Chem. B* **2022,** *126,* 217–228. doi:10.1021/acs.jpcb.1c09180
262. Nadon, J.-F.; Rochon, K.; Grastilleur, S.; Langlois, G.; Dao, T. T. H.; Blais, V.; Guérin, B.; Gendron, L.; Dory, Y. L. *ACS Chem. Neurosci.* **2017,** *8,* 40–49. doi:10.1021/acschemneuro.6b00163
263. Takeuchi, Y.; Kamezaki, M.; Kirihara, K.; Haufe, G.; Laue, K. W.; Shibata, N. *Chem. Pharm. Bull.* **1998,** *46,* 1062–1064. doi:10.1248/cpb.46.1062
264. Jaun, B.; Seebach, D.; Mathad, R. I. *Helv. Chim. Acta* **2011,** *94,* 355–361. doi:10.1002/hlca.201100023
265. Hunter, L.; Jolliffe, K. A.; Jordan, M. J. T.; Jensen, P.; Macquart, R. B. *Chem. – Eur. J.* **2011,** *17,* 2340–2343. doi:10.1002/chem.201003320
266. March, T. L.; Johnston, M. R.; Duggan, P. J.; Gardiner, J. *Chem. Biodiversity* **2012,** *9,* 2410–2441. doi:10.1002/cbdv.201200307
267. Hunter, L.; Butler, S.; Ludbrook, S. B. *Org. Biomol. Chem.* **2012,** *10,* 8911–8918. doi:10.1039/c2ob26596f
268. Peddie, V.; Butcher, R. J.; Robinson, W. T.; Wilce, M. C. J.; Traore, D. A. K.; Abell, A. D. *Chem. – Eur. J.* **2012,** *18,* 6655–6662. doi:10.1002/chem.201200313
269. Hassoun, A.; Grison, C. M.; Guillot, R.; Boddaert, T.; Aitken, D. J. *New J. Chem.* **2015,** *39,* 3270–3279. doi:10.1039/c4nj01929f
270. Mansour, F.; Hunter, L. Synthesis and applications of backbone-fluorinated amino acids. In *Fluorine in Life Sciences: Pharmaceuticals, Medicinal Diagnostics, and Agrochemicals;* Haufe, G.; Leroux, F., Eds.; Progress in Fluorine Science; Academic Press: London, UK, 2019; pp 325–347. doi:10.1016/b978-0-12-812733-9.00009-x
271. Mathad, R. I.; Gessier, F.; Seebach, D.; Jaun, B. *Helv. Chim. Acta* **2005,** *88,* 266–280. doi:10.1002/hlca.200590008
272. Lawer, A.; Hunter, L. *Eur. J. Org. Chem.* **2021,** 1184–1190. doi:10.1002/ejoc.202001619
273. Patel, A. R.; Lawer, A.; Bhadbhade, M.; Hunter, L. *Org. Biomol. Chem.* **2024,** *22,* 1608–1612. doi:10.1039/d3ob02016a
274. Gimenez, D.; Aguilar, J. A.; Bromley, E. H. C.; Cobb, S. L. *Angew. Chem., Int. Ed.* **2018,** *57,* 10549–10553. doi:10.1002/anie.201804488
275. Appavoo, S. D.; Huh, S.; Diaz, D. B.; Yudin, A. K. *Chem. Rev.* **2019,** *119,* 9724–9752. doi:10.1021/acs.chemrev.8b00742

276. Au, C.; Gonzalez, C.; Leung, Y. C.; Mansour, F.; Trinh, J.; Wang, Z.; Hu, X.-G.; Griffith, R.; Pasquier, E.; Hunter, L. *Org. Biomol. Chem.* **2019,** *17,* 664–674. doi:10.1039/c8ob02679c
277. Hu, X.-G.; Thomas, D. S.; Griffith, R.; Hunter, L. *Angew. Chem., Int. Ed.* **2014,** *53,* 6176–6179. doi:10.1002/anie.201403071
278. Díaz, N.; Suárez, D. *J. Chem. Inf. Model.* **2021,** *61,* 223–237. doi:10.1021/acs.jcim.0c00746
279. Ariawan, A. D.; Webb, J. E. A.; Howe, E. N. W.; Gale, P. A.; Thordarson, P.; Hunter, L. *Org. Biomol. Chem.* **2017,** *15,* 2962–2967. doi:10.1039/c7ob00316a
280. Burade, S. S.; Saha, T.; Bhuma, N.; Kumbhar, N.; Kotmale, A.; Rajamohanan, P. R.; Gonnade, R. G.; Talukdar, P.; Dhavale, D. D. *Org. Lett.* **2017,** *19,* 5948–5951. doi:10.1021/acs.orglett.7b02942
281. Kim, S.-Y.; Lee, J.; Kim, S. K.; Choi, Y. S. *Chem. Phys. Lett.* **2016,** *659,* 43–47. doi:10.1016/j.cplett.2016.06.083
282. Tomita, R.; Al-Maharik, N.; Rodil, A.; Bühl, M.; O'Hagan, D. *Org. Biomol. Chem.* **2018,** *16,* 1113–1117. doi:10.1039/c7ob02987j
283. Thiehoff, C.; Holland, M. C.; Daniliuc, C.; Houk, K. N.; Gilmour, R. *Chem. Sci.* **2015,** *6,* 3565–3571. doi:10.1039/c5sc00871a
284. Thiehoff, C.; Schifferer, L.; Daniliuc, C. G.; Santschi, N.; Gilmour, R. *J. Fluorine Chem.* **2016,** *182,* 121–126. doi:10.1016/j.jfluchem.2016.01.003
285. Santschi, N.; Thiehoff, C.; Holland, M. C.; Daniliuc, C. G.; Houk, K. N.; Gilmour, R. *Organometallics* **2016,** *35,* 3040–3044. doi:10.1021/acs.organomet.6b00564
286. Axford, J.; Sung, M. J.; Manchester, J.; Chin, D.; Jain, M.; Shin, Y.; Dix, I.; Hamann, L. G.; Cheung, A. K.; Sivasankaran, R.; Briner, K.; Dales, N. A.; Hurley, B. *J. Med. Chem.* **2021,** *64,* 4744–4761. doi:10.1021/acs.jmedchem.0c02173
287. Juaristi, E.; Notario, R. *J. Org. Chem.* **2016,** *81,* 1192–1197. doi:10.1021/acs.joc.5b02718
288. Duan, T.; Gao, J.; Babics, M.; Kan, Z.; Zhong, C.; Singh, R.; Yu, D.; Lee, J.; Xiao, Z.; Lu, S. *Sol. RRL* **2020,** *4,* 1900472. doi:10.1002/solr.201900472
289. Huang, H.; Yang, L.; Facchetti, A.; Marks, T. J. *Chem. Rev.* **2017,** *117,* 10291–10318. doi:10.1021/acs.chemrev.7b00084
290. Britton, R.; Gouverneur, V.; Lin, J.-H.; Meanwell, M.; Ni, C.; Pupo, G.; Xiao, J.-C.; Hu, J. *Nat. Rev. Methods Primers* **2021,** *1,* 47. doi:10.1038/s43586-021-00042-1

License and Terms